Science

2 September 2005

Vol. 309 No. 5740
Pages 1441–1632 $10

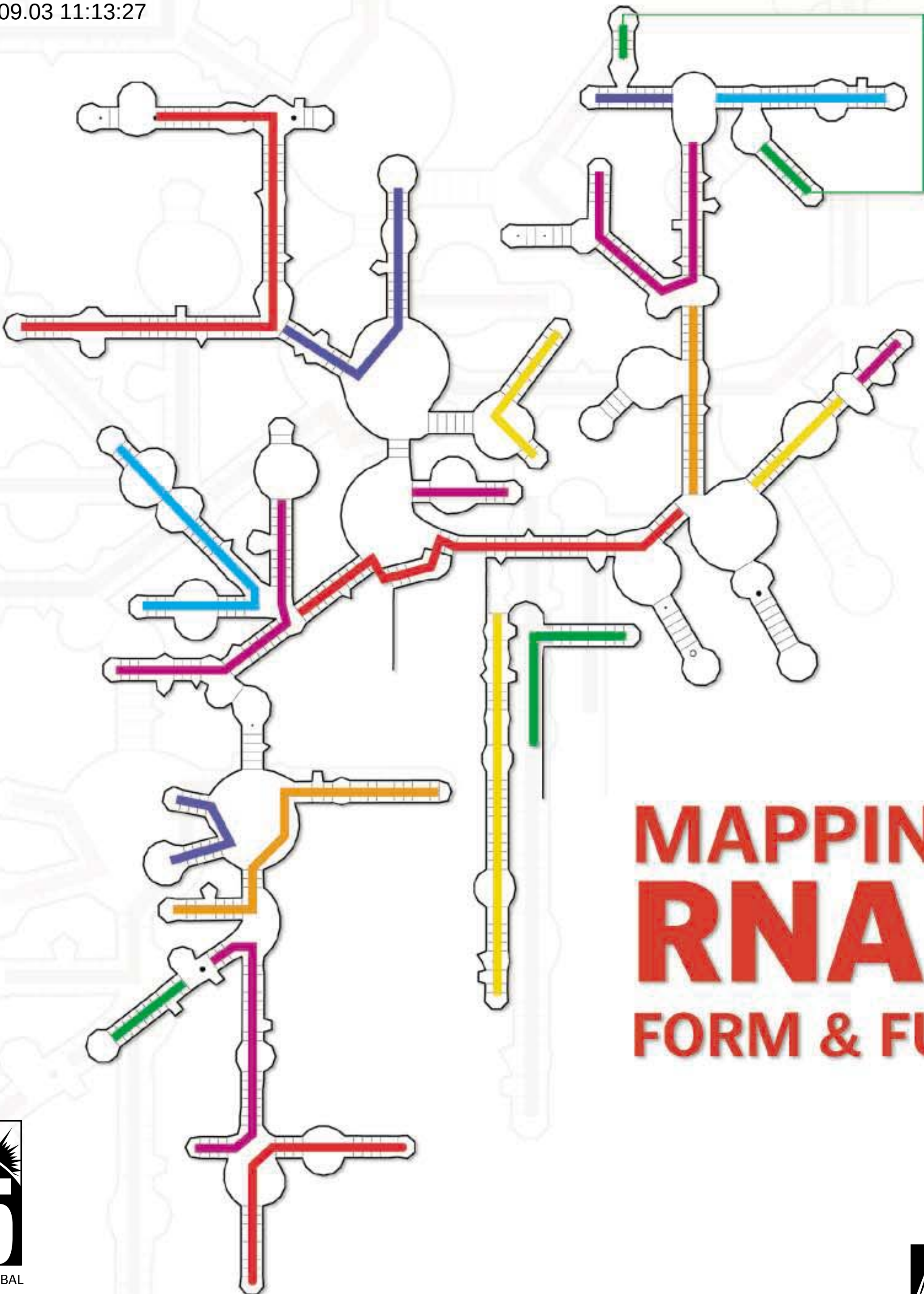

MAPPING RNA FORM & FUNCTION

125 YEARS OF GLOBAL Science

AAAS

cell sciences . . . experiment, discover, understand.

www.cellsciences.com

Cytokine Center

Browse our web site containing over 1300 recombinant cytokines, growth factors, chemokines and neurotrophins. Daily shipping and competitive pricing are offered. Bulk quantities of many proteins available. Also offered are corresponding antibodies and ELISA kits. Let us help you find your reagents.

Human Proteins

4-1BBL
4-1BB Receptor
6 Ckine
gAcrp30/Adipolean
Activin A
Adiponectin
AITRL
Alpha-Feto Protein (AFP)
Angiopoietin-1 (Ang-1)
Angiopoietin-2 (Ang-2)
Angiostatin K1-3
Annexin-V
apo-SAA
Apoliprotein A-1
Apoliprotein E2
Apoliprotein E3
Apoliprotein E4
Artemin
ATF2
B-type Natriuretic Protein
BAFF
BCA-1
BCMA
BD-1
BD-2
BD-3
BDNF
BMP-2
BMP-7
BMP-13
BMP-14
sBMPR-1A
BRAK
Breast Tumor Antigen
C-Reactive Protein (CRP)
c-Src
Carcino-embryonic Antigen
Cardiotrophin-1
Caspase-3
Caspase-6
CD14
CD22
sCD40Ligand/TRAP
sCD95/sFas Ligand
sCD105/Endoglin
sCD119
Chorionic Gonadotropin
CNTF
CREB
CTACK/CCL27
CTGF
CTGFL/WISP-2
CTLA-4/Fc
CXCL16
E-selectin
EGF
Elafin/SKALP
EMAP-II
ENA-78
Endostatin
Enteropeptidase
Eotaxin
Eotaxin-2
Eotaxin-3 (TSC)
Erk-2
Erythropoietin (EPO)
Exodus-2
Fas Ligand
Fas Receptor
FGF-acidic
FGF-basic
FGF-4
FGF-5
FGF-6
FGF-7/KGF
FGF-8
FGF-9
FGF-10
FGF-16
FGF-17
FGF-18
FGF-19
FGF-20
sFGFR-1 (IIIc)/Fc Chimera
sFGFR-2 (IIIc)/Fc Chimera
sFGFR-3/Fc Chimera
sFGFR-4/Fc Chimera
sFlt-1 (native)
sFlt-1 (D3)
sFlt-1 (D4)
sFlt-1 (D5)
sFlt (D7)/Fc
Flt3-Ligand
sFlt-4
sFlt-4/Fc Chimera
Follicle Stimulating Hormone
Fractalkine/CX3C
G-CSF
PEG-G-CSF
Galectin-1
Galectin-3
Gastrointestinal Cancer Antigen
GCP-2
GDF-3
GDNF
GM-CSF
GRO-α
GRO-β
GRO-γ
GRO/MGSA
Growth Hormone
Growth Hormone 20K
Growth Hormone (Placental)
Growth Hormone BP
GH Releasing Hormone
HCC-1
HGF
HRG1-β1
I-309
I-TAC
IFN-α
IFN-α 1
IFN-α 2
IFN-α 2a
PEG-IFN-α 2a
IFN-α 2b
PEG-IFN-α 2b
IFN-α 4a
IFN-α 4b
IFN-α A
IFN-α B2
IFN-α C
IFN-α D
IFN-α F
IFN-α G
IFN-α H2
IFN-α I
IFN-α J1
IFN-α K
IFN-α WA
IFN-β
IFN-β 1a
IFN-β 1b
IFN-γ
IFN-γ sR Chain 1
IFN-κ
IFN-λ 2
IFN-ω
Leukocyte IFN
IGF-I
Long R^3 IGF-I
IGF-II
proIGF-II
IGFBP-1
IGFBP-2
IGFBP-3
IGFBP-4
IGFBP-5
IGFBP-6
IGFBP-7
IκBα
IL-1α
IL-1β
IL-2
sIL-2 Receptor-α
IL-3
IL-4
sIL-4 Receptor
IL-5
IL-6
sIL-6 Receptor
IL-7
IL-8 (72 a.a.)
IL-8 (77 a.a.)
IL-9
IL-10
IL-11
IL-12
IL-12p40
IL-13
IL-13 analog
IL-15
IL-16 (121 a.a.)
IL-16 (130 a.a.)
IL-17
IL-17B
IL-17D
IL-17E
IL-17F
IL-19
IL-20
IL-21
IL-22
Insulin
IP-10
JNK2α1
JNK2α2
sKDR (D7)
sKDR/Fc Chimera
KGF
LAG-1
LALF Peptide
LBP
LBP Natural, Purified
LBP Peptide
LD-78β
LEC/NCC-4
Leptin
LeukinFeron
Leuprolide
Leutenizing Hormone Releasing Hormone
LIF
LIGHT
sLYVE-1
Lymphotactin
M-CSF
MCP-1 (MCAF)
MCP-2
MCP-3
MCP-4
MDC (67 a.a.)
MDC (69 a.a.)
MEC
Mek-1
Menopausal Gonadotrophin
Midkine
MIG
MIP-1α
MIP-1β
Viral MIP-2
MIP-3
MIP-3α
MIP-3β
MIP-4 (PARC)
MIP-5
Myostatin (GDF-8)
Myostatin-Propeptide
NAP-2
Neurturin
beta-NGF
NFAT-1
NOGGIN
NP-1
NT-1/BCSF-3
NT-3
NT-4
Oncostatin M
Osteoprotegerin (OPG)
Ovarian Cancer Antigen
p38-α
PDGF-AA
PDGF-AB
PDGF-BB
Persephin
PF-4
PIGF-1
PIGF-1/His
PIGF-2
Pleiotrophin
PLGF-1
Polymyxin B (PMB)
PRAS40
Prokineticin-2
Prolactin
PTHrP
sRANK
sRANKL
RANTES
RELM-β
Resistin
apo-SAA
SCF
SCF/C-kit Ligand
SCGF-α
SCGF-β
SDF-1α
SDF-1β
SHH
c-Src
STAT1
TACI
TARC
TECK
TFF2
TGF-α
TGF-β1
TGF-β2
TGF-β3
Thymosin α1
sTIE-1/Fc Chimera
TL-1A
TNF-α
TNF-β
sTNF-receptor Type I
sTNF-receptor Type II
TPO
TRAIL/Apo2L
sTRAIL R-1 (DR4)
sTRAIL R-2 (DR5)
Tumor Suppressor p53
TWEAK
TWEAK Receptor
Urokinase
EG-VEGF
VEGF121
VEGF165
Orf Virus VEGF-E
Orf Virus HB-VEGF-E
WISP-1
WISP-2
WNT-1

Mouse Proteins

Acrp30
April
BLC/BCA-1
C-10
Cardiotrophin-1
CD14
sCD40 Ligand/TRAP
CD105/Endoglin
CTACK/CCL27
CXCL16
EGF
Eotaxin
Eotaxin-2
Exodus-2
FGF-9
FGF-basic
Flt3-Ligand
G-CSF
GM-CSF
GRO-β/MIP-2
GRO/KC/CINC-1
I-TAC
IFN-α
IFN-α A
IFN-β
IFN-γ
IFN-γ sR chain 1
IFN-λ 2
IGF-I
IGFBP-5
IL-1α
IL-1β
IL-2
IL-3
IL-4
IL-6
IL-7
IL-9
IL-10
IL-12
IL-12p40
IL-13
IL-15
IL-17
IL-20
IL-22
IP-10
I-TAC
JE (MCP-1)
KC
LBP
Leptin
LIGHT
Limitin
LIX
sLYVE-1
M-CSF
MCP-2
MCP-3
MCP-5
MDC
MEC
MIG
MIP-1 α
MIP-1 β
MIP-1 γ
MIP-2
MIP-3 α
MIP-3 β
NGF
sRANKL
RANTES
RELM-α
RELM-β
Resistin
SCF
SDF-1α
SDF-1β
SF20
TNF-alpha
TPO
VEGF164

Antigen affinity purified polyclonal antibodies are available to most cytokine products.

480 Neponset Street, Building 12A, Canton, MA 02021 • TEL (781) 828-0610 • EMAIL info@cellsciences.com

CALL TOLL FREE (888) 769-1246 • FAX (781) 828-0542 • VISIT www.cellsciences.com

High-performance features come standard.

The best real-time PCR system just got better.

Stratagene's Mx3005P™ Real-Time PCR System sets the next benchmark in real-time PCR with new high-performance features, increased flexibility to support more applications and chemistries, and affordable pricing for the individual researcher (€29,900 list price*).Real-time PCR systems starting at €24,950 list price*.

- **The *only* instrument with five (5) color multiplex capability and user-selected filters**
- **Novel custom filter path selection for FRET probe chemistries**
- **Includes Beacon Designer™ oligo design software**

Need More Information? Give Us A Call:

Stratagene USA and Canada
Order: (800) 424-5444 x3
Technical Services: (800) 894-1304

Stratagene Europe
Order: 00800-7000-7000
Technical Services: 00800-7400-7400

Stratagene Japan K.K.
Order: 03-5159-2060
Technical Services: 03-5159-2070

www.stratagene.com

Practice of the patented polymerase chain reaction (PCR) process requires a license. The Mx3005P™ real-time PCR system is an Authorized Thermal Cycler and may be used with PCR licenses available from Applied Biosystems. Its use with Authorized Reagents also provides a limited PCR license in accordance with the label rights accompanying such reagents.

Beacon Designer™ is a trademark of PREMIER Biosoft International

*Pricing only available in Benelux, France, Germany, Austria, and Switzerland.

STRATAGENE®

Science

Volume 309
2 September 2005
Number 5740

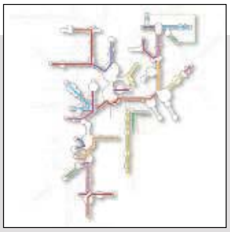

SPECIAL ISSUE

MAPPING RNA FORM AND FUNCTION

Secondary structures of 16S ribosomal RNA and transfer RNA, showing their respective base-pairing schemes. Colored bars indicate end-to-end stacking of individual helices to form longer, continuous coaxial arms. [Image: A. Baucom and H. Noller]

INTRODUCTION
1507 In the Forests of Dark Matter

REVIEWS
1508 RNA Structure: Reading the Ribosome
H. F. Noller
1514 From Birth to Death: The Complex Lives of Eukaryotic mRNAs
M. J. Moore
Poster: RNA Silencing
1519 Ribo-gnome: The Big World of Small RNAs
P. D. Zamore and B. Haley

VIEWPOINTS
1525 It's a Small RNA World, After All
M. W. Vaughn and R. Martienssen
related Report page 1567
1527 The Functional Genomics of Noncoding RNA
J. S. Mattick
related Report page 1570
1529 Fewer Genes, More Noncoding RNA
J.-M. Claverie
related Reports pages 1559 and 1564
1530 Capping by Branching: A New Ribozyme Makes Tiny Lariats
A. M. Pyle
related Report page 1584

Related Science Express Report by M. Brengues et al.; Research Article page 1534; Reports pages 1559 to 1590

For related online content in SAGE KE and STKE, see page 1451 or go to www.sciencemag.org/sciext/rna/

DEPARTMENTS
1451 SCIENCE ONLINE
1453 THIS WEEK IN SCIENCE
1457 EDITORIAL *by Alison Jolly*
The Last Great Apes?
related News story page 1468; Perspectives pages 1498 and 1499; Science Express Report by P. Khaitovich et al.
1459 EDITORS' CHOICE
1464 CONTACT SCIENCE
1467 NETWATCH
1591 NEW PRODUCTS
1596 SCIENCE CAREERS

NEWS OF THE WEEK
1468 GENOMICS
Chimp Genome Catalogs Differences With Humans
related Editorial page 1457; Perspectives pages 1498 and 1499; Science Express Report by P. Khaitovich et al.
1469 BIOETHICS
Final NIH Rules Ease Stock Limits
1471 EUROPEAN POLITICS
Germany Poised to Elect First Scientist-Chancellor
1471 SCIENCESCOPE
1472 SPACE-BASED ASTRONOMY
Scientists Scramble to Curb Webb Overruns
1472 U.S. MILITARY INSTALLATIONS
Base Commission Alters Pentagon's Wishes on Labs
1473 SCIENTIFIC DATABASES
NIH, Chemical Society Look for Common Ground
1475 BIODEFENSE
Microbiologist Resigns After Pitch for Antianthrax Product

1476

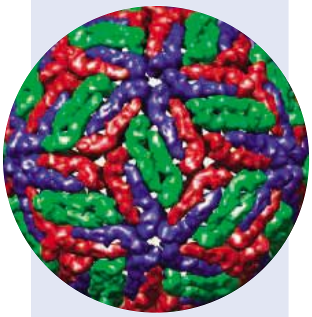

1495

1475 INFECTIOUS DISEASES
Homeland Security Ponders Future of Its Animal Disease Fortress

NEWS FOCUS
1476 PRENATAL DIAGNOSIS
An Earlier Look at Baby's Genes
1479 NUCLEAR WEAPONS
Laser Facility Faces Burning Questions Over Cost, Technology
1481 THE LAW
Vioxx Verdict: Too Little or Too Much Science?
1482 COSMOLOGY
The Quest for Dark Energy: High Road or Low?
1485 RANDOM SAMPLES

LETTERS
1489 **The Perils of Increased Aquaculture** *D. A. Mann.* **Notes and Double-Knocks from Arkansas** *R. A. Charif* et al. **Nature Makes a Difference in the City** *J. G. Tundisi.* **Einstein's Interoffice Memo?** *R. Noll.* **Aggressive, or Just Looking for a Good Mate?** *A. D. Aisenberg*
1491 Corrections and Clarifications

BOOKS *ET AL.*
1493 SCIENCE AND RELIGION
Before Darwin Reconciling God and Nature; **The Watch on the Heath** Science and Religion Before Darwin
K. Thomson, reviewed by A. Cutler
1494 MOVIES: NATURAL HISTORY
March of the Penguins
L. Jacquet, reviewed by D. Kennedy

ESSAY
1495 GLOBAL VOICES OF SCIENCE
Deciphering Dengue: The Cuban Experience
M. G. Guzmán

125 YEARS OF GLOBAL Science

Contents continued

Science

Perspectives

1498 **Natural History**
Beyond the Chimpanzee Genome: The Threat of Extinction *M. D. Hauser* *related Editorial page 1457; News story page 1468; Perspective page 1499;* Science *Express Report by P. Khaitovich* et al.

1499 **Genomics**
Thoughts on the Future of Great Ape Research *E. H. McConkey and A. Varki* *related Editorial page 1457; News story page 1468; Perspective page 1498;* Science *Express Report by P. Khaitovich* et al.

1501 **Physics**
Manipulating Magnetism in a Single Molecule *M. F. Crommie* *related Report page 1542*

1502 **Physics**
Reduced Turbulence and New Opportunities for Fusion *K. Krushelnick and S. Cowley*

Science Express www.sciencexpress.org

Evolution: Parallel Patterns of Evolution in the Genomes and Transcriptomes of Humans and Chimpanzees
P. Khaitovich et al.
Similar genes are expressed in many organs of the chimp and human; those expressed in the testes have evolved considerably in both species, as have those expressed in the human brain. *related Editorial page 1457; News story page 1468; Perspectives pages 1498 and 1499*

Cell Biology: Movement of Eukaryotic mRNAs Between Polysomes and Cytoplasmic Processing Bodies
M. Brengues, D. Teixeira, R. Parker
Cytoplasmic organelles called P-bodies cannot only degrade messenger RNA but can store it for later release into the protein translation machinery.

Developmental Biology: Direct Isolation of Satellite Cells for Skeletal Muscle Regeneration
D. Montarras, J. Morgan, C. Collins, F. Relaix, S. Zaffran, A. Cumano, T. Partridge, M. Buckingham
Satellite muscle cells isolated from the diaphragm of a healthy mouse can restore function when grafted into muscles of a dystrophic mouse.

Applied Physics: Coherent Manipulation of Coupled Electron Spins in Semiconductor Quantum Dots
J. R. Petta et al.
Fast electrical pulses can be used to manipulate, exchange, and prolong the spin state of electrons in a pair of quantum dots, representing a quantum logic gate.

Technical Comment Abstracts

1492 **Paleontology**
Comment on "Independent Origins of Middle Ear Bones in Monotremes and Therians" (I)
G. S. Bever, T. Rowe, E. G. Ekdale, T. E. Macrini, M. W. Colbert, A. M. Balanoff
full text at www.sciencemag.org/cgi/content/full/309/5740/1492a

Comment on "Independent Origins of Middle Ear Bones in Monotremes and Therians" (II)
G. W. Rougier, A. M. Forasiepi, A. G. Martinelli
full text at www.sciencemag.org/cgi/content/full/309/5740/1492b

Response to Comments on "Independent Origins of Middle Ear Bones in Monotremes and Therians"
T. H. Rich, J. A. Hopson, A. M. Musser, T. F. Flannery, P. Vickers-Rich
full text at www.sciencemag.org/cgi/content/full/309/5740/1492c

Brevia

1533 **Virology:** Major Biocontrol of Plant Tumors Targets tRNA Synthetase
J. S. Reader, P. T. Ordoukhanian, J.-G. Kim, V. de Crécy-Lagard, I. Hwang, S. Farrand, P. Schimmel
A biocontrol agent for the crown gall virus acts by inactivating the transfer RNA synthetase for leucine, an approach that might be useful in targeting other plant diseases.

Research Article

1534 **Structural Biology:** Inositol Hexakisphosphate Is Bound in the ADAR2 Core and Required for RNA Editing
M. R. Macbeth, H. L. Schubert, A. P. VanDemark, A. T. Lingam, C. P. Hill, B. L. Bass
An enzyme that "edits" messenger RNA by converting adenosine to inosine contains an essential inositol hexakisphosphate at its core, possibly to stabilize a protein fold.

Reports

1539 **Materials Science:** Single-Molecule Torsional Pendulum
J. C. Meyer, M. Paillet, S. Roth
A metal block suspended on a single-walled carbon nanotube, which acts as a spring, forms a torsional pendulum that is visible in the optical microscope.

1542 **Physics:** Controlling the Kondo Effect of an Adsorbed Magnetic Ion Through Its Chemical Bonding
A. Zhao, Q. Li, L. Chen, H. Xiang, W. Wang, S. Pan, B. Wang, X. Xiao, J. Yang, J. G. Hou, Q. Zhu
Changing the local chemical environment of a cobalt ion adsorbed on a gold surface can lead to strong coupling between its magnetic moment and conduction electrons. *related Perspective page 1501*

1545 **Materials Science:** The Ultrasmoothness of Diamond-like Carbon Surfaces
M. Moseler, P. Gumbsch, C. Casiraghi, A. C. Ferrari, J. Robertson
Diamond-like films produced from a hail of high-energy carbon atoms are extremely smooth because locally induced particle currents smooth out hills and valleys.

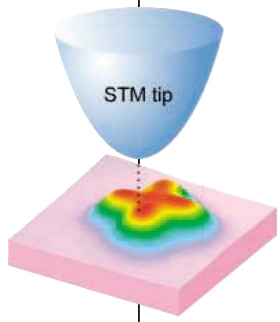

1501 & 1542

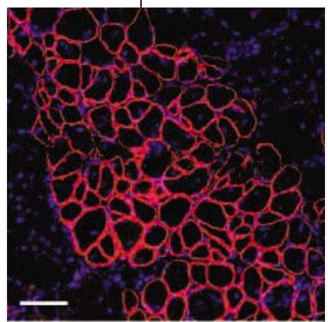

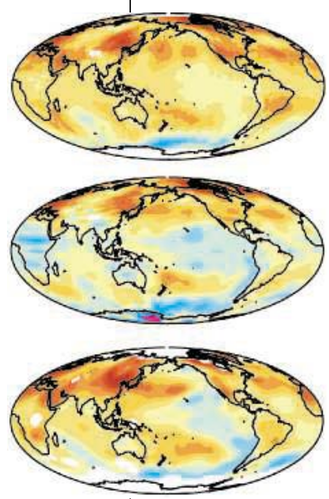

1548

Contents continued

Reports continued

1548 **Atmospheric Science:** The Effect of Diurnal Correction on Satellite-Derived Lower Tropospheric Temperature
C. A. Mears and F. J. Wentz
After modification of an erroneous diurnal correction, a reconstruction of recent atmospheric warming of the lower troposphere from satellite data now agrees with that inferred from measurements at the surface.

1551 **Atmospheric Science:** Amplification of Surface Temperature Trends and Variability in the Tropical Atmosphere
B. D. Santer et al.
Results of modeling recent temperature changes in the tropical troposphere agree with satellite data that indicate more warming than earlier observations.

1556 **Atmospheric Science:** Radiosonde Daytime Biases and Late–20th Century Warming
S. C. Sherwood, J. R. Lanzante, C. L. Meyer
Temperature measurements by weather balloons in the troposphere failed to reveal the extent of warming because of an uncorrected artifact in new instrumentation.

1559 **Molecular Biology:** The Transcriptional Landscape of the Mammalian Genome
The FANTOM Consortium and RIKEN Genome Exploration Research Group and Genome Science Group (Genome Network Project Core Group)
Examination of RNA transcripts from the mouse genome defines transcriptional boundaries and identifies new complementary DNAs, proteins, and noncoding RNAs. *related Viewpoint page 1529*

1564 **Molecular Biology:** Antisense Transcription in the Mammalian Transcriptome
RIKEN Genome Exploration Research Group and Genome Science Group (Genome Network Project Core Group) and the FANTOM Consortium
Some pairs of complementary RNA transcripts are expressed discordantly in the mouse genome, as expected, whereas others are regulated together. *related Viewpoint page 1529*

1567 **Genetics:** Elucidation of the Small RNA Component of the Transcriptome
C. Lu, S. S. Tej, S. Luo, C. D. Haudenschild, B. C. Meyers, P. J. Green
An extensive analysis of transcribed RNAs in the plant *Arabidopsis* identifies 10 times more small RNAs than had previously been described. *related Viewpoint page 1525*

1570 **Molecular Biology:** A Strategy for Probing the Function of Noncoding RNAs Finds a Repressor of NFAT
A. T. Willingham et al.
A screen for the function of noncoding RNAs in human cells identifies an RNA repressor that probably regulates movement of a transcription factor into the nucleus. *related Viewpoint page 1527*

1573 **Molecular Biology:** Inhibition of Translational Initiation by Let-7 MicroRNA in Human Cells
R. S. Pillai et al.
A human microRNA regulates gene expression by inhibiting translation initiation, possibly by binding to the cap structure at the 5′ end of the targeted messenger RNA.

1577 **Molecular Biology:** Modulation of Hepatitis C Virus RNA Abundance by a Liver-Specific MicroRNA
C. L. Jopling, M. Yi, A. M. Lancaster, S. M. Lemon, P. Sarnow
Hepatitis C virus exploits a host-encoded microRNA to increase its levels of its own RNA, suggesting new approaches to antiviral therapy.

1581 **Molecular Biology:** Recombination Regulation by Transcription-Induced Cohesin Dissociation in rDNA Repeats
T. Kobayashi and A. R. D. Ganley
Transcription of noncoding sequences between the genes for ribosomal RNA dissociates an inhibitory protein, promoting an increase in the number of rRNA genes.

1584 **Molecular Biology:** An mRNA Is Capped by a 2′,5′ Lariat Catalyzed by a Group I–Like Ribozyme
H. Nielsen, E. Westhof, S. Johansen
A natural ribozyme can generate a lariat-shaped structure at one end of a messenger RNA molecule, perhaps to serve as its protective cap. *related Viewpoint page 1530*

1587 **Structural Biology:** Structural Evidence for a Two-Metal-Ion Mechanism of Group I Intron Splicing
M. R. Stahley and S. A. Strobel
A catalytically active RNA intermediate uses the same arrangement of two magnesium ions to transfer phosphates, as is found in many protein phosphotransferases.

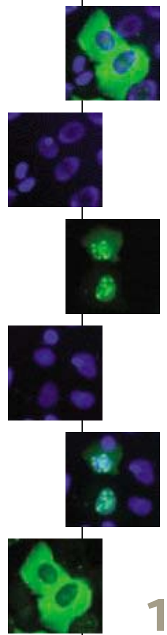

1527 & 1570

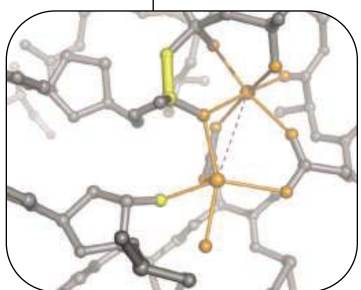

1587

AAAS
ADVANCING SCIENCE, SERVING SOCIETY

SCIENCE (ISSN 0036-8075) is published weekly on Friday, except the last week in December, by the American Association for the Advancement of Science, 1200 New York Avenue, NW, Washington, DC 20005. Periodicals Mail postage (publication No. 484460) paid at Washington, DC, and additional mailing offices. Domestic individual membership and subscription (51 issues): $135 ($74 allocated to subscription). Domestic institutional subscription (51 issues): $550; Foreign postage extra: Mexico, Caribbean (surface mail) $55; other countries (air assist delivery) $85. First class, airmail, student, and emeritus rates on request. Canadian rates with GST available upon request, GST #1254 88122. Publications Mail Agreement Number 1069624. **Printed in the U.S.A.**

Change of address: allow 4 weeks, giving old and new addresses and 8-digit account number. **Postmaster:** Send change of address to *Science*, P.O. Box 1811, Danbury, CT 06813–1811. **Single copy sales:** $10.00 per issue prepaid includes surface postage; bulk rates on request. **Authorization to photocopy** material for internal or personal use under circumstances not falling within the fair use provisions of the Copyright Act is granted by AAAS to libraries and other users registered with the Copyright Clearance Center (CCC) Transactional Reporting Service, provided that $15.00 per article is paid directly to CCC, 222 Rosewood Drive, Danvers, MA 01923. The identification code for *Science* is 0036-8075/83 $15.00. *Science* is indexed in the *Reader's Guide to Periodical Literature* and in several specialized indexes.

Contents continued

Science
www.scienceonline.org

sciencenow www.sciencenow.org DAILY NEWS COVERAGE

Keeping the Young from Dying Old
Cancer drug may prevent premature aging in children.

New Nanocoating Foils Fog
Tiny glass particles may leave traditional defoggers in the mist.

Ice, Served Warm
Scientists create icelike sheet at room temperature.

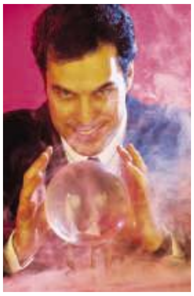

A murky scientific job market.

science's next wave www.nextwave.org CAREER RESOURCES FOR YOUNG SCIENTISTS

POSTDOC NETWORK: **A Cloudy Crystal Ball** *B. L. Benderly*
Two studies paint divergent pictures of the future of America's scientific labor market.

US: Science from the Balcony *C. Cohen and S. Cohen*
Developing a different perspective on people problems is a necessary skill for scientists.

EUROPE: **Getting a Group Leader Position and a Chair of Excellence** *E. Pain*
Young Greek researcher Lena Alexopoulou won dual accolades in 2004.

MISCINET: **Speaking the Language of Computers** *C. Choi*
A recent high school graduate of the Baltimore Polytechnic Institute won a top prize in the 2005 Intel Science Talent Search.

GRANTSNET: **September 2005 Funding News** *Edited by S. Martin*
Get the latest index of funding, scholarships, fellowships, and internships for postdocs and students.

science's sage ke www.sageke.org SCIENCE OF AGING KNOWLEDGE ENVIRONMENT

Related Mapping RNA section page 1507

▶ PERSPECTIVE: **Interfering with Longevity** *S. S. Lee*
RNA interference has transformed aging-related research in worms.

NEWS FOCUS: **Another Knock Against Cholesterol** *M. Leslie*
Artery clogger might promote Alzheimer's disease when damaged.

NEWS FOCUS: **Numb Together** *R. J. Davenport*
Bone marrow cells deaden neurons in diabetes.

Slithering toward long life with RNAi.

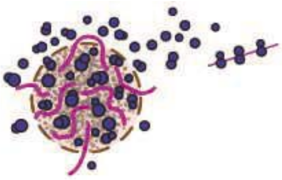

Activating an RNA granule.

science's stke www.stke.org SIGNAL TRANSDUCTION KNOWLEDGE ENVIRONMENT

Related Mapping RNA section page 1507

▶ EDITORIAL GUIDE: **Focus Issue—RNA, a Multifunctional Molecule** *N. R. Gough and E. M. Adler*
RNA increases genomic complexity and regulates gene expression.

▶ PERSPECTIVE: **MicroRNA-Dependent Trans-Acting siRNA Production** *H. Vaucheret*
A new class of endogenous small RNAs, tasiRNAs, establishes a link between the miRNA and siRNA pathways.

▶ TEACHING RESOURCE: **A Journal-Club Discussion of Regulation by MicroRNA** *D. C. Weinstein*
Design a student discussion to critically evaluate the primary literature regarding microRNA.

▶ TEACHING RESOURCE: **A Model for Local Regulation of Translation Near Active Synapses** *K. S. Kosik and A. M. Krichevsky*
This animation illustrates how RNA granules may contribute to synaptic plasticity.

Separate individual or institutional subscriptions to these products may be required for full-text access.

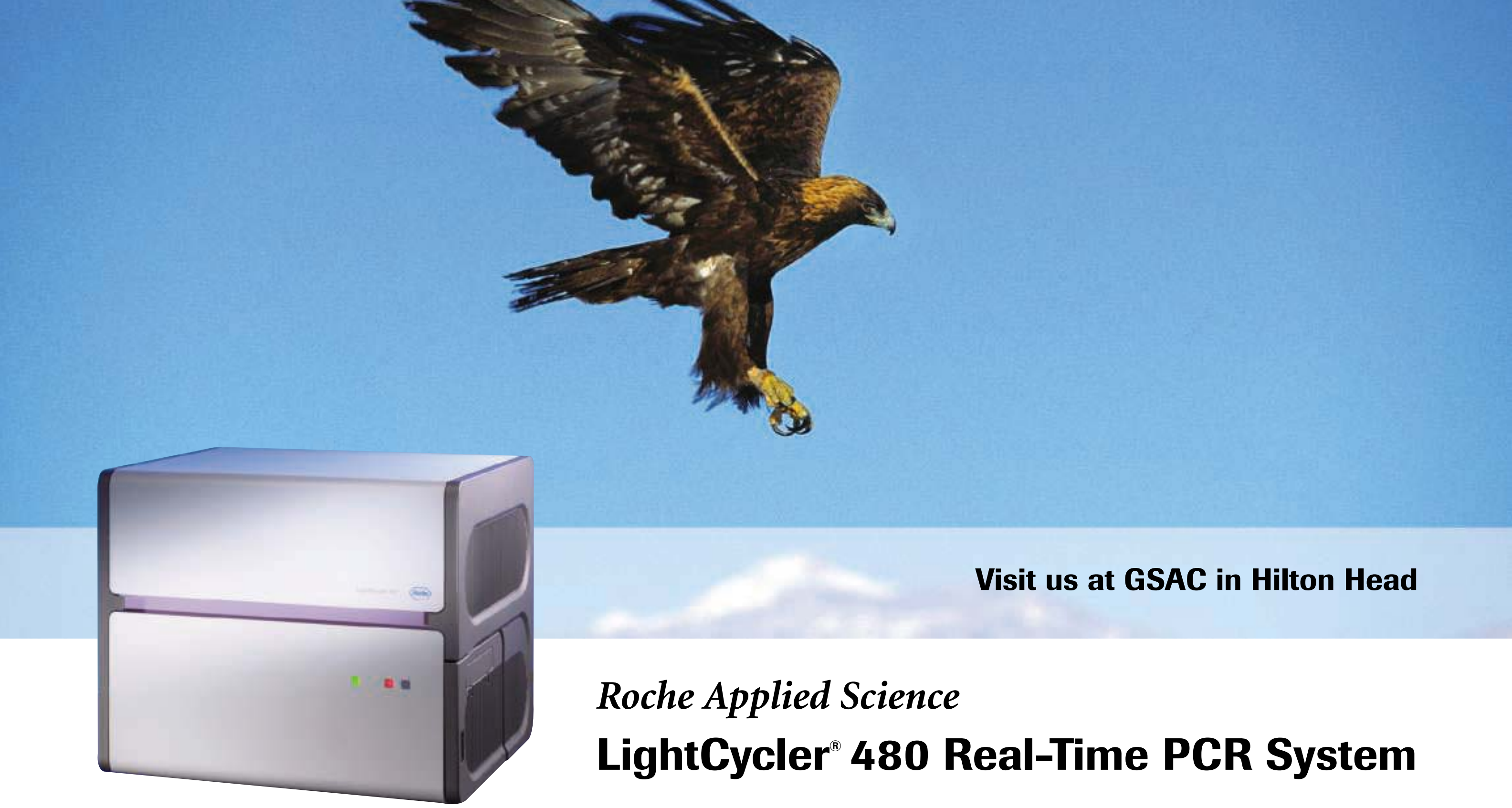

Roche Applied Science

LightCycler® 480 Real-Time PCR System

Rapid by nature,
accurate by design

▲ LightCycler® 480 Thermoblock for 96 or 384 wells, easily exchanged by users within minutes.

For years, Roche has provided real-time automated PCR solutions you can count on. Now, you can obtain the proven performance and benefits of the original LightCycler® System in a 96- or 384-well instrument platform for high-throughput applications – the new **LightCycler® 480 Real-Time PCR System**.

Speed – Save time without sacrificing the quality of your results – precise, high-speed temperature changes maximize specificity and yield.

Accuracy – Benefit from our novel thermal block and data-capture technologies to eliminate edge-effects for outstanding accuracy and precision.

Versatility – Combine 5 excitation and 6 detection channels, multiple probe formats, proven analysis software, and true master mix reagents to meet your specific application needs.

Compatibility – Take advantage of the instrument's automation and LIMS capabilities to interface with your current systems and future workflows.

Visit ***www.roche-applied-science.com/lightcycler480*** for more information.

In Development. Planned introduction: September, 2005.

For general laboratory use.
Not for use in diagnostic procedures.

The LightCycler® is an Authorized Thermal Cycler. Purchase and use of the LightCycler®, in conjunction with Authorized Reagents, provides a limited license for use of the PCR process in life science research. No rights for any application, including any *in vitro* diagnostic application, are conveyed expressly, by implication or by estoppel under patents owned by Roche Molecular Systems, Inc., F. Hoffmann-La Roche Ltd, or Applera Corporation claiming homogeneous or real-time amplification and detection methods.

LIGHTCYCLER is a trademark of Roche.

The technology used for the LightCycler® System is licensed from Idaho Technology, Inc., Salt Lake City, UT, USA.

Roche Diagnostics

Roche Diagnostics GmbH
Roche Applied Science
68298 Mannheim
Germany

edited by Stella Hurtley and Phil Szuromi

Lapse in Understanding

Some reconstructions of recent warming in the troposphere based on satellite data have indicated that the troposphere has warmed since 1979 (when the data were initially collected) at a rate considerably less than that, which should be expected from surface temperature measurements. Three studies (all published online 11 August 2005) reassess these data and reconstructions in favor of the surface temperature trends. **Mears and Wentz** (p. 1548) identify an error in the diurnal correction that has been applied to the satellite data, and derive a physically consistent one of the opposite sign, whose application brings into agreement a newer reconstruction of tropospheric warming, model calculations, and surface temperature measurements. **Sherwood *et al.*** (p. 1556) show that a spurious temporal trend was introduced into tropospheric temperature profiles recorded by radiosondes through changes in instrumentation made over time that involved solar heating of the instrument above ambient temperature. Correction for this bias brings many of the radiosonde data into better agreement with models and the surface temperature record, particularly in the tropics, where the disagreement between surface and expected tropospheric temperatures was most pronounced. **Santer *et al.*** (p. 1551) examined patterns of the amplification of surface temperature trends in the tropical troposphere using 19 different models. They show that the reconstructions used to argue that the troposphere was not warming are inconsistent with our understanding of the physical processes that control the vertical temperature structure of the atmosphere (the lapse rate).

Hard but Smooth

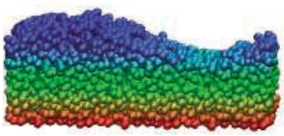

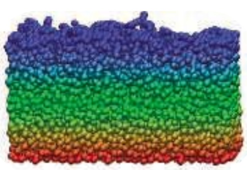

High-energy carbon atoms can be deposited onto a substrate to form a hard diamondlike coating that can provide wear resistance in applications ranging from hard drive to hip joints. Despite the energetic conditions of their formation, these films are extremely smooth—the roughness can be as low as 0.1 nanometers on a lateral area of 1 square micrometer (equivalent of millimeter-scale bumps on a soccer field). Using a combination of atomistic and continuum modeling, **Moseler *et al.*** (p. 1545) show that when the carbon atoms are implanted, they generate particle currents that smooth out neighboring hills and valleys.

Mining the Mammalian Genome and Transcriptome

Analyses of the mammalian genome sequence and its corresponding transcriptome have revealed a complex assembly of information that provides great diversity through its varied sequence elements. **Hayashizaki *et al.*** (p. 1559) use a combination of approaches [complementary DNA (cDNA) isolation, 5′ and 3′-end sequencing of cDNAs, and ditag sequencing] to reveal a large number of novel cDNAs, noncoding RNAs, and proteins, as well as information about overlapping transcripts, alternative sites for transcription initiation and termination, and elements for splicing variation. In a second paper, **Hayashizaki *et al.*** (p. 1564) explored sense/antisense (S/AS) expression and found that the density of S/AS transcripts varies across the genome; about 72% of all transcription units overlapping with expression of the opposite strand. S/AS pairs can be coregulated or can be reciprocally or discordantly regulated.

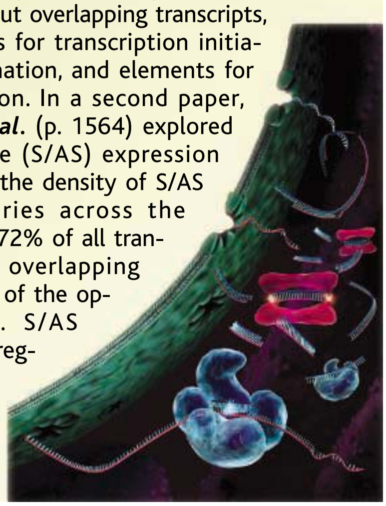

Twisting a Fine Wire

By linking a single-walled carbon nanotube to a macroscale metal block, **Meyer *et al.*** (p. 1539) have created a torsional pendulum whose end is visible in an optical microscope that rotates about a single molecule. When placed in a transmission electron microscope, the pendulum twists because of charging of the metal block. Oscillations set up by thermal effects can also be discerned. This experimental setup can also be used to determine the helicity of the carbon nanotube in diffraction experiments.

Cut and Couple

In the Kondo effect, localized spins, such as magnetic impurities in nonmagnetic metal, can couple to conduction electrons and cause resistivity to increase with decreasing temperature. **Zhao *et al.*** (p. 1542; see the Perspective by **Crommie**) show that the effect of the magnetic moment of a single adsorbed magnetic atom can be changed by altering its chemical environment. Using a scanning tunneling microscope (STM) as a probe, they observed no Kondo effects when cobalt phthalocyanine (CoPc) was adsorbed on the (111) surface of gold. However, when they used the STM tip to dehydrogenate the Pc ligand, the local magnetic moment of the Co ion interacted with surface Au electrons to produce a Kondo effect with a high Kondo temperature (~200 kelvin).

Small RNA Assay of *Arabidopsis*

Small noncoding RNAs, in the form of small interfering RNAs (siRNAs, intermediates in RNA interference) and microRNAs (miRNAs), play vital roles in eukaryotes' cell biology, but are by their very nature difficult to detect. **Lu *et al.*** (p. 1567) have now thoroughly characterized small RNAs in the plant *Arabidopsis* through a massively parallel signal sequencing of more than 2 million such RNAs. Although they identify many siRNAs, particularly from transposons, centromeric regions, and other repeats, few are associated with overlapping antisense transcripts, which suggests that antisense transcription may regulate gene expression mainly through transcriptional interference. They also identify a significant number of new miRNAs but generally do not find evidence for miRNA transitivity.

CONTINUED ON PAGE 1455

CREDITS (TOP TO BOTTOM): HAYASHIZAKI *ET AL.*; MOSELER *ET AL.*

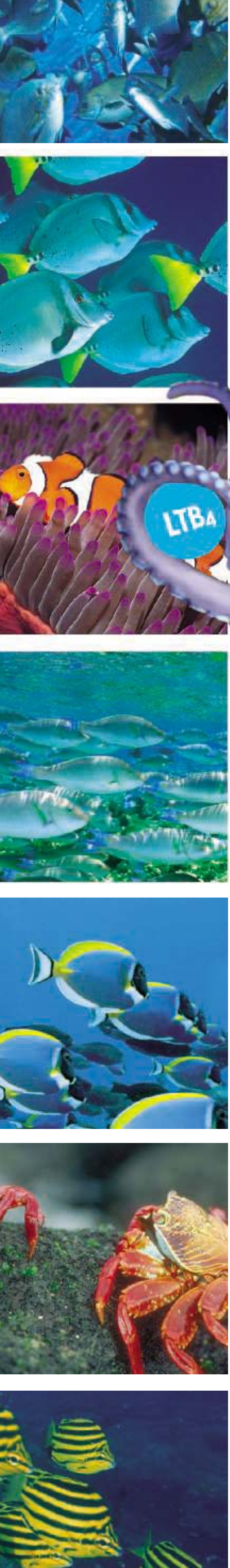

a spectacular variety of immunoassays and cell-signaling kits

PGE_2 ELISA (2-hr assay)
Leukotriene C_4 EIA
Thromboxane B_2 EIA
Leukotriene B_4 EIA
8-Isoprostane EIA
CGRP ELISA
Cyclic GMP EIA
Glutathione Assay
Cyclic AMP EIA
PGE_2 EIA
Corticosterone EIA
TNFα (human) ELISA
SOD Assay
LPO Assay

Insulin EIA
PGE_2 FPIA
Cortisol EIA
Catalase Assay
Substance P ELISA
PGE-Metabolite EIA
PAF Acetylhydrolase Assay
Glutathione Peroxidase Assay
Interleukin-6 (human) ELISA
Testosterone EIA
6-keto $PGF_{1\alpha}$ EIA
Endothelin EIA
Histamine EIA
PGD_2-MOX EIA
$cPLA_2$ Assay
Leptin ELISA
11-dehydro Thromboxane B_2 EIA
Creatinine Assay
Estradiol EIA
Interleukin-1β (human) ELISA
Antioxidant Assay
Nitrate/Nitrite Assay
Glutathione S-Transferase Assay
$iPF_{2\alpha}$-VI EIA
Aldosterone EIA
Enterolactone EIA
HDAC Assay
Renin Inhibitor Assay
Protein Carbonyl Assay
Ghrelin (Active) ELISA
PGD_2 FPIA
Vitellogenin ELISA
Leukotriene E_4 EIA

and many more...

Cayman CHEMICAL

www.caymanchem.com/kits

New Platforms for Cayman's Eicosanoid Assays

Several of Cayman's eicosanoid assays are being optimized for use on both the Luminex® and Meso Scale Discovery™ platforms. Both systems offer multiplexing capabilities for the measurement of several analytes from a single sample. Contact our sales or technical staff to discuss the application of these assays for your sample analysis needs.

MSD® Meso Scale Discovery

PGE_2
PGD_2
TXB_2

Luminex®

PGE_2
PGD_2
TXB_2
LTB_4
11-dehydro TXB_2
cysteinyl leukotrienes

CONTINUED FROM 1453

Noncoding RNAs at Work

One type of the small noncoding RNAs (ncRNAs), microRNAs (miRNAs), are about 21 nucleotides in length and are believed to regulate gene expression either through messenger RNA (mRNA) cleavage or by translational repression. **Pillai *et al.*** (p. 1573, published online 4 August 2005) show that in human cells, the miRNA let-7 represses gene expression by inhibiting translation initiation of capped mRNAs, rather than through a degradation mechanism. This repressive machinery appears to be localized to cytoplasmic processing (P) bodies, where mRNAs are stored or degraded. A large fraction of eukaryotic genomes are transcribed into ncRNAs, some of which, such as miRNAs or the much larger Xist ncRNA, have known functions. However, the great majority of ncRNAs are of unknown functional significance. **Willingham *et al.*** (p. 1570) have developed a method for identifying functional ncRNAs—looking for evolutionary conservation and using a battery of cell-based RNA-interference assays—and have characterized the noncoding repressor of NFAT (NRON) that represses the transcription factor NFAT (nuclear factor of regulated T cells), probably though modulation of NFAT's cellular localization.

Trapped by an Editor

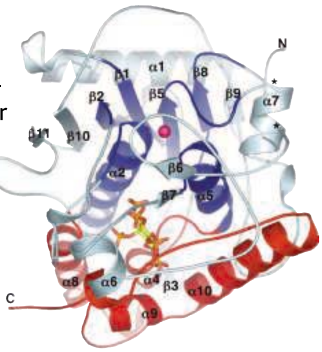

A family of RNA editing enzymes, adenosine deaminases that act on RNA (ADARs), is important for proper neuronal function and are implicated in the regulation of RNA interference. **Macbeth *et al.*** (p. 1534) determined the crystal structure of human ADAR2 at 1.7 angstrom resolution. Surprisingly, inositol hexakisphosphate (IP_6) is buried within the fold of the enzyme core. Activity assays show that IP_6 is required for hADAR2 activity and for the activity of a yeast RNA editing enzyme, ADAT1.

Small Takeover, Big Gain

Viruses exploit host functions in many ways in order to replicate. Identified functions now include taking over host-encoded microRNAs (miRNAs) that play a crucial role in RNA interference, a recently discovered mechanism of gene regulation. Studying the human pathogen hepatitis C virus (HCV), **Jopling *et al.*** (p. 1577) show that a host miRNA that is abundantly expressed in the liver, where the virus replicates, interacts with the 5′ noncoding region of the viral RNA. This interaction leads to an increase in HCV RNA and possibly contributes to viral persistence in the liver. Inactivation of this miRNA could be a useful therapeutic strategy for HCV, which is estimated to affect 170 million people worldwide.

Similarities in Splicing

Group I self-splicing introns have been thought to be distinct from their group II cousins and messenger RNA (mRNA) splicing reactions in not generating a lariat (looped) intermediate that is subsequently removed from the spliced product. **Nielsen *et al.*** (p. 1584) show a group I–like ribozyme from the slime mold *Didymium iridis* also produces a lariat. The DiGIR1 ribozyme cleaves its RNA target to form a microlariat at the extreme 5′ end of its parent homing endonuclease mRNA. The lariat might function in an analogous manner to the cap found on regular polymerase II mRNAs. The evolution of the GIR1 ribozyme might parallel a possible step in the evolution of mRNA splicing. Biochemical studies of group 1 intron splicing have shown that both of its chemical steps require divalent metal ions, and several metal ligands have been identified. Mechanisms involving either two or three metal ions have been proposed. **Stahley and Strobel** (p. 1587) have determined the structure of an intron splicing intermediate that is active in catalyzing exon ligation. The active site contains two Mg^{2+} ions that coordinate all six of the biochemically identified ligands. Thus, an RNA phosphotransferase can function through a two-metal-ion mechanism.

CREDIT: MACBETH *ET AL.*

The Last Great Apes?

Forty years ago, adolescent Figan set off confidently into the woods of Tanzania as though he knew of a food source even richer than the bananas near Jane Goodall's camp. Older and stronger chimpanzees would follow him away. Then he'd lose them and circle back to gorge himself on bananas. One day, a high-ranking male turned up in the meantime and sat eating, in full possession of the site. When Figan returned he stared for a few seconds at the unchallengeable male, then threw a tantrum, screaming and hitting the ground. Figan finally left camp unfed, his screams still echoing behind him.

Forty years ago, behavioral scientists hardly believed that story. We had schooled ourselves to think of animals as devoid of foresight and powered by mechanical "drives" that didn't count as emotions. The pioneers of ape field study—the Japanese researchers Itani, Nishida, and Kano; the "Trimates" Goodall, Fossey, and Galdikas; and the British Broadcasting Corporation films by Attenborough—taught us instead to trust our own evolved empathy. We now know that apes may actively encourage or deceive each other, transmit learned tool cultures, gang-kill rivals, or adopt motherless orphans. Above all, each is an individual who is politically astute or brutal, nurturing or careless, playing his or her own role in a complicated society. Now we look into the eyes of an ape and see someone looking back.

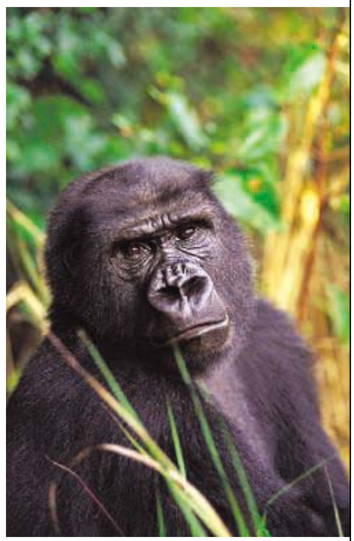

Does our empathy lead to action? Roughly 100,000 gorillas, 100,000 chimpanzees, 10,000 bonobos, and 30,000 orangutans survive today in the wild. Some forms are critically endangered: About 200 Cross River gorillas remain in Nigeria and Cameroun; about 6000 Sumatran orangutans survive, swinging their full-body orange dreadlocks. All the great apes of the world together number less than the human population of Brighton, England; the most numerous species, less than the people of Abilene, Texas.

Apes lose their lives to logging and clearing and bushmeat hunters. They are shot by raiding armies. Half of the countries of Africa and Asia where apes live have suffered recent wars or natural disasters. Perhaps 80 or 90% of lowland eastern gorillas disappeared during the fighting in Congo in the past 3 years. The 26 December 2004 tsunami that devastated Aceh, Sumatra, will put ever-greater pressure on Sumatra's Gunung Leuser National Park. One population of the park's orangutans lived at the highest known density of the orange apes—high enough for them to associate with each other and pass on social traditions of tool use, unlike any other wild orangutans. However, Gunung Leuser is estimated to lose up to 1000 orangutans per year to logging and warfare.

There is hope, though. The gorillas of the Virunga Volcanoes were spared during the Rwandan genocide, when some 800,000 people died. Dedicated foreign and Rwandan conservationists have made ecotourism a major source of foreign exchange and have spread education about the gorillas' cash value as well as their similarity to human beings. People in any country can be proud of great apes in their midst, but only with the support of those who can afford to help.

The Great Ape Survival Project (GRASP) links the 23 ape range-state governments with all the different organizations working for great apes, as well as with the United Nations (UN) Environment Programme and the UN Educational, Scientific and Cultural Organization. Is this just another layer of bureaucracy? No. GRASP is a heroic effort to aid global treasures on a global scale. Each separate forest and its denizens can only be saved locally, and each needs the backing of its own country's people and government. In turn, each government needs to appreciate the importance of what it holds. Politicians are not impressed by wildlife that doesn't lobby and doesn't vote. GRASP is the coordinating lobby in favor of humankind's nearest relatives.

The sequencing of the chimpanzee genome* is a huge step toward discovering how building blocks of information are assembled to construct either ape or human. Even so, geneticists are all too aware that a genome is only part of the story of an individual, let alone a species. The nature of genetic variability between individuals, populations, and species can and will find objective measures, but the future of individuals, populations, and species will never be solved by genetics.

It will only be solved by action—practical political action based on respect for other individuals—even if those individuals are only almost human.

Alison Jolly

Alison Jolly is a visiting senior scientist at Sussex University in Brighton, UK.

*The initial sequence of the chimpanzee genome and its comparison with the human genome has been published in *Nature* **437**, 69 (2005).

10.1126/science.1111873

CREDIT: KARL AMMANN/GETTY IMAGES

EDITORS' CHOICE

edited by Gilbert Chin

MICROBIOLOGY

In Living Color

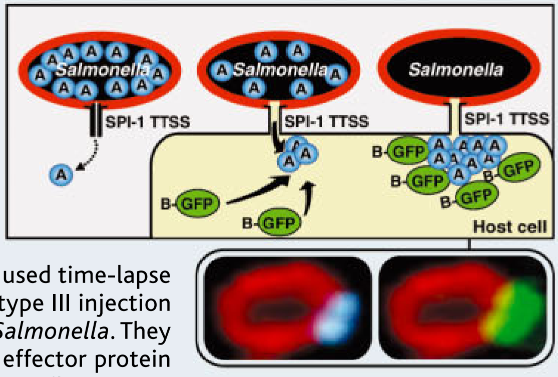

Injection of SipA (blue) and detection by GFP-InvB (green).

Gram-negative bacteria, such as *Salmonella*, use a specialized secretion system (type III) to inject target eukaryotic cells with bacterial effector proteins that subvert the target cell's machinery and promote bacterial virulence. Schlumberger *et al.* have used time-lapse microscopy to follow in real time the type III injection of mammalian tissue culture cells by *Salmonella*. They observed the delivery of the bacterial effector protein SipA into the host cytosol using a green fluorescent protein (GFP) fusion to InvB (a binding partner of SipA) to measure the kinetics of arrival. Bacteria were mixed with mammalian cells, and individual bacterium-cell interactions were monitored to see how much SipA remained in the bacterium. After the initial attachment, effector protein was transported into the target cell over the subsequent 1 to 10 min, leaving the bacterium virtually devoid of SipA. The results vividly illustrate the efficiency of the type III secretion system, a key weapon in the establishment of a niche for bacterial multiplication. — SMH

Proc. Natl. Acad. Sci. U.S.A. **102**, 12548 (2005).

PSYCHOLOGY

An Unsteady State

Neuroticism has often been linked with instability, manifest as a tendency to worry excessively, to respond to similar situations in a variable fashion, or to cope poorly when emotionally stressed. What might be the neural mechanisms underlying the expression of this trait, and would they affect high- or low-level cognitive processes? Previous studies have begun to address the extent of trial-to-trial variation in neuronal firing rates and patterns, as well as the behavioral consequences of that variability.

Robinson and Tamir have used a nested series of reaction time tasks—requiring (i) stimulus detection, (ii) stimulus detection and discrimination or (iii) stimulus detection and discrimination and response selection—and find that mean reaction time increases, as expected, over this series. In contrast, self-reported neuroticism did not correlate with mean reaction time but did correlate with the standard deviation of reaction time across all three tasks. They suggest that individuals scoring high on neuroticism, even though motivated or conscientious, may suffer from unreliable or inefficient low-level cognitive processing, which contributes to less stable and successful behavior. — GJC

J. Pers. Soc. Psych. **89**, 107 (2005).

MATERIALS SCIENCE

Capturing the Fine Details

Titanium has long been used as an orthopedic implant material because it is strong and relatively light. Many studies have shown in vitro that when the surface oxide layer is rough, osteoblasts (the bone-forming cells) deposit more calcium. However, these studies have not determined whether the enhanced activity is due to the surface roughness, crystallinity, crystal phase, or surface chemistry of the nanostructured material.

Pallin *et al.* generated surface replicas using poly-lactic-*co*-glycolic acid (PLGA) to capture the roughness of conventional and nanostructured titania. In experiments with osteoblasts, both adhesion and proliferation were greater on the nanostructured titania and the PLGA replicas. The higher number of surface atoms, defects, and surface electron delocalizations may influence the initial cell-surface interactions and thus lead to the improved adhesion. An examination of samples from a bovine femur showed roughness values comparable to that of nanostructured titania, supporting the role of texture in affecting bone growth. — MSL

Nanotechnology **16**, 1828 (2005).

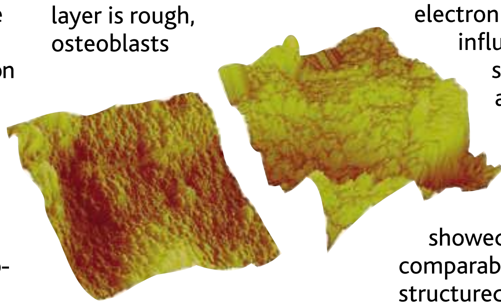

Atomic force microscopy of nanophase titania (left) and a PLGA replica (right).

CHEMISTRY

Reviving Bohr Molecules

Before the Heisenberg-Schrödinger formulation of quantum mechanics, the semi-classical Bohr-Sommerfeld theory successfully accounted for quantized properties such as the energy levels in the hydrogen atom. However, the forcing of closed orbits for particle motion ran afoul of the uncertainty principle. Recently, the use of D scaling, in which the motion of each particle is described by a vector in D dimensions, was used to reintroduce the uncertainty principle to this earlier theory. When properly done, such equations reduce to the correct Schrödinger form for $D = 3$ but can still be solved in the more tractable $D \rightarrow \infty$ limit. This D scaling approach was applied successfully to atoms but did not yield bound states for molecules.

Svidzinsky *et al.* have developed a D scaling description that fully quantizes one of the angles describing the interelectron coordinates and properly weights the contribution of electron-electron repulsion. After application of a leading correction term in $1/D$, the potential energy curves for the lowest singlet, triplet, and excited states of H_2 are in good agreement with accepted values after minimal numerical calculation. The procedure also yields reasonable agreement for the ground state of BeH. — PDS

Phys. Rev. Lett. **95**, 080401 (2005).

NEUROSCIENCE

One Singular Sensation

While not everyone enjoys the zing that garlic imparts to culinary fare, a variety of cultures—dating back to the ancient Egyptians—have firmly believed that the herb

CONTINUED ON PAGE 1461

CREDITS: (TOP) SCHLUMBERGER *ET AL.*, *PROC. NATL. ACAD. SCI. U.S.A.* **102**, 12548 (2005); (BOTTOM) PALLIN *ET AL.*, *NANOTECHNOLOGY* **16**, 1828 (2005)

CONTINUED FROM 1459

has extraordinary medicinal powers. Although its health benefits remain somewhat contentious, garlic is currently marketed as an alternative therapy for high blood pressure, high cholesterol levels, excessive blood clotting, and many other disorders. Garlic's pungent taste and odor are due to sulfur-containing components such as allicin, whose physiological mechanism of action has been unclear.

Bautista *et al.* and Macpherson *et al.* show that allicin activates an excitatory ion channel called TRPA1, which is expressed on sensory neurons involved in innervation of the skin, tongue, and other tissues, including vascular smooth muscle. Based on experiments with isolated rat arteries, Bautista *et al.* propose that allicin-induced excitation of these neurons causes release of peptides that mediate vasodilation, which could potentially explain garlic's effect on blood pressure. Interestingly, the TRP family of ion channels had previously been identified as the molecular target of ingredients in other spicy foods such as chili peppers, wasabi, and yellow mustard, suggesting that these compounds all activate a common pathway. — PAK

Proc. Natl. Acad. Sci. U.S.A. **102**, 12248 (2005); *Curr. Biol.* **15**, 929 (2005).

CHEMISTRY

Magnetic Catalysts

In the chemical synthesis of drugs, the route via homogeneous catalysis by metal complexes is plagued by the challenge of separating residual toxic metal from the product. Binding the catalyst to a heterogeneous support can simplify this purification step, but at the expense of reducing the mixing efficiency between catalyst and reagent.

Hu *et al.* have found a compromise by fusing a ruthenium catalyst to magnetite (Fe_3O_4) nanoparticles. The tiny particles mix efficiently with molecular reagents and would ordinarily be hard to remove by filtration, but by holding a small magnet to the flask, the authors can retain the catalyst and decant the product. The Ru complex, a variant of Noyori's binaphthyl-based asymmetric hydrogenation catalyst, was attached to 8-nm-diameter particles through a phosphonate group. A range of aromatic ketones were reduced quantitatively to alcohols at room temperature and 0.1 mol % catalyst loading, with enantiomeric excesses ranging from 77 to 98%, and the catalyst could be recycled 10 times without loss of activity. — JSY

J. Am. Chem. Soc. 10.1021/ja053881o (2005).

HIGHLIGHTED IN *SCIENCE*'S SIGNAL TRANSDUCTION KNOWLEDGE ENVIRONMENT

Science's stke www.stke.org

Geometry of Cell Proliferation

Localized differences in cell proliferation can help sculpt tissues during morphogenesis and produce the complex structures found in mature organisms. In some cases, however, changes in tissue structure occur before changes in cell proliferation. To show that geometry could itself feed back and regulate cell proliferation, Nelson *et al.* cultured bovine pulmonary artery endothelial cells on small fibronectin-coated islands surrounded by non-adhesive regions. Examination of cell growth on islands of different sizes and shapes—or on undulating surfaces—revealed distinctive and nonuniform patterns of proliferation. A finite element model predicted that cell proliferation would be greatest in regions of high mechanical stress; this was confirmed by culturing cells on a force sensor array that allowed traction forces to be measured directly. Pharmacological inhibition of Rho kinase, myosin light-chain kinase, or nonmuscle myosin II ATPase (to decrease tension generated through the cytoskeleton), or disruption of cadherin-mediated intercellular adhesions, attenuated gradients of cell proliferation, whereas expression of a constitutively active RhoA mutant enhanced them. — EMA

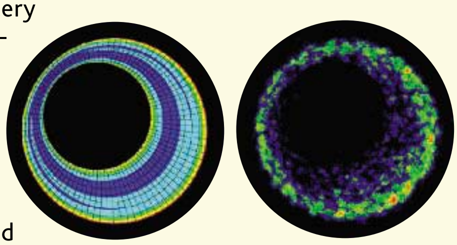

Cell proliferation (red, high; violet, low) in the model (left) and in the dish (right).

Proc. Natl. Acad. Sci. U.S.A. **102**, 11594 (2005).

CREDITS: NELSON *ET AL.*, *PROC. NATL. ACAD. SCI. U.S.A.* **102**, 11594 (2005)

GENETIC

IMAGINE SOLVING

YOUNG SCIENTIST AWARD

ABOUT THE SPONSORS:

GE Healthcare
GE Healthcare helps predict, diagnose, inform and treat so that every individual can live life to the fullest. GE Healthcare employs more than 42,500 people in more than 100 countries and is one of the world's leading suppliers of transformational medical technologies.

AAAS/Science
As well as publishing the journal *Science*, AAAS is an international non-profit organization dedicated to advancing science around the world by serving as an educator, leader, spokesperson and professional association.

www.sciencemag.org

Science

1200 New York Avenue, NW
Washington, DC 20005
Editorial: 202-326-6550, FAX 202-289-7562
News: 202-326-6500, FAX 202-371-9227

Bateman House, 82-88 Hills Road
Cambridge, UK CB2 1LQ
+44 (0) 1223 326500, FAX +44 (0) 1223 326501

Subscription Services For change of address, missing issues, new orders and renewals, and payment questions: 800-731-4939 or 202-326-6417, FAX 202-842-1065. Mailing addresses: AAAS, P.O. Box 1811, Danbury, CT 06813 or AAAS Member Services, 1200 New York Avenue, NW, Washington, DC 20005

Institutional Site Licences please call 202-326-6755 for any questions or information

Reprints: Author Inquiries 800-635-7181
Commercial Inquiries 803-359-4578
Corrections 202-326-6501

Permissions 202-326-7074, FAX 202-682-0816

Member Benefits Bookstore: AAAS/BarnesandNoble.com bookstore www.aaas.org/bn; Car purchase discount: Subaru VIP Program 202-326-6417; Credit Card: MBNA 800-847-7378; Car Rentals: Hertz 800-654-2200 CDP#343457, Dollar 800-800-4000 #AA1115; AAAS Travels: Betchart Expeditions 800-252-4910; Life Insurance: Seabury & Smith 800-424-9883; Other Benefits: AAAS Member Services 202-326-6417 or www.aaasmember.org.

science_editors@aaas.org (for general editorial queries)
science_letters@aaas.org (for queries about letters)
science_reviews@aaas.org (for returning manuscript reviews)
science_bookrevs@aaas.org (for book review queries)

Published by the American Association for the Advancement of Science (AAAS), *Science* serves its readers as a forum for the presentation and discussion of important issues related to the advancement of science, including the presentation of minority or conflicting points of view, rather than by publishing only material on which a consensus has been reached. Accordingly, all articles published in *Science*—including editorials, news and comment, and book reviews—are signed and reflect the individual views of the authors and not official points of view adopted by the AAAS or the institutions with which the authors are affiliated.

AAAS was founded in 1848 and incorporated in 1874. Its mission is to advance science and innovation throughout the world for the benefit of all people. The goals of the association are to: foster communication among scientists, engineers and the public; enhance international cooperation in science and its applications; promote the responsible conduct and use of science and technology; foster education in science and technology for everyone; enhance the science and technology workforce and infrastructure; increase public understanding and appreciation of science and technology; and strengthen support for the science and technology enterprise.

Information for Contributors

See pages 135 and 136 of the 7 January 2005 issue or access www.sciencemag.org/feature/contribinfo/home.shtml

NetWatch

edited by Mitch Leslie

RESOURCES

Gauging Nanotech Risks

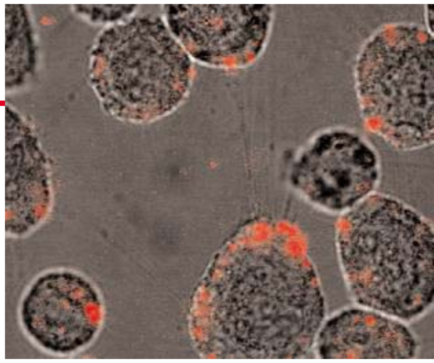

From stain-resistant pants that repel liquids with tiny bristles to tennis rackets reinforced with carbon nanotubes, more products that rely on nanotechnology are hitting the market. But investigation of possible hazards from nanomaterials has lagged (*Science*, 1 July 2005, p. 36). To assess the state of the research, visit this new database of nanotech's risks. A joint project of the International Council on Nanotechnology and Rice University's Center for Biological and Environmental Nanotechnology (CBEN) in Houston, Texas, the site compiles abstracts for hundreds of nanoparticle-related environmental health and safety studies dating back to 1962. For example, you can locate recent papers on the possible harm to cells from quantum dots, minute semiconductor crystals deployed to pinpoint cancer (above), and track molecular movements. "The real value added here is that the research is being interpreted [and catalogued] by people who understand nanoparticles," says Kevin Ausman, co-executive director of CBEN. Targeted initially at scientists, the database will eventually include summaries for the general public and the media.

icon.rice.edu/research.cfm

RESOURCES

A Drying Trend

Seven years of below-normal precipitation have slashed the amount of water in the Missouri River by nearly one-third, threatening wildlife and disrupting transportation, power generation, and agriculture. Researchers and the general public can find out whether dry conditions will persist in the Midwest and elsewhere in the country at the Drought Monitor, hosted by the University of Nebraska, Lincoln. The site unites information from federal and academic sources to produce assessments of current drought conditions along with predictions. For example, experts foresee more rain across the Midwest but continuing drought in the Northwest.

www.drought.unl.edu/dm/index.html

EXHIBITS

First Impressions

After their ships hove into Sydney Harbor in January of 1788, the first British colonists in Australia ran low on food and supplies. But they still managed to render some 600 drawings and paintings of the unexplored continent's landscape and natural history. Browse these early views of Oz at the First Fleet Artwork Collection from the Natural History Museum in London. The Rembrandt of the colony's artists is Thomas Watling, a trained painter who had previously applied his talent as a forger. For zoologists and botanists, the works capture some of the first views of Australia's unusual plants and animals. For anthropologists, illustrations such as this portrait of an aboriginal man named Balloderree (right) provide the only records of the local Eora people, who died out within 20 years of the settlers' landing.

internt.nhm.ac.uk/jdsml/nature-online/first-fleet/

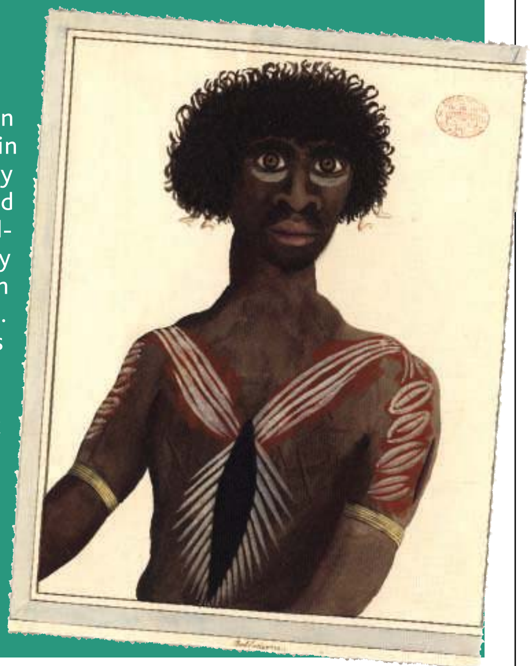

EDUCATION

Way Out Molecules

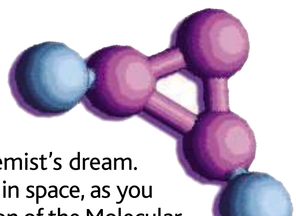

Cloaked by an atmosphere teeming with methane, carbon monoxide, and many other molecules, Saturn's hefty moon Titan is an astrochemist's dream. But interesting compounds also linger elsewhere in space, as you can see at The Astrochymist created by David Woon of the Molecular Research Institute in Mountain View, California. Two tables summarize the molecules researchers have detected on our solar system's planets and moons. The tally for Titan, for example, stands at 14—more than twice as many as on Mars. Other listings furnish similar information about stars, comets, and interstellar space. The site also offers a news archive and an "astromolecule of the month" feature that profiles examples such as the reactive cyclopropenylidene (above), which might spawn other space compounds.

www.molres.org/astrochymist/

DATABASE

Broken Genes

Many changes, such as a lost DNA segment or stretches of flipped nucleotides, can corrupt genes and cause disease. The Human Gene Mutation Database, hosted by Cardiff University in the United Kingdom, identifies the errors that contribute to a long list of ailments—from the rare immune disorder Chediak-Higashi syndrome to common maladies such as type II diabetes. The expanding clearinghouse lists more than 47,000 disease-linked glitches in our DNA, all gleaned from published papers. Users can search the database by gene or by illness. The results, organized by type of mutation, connect to PubMed abstracts.

www.hgmd.org/

Send site suggestions to netwatch@aaas.org. Archive: www.sciencemag.org/netwatch

CREDITS (TOP TO BOTTOM): RICE UNIVERSITY; NATIONAL SCIENCE FOUNDATION; NATIONAL HISTORY MUSEUM, LONDON

NEWS

This Week

PAGE 1471
Good chemistry?

1473
Dueling databases

GENOMICS

Chimp Genome Catalogs Differences With Humans

Anyone who has ever looked into the eyes of a chimpanzee has wondered what separates them from us. Now, in a raft of papers in this week's *Nature* and other journals, including *Science* (see pp. 1457, 1498, and 1499), international teams of researchers present a genetic answer to that question.

Scientists produced a rough draft of the chimpanzee DNA sequence, and aligned it with the human one, and made an intimate comparison of the chimp and human genomes. "It's wonderful to have the chimp genome," says geneticist Mark Adams of Case Western Reserve University in Cleveland, Ohio, who was not on the papers. "It's the raw material … to figure out what makes us unique."

The papers confirm the astonishing molecular similarity between ourselves and chimpanzees. The average protein differs by only two amino acids, and 29% of proteins are identical. The work also reveals that a surprisingly large amount of genetic material—2.7% of the genomes—has been inserted or deleted since humans and chimps went their separate evolutionary ways 6 million years ago.

But those hoping for an immediate answer to the question of human uniqueness will be disappointed. "We cannot see in this why we are phenotypically so different from the chimps," says Svante Pääbo of the Max Planck Institute of Evolutionary Anthropology in Leipzig, Germany, a co-author on one *Nature* paper and leader of a study in *Science* comparing gene expression in chimps and humans (see www.sciencemag.org/cgi/content/abstract/1108296). "Part of the secret is hidden in there, but we don't understand it yet."

Instead, the papers delve deeply into the genomic differences between us and our closest living relatives, revealing a flurry of relatively recent insertions and deletions in both human and chimp DNA, and mutational hotspots near the ends of chromosomes. "[A] genome is like the periodic table of the elements," says Ajit Varki of the University of California, San Diego. "By itself it doesn't tell you how things work—it's the first step along a long road."

The researchers in the Chimpanzee Sequencing and Analysis Consortium deciphered DNA taken from an adult male named Clint; the draft sequence was announced but not formally published in 2003. Now the team, led by Robert Waterston of the University of Washington (UW), Seattle, confirms in *Nature* the oft-cited statistic that on average only 1.23% of nucleotide bases differ between chimps and humans.

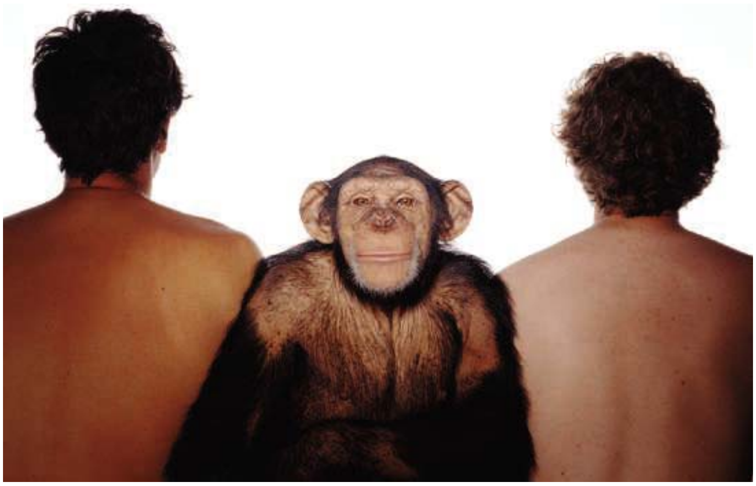

All in the family. Genome data reveal a few surprising differences between chimps and humans but overall confirm our close kinship.

But as suggested by earlier work on portions of the chimp genome, other kinds of genomic variation turn out to be at least as important as single nucleotide base changes. Insertions and deletions have dramatically changed the landscape of the human and chimp lineages since they diverged. Duplications of sequence "contribute more genetic difference between the two species—70 megabases of material—than do single base pair substitutions," notes Evan Eichler, also of UW, Seattle, who led a team analyzing the duplications. "It was a shocker, even to us."

The total genetic difference between humans and chimps, in terms of number of bases, sums to about 4% of the genome. That includes 35 million single base substitutions plus 5 million insertions or deletions (indels), says Waterston.

Somewhere in that catalog of 40 million evolutionary events lie the changes that made us human. But where? In another *Nature* paper, a team led by Barbara Trask of UW, Seattle, and the Fred Hutchinson Cancer Research Center reports that almost half of the indels in the regions near the ends of chromosomes are unique to humans. Many of the insertions contain gene duplications, which in other organisms have fostered evolutionary novelty by allowing one copy of a gene to adapt to a new function without disrupting the original. "It'll be very exciting to see how many indels actually made a difference in our own evolution," says David Haussler of the University of California, Santa Cruz.

To narrow the number of genes that might have been favored in the primate lineage, Waterston's team searched for genes evolving more rapidly than the background rate of mutation. Among both human and chimp lineages, genes involved in ion transport, synaptic transmission, sound perception, and spermatogenesis stood out. The researchers also used the chimp data to identify 585 genes evolving more quickly in people, including genes involved in defense against malaria and tuberculosis. And they uncovered a handful of regions of the human genome that may have been favored in "selective sweeps" relatively recently in human history; one region contains the *FOXP2* gene, proposed to be important in the evolution of speech.

Overall, however, "the vast majority of changes between humans and chimps appear to be neutral, and there's no smoking gun on which are the important changes for making us human," says Adams.

One notable finding was that the fastest evolvers among human proteins are transcription factors, which regulate gene expression. Thirty years ago, Mary-Claire King and Allan Wilson proposed that altered gene regulation could solve the paradox of how a few genetic changes drove the wide anatomic and behavioral gulf between humans and chimps. "That's how you could get lots of morphological change without much nucleotide substi-

CREDIT: JAMES BALOG/GETTY IMAGES

Focus

1476 Fateful fetal information

1481 Viox on trial

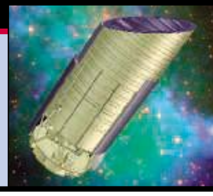

1482 A dark secret

tution. But there's been no evidence for it until now," says Eichler. Given the chimp data, "people will rethink the regulatory hypothesis," predicts Huntington Willard of Duke University in Durham, North Carolina.

Another *Nature* paper addresses a controversy about whether the human Y chromosome will vanish within some 10 million years. Geneticist David Page of the Whitehead Institute in Cambridge, Massachusetts, and colleagues report the detailed sequence of the "X-degenerate" region of the chimp Y, which contains functional genes once paired with those on the X but now being slowly eroded by deleterious mutations. Page's team then compared human and chimp Ys to see whether either lineage has lost functional genes since they split.

The researchers found that the chimp had indeed suffered the slings and arrows of evolutionary fortune. Of the 16 functional genes in this part of the human Y, chimps had lost the function of five due to mutations. In contrast, humans had all 11 functional genes also seen on the chimp Y. "The human Y chromosome hasn't lost a gene in 6 million years," says Page. "It seems like the demise of the hypothesis of the demise of the Y," says geneticist Andrew Clark of Cornell University in Ithaca, New York.

Although the chimp genome should be a boon for biomedical studies, an accompanying *Nature* commentary by Varki and colleagues calls for moderation, using principles generally similar to those that guide human experimentation. The similarity of the two genomes underscores the importance of an ethical approach to our closest living cousins, says Waterston. –ELIZABETH CULOTTA

BIOETHICS

Final NIH Rules Ease Stock Limits

The National Institutes of Health (NIH) in Bethesda, Maryland, has relaxed ethics rules issued 6 months ago that many feared would drive talent away from the agency. NIH Director Elias Zerhouni last week announced that the agency's final rules would no longer require all employees to limit their stock in biotech or drug companies. But NIH will retain a blanket ban on consulting for industry.

The revised rules seem to please both NIH scientists and outside critics. "Dr. Zerhouni has done an admirable job addressing a difficult yet critical issue," said House Energy and Commerce Committee chair Joe Barton (R–TX), whose committee held several hearings on the subject.

The rules appear to end a controversy that has roiled NIH since late 2003, when the *Los Angeles Times* raised questions about several senior NIH researchers who had been paid large sums to consult for drug or biotech companies. NIH eventually found at least 44 cases in which researchers didn't receive proper ethics approval and nine possible criminal violations. To address the problem, Zerhouni issued interim ethics rules in February 2005 that banned all biomedical consulting—even for nonprofits—and limited all employees' ownership of drug company stock (*Science*, 11 February, p. 824).

The interim rules outraged many NIH employees. Some senior intramural scientists cited the rules as a factor in their departure, one institute director threatened to leave, and a newly hired one delayed his arrival.

After receiving 1300 mostly critical comments, NIH "decided to adjust in terms of degree," Zerhouni told reporters. Stock limits will now apply only to about 200 senior staff, including directors and other top managers of NIH's 27 institutes and centers. By next February, these employees and their families must limit their stock to $15,000 in any one company "significantly involved" in biomedicine. Previously, this limit would have applied to 12,000 lower-level employees, and about 6000 senior staff would have had to divest all their drug company stock. Those senior staff and clinicians will now have to report their holdings for review.

NIH will no longer ban work done for associations, such as serving as an officer of a scientific society. The final rules also allow compensation for reviewing scientific grants and for giving a single lecture—the interim rules exempted only entire courses—and make clear that approval is not needed for hobbies, such as coaching youth soccer.

Tight reins. NIH Director Elias Zerhouni says final rules are "most restrictive" in the field.

CREDIT: MARTY KATZ

The NIH Assembly of Scientists' executive committee "is very pleased" by the changes, says member Cynthia Dunbar of the National Heart, Lung, and Blood Institute. "Morale should improve markedly," she adds. Howard Garrison of the Federation of American Societies for Experimental Biology expressed relief that NIH scientists can maintain ties to professional associations.

Dunbar says concerns remain that the industry consulting ban will harm recruitment and retention. Zerhouni says he decided to retain the ban after concluding NIH doesn't have "adequate systems" to prevent abuses. He added, however, that NIH intends to review the rule within a year. Although NIH scientists can still work with companies through cooperative agreements, some outside biomedical leaders suggest that's not enough: "It is also important to continue to seek ways to foster appropriate interactions with" industry researchers, says Phil Pizzo, dean of the Stanford University School of Medicine, who served on a 2004 NIH advisory panel that favored allowing some industry consulting.

Not everyone thinks the final rules solve NIH's ethics problems. "There's a whole variety of things involving laundered money going to people whose views are favorable," such as drug company-sponsored education courses, says Sidney Wolfe, of the Washington, D.C.–based watchdog group Public Citizen. But Zerhouni defended the new plan as "the most restrictive of any rules we know about in the world of biomedical research." The final regulation was to take effect this week when it was published in the *Federal Register*.

–JOCELYN KAISER

EUROPEAN POLITICS

Germany Poised to Elect First Scientist-Chancellor

BERLIN—German opinion polls predict that the country will elect its first chancellor trained in the natural sciences later this month. A victory for the Christian Democratic Union (CDU) on 18 September over the ruling Social Democrats would mean a government led by Angela Merkel, who holds a Ph.D. in physical chemistry—a result that could produce significant changes for German scientists.

Merkel has been a politician for longer than she worked as a scientist, and her training is seldom mentioned in a campaign dominated by economic issues. More is being made of two other milestones stemming from a CDU victory: the country's first female chancellor and the first from the former East Germany. But some scientists hope that Merkel's previous career, and the fact that her husband is a well-respected chemistry professor, might give them a sympathetic ear in the chancellery—and boost science's profile. "The first natural scientist as a chancellor would be a wonderful message for the country," says biologist Hubert Markl of the University of Constance, former head of Germany's Max Planck Society and its DFG funding agency.

Markl is quick to add that the current chancellor, Gerhard Schröder, is also "very pro-innovation," and party politics is likely to play a larger role in shaping science policy than the next chancellor's Ph.D. For example, if Schröder pulls off a come-from-behind victory, scientists hoping to work with human embryonic stem (ES) cells could get a boost. Schröder has said that he would like the Bundestag to revisit the laws that ban research on embryos and allow scientists to import only those ES cell lines derived before 1 January 2002.

The CDU provided much of the support for this legislation, and while Merkel has been quiet on the subject, several high-ranking party members have said that there would be no move to relax the law in a CDU-led government. That stance might be challenged, however, by the CDU's preferred coalition partners, the Free Democrats (FDP). Like Schröder, the FDP favor relaxed laws that would allow derivation of human ES cells and human nuclear transfer experiments.

The potential coalition partners have fewer disagreements on two other hot scientific issues: nuclear power and genetically modified crops. Both the CDU and FDP support a relaxing of the current government's policy of phasing out all nuclear power plants by 2020. Some say this policy, pushed by the government coalition member Green Party, has made it difficult for nuclear physics departments in Germany to attract students.

Both the CDU and FDP say they would relax restrictions on genetically modified crops. The Greens have supported tough curbs on the technology, pushing through a law that holds planters legally responsible for pollen that escapes and contaminates a neighboring field (*Science*, 25 June 2004, p. 1887). Scientists say that the measure effectively rules out all field research with genetically modified plants. Several politicians expect a more permissive law to be high on the agenda of a CDU-FDP coalition.

Quantum leap. Angela Merkel, who studied physics and quantum chemistry, is likely to be Germany's next chancellor.

CREDIT: INA FASSBENDER/REUTERS

All parties agree on the need to boost science funding, a step the Bundestag took this summer by passing a 5-year, \$2.8 billion science spending package (*Science,* 1 July, p. 33). The CDU says that it wants to go even further, adding \$1.25 billion over 4 years so the DFG can fund overhead costs.

What voters are most concerned about, however, is whether Merkel can tackle the country's economic woes. At least some observers say her scientific training might be an advantage. Last month, the influential *Süeddeutsche Zeitung* wrote that Merkel had demonstrated both meticulousness and tenacity in her 1986 dissertation on the calculation of rate constants in hydrocarbon decomposition reactions. Such qualities, the paper said, could be usefully applied to the equally complex problems facing Germany.

–GRETCHEN VOGEL

ScienceScope

Scientist Quits Climate Panel

A climate researcher resigned in protest last week from a federal panel about to release its report on recent temperature trends.

Roger Pielke Sr., of Colorado State University, Fort Collins, had been a member of the 22-person panel currently assessing conflicting temperature trends from Earth's surface, balloons, and satellites for the federal Climate Change Science Program. Pielke says he threw in the towel because the committee failed to be "inclusive" and improperly eliminated consideration of regional temperature trends. The report, which is expected out within a few weeks, "is much too narrow," he says. Factors such as land-use changes, in addition to greenhouse gases, are driving recent warming, Pielke has advocated. Leaders of the panel would not comment, but fellow panel member Chris Forest of the Massachusetts Institute of Technology says that the report's 70-page limit ended up excluding the diversity of viewpoints that Pielke wanted to see.

A U.S. hurricane expert in January said that politicization of the scientific process was behind his decision to resign from an international climate change panel (*Science*, 28 January, p. 501). But Pielke says his difference of opinion was not related to politics. –RICHARD A. KERR

NIH Overhaul Still Fermenting

A new version of a draft bill to streamline the management of the National Institutes of Health (NIH) leaves many issues unresolved, say advocacy groups.

The House Energy and Commerce Committee wants to give the NIH director more authority as part of a reauthorization of NIH's programs, with a bill to be introduced as soon as next month. But a July draft drew concerns that it would undermine the autonomy of NIH's 27 institutes and centers (*Science*, 22 July, p. 545). A new draft released last week creates a "common fund" for trans-NIH initiatives but lets institutes award the grants. But, controversially, the plan still groups NIH entities into two funding clusters and doesn't specify how individual budgets would be set. And lawmakers have not explained how much of institutes' budgets would go to the "common fund"—5% is often discussed. "There are still a lot of questions," says Dave Moore of the Association of American Medical Colleges.

–JOCELYN KAISER

SPACE-BASED ASTRONOMY

Scientists Scramble to Curb Webb Overruns

NASA plans to reduce the sensitivity of the successor to the Hubble Space Telescope to beat back rising costs that threaten to overwhelm the project. But despite a wealth of suggestions from scientists on how to cut costs, the agency likely will still face a shortfall of more than $500 million of the $3.5 billion needed to build, launch, and operate the James Webb Space Telescope (JWST).

The trouble surfaced this spring, when agency officials found a $1 billion overrun in the project that they blamed on a host of technical issues (*Science*, 13 May, p. 935). A panel convened to examine the crisis last week recommended several ways to minimize the shortfall and avoid future cost increases. As a result of the cost-cutting measures, NASA science chief Mary Cleave has tentatively given the project a green light pending a final decision by NASA administrator Mike Griffin, telescope officials say. NASA is also projecting a 2-year slip in the launch, to 2013.

The higher price tag could not come at a worse time for a science program choking on the costs of another space shuttle mission to Hubble, overruns in other science efforts, and the seemingly endless woes of the space shuttle program. Still, a 2001 report by the National Academy of Sciences labeled JWST the top priority for astronomy and astrophysics in the coming decade. NASA officials also remember well the uproar following the attempt by former NASA chief Sean O'Keefe to cancel a Hubble shuttle servicing mission—a decision Griffin reversed.

JWST scientists remain adamant that dramatic cuts to the size of the mirror or the major instruments are not an acceptable option. But the science panel, led by astronomer Peter Stockman and JWST scientist Mattias Mountain, both of Baltimore, Maryland's Space Telescope Science Institute (Mountain was recently named its director), did find significant savings in other areas.

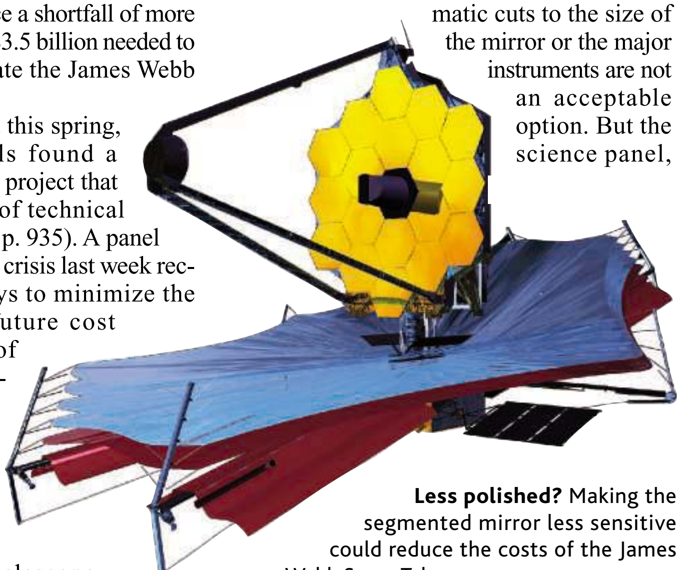

Less polished? Making the segmented mirror less sensitive could reduce the costs of the James Webb Space Telescope.

The mirror is designed to capture wavelengths from 0.6 to 28 microns. But thanks to advances in adaptive optics that can screen out perturbations in the Earth's atmosphere, the team agreed that the lower limit could be raised to 1.7 microns. That change would require one less cycle of polishing, at a savings of $150 million. Although the telescope would be less capable of observing at shorter wavelengths, future ground-based telescopes could compensate, says Eric Smith, JWST program scientist at NASA. That change disturbs some scientists, like Robert O'Dell of Vanderbilt University in Nashville, Tennessee. He says that degrading JWST's performance will make studies of nebulae and star formation now possible with Hubble more difficult.

Relaxing stringent requirements designed to limit dust on the mirror could save a similar amount in test-related hardware, says Stockman. And the telescope likely would require one less testing cycle, knocking off another $100 million.

Although the major instruments would not dramatically change, the team did recommend saving weight, mass, and support costs by dropping one portion of the Canadian fine guidance sensor designed to image at shorter wavelengths. A small French-made coronagraph could also be abandoned if necessary, the team said. NASA has yet to discuss those options with Canadian or French officials.

The savings could total $430 million, Stockman estimates, and significantly reduce future risk, which also saves money. "I don't think we're going to find $1 billion," adds Smith. "But hundreds of millions … is most welcome." –ANDREW LAWLER

U.S. MILITARY INSTALLATIONS

Base Commission Alters Pentagon's Wishes on Labs

A federal panel tasked with restructuring U.S. military facilities delivered a mixed bag to researchers last week.

The Armed Forces Institute of Pathology (AFIP) in Washington, D.C., got a reprieve from a recommendation to shut down most of its functions (*Science*, 20 May, p. 1101), and the Army's Night Vision Lab in Fort Belvoir, Virginia, fought off a move to Aberdeen Proving Ground in northeastern Maryland. But the Army signal processing research and electronics laboratories at Fort Monmouth, New Jersey, are headed to that site.

The Base Realignment and Closure (BRAC) process, last completed in 1995, drew up a list of hundreds of closures and restructurings in the military's vast network of bases, labs, and offices. The commission voted last week, and its recommendations, which include major closings in Texas and Georgia, now go to the White House and then to Congress.

The Defense Department recommended in May that the president "de-establish" the AFIP except for its museum and tissue repository. The College of American Pathologists and other groups lobbied the BRAC commission to save the $100 million a year, 820-staff pathology institute, arguing that the research staff was essential for roles such as helping prepare for bioterror attacks. The panel's decision that its functions "be absorbed" into other federal or civilian facilities is a "glimmer of good news, but the devil is in the details," says former lab pathologist William Travis, who left AFIP this year for Memorial Sloan-Kettering Cancer Center in New York City.

One question is whether AFIP will stay intact and move to a new building, he says. At least one piece is already splitting off: The chair of veterinary pathology announced last week that his department expects to move to an annex in Silver Spring, Maryland. A conference this week was to explore the future of its renowned 3 million-case tissue repository in light of the proposed breakup.

Lobbying against the move to Maryland, former Fort Monmouth research director Robert Giordano cited a poll that showed that only 20% of the 5000 technical civilian staff would follow the lab. The resulting "brain drain," he warned, would decimate crucial military research positions. Similar arguments were made against the move of the night vision lab, which conducts work in lasers, radar, and infrared light.

–JOCELYN KAISER AND ELI KINTISCH

CREDIT: NASA

SCIENTIFIC DATABASES

NIH, Chemical Society Look for Common Ground

U.S. government officials and a scientific society are batting ideas back and forth on how to keep a new federal chemical database from overlapping with an existing private one. So far, they are still searching for common ground.

A dispute between the National Institutes of Health (NIH) and the American Chemical Society (ACS) broke out after NIH's National Center for Biotechnology Information (NCBI) last fall launched PubChem, a database of small molecules with potential use as biological probes or as drugs, including data from a new screening initiative. ACS complained to NIH and Congress that PubChem's listing of chemical structures, though modest in size so far, duplicated its Chemical Abstracts Service (CAS) Registry, a massive, subscription-only chemical database that is a critical source of income for the society. Earlier this year, after discussing whether NIH should scale back the scope of PubChem, the House and later the Senate instead asked NIH to "work with private sector providers to avoid unnecessary duplication and competition" (*Science*, 17 June, p. 1729).

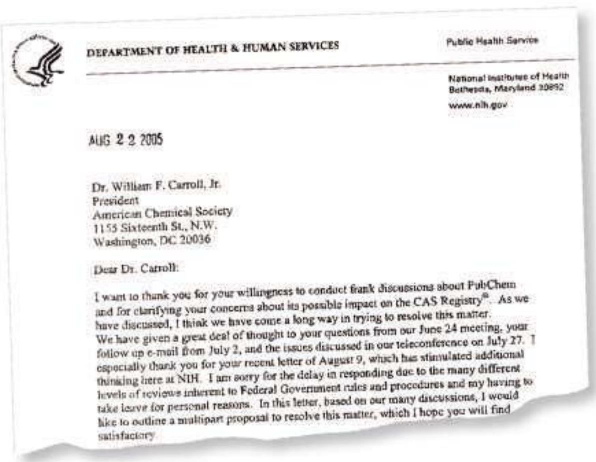
DEPARTMENT OF HEALTH & HUMAN SERVICES

Public Health Service

National Institutes of Health
Bethesda, Maryland 20892
www.nih.gov

AUG 2 2 2005

Dr. William F. Carroll, Jr.
President
American Chemical Society
1155 Sixteenth St., N.W.
Washington, DC 20036

Dear Dr. Carroll:

I want to thank you for your willingness to conduct frank discussions about PubChem and for clarifying your concerns about its possible impact on the CAS Registry®. As we have discussed, I think we have come a long way in trying to resolve this matter. We have given a great deal of thought to your questions from our June 24 meeting, your follow up e-mail from July 2, and the issues discussed in our teleconference on July 27. I especially thank you for your recent letter of August 9, which has stimulated additional thinking here at NIH. I am sorry for the delay in responding due to the many different levels of reviews inherent to Federal Government rules and procedures and my having to take leave for personal reasons. In this letter, based on our many discussions, I would like to outline a multipart proposal to resolve this matter, which I hope you will find satisfactory.

Paper trail. NIH's Elias Zerhouni countered the American Chemical Society's offer to build NIH a chemical database.

CREDIT: NIH

In early August, ACS president William Carroll made NIH an offer: The society would donate $10 million and up to 15 staff members over 5 years to build NIH a free database of chemicals with attached bioassay data. NIH expressed many concerns about the proposal, however, in a four-page letter to Carroll from NIH Director Elias Zerhouni.

In the 22 August letter, Zerhouni notes that NIH wants to integrate PubChem with other public biomedical databases, which NCBI staff—not a chemistry organization—"are in an ideal and unique position" to do. NIH is also concerned about which molecules ACS would include, arguing that the database cannot be limited to compounds with biological data because such bioactivity may remain to be discovered. In addition, Zerhouni explains, the plan would violate federal rules requiring that any such agreement be open to bidding from other companies.

Zerhouni offered a six-part "alternative structure" that would avoid overlap between PubChem and CAS but strengthen the ties between the two databases. Among those changes, NIH would pay ACS to make sure PubChem entries contain the same numbers that CAS uses to register each molecule to "maximize the interactiveness" of the two databases. NIH would agree not to include nonbiomedical information that CAS now offers, such as chemical reactions and patents. NIH also wants to set up a working group, with chemical database companies as members, that would offer NCBI advice on how to run PubChem.

The letter says NIH is open to developing a "retrospective process" for removing chemicals from PubChem that are deemed of no use for biomedical research. NIH officials have noted in the past that it would be very hard to rule out any chemicals. For example, ACS initially claimed that an explosive called HDX should not be included in PubChem, but an NCBI official pointed out that the National Cancer Institute has found that HDX has activity in antitumor assays.

Both sides say they are committed to finding a compromise. In a 23 August letter to ACS members, Carroll says the society is "studying" this proposal but maintains that NIH should "[take] advantage of the CAS Registry." ACS spokesperson Nancy Blount said that a national ACS meeting in Washington, D.C., earlier this week prevented society officials from speaking with *Science*, but that ACS will "continue to have the best interest of science in mind." Likewise, NIH spokesperson John Burklow says that "we are hopeful our proposals will resolve the issues."

–JOCELYN KAISER

ScienceScope

WHO Tamiflu Stockpile Grows

PARIS—The World Health Organization (WHO) last week said it had received a donation of 3 million 5-day treatment courses of the anti-influenza drug oseltamivir, better known as Tamiflu, from Swiss drugmaker Roche. The drugs could help avert, or at least slow, a flu pandemic, the agency says.

Two recently published models show that a combination of quarantine measures and the widespread administering of oseltamivir could halt a nascent pandemic. But that would require a stockpile of several million treatments (*Science*, 5 August, p. 870). Despite Roche's gift, countries still need to stock up themselves, WHO warns.

–MARTIN ENSERINK

Japan Expects Budget Squeeze

The Japanese cabinet has indicated that it will not spare science in its efforts to shrink total governmental spending by 3% next year, and polls indicate the incumbent coalition is likely to survive the 11 September elections. But Japan's Ministry of Education has optimistically requested a 9.5% increase in science-related spending, to $8.3 billion, for the fiscal year beginning next April. Plans include a new supercomputer and work on an x-ray laser for protein crystallography and other uses. "It's impossible to know at this point" the science budget's fate, says Takafumi Goda, the Ministry of Education's budget director.

–DENNIS NORMILLE

Climate (Policy) Shifts

Environmentalists cleared a legal hurdle last week in a court battle over climate change impacts. Advocacy groups and several western federal cities had sued in 2002 to force the Export-Import Bank and the Overseas Private Investment Corporation, which fund power projects, to conduct environmental assessments on climate change. Last year, the U.S. government asked the federal court in the northern district of California to throw out the lawsuit, but Judge Jeffrey White has ruled that the "reasonably probably" climate impacts were sufficient to allow the case to proceed.

Meanwhile, *The New York Times* reported progress by a nine-state consortium—including New York and Massachusetts—on a regional greenhouse cap and trade system that would freeze emissions and reduce them by 10 percent by 2020. The regional system is expected to be finalized this month.

–ELI KINTISCH

Biotechnology Lab, Gaithersburg, MD: Thursday, August 18th, 10:38 AM

The drug you need.

What if it was possible for consulting services and IT solutions to set in motion the discovery and development of targeted drugs that are safer and more effective?

As you read this, our consultants are helping companies transform their R&D processes to support the discovery and development of more targeted treatments that work better for patients with common genetic characteristics. IBM and IBM Business Partners can deliver the IT infrastructure and solutions you need to help manage the integration of clinical and genomic data and to enhance security for access to publicly available biomedical information. So you can understand the underlying molecular mechanisms of disease, select patient populations for smaller and more effective clinical trials, and ultimately transform the paradigm of medicine. IBM Information Based Medicine – innovation that matters. Learn more at **ibm.com**/lifesciences/genomics

BIODEFENSE

Microbiologist Resigns After Pitch for Antianthrax Product

A scientist's enthusiastic endorsement of a skin lotion against anthrax has ended his career at the University of Texas Medical Branch (UTMB) at Galveston. On 17 August, John Heggers, a microbiologist and plastic surgeon specializing in burn treatment, resigned after the university's Scientific Integrity Committee (SIC) concluded he engaged in "egregious" misconduct by making "false and excessive statements" about the purported antianthrax lotion, a blend of citrus oils, plant herbs, and seed bitters that sells at $179 for half a liter.

On 1 February 2005, the report says, Heggers wrote a letter on UTMB letterhead to Bio-Germ, the Dallas company that produces the lotion, in which he said his research had demonstrated the product's efficacy and safety; "we believe it will be successful against Smallpox, the Plague, and other pathogens possibly used by terrorists" as well, he wrote, adding that the lotion "should be rolled out to our Nation's First Responders, Military and, as soon as possible, to the citizenry of our Country." Bio-Germ posted the letter on its Web site, according to the 29 June university investigation, along with a videotaped interview in which Heggers made similar statements.

Heggers, 72, has been at UTMB for 17 years and had a co-appointment at the Shriners Burns Hospital; he was not involved in UTMB's sizable federally funded biodefense program. He did carry out one anthrax study, but the committee says it did not support his claims. In a 2004 paper in the online *Journal of Burns and Wounds*, Heggers described tests of several topical antibacterials, "nutriceuticals," and herbal products against strains of *Bacillus anthracis*, which causes anthrax. The paper claims that the Bio-Germ lotion and many other products killed the microbes, but the result is irrelevant, the panel says, because the tests used vegetative *B. anthracis* growing in a petri dish, not the spore form used in weaponized anthrax. Heggers has no data on plague and smallpox, according to the panel, which calls his recommendation for mass deployment of the lotion "utterly irresponsible scientifically." The SIC says Bio-Germ paid Heggers's expenses to attend several meetings about homeland security but no honoraria. Two of Heggers's co-authors, Johnny Peterson and Ashok Chopra, say they did not see the manuscript of the paper in the *Journal of Burns and Wounds* before it was posted and found its conclusions "misleading." The paper was removed from the journal's Web site in early June, they say.

All you need. Bio-Germ says its $249 Protection Kit, which includes antianthrax lotion (also sold separately), provides "an effective shield against infection from anthrax."

CREDIT: BIO-GERM PROTECTION 2005

Heggers could not be reached for comment. But in a 15 July letter to UTMB President John Stobo, Heggers claimed that the university had been "intimidated" by the *Dallas Morning News*, which first reported the story, and that the panel was not qualified to judge him. In his 17 August resignation letter to Stobo (copies of both letters were made available to *Science*), Heggers acknowledged "several misstatements." In an e-mail to a *News* reporter he attached to the resignation letter, Heggers said, "on reflection, I think my hope and enthusiasm outran my scientific caution."

At UTMB's request, Heggers's testimonials have been removed from Bio-Germ's Web site. "It's an embarrassment," says David Walker, executive director of UTMB's Center of Biodefense and Emerging Infectious Diseases. –MARTIN ENSERINK

INFECTIOUS DISEASES

Homeland Security Ponders Future of Its Animal Disease Fortress

The Alcatraz of animal diseases may come ashore. Last week, the U.S. Department of Homeland Security (DHS) announced that the Plum Island Animal Disease Center (PIADC)—which studies the most devastating agricultural diseases on a tiny speck in the Atlantic off Long Island, New York—will be replaced by a new facility that may be located elsewhere. The state's politicians, who oppose expanding the lab's remit but don't want it to close, immediately blasted the proposal. But some scientists say they would welcome leaving the remote, impractical location.

DHS took over responsibility for Plum Island from the U.S. Department of Agriculture in 2002. In a fact sheet issued last week, the department said the 50-year-old lab is "nearing the end of its lifecycle" and will be replaced by a new National Bio and Agrodefense Facility (NBAF) with a stronger focus on bioterrorism. DHS is launching a study to determine the facility's mission, its preferred location, and whether it needs a biosafety level 4 (BSL-4) lab, the highest level of biological containment. The study should be completed by 2006, and the facility could open in 2011.

Few contest that the dilapidated complex at Plum Island needs an extreme makeover. But adding a BSL-4 facility, or moving it, is controversial. Because most of the diseases studied there—such as foot-and-mouth disease and classical swine fever—don't infect humans, the lab operates at BSL-3 plus, which resembles BSL-4 except that researchers don't wear space suits. Scientists have long argued that the U.S. needs a BSL-4 facility for agricultural diseases to allow the study of agents, such as the Nipah and Hendra viruses, that sicken farm animals as well as humans.

But Long Island residents and local politicians fear an escape of the deadly viruses and have resisted those plans (*Science*, 26 May 2000, p. 1320). In 2003, former DHS secretary Tom Ridge assured Sen. Hillary Clinton (D–NY) and Rep. Timothy Bishop (D–NY) that no BSL-4 would be built on Plum Island—a promise DHS says it will honor. Clinton and Bishop want the facilities upgraded, they wrote "in distress" to DHS secretary Michael Chertoff last week, not moved off the island.

A DHS spokesman says that all options are still on the table—including building a new lab without a BSL-4 on Plum Island. But Harley Moon, an emeritus professor at Iowa State University in Ames who directed Plum Island in the mid-1990s, says moving the lab ashore would be the best option for several reasons. Operating the lab on an island is expensive, he says, the researchers are "intellectually isolated," and Long Island's high cost of living hinders recruitments. Moon suggests moving it to an agricultural research center, such as those in Georgia, Colorado, or Iowa, where "the community and the policy makers understand the importance of the lab's mission."

–MARTIN ENSERINK

The increasing ability to analyze fetal DNA from maternal blood should lead to better prenatal diagnoses of genetic disease—and confront future parents with tough information and choices

An Earlier Look At Baby's Genes

The smiling, dark-haired woman chatting with Katie Couric on NBC's popular *Today* show explains why she wants to know the sex of her third baby just 7 weeks into her pregnancy. Holly Osburn of Glastonbury, Connecticut, the mother of two daughters, says her house is full of pink, purple, and green, and "we're anxious to find out if we're going to … maybe have to paint the nursery blue."

So Osburn has sent dried spots of her blood to a Massachusetts company offering Baby Gender Mentor, a new $275 test that promises to detect a fetus's sex from maternal blood as early as 5 weeks after conception. After Couric conducts a discussion with a physician about the pros and cons of the test, a spokesperson for a company selling it online delivers the big news live to millions of viewers: It's a girl! Osburn's smile wavers. "Another one," she says. Then she regains her composure, assuring the TV audience that "a third is great."

While watching this in June, "my jaw dropped," says Diana Bianchi, a prenatal geneticist at Tufts University School of Medicine in Boston and one of a small number of researchers who have spent more than a decade trying to detect sex and genetic disorders from fetal cells and DNA in a mother's blood. She notes that "at home" fetal DNA tests such as Baby Gender Mentor aren't yet considered scientifically and ethically vetted. "I'm concerned about whether this is ready for prime time," says Bianchi.

Ready or not, noninvasive fetal diagnosis is here. Tests based on fetal DNA circulating in a woman's blood are expected to replace invasive prenatal tests, such as amniocentesis, that are typically done later in pregnancy and pose a small risk of miscarriage. Researchers have already used fetal DNA from maternal blood to successfully test for genes inherited from a father that cause diseases such as cystic fibrosis and the blood disorder thalassemia. They are now refining their techniques and moving on to bigger challenges, such as identifying Down syndrome. If this work pans out, fetal genetic testing could be as cheap and routine as many other diagnostic tests, such as ones for HIV, says molecular biologist Sinuhe Hahn of the University Women's Hospital in Basel, Switzerland.

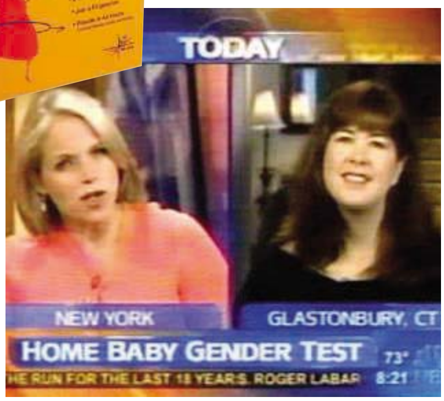

Broadcast news. Through a new test (*inset*), expectant mother Holly Osburn, along with Katie Couric and *Today* viewers, learned the apparent gender of her 7-week-old fetus.

Earlier and easier fetal DNA testing will certainly raise ethical questions. For example, some researchers worry that gender tests will lead to abortions by parents who desire a baby of a specific gender. The ethically explosive applications extend beyond sex selection. If fetal DNA testing can one day routinely reveal whether an early fetus has genes that predispose it to cancer or other diseases, parents-to-be could be facing much more difficult decisions than what color to paint the nursery.

For now, researchers are grappling with how to get a clear, consistent signal from a relatively few molecules of fetal DNA sequence floating in a sea of maternal DNA. When a diagnosis could lead parents to end a pregnancy, they note, accuracy is crucial. "It's very important that we get it right," says medical geneticist Maj Hulten of the University of Warwick, U.K.

One in a million

Researchers have known for more than 3 decades that a few fetal cells of various types are present in a pregnant woman's blood. While there may only be about two to six fetal cells per milliliter of blood during pregnancy, some of these cells can linger for several decades after birth and may even contribute to postnatal tissue repair or disease in the mother *(Science*, 21 June 2002, p. 2169). The first proof that such cells could be used to diagnose a fetal condition came in 1991 from Joe Leigh Simpson's lab at Baylor College of Medicine in Houston, Texas. Using an antibody called CD71 that tends to bind to red blood cells of fetal origin, his team separated these cells from most maternal blood cells. They then used fluorescence in situ hybridization (FISH), in which colored probes bind to chromosomes, to detect Down syndrome, which is caused by an extra chromosome 21, and another chromosomal disorder.

Other labs soon reported similar results, exciting researchers who saw the technique as a promising alternative to amniocentesis and chorionic villus sampling (CVS). These diagnostic tests, which collect fetal cells by inserting a needle into the womb either late in the first trimester or during the second trimester, carry up to a 1% risk of miscarriage. In 1994, the National Institute for Child Health and Development (NICHD) launched a validation study in which five labs used fetal cells from maternal blood to look for Down syndrome in 2744 pregnancies. The results, published in 2002, were just modestly encouraging: The researchers found only enough fetal cells to detect 74% of Down syndrome cases. In contrast,

CREDITS (TOP TO BOTTOM): G. MOSCOSO/PHOTO RESEARCHERS INC.; (INSET) ACU-GEN BIOLAB INC.

CVS and amniocentesis are 99% accurate.

The authors of the NICHD study concluded that the current techniques—which involve physically separating the fetal and maternal cells—would have to improve before blood-borne fetal cells could provide reliable diagnoses. The key will be an antibody or other compound that can more efficiently separate out the fetal cells, which make up only about one out of every million cells in a mother's blood, says Simpson. "Once that occurs, the field will turn around overnight," he says.

A few teams, including Simpson's at Baylor, and at least two companies are also pursuing an alternative approach, attempting to isolate fetal cells, called trophoblasts, from cervical swabs of pregnant women. The trophoblasts make up about 1 in 100,000 cells in a swab, and so should be easier to distinguish from maternal cells than fetal blood cells, says Farideh Bischoff of Simpson's group. Yet to be proved is whether researchers can extract enough cells without sampling so high in a woman's cervix that the technique becomes invasive, Bianchi notes.

Free and easy

Noninvasive fetal testing took off in a new direction several years ago after Dennis Lo, now at the Chinese University of Hong Kong, and co-workers discovered that maternal blood contains more than fetal cells. There's also fetal DNA floating freely, outside of cells, he found. Lo was inspired to look by two 1996 *Nature Medicine* articles on detecting tumor DNA in the blood of cancer patients. He reasoned that like a tumor, the fetus-derived placenta is a fast-growing tissue that might shed DNA.

The hunch paid off: Using a form of polymerase chain reaction (PCR) to detect a gene called *SRY* on the Y chromosome of male fetuses, Lo's group reported in 1998 that fetal DNA is much more plentiful in a future mom's bloodstream than are fetal cells. Levels rise during pregnancy to as much as 3% to 6% of the cell-free DNA in a mother's plasma, then plummet in 2 hours after a baby is born. The fetal DNA seems to come mainly from the placenta, Bianchi and others have shown.

Lo's group soon showed that this fetal DNA could be used to diagnose potentially lethal conflicts in Rh factor, a protein on the surface of red blood cells. If an Rh-negative woman carries an Rh-positive fetus, her immune system can create antibodies against the baby's blood cells, causing anemia for the fetus. This sensitization can be prevented by injecting the pregnant mother at certain points in pregnancy with Rh immunoglobulin, a step often taken as a precaution without knowing the fetus's Rh status. But many research groups have now shown they can reliably test the blood of Rh-negative pregnant women for fetal DNA that reveals the functional form of the *Rh* gene. Such a test has been offered since 2001 by a few research labs in Europe.

Several groups have since reported they can detect other disease mutations passed on from the father, such as ones causing cystic fibrosis, beta-thalassemia, a type of dwarfism, and Huntington's disease. The results haven't always been reproducible, partly because smaller mutations are difficult to pick up from a mixture of fetal and maternal DNA. Other promising findings are still being debated. Lo's group reported in 2000 that intact fetal DNA in fragments of dying cells could be analyzed for Down syndrome, and last year a biotech company claimed that treating maternal blood with formaldehyde could boost the amount of fetal DNA recovered. Only some labs have been able to replicate these experiments.

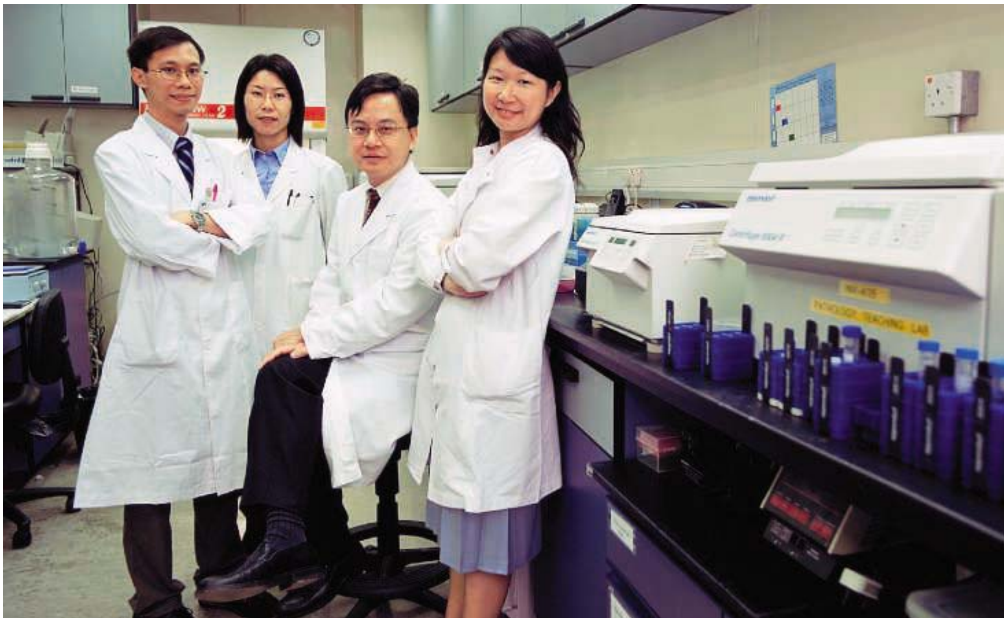

Detective squad. Dennis Lo (*center*) and his group at Chinese University of Hong Kong have pioneered noninvasive prenatal testing using cell-free fetal DNA.

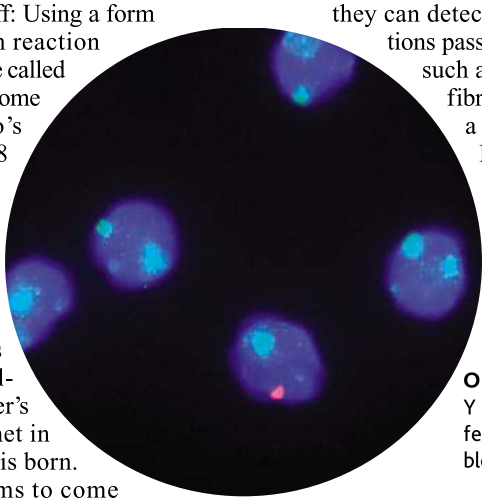

Oh, boy. Red marks the Y chromosome in a male fetal cell amid maternal blood cells.

CREDITS (TOP TO BOTTOM): THE CHINESE UNIVERSITY OF HONG KONG; T. BABOCHKINA/UNIVERSITY WOMEN'S HOSPITAL, SWITZERLAND

Two advances in the past year have clearly boosted the potential reliability of fetal DNA tests, however. Both involved studies looking for mutations that trigger beta-thalassemia, which leads to severe anemia and is most common in people of Asian and Mediterranean descent. Last summer, a report in the *Proceedings of the National Academy of Sciences* by Lo's team and the San Diego–based firm Sequenom Inc. said that inherited beta-thalassemia point mutations could be diagnosed in 12 fetuses much more reliably if mass spectrometry and PCR, rather than PCR alone, were used to analyze the fetal DNA.

Earlier this year in the *Journal of the American Medical Association*, Hahn's team in Basel reported another approach for detecting beta-thalassemia mutations comprising a single nucleotide change. The group took advantage of a finding by Lo's group that the fragments of fetal DNA found in the mother's blood are typically less than 300 basepairs in size, compared with more than 500 basepairs for cell-free maternal DNA. By using electrophoresis to increase the ratio of the shorter segments in blood samples, the Swiss team successfully detected the presence or absence of four common beta-thalassemia point mutations in 28 of 31 fetuses. While the mass spectrometer needed for the Sequenom-Lo method costs \$300,000, the Swiss team notes that its approach could cost as little as \$8 per sample, within the economic reach of developing countries.

Several teams are now racing to try these techniques—or combine them—to reliably detect cystic fibrosis and other genetic dis-

eases, says Hahn. "They will open up a lot of new applications," Lo agrees.

One major caveat is that the studies so far have only been able to detect mutations passed on by the father. Because there's not yet a way to completely separate fetal DNA from the maternal DNA in a woman's blood, it's not possible to tell if a mutation possessed by the mother has been inherited by the fetus or if researchers are just seeing the mother's DNA. One possible solution may be an epigenetic marker, such as methylated groups attached to a gene, that distinguishes fetal DNA from a mother's. Lo's group showed in 2002 that they could make such a distinction. Another potential strategy is to use messenger RNA molecules produced only by the fetus and not the mother. Several groups have recently shown, for example, that RNA produced by placental genes can be detected in maternal blood.

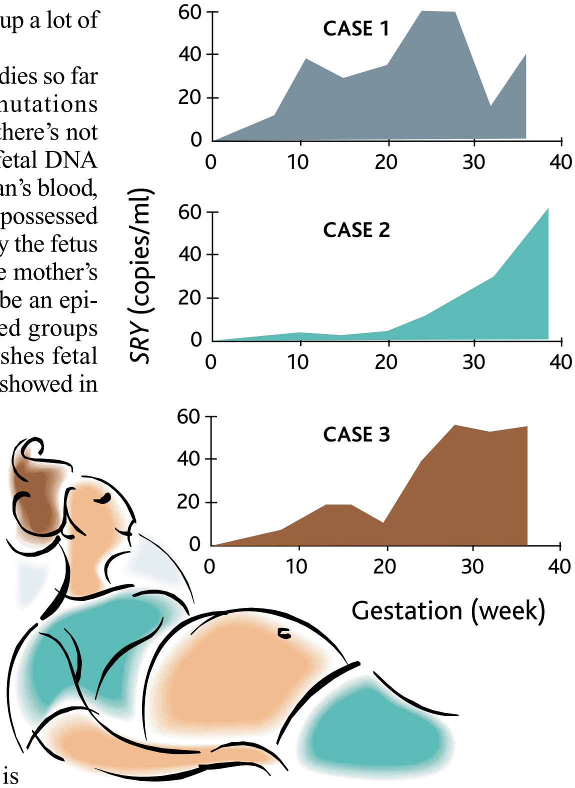

Baby signs. Cell-free fetal DNA levels rise during pregnancy, as shown in three future moms.

Seeing double

Diagnosing Down syndrome noninvasively through fetal DNA is the big prize luring researchers. The potential demand for such a test is huge, says Boston University's Charles Cantor, chief scientific officer of Sequenom Inc., because the rate of Down syndrome is at least 1 in 270 for mothers over 35. Doctors can screen for the disorder in the first trimester by using ultrasound to measure the dimensions of the fetus's neck and checking the levels of several protein markers in maternal blood; this combination picks up 85% of cases, albeit with a false positive rate of 2% to 6%. The International Down Syndrome Screening group last year called for this noninvasive strategy to be offered to all women, but a firm diagnosis still requires subsequent amniocentesis or CVS. The $1000 or more cost of these two tests limits routine use to women over 35, which means most Down syndrome births now occur in younger women.

Yet while Down syndrome is easy to detect if fetal cells are in hand, it's harder using cell-free DNA. The reason is that this condition is caused by an extra chromosome, rather than a mutation that can be detected with PCR. So far, for Down syndrome, fetal DNA can be used to only slightly improve screening: Overall fetal DNA levels are higher in women carrying fetuses with Down syndrome and some other aneuploidies. Adding a fetal DNA quantity test to other serum markers for Down syndrome would boost the detection rate from 81% to 85%, Bianchi's group has shown.

Still, the real prize is a straightforward, noninvasive fetal DNA diagnostic for Down syndrome that's as accurate as amniocentesis and CVS. One possible solution is to discover an epigenetic marker for Down syndrome that would allow Down-specific DNA sequences to be amplified with PCR. Another is to look for fetal mRNA from a gene expressed by chromosome 21 but not by the mother's cells. Cantor estimates that two dozen groups are working on the problem and predicts it will be solved in 3 years.

Ethical minefield

Indeed, while research on noninvasive fetal testing is very competitive—Lo and other investigators have certainly applied for many patents—cooperation is common. Cross-lab studies like the one sponsored by NICHD have nurtured the field, and they are continuing thanks to a new 5-year, €12 million European Union project called Special Advances in Fetal Evaluation (SAFE) that involves 52 institutional partners. "I think this is a positive example of a new technology being rigorously investigated before it filters into practice," says gynecologist Wolfgang Holzgreve of the Basel group.

The need for caution makes some scientists uncomfortable with Baby Gender Mentor. The company offering the test, Acu-Gen Biolabs in Lowell, Massachusetts, claims it works at 5 weeks of gestation at 99.9% accuracy. But Bianchi questions that figure, noting that a cross-lab study of gender detection published last year found that sensitivity varied widely among labs. A company spokesperson says the 99.9% figure is based on 20,000 births but notes that the company won't publish results until it has patented its technology.

There's little chance for outside experts to scrutinize that accuracy claim. Food and Drug Administration approval is not needed as long as the blood sample goes to a lab and the test is sold as a service rather than as a kit. Like other genetic tests, "[this] is opening up gaps in the oversight system," says Kathy Hudson, director of the Genetics and Public Policy Center at Johns Hopkins University in Baltimore, Maryland. It's not just the U.S. that does not regulate such testing. A Canadian company called Paragon Genetics has been offering a fetal DNA gender test for more than 2 years. The firm's quiet marketing of it hasn't drawn as much criticism as Baby Gender Mentor, in part because it follows the practice of many fetal DNA researchers by using fresh maternal blood, instead of dried blood spots. It also suggests that samples be taken 10 weeks into pregnancy.

As for concerns that some couples could use fetal DNA gender tests to end a pregnancy, Paragon Genetics lab director Yuri Melekhovets argues that parents can already do that based on ultrasound tests early in the second trimester. Still, Lo's group has gone so far as to stipulate in licensing agreements with companies that its technology can't be used for sex selection. The SAFE project, meanwhile, is funding a study of the implications of using early fetal DNA testing, especially if costs fall enough to make it feasible for couples in countries such as India and China where female children may be viewed as less desirable. "Especially in 'one child' countries, there is a risk that this [test] can be abused," says Hulten, the SAFE project's coordinator.

Another troubling ethical issue for some is how abortion rates could be affected by the advent of widespread, accurate fetal DNA testing for many genetic diseases. Although abortions may increase, Bianchi points out that mothers who keep a child with a disease could also benefit from the prenatal diagnosis. A survey by her group found that mothers who went to term after learning that they were carrying a fetus with Down syndrome were better able to cope psychologically once the child was born than mothers who learned of their baby's disorder at birth. Based on that finding, if fetal DNA testing fully comes of age, it may provide many potential parents with news that's difficult to hear, but it could also give them time to decide what's right for them and accept their decision.

–JOCELYN KAISER

SOURCE: D. LO, *AM. HUM. GENET.* **62**, 768–775 (1998); ILLUSTRATION: JUPITER IMAGES

Laser Facility Faces Burning Questions Over Cost, Technology

The National Ignition Facility is the world's biggest laser. So maybe it's no surprise that sparks are flying over its fate

Nobody ever said recreating a thermonuclear explosion in a laboratory was going to be easy. But this year, the Department of Energy's (DOE) long-troubled National Ignition Facility (NIF) has suffered a series of political and fiscal blows that threaten to sink the stadium-sized laser. With doubts recently raised about the project's technical progress, Congress must decide whether to give DOE enough money to continue building the \$3.5 billion facility, housed at Lawrence Livermore National Laboratory in California.

NIF is the linchpin of DOE's \$5.5-billion-a-year stockpile stewardship research program—an effort to use science to assure the effectiveness of existing nuclear weapons without actually testing them. Its 192 lasers are designed to heat a pea-sized capsule of heavy hydrogen 100 million degrees to achieve a fusion reaction simulating the guts of a nuclear warhead. Although the project has spent 80% of its estimated budget, only eight of the 192 lasers are operational, and a recent report by the Jasons, an elite outside group, says there is "substantial technical risk" of not achieving fusion ignition by DOE's stated 2010 goal.

The Bush Administration has requested another \$337 million for 2006, an amount that the House of Representatives endorsed before the Senate slashed it to \$103 million in June. While the lower funding level would effectively kill the project, NIF project head Ed Moses is optimistic. "We've been through this before, and we'll get through it again," he says.

Approved in 1993, NIF has never had a smooth ride. The nuclear weapons community has long been divided on its usefulness for assessing U.S. nukes, and the project, initially pegged at \$2 billion, is 3 years past its original planned completion date. In 2000, management scandals led to a reshuffling. Last year, after DOE pushed the target ignition date back to 2014, Senator Pete Domenici (R–NM), a recurrent foe and chair of the spending panel that controls DOE's budget, threatened to "do everything in my power" to force the lab to confront "pressing technical issues." Lab officials subsequently altered their schedule to achieve ignition by 2010.

Still, a string of review boards have blessed its mission. Just last year, for example, a review by the Defense Science Board concluded that "[L]aser performance parameters … have been demonstrated." And Livermore Director Michael Anastasio says, "I believe the project is going well."

Bright idea. Energy Secretary Samuel Bodman (*right*) tours NIF with Livermore's Ed Moses.

CREDIT: U.S. DEPARTMENT OF ENERGY

The Jasons's report, delivered in June, takes another look at the lasers, which have been used for 400 shots, as part of its inquiry into whether NIF will be ready by 2010. NIF scientists point to successful results separately using the three kinds of so-called "beam smoothing" devices, during which proper focus and laser spot-size were achieved. But the report urges the project to demonstrate that the three techniques can work simultaneously, at full energy and high frequency.

Arrayed in a 10-meter sphere, the activated lasers turn the target into a plasma, which can reflect some laser light in a phenomenon known as backscattering. The Jasons's report says the problem is "a serious potential risk" and calls for more study, including real tests of the system. But NIF doesn't plan to do those tests, since managers have halted further laser-target experiments until all 192 lasers are built.

The Jasons also said that Livermore's decision to conduct the first experiments in 2010 at 1.0 megajoules (MJ) rather than the intended operating level of 1.8 MJ would reduce their chances of success. The reduction, NIF managers say, will let them ramp up gradually, but critics say the real goal is to protect expensive optics. The full 1.8 MJ allow use of larger, more robust targets. With smaller targets, the Jasons fear, irregularities such as asymmetrical squeezing may prevent ignition. Critics as well as supporters also now worry that the laser won't be able to deliver full power. "The laser operates at one-third the total energy without damage," says plasma physicist Stephen Bodner, a consultant to the Jasons's study and longtime NIF critic.

Despite its criticism, the panel wants the project to be completed, says Jasons study leader David Hammer of Cornell University in Ithaca, New York, noting the report hailed engineering feats including diagnostics and other supporting technologies. In fact, NIF Associate Director George Miller predicts that getting the 192 lasers, the target, and the diagnostics working correctly together will pose a more formidable challenge than reaching 1.8 MJ. As for the backscattering, he says the plasma encountered in the early tests is different from what they'll encounter in the final product. "To create ignition-relevant plasmas, you have to complete NIF," Miller said in an e-mail. Lab officials also believe that the smoothing performance shown in separate tests is adequate because the three techniques do not interact. But they acknowledge a full-power test shot with all three smoothing techniques simultaneously won't be performed until early next year.

Within Congress, Sen. Dianne Feinstein (D–CA) is expected to lead the charge for full funding. Domenici is unhappy that other laboratory stockpile stewardship programs—several of which, NIF supporters note, are located in his home state—are being cut to fund NIF. So more funds for those programs could win him over. Congressional supporters also hope the White House will step in. In February, DOE Secretary Samuel Bodman called NIF the "core" of U.S. stockpile stewardship; now Bodman's spokesperson says the secretary needs to learn more about the project. The administration also failed to react officially to the Senate cuts. To survive, the biggest laser ever built just might need a little more firepower.

–Eli Kintisch

Vioxx Verdict: Too Little or Too Much Science?

A widow's victory in the first of thousands of cases against Merck's pain reliever sidesteps important questions about the drug and a patient's death

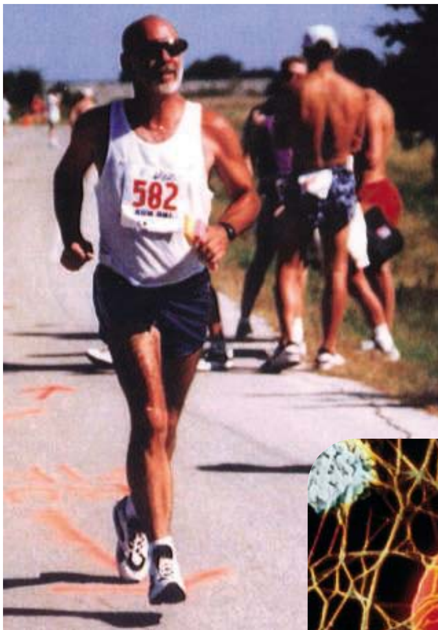

Running question. Whether arrhythmic victim Robert Ernst also suffered a blood clot (*inset*) went unanswered at the trial.

CREDITS (TOP TO BOTTOM): ASSOCIATED PRESS; MANFRED KAGE/PETER ARNOLD INC.

In her closing argument last month in a Texas courtroom, Merck lawyer Gerry Lowry said that science is "what this [Vioxx] case is all about." The team representing the pharmaceutical giant presented reams of data to show that Vioxx was not to blame in the death of the plaintiff's husband, a 59-year-old triathelete. So when 10 of 12 jurors decided that Merck was guilty of producing and marketing a drug that could be deadly, some reports painted the outcome as a triumph of hot emotion over cold facts.

But observers say that neither legal team dealt forthrightly with two important scientific questions: How safe are Vioxx and similar drugs, and did the victim, a Wal-Mart employee named Robert Ernst, actually die from one of the drug's known side effects? "Both sides avoided the scientific complexity," says Garret FitzGerald, a cardiologist and pharmacologist at the University of Pennsylvania in Philadelphia who has criticized COX-2 inhibitors, the class of drugs to which Vioxx belongs, despite having received research funding from Merck. That complexity, which received only minimal attention during the 5-week trial, centers on how Vioxx affects the heart—and how new techniques can pinpoint death by blood clot even if it's not visible during a standard autopsy.

Carol Ernst's suit on behalf of her husband, who died in 2001 after taking Vioxx for 8 months, is one of more than 4000 pending suits against the one-time blockbuster drug that Merck pulled from the market last September after a study showed an increased risk of heart attacks and strokes. The jury's brief deliberations and the size of the verdict—$253 million, some 10 times what Texas law allows—led some observers to conclude that jurors disregarded the factual evidence in favor of emotional arguments put forth by the plaintiff's attorney Mark Lanier. "The jury never quite got it—a lot of people just don't want to hear data," says Thomas Wheeler, a pathologist at Baylor College of Medicine in Houston, Texas, who testified as a paid witness on Merck's behalf. In fact, jurors told the *Wall Street Journal* after the verdict that the science presented during the trial "sailed right over their heads."

But questioning the jury's scientific competence—a majority had high school educations—may be missing a more important issue. "It is all too easy to blame the jury for being stupid," says Shari Diamond, a research psychologist and law professor at Northwestern University in Chicago. She and others believe the jury was convinced by studies showing that Vioxx can cause abnormally high rates of heart attack and stroke. Neil Vidmar, a law professor and psychologist at Duke University in Durham, North Carolina, adds that although "science seemed to be the issue" during the trial, "I suspect the strongest evidence [against the defense] was that Merck had covered up." Internal memos and e-mails cited in the trial show that Merck scientists were aware of cardiovascular concerns about Vioxx long before a 2000 article in *The New England Journal of Medicine* first raised the issue publicly.

Unlike older anti-inflammatory drugs, Vioxx and other COX-2 inhibitors are thought less likely to upset the stomach or cause gastric bleeding. The compounds—which include Pfizer's Bextra and Celebrex—inhibit on a narrower set of inflammatory enzymes than their painkilling predecessors do. That action, researchers believe, may instigate and accelerate blood clotting that could lead to heart attacks and strokes (*Science*, 15 October 2004, p. 384).

However, Ernst's death certificate listed arrhythmia rather than a heart attack brought on by a blood clot. Vioxx or other COX-2 drugs have not been associated in any study with arrhythmia. And the autopsy showed no signs of clotting that could have generated a heart attack. Wheeler, a pathologist who has specialized in prostate rather than heart research, told the jury that Vioxx could not have been responsible for Ernst's death. "And I stand by that," he told *Science* last week.

But FitzGerald and others aren't so sure. Although there was no evidence of a clot, he says, "that doesn't mean [Ernst] didn't have one." Eric Topol, a cardiovascular researcher at the Cleveland Clinic in Ohio who has been a vocal critic of Vioxx, notes that clots traditionally have been difficult to track because they sometimes dissolve only to reform. "This is not a static phenomenon." Clots also can embolize, or shower downstream, leaving little trace. It's even possible to find clues of a vanished clot using microscopic examinations of heart tissue, a method pioneered by the late Michael Davies.

Such a fine-tuned autopsy was not performed on Ernst. As a result, says Topol, "they spent 5 weeks discussing the wrong topic. The issue was [what causes] sudden cardiac death, not [that Ernst suffered an] arrhythmia." The sharp distinction Merck tried to draw was blurred by testimony from the coroner Maria Araneta that a blood clot may have been dislodged and dissolved during attempts to save Ernst's life.

Merck's general counsel Kenneth Frazier said after the trial that "the jury was allowed to hear testimony that was not based on reliable science and that was irrelevant." He vowed to appeal that case, in part on that basis, and to fight some 4200 pending cases "one by one," although last week he told *The New York Times* that Merck might be willing to settle select cases.

Yet even if upcoming trials involve heart attack and stroke victims, they inevitably will require sorting through many complex factors, says Topol. And a courtroom, Wheeler notes, is a difficult place to debate complicated research issues. So even if science is what the Vioxx debate is all about, it's a strain developed for the courtroom, not the lab.

–ANDREW LAWLER

The Quest for Dark Energy: High Road or Low?

A space telescope could reveal the mysterious stuff that is blowing the universe apart—if those on the ground don't do it first

Seven years ago, astrophysicists asked a simple question: "How far?" The answer overturned our understanding of the cosmos.

Since 1929, researchers had known that the universe is expanding. But they assumed the expansion is slowing as the universe's own gravity tugs against it. Two teams set out to observe the slowing by measuring the distances to exploding stars known as supernovae. To the researchers' surprise, the farthest supernovae were farther than expected. That meant the expansion of the universe is accelerating as if driven by some weird space-stretching "dark energy."

"When we first saw the result, I assumed our data was miscalibrated," recalls Saul Perlmutter of Lawrence Berkeley National Laboratory and the University of California, Berkeley. But within a few years, studies of the afterglow of the big bang—the "cosmic microwave background"—and other measurements bolstered the case for dark energy and showed that it accounts for a whopping two-thirds of the universe. "The amazing thing about this discovery is how quickly people accepted it," Perlmutter says.

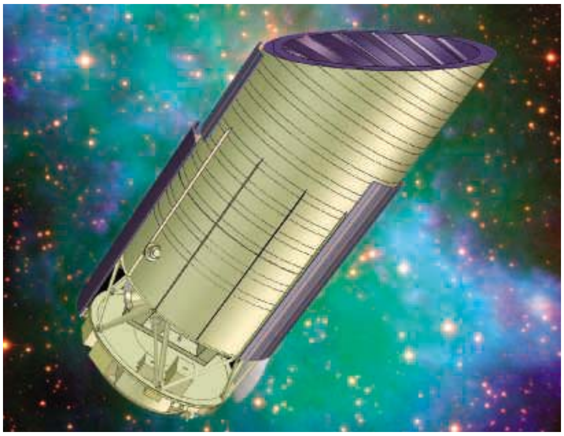

Don't look down. A proposed space telescope such as SNAP (*top*) faces competition from today's ground-based telescopes such as the Canada-France-Hawaii Telescope on Mauna Kea.

CREDITS (TOP TO BOTTOM): ROBIN LAFEVER/LBNL; J.-C. CUILLANDRE/CFHT

Yet researchers still don't know what the mysterious stuff is. They believe the answer lies in observing thousands of supernovae and millions of galaxies. Sometime in the next decade, NASA and the U.S. Department of Energy (DOE) are expected to launch a $600-million space telescope designed to measure dark energy, the Joint Dark Energy Mission (JDEM).

But even as they lay their plans for the satellite, researchers are debating whether they could hammer out key properties of dark energy with observations from the ground. NASA, DOE, and the U.S. National Science Foundation have received dozens of proposals for measuring dark energy from terra firma, and the agencies have assembled a Dark Energy Task Force to evaluate them and report back by year's end. The task force's report will help the agencies set their near-term priorities and will inform another panel studying proposed methods and technologies for JDEM.

Figuring out what can be done from the ground may be key to keeping JDEM affordable. "Clearly, you should only do from space what you have to do from space," says Rocky Kolb, a cosmologist at the Fermi National Accelerator Laboratory in Batavia, Illinois, and chair of the task force. But deciding what's best done where is tricky, says Charles Bennett, an astrophysicist at Johns Hopkins University in Baltimore, Maryland, and co-chair of the JDEM science definition team. "We don't know what dark energy is, and there are different ways to measure it and different aspects to measure," Bennett says. "There are unknowns in all directions."

Weird and weirder

So far theorists have dreamed up three ideas of what dark energy might be, each one a challenge to the current conception of the universe, says Sean Carroll, a theoretical physicist at the University of Chicago. "There are no uninteresting possibilities," Carroll says, "which is what makes it so exciting."

Perhaps the simplest explanation is that dark energy is part of the vacuum itself, so that space naturally tends to stretch as if driven by some inherent constant pressure. In 1917, Albert Einstein proposed such a pressure, or "cosmological constant," to counteract gravity and keep the universe from imploding. He later abandoned the notion as unnecessary when astronomers found that the universe is in fact expanding. But Einstein's orphaned idea may be the thing that drives the acceleration of the universe.

If so, it will vex particle physicists. For decades they've known that, thanks to quantum mechanics, the vacuum roils with particles popping in and out of existence, and that such "virtual" particles give the vacuum an energy that could serve as the cosmological constant. Unfortunately, the energy physicists calculate is far too big to fit the data. In the past, theorists have assumed for the sake of simplicity that some still-unknown principle cancels everything out to make the vacuum energy add up to zero. If there is a cosmological constant, Carroll says, that tidy fix won't work.

Alternatively, the dark energy might come from some sort of particle or interaction that propagates through space much as light does and provides the space-stretching push. Such "quintessence" theories skirt the problem with the vacuum energy, but they run into difficulties with other aspects of particle physics. For one, theorists must explain why the new particles don't interact with those already familiar to us.

Finally, the accelerated expansion might not be driven by dark energy at all. Rather it could signal that across billions of light-years, gravity no longer works as Einstein's general theory of relativity predicts it should. "It's very hard to change gravity on large distances without changing it at short distances, too," says Gia Dvali, a theoretical physicist at New York University. But that's a good thing, he says, because it means that theories that modify gravity may be easier to test.

Researchers hope to distinguish between the possibilities by measuring simply how the density of dark energy changed as the uni-

verse expanded. If dark energy is a cosmological constant, then the density should have remained constant (see figure, below). And if the density varied, then dark energy must be something else. To tell the difference, researchers must trace the history of the expansion of the universe, which is encoded in the ancient light from far-flung stars.

How red? How far?

The quest boils down to asking two questions about some astronomical object, such as a supernova or a cluster of galaxies: How far away is it? And how red is its light? The record of the universe's expansion lies in the combination of the two answers, the so-called "distance-redshift relation."

As space expands, light zipping through it stretches to longer and redder wavelengths, much as sound waves in a slide whistle shift to lower pitches as the whistle's plunger descends. Light's wavelength increases more quickly if space is stretching faster. So to accumulate a given amount of stretch, or "redshift," light would have had to travel longer and farther if the universe had expanded more slowly billions of years ago than if the universe had always expanded at its current rate. Astronomers first glimpsed dark energy by noting that supernovae whose light had been stretched by 20% to 100%—that is, with redshifts of 0.2 to 1.0—were farther away than expected (*Science*, 27 February 1998, p. 1298). The leading proposals for JDEM—designs named SNAP, JEDI, and Destiny—all aim to measure thousands of supernovae with redshifts as high as 1.7.

But instead of a supernova, the object in question could be the distance between galaxies, says Daniel Eisenstein, a cosmologist at the University of Arizona in Tucson. Because of a phenomenon known as "baryon acoustic oscillations," galaxies show a slight tendency to space themselves at a specific distance. That distance, about 500 million light years, is determined by how far sound waves traveled in the plasma that filled the primordial universe before atoms formed. By surveying millions of galaxies of a given redshift and measuring how far apart they appear in the sky, researchers can determine their distance and deduce the distance-redshift relation, Eisenstein says.

Galaxies might also reveal the evolution of dark energy through a more subtle effect. From studies of the cosmic microwave background, researchers know that almost all the matter in the universe is undetected "dark matter," which fills space with vast filaments that contain the galaxies. Gravity from those threads bends light from more distant galaxies and distorts their appearance so that neighboring galaxies in the sky seem to line up (*Science*, 17 March 2000, p. 1899). Such "weak gravitational lensing" depends on the distances to the dark-matter "lens" and the observed galaxy. So by comparing the lensing of millions of galaxies at different redshifts, researchers hope to decipher the distance-redshift relation.

Finally, researchers might probe dark energy simply by counting clusters of galaxies in a patch of the sky, says Joseph Mohr, an astronomer at the University of Illinois, Urbana-Champaign. The number of clusters at a given redshift reveals how much volume the patch contains, and the size of the patch in the sky reveals how far away it is, just what cosmologists need to know to trace the expansion.

The ups and downs

The question now is where best to make the observations. All agree that supernovae with redshifts greater than 1 can be studied only from space because their light stretches to infrared wavelengths that would get lost in the infrared glare of the atmosphere. Beyond that, consensus vanishes.

"If you're looking at stellar objects, you're better off in space," says Anthony Tyson, an astrophysicist at the University of California, Davis. "If you're looking at galaxies, you're better off on the ground." Tyson leads the team developing the Large Synoptic Survey Telescope (LSST), a ground-based behemoth with an 8.4-meter mirror and a camera with 3 billion pixels, which if funded could take its first look at the sky in 2012 (*Science*, 27 August 2004, p. 1232). Imaging the entire sky and some 3 billion galaxies, LSST should best space-based measurements of weak lensing and baryon acoustic oscillations, Tyson claims.

But others say such cut-and-dried standards are too simplistic. For example, atmospheric distortions can mimic weak lensing, says Gary Bernstein, a cosmologist at the University of Pennsylvania in Philadelphia. So a space-based weak-lensing study might do better than LSST even if it counted only a few hundred-million galaxies. Similarly, the redshifts of galaxies are harder to measure from the ground, says Arizona's Eisenstein, so earthbound baryon acoustic oscillation measurements could prove impractically slow.

Given the uncertainties, researchers have proposed different strategies for JDEM. The infrared Destiny space telescope would measure only supernovae, says Jon Morse, an astrophysicist at NASA's Goddard Space Flight Center in Greenbelt, Maryland. "Destiny is focused like a laser on this one problem," he says. But that's taking a risk, says Yun Wang, a cosmologist at the University of Oklahoma in Norman and leader of the JEDI project. "We still don't know that supernovae will give you the precision you need to really know what dark energy is," she says. JEDI and SNAP would measure supernovae, weak lensing, and baryon oscillations.

The biggest uncertainties surrounding JDEM may be more political than technical. Both NASA and DOE list JDEM as a priority, but neither has committed to building it. Researchers say they're ready to start now, for a launch before 2011. But JDEM may not launch until 2017. And in the meantime, ground-based measurements will continue to whittle away at our ignorance—and JDEM's potential scientific impact.

"You shouldn't look at a space mission as an improvement over what you know today," says Johns Hopkins's Bennett. "You should look at it as an improvement over what you'll know tomorrow." But as tomorrow gets pushed further into the future, such prognostications grow as murky as the nature of dark energy itself.

–ADRIAN CHO

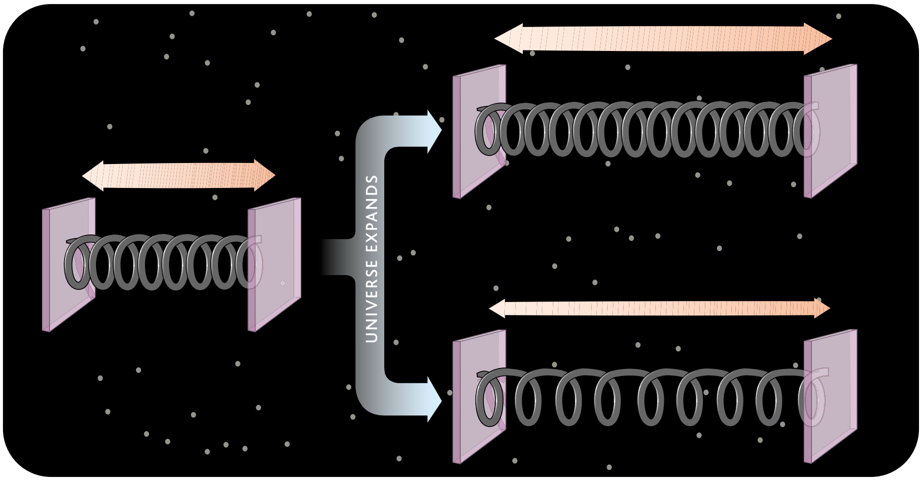

Loaded question. Dark energy acts like a spring that stretches space. If it's a cosmological constant, the spring grows with space to maintain a constant push (*top*). Otherwise, the push may vary (*bottom*).

CREDIT: C. BICKEL/*SCIENCE*

The power of small.

It's a small world.
The NanoDrop® Spectrophotometer has the power to analyze it.

1 µl samples · No dilutions · No cuvettes · Full spectrum

- **Nucleic Acid** concentration and purity measurements (from a 2ng/µl detection limit up to 3700ng/µl for dsDNA)
- **Microarray** nucleic acid and dye concentrations to determine labeling efficiency (Cy3, Cy5, Alexa Fluor dyes . . .)
- **Protein**, labeled and unlabeled, concentration and purity measurements (A280, protein arrays, Bradford, BCA, Lowry, antibody conjugates, metallo-proteins . . .)
- **General UV/Vis Spectrophotometry**

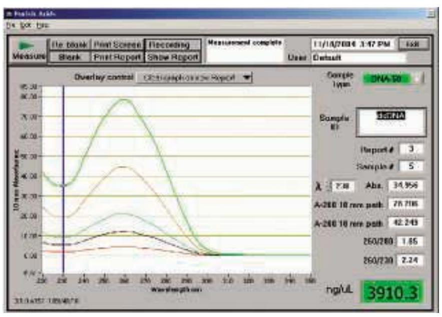

Measurement is as easy as pipette and read. The sample is read using two different path lengths (1mm and 0.2mm) to achieve an extensive dynamic range that virtually eliminates the need for dilutions. Then just a quick wipe clean and you're ready for your next sample. What could be easier—or more powerful?

Ready to experience the power of small? Contact us today and find out what our satisfied users worldwide have to say about the NanoDrop® ND-1000 Spectrophotometer.

FREE one week evaluation

Call for details.

(302) 479-7707 www.nanodrop.com

NanoDrop
when every drop counts.

RANDOM SAMPLES

Edited by Constance Holden

Sleepless and Sharp

Researchers have found that a drug that enhances mental alertness may also hold promise for helping shift workers and others battle sleepiness.

The drug, CX717, is an ampakine, one of a class of synthetic compounds that amplify the signal of glutamate, a neurotransmitter important for learning and memory. Sam Deadwyler, a neuroscientist at Wake Forest University School of Medicine in Winston-Salem, North Carolina, wondered if ampakines could help in his search for strategies to prevent sleep deprivation in pilots. He and his colleagues found that when given the drug, monkeys kept awake for 30 to 36 hours outdid their well-rested, drug-free counterparts in cognitive tests. And brain scans showed that unlike other stimulants, the drug worked selectively, increasing activity only in the areas activated during the mental tasks, the researchers reported 22 August in *PLoS Biology*.

CX717 may have similar effects in humans. The manufacturer, Cortex Pharmaceuticals in Irvine, California, says in a small pilot study the drug improved mental function in young men kept awake for 27 hours. The Defense Department is now starting a trial to test the drug with shift workers.

"This could have very large social and economic consequences," says ampakine inventor Gary Lynch of the University of California, Irvine. He says a similar drug, Modafinil, affects different brain systems—those regulating sleep—so "the [two] drugs will probably find quite different uses."

Eye on the Tiger

East-West differences are mirrored by differnces in perceptual processes, new research shows. Richard Nisbett, a social psychologist at the University of Michigan in Ann Arbor, and colleagues have shown that Chinese and American students differ in the way they look at and remember a complex visual scene.

Wearing headsets with a built-in eye-movement tracker, 25 American and 27 Chinese graduate students were asked to observe 36 pictures—each with an object against a realistic background, such as a tiger in a forest—for three seconds each. The Americans zoomed in on the foreground object earlier and for a longer time than did the Chinese, who spent more time taking in the background and less time studying the object, Nisbett's team reports online this week in *Proceedings of the National Academy of Sciences*. The Chinese thus tended to recall background more accurately, whereas Americans remembered more about the central object.

"As best I know, this is the first example clearly documenting [cultural differences in] where people look when they're encoding a scene," says Daniel Simons, a cognitive psychologist at the University of Illinois at Urbana-Champaign. Nisbett suggests that the study reflects more general differences. East Asians have a more holistic, relational outlook on the world, whereas Americans are more individualistic and object-oriented, he says.

Animal Wars

As the battle between animal rights activists and researchers continues to escalate in the United Kingdom, 500 U.K. scientists and doctors, including 3 Nobel laureates, have signed a petition in favor of the use of animals in research.

The petition comes on the heels of a decision by a small farm in central England that supplied guinea pigs for researchers to fold the business after 6 years of harassment by activists who last fall dug up the remains of the mother-in-law of one of the farm owners. Andrew Gay, a spokesman for Huntingdon Life Sciences, a longtime target of antivivisectionists, says the assault on the farm "marks a definite change in tactics" as protestors turn from large institutions to more vulnerable small outfits—"the soft underbelly of the life sciences."

Proponents of animal rights have been stepping up their activities in defiance of a new U.K. law that calls for substantial prison terms for anyone interfering with life science facilities or their providers. Signers of the petition, organized by the London-based Research Defense Fund, say they will not be intimidated. "We would rather not use animals, and we try hard to find alternatives," says Robin Lovell-Badge, a geneticist at the National Institute for Medical Research in London.

The animal rights battle may be further inflamed by plans to genetically engineer monkeys to develop Huntington's disease, announced last week by Yerkes Primate Center. Coincidentally, animal rights groups at an international conference in Berlin last week came out with a new petition calling for a global ban on experimentation with primates.

Astronomers ID Adams Snap

Astronomers say they have pinpointed the exact time and place that Ansel Adams took his famous photograph in California's Yosemite National Park. *Autumn Moon, the High Sierra from Glacier Point*, is known only to have been taken some time in the 1940s. A team led by Donald Olson at Texas State University in San Marcos concluded, after scouring maps, weather records, lunar tables, astronomical software, and a recently uncovered color version of the photograph, that it was taken near a geology hut on 15 September, 1948, at approximately 7:03 p.m. At right is a long-exposure photo the scientists took at the site. Their report will be in the October issue of *Sky and Telescope*.

CREDITS (TOP TO BOTTOM): *PNAS*; BRIGITTE SPORRER/ZEFA/CORBIS; RUSSELL DOESCHER/TEXAS STATE UNIVERSITY

PEOPLE

Edited by Yudhijit Bhattacharjee

JOBS

Hot seat. A 19-year veteran of Brookhaven National Laboratory in Upton, New York, has become the first woman to chair its physics department. A particle theorist with 134 publications to her credit, Sally Dawson, 50, will lead a staff of 260 and oversee a budget of nearly $60 million.

Dawson, now acting chair, assumes the helm of a struggling department. Last month, the National Science Foundation canceled a pair of high energy physics experiments to be built at the lab (*Science*, 19 August, p. 1163), and there's a cloud over the lab's flagship Relativistic Heavy Ion Collider, a particle smasher that studies nuclear physics (*Science*, 24 June, p. 1852). Dawson's skills as a consensus builder should help her guide the department through its troubles, says Yannis Semertzidis, an experimental physicist at Brookhaven. "She listens to you sincerely, and she has great enthusiasm for physics," he says. "She understands that the way out of the mess is physics, not politics."

Ideas man. Peter McPherson says that his first task as the new president of the National Association of State Universities and Land-Grant Colleges (NASULGC) is to halt "the gradual defunding" of public universities by state legislators. McPherson, 64, has watched that trend for the past 11 years as president of Michigan State University. There he learned the value of finding other sources of revenue, a skill that he plans to share with NASULGC's 215 members.

"Ideas move things, and money can follow," says McPherson. He will take over from Peter McGrath, who's leaving at the end of 2005 after 14 years atop the association.

MISFORTUNES

Shark attack. A marine field trip turned tragic last week near Adelaide, Australia. Jarrod Stehbens, 23, was diving with another research assistant off a reef about 2 kilometers offshore to collect cuttlefish eggs as part of a research project on the population structure of the species *Sepia apama*, which has been threatened by fishing. When the pair was about to emerge from the water, they were attacked by what was likely a great white shark. The other diver managed to surface and was pulled from the water by two researchers on the boat, but Stehbens was dragged down and vanished. Stehbens graduated last month from the University of Adelaide and was about to begin a Ph.D. program in marine ecology at the Alfred-Wegener Institute for Polar and Marine Research in Helgoland, Germany.

POLITICS

Holding course. Mohammad-Mehdi Zahedi, an expert on fuzzy mathematics at the Shahid Bahonar University of Kerman, has been named Iran's new science minister. But Zahedi is not expected to deviate far from the course laid by his predecessor, Ja'far Tofiqi, who championed big-science projects in high-energy physics, astronomy, and biotechnology in the country's $900 million science portfolio. "It's too early to say anything," says deputy research minister Reza Mansouri, an astrophysicist, who nonetheless predicts only minor fluctuations in science policy. Zahedi, whose appointment was confirmed by Iran's Parliament last week, could not be reached for comment.

Iranian researchers are more worried about the policies of the country's new president, the ultraconservative Mahmoud Ahmadinejad. They say that a potential rollback of social reforms and a chill in relations with the West provoked by Iran's nuclear ambitions are greater threats to Iranian science than any potential changes brought about by Zahedi.

RISING STARS

Not old enough. 14-year-old Yinan Wang is the latest child prodigy to be offered a university place in the U.K. Could he also be the last?

Unable to speak English when he arrived in the U.K. from China two years ago, math and physics whiz Wang is now on his way to Oxford to study materials science. But a new U.K. law, passed in March, states that all those working with children have a legal duty to protect them. In recent years, Oxford was the only British university to accept children as young as 12. But it will probably no longer do so. The new law would mean expensive training and screening of any personnel coming into contact with these youth, who would not be allowed to live with other students. Admissions officials are considering establishing a minimum age of 17, according to a spokesperson.

That would be unfortunate, says mathematician Ruth Lawrence, who was 12 when she went to Oxford in 1982. Lawrence, now at Hebrew University in Jerusalem, believes parents or guardians should keep track of their children as her father did when she was at Oxford. "Universities should not be turned from wellsprings of knowledge into caretakers for students."

Got any tips for this page?
E-mail people@aaas.org

CREDITS (TOP TO BOTTOM): MAYA LINNELL, *THE SOUTH EASTERN TIMES*, SOUTH AUSTRALIA; THE BROOKHAVEN NATIONAL LABORATORY; MSU

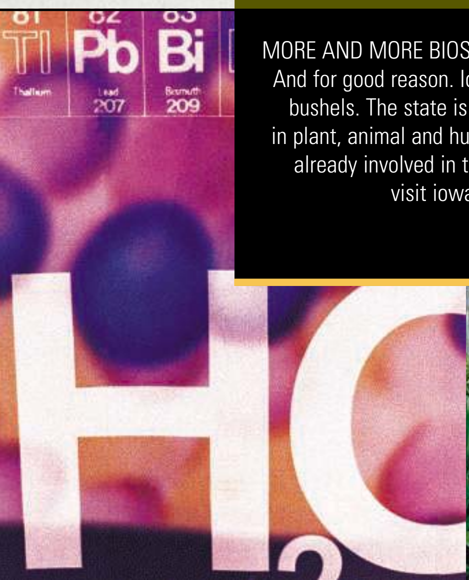

Tl
Pb
Bi
Lead
207
Bismuth
209

The Perils of Increased Aquaculture

IN A RECENT OPINION PIECE DISTRIBUTED TO U.S. newspapers, Conrad Lautenbacher, the Administrator of the National Oceanic and Atmospheric Administration (NOAA) argued in favor of the National Offshore Aquaculture Act of 2005 ("A boost for aquaculture?", Random Samples, 17 June, p. 1738). This Act would give NOAA responsibility for permitting offshore aquaculture operations up to 200 miles from shore in U.S. waters.

The arguments in favor of promoting expanded aquaculture include meeting market demand for seafood and decreasing the seafood "trade deficit." Aquaculture's potential for solving these problems is debatable, and many concerns must still be addressed and acknowledged openly.

The U.S. Commission on Ocean Policy report (*1*) recommended that NOAA serve as the lead agency for permitting an expanded aquaculture program. Although this makes sense, the agency should not overemphasize the potential benefits and downplay the potential hazards, which include serious environmental consequences such as pollution from aquaculture waste, potential marine mammal entanglements, escapement of aquaculture species into the wild, and spread of disease. Furthermore, if we culture carnivorous species that rely on fish meal as a food source, this could have the unintended consequence of increasing fishing pressure on fish meal species.

NOAA should not lose sight of the other aquaculture recommendations of the Commission. One of the most important of these is coordination with the United Nations Food and Agriculture Organization (FAO) "to encourage and facilitate worldwide adherence to the aquaculture provisions of the Code of Conduct for Responsible Fisheries." Importing food raised through aquaculture from other countries that sacrifice their environments does little to enhance marine ecosystems worldwide.

What is most worrisome is what is not being discussed. Many of the important recommendations of the U.S. Commission on Ocean Policy may face the worst fate of all—being ignored.

DAVID A. MANN
College of Marine Science, University of South Florida, 140 Seventh Avenue South, Saint Petersburg, FL 33701–5016, USA.

Reference

1. U.S. Commission on Ocean Policy, *An Ocean Blueprint for the 21st Century Final Report* (U.S. Comission on Ocean Policy, Washington, DC, 2004) (see www.oceancommission.gov).

Notes and Double Knocks from Arkansas

IN THE SEARCH FOR IVORY-BILLED WOOD-peckers (*Campephilus principalis*) in the Big Woods region of eastern Arkansas ["Ivory-billed woodpecker (*Campephilus principalis*) persists in continental North America," Reports, 3 June, p. 1460], our unattended digital autonomous recording units (ARUs) recorded over 17,000 hours of ambient sound at 153 sites between 18 December 2004 and 31 May 2005. Review and analysis of these recordings are ongoing, and a full account will be published when analyses are complete. Here we briefly describe examples of the possible nasal "kent" notes and "double-knock" display drums mentioned in our Report and provide them as supporting online material (SOM) (*1*).

A painting of the ivory-billed woodpecker and the device used to record its calls.

On four different mornings in January 2005, a single ARU in the White River National Wildlife Refuge (NWR) recorded a sequence of kent-like vocalizations. The four sequences, which lasted 8 to 41 s and contained between 11 and 26 notes, are extremely similar; the recording of 29 January (audio S2) is typical of them. In the same area, experienced observers have heard blue jays (*Cyanocitta cristata*) produce atypical notes resembling these ARU recordings. Quantitative comparisons of these kent-like sounds with sounds of known ivory-bills (SOM text; audio S1), white-breasted nuthatch (*Sitta carolinensis*), and the most kent-like notes of blue jay in the collection of the Cornell Laboratory of Ornithology's Macaulay Library indicate that the notes recorded by the ARU are most similar to those of ivory-bills.

Sounds that are strikingly similar to the double knocks of other *Campephilus* woodpeckers (SOM text; audio S3) were recorded by ARUs in several areas of the White River and Cache River NWRs. One recording (audio S4), made 1.3 km from the site of the kent-like notes discussed above at 0645 local time on 24 January, includes a low-amplitude, apparently distant double knock followed 3.5 s later by a higher-amplitude, apparently closer double knock. Although the sequence and cadence of this recording match an exchange between two individuals of a *Campephilus* woodpecker, the relative amplitude of the separate strikes in each double knock is atypical (SOM text).

Additional descriptions and discussion of our acoustic data are available at www.birds.cornell.edu/ivory/field/listening. Further acoustic monitoring and field observation (including intensive efforts to record a large sample of the vocal repertoire of local blue jays) are planned for the areas where these recordings were made.

RUSSELL A. CHARIF,[1] KATHRYN A. CORTOPASSI,[1] HAROLD K. FIGUEROA,[1] JOHN W. FITZPATRICK,[1] KURT M. FRISTRUP,[1] MARTJAN LAMMERTINK,[1] M. DAVID LUNEAU JR.,[2] MICHAEL E. POWERS,[1] KENNETH V. ROSENBERG[1]
[1]Cornell Laboratory of Ornithology, Cornell University, 159 Sapsucker Woods Road, Ithaca, NY 14850, USA. [2]Department of Engineering Technology and Department of Information Technology, University of Arkansas at Little Rock, Little Rock, AR 72204, USA.

Reference

1. The SOM is available on *Science* Online at www.sciencemag.org/cgi/full/309/5740/1489c/DC1.

Nature Makes a Difference in the City

THE EDITORIAL "NATURE IN THE METROPOLIS" by P. Crane and A. Kinzig (27 May, p. 1225) called attention to the importance of nature in the modern metropolis and to the role of green cities in developing sustainable urban environments; in this context, São Paulo was mentioned. With a population of almost 21 million, São Paulo's metropolitan area includes relatively large fragments of

CREDITS: (PAINTING) LARRY CHANDLER; (PHOTO) SUSAN SPEAR, CORNELL LABORATORY OF ORNITHOLOGY

São Paulo, Brazil

Atlantic rain forest (*1*). These fragments are important in controlling water pollution and eutrophication of the water supply reservoirs serving the area. Forests and peri-urban area wetlands around the reservoirs remove phosphorus and nitrogen, thus contributing to diminishing water treatment costs. These and other natural ecosystems are indispensable in maintaining water quality within acceptable levels in the metropolitan region. In addition, as demonstrated by air pollution studies (*2*), these features collectively form a multifaceted filter, which contributes to regional air quality. Therefore, the conservation and, hopefully, eventual expansion of this biosphere reserve with its associated natural ecosystems, are crucial in preserving the quality of life in metropolitan São Paulo.

JOSÉ GALIZIA TUNDISI
International Institute of Ecology, Rua Bento Carlos, 750, São Carlos 13560.660, SP, Brazil.

References

1. J. G. Tundisi *et al.*, *Hydrobiologia* **500**, 231 (2003).
2. J. G. Tundisi, *Sci. Am. Brazil* **30**, 45 (2005).

Einstein's Interoffice Memo?

THE FOLLOWING IS REPUTED TO HAVE BEEN found in the files of the Swiss Patent Office.

21 September 1904
TO: Patent Office Headquarters
FROM: Albert Einstein
SUBJECT: Commercial Prospects for My Research

I am responding to your request for more information concerning my proposed research for the coming year. In particular, you asked me to describe the prospects for the economic development of Switzerland that will arise from my current work. You have also asked me to explain my work and its commercial prospects in terms that are understandable to the typical Swiss voter.

I am working on three related topics: Brownian motion, the theory of relativity, and the photoelectric effect. Although the work on all three is far from complete, I believe that it is not too soon to see great commercial prospects for Switzerland in at least two of these projects.

Brownian motion is the movement of small particles that float in a liquid. No one is quite sure why these little fellows jump around so much, but previous research confirms that their motions are random. My research is based on the idea that liquids are composed of tiny little pieces of matter, so small that they cannot be seen by the most powerful microscope, and that these little beggars are always jumping around. Occasionally, they bump into the specks floating in the liquid, causing the specks to jump, too.

The commercial prospects here depend on finding a way to control and make use of the jumping specks. If my research is successful, we may be able to create new types of liquids and specks that cause specks to jump around more frequently and in entertaining ways. If so, bartenders will be able to sell beer and schnapps with colorful bouncing specks. Maybe we can find ways to get the specks to sparkle or explode when they are bumped, in ways that are not damaging to the intestinal track of the consumer. If I am allowed to patent a device that implements this idea, I commit to licensing it only to Swiss brewers and distillers, so that Switzerland can dominate the world market in these products.

The theory of relativity is an attempt to integrate time, distance, matter, and energy into a unified theory of everything. My progress here is slow, and so I have decided to leave out gravity for this version. I am now concentrating on the implications of the fact that light, unlike other forms of energy, travels at the same speed in all mediums, even a vacuum. This seems to imply that if several people see the same light, it will travel in relation to each one at the same speed, even if they are moving in relation to each other.

The commercial prospects of this work are enormous. If I can prove one or two more conjectures, the implication will be that it is possible to grow younger if we just travel fast enough. The implications for the Swiss travel industry are staggering. If I can use this theory to build a device for traveling to youthfulness, I will patent it in Switzerland and grant licenses only to Swiss travel agencies to offer such excursions to the public.

The photoelectric effect refers to the fact that under some conditions, one can generate electricity by shining light on matter. My research pursues some implications of my conjecture that energy, too, is comprised of little tiny things and that these explain how light is transformed into electricity.

I have thought long and hard about the commercial implications of this project,

CREDIT: JEREMY WOODHOUSE/GETTY IMAGES/THE IMAGE BANK

but, sadly, I have not been able to see any. Electricity is useful for lights and trolleys, but its commercial potential does not seem particularly great. Moreover, Edison and Westinghouse have been successfully pursuing other means of producing it rather than shining lights on certain materials. My initial thought was that one could manufacture an electric light that would shine on your newspaper as you walked down the street, but I now realize that for this to work it would have to be light out anyway. Perhaps I should abandon this project in favor of the others because its commercial prospects are so dim.

ROGER NOLL

Department of Economics, Stanford University, Stanford, CA 94305, USA.

Aggressive, or Just Looking for a Good Mate?

IN HER ARTICLE "STRONG PERSONALITIES CAN pose problems in the mating game" (News Focus, 29 July, p. 694), E. Pennisi discusses whether aggressiveness, which helps individuals survive, can also impair reproductive success. Extremely aggressive female fishing spiders are mentioned as an example.

Fishing spiders are closely related to lycosid spiders. Lycosid individuals are active hunters, and the females are bigger and more aggressive than males.

Schizocosa malitiosa is a common Uruguayan lycosid. In this species the male performs a conspicuous display (*1*), then struggles with the female, their front legs in contact. Mount takes place only if the male is allowed to climb on top of the female. Males that fail are actively chased away and occasionally cannibalized.

Recent work on *S. malitiosa*, where virgin females were exposed to males (*2*), shows that the most aggressive females, which rejected and attacked three or four males consecutively until finally accepting one, hatching a higher number of spiderlings than "docile" females, which succumbed to their first partner.

Are the females showing uncontrollable aggressiveness or instead estimating their partners' condition? The benefits of boldness in hunting and defending territories could be of use in mate selection, with well-nourished females being more choosy, selecting males that can probably transmit the "good-persuader" condition to progeny.

ANITA D. AISENBERG

Laboratorio de Etología, Ecología y Evolución, Instituto Clemente Estable, Avenida Italia 3318, Montevideo 11400, Uruguay.

References

1. F. G. Costa, *Rev. Brasil. Biol.* **35**, 359 (1975).
2. A. D. Aisenberg, F. G. Costa, *Ethology* **111**, 545 (2005).

CORRECTIONS AND CLARIFICATIONS

Random Samples: "Bombs away… and back" (5 Aug., p. 872). Because of a reporting error, the story incorrectly identified John Rhoades of Bradbury Science Museum in Los Alamos, NM as John Wheaton.

News Focus: "Looted tablets pose scholar's dilemma" by A. Lawler (5 Aug., p. 869). The number of scholars who signed a resolution against working on possibly looted tablets was incorrectly stated. Forty-six scholars signed the document just after the meeting and an additional 26 have since signed on. The total attendance at the meeting was 130.

News Focus: "Preventing Alzheimer's: a lifelong commitment?" by J. Marx (5 Aug., p. 864). Francine Grodstein's name was misspelled in the article.

Editors' Choice: "Who's the most proficient of all?" (5 Aug., p. 852). The enzyme that achieves the greatest rate enhancement, without the aid of cofactors or metals, is orotidine 5′-monophosphate decarboxylase, and not ornithine 5′-monophosphate decarboxylase. The citation should read "*J. Am. Chem. Soc.* **126**, 6932 (2004); 10.1021/ja0525399 (2005)."

TECHNICAL COMMENT ABSTRACTS

COMMENT ON "Independent Origins of Middle Ear Bones in Monotremes and Therians" (I)

Gabe S. Bever, Timothy Rowe, Eric G. Ekdale, Thomas E. Macrini, Matthew W. Colbert, Amy M. Balanoff

At least three hypotheses regarding the evolution of the mammalian ear can be formulated based on the information provided by Rich *et al*. (Reports, 11 Feb. 2005, p. 910). Only one of these hypotheses, which requires a single species to be polymorphic for the mammalian ear and is based on an assumed systematic affinity, supports an independent origin.

Full text at www.sciencemag.org/cgi/content/full/309/5740/1492a

COMMENT ON "Independent Origins of Middle Ear Bones in Monotremes and Therians" (II)

G. W. Rougier, A. M. Forasiepi, A. G. Martinelli

Based on a new fossil specimen of the Early Cretaceous monotreme *Teinolophos trusleri,* Rich *et al*. (Reports, 11 Feb. 2005, p. 910) argued that middle ear bones formed independently in monotreme and therian mammalian lineages. We contend that known specimens of *Teinolophos* provide insufficient evidence to overturn the comparative, embryological, and paleontological evidence that support their homology.

Full text at www.sciencemag.org/cgi/content/full/309/5740/1492b

RESPONSE TO COMMENTS ON "Independent Origins of Middle Ear Bones in Monotremes and Therians"

T. H. Rich, J. A. Hopson, A. M. Musser, T. F. Flannery, P. Vickers-Rich

Derived molar resemblances demonstrate that *T. trusleri* is a monotreme. All *Teinolophos* jaws, including holotype, possess a mandibular trough, which in basal mammaliaforms contains postdentary bones homologous to mammalian ear bones. *Teinolophos* shows features expected in transitional forms losing contact of ear bones with the mandible and phylogenetic evidence supports independent freeing of the ear bones from the jaw in monotremes and therian mammals.

Full text at www.sciencemag.org/cgi/content/full/309/5740/1492c

Letters to the Editor

Letters (~300 words) discuss material published in *Science* in the previous 6 months or issues of general interest. They can be submitted through the Web (www.submit2science.org) or by regular mail (1200 New York Ave., NW, Washington, DC 20005, USA). Letters are not acknowledged upon receipt, nor are authors generally consulted before publication. Whether published in full or in part, letters are subject to editing for clarity and space.

SCIENCE AND RELIGION

200 Years of Accommodation

Alan Cutler

Can science and religion be reconciled? That is a perennial question, and one I doubt will ever be definitively answered. After all, we first need to ask, which science? which religion? And even then the parties involved often can't be neatly sorted into two contending camps.

Before Darwin
Reconciling God and Nature
Keith Thomson

Yale University Press, New Haven, CT, 2005. 328 pp. $27. ISBN 0-300-10793-5.

The Watch on the Heath
Science and Religion Before Darwin

HarperCollins, London, 2005. £20. ISBN 0-00-713313-8.

For the 17th-century founders of modern science—especially those in England such as Robert Boyle, John Ray, and Isaac Newton—the pertinent question was not whether science and religion could be reconciled. It was whether science and atheism could be reconciled, and the answer seemed to be a definitive no. The theistic beliefs of Boyle and his contemporaries predicted a rational order beneath the apparent chaos of nature, and, lo, that was what they found. We moderns cannot easily imagine the emotional and intellectual impact this must have had on these already religious men. At the sight of the intricate structure of an insect eye under his newfangled microscope, even the not especially pious Robert Hooke was moved. Anyone stupid enough to think such things were "a production of chance," he wrote, must be "extremely depraved" or "they did never attentively consider and contemplate the works of the Almighty" (*1*).

Thanks to Charles Darwin, we now can explain biological complexity in terms of a theory that does, in fact, rely on a measure of chance. But before Darwin, no such explanation was available. That nature reflected divine wisdom seemed obvious, at least among those who attentively considered and contemplated it, and out of this idea came a hybrid of science and religion called "natural theology." Natural theology is sometimes depicted as religion's desperate attempt to cling to the coattails of science. Although that description may fit in some cases, a little perspective is in order. At the time when Hooke peered through his microscope, what we now call science had produced few if any tangible benefits to society. Its virtuosos were more often satirized than lionized. (Hooke was mercilessly lampooned on the London stage as "Dr. Gimcrack.") Through the early years of modern science, the link with religion helped legitimize the investigation of nature as a serious and worthwhile endeavor.

In *Before Darwin: Reconciling God and Nature*, Keith Thomson chronicles the changing fortunes of natural theology from its first flowering in the work of John Ray to its fatal (or, depending on your point of view, near-fatal) encounter with Darwinian evolution. Thomson, an emeritus professor of natural history at the University of Oxford, focuses particularly on the work of English cleric William Paley. It is an apt choice not only because Paley's book *Natural Theology* is generally considered the definitive work in the genre, but because of the book's impact on one of its readers: the young Charles Darwin (*2*).

Although Paley was no scientist, he was a skilled logician and a zealous compiler of biological facts. He is most famous for the analogy of the watch, which appeared in the introduction of his book. Suppose one happened to find a watch upon the ground, he wrote. Would not its intricate mechanism imply "that the watch must have had a maker…who comprehended its construction, and designed its use"? Nature, so the argument went, is vastly more complex and perfect than any human contrivance. (Hooke's microscope had already revealed how pathetically crude even the finest needles were compared to the appendages of a common flea.) Reason leads us to the inevitable conclusion that nature must also have a maker, but one infinitely wiser and more skilled than a human watchmaker. In other words, not just a creator, but a Creator.

This is the argument from design, which philosophers have generally found unconvincing. But if Darwin, who encountered Paley's book as a student, was typical, most readers found the logic ironclad. "*Natural Theology* gave me as much delight as did Euclid," confessed Darwin in his autobiography. His enthusiasm was to fade, of course, with momentous consequences.

What Paley saw as the biggest threat to his brand of natural theology, Thomson notes, were the atheistic theories of evolution bandied about by Erasmus Darwin (Charles's grandfather) and other unorthodox thinkers. Paley's dispute with them did not exactly constitute a clash between science and religion, because these mystical ideas were scarcely more scientific than Paley's. And when Charles Darwin came up with a theory of evolution that did meet the standards of science, he probably borrowed as much from Paley as from previous evolutionists. Thomson argues persuasively that Darwin likely first encountered Thomas Malthus's grim statistics on population growth in Paley's book. But where Paley saw the weeding out of unfit variants as a force of stability, Darwin saw it instead as a mechanism of evolutionary change.

According to Thomson, it was principally Darwin's theory that, by removing the necessity of a designer, doomed natural theology. In this sense, *Before Darwin* is a fairly conventional Darwin-versus-the-theologians account

Jacopo Tintoretto's *Creation of the Animals* (*c.* 1550).

CREDIT: MAURO MAGLIANI/© ALINARI ARCHIVES/CORBIS

The reviewer is the author of *The Seashell on the Mountaintop*, a biography of Nicholas Steno. E-mail: ahcutler@aol.com

of the relationship between science and religion. Bishop Samuel Wilberforce even makes his obligatory appearance to be smitten in debate by Thomas Henry Huxley. But Thomson shows that there is more to the story. Whereas most modern readers of *Natural Theology* probably don't venture much beyond the opening pages and the watch metaphor, Thomson sifts through Paley's entire argument. In looking for purpose and design in every aspect of the world, even human misery and the worst social inequality, Paley presented an image of God as a compassionless technocrat. Natural theologians had long been criticized for emphasizing God the Creator over God the Redeemer. Paley's book nowhere mentions Jesus. When Darwin grieved over the death of his beloved daughter at the age of ten, Paley's watchmaker God was cold comfort at best. It was this, as much as any intellectual argument, that undermined Darwin's Christian faith. Natural theology's theology was ultimately as unsatisfying as its science.

Thomson summarily dismisses the efforts of William Whewell and others to reconcile evolution and theology, stating flatly that "Although many tried, it was not possible to enlist natural selection on the side of the angels by construing it as the result of God-given natural laws." I wish the author had allowed Whewell, right or wrong, to say his piece. In a book subtitled "Reconciling God and Nature," evolution's friends across the aisle deserve the same consideration as its enemies.

Thomson devotes only a few pages to the modern-day incarnation of natural theology, the intelligent design movement. This is enough. The answers to their arguments are basically the same as the answers to Paley's. But that is what makes *Before Darwin* a timely book, as the perennial debates about science and religion go on and on.

References and Notes

1. The quote appears in S. Shapin, *The Scientific Revolution* (Univ. Chicago Press, Chicago, 1996).
2. W. Paley, *Natural Theology: Or, Evidence of the Existence and Attributes of the Deity* (London, 1802). (As Thomson notes, it was probably the 1826 edition that Darwin read as a student.)

10.1126/science.1116362

MOVIES: NATURAL HISTORY

Emperors on the Ice

March of the Penguins
by Luc Jacquet

Warner Independent Pictures, Burbank, CA, and National Geographic Feature Films, Washington, DC, 2005. 80 minutes. www.marchofthepenguins.com

It is rare that a nature film becomes so popular that, in the terms of the trade, it "moves uptown" from art theatres to the revenue-generating sites. *March of the Penguins* succeeds because it is beautifully photographed, because the birds are almost endearingly charming, and because the story has the kind of high drama we associate with mysteries—or perhaps extreme sports.

What a relief to review a film the entire plot of which, right up to the ending, can be revealed without spoiling any surprises for the prospective viewer. The story narrator Morgan Freeman tells is this: Emperor penguins (*Aptenodytes forsteri*), the largest of the penguins, live in the Antarctic seas, where they find plenty of krill, their favored food. But there they also encounter nasty predators, like leopard seals (*Hydrurga leptonyx*). In addition, the thin ice on the margins of these cold seas is not a good place to breed and rear young. The adults of both sexes therefore make pilgrimages, walking distances of up to 110 kilometers to interior sites on the ice, where they pair up and breed. About two months later, in the austral autumn, females produce a large egg, which they then transfer to their partners in a delicate, well-practiced, feet-to-feet maneuver. The males then incubate the eggs in a protective feathered pouch while their mates make the return march to the sea. The females have invested heavily in their big eggs, and they are hungry and tired. But most of them reach the water and will feed for weeks to fatten up. Then it's back to the breeding ground, where the males have endured winter storms, the French cinematographers have demonstrated that they are as tough as they are talented, and—voilà!—most of the eggs have hatched.

After some touching reunions, the elegance of this high-risk behavioral orchestration becomes clear. The females return just in time to feed the chicks. But in case there's a slip, the half-starved male has a tiny emergency tank—a few drops of regurgitate to tide the chick over for a day or two. Now spring is imminent again, and growth is the name of the game. Watching feeding by regurgitation is not for everyone, but it helps one appreciate the metabolic marvel of how much nutrition a female emperor penguin can mobilize and deliver. The chicks get bigger and fuzzier, while the males march back to the sea to load up again. (Actually, although "march" makes a nice title for this film, the actual means of locomotion is waddle/belly flop/waddle, which might not sell as well.) At this point, the filmmaker introduces some drama: a lone southern giant petrel (*Macronectes giganteus*) appears and makes several passes at the big chicks. Although giant petrels are the principal predator of emperor chicks, this bird looked so overmatched that I didn't quite get the feeling of incipient tragedy.

But the film is so wonderful that caviling is out of place. The march of these magnificent birds is compelling, in its improbability and in its quality as spectacle. In terms of orderly, migrating legions of animals, the spectacle might remind us of the wildebeests (*Connochaetes taurinus*) of East Africa—but these Antarctic migrants are covering much of their journey on empty stomachs. For me the most fascinating part of the story is that over time scales ranging from millennia to millions of years, the climate of Antarctica has changed. The icy continent was once vegetated, and over the last few hundred thousand years there have been extensive shifts in the relation between ocean margins and the interior. Thus the penguins have had to modify their behavior to keep pace with changing topography. Indeed, just as the film ends the males return, well fed. And in a piece of exquisite timing, the ice margin has retreated to a point much closer to the breeding ground. So parents and young can take the shorter trip to sea together, and viewers get to witness the youngsters' first dives.

These birds have evolved a majestic stereotyped sequence of unlikely, high-risk behaviors that deals beautifully with current conditions. But conditions weren't always as they now are, and what the film can only hint at is that the penguins' march is improbable and strange precisely because it bears the imprint of its own evolutionary responses to changing conditions.

By all means see *March of the Penguins*. Better still, you can accomplish a good work by inviting an advocate for "intelligent design" to accompany you. After the show, buy him or her a beer, and ask for an explanation of just what the Designer had in mind here.

—DONALD KENNEDY

10.1126/science.1118709

ESSAY

GLOBAL VOICES OF SCIENCE

Deciphering Dengue: The Cuban Experience

María G. Guzmán

By the 1960s, vaccines and antibiotics had so reduced the incidence of such deadly diseases as smallpox, poliomyelitis, and acute rheumatic fever that the public health community was basking in a "comfort zone." This comfort was shattered beginning in the 1980s with the emergence of new infectious diseases, among them HIV/AIDS, severe acute respiratory syndrome (SARS), and avian flu, and the reemergence of diseases once considered scourges of the past,* including West Nile fever and dengue, a devastating disease to which I have devoted much of my professional life.

This yearlong essay series celebrates 125 years of *Science* by inviting researchers from around the world to provide a regional view of the scientific enterprise. Series editor, Ivan Amato

Factors involved in the emergence of infectious diseases are complex and interrelated. Epidemiological evidence shows that social and economic factors such as poverty, social exclusion, health systems, environments, food security, water and sanitation, and education are of utmost importance.*† Public health infrastructure, including disease surveillance, disease prevention, communication, and financial support, are crucial for facing threats posed by emerging infectious disease.

Almost 50 years ago, a small Caribbean country, the Republic of Cuba, embarked on a plan to accelerate development of its education, public health, and science sectors, a policy that has prepared the country for the new global context of emerging and returning diseases. At the end of the 1950s, Cuba had approximately 10 million inhabitants and no more than 3000 physicians. Now a population of about 11 million is served by a health system that includes more than 70,000 medical doctors.

This buildup has been serving the population well. Poliomyelitis and malaria were eradicated in 1962 and 1967, respectively. In the 1970s, tetanus neonatorum (which afflicts newborns) and diphtheria became a worry of the past for Cubans. A national regimen of 13 vaccines led, in the mid-1990s, to the elimination of measles, rubella, and mumps and to the control of tetanus, meningococcal disease, hepatitis B, leptospirosis, and other diseases. The rates of contracting meningococcal disease and dying from it diminished by 93% and 98%, respectively, and the rate of hepatitis B infection has been cut by 97% in children younger than 15 years of age. Although the incidence of tuberculosis is increasing worldwide, with some countries having reported rates in recent years well above 100 cases per 100,000 inhabitants, Cuba has a low rate of 6.6 cases per 100,000 inhabitants, and the cases that we do see are treatable. Deaths due to diarrhea were reduced by more than 95%.

In general, mortality from infectious and parasitic diseases in Cuba is only 6.5%, with most of the deaths due to influenza and pneumonia. According to the World Health Organization's World Health Report, 1998, infectious and parasitic diseases caused one-third of all deaths in the world in 1997 and 43% of deaths in the developing world. The low rate in Cuba is possible because of the high educational and health levels of the country.

The steady improvement of Cuba's health system over the past half-century has been complemented by a buildup of the country's scientific strength, particularly in the biomedical sciences. At the beginning of the 1960s, there were only four experimental stations (all of them dedicated to the study and improvement of sugar cane) and three universities, and illiteracy was widespread. Today, there are more than 700,000 graduates at 60 universities, which are host to 220 science and technology centers. In 2003, these institutions employed nearly 78,000 Cubans, almost two-thirds of them scientists and technicians and 52% of them women.

A Scientist Grows in Havana

As a little girl, I found myself within this improving health system and educational infrastructure, and I grew up with the idea that I could become a scientist. Early on, I dreamed about studying astronomy. I was impressed by the planets that I could see in the sky, as well as the other worlds I couldn't see. However, I was caught up in the rapid changes of Cuban society, particularly those related to the development of biomedicine. As a result, I shifted my studies toward medicine.

After I received my medical degree from Havana University in 1975, I started working

CREDIT: OGOBARA DOUMBO

María G. Guzmán
Cuba

María G. Guzmán, head of the virology department at the Tropical Medicine Institute Pedro Kourí (IPK), in Havana, Cuba, has more than 20 years of experience working on virology. With her husband and a group of distinguished collaborators, her work on dengue viruses in Cuba and abroad has contributed to knowledge of the pathogenesis, diagnosis, epidemiology, and clinical progression of this disease. She is a member of the Cuban Academy of Science, a Fellow of the Academy of Sciences for the Developing World (TWAS), and director of the PAHO/WHO Collaborating Center for Viral Diseases. More recently, she has taken over the helm of the PAHO/WHO Collaborating Center for the Study of Dengue and Its Control and become a member of the Foundation Council of the Global Forum for Health Research. She is a member of several expert committees at the Pan American Health Organization (PAHO), World Health Organization (WHO), and the Special Programme for Research and Training in Tropical Diseases (TDR).

All essays and interactive features appearing in this series can be found online at www.sciencemag.org/sciext/globalvoices/

as an investigator at the virology laboratory of the Centro Nacional de Investigaciones Cientificas (CNIC) in Havana. This scientific institution was founded in 1965 and it has been crucial for the development of Cuban science ever since. Many of the scientific leaders of the country's main research centers—including the Centro de Ingeniería Genética y Bioteclogía (CIGB), Instituto Finlay (for vaccine development), Centro de Inmunoensayos (for the development of diagnosis technology), and Instituto de Medicina Tropical "Pedro Kourí" (IPK) (for the surveillance, research, and control of infectious and parasitic diseases)—were trained at CNIC.

At CNIC, I honed my skills in research and analytic thinking and in 1980 I moved to the virology laboratory at IPK. There was no better place for a person who wanted to devote her efforts to fighting infectious diseases.

In May 1981, my country was befallen with a public health crisis, one that would decide my professional future. The first epidemic of dengue hemorrhagic fever/dengue shock syndrome (DHF/DSS) anywhere in the Americas took hold in Cuba. DHF/DSS is the most lethal form of disease resulting from infection with the dengue virus (see the figure), a member of the viral family Flaviviridae that is transmitted from person to person via mosquitoes, mostly in the Tropics where these vectors thrive. Most people who get infected develop a fever and a rash, but recover in about 5 days. About 1 in 20 of those who develop a hemorrhagic form of the fever die, and of those who develop dengue shock syndrome, 40% die.[‡]

Previously, only 60 DHF/DSS cases had been observed in the Americas. In the 1981 epidemic in Cuba, more than 344,000 cases were reported, of which 10,000 were deemed severe and very severe. There were 158 fatalities. All but 57 of these were children, a chilling factor that only added to the national dread elicited by this epidemic. Once the first cases were detected, I found myself—despite my youth and inexperience—playing a crucial national role in the diagnosis of a severe viral disease that had been relatively unknown in Cuba or the region before. (Although a milder dengue epidemic had been reported in Cuba in 1977–1978, I was not involved in the country's scientific and medical response at that time.)

Our serological and virological examinations quickly revealed that the 1981 outbreak was due to the dengue 2 virus, one of the four serotypes known. In addition to studying the severe cases during the epidemic, we developed protocols for diagnosing the disease, which can be confused with other infections, and we established disease surveillance methods.

Even as Cuban health care workers were succeeding in checking the spread of the virus, using mosquito eradication and other techniques, a new phase in my scientific career was just beginning. Rather than leaving the dengue virus behind, I devoted my research to it. After all, this outbreak that I had just witnessed represented a globally significant turning point in the disease's history.

The Whole Dengue

Among my first tasks were to clinically describe DHF/DSS in the adults who contracted the disease, define and confirm some risk factors for progressing to the more severe form of the disease, and conduct a genetic study of the dengue 2 strain. I would later find this work to be helpful, during DHF/DSS epidemics in Cuba in 1997 (dengue 2) and 2001–2002 (dengue 3).

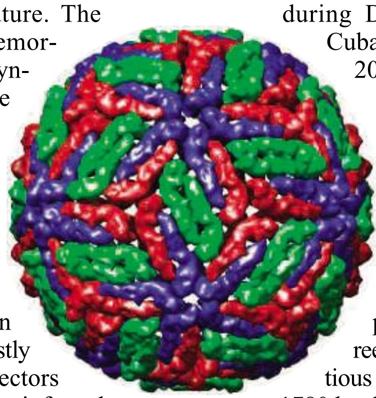

Bad ball. A computer portrait of the dengue virus indicates several types of protein constituents in the virus's shell.[¶]

Dengue disease is considered one of the best contemporary examples of the emergence or reemergence of a viral infectious disease. First described in 1780 by the Philadelphia physician Benjamin Rush during an epidemic in his city at that time, many epidemics have been reported since then. Currently, the distribution of dengue is worldwide. Caused by any of the four dengue serotypes and mainly transmitted by the *Aedes aegypti* mosquito, the disease is observed in two main clinical forms: the mild disease called dengue fever (DF) and the severe syndrome, DHF/DSS.

In the last 30 years, the incidence of the disease has been increasing. The first cases of DHF/DSS were reported in Southeast Asia and the Western Pacific (during the 1950s and the 1960s) and then later in the American region. Factors such as substandard housing, poor water supplies, and the spread of dengue viruses between populations have directly contributed to the reemergence of the disease.

Soon after the clinical recognition of DHF/DSS, Scott. B. Halstead, then at the University of Hawaii's School of Medicine, and others argued that those most at risk for developing this severe form of dengue disease are those who already had been infected by one dengue serotype and then subsequently become infected with a different serotype. Others proposed that viral virulence is the key risk factor.[§||]

Following the 1981 outbreak in Cuba, I, along with Gustavo Kourí, my collaborator and husband (and son of the founder of IPK), and a group of distinguished scientists, including Susana Vasquaz, dedicated our work to uncovering risk factors for DHF/DSS. Our epidemiological, virological, and clinical investigations have led to important new observations. For one thing, in studies of three well-defined DHF/DSS epidemics in Cuba—in 1981, 1997, and 2001–2002—we confirmed that secondary infection was a significant factor in more than 97% of the severe cases. We made two other particularly important epidemiological observations that support the role of the secondary infection. One of them was that no severe and fatal DHF/DSS cases were observed among 1- to 2-year-olds during the 1981 epidemic. Because they were not born until after the first epidemic of DF caused by the dengue 1 virus in 1977, they could only have experienced a primary infection during the 1981 epidemic. We also found that no cases of DHF/DSS were observed among children during the 1997 and 2001–2002 epidemics. These children were born in a period free of dengue transmission (1982–1996) and so also were only at risk of a primary dengue infection.

Another relevant finding, which our group reported in 2000, is the influence of the interval between dengue infections. In contrast with early epidemiological studies that predicted that DHF/DSS would ensue only if the primary and secondary infections occurred within an interval of 5 years, our studies have demonstrated a marked increase in severity with longer intervals between an initial dengue 1 and a secondary dengue 2 infection. Supporting this result is our recent demonstration that certain lymphocytes, a type of immune cell, can retain a "memory" of a dengue infection that occurred 20 years earlier. These observations suggest that once an individual is infected by dengue 1 virus, that person could be susceptible to developing the severe disease for decades. The message to vaccine developers is clear: A dengue vaccine needs to elicit long-lasting protection against the four dengue serotypes, or else the vaccine itself could sensitize individuals who are subsequently infected to mount a severe immune response.

In some of our other research into risk factors for severe dengue, we have found that individuals with chronic diseases such as bronchial asthma, diabetes mellitus, and sickle cell anemia have a higher likelihood of

developing DHF/DSS. Age too is a risk factor. We have demonstrated a much higher risk of developing the severe disease during a secondary infection in infants and children as compared with adults. For children aged 3 to 14 years with secondary infections, the death rate was 14.5-fold higher than in young adults aged 15 to 39 years (see the figure).

Not many researchers have looked into how ethnicity and genetics relate to the risk of developing DHF/DSS. Our investigations into these issues have suggested that whites are at particular risk as compared with blacks. In my country's three epidemics since the late 1970s, DHF/DSS was predominantly observed in whites. Currently, Beatriz Sierra and Gissel Garcia, two of our immunologists, are studying the genes that may predispose individuals to the development of DF and DHF/DSS.

Meanwhile, others in our group are working on biological and genetic characterizations of the viruses that have been isolated in the Cuban dengue epidemics. With the help of Delfina Rosario and Rosmari Rodríguez Roche, we have demonstrated that viruses linked to DHF epidemics belong to an Asian genotype. In a more detailed study of genetic changes in the dengue 2 virus during the 1997 epidemic, we documented a pattern of sequence evolution in some genes, and a remarkable conservation both of genes coding for structural proteins, as well as of the noncoding regions in the genome. We are currently trying to decipher the implications of these findings.

In addition to the human and viral genes important in dengue infections, we are looking into the role of the humoral and cellular immune response in the development of DHF/DSS. With the collaboration of Ana B. Perez and Mayling Alvarez, two young researchers in our group, we have obtained preliminary data on the influence of heterotypic neutralization—in which antibodies elicited against one dengue serotype can react also with another serotype—to mitigate the severity of the severe form of the disease. Our results suggest that heterotypic dengue antibodies decline over time, a phenomenon that could explain why secondary infections often appear worse as more time passes since the primary infections. Also, we demonstrated the association of increased levels of interleukin-10 in dengue patients with a secondary infection, suggesting an important role of this cytokine in the pathogenesis of dengue. This observation provided the first "in vivo" evidence of a direct relationship between secondary dengue infection and the development of a noninflammatory immune response, opening yet another new avenue of research.

We have made several attempts to synthesize what is known about dengue pathogenesis into testable hypotheses about why some outbreaks lead to DHF/DSS epidemics. In one of these, published in 1987, my husband and I integrated epidemiological factors (high vector density, high virus circulation, and a susceptible population at risk of a secondary dengue infection), host factors (age, gender, ethnicity, chronic diseases, preexistence of dengue antibodies, interval between infections, and genetics), and viral factors (serotype, strains, and genotypes) into one multifactorial analysis to facilitate the evaluation of the risk of a given population.

More recently, I, my husband, and Scott Halstead—now working for the South Korea–based Pediatric Dengue Vaccine Initiative—published a hypothesis in an attempt to explain the significant monthly increases in severity during the Cuban dengue epidemics. Specifically, a significant increase in the proportion of DHF/DSS cases and in fatality rates for both DF and DHF/DSS was observed during the 1981 and 1997 epidemics. In our "escape mutant" hypothesis, we conjecture that the occurrence of heterotypic dengue neutralizing antibodies after a primary dengue 1 infection later serves, during a subsequent infection with dengue 2 virus, as a selection mechanism that favors "neutralizing-escape mutants" of the dengue 2 virus. This can bring on more severe sickness.

Dengue to Come

The world needs a dengue vaccine. Our group is now collaborating with CIGB on a project whose goal is to obtain a recombinant vaccine candidate to dengue viruses. With the collaboration of Mayra Mune, a molecular immunologist, for the first time we have evaluated in monkeys the usefulness of a recombinant protein expressed in yeast *Pichia pastoris*. We observed a rise both in neutralizing antibodies against dengue and partial protection to challenges with the wild-type virus. Also, our preliminary evaluations of a dengue protein fragment are showing promise in eliciting protective immune responses in animals.

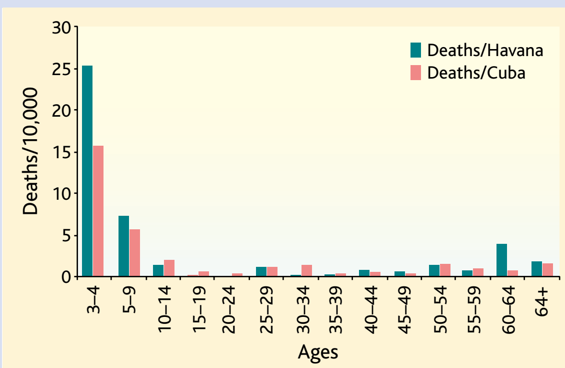

Dengue's ageism. In Cuban epidemics of dengue fever, the very young succumbed most readily to a severe form of the disease.

CREDIT: M. GUZMAN *ET AL.*

Although dengue has dominated my research portfolio, I have been able to collaborate with my colleagues in the study of a number of the most medically important infectious diseases. As the national reference center for viral diseases, our virology department at IPK is charged with the diagnosis and surveillance of, and research into, hepatitis, measles, rubella, and mumps, as well as respiratory, enteroviral, and sexually transmitted diseases, among others. Current international events have obliged us to include in our portfolio new viral infections, such as West Nile fever, SARS, and avian flu, among others.

Founded in 1937 by Pedro Kourí, the famous Cuban parasitologist, IPK now gathers in one place the main disciplines involved in the study of infectious and parasitic diseases. In this setting that combines high scientific quality and collegiality, we have been able to assemble a multidisciplinary group for dengue research that has recently been recognized as a new PAHO/WHO Collaborating Center for the Study of Dengue and Its Control. It is gratifying to be able to share our insights and discoveries with others in what is becoming a global fight against this disease.

References and Notes

*B. L. Ligon, *Semin. Pediatric Infect. Dis.* **15**, 199 (2004).
†S. S. Morse, *Emerg. Infect. Dis.* **1**, 7 (1995).
‡www.stanford.edu/group/virus/flavi/2000/dengue.htm
§S. B. Halstead, *Yale J. Biol. Med.* **40**, 350 (1970).
||L. Rosen, *Rev. Infect. Dis.* **11**, S840 (1989).
¶Image produced using the UCSF Chimera visualization package from the Resource for Biocomputing, Visualization, and Informatics at the University of California, San Francisco (www.cgl.ucsf.edu/chimera).

Acknowledgement: As a woman scientist in Cuba, I have received official, social, and family support for my scientific development. I am especially grateful to my mother for attending to my family with love and care, my husband for encouraging me to pursue my dreams, and my son, who has often felt my absence.

The author is in the Virology Department, PAHO/WHO Collaborating Center for Viral Diseases and PAHO/WHO Collaborating Center for the Study of Dengue and Its Control, Instituto de Medicina Tropical "Pedro Kourí" Autopista Novia del Mediodia, Km 6½, Post Office Box Mariano 13, Habana, Cuba. E-mail: lupe@ipk.sld.cu

10.1126/science.1115177

NATURAL HISTORY

Beyond the Chimpanzee Genome: The Threat of Extinction

Marc D. Hauser

I have had the privilege of watching chimpanzees for many hours in their natural habitat in Africa and in a variety of zoo settings. They are magnificent animals. Watching them is unlike watching any other nonhuman creature. When a chimp looks back at you, your soul has been penetrated. You feel as though your inquisitiveness has been volleyed back, no words or actions exchanged.

The unveiling of the chimpanzee genome (*1*) presents a unique opportunity to systematically explore how and why we diverged from our closest living relatives. Perhaps, once and for all, we can begin to figure out the meaning of the tiny differences in DNA between our respective species. Perhaps we will learn how small differences in the code of life enabled us—but not chimpanzees—to cook soufflés, create symphonies, translate our own voyages into maps, build ever more complicated artifacts, and write plays that reflect the social intricacies of our lives. But none of this will have any meaning unless we understand what it is like to be a chimpanzee. Humans are unique, and so too is every other species on this planet. But characterizations of uniqueness only make sense in light of a comparative record, one that documents the anatomy, physiology, and behavior of other species.

A map of the genome provides one layer of description. It is a meaningless layer without equally rich descriptions of how genes enable each species to make a living, escape predators, fend off competitors, build allies, and produce babies. In this sense, my greediness to understand extends beyond the chimpanzee genome to that of its closest genetic relative, the bonobo. Although remarkably similar on many levels, bonobos differ from chimpanzees—and resemble humans—in important parts of their skeletal anatomy, brain physiology, sexual behavior, and temperament. In many ways we are "chimpobos," a hybrid ape.

Thanks to the pioneering work of Jane Goodall [see the figure; (*2*)] and the many primatologists who have enriched her work since, we now have a detailed description of chimpanzee life. The general public's impression of this life is, however, highly colored by the documentaries presented on television. These focus on the brutality of their hunting and intercommunity killings, or on their exceptional talents with tools. But if you take a snapshot of chimpanzee life at a random moment, here's what you see: eating, sleeping, or grooming.

Watching a chimpanzee eat may not be the most exhilarating experience for even the most die-hard field biologist, but by documenting what these animals eat, when, how, and for how long, scientists have unlocked some extraordinary mysteries. When chimpanzees are infected with certain pathogens, such as the nematodes that attack them in the Mahale Mountains of Tanzania, they consume plants that act as either chemical or physical defenses. For other ailments, including constipation, lethargy, and lack of hunger, they eat the bitter pith of a plant; this same plant is used across Africa as a local cure for humans infected with bilharzia and malaria. These discoveries, made possible by painstaking observations, have ignited an entire field of inquiry: searching for new remedies in the plant life that surrounds us (*3*).

Detailed observations of their eating habits also reveal an exceptionally diverse tool technology (*4*). On the basis of studies spanning the natural range of chimpanzees in eastern and western Africa, we now know that different populations use different tools to gain access to their local resources. Some use sticks to extract termites, others use rocks to crack open hard nuts, and yet others use tree bark as sandals to climb over the thorny needles of trees that hold a delectable fruit. The variation among populations is not due to genes, but rather to the capacity for social learning that the genes have built. What we see when we watch a chimpanzee population is a microculture—one that has developed its own unique signature, evidenced by distinctive tool technologies and, in many cases, equally distinctive social gestures (*5*).

When chimpanzees eat, sometimes they do so in the midst of several other community members, and sometimes they do so alone. Here, sex differences emerge. Males live in their natal groups for life, whereas females leave once they reach reproductive maturity. When you watch chimpanzees in the wild, it is not uncommon to find an adult female, either alone or with her offspring. Seeing a male alone is rare. Many of the males in a community are brothers. They hunt together, cooperate to form alliances against other members of the community, and often go off on patrols to defend their turf against often violent neighbors. Like our own species, but unlike their close relative the bonobo, chimpanzee males are extremely aggressive toward their neighbors. If members of one community have outnumbered a foe, they will attack and kill a member of another community who has wandered too far from home (*6*, *7*); some of the calculations used in making such group decisions may be carried out with the chimps' exquisite mathematical prowess (*5*, *8*). Watching such kills is chilling. It is too close for comfort.

When chimpanzees cluster into social groups, the political strategizing that goes on reflects planning, power, and peace offerings (*9*). Studies in the wild and in cap-

Understanding our relatives. Jane Goodall observes a family of chimpanzees.

CREDIT: KARL AMMANN/CORBIS

The author is in the Departments of Psychology, Organismic and Evolutionary Biology, and Biological Anthropology, Harvard University, Cambridge, MA 02138, USA. E-mail: mdh@wjh.harvard.edu

tivity, especially the latter, have revealed that individuals both compete and cooperate by making inferences about what others know and intend (*10*, *11*). These studies have revolutionized our understanding of what chimpanzees think and feel, raising profound philosophical questions about the nature of thought without language, as well as ethical questions concerning the rights and welfare of these animals (*12*).

Constraining our continued understanding of this wonderful animal is one annoying hurdle: our own species. In the very near future, we may ironically face the possibility of having a detailed map of the chimpanzee genome, but no individuals to study. Illegal hunting, the bushmeat trade, and deforestation are destroying chimpanzee populations (see, for example, www.chimpcollaboratory.org). If the same amount of effort that is going into genetic analyses went into chimpanzee conservation and behavioral biology, not only would we save this species from extinction, but we would write the most detailed story of our past—as rich as the Bible, but grounded in science.

References and Notes

1. The Chimpanzee Sequencing and Analysis Consortium, *Nature* **437**, 69 (2005).
2. J. Goodall, *The Chimpanzees of Gombe: Patterns of Behavior* (Belknap/Harvard, Cambridge, MA, 1986).
3. M. A. Huffman, R. W. Wrangham, in *Chimpanzee Cultures*. R. W. Wrangham, W. C. McGrew, F. B. M. de Waal, P. G. Heltne, Eds. (Harvard Univ. Press, Cambridge, MA, 1994), pp. 129–148.
4. A. Whiten *et al*., *Nature* **399**, 682 (1999).
5. T. Matsuzawa, *Primate Origins of Human Cognition and Behavior* (Springer-Verlag, Berlin, 2002).
6. M. L. Wilson, M. D. Hauser, R. W. Wrangham, *Anim. Behav.* **61**, 1203 (2001).
7. R. W. Wrangham, D. Peterson, *Demonic Males* (Houghton Mifflin, New York, 1996).
8. M. D. Hauser, *Wild Minds: What Animals Really Think* (Holt, New York, 2000).
9. F. B. M. de Waal, *Chimpanzee Politics: Power and Sex Among Apes* (Harper & Row, New York, 1982).
10. D. Premack, A. Premack, *Original Intelligence* (McGraw-Hill, New York, 2002).
11. M. Tomasello, J. Call, B. Hare, *Trends Cognit. Sci.* **7**, 153 (2003).
12. P. Cavalieri, P. Singer, *The Great Ape Project: Equality Beyond Humanity* (St. Martin's, New York, 1994).
13. I thank three of my closest colleagues for comments on this essay: F. de Waal, B. Hare, and R. Wrangham.

10.1126/science.1111421

GENOMICS

Thoughts on the Future of Great Ape Research

Edwin H. McConkey and Ajit Varki

When the Human Genome Project was established in 1991, the planners wisely included sequencing the genomes of model organisms in the project's goals. At that time, the only nonhuman mammalian genome scheduled for sequencing was that of the laboratory mouse. Although the relevance of the mouse genome for interpreting the human sequence was beyond dispute, some biologists were disappointed that no nonhuman primate genome had been included. The remarkable similarity of the chimpanzee genome to that of humans was already predicted from overall DNA comparisons, and it seemed clear that questions about the genetic basis for human uniqueness would eventually require detailed comparisons with the genomes of great apes (*1*), our closest evolutionary relatives. A formal presentation of the need for sequencing the chimpanzee genome was published in 1997 (*2*). Soon thereafter it was pointed out (*3*) that there should also be a project to increase our knowledge of the great ape "phenome" (the complete body of information about an organism's phenotype under various environmental conditions), about which very little is known. Scientists from a variety of disciplines rallied in support of sequencing the chimpanzee genome, also citing biomedical reasons and the potential importance for proper care and conservation of great apes (*4*, *5*).

E.H. McConkey is in the Department of Molecular, Cellular and Developmental Biology, University of Colorado, Boulder, CO 80309, USA. E-mail: mcconkey@colorado.edu A. Varki is in the Departments of Medicine and Cellular and Molecular Medicine, University of California, San Diego, La Jolla, CA 92039, USA. E-mail: a1varki@ucsd.edu

We now have a draft sequence of the common chimpanzee genome (*Pan troglodytes*) and a detailed comparison with the human genome (*6*). The results include extensive information on comparative genomics, such as the number of single base pair and insertion/deletion differences and transposable elements unique to either human or chimpanzee. The report clarifies much previously conflicting or confusing information in existing human nucleotide sequence databanks and addresses several important questions about genomic and population evolution mechanisms. It also adopts a rational orthologous chromosomal numbering system to facilitate comparisons of human and ape genomic organization (*7*).

Can we now provide a DNA-based answer to the fascinating and fundamental question, "What makes us human?" Not at all! Comparison of the human and chimpanzee genomes has not yet offered any major insights into the genetic elements that underlie bipedal locomotion, a big brain, linguistic abilities, elaborated abstract thought, or any other unique aspect of the human phenome. This state of affairs may seem disappointing, but it is merely the latest example of a generalization that genomics research has already established—interpretation of DNA sequences requires functional information from the organism that cannot be deduced from sequence alone. Functional genomics investigations must determine where a gene is expressed within an organism, when it is expressed during development and life history, and what the level of expression is at various times. Furthermore, these data must be integrated with information about the related phenotypes, as well as critical environmental influences under which the genotype generates the phenotype (see the figure).

There are three general reasons for substantially increasing research on chimpanzees (and the other great apes—bonobos, gorillas, and orangutans): First, to understand the contribution of genomic DNA to human and great ape evolution; second, to improve our understanding of human and ape phenomes (at all levels, from molecular to behavioral to states of diseases); and third, to help preserve populations of these important human relatives. These goals must be pursued in the face of challenging ethical issues that still need to be resolved by open debate.

Understanding the genetic basis of uniquely human traits will require increasing the accuracy and completeness of the currently available chimpanzee genome sequence, as well as sequencing other primate genomes as out-groups. The genomes of the orangutan and the rhesus macaque are currently being sequenced, but other genomes are needed to obtain a complete picture. Among other benefits, such multispecies comparisons are essential for identifying human-specific coding and regulatory regions.

A parallel requirement is the comparison of human gene expression with those of chimpanzees and other primates. There are formidable obstacles to achieving this goal, the most obvious of which is obtaining experimental material from great apes. It is not ethically acceptable to sacrifice a great ape simply to obtain tissue samples.

Studies of great apes should follow guidelines generally similar to those for research on human subjects. Thus, there is a need for new funding to support development of a network among current holders of captive great apes (including primate facilities, great ape sanctuaries, and zoos) to guarantee that tissue samples can be obtained quickly from each great ape that dies of natural causes, or has to be euthanized because of incurable suffering. Autopsy samples need to be preserved for histological analysis and used as source materials for studies of gene expression and cDNA libraries. Such samples can also be used for a wide variety of other "omic" comparisons (including proteomics, glycomics, and lipomics). Because every tissue is made up of multiple cell types, such approaches can still miss important differences in minor cell types. Thus, parallel histological comparisons must occur, using multiple probes to detect differences.

Examination of adult tissues, however, will still not allow us to understand gene expression and its consequences during development, which may well be the time when many of the crucial differences between humans and the great apes are expressed. This concept was suggested decades ago by King and Wilson (*8*), and studies since then have given us no reason to reject that hypothesis. Analysis of gene expression during prenatal development can be approached with three experimental strategies: transgenesis, stem cells, and direct study of developmental samples.

Transfer of human genes into mice has been fundamental to the analysis of human gene function. Comparative analysis of human and chimpanzee orthologous genes in transgenic mice is now certain to be pursued. Of course, there are limits to what one can deduce about the phenotypic effects of human or ape genes in mice. This is particularly true for the brain, skin, innate immune system, and reproductive system, wherein primates have undergone considerable functional divergence from rodents. However, ethical, fiscal, and practical considerations will make the idea of transgenic apes moot. Thus, we should expect that the need for transgenic monkeys will arise, and deciding on the ideal model for such experiments will not be easy. Given ethical and practical issues and the longer generation-time of monkeys, such studies will require much thought, patience, and long-term funding.

Embryonic stem cell cultures from humans are a subject of intense interest. Although creation of stem cell lines from ape embryos will be just as difficult technically, it represents a feasible experimental approach that causes no lasting harm to the animals from which gametes are obtained for in vitro fertilization. As technical progress is made with human stem cells, this knowledge can be applied to chimpanzee stem cells, providing a major source of information on gene expression in several embryonic and differentiated cell types, during various stages of in vitro development. If current approaches to tissue and organ engineering with human stem cells are successful, parallel studies of chimpanzee equivalents could provide further resources to study expression of genes and gene products and contribute to treatment of great ape diseases in the future.

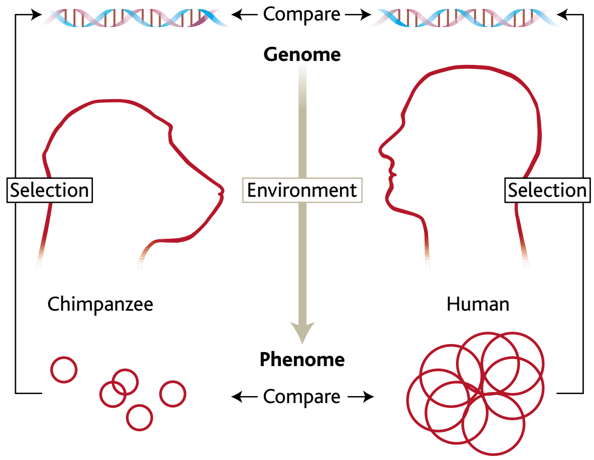

What makes us human? This question may be answered by comparison of human and chimpanzee genomes and phenomes, and ultimately those of other primates. To this end, we need to understand how genotype generates phenotype, and how this process is influenced by the physical, biological, and cultural environment.

Material for direct analysis of gene expression during embryonic development can, in principle, be obtained by controlled breeding and surgical termination of pregnancies. This approach is already well established for monkeys such as the rhesus macaque. A thorough study of gene expression during monkey embryonic development would be expensive, but it should be undertaken (*9*), perhaps only after studies of transgenic mice and chimpanzee stem cells have defined critical experimental questions that cannot be otherwise answered. We do not envision this being done with great apes because of ethical and practical considerations. As with humans, however, great ape samples may become available in the course of birth control or medical care.

The second reason for expanding research on chimpanzees and other apes is the lack of information on their phenotypes (*3*). The utility of the human genome has been greatly aided by our vast knowledge of the human phenome in areas ranging from anatomy to cognitive function. In contrast, our knowledge of the great ape phenome is inadequate, except in a few arenas such as behavior and ecology. Worse, extant information on great apes is in many scattered sources spanning the last century, and some accepted "facts" actually represent folklore derived from misinterpretations or assumptions made in popular science literature. Thus, there is no easy way to reliably ascertain all the known and unknown differences between humans and great apes. One possibility (*10*) is to develop a Web-based "Museum of Comparative Anthropogeny" that would catalog information about human-specific differences from great apes that is scattered throughout the literature. Having a centralized resource of such information could lead to new conceptual insights and multidisciplinary interactions and also point to ethically acceptable studies that would help to explain human-ape differences. Regardless, interpreting the results of functional genomics studies will require more information about ape phenomes. Thus, there should be substantially increased funding for studies on great ape anatomy, physiology, biochemistry, neurobiology, cognitive functions, behavior, and ecology. All such research should be done following ethical principles like those currently used in human studies. Much can also be learned in the course of providing outstanding medical care, as has been the case for humans. Increased knowledge about ape phenomes will likely be helpful for understanding some human diseases (*5*).

The third reason for expanding research on chimpanzees and other great apes is that the more we know about these species, the better we can care for them. This will be particularly important for captive apes, but could also have an impact on maintaining healthy wild populations (for example, by vaccinating them against human diseases). In this regard, making practical use of all the functional and behavioral knowledge arising from such research will require a significant increase in financial support for the optimal maintenance of captive great apes, and to facilitate survival of currently endangered wild populations. One way to coordinate funding for ape research and care is to create a Great Ape Conservation Trust that would receive 10% of all grant funds awarded by government agencies for research on ape genomes, phenomes, or behavior. The Trust could be administered by an agency that does not award research grants; instead, it would

CREDIT: PRESTON HUEY/*SCIENCE*

award grants only for the support of captive animals and the conservation of wild populations. The agency that administers the Trust could be either a governmental or nongovernmental group that already exists, or a new organization with representatives from various interest groups, particularly those with firsthand knowledge about conservation issues. The Trust could also be authorized to solicit and receive funds from nongovernmental sources.

With the sequencing of the chimpanzee genome, we have now reached the end of the beginning, and can start down the long road toward fully understanding our relationships to these closest evolutionary cousins. If the road is taken with intellectual and ethical care, there is much to gain, for both them and us.

References and Notes

1. The term "great ape" is used here in the colloquial sense. In the commonly used classification, these species are now grouped with humans in the family Hominidae, and humans belong to the tribe Hominini, along with chimpanzees and bonobos.
2. E. H. McConkey, M. Goodman, *Trends Genet.* **13**, 350 (1997).
3. A. Varki *et al.*, *Science* **282**, 239 (1998).
4. E. H. McConkey, A. Varki, *Science* **289**, 1295 (2000).
5. A. Varki, *Genome Res.* **10**, 1065 (2000).
6. Chimpanzee Sequencing and Analysis Consortium, *Nature* **437**, 69 (2005).
7. E.H. McConkey, *Cytogenet. Genome Res.* **105**, 157 (2004).
8. M.C.King, A. C. Wilson, *Science* **188**, 107 (1975).
9. E. H. McConkey, *Trends Genet.* **18**, 446 (2002).
10. M. V. Olson, A. Varki, *Science* **305**, 191 (2004).

11. The opinions expressed are strictly those of the authors. We thank K. Krauter, J. Moore, P. Gagneux, and N. Varki for helpful comments. Supported by the G. Harold and Leila Y. Mathers Charitable Foundation.

10.1126/science.1113863

PHYSICS

Manipulating Magnetism in a Single Molecule

Michael F. Crommie

The size of magnetic objects that can be manipulated in condensed-matter environments has decreased over the last 50 years, from bulk ferromagnets to thin films, nanocrystals, clusters, and now to single atoms and molecules (*1–7*). The single-atom or single-molecule regime is especially interesting because magnetism arises in this case from very few unpaired electronic spins and is thus quantum mechanical in nature. This property opens new opportunities that range from basic quantum impurity studies to quantum information and spintronics applications (*8*). Molecular systems, in particular, provide a useful means for "packaging" quantum spin centers, because molecules are structurally and electronically very flexible (*7*). This is readily seen in the work of Zhao *et al.* (*9*) on page 1542 of this issue. They show that it is possible to tune the spin behavior of a magnetic cobalt ion trapped within a single molecule by pruning the ligands of the molecule with the tip of a scanning tunneling microscope (STM).

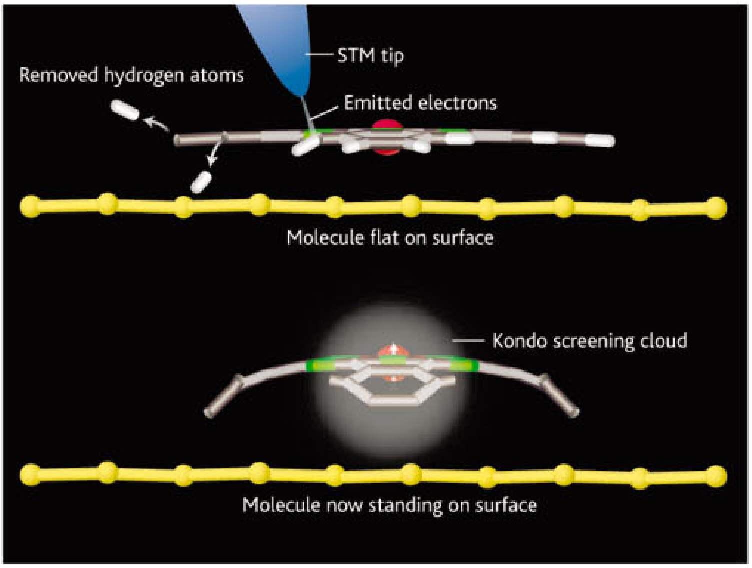

Molecular magnetic surgery. (Top) An STM tip is used to snip hydrogen atoms from a single cobalt phthalocyanine molecule lying on a gold surface. **(Bottom)** The trimmed molecule protrudes from the surface and is surrounded by a cloud of electrons that represent the Kondo screening cloud about the cobalt ion spin.

Zhao *et al.* observed this behavior by tunneling electrons from the tip of an STM into a single cobalt phthalocyanine (CoPc) molecule sitting on a gold surface, thereby performing a type of local electron spectroscopy. For pristine CoPc molecules they observed the d-orbital of the inner cobalt ion to be an energetically broad resonance lying below the Fermi energy (E_F, the energy of the highest occupied electronic level). After plucking hydrogen atoms from the periphery of the molecule with their STM, however, the broad d-resonance was replaced by a much narrower resonance pinned at E_F, indicating a change in the magnetic nature of the molecule (see the figure).

Monitoring the d-orbital of a magnetic nanostructure in this way allows one to study its magnetic properties. This is because magnetism in transition-metal ions (like the cobalt ion in CoPc) arises from unpaired spins residing in d-orbitals. When a single cobalt atom or cobalt-carrying molecule contacts a metal surface, the d-orbital hybridizes with the continuum states of the surface and broadens energetically into a resonance. If the resonance shifts below E_F, then electrons are transferred to the d-level, whereas if the resonance shifts above E_F, then charge is pulled out of it. The magnetic moment of the ion depends on how the d-orbital is filled with electrons, but the precise filling is difficult to determine when only a limited energy range is experimentally accessible.

This is where a subtle phenomenon known as the Kondo effect proves useful. The Kondo effect (*10*) describes the process by which electrons from a surrounding substrate magnetically screen the spin of a magnetic ion. This effect is driven by an interaction between the localized spin of the ion and the itinerant spins of the substrate, and induces the magnetic ion to effectively "capture" an electron spin from the substrate and loosely bind it in a net-zero-spin configuration (that is, the two spins cancel). The signature of the new bound state is a narrow resonance (the Kondo resonance) that appears at E_F and whose width (the Kondo temperature) gives a measure of the captured spin's binding energy (*10*). Historically, this effect has been observed in bulk materials containing magnetic impurities because a change in the density of states at E_F can significantly affect bulk properties such as magnetization, specific heat, and conductivity. More recently, the Kondo effect has been

The author is in the Physics Department, University of California, Berkeley, CA 94720, USA, and the Materials Sciences Division, Lawrence Berkeley National Laboratory, Berkeley, CA 94720, USA. E-mail: crommie@berkeley.edu

observed by STM for single atoms at surfaces in various configurations (*2–6*). Such Kondo physics play a role whenever localized spins interact with conduction electrons (*11*, *12*).

In their work with CoPc, Zhao *et al.* interpret the onset of the narrow resonance at E_F for their pruned (that is, dehydrogenated) molecules as a sign of the Kondo effect, and thus proof that the dehydrogenated molecules have a well-defined magnetic moment. This is in contrast to their pristine CoPc molecules, which show no Kondo resonance and are believed to be nonmagnetic. This central result is interesting because it demonstrates an ability to change the magnetic state of a molecule by directly modifying its structure via single-molecule manipulation. Mechanical (*13*) and electronic (*14*) properties of individual molecules have been manipulated previously, but the modification of single-molecule spin properties by Zhao *et al.* takes such manipulations to a new level. Their results are also somewhat surprising because they observe a Kondo temperature for the dehydrogenated molecule that is even higher than the Kondo temperature observed previously for bare cobalt atoms sitting on a similar substrate (*2*). Typically the Kondo temperature increases when an ion is more strongly contacted to a substrate (that is, more strongly electronically screened and/or hybridized with the substrate's continuum states). The results imply that the modified phthalocyanine molecular cage connects the interior cobalt atom more strongly to substrate electrons than if the atom were sitting on the substrate unadorned.

This counterintuitive result highlights how STM single-molecule studies help us to understand how molecules might be used to connect the electrodes of future electronic and spintronic devices. Currently, one of the greatest questions in molecular electronics is what happens at the contact between a molecule and a metal electrode. Many interesting effects have been observed in molecular transport experiments, including the Kondo effect (*15–17*), but the microscopic basis of much of this behavior remains a mystery. Experiments such as that reported by Zhao *et al.* form a beautiful complement to transport measurements because they provide direct microscopic evidence of how specific, well-characterized molecular contact configurations lead to different electronic and spin behaviors.

There are many exciting future possibilities in this area, including the exploration of other classes of magnetic molecules that show different spin behaviors. One example is molecules having high magnetic anisotropy energy ["single molecule magnets" (*7*)]. These molecules exhibit well-defined spin-up and spin-down states and have been suggested for numerous applications ranging from quantum information processing to data storage (*7*). Controlling spin at the single-molecule scale in these and related systems promises a new level of control in magnetic nanostructures.

References

1. F. J. Himpsel, J. E. Ortega, G. J. Mankey, R. F. Willis, *Adv. Phys.* **47**, 511 (1998).
2. V. Madhavan, W. Chen, T. Jamneala, M. F. Crommie, N. S. Wingreen, *Science* **280**, 567 (1998).
3. J. Li, W.-D. Schneider, R. Berndt, B. Delley, *Phys. Rev. Lett.* **80**, 2893 (1998).
4. H. C. Manoharan, C. P. Lutz, D. M. Eigler, *Nature* **403**, 512 (2000).
5. N. Knorr *et al.*, *Phys. Rev. Lett.* **88**, 096804 (2002).
6. A. J. Heinrich, J. A. Gupta, C. P. Lutz, D. M. Eigler, *Science* **306**, 466 (2004).
7. J. R. Long, in *Chemistry of Nanostructured Materials*, P. Yang, Ed. (World Scientific, Hong Kong, 2003), pp. 291–315.
8. I. Zutic, *Rev. Mod. Phys.* **76**, 323 (2004).
9. A. Zhao *et al.*, *Science* **309**, 1542 (2005).
10. A. C. Hewson, *The Kondo Problem to Heavy Fermions* (Cambridge Univ. Press, Cambridge, 1993).
11. D. Goldhaber-Gordon *et al.*, *Nature* **391**, 156 (1998).
12. S. M. Cronenwett, T. H. Oosterkamp, L. P. Kouwenhoven, *Science* **281**, 540 (1998).
13. F. Moresco *et al.*, *Phys. Rev. Lett.* **86**, 672 (2001).
14. R. Yamachika, M. Grobis, A. Wachowiak, M. F. Crommie, *Science* **304**, 281 (2004).
15. J. Park *et al.*, *Nature* **417**, 722 (2002).
16. W. Liang *et al.*, *Nature* **417**, 725 (2002).
17. L. H. Yu, D. Natelson, *Nano Lett.* **4**, 79 (2004).

10.1126/science.1117039

PHYSICS

Reduced Turbulence and New Opportunities for Fusion

Karl Krushelnick and Steve Cowley

Fusion has long been considered the energy source of the future—since its fuel supply (deuterium and lithium) is virtually limitless and the environmental impact is minimal. However, although fusion is a spectacularly successful energy source for the Sun, the practicalities of producing useful amounts of fusion energy in a laboratory on Earth are technically challenging—primarily because of the difficulty of confining a plasma (an ionized gas) heated to the hundred million degree Celsius temperatures necessary to induce nuclear fusion reactions. Recent findings about plasma behavior in such conditions, however, have led to new hope that the control of fusion plasmas may become much easier.

Enhanced online at www.sciencemag.org/cgi/content/full/309/5740/1502

The use of magnetic "bottles" to confine thermonuclear plasmas for fusion has been an active area of research since 1946 when Thomson and Blackman obtained a British patent for this concept (*1*). Enormous progress has been made since that time. The critical parameter, termed the energy confinement time, measures the time taken for the plasma energy to leak out of the magnetic bottle. In a fusion reactor this energy must be replaced by heat produced in the fusion reactions. The energy confinement time achieved in experiments has increased by six orders of magnitude since the 1960s. Today scientists are confining plasmas with temperatures around a hundred million degrees Celsius for many seconds in a toroidal (donut-shaped) magnetic field configuration called a tokamak. Despite such progress, the theoretical understanding of the physical causes of the leakage—so-called anomalous transport—is incomplete, and experimental techniques to reduce it are still being developed.

In an idealized situation, the motion of charged particles in a strong magnetic field is restricted to a tight spiral around the field lines. In a plasma, these particles will escape in the direction perpendicular to the field lines via a random walk as a result of infrequent collisions with one another (with the step size being the radius of the spiral). However, such "classical" diffusion of particles and thermal energy across magnetic fields lines should be about a thousand times slower than that actually observed in experiments. Indeed, if plasma confinement were as efficient as classical theory suggests, it is likely that fusion power stations would now dot the landscape and climate change would not be a particularly important issue.

Consequently, the experimentally observed diffusion rate was famously termed "anomalous transport" due to the lack of understanding of the physics behind this effect. Anomalous transport is a ubiquitous phenomenon in astrophysical, geophysical, and laboratory plasmas since it

The authors are in the Department of Physics, Imperial College London, London SW7 2AZ, UK. S. Cowley is also in the Department of Physics and Astronomy, University of California–Los Angeles, Los Angeles, CA 90095, USA. E-mail: kmkr@imperial.ac.uk, steve.cowley@imperial.ac.uk

turns out that plasmas are not quiescent or classical at all, but are always quivering with small-scale fluctuations in all of their parameters—density, temperature, and even the local microscopic magnetic and electric fields. It was clear by the late 1970s that these turbulent fluctuations in a tokamak were driven by the high-pressure plasma in the center expanding into the low-pressure outer regions. The fluctuating, turbulent, electric and magnetic fields move the particles across the mean field in convective eddylike motions—much more quickly than classical diffusion. The transport of heat and particles across the field is effectively a random walk with an enhanced step length and short correlation time. The density fluctuations in a computer simulation of a tokamak can be seen in the figure. The eddies are characteristically elongated along the field lines and have small-scale lengths perpendicular to the field.

The complexity of this turbulence is immense. For example, the shape of the magnetic bottle, the profiles of plasma density and temperature within the bottle, and the microscopic dynamics of both ions and electrons all play critical roles (*2–4*). Furthermore, the turbulence can exist on many different spatial scales simultaneously. Indeed, it is also possible that turbulence excited in one region of the plasma can produce transport in another. A concerted effort to measure, understand, and model the turbulence has brought significant results in recent years. One of the most important is the development of sophisticated computational models (*5–8*)—the figure, for example, was produced with such a model. These models make quantitatively accurate predictions in many situations. However, some of the most exciting experimental results, in which turbulence has been observed to be substantially reduced, cannot yet be accurately predicted by the codes.

The first such observation occurred in 1982 at the ASDEX experiment at the Max-Planck Institute for Plasma Physics near Munich, Germany—where the so-called H-mode (or high-confinement mode) for tokamak operation was discovered (*9*). It was found that when the heat leaking out of the plasma reached a critical threshold, a radial electric field, a plasma velocity gradient, and a steep pressure gradient spontaneously arose at the edge of the plasma. This led to a dramatic enhancement of the confinement time and was presumed to be the result of a reduction in turbulent transport at the edge. This was consequently termed an "edge transport barrier," which kept plasma particles and thermal energy from escaping to the material walls of the device. It was surprising and gratifying to the researchers that—almost by itself—the plasma had found a way to reduce the turbulence, if only in a small region of the plasma.

It was subsequently discovered, in the 1990s, that such transport barriers do not only exist at the edge of the plasma, but can also be produced in the interior regions of the plasma (so-called internal transport barriers, ITBs) (*10*). These transport barriers in the core can be induced by rapid localized changes to the "twist" of the magnetic fields of the tokamak (reversed magnetic shear) or to the plasma drift velocity (velocity shear). ITBs have enabled access to enhanced performance regimes of these tokamaks and have generated much excitement throughout the research community. However, precise measurements of the reduction of turbulence in one of these ITBs near the core region has been very difficult. In fact, only recently have experimental techniques been developed to determine which components of the turbulence are being suppressed within a transport barrier.

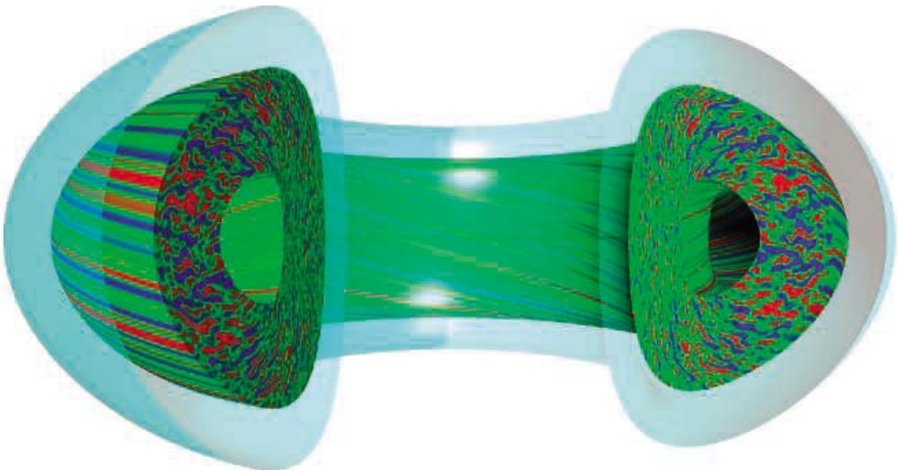

A new twist. Gyro-kinetic simulation of plasma density fluctuations in a shaped tokamak. Image shows a cut-away view of the density fluctuations (red/blue colors indicate positive/negative fluctuations). The blue halo is the last closed magnetic flux surface in the simulated tokamak.

CREDIT: JEFF CANDY/GENERAL ATOMICS CORP.

New measurements at the JT-60U tokamak in Japan by a team led by Nazikian from the Princeton Plasma Physics Laboratory have used microwave reflectometry to determine that the density correlation length of the plasma fluctuations is reduced substantially during the establishment of an internal transport barrier—from about 20 cm to 4 mm—and that this corresponds to a reduction in turbulence (*11*). The radius of the plasma is about 1 m in JT-60U.

The recent discoveries about turbulence and control of turbulent transport through transport barriers and progress in both experimental measurements and improved (predictive) simulation capabilities are now leading to renewed optimism for fusion as an energy source and confidence that new designs for fusion experiments will indeed work. However, the large-scale "reactor-relevant" experiments in which many of these discoveries were made—the Joint European Torus (JET) in the United Kingdom, JT-60U in Japan, and the Tokamak Fusion Test Reactor (TFTR) in the United States—were constructed more than 20 years ago. The next critical step in fusion research is the International Thermonuclear Experimental Reactor (ITER), a US$5 billion project, which is planned to be operational in 2015 in Cadarache, France (*12–16*). Edge transport barriers are key to ITER achieving a "burning" fusion plasma. Advanced operational regimes using internal transport barriers are also planned for ITER.

Such experiments may enable fusion power to be economical sooner than anyone has previously thought. For the past 40 years, some have criticized the fusion community for perpetually claiming to be only 30 years away from realizing success. As of today, fusion power may be much closer than that.

References and Notes

1. Original patent reproduced in M. G. Haines, *Plasma Phys. Control. Fusion* **38**, 643 (1996).
2. W. Horton, *Rev. Mod. Phys.* **71**, 735 (1999).
3. T. L. Rhodes *et al.*, *Phys. Plasmas* **9**, 2141 (2002).
4. X. Garbet *et al.*, *Plasma Phys. Control. Fusion* **46**, B557 (2004).
5. A. Dimits *et al.*, *Phys. Rev. Lett.* **77**, 71 (1996).
6. Z. Lin *et al.*, *Science* **281**, 1835 (1998).
7. W. Dorland *et al.*, *Phys. Rev. Lett.* **85** 5579 (2000).
8. J. Candy, R. E. Waltz, *Phys. Rev. Lett.* **91**, 045001(2003).
9. F. Wagner *et al.*, *Phys. Rev. Lett.* **49**, 1408 (1982).
10. Y. Koide *et al.*, *Phys. Rev. Lett.* **72**, 3662 (1994).
11. R. Nazikian *et al.*, *Phys. Rev. Lett.* **95**, 135002 (2005).
12. R. Aymar, P. Barabaschi, Y. Shimomura, *Plasma Phys. Control. Fusion* **44**, 519 (2002).
13. X. Litaudon *et al.*, *Plasma Phys. Control. Fusion* **46**, A19 (2004).
14. The ITER Web page is at www.iter.org.
15. D. Clery, D. Normile, *Science* **309**, 28 (2005).
16. D. King, *Nature* **428**, 891 (2004).

10.1126/science.1113477

INTRODUCTION

In the Forests of RNA Dark Matter

For a long time, RNA has lived in the shadow of its more famous chemical cousin DNA and of the proteins that supposedly took over RNA's functions in the transition from the "RNA world" to the modern one. The shadow cast has been so deep that a whole universe (or so it seems) of RNA—predominantly of the noncoding variety—has remained hidden from view, until recently.

Nor is RNA quite so inert or structurally constrained as its cousin; its conformational versatility and catalytic abilities have been implicated at the very core of protein synthesis and possibly of RNA splicing. Noller (p. 1508) discusses how the basic building block of RNA—the double helix—has been fashioned into the intricate "protein-like" three-dimensional surfaces of the ribosome. A further parallel between RNA and protein is revealed in the structure of an RNA group I self-splicing intron, which uses an arrangement of two metal ions for phosphoryl transfer much like that seen in many protein enzymes (p. 1587). Another group I–like intron catalyzes the formation of a tiny RNA lariat, a reaction strikingly similar to one seen in group II introns and spliceosomal introns (pp. 1584 and 1530). This unusual lariat, at the very 5′ end of the resultant mRNA, is suggested to help protect the mRNA from degradation. The dynamics of the RNA messages passed between nucleus and cytoplasm provide a complex and sophisticated layer of regulation to gene expression, covered by Moore (p. 1514), who describes the teams of proteins that escort and regulate mRNA throughout the various stages of its life (and death). Death for many mRNAs occurs in cytoplasmic foci called P-bodies, which can also act as temporary storage depots for nontranslating mRNAs (see the *Science* Express Report by M. Brengues *et al.*).

Small noncoding microRNAs (miRNAs) have been found in such abundance that they have been christened the "dark matter" of the cell, a view reinforced by an analysis of the small RNAs found in *Arabidopsis* (pp. 1567 and 1525). The role of miRNAs and of their close cousins small interfering RNAs (siRNAs) in RNA silencing is discussed by Zamore and Haley (p. 1519), and illustrated in the poster pullout in this issue and in research showing that miRNAs can repress the initiation of translation (p. 1573) and, intriguingly, can also increase mRNA abundance (p. 1577). [See also this week's online Science of Aging Knowledge Environment (SAGE KE) and Signal Transduction Knowledge Environment (STKE)]. The phrase "dark matter" could well be ascribed to noncoding RNA in general. The discovery that much of the mammalian genome is transcribed, in some places without gaps (so-called transcriptional "forests"), shines a bright light on this embarrassing plentitude: an order of magnitude more transcripts than genes (pp. 1559, 1564, and 1529). Many of these noncoding RNAs (p. 1527) are conserved across species, yet their functions (if any) are largely unknown: A cell-based screen shows one, NRON, to be a regulator of the transcription factor NFAT (p. 1570). Of course, in some cases it is the act of transcription that is the regulatory event, as in the case of the transcriptional regulation of recombination (p. 1581). Finally, even the coding and base-paring capacity of RNA can be altered—by RNA editing, in which bases in the RNA are changed on the fly. Analysis of editing enzymes (p. 1534) reveals that the cell-signaling molecule IP_6 is required for their editing activity.

–GUY RIDDIHOUGH

CREDIT: Y. HAYASHIZAKI AND K. SHIMOKAWA

CONTENTS

REVIEWS

1508 **RNA Structure: Reading the Ribosome**
H. F. Noller

1514 **From Birth to Death: The Complex Lives of Eukaryotic mRNAs**
M. J. Moore

Poster: RNA Silencing

1519 **Ribo-gnome: The Big World of Small RNAs**
P. D. Zamore and B. Haley

VIEWPOINTS

1525 **It's a Small RNA World, After All**
M. W. Vaughn and R. Martienssen

1527 **The Functional Genomics of Noncoding RNA**
J. S. Mattick

1529 **Fewer Genes, More Noncoding RNA**
J.-M. Claverie

1530 **Capping by Branching: A New Ribozyme Makes Tiny Lariats**
A. M. Pyle

See also related* Science *Express Report by M. Brengues* et al.*; Research Article p. 1534; Reports pp. 1559 to 1590; SAGE KE and STKE material on p. 1451 or at www.sciencemag.org/sciext/rna/

Science

RNA Structure: Reading the Ribosome

Harry F. Noller

The crystal structures of the ribosome and its subunits have increased the amount of information about RNA structure by about two orders of magnitude. This is leading to an understanding of the principles of RNA folding and of the molecular interactions that underlie the functional capabilities of the ribosome and other RNA systems. Nearly all of the possible types of RNA tertiary interactions have been found in ribosomal RNA. One of these, an abundant tertiary structural motif called the A-minor interaction, has been shown to participate in both aminoacyl-transfer RNA selection and in peptidyl transferase; it may also play an important role in the structural dynamics of the ribosome.

As awareness of the biological importance of RNA continues to unfold, the ways in which the structural properties of RNA enable its functional capabilities are becoming all the more interesting. For more than 20 years, our understanding of RNA structure was based almost entirely on the x-ray crystal structure of the 25-kD transfer RNA (tRNA), which appeared in 1974 (*1*, *2*). The widespread lack of success in obtaining useful crystals of other RNA molecules discouraged efforts to solve new structures of more complex RNA molecules. Except for x-ray structures of the smaller hammerhead ribozyme (*3, 4*) no new RNA structures of comparable size appeared until the 160-nucleotide (nt) P4-P6 domain of the group I ribozyme, in 1996 (*5*). Only 4 years later, the first high-resolution x-ray crystal structures of the ribosomal subunits emerged (*6*–*8*), suddenly increasing information on RNA structure by two orders of magnitude (Fig. 1) (*9*, *10*). It is now possible to see directly how RNA can be folded into this breathtakingly intricate and graceful globular 2.5-MD structure containing over 4500 nt and more than 50 proteins, related versions of which are responsible for synthesis of proteins in all cells. The lessons learned from these structures not only address the function and assembly of ribosomes but provide an enormous database for interpreting and predicting the structures of the numerous other cellular RNAs and ribonucleoproteins (RNPs), giving new insights into the structural basis of RNA function as well as how life might have originated in an RNA world (*11*).

Lessons from tRNA

Many principles of RNA structure were gleaned from the structure of the 76-nt $tRNA^{Phe}_{yeast}$ (*1*, *2*). It showed that RNA forms double-helical structures with Watson-Crick base pairing but also that the presence of ribose in RNA has a profound influence on its structure. tRNA was found to contain many noncanonical base pairs, and even base triples, that allow it to fold into its unique three-dimensional structure. Inspection of its structure reveals a strong tendency for its strands to follow an A-helical path, even in non-base-paired regions. For example, hairpin turns are accomplished not by incremental bends in the RNA chain but by abrupt local changes in direction, usually centered around one or two nucleotides. A commonly observed motif is the U turn, seen in the anticodon loop of tRNA, which involves hydrogen bonding of the N3 position of a uridine with the phosphate group of a nucleotide three positions downstream, causing an abrupt reversal in direction of the RNA chain. The tRNA structure also revealed the coaxial stacking of RNA helices: The 7-base-pair (bp) acceptor stem stacks on the 5-bp T stem to form one continuous A-form helical arm of 12 bp (Fig. 2B). The other two helices, the D stem and anticodon stem, also stack, although imperfectly, to form a second helical arm. The two coaxially stacked arms form the familiar L form of tRNA (Fig. 1). Coaxial stacking is a common feature of RNA and is widespread in rRNA, where continuous coaxial stacking of as many as 70 bp is found (Fig. 2). In spite of the wealth of information provided by the 76-nt tRNA, many other common features of RNA structure were absent.

The Post-tRNA Renaissance

In the absence of new RNA crystals, nuclear magnetic resonance (NMR) spectroscopists began to solve the structures of small RNAs, quickly adding to the diversity of known RNA folding motifs (*12*). The ability of small ligands to stabilize or rearrange RNA structure was exemplified by the dramatic structural rearrangement of the HIV TAR RNA induced by binding a single arginine residue (*13*).

One of the first rRNA structures obtained by NMR spectroscopy was the sarcin-ricin loop (SRL) of 28S rRNA (*14*), a structure that interacts with elongation factors EF1 and EF2 and is targeted by the lethal ribotoxins α-sarcin and ricin. The compact 29-nt structure was found to contain several purine-purine base pairs, a tetraloop, and a bulged guanosine adjacent to a reverse Hoogsteen A-U pair. It is stabilized by stacking of bases from opposite strands (termed cross-strand stacking) and H-bonding between imino protons of guanines and phosphate oxygens. The zig-zag fold of its backbone (the S turn), along with its other features, have been identified as recurring motifs in RNA structures.

Although NMR spectroscopy sidestepped the difficult problem of crystallizing RNA, it is limited to structural analysis of molecules with an upper size limit of about that of tRNA. This led

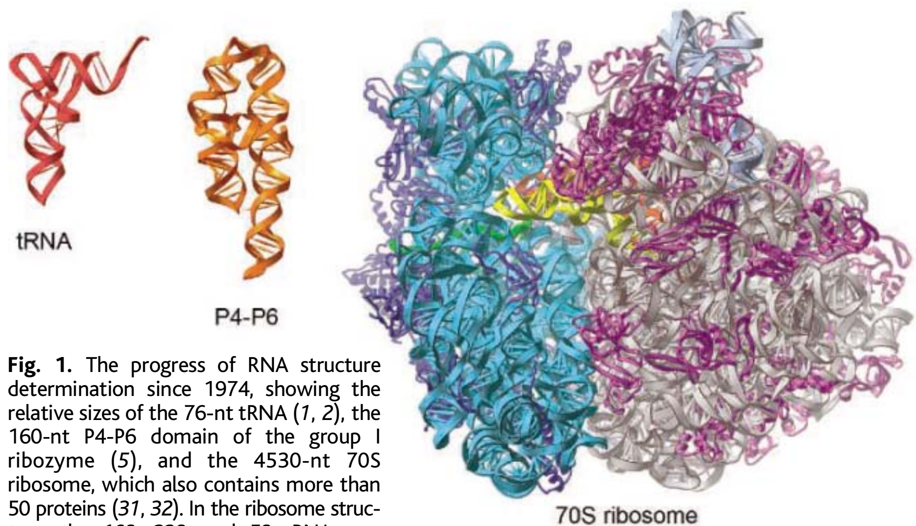

Fig. 1. The progress of RNA structure determination since 1974, showing the relative sizes of the 76-nt tRNA (*1*, *2*), the 160-nt P4-P6 domain of the group I ribozyme (*5*), and the 4530-nt 70S ribosome, which also contains more than 50 proteins (*31*, *32*). In the ribosome structure, the 16S, 23S, and 5S rRNAs are colored cyan, gray, and gray-blue, respectively, and the small and large subunit ribosomal proteins are dark blue and magenta, respectively. Two tRNAs (yellow and orange) and a mRNA (green) are visible inside the ribosome.

Center for Molecular Biology of RNA, Department of Molecular, Cell, and Developmental Biology, Sinsheimer Laboratories, University of California, Santa Cruz, Santa Cruz, CA 95064, USA.

to an increased effort to improve methods for RNA crystallization (*15*). An encouraging sign was the appearance of the first crystal structures of a catalytic RNA, the hammerhead ribozyme, solved first as an RNA-DNA chimera and subsequently as an all-RNA structure (*3*, *4*). Both structures revealed essentially the same fold, with three helices arranged in a Y configuration containing a U turn at the three-helix junction. Scott and coworkers have gone on to solve the structures of four additional constructs by using strategies that trap the hammerhead ribozyme in different states of its catalytic cycle, revealing for the first time a detailed high-resolution "movie" of the mechanism of action of a catalytic RNA (*16*). Since the hammerhead structure, crystal structures of three more ribozymes have been solved, including the hepatitis delta virus ribozyme (*17*), the hairpin ribozyme (*18*), and the group I self-splicing intron (*19–21*), providing the structural basis for understanding their respective catalytic mechanisms.

The first RNA structure to be solved that exceeded the size of tRNA was the 160-nt P4-P6 domain of the *Tetrahymena* group I intron at 2.8 Å resolution (*5*). It consists of two extended coaxial helical elements connected at one end by an internal loop containing a 150° bend (Fig. 1). For the first time, examples could be seen of the kinds of RNA-RNA interactions that are used to stabilize the packing of RNA helices into larger, more complex globular structures. One of these has been named the A-minor motif (*22*), one of the most abundant long-range interactions in rRNA, in which single-stranded adenosines make tertiary contacts with the minor grooves of double helices. A-minor interactions also play important functional roles. Helix-helix interactions were also formed by ribose zippers involving H bonding between the 2′-hydroxyl group of a ribose in one helix and the 2′-hydroxyl and the 2-oxygen of a pyrimidine base (or the 3-nitrogen of a purine base) of the other helix between their respective minor groove surfaces. In addition, close approach of phosphates was often mediated by bound hydrated magnesium ions. A recurring motif in the P4-P6 structure, called the A platform, positions adenines side by side in a pseudo–base pair within a helix, opening the minor groove for interactions with nucleotides from noncontiguous RNA strands.

rRNA Secondary Structure Prediction

Long before the first ribosome crystal structures appeared, the essential features of rRNA secondary structures were correctly predicted by using comparative sequence analysis (*23–25*). At about this same time, Michel and colleagues used a similar approach to establish the secondary structures of group I introns (*26*). Comparative analysis establishes base pairing by identification of compensating base changes in complementary nucleotides between two or more sequences. This approach was first explicitly applied by Fox and Woese (*23*), who, studying 5S rRNA sequences as phylogenetic markers, realized there was a common secondary structure that was compatible with several different sequences. Comparative analysis was used on the large 16S and 23S rRNAs from the outset; consequently, their main secondary structure features were deduced rather quickly (*24*, *25*), to be confirmed crystallographically some 20 years later. Even some rRNA tertiary interactions were discovered by comparative analysis (*27*, *28*), as had been the case earlier for tRNA (*29*). The secondary structures of most globular RNAs have been determined by comparative analysis, including ribonuclease (RNase) P RNA, the group I and group II self-splicing introns, snRNAs, and telomerase RNA. For some RNAs, such as in vitro–selected RNA aptamers and ribozymes, a lack of phylogenetic sequence information has been overcome by introducing base variation with the use of either site-directed or random mutagenesis (*30*).

About 60% of the nucleotides in the large rRNAs are involved in Watson-Crick base pairing. However, the unpaired bases are not distributed evenly among the four bases. In *Escherichia coli* 16S rRNA, for example, the proportions of unpaired bases for G, C, and U are 31%, 29%, and 33%, respectively, whereas 62% of As are unpaired (*27*), a tendency that extends to other functional RNAs. The preponderance of unpaired adenosines reflects their participation in special tertiary interactions.

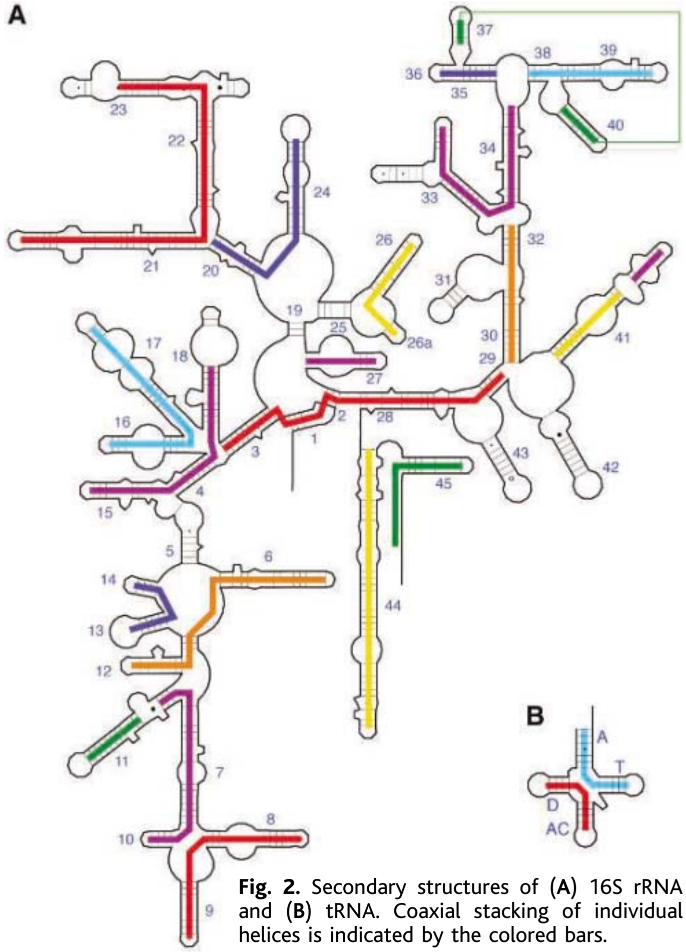

Fig. 2. Secondary structures of (**A**) 16S rRNA and (**B**) tRNA. Coaxial stacking of individual helices is indicated by the colored bars.

Implications for RNA Tertiary Structure

The ribosome and its subunits are the largest asymmetric structures that have been solved so far by crystallography. The 2.4 Å *Halocarcula marismortui* 50S subunit structure (*8*) and the ~3 Å *Thermus thermophilus* 30S subunit structure (*6*, *7*) provided the first detailed views of the molecular interactions that are responsible for the structures of both ribosomal subunits. A 5.5 Å structure of a functional complex of the *T. thermophilus* 70S ribosome revealed the positions of the tRNAs and mRNA and their interactions with the ribosome, as well as the features of the intersubunit bridges (*31*, *32*). Many co-crystals of ribosomes and subunits containing tRNA and mRNA fragments, protein factors, and antibiotics have now been solved in an effort to understand the mechanism of translation (*33*). These analyses have been complemented by extensive cryogenic electron microscopy (cryo-EM) reconstruction studies, which have led to lower-resolution structures for many functional complexes of the ribosome that have so far defied crystallization (*34*).

Many long-standing questions were immediately resolved by the crystal structures. A critical issue was whether the rRNA merely serves as a structural scaffold, or whether it is directly involved in ribosomal function. The structures showed that rRNA in fact does both of these things, creating the structural framework for the ribosome, and at the same time forming the main features of its functional sites, confirming that the ribosome is indeed a ribozyme (*35*).

It was already clear from the secondary structures of 16S and 23S rRNA that they are organized into domains of a few hundred nu-

cleotides each, four for 16S rRNA and six for 23S rRNA (*24*, *25*). The three major domains of 16S rRNA were assigned to the head, body, and platform features of the low-resolution EM structure for the 30S subunit (*36*, *37*), and this has been confirmed by crystallography (*6*, *7*). Their structural autonomy appears to facilitate their independent movement during translation. The six domains of 23S rRNA are more closely packed against one another (*8*) and were not distinguishable as separate domains of the 50S subunit at low resolution.

Comparative analysis of 16S and 23S rRNA secondary structure also provided a sense of the allowed variation in the sizes of the different helical elements (*24*, *25*, *27*). Some helices are strictly conserved in length, showing no phylogenetic variation. Others vary, showing both shorter and longer versions relative to *E. coli* in different phylogenetic branches. In some cases, shortening but not lengthening is permitted. These observations can now be interpreted in view of the three-dimensional structures. Variable-length helices are always found on the surface, distant from the functional center of the ribosome, with their extensible ends pointing into the solvent. Ones that can be shortened, but not lengthened, have ends whose maximum lengths are restricted by potential clash with other structural elements.

The hundreds of individual rRNA helices in the ribosome allow us to draw new generalities about RNA secondary structure. Most rRNA helices terminate at both ends in G-C pairs. As predicted from sequence analysis and chemical probing studies, noncanonical A-G pairs often flank the ends of helices (*38*, *39*). The crystal structures show that they are most commonly sheared A-G pairs, as well as Watson-Crick-like A-G imino pairs (*40*, *41*). As first observed for tRNA, bases that fall into nonhelical (so-called single-stranded) regions of the secondary structure are typically found to be highly structured, participating in H bonding and stacking interactions with other elements of the RNA. Of the 25 possible kinds of noncanonical base pairs involving two or more hydrogen bonds (*40*, *41*), 20 are found in the ribosome. For example, the sheared A-G pair is represented 20 times in 16S rRNA and 46 times in 23S rRNA, and there are 7 and 22 examples, respectively, of the reverse Hoogsteen A-U pair. Westhof and co-workers have made a comprehensive study of the kinds of noncanonical interactions that appear in RNA and their geometric and stereochemical classification (*42*, *43*).

Among the most interesting structural motifs are the A-minor interactions, of which hundreds of examples are found in rRNA (*22*). In these motifs, single-stranded adenosines reach into the minor groove of a helix, making both H bonding and van der Waals contacts. They are not simply base-base interactions, but nucleoside-nucleoside interactions, because crucial contacts are also made with the riboses as well as the bases (Fig. 3). Pairs of consecutive A-minor interactions are often found, in which two adjacent adenosines sequentially form type II and type I interactions (although some type II interactions are also made by guanosines) with adjacent base pairs (Fig. 3, A and B), which are typically G-C pairs. Although they form many important structural contacts, they are also intimately involved in ribosome function. For example, the 3′-terminal adenosines of both the A- and P-site tRNAs are positioned in the peptidyl transferase site by A-minor interactions with 23S rRNA (*35*). An elegant RNA-based mechanism using the A-minor motif occurs in the decoding site of the 30S subunit (*44*), where the stereochemical fit of codon-anticodon pairing is monitored by A-minor interactions between A1492 and A1493 of 16S rRNA (supported by additional interactions from G530) and the minor groove surface of the codon-anticodon helix (Fig. 3, C to E). The prevalence of A-minor interactions in rRNA helps to account for the overrepresentation of single-stranded adenosines in rRNA secondary structures.

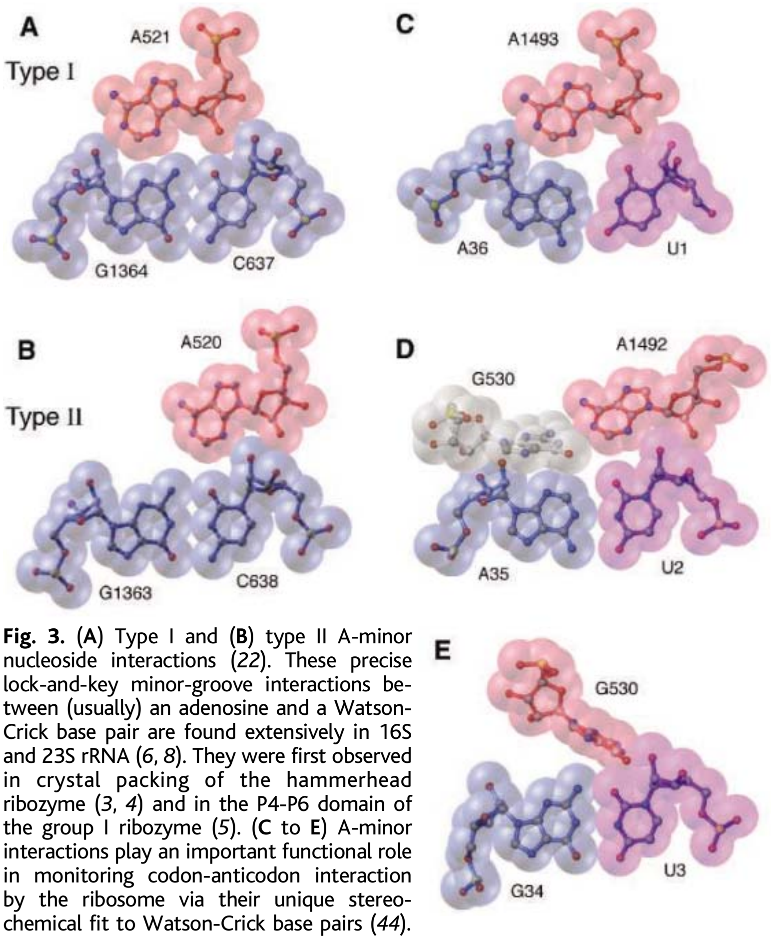

Fig. 3. (**A**) Type I and (**B**) type II A-minor nucleoside interactions (*22*). These precise lock-and-key minor-groove interactions between (usually) an adenosine and a Watson-Crick base pair are found extensively in 16S and 23S rRNA (*6*, *8*). They were first observed in crystal packing of the hammerhead ribozyme (*3*, *4*) and in the P4-P6 domain of the group I ribozyme (*5*). (**C** to **E**) A-minor interactions play an important functional role in monitoring codon-anticodon interaction by the ribosome via their unique stereochemical fit to Watson-Crick base pairs (*44*).

About half of the helices in rRNA terminate in hairpin loops. In *T. thermophilus* 16S rRNA, 17 of its 32 hairpin loops are tetraloops (Fig. 2), first identified as the most common type of hairpin loop in rRNA by inspection of their phylogenetically derived secondary structures (*45*). As found for many RNAs, the GNRA tetraloop is most common in rRNA, representing about half of the observed tetraloops. The other hairpin loops use a variety of strategies to execute their turns. In 16S rRNA, there are five examples of U turns, and G turns are also found, in which the stabilizing hydrogen bond to the backbone phosphate is made from the N1 position of a guanine base; these include the G turns that are an intrinsic feature of GNRA tetraloop structures. Indeed, G(N1)-phosphate H bonds are widespread, making many kinds of base-backbone interactions in addition to G turns, of which there are dozens of examples in both 16S and 23S rRNA.

It has been said that "tRNA looks like Nature's attempt to make RNA do the job of a protein" (*46*). rRNA takes this notion to the extreme, representing the limit of what can be done to make a globular, functional molecule out of RNA, beyond which nature has resorted to proteins. The basic building block of RNA structure, the double helix, greatly restricts the ability of RNA to form globular structures because of its rigidity and limited geometry. How then, does RNA manage to form a structure such as the ribosome, with its complex, curving three-dimensional surfaces, stereospecific binding pockets, and other intricate molecular features? Almost all rRNA helices contain seven or fewer contiguous Watson-Crick base pairs, in spite of the fact that the overall dimensions of the ribosome (~250 Å) would in principle allow for continuous heli-

ces of as many as 80 bp. A general strategy found throughout the ribosome is to connect these short helices by bulge loops or internal loops of unequal length, introducing bends that allow a high degree of structural curvature. The connecting loops themselves are highly structured, rich in noncanonical base pairs as well as base-phosphate and base-ribose interactions that constrain the geometries of the individual bends. Indeed, bases that are not involved in either Watson-Crick or some kind of noncanonical interaction are very rare, explaining why so few bases are reactive toward chemical probes and their inability to hybridize with oligonucleotide probes. Some of the connecting loop features have been recognized as recurring motifs in RNA structure: for example, the S turn motif and the kink turn that creates a sharp 120° angle between two adjacent helices (*47*).

These irregular compound helices are packed against one another to form the final globular structure. Earlier, it was thought that RNA-RNA packing would be mediated by the basic ribosomal proteins to alleviate charge repulsion between the high density of negatively charged phosphate groups lining the RNA backbone. It was therefore surprising to find extensive regions of closely packed RNA helices containing little or no protein. Packing of RNA structural elements is of special interest in the functional sites, which are mostly devoid of proteins. In fact, ribosomal proteins are found mainly on the outer surface of the ribosome, although many of them contain long, unstructured tails that penetrate the RNA (*48*, *49*). Not surprisingly, both divalent and monovalent cations as well as polyamines, which have long been known to be essential for the structural and functional integrity of ribosomes, mediate RNA-RNA packing interactions in the ribosome, helping to neutralize phosphate-phosphate repulsion (*50*). The ribose zipper (*5*) is yet another strategy that is used for packing the minor grooves of rRNA helices against each other.

Folding of RNA differs in many ways from that of proteins. There are only four types of nucleotide monomers; there are six backbone torsion angles, instead of two; and RNA structure is not nucleated by a hydrophobic core, as are most proteins. Instead, RNA folding uses the two principle devices that were first seen in the double-helical structures of DNA and RNA: hydrogen bonding and base stacking.

An example of how noncanonical H-bonded interactions can direct the packing of RNA helices is the helix 6–helix 8 interaction in 16S rRNA (*6*) (Fig. 4). These two helices pack against each other at a 90° angle, via their respective minor-groove surfaces. They are positioned by two layers of coplanar bases that form two exquisitely stereospecific H-bonded networks. Both layers contain central A-minor interactions in which adenosines in helix 8 bind to receptors in helix 6, forming the heart of the interhelical connection. The upper (yellow) layer is formed by interaction of the minor-groove side of a Watson-Crick G-C pair in helix 6 through a type II A-minor interaction with the adenosine of a noncanonical Hoogsteen base pair in helix 8. The lower (red) layer is formed from a noncanonical A-G-G base triple, of which one of the guanosines forms the receptor for a Type I A-minor interaction from an adenosine involved in a noncanonical A-C pair in helix 8. The positions of both of the A-minor adenosines are constrained by their additional base-base interactions, tightly restricting the overall geometry. It seems counterintuitive that this apparently coplanar arrangement of bases results in a 90° packing angle between the two helices. This is the result of three effects: first, the bases of RNA helices are tilted at an angle to the helical axis; second, the adenine bases in A-minor interactions typically form ~30° angles with the planes of their receptor bases; and third, the adenines are held at an angle to helix 8 by additional noncanonical base-base interactions.

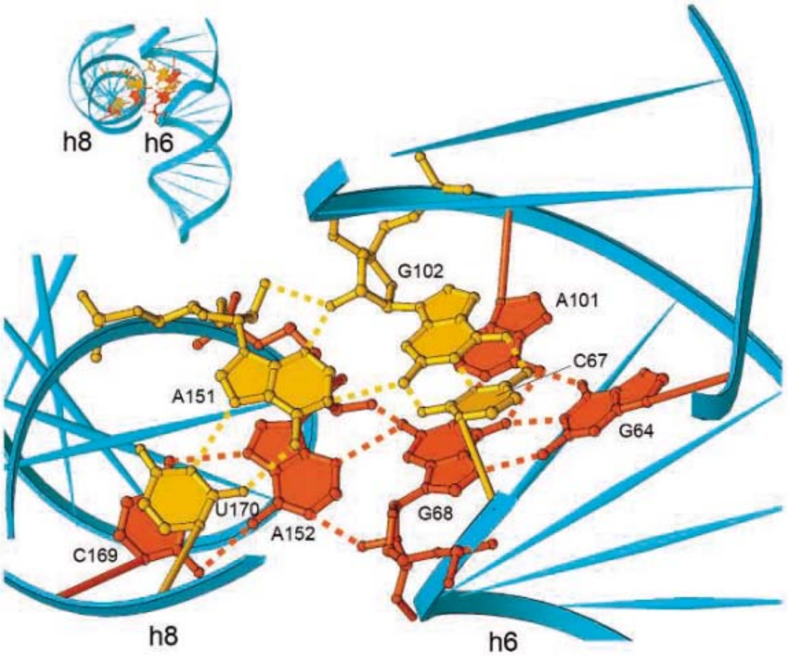

Fig. 4. An example of how the ribosome packs two helices (h6 and h8) in 16S rRNA together at right angles to each other (6). Two layers of nucleotides (yellow and red) form extensive hydrogen-bonded networks (dotted lines) that precisely locate the two helices. In the top (yellow) layer, nucleotide A151 in h8 makes a type II A-minor interaction with the G102-C67 base pair in h6, itself bolstered by a Hoogsteen pair with U170. In the bottom (red) layer, A152 of h8 makes a type I A-minor interaction with a Watson-Crick-like pair between G68 and A101 of h6. Both A152 and its A-G receptor are bolstered by additional noncanonical base pairings with C169 and G64.

In addition to coaxial stacking of helices, the ribosome contains some remarkable examples of base stacking of unpaired bases, such as in the noncanonical structure known as helix 70 in 23S rRNA (Fig. 5). Helix 70 is located at the subunit interface of the 50S subunit near the geometric center of the ribosome (*8*). It forms the attachment point for helix 69, which interacts with both the A- and P-site tRNAs, as well as forming a bridge to the decoding site of 16S rRNA (*31*, *32*). Its compact, 23-nucleotide structure is a tour de force of noncanonical complexity and is one of the most conserved features of rRNA. It contains no fewer than four systems of stacked bases, one of which is bifurcated to form a short fifth stack. Although helix 70 superficially resembles a normal RNA helix, it in fact contains only a single canonical Watson-Crick base pair (G1964-C1934). Although its role in translation is not known, the projection of bases A1966 and U1944 into the minor grooves of the functionally important helices 93 and 92, respectively, are suggestive of some relationship to the peptidyl transferase activity of the ribosome.

rRNA folds correctly only by assembling with ribosomal proteins, which appear to stage the order of folding of rRNA during ribosome assembly to avoid losing improperly folded ribosomes in kinetic traps. Their role in translational function appears to be subordinate to that of rRNA, helping to improve the efficiency and accuracy of mechanisms that are based on RNA. This view is supported by their location mainly on the exterior of the ribosome, away from the functional subunit interface region (*6*–*8*, *31*, *32*). Further evidence comes from the observation that at least one-third of the ribosomal proteins can be deleted singly without conferring a lethal phenotype (*51*). Nearly all ribosomal proteins interact directly with rRNA, and few have contact with other ribosomal proteins. They are typically small and basic, representing a diverse collection of structural types that span the range of known protein folds, giving the

impression that they were recruited to the ribosome in many independent evolutionary events. As mentioned above, some ribosomal proteins have long, unstructured tails that penetrate, and co-assemble with, the rRNA (*48*, *49*). The C-terminal tails of proteins S9 and S13 contact the anticodon stem loop of tRNA in the 30S P site; cells in which the S9 and S13 tails have been deleted are viable, showing that these interactions are not essential for ribosome function (*52*). In keeping with their diverse structures, their rRNA binding sites are comparably diverse, comprising both helical and loop features; unlike DNA-binding proteins, ribosomal proteins mainly recognize higher-order structural features of rRNA, rather than base sequence (*48*, *49*). Binding to rRNA helices occurs preferentially on their minor-groove surfaces. Apart from contributing to the neutralization of negative charges on the rRNA backbone, ribosomal proteins are known to stabilize certain tertiary folds (*53*) and to help fix the relative orientation of helices at multihelix junctions (*54*). Indeed, proteins may have initially evolved to extend the structural repertoire of RNA in an RNA world (*55*).

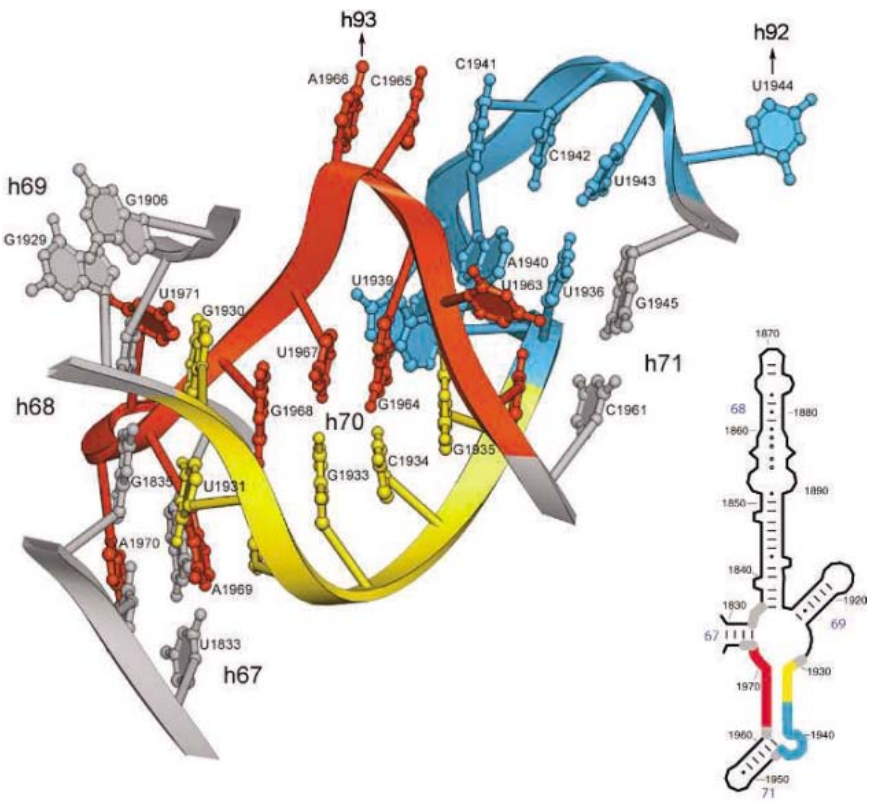

Fig. 5. Helix 70 of 23S rRNA (*8*) contains four different systems of stacked bases and contains only a single canonical Watson-Crick base pair (G1964-C1934). Its structure positions U1944 and A1966 to interact with the minor grooves of helices 92 and 93 in the peptidyl transferase region of the 50S subunit.

Ribosome Dynamics

Ribosomes are molecular machines, whose moving parts enable the dynamic process of translation. Each tRNA traverses a distance of more than 130 Å from the time it enters the ribosome as an aminoacyl-tRNA until it is released as a deacylated tRNA (*31*, *32*, *56*); it was anticipated that such large-scale tRNA movement must be matched by corresponding movements in the ribosome. Evidence for this, ranging from local conformational changes to relative movement of the 30S and 50S subunits, comes from structural changes that are observed between different crystal structures (*31*, *32*, *44*, *57*–*59*) and from cryo-EM studies of ribosomes trapped in different functional states (*34*, *60*, *61*).

An example of a local rearrangement is the flipping of bases G530, A1492, and A1493 in the 30S decoding site to monitor the accuracy of codon-anticodon interaction (*44*) (Fig. 3, C to E). Accompanying this local change is a larger-scale movement, in which the 30S subunit goes from an open to a closed conformation that is induced by binding of a cognate tRNA (*44*, *62*, *63*). It is believed that the energy derived from binding the cognate tRNA compensates for the energetic costs of the transition to the closed form. The altered conformation of the 30S subunit may affect the interactions between the aminoacyl-tRNA·EF-Tu· guanosine triphosphate (GTP) ternary complex and the conserved sarcin-ricin loop of 23S rRNA in the 50S subunit, leading to acceleration of GTP hydrolysis and accommodation of aminoacyl-tRNA (*62*, *63*).

An example of a larger-scale movement is that of the L1 arm of the 50S subunit. Exit of the E site–bound deacylated tRNA is obstructed by protein L1 and the extended arm of 23S rRNA to which it is bound (*32*). In addition, the observed contact with the elbow of tRNA bound in the P/E state (*64*) requires movement of the L1 arm by about 20 Å (*65*). In the *Dinococcus radiodurans* 50S crystal structure (*59*), the position of the L1 arm is shifted downward by about 20 Å relative to that seen in the *T. thermophilus* crystal and the *E. coli* cryo-EM structures, sufficient to allow release of the tRNA.

Coupled movement of tRNA and mRNA occurs during the EF-G–catalyzed process of translocation, the most dynamic of ribosomal functions. Translocation takes place in at least two steps, the first of which mainly involves movement of the acceptor arms of tRNA relative to the 50S subunit. This results in tRNAs bound in hybrid states, in which their anticodon ends remain in their original positions in the A and P sites of the 30S subunit while their acceptor ends move to the P and E sites of the 50S subunits (*64*). In the second step, the anticodon ends move to the P and E sites of the 30S subunit, coupled to movement of the mRNA, completing the translocation of tRNA from the A to P and P to E sites. Structural changes accompanying translocation have been analyzed by comparison of cryo-EM reconstructions in which ribosomes were trapped in the pre- and posttranslocation states (*60*, *61*). Pretranslocation or posttranslocation ribosomes, containing peptidyl-tRNA bound to the A site or P site, respectively, were bound with EF-G and a nonhydrolyzable GTP analog or guanosine diphosphate (GDP). These experiments show structural differences between the pre- and posttranslocation states of the ribosome corresponding to a rotational movement of about 6° between the 30S and 50S subunits, causing relative displacements of as much as 20 Å at their extremities. This movement is accompanied by other structural changes, including rearrangement of intersubunit bridge contacts between the head of the 30S subunit and the central protuberance of the 50S subunit, as well as a 20 Å displacement of the L1 arm. On the basis of these observations, Frank and co-workers have proposed a ratchet model for translocation, in which rotational movement between the subunits and movement of the L1 arm, coupled with alternate binding and release of the two ends of the tRNA, is used to drive movement of tRNA and mRNA through the ribosome (*60*, *61*). GTP hydrolysis is coupled to translocation under normal cellular conditions, although the first step of translocation leading to formation of hybrid states can proceed spontaneously in vitro after peptide bond formation (*64*). Furthermore, the observation that a complete single round of highly accurate

translocation can proceed in the absence of EF-G and GTP, stimulated by the antibiotic sparsomycin (*66*), indicates that translocation is an inherent property of the ribosome itself.

Although the resolution of cryo-EM reconstructions is insufficient to draw detailed conclusions about the mechanism of translocational dynamics, it is likely to be yet another function of rRNA. A puzzle is how large-scale movements, such as those of translocation, which must occur at the rate of about 20 per second, avoid the potential kinetic barriers that would be expected from making and breaking of the many molecular interactions that maintain the precise geometry of the different conformational states needed for accurate translation. Helical switches, in which certain RNA sequences alternate between two different structures by base pairing with different complementary strands, have two disadvantages. First, disruption of an RNA helix has a high energy of activation, and second, it leads to single-stranded intermediates that lack the necessary rigidity to maintain precise geometry. Helical switches have not been found in ribosomes, perhaps for these reasons. The ideal dynamic interactions would thus be ones whose disruption and formation have relatively low activation barriers, maintain their local conformations in the disrupted state, and form with precise stereochemistry. The abundant A-minor interactions fit this description well. We have already seen that they participate in dynamic yet precise interactions in aminoacyl-tRNA selection and in the peptidyl transferase active site (Fig. 3) (*35*, *44*). The crystallographic evidence suggests that involvement of A-minor interactions in ribosomal dynamics may be much more widespread.

The 3.0 Å crystal structure of the isolated 30S subunit shows that there are about 55 A-minor interactions, or potential A-minor interactions, in 16S rRNA (Fig. 6). They are typically found in consecutive pairs consisting of a type II interaction followed by a type I interaction. The vast majority of them are long-range interactions; i.e., they connect parts of the secondary structure that lie in different domains or subdomains of the RNA. In contrast, the other base-base and base-backbone tertiary interactions are overwhelmingly local (*67*). Most intriguing is that eight of the sets of A-minor examples in Fig. 6 have optimal geometries except that the adenosines are out of contact range from their putative helical receptors. This suggests that these eight sets of potential A-minor contacts could play a role in the conformational dynamics of the 30S subunit. Direct support for formation of one of them comes from the electron density map of the *T. thermophilus* 70S ribosome (*32*), in which the potential interaction between helix 13 and helix 44 (Fig. 6) is clearly formed. Intriguingly, most of these potentially dynamic interactions are positioned immediately adjacent to features of 16S rRNA that form intersubunit bridges (Fig. 6) (*32*); this observation is consistent with their possible involvement in translocation, in which molecular rearrangements at the subunit interface are known to occur (*60*, *61*).

Conclusions

We have now seen enough RNA structures to infer some generalities about what we can expect to find in other RNAs. We have probably seen most, if not all of the possible local RNA folding motifs (*10*); U turns, T loops, S turns, kink turns, hook turns, A minor interactions, A platforms, and tetraloops are all recurring features of the structures of globular RNAs. Together with the A-form double helix and the more than 20 types of noncanonical base pairs, we can now say that these comprise the building blocks of RNA architecture. It has been shown that we can already predict with good accuracy the occurrence of many of these structural features with the use of only sequence information. With the availability of many thousands of rRNA sequences plus examples of their high-resolution crystal structures, it may be possible to further extend the rules for prediction of RNA structure by using sophisticated bioinformatic approaches. Lastly, and most importantly, the ribosome is a dynamic structure, no doubt facilitated by the inherent flexibility of its RNA. The functional capabilities of a number of cellular RNAs, including the hammerhead ribozyme, group I intron, and spliceosomal RNAs also appear to depend on their structural dynamics (*68*). There is little doubt that the ribosome will continue to help us understand the strategies by which RNA structure enables movement and biological function.

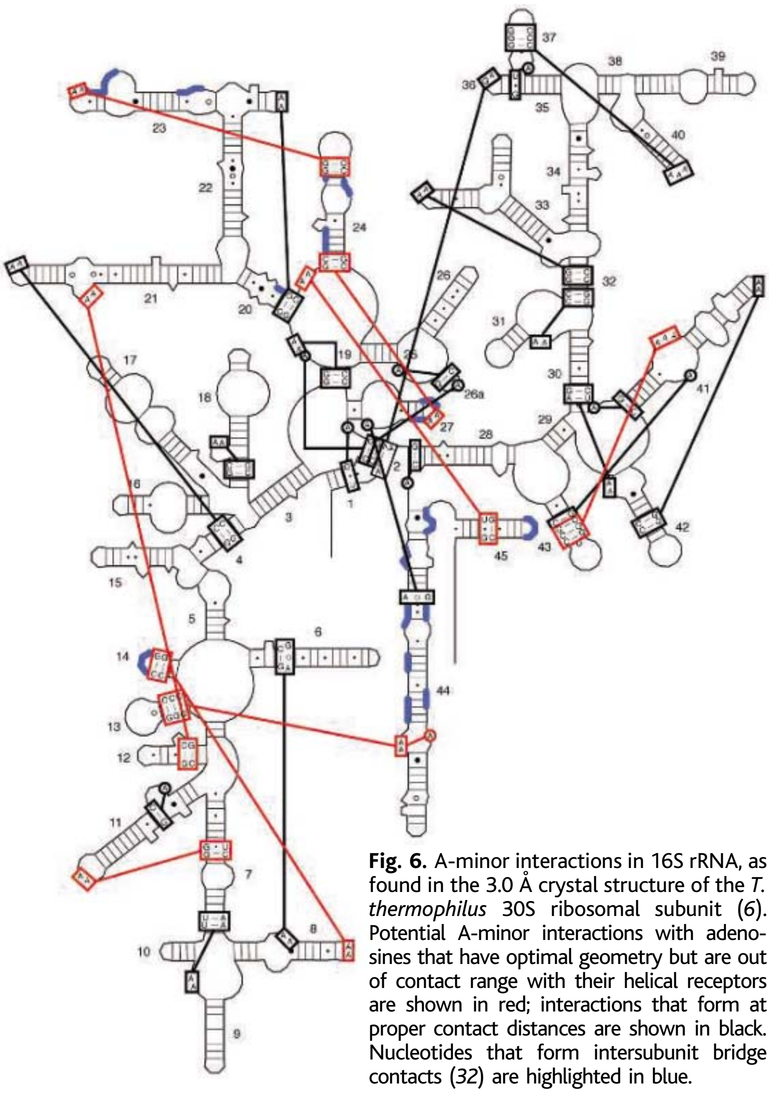

Fig. 6. A-minor interactions in 16S rRNA, as found in the 3.0 Å crystal structure of the *T. thermophilus* 30S ribosomal subunit (*6*). Potential A-minor interactions with adenosines that have optimal geometry but are out of contact range with their helical receptors are shown in red; interactions that form at proper contact distances are shown in black. Nucleotides that form intersubunit bridge contacts (*32*) are highlighted in blue.

References and Notes

1. J. D. Robertus *et al.*, *Nature* **250**, 546 (1974).
2. S. H. Kim *et al.*, *Science* **185**, 435 (1974).
3. H. W. Pley, K. M. Flaherty, D. B. McKay, *Nature* **372**, 68 (1994).
4. W. G. Scott, J. T. Finch, A. Klug, *Cell* **81**, 991 (1995).
5. J. H. Cate *et al.*, *Science* **273**, 1678 (1996).
6. B. T. Wimberly *et al.*, *Nature* **407**, 327 (2000).
7. F. Schluenzen *et al.*, *Cell* **102**, 615 (2000).
8. N. Ban, P. Nissen, J. Hansen, P. B. Moore, T. A. Steitz, *Science* **289**, 905 (2000).
9. V. Ramakrishnan, *Cell* **108**, 557 (2002).
10. P. B. Moore, T. A. Steitz, *Annu. Rev. Biochem.* **72**, 813 (2003).
11. R. F. Gesteland, T. R. Cech, J. F. Atkins, Eds., *The RNA World* (Cold Spring Harbor Laboratory Press, Cold Spring Harbor, NY, ed. 2, 1999).
12. O. C. Uhlenbeck, A. Pardi, J. Feigon, *Cell* **90**, 833 (1997).
13. J. D. Puglisi, R. Tan, B. J. Calnan, A. D. Frankel, J. R. Williamson, *Science* **257**, 76 (1992).
14. A. A. Szewczak, P. B. Moore, Y. L. Chang, I. G. Wool, *Proc. Natl. Acad. Sci. U.S.A.* **90**, 9581 (1993).
15. J. A. Doudna, C. Grosshans, A. Gooding, C. E. Kundrot, *Proc. Natl. Acad. Sci. U.S.A.* **90**, 7829 (1993).
16. Movie is available online (http://chemistry.ucsc.edu/~wgscott/pubs/movies2.html).

17. A. R. Ferre-D'Amare, K. Zhou, J. A. Doudna, *Nature* **395**, 567 (1998).
18. P. B. Rupert, A. R. Ferre-D'Amare, *Nature* **410**, 780 (2001).
19. P. L. Adams, M. R. Stahley, A. B. Kosek, J. Wang, S. A. Strobel, *Nature* **430**, 45 (2004).
20. F. Guo, A. R. Gooding, T. R. Cech, *Mol. Cell* **16**, 351 (2004).
21. B. L. Golden, H. Kim, E. Chase, *Nat. Struct. Mol. Biol.* **12**, 82 (2005).
22. P. Nissen, J. A. Ippolito, N. Ban, P. B. Moore, T. A. Steitz, *Proc. Natl. Acad. Sci. U.S.A.* **98**, 4899 (2001).
23. G. W. Fox, C. R. Woese, *Nature* **256**, 505 (1975).
24. C. R. Woese *et al.*, *Nucleic Acids Res.* **8**, 2275 (1980).
25. H. F. Noller *et al.*, *Nucleic Acids Res.* **9**, 6167 (1981).
26. F. Michel, A. Jacquier, B. Dujon, *Biochimie* **64**, 867 (1982).
27. R. R. Gutell, B. Weiser, C. R. Woese, H. F. Noller, *Prog. Nucleic Acid Res. Mol. Biol.* **32**, 155 (1985).
28. R. R. Gutell, H. F. Noller, C. R. Woese, *EMBO J.* **5**, 1111 (1986).
29. M. Levitt, *Nature* **224**, 759 (1969).
30. R. Green, A. D. Ellington, J. W. Szostak, *Nature* **347**, 406 (1990).
31. J. H. Cate, M. M. Yusupov, G. Z. Yusupova, T. N. Earnest, H. F. Noller, *Science* **285**, 2095 (1999).
32. M. Yusupov *et al.*, *Science* **292**, 883 (2001).
33. For example, (*57*, *69*, *70*).
34. J. Frank, *Biopolymers* **68**, 223 (2003).
35. P. Nissen, J. Hansen, N. Ban, P. B. Moore, T. A. Steitz, *Science* **289**, 920 (2000).
36. H. F. Noller, C. R. Woese, *Science* **212**, 403 (1981).
37. R. Brimacombe, P. Maly, C. Zwieb, *Prog. Nucleic Acid Res. Mol. Biol.* **28**, 1 (1983).
38. D. Moazed, S. Stern, H. F. Noller, *J. Mol. Biol.* **187**, 399 (1986).
39. T. Elgavish, J. J. Cannone, J. C. Lee, S. C. Harvey, R. R. Gutell, *J. Mol. Biol.* **310**, 735 (2001).
40. M. E. Burkard, D. H. Turner, I. Tinoco Jr., in (*11*), pp. 675–685.
41. W. Saenger, *Principles of Nucleic Acid Structure* (Springer-Verlag, New York, 1984).
42. N. B. Leontis, E. Westhof, *Curr. Opin. Struct. Biol.* **13**, 300 (2003).
43. A. Lescoute, N. B. Leontis, C. Massire, E. Westhof, *Nucleic Acids Res.* **33**, 2395 (2005).
44. J. M. Ogle *et al.*, *Science* **292**, 897 (2001).
45. C. R. Woese, S. Winker, R. R. Gutell, *Proc. Natl. Acad. Sci. U.S.A.* **87**, 8467 (1990).
46. F. H. C. Crick, *Cold Spring Harb. Symp. Quant. Biol.* **31**, 3 (1966).
47. D. J. Klein, T. M. Schmeing, P. B. Moore, T. A. Steitz, *EMBO J.* **20**, 4214 (2001).
48. D. E. Brodersen, W. M. Clemons Jr., A. P. Carter, B. T. Wimberly, V. Ramakrishnan, *J. Mol. Biol.* **316**, 725 (2002).
49. D. J. Klein, P. B. Moore, T. A. Steitz, *J. Mol. Biol.* **340**, 141 (2004).
50. D. J. Klein, P. B. Moore, T. A. Steitz, *RNA* **10**, 1366 (2004).
51. E. R. Dabbs, *J. Bacteriol.* **140**, 734 (1979).
52. L. Hoang, K. Fredrick, H. F. Noller, *Proc. Natl. Acad. Sci. U.S.A.* **101**, 12439 (2004).
53. S. Stern, T. Powers, L.-M. Changchien, H. F. Noller, *Science* **244**, 783 (1989).
54. J. W. Orr, P. J. Hagerman, J. R. Williamson, *J. Mol. Biol.* **275**, 453 (1998).
55. H. F. Noller, *RNA* **10**, 1833 (2004).
56. R. K. Agrawal *et al.*, *J. Cell Biol.* **150**, 447 (2000).
57. A. P. Carter *et al.*, *Science* **291**, 498 (2001); published online 4 January 2001 (10.1126/science.1057766).
58. H. F. Noller, A. Baucom, *Biochem. Soc. Trans.* **30**, 1159 (2002).
59. J. Harms *et al.*, *Cell* **107**, 679 (2001).
60. J. Frank, R. K. Agrawal, *Nature* **406**, 318 (2000).
61. M. Valle *et al.*, *Cell* **114**, 123 (2003).
62. J. M. Ogle, F. V. Murphy, M. J. Tarry, V. Ramakrishnan, *Cell* **111**, 721 (2002).
63. J. M. Ogle, A. P. Carter, V. Ramakrishnan, *Trends Biochem. Sci.* **28**, 259 (2003).
64. D. Moazed, H. F. Noller, *Nature* **342**, 142 (1989).
65. H. F. Noller, M. M. Yusupov, G. Z. Yusupova, A. Baucom, J. H. Cate, *FEBS Lett.* **514**, 11 (2002).
66. K. Fredrick, H. F. Noller, *Science* **300**, 1159 (2003).
67. Global searches for RNA tertiary interactions, including A-minor interactions, in 16S (4) and 23S (6) rRNA were carried out by using CASTER (*71*).
68. E. A. Doherty, J. A. Doudna, *Annu. Rev. Biochem.* **69**, 597 (2000).
69. L. Ferbitz, T. Maier, H. Patzelt, B. Bukau, E. Deuerling, N. Ban, *Nature* **431**, 590 (2004).
70. J. L. Hansen, J. A. Ippolito, N. Ban, P. Nissen, P. B. Moore, T. A. Steitz, *Mol. Cell* **10**, 117 (2002).
71. CASTER, A. Baucom, Univ. California Santa Cruz, 2005.
72. I thank A. Baucom for preparation of molecular graphics figures and W. G. Scott for discussions. Work in the author's laboratory was supported by grants from the NIH and the NSF. H.N. is a paid member of the scientific advisory board of and owns equity in the biopharmaceutical company Rib-X, which is involved in antibiotic development.

10.1126/science.1111771

REVIEW

From Birth to Death: The Complex Lives of Eukaryotic mRNAs

Melissa J. Moore

Recent work indicates that the posttranscriptional control of eukaryotic gene expression is much more elaborate and extensive than previously thought, with essentially every step of messenger RNA (mRNA) metabolism being subject to regulation in an mRNA-specific manner. Thus, a comprehensive understanding of eukaryotic gene expression requires an appreciation for how the lives of mRNAs are influenced by a wide array of diverse regulatory mechanisms.

Many written accounts of eukaryotic gene expression might start something like this: "Messenger RNAs (mRNAs) are the central conduits in the flow of information from DNA to protein. In eukaryotes, mRNAs are first synthesized in the nucleus as pre-mRNAs that are subject to 5′-end capping, splicing, 3′-end cleavage, and polyadenylation. Once pre-mRNA processing is complete, mature mRNAs are exported to the cytoplasm, where they serve as the blueprints for protein synthesis by ribosomes and then are degraded." Like a short obituary, however, this dry and simplistic description captures nothing of the intricacies, intrigues, and vicissitudes defining the life history of even the most mundane mRNA. In addition, of course, some mRNAs lead lives that, if not quite meriting an unauthorized biography, certainly have enough twists and turns to warrant a more detailed nucleic acid interest story. It is these intricacies, and our recent progress in understanding them, that are the subject of this review. We will follow the lives of eukaryotic mRNAs from the point at which they are birthed from the nucleus until they are done in by gangs of exonucleases lying in wait in dark recesses of the cytoplasm. Along the way, mRNAs may be shuttled to and from or anchored at specific subcellular locations, be temporarily withheld from the translation apparatus, have their 3′ ends trimmed and extended, fraternize with like-minded mRNAs encoding proteins of related function, and be scrutinized by the quality-control police. Although some of these processes were originally thought to affect only select mRNA populations or be largely limited to highly specialized cell types like germ cells and neurons, recent work suggests that the majority of mRNAs in multiple cell types are subject to a diverse array of regulatory activities affecting essentially every aspect of their lives.

Department of Biochemistry, Howard Hughes Medical Institute, Brandeis University, 415 South Street, Waltham, MA 02454. E-mail: mmoore@brandeis.edu

The mRNP as a Posttranscriptional Operon

Throughout their lifetimes, mRNAs are escorted by a host of associated factors, some of which remain stably bound while others are subject to dynamic exchange (Table 1). Together with mRNA, this complement of proteins and small noncoding RNAs [e.g., microRNAs (miRNAs)] constitute the messenger ribonucleoprotein particle (mRNP). It is the unique combination of factors accompanying any particular mRNA, as well as their relative positions along the transcript, that dictates almost everything that happens to that mRNA in the cytoplasm. In budding yeast, it is estimated that ~570 different proteins have the capacity to bind RNA (*1*). This number is no doubt considerably larger in humans, because a single type of RNA binding domain, the RNA recognition motif (RRM), is represented in

Table 1. mRNP cheat sheet.

CBC20/80	The nuclear cap binding complex. A heterodimer of 20 and 80 kD subunits. Joins the mRNP coincident with cap formation during transcription and facilitates pre-mRNA splicing. In the cytoplasm, can serve as a translation initiation factor through interactions with eIF4G but is ultimately replaced by eIF4E.
eIF4E	Eukaryotic translation initiation factor 4E. The major cytoplasmic cap binding protein. Target of many translational regulators [eIF4E binding proteins (4E-BPs)] that disrupt its interaction with eIF4G.
eIF4G	Eukaryotic translation initiation factor 4G. A large scaffolding protein that can simultaneously interact with cap binding proteins, PABPCs, and eIF3 bound to the small ribosomal subunit.
PABPN1	The nuclear poly(A) binding protein. Binds poly(A) by a single RNA recognition motif (RRM) and an arginine-rich C-terminal domain. In budding yeast, the evolutionarily unrelated Nab2 protein serves this role.
PABPCs	Cytoplasmic poly(A) binding proteins. Single-celled eukaryotes contain a single PABPC, whereas human cells contain four. All PABPCs bind poly(A) RNA through four RRMs.
HnRNP proteins	A diverse set of factors loosely defined as all proteins associating with heterogeneous nuclear RNA (hnRNA, made up of pre-mRNA and nuclear mRNA) that are not stable components of other RNP complexes, such as small nuclear RNPs (snRNPs). Some hnRNP proteins accompany mRNAs to the cytoplasm; others are confined to the nucleus.
EJC	The exon junction complex. A set of proteins loaded onto mRNAs upstream of exon-exon junctions as a consequence of pre-mRNA splicing and which accompanies the spliced mRNA to the cytoplasm.
SR proteins	A family of structurally related, nuclear RNA binding proteins containing an RRM and a domain rich in serines and arginines (RS domain). The serines in the RS domain serve as sites of dynamic phosphorylation. Some SR proteins accompany mRNAs to the cytoplasm; others are confined to the nucleus. Many SR proteins play key roles in pre-mRNA splicing.
Y-box proteins	A family of multifunctional nucleic acid binding proteins containing a "cold-shock" domain. Along with PABPCs, Y-box proteins constitute the major mRNP structural components in somatic cells. They are thought to bind along the body of the message and have a packaging role that modulates translational activity. In *Xenopus* oocytes, Y-box proteins FRGY2 and mRNP3 are major components of stored mRNPs.
TIA-1/TIAR	Structurally related RNA binding proteins consisting of three RRMs and a C-terminal prionlike domain. The prionlike domain is thought to self-oligomerize in vivo and drive the formation of stress granules.
miRNAs	MicroRNAs. Small noncoding RNAs that imperfectly base-pair with recognition sites in 3′ UTRs. In combination with RISC (RNA-induced silencing complex), miRNAs negatively regulate protein synthesis by the cognate mRNA.

nearly 500 different human genes (*2*). Other common RNA binding motifs include the KH domain, the double-stranded RNA binding domain (dsRBD), zinc fingers, RGG boxes, and the Pumilio homology domain found in PUF proteins (*3*, *4*). The human genome has also been estimated to encode more than 400 different miRNAs targeting transcripts from ~5,000 different genes, or ~20% of the genome (*5*–*7*).

A few mRNP components target the two elements common to almost every message: the 7-methylguanosine cap found at the 5′ end of all RNA polymerase II transcripts and the poly(A) tail comprising most mRNA 3′ ends (*8*, *9*). Others, such as the abundant mRNA-packaging Y-box proteins, appear to associate along the length of transcripts in a largely sequence-independent manner (*10*). Yet another set, exemplified by the exon junction complex (EJC), is loaded at specific positions independent of sequence (*11*). The majority of mRNA binding factors, however, target particular structures or sequences present in some mRNAs but not others. Such specific recognition elements most commonly occur in the untranslated regions (UTRs) at the 5′ and 3′ ends of the message.

Individual mRNP components can be thought of as adaptors that allow mRNAs to interface with the numerous intracellular machineries mediating their subcellular localization, translation, and decay, as well as the various signal transduction systems. Some adaptors make positive interactions and thereby serve as activators of a particular process, whereas others disrupt the positive interactions and act as repressors. By containing binding sites for diverse adaptors, individual mRNAs can respond to myriad inputs, allowing their expression to be exquisitely fine-tuned to changing conditions. These changing conditions can also alter the levels and RNA binding properties of the adaptors, transforming the subpopulations of mRNAs to which they bind. The result is an elaborate web of regulatory networks of equal, if not greater, complexity to those controlling initial mRNA synthesis (*12*, *13*). Indeed, eukaryotic mRNPs have been likened to "posttranscriptional operons" that serve to markedly expand the regulatory plasticity of our unexpectedly small genomes (*12*). The importance of such posttranscriptional regulatory mechanisms in the control of eukaryotic gene expression is highlighted by the wide variability in the degree to which mRNA and protein abundances correlate in vivo (*14*, *15*). Thus, changes in mRNA levels, as measured by microarrays, for example, cannot be presumed to reflect proportionate changes in protein abundance or activity.

A key assertion of the posttranscriptional operon model is that mRNAs encoding functionally related proteins should be coordinately regulated by specific mRNP components recognizing sequence elements common to that set of mRNAs (*12*). Evidence that this may be the case on a genome-wide scale was recently provided by a study identifying the complement of mRNAs bound to each of the five individual Puf proteins in *Saccharomyces cerevisiae* (*16*). The Puf proteins are a family of structurally related cytoplasmic mRNP proteins that have been implicated in the control of mRNA translation and stability through binding sites in the 3′ UTR. In all, 12% of known or predicted yeast mRNAs were found to stably associate with one or more of these proteins, although the vast majority (645 out of 735) bound only one. Notably, each Puf protein exhibited a highly skewed distribution of bound mRNAs: Puf1p and Puf2p bound mostly mRNAs encoding membrane-associated proteins, Puf3p almost exclusively targeted messages for nuclear-encoded mitochondrial proteins, and Puf4p and Puf5p associated primarily with transcripts encoding proteins bound for the nucleus. In several cases, a majority of the subunits comprising a particular multiprotein machine, such as the mitochondrial ribosome and a number of nuclear chromatin modification complexes, were encoded by mRNAs "tagged" by a single Puf protein. Together with earlier data (*12*), these new results (*16*) strongly support the idea that the expression of proteins with common functional themes or subcellular distributions is coordinated by large-scale regulatory networks operating at the mRNP level.

Nuclear mRNP Embryology and Export

Many components of the cytoplasmic mRNP are first recruited in the nucleus, coincident with transcription and pre-mRNA processing. Such factors include the nucleocytoplasmic shuttling hnRNP (heterogeneous nuclear RNP) and SR (serine/arginine rich) proteins as well as the EJC (*11*, *17*, *18*) (Table 1). Both hnRNP and SR proteins recognize short consensus sequences through their RNA binding domains (*17*); the SR proteins additionally contain a domain rich in Arg-Ser dipeptides that can variously interact with proteins or RNA and is subject to dynamic phosphorylation (*18*). The

EJC is a set of proteins deposited onto spliced mRNAs by the process of pre-mRNA splicing. Unlike other known mRNP components, the EJC is loaded in a position-dependent, but sequence-independent, manner. EJC deposition sites are about 20 to 25 nucleotides upstream of exon-exon junctions, the sites where introns resided in the pre-mRNA. Intriguingly, the downstream consequences of EJC deposition are highly dependent on EJC location along the mRNA—EJCs inside the open reading frame (ORF) can positively influence translation, whereas EJCs in the 3′ UTR can target the bound mRNA for rapid destruction via nonsense-mediated mRNA decay (NMD) (*11*). It was recently found that certain SR proteins can recapitulate both of these effects, although the extent to which this is dependent on SR protein position along the mRNA remains to be elucidated (*18*).

A key issue regarding mRNP composition is how the complement of bound factors evolves as an mRNA proceeds through the various stages of its life. The first major change in mRNP composition occurs as mRNAs are birthed from the nucleus through the nuclear pore complex (NPC) (Fig. 1). The NPC is a mammoth, eight-fold symmetric supramolecular assembly (50 to 125 MD) that serves as the molecular gatekeeper for movement of proteins and protein-RNA complexes between the nucleus and cytoplasm (*19*). Some nuclear-acquired mRNP proteins, such as the mRNA export adaptors and receptors responsible for targeting the nuclear mRNP to the NPC, are shed as a consequence of the birthing process. In general, export adaptors are mRNA binding proteins that serve to bridge the mRNA to one or more receptor proteins, which in turn contact components of the NPC. Like other nuclear-acquired mRNP proteins, these adaptors and receptors are recruited cotranscriptionally, but they dissociate from the mRNA either as it is transiting the pore or soon after reaching the cytoplasm (*20*). In the case of the yeast adaptor and SR-like protein Npl3p, this dissociation is triggered by its cytoplasmic phosphorylation, which serves to destabilize its interaction with both the mRNA and the export receptor NXF1/Mex67p. Reimport and nuclear dephosphorylation of Npl3p creates a regulated RNA binding-and-release cycle capable of imparting overall directionality to the mRNA export process (*18*, *21*).

Other nuclear-restricted mRNP components might be removed by DExH/D-box proteins, a family of RNA binding nucleotide triphosphatases, some of which can remove secondary structures and/or bound proteins from RNA (*22*). One such protein is the essential mRNA export factor Dbp5p, which is recruited to mRNPs both cotranscriptionally and as they transit the pore (*23*). It has been suggested that Dbp5p assists in "remodeling" the mRNP during nuclear export, possibly by facilitating binding of new cytoplasmic mRNP factors as it bumps off other proteins that return to the nucleus. If this is the case, however, it is unclear how Dbp5p would be prevented from indiscriminately removing the many nuclear-acquired proteins known to remain associated with the cytoplasmic mRNP. An alternate role for Dbp5p is suggested by its strong interactions with the long fibrils extending away from the cytoplasmic face of the NPC. By simultaneously binding the mRNA and these fibrils, Dbp5p might instead serve to prevent the mRNP from backsliding into the nucleus as it exits the pore and thereby contribute to export directionality.

To date, the only mRNPs that have been caught in the act of transiting the pore are the gigantic Balbiani ring mRNPs (*24*). Balbiani ring mRNAs 1 and 2 of the dipteran *Chironomus tentans* are each >30,000 nucleotides long. This immense size, coupled with their extremely high expression levels in larval salivary glands, has enabled direct electron microscopic visualization of Balbiani mRNP docking and translocation through the NPC. In the nucleoplasm, Balbiani ring mRNPs exist as tightly packed ringlike structures. Upon docking with the NPC, these ring structures partially unfold, allowing the mRNA to enter the pore 5′ end first. As soon as their 5′ ends begin to protrude into the cytoplasm, Balbiani ring mRNAs are engaged by the translation machinery, with multiple ribosomes often visible attached to mRNAs still transiting the pore. It should be noted, however, that this one-at-a-time, 5′-end-first birthing order of Balbiani ring mRNPs does not necessitate that this is how all mRNPs emerge from the nucleus; lesser mRNPs could well be born as multiples or even in a breach position. Many mRNAs destined for particular subcellular locations appear to travel in multi-mRNA packets or particles. Currently it is unknown whether these particles first form in the cytoplasm after mRNP export, or whether they are initially assembled in the nucleus and are then exported to the cytoplasm en masse. Other data support the idea that mRNAs might not always emerge 5′ end first. For example, neither the 7-methylguanosine 5′ cap structure nor the nuclear 5′ cap binding complex (CBC20/80) is essential for mRNA export in budding yeast, and injection of large amounts of cap analog only minimally affected mRNA export in *Xenopus* oocytes (*25*). Further, mRNA export adaptors are apparently recruited along the length of nascent transcripts rather than being concentrated near 5′ ends (*26*). Finally, consistent with a crucial role for the poly(A) tail in mRNA export, the nuclear poly(A) tail-binding proteins in both metazoans and budding yeast have known interactions with export receptors and NPC components (*9*). Indeed, a provocative possibility is that simply because of their gigantic size and their need to be efficiently recruited to the endoplasmic reticulum (which constitutes the cytoplasmic face of the nuclear envelope and into which proteins bound for secretion are extruded), Balbiani ring mRNPs may have evolved specific mechanisms ensuring 5′-end-first delivery that are not employed by the bulk of cellular mRNPs.

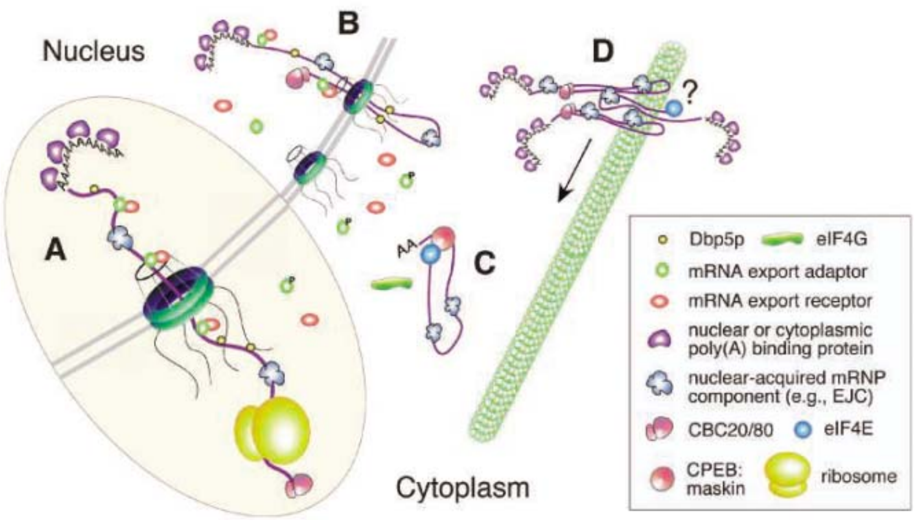

Fig. 1. Schematic of mRNA export and alternate mRNA fates in the cytoplasm. Export through the NPC requires export adaptors and receptors as well as Dbp5p. Some mRNAs are exported 5′ end first and are immediately engaged by ribosomes (**A**), whereas others may be exported by a non-5′-end-first mechanism (**B**). Once in the cytoplasm, some mRNPs are stored in a translationally silent state (**C**), and others are transported to specific subcellular locations along the cytoskeleton (**D**).

From Birth to Baptism: Engaging the Translation Apparatus

Although CBC20/80 is not essential for mRNA export, it can serve as an initiation factor for protein synthesis. Like the Balbiani ring mRNAs, many mRNAs enter the translationally active pool immediately upon export to the cytoplasm. At this stage, the 5′ cap is still largely bound by the nuclear CBC20/80 com-

plex, whereas the poly(A) tail carries a mixture of nuclear and cytoplasmic poly(A) binding proteins PABPN1 and PABPCs (Table 1). In this newly exported mRNP, CBC20/80 can functionally interact with translation initiation factor 4G (eIF4G), which serves to recruit the small ribosomal subunit and initiate $5' \rightarrow 3'$ scanning along the 5′ UTR for an AUG start codon (*27*). Once the start codon is identified, the large ribosomal subunit is engaged to form an 80S complex competent for protein synthesis.

Another major change in mRNP composition necessarily occurs upon the first passage of the 80S ribosome along the mRNA—the so-called "pioneering round" of translation (*28*). Threading of the mRNA through the narrow space between the two ribosomal subunits strips away any remaining nuclear-acquired mRNP proteins, such as EJCs, residing inside the ORF. At some point, CBC20/80 and PABPN1 are also replaced by eIF4E (the major cytoplasmic cap-binding protein) and PABPCs, respectively. Whether these exchanges require any special mechanisms, such as the phosphorylation that promotes dissociation of Npl3p from newly exported mRNPs, or whether they occur simply as a consequence of mass action, is unknown. Regarding the second possibility, the low cytoplasmic concentrations of CBC20/80 and PABPN1 coupled with the high concentrations of eIF4E and PABPCs could naturally lead to the latter set replacing the former, given reasonable dissociation rates. In any event, once the transition is complete, a network of simultaneous interactions between the 5′ cap, eIF4E, eIF4G, PABPCs, and the poly(A) tail results in functional circularization of the message (Fig. 2), an arrangement thought to facilitate translational control by regulatory elements in the 3′ UTR, promote efficient ribosome reinitiation during active translation, and protect both ends of the transcript from the mRNA degradation machinery (*9*).

Upon export, not all mRNAs immediately enter the translationally active pool. Many are held instead in a translationally quiescent state awaiting either proper subcellular localization or some signal that the timing is now right to make protein. In early metazoan embryos, for example, no new transcription occurs until after several cell divisions. Therefore, the oocyte must accumulate and store all the mRNAs required for early development. In immature frog oocytes, a number of these maternal mRNAs are translationally silenced through a mechanism involving substantial shortening of their poly(A) tails from their initial nuclear length of 200 to 250 adenosines to a mere 20 to 40 bases. This shortening is modulated by CPEB, a protein that recognizes the so-called cytoplasmic polyadenylation element (CPE) in the 3′ UTR. CPEB also interacts with Maskin, a protein that competes with eIF4G for binding to eIF4E. In the context of a short poly(A) tail, which cannot effectively recruit PABPCs or eIF4G, the Maskin-eIF4E interaction inhibits translation. When the oocytes are induced to complete meiosis, CPEB becomes phosphorylated; in this phosphorylated form, CPEB stimulates readdition of the poly(A) tail by cytoplasmic poly(A) polymerases. The longer poly(A) tails rebind PABPCs, which in turn recruit eIF4G to initiate translation (*29*).

The CPEB-Maskin-eIF4E interaction is just one example of translational regulation by so-called "4E inhibitory proteins," which target the eIF4E-eIF4G interface. Some 4E inhibitory proteins like Maskin are tethered to a cis element in the 3′ UTR and therefore act only on mRNAs containing that element. Another class, the "4E binding proteins" (4E-BPs), are not tethered and therefore act more globally by sequestering any available eIF4E; this results in preferential translational inhibition of mRNAs that normally require high eIF4E levels. In addition to the control of development and cell growth, variants of this general translational regulatory scheme have been implicated in tumor suppression as well as the control of localized protein synthesis at neuronal synapses, which is believed to be essential for long-term potentiation (LTP) and memory consolidation (*29*).

A currently open question about translationally quiescent mRNPs has been whether they undergo a "pioneering round" of translation driven by CBC20/80 before entering their translationally silent phase. At least for one mRNA, this appears not to be the case. Proper localization and regulated translation of oskar mRNA at the posterior pole of *Drosophila* oocytes is essential for germline and abdomen formation in the future embryo. During transport from its sites of production in nurse cells to the posterior pole of the oocyte, oskar mRNA is translationally silenced by a 3′-UTR-tethered 4E inhibitory protein, Cup (*29*). In addition to sequences in the 3′ UTR, oskar mRNA localization requires deposition of an EJC within the ORF, and the bound EJC proteins accumulate along with oskar mRNA at the posterior pole (*30*). If oskar mRNA were subject to a pioneering round of translation before translational silencing and transport, then the EJC would be expected to be removed in the nurse cells and be unable to participate in mRNP localization or colocalize with oskar mRNA at the posterior pole. Further, the observation that translational silencing of oskar during transport involves a 4E inhibitory protein supports the idea that exchange of CBC20/80 for eIF4E at the cap can occur independent of any pioneering round of translation.

Location, Location, Location

Oskar is but one example of a plethora of localized mRNPs. Such localization, usually coupled with regulated translation, serves to restrict synthesis of the encoded protein to a specific subcellular compartment. For example, repression of mating-type switching by *S. cerevisiae* daughter cells is facilitated by localizing the mRNA encoding Ash1p, a transcriptional repressor, to the developing bud tip. In all, 24 transcripts have been shown to localize to the bud tip and 8 to the vicinity of yeast mitochondria (*31*). In metazoans, regulated translation of localized mRNAs is particularly rife in highly polarized cells such as oocytes and neurons. Fully one-tenth of randomly selected *Drosophila* ovarian mRNAs localize to the anterior pole of the oocyte, and ~400 different mRNAs have been identified in mammalian neuronal dendrites (*32*).

Mechanisms for mRNA localization include active transport along the cytoskeleton, diffusion and anchoring, local protection from degradation, and local synthesis by subsets of nuclei in syncytial cells. In many instances, a combination of mechanisms work on a single transcript. For example, oskar mRNA is transported along microtubules by kinesin and then becomes anchored at the posterior pole by its own gene product. Another posterior pole mRNA, nanos, achieves its localization pattern by diffusion and anchoring, along with regional stabilization. Some localized mRNAs travel as individual mRNPs, whereas others appear to migrate as higher order RNP structures or particles. In neurons, such particles have been estimated to contain ~30 mRNAs and have diameters up to 1 μm (*32*).

Although mRNA localization and regulated translation have been most intensively studied in specialized cells such as oocytes and neurons, it now appears that many mRNAs may exhibit asymmetric localization even in somatic cells. One particularly well-characterized example is β-actin mRNA, which localizes to sites of actin polymerization at the leading edges of crawling cells (*33*). Local β-actin

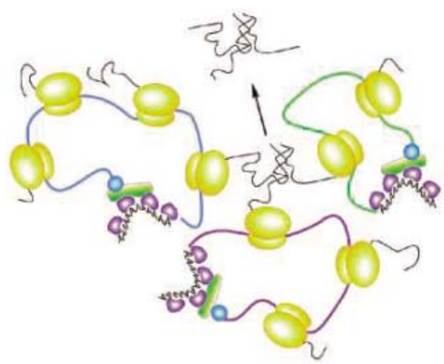

Fig. 2. Schematic showing cotranslational assembly of a protein complex encoded by a family of colocalized mRNAs. Functional circularization of mRNAs by a network of interactions between eIF4E, eIF4G, and PABPs promotes efficient translation by polyribosomes. Physical juxtaposition of mRNAs encoding individual components of the complex may facilitate cotranslational polypeptide interaction and complex assembly.

RNA SILENCING

A journey into the RNA silencing world

Small noncoding RNAs have rapidly become the "rising star" of biology. The first member of the class of small RNAs known as microRNAs (miRNAs) was initially discovered as a key regulator of larval development in the nematode *Caenorhabditis elegans* (see the Review by Zamore and Haley. Since then, numerous miRNAs have been identified in a wide range of metazoans. A second related class of small noncoding RNAs are the small interfering RNAs (siRNAs), first seen in plants associated with gene silencing but later found in organisms ranging from yeast to humans. These two classes of small noncoding RNAs are now known to maintain genome stability, defend against invading nucleic acids (such as viruses), and regulate gene expression in a multitude of biological processes (such as cell proliferation and differentiation). Recent evidence also strongly suggests that the misregulation of miRNAs plays a role in cancer and other diseases. At the same time, synthetic siRNAs are now widely used as a molecular tool to easily and rapidly assay gene function in a wide range of biological systems, including whole-genome screening, and siRNAs are even being considered as therapeutic tools to combat diseases such as cancer.

We have created this poster to help readers of *Science* navigate the ins and outs of the core mechanism of small RNA silencing, as well as many of the associated phenomena—such as spreading of the silencing effect, viral defense, and even its role in genome deletion. We highlight these biological pathways in a diverse range of experimental organisms, and include descriptions of the key steps and cellular components.

The poster is, inevitably, merely a snapshot of our (still limited) comprehension of the process of RNA silencing, circa July 2005, and parts will be superseded quickly, given the breakneck speed of research in this area. The poster illustrates how much more work needs to be done to fully understand these RNA-based biological pathways—the challenge awaits! For a detailed account of the history and biology of small RNAs, see the Review by Zamore and Haley.

Welcome to the world of RNA silencing, and be careful! You are likely to find a small noncoding RNA implicated in your favorite biological process… sooner or later.

M. J. Simard and G. Hutvagner

Authors

Martin J. Simard, Laval University Cancer Research Center, Quebec, Canada.

György Hutvagner, University of Dundee School of Life Sciences, Scotland, UK

Science coordinators

Guy Riddihough, Katrina L. Kelner

Illustration

Katharine Sutliff

Design and Production

Nathalie Cary, Marcus Spiegler, Joshua Moglia

Science

Science

This poster is sponsored by: Ambion® THE RNA COMPANY®

RNA SILENCING

Spreading A PRIMITIVE "IMMUNE SYSTEM"

RNA silencing can spread from cell to cell in plants and confer a sort of plant-wide immunity to viruses. In the nematode *C. elegans*, silencing can be transmitted from generation to generation.

Plant

Nematode

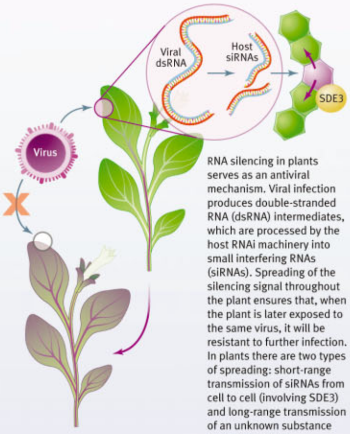

RNA silencing in plants serves as an antiviral mechanism. Viral infection produces double-stranded RNA (dsRNA) intermediates, which are processed by the host RNAi machinery into small interfering RNAs (siRNAs). Spreading of the silencing signal throughout the plant ensures that, when the plant is later exposed to the same virus, it will be resistant to further infection. In plants there are two types of spreading: short-range transmission of siRNAs from cell to cell (involving SDE3) and long-range transmission of an unknown substance through phloem.

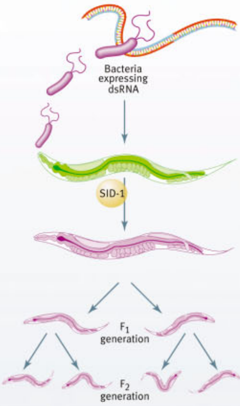

C. elegans can take up dsRNAs by ingestion of bacteria expressing dsRNA molecules (which requires a cellular factor called SID-1); by being soaked in a solution containing dsRNA; or by being injected with dsRNA into the body cavity. Gene silencing spreads to most cells of the animal, with the exception of neurons. Moreover, RNA silencing can be passed on for several generations. The physiological role of spreading in *C. elegans* is unknown.

RNAi Suppressors VIRUSES STRIKE BACK

Some viruses have evolved endogenous proteins that interfere with the gene silencing machinery, as a countermeasure to attenuate host antiviral defenses.

Plant

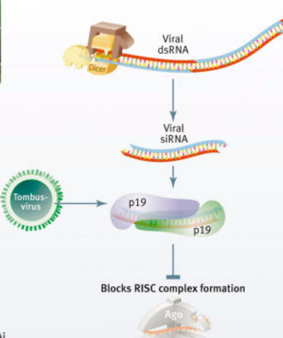

Plant and likely animal cells direct siRNAs against invading viruses to prevent or slow viral replication. In the ongoing arms race between host and pathogen, many plant and some animal viruses in turn have evolved proteins, suppressors of gene silencing, which interfere with different steps of the RNAi machinery.

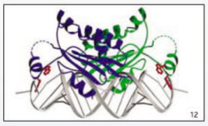

The best-characterized silencing suppressor is the p19 protein (above) of the Tombusvirus family, which infects plants. Homodimerized p19 sequesters siRNA, preventing the formation of active RISC and consequent silencing.

Hc-Pro, the RNAi suppressor of the Potyvirus family, which infects plants, blocks RISC activity rather than affecting RISC formation.

MicroRNAs MICROCONTROLLERS OF MULTIPLE PATHWAYS

These noncoding genes, found in nearly every eukaryotic organism, are often highly conserved through evolution and are involved in regulation of a diverse range of biological pathways.

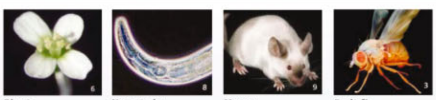

Plant Nematode Mouse Fruit fly

MicroRNAs are encoded in the genome and produced by the maturation of a hairpin-shaped RNA transcript. These RNAs are key regulators of many biological processes such as development (see example in Zebrafish at top right), cell proliferation, apoptosis, morphogenesis, oncogenesis (see example in mouse at bottom right), and hematopoiesis. In animals, they generally work by blocking protein synthesis or destabilizing mRNA. In contrast, miRNAs from plants and some from animals predominantly induce mRNA degradation and are important for plant siRNA formation. They also act as defense mechanisms by targeting RNA from viruses, leading to silencing of viral protein expression. MicroRNAs produced by viruses can also affect expression of host genes.

Ventral view of mir-140 expression in Zebrafish embryos.

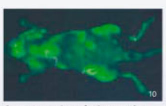

Overexpression of mir-17-19b clusters accelerates lymphomas formation in mice.

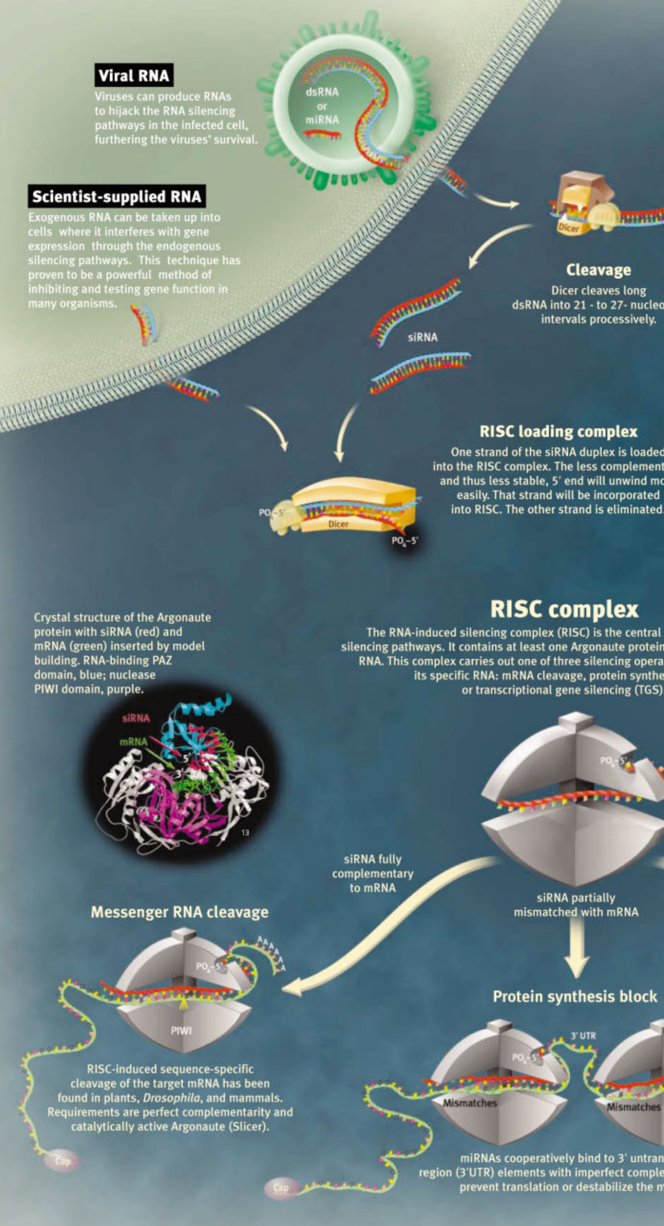

Viral RNA

Viruses can produce RNAs to hijack the RNA silencing pathways in the infected cell, furthering the viruses' survival.

Scientist-supplied RNA

Exogenous RNA can be taken up into cells where it interferes with gene expression through the endogenous silencing pathways. This technique has proven to be a powerful method of inhibiting and testing gene function in many organisms.

Cleavage

Dicer cleaves long dsRNA into 21 - to 27- nucleo intervals processively.

RISC loading complex

One strand of the siRNA duplex is loaded into the RISC complex. The less complement and thus less stable, 5' end will unwind mo easily. That strand will be incorporated into RISC. The other strand is eliminated.

Crystal structure of the Argonaute protein with siRNA (red) and mRNA (green) inserted by model building. RNA-binding PAZ domain, blue; nuclease PIWI domain, purple.

RISC complex

The RNA-induced silencing complex (RISC) is the central silencing pathways. It contains at least one Argonaute protein RNA. This complex carries out one of three silencing opera its specific RNA: mRNA cleavage, protein synthe or transcriptional gene silencing (TGS)

siRNA fully complementary to mRNA

siRNA partially mismatched with mRNA

Messenger RNA cleavage

RISC-induced sequence-specific cleavage of the target mRNA has been found in plants, *Drosophila*, and mammals. Requirements are perfect complementarity and catalytically active Argonaute (Slicer).

Protein synthesis block

miRNAs cooperatively bind to 3' untran region (3'UTR) elements with imperfect comple prevent translation or destabilize the m

	Vertebrate Mouse	Fruit fly *Drosophila melanogaster*	Nematode *Caenorhabditis elegans*
Argonaute Core protein Some with catalytic activity	Ago1 Ago2 (endonuclease) Ago3 Ago4	Aubergine (Stellate silencing, heterochromatin silencing) Ago1 (miRNA) piwi (heterochromatin, cosuppression) Ago2 (siRNA)	RDE-1 (RNAi) ALG-1 and ALG-2 (miRNA) PPW-2 (transposon silenci PPW-1 (germline RNAi)
RNAse III dsRNA-specific nucleases	Dicer (RNAi and miRNA, essential) Drosha (miRNA)	Dicer-1 (miRNA) Dicer-2 (RNAi) Drosha (miRNA)	DCR-1 (RNAi, miRNA) Drosha (miRNA)
Helicases Destabilize dsRNAs	Gemin3 (miRNP) (miRNA)	Spindle-E (Stellate silencing, heterochromatin) Armitage (RISC formation)	DRH-1/DRH-2 (RNAi) SMG-2 (RNAi) MUT-14 (transposon silenc germline RNAi)
RdRp RNA-dependent RNA polymerases			RRF-1 (somatic RNAi) EGO-1 (germline RNAi) RRF-3 (RNAi silencer)
dsRNA binding proteins RNAse III associated	DGCR8 TRBP	R2D2 (siRNA) Pasha (pre-miRNA) Loquacious (miRNA)	RDE-4 (RNAi)
Others	Tudor-SN (RNAi and miRNA) Exportin-5 (miRNA transporter) Gemin4 (miRNA)	VIG (RNAi and miRNA) FXR (RNAi and miRNA) Tudor-SN (RNAi and miRNA)	ERI-1 (RNAi) RDE-3 (RNAi) SID-1 (RNA transporter, R MUT-7 (cosuppression, ge MUT-8 (transposon silenci VIG-1 (miRNA) TSN-1 (miRNA)

Small RNAs from both inside and outside the cell are processed by the RNA interference (RNAi) machinery to inhibit genes and proteins by cleaving messenger RNAs, blocking protein synthesis, or inhibiting transcription.

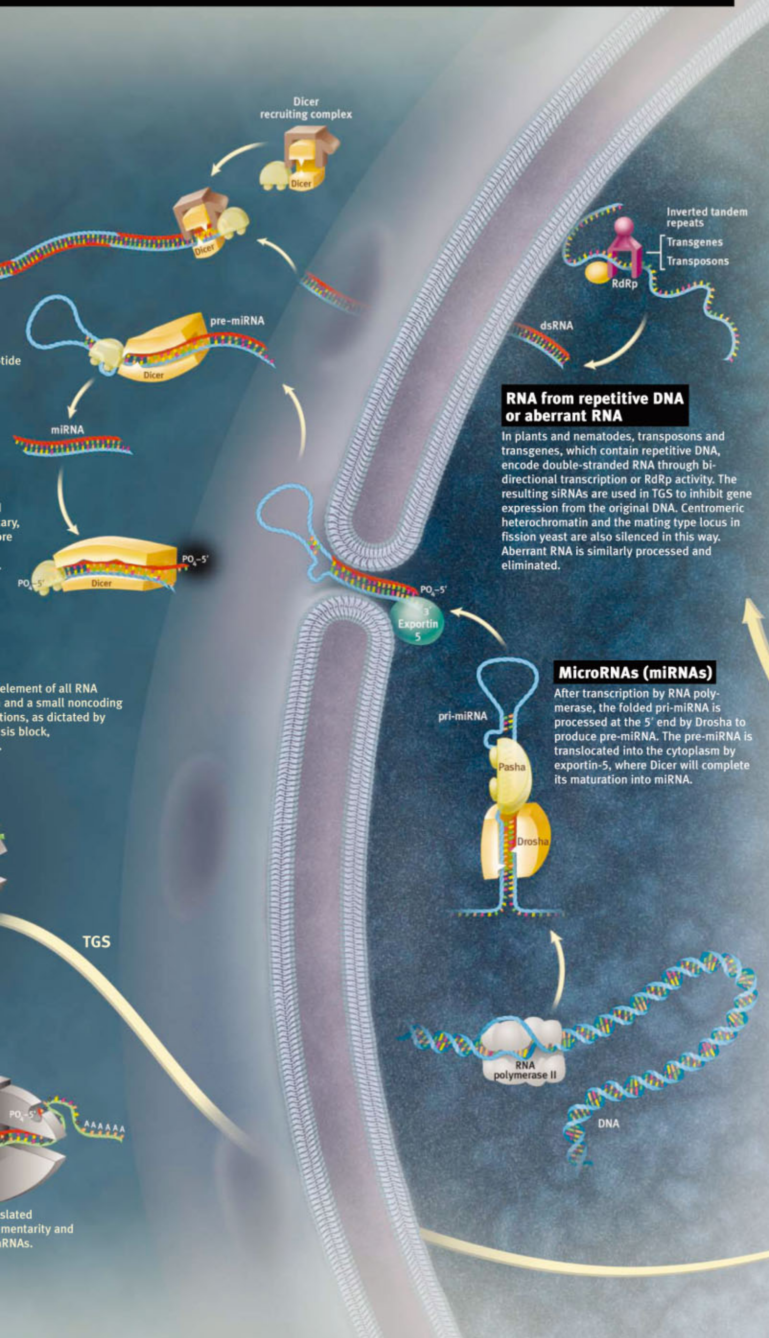

tide

ary,
re

element of all RNA
and a small noncoding
tions, as dictated by
sis block,

slated
mentarity and
RNAs.

RNA from repetitive DNA or aberrant RNA

In plants and nematodes, transposons and transgenes, which contain repetitive DNA, encode double-stranded RNA through bidirectional transcription or RdRp activity. The resulting siRNAs are used in TGS to inhibit gene expression from the original DNA. Centromeric heterochromatin and the mating type locus in fission yeast are also silenced in this way. Aberrant RNA is similarly processed and eliminated.

MicroRNAs (miRNAs)

After transcription by RNA polymerase, the folded pri-miRNA is processed at the 5' end by Drosha to produce pre-miRNA. The pre-miRNA is translocated into the cytoplasm by exportin-5, where Dicer will complete its maturation into miRNA.

DNA Elimination RNA-DIRECTED GENOME SHREDDING

In this unusual process that may function as a germline defense mechanism, small "scan" RNAs generated by an RNAi-like process direct the elimination of DNA segments.

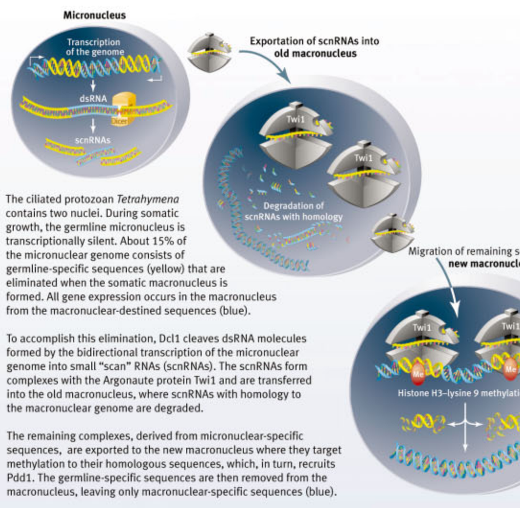

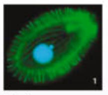

Tetrahymena

The ciliated protozoan *Tetrahymena* contains two nuclei. During somatic growth, the germline micronucleus is transcriptionally silent. About 15% of the micronuclear genome consists of germline-specific sequences (yellow) that are eliminated when the somatic macronucleus is formed. All gene expression occurs in the macronucleus from the macronuclear-destined sequences (blue).

To accomplish this elimination, Dcl1 cleaves dsRNA molecules formed by the bidirectional transcription of the micronuclear genome into small "scan" RNAs (scnRNAs). The scnRNAs form complexes with the Argonaute protein Twi1 and are transferred into the old macronucleus, where scnRNAs with homology to the macronuclear genome are degraded.

The remaining complexes, derived from micronuclear-specific sequences, are exported to the new macronucleus where they target methylation to their homologous sequences, which, in turn, recruits Pdd1. The germline-specific sequences are then removed from the macronucleus, leaving only macronuclear-specific sequences (blue).

Transcriptional Gene Silencing (TGS)

CONTROL OF THE CHROMATIN STATE

Small noncoding RNAs silence expression of genes with homologous sequences by preventing transcription at the DNA. TGS inhibits gene transcription by forming heterochromatin or promoting methylation.

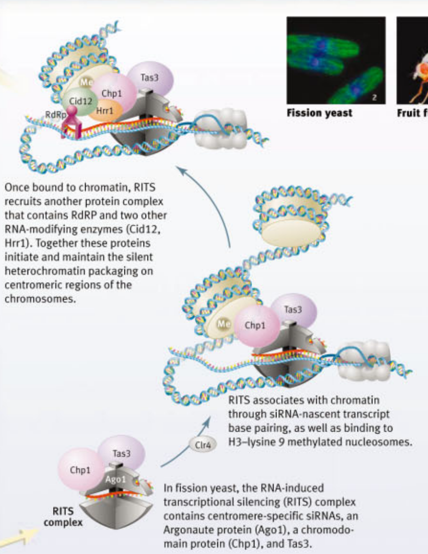

Fission yeast | Fruit fly | Plant

Once bound to chromatin, RITS recruits another protein complex that contains RdRP and two other RNA-modifying enzymes (Cid12, Hrr1). Together these proteins initiate and maintain the silent heterochromatin packaging on centromeric regions of the chromosomes.

RITS associates with chromatin through siRNA-nascent transcript base pairing, as well as binding to H3–lysine 9 methylated nucleosomes.

In fission yeast, the RNA-induced transcriptional silencing (RITS) complex contains centromere-specific siRNAs, an Argonaute protein (Ago1), a chromodomain protein (Chp1), and Tas3.

In fruit flies, RNAi-associated genes such as *piwi* and *aubergine* (two Argonaute proteins) and *spindle-E* (an RNA helicase) are involved in TGS. Mutation in these genes results in a loss of heterochromatin. *Piwi* also has a central role in cosuppression in flies.

In plants, TGS often involves DNA methylation. siRNAs are implicated in the de novo methylation of gene sequences—including non-CG methylation and CNG methylation by different complexes.

Stellate Silencing RNAi DOIN' IT NATURALLY

Silencing of the repetitive Stellate genes in *Drosophila melanogaster*, which is necessary for male fertility, was the first example of endogenous dsRNA-mediated gene repression.

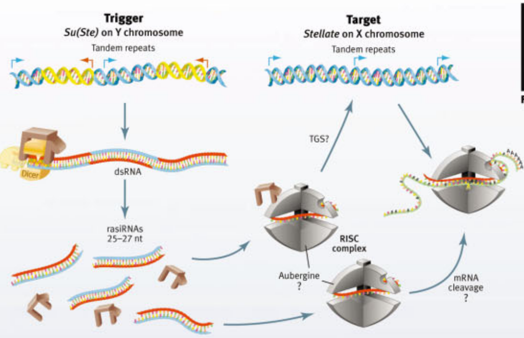

Fruit fly

In the testis of male fruit flies, overexpression of the repetitive *Stellate* genes on the X chromosome is prevented by the *Suppressor of Stellate* [*Su(Ste)*] locus on the Y chromosome. Overlapping sense and antisense RNAs are generated from the Su(Ste) locus, which form dsRNAs. Dicer processes these dsRNAs into short repeat-associated siRNAs (rasiRNAs), with the possible assistance of two RNA helicases Spindle-E and Armitage, and the dsRNA binding protein Loquacious. The rasiRNAs are probably incorporated into a RISC-like complex with Aubergine, an Argonaute homolog, which silences the *Stellate* genes.

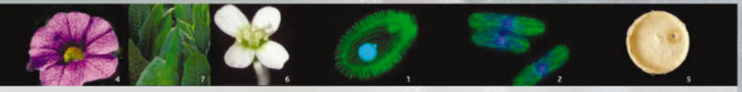

	Plant Petunia, Tobacco, *Arabidopsis thaliana*	*Tetrahymena*	Fission yeast *Schizosaccharomyces pombe*	*Neurospora crassa*
ng)	AGO1 (miRNA, PTGS*) AGO4 (heterochromatin)	Twi1	Ago1	QDE-2 (Quelling)
	DCL1 (miRNA) DCL2 (virus related) DCL3 (heterochromatin)	Dicer (DCL1)	Dcr1	
cing,	SDE3 (VIGS, PTGS*)		Hrr1	
	SGS2/SDE1/RDR6 (virus, PTGS*) RDR1 (virus PTGS*) RDR2 (chromatin silencing)		Rdp1	QDE-1 (Quelling)
	Hyl1 (miRNA) DRB4			
NAi) rmline RNAi) ng, RNAi)	HEN1 (miRNA, RNA methylase) SGS3 (PTGS*) SDE4/Pol IV subunits (RNAi) HASTY (miRNA transporter)	Pdd1	Cid12	QDE-3 (Quelling)

*PTGS, posttranscriptional gene silencing

THE COMPLETE miRNA SOLUTION PROVIDER™

microRNA Experimental Overview

As a unique class of small RNA molecules, miRNAs require special tools for accurate and sensitive analysis. Ambion's scientists have developed a portfolio of products that provide a complete solution to accelerate identification and characterization of this gene class. These tools will help you uncover the relationship between mRNA and protein expression, potentially leading to a new segment of targets for diagnostics and therapeutics.

Isolation and Enrichment

Isolation of Small RNAs

The first step in the analysis of miRNAs is purification from a biological sample. Most RNA isolation kits were developed to recover messenger RNA, while ignoring smaller molecules such as microRNA. The *mir*Vana™ miRNA isolation products are optimized to isolate all RNA species, including small RNA (less than 200 nt). The flashPAGE™ Fractionator can then be used to isolate RNA 10-14 nt in size, including mature miRNA.

PRODUCTS

- *mir*Vana™ miRNA Isolation Kit
- "miRNA Certified" FirstChoice® Total RNA
- *mir*Vana™ PARIS™ Kit
- flashPAGE™ Fractionator
- RecoverAll™ Total Nucleic Acid Isolation Kit for FFPE

Detection & Quantification

Global miRNA Expression

miRNA Microarray Profiling

The expression levels of miRNAs vary between tissues and developmental stages, and several miRNAs appear to be down-regulated in patients with chronic lymphocytic leukemia, colonic adenocarcinoma, and Burkitt's lymphoma. Evaluation of the global expression patterns of miRNAs provides key opportunities to identify regulation points for many different biological processes.

PRODUCTS

- *mir*Vana™ miRNA Bioarrays for Detection and Quantification
- *mir*Vana™ miRNA Array Probe Set
- *mir*Vana™ miRNA Array Labeling Kit

Specific miRNA Expression

Sensitive Detection of Specific miRNAs

Specialized tools provide sensitive, quantitative detection of miRNAs. These detection products provide highly accurate analysis of specific miRNAs, which is critical for the verification of data from microarray profiling or in-depth analysis of a small number of specific miRNAs.

PRODUCTS

- *mir*Vana™ qRT-PCR Detection Kit
- *mir*Vana™ miRNA Detection Kit
- *mir*Vana™ Probe and Marker Kit
- *mir*Vana™ miRNA Probe Construction Kit

Functional Analysis

Functional Studies

MicroRNA functional analysis can be performed with protocols that are similar to standard genes. Up-regulation of the miRNAs can be conducted to identify gain-of-function phenotypes; down-regulation or inhibition can be conducted to identify loss-of-function phenotypes. The combination of up- and down-regulation can be used to identify genes that are regulated by specific miRNAs as well as to identify cellular processes that are affected by specific miRNAs.

PRODUCTS

- Pre-miR™ miRNA Precursor Molecules
- siPORT™ *NeoFX*™ Transfection Agent
- Anti-miR™ miRNA Inhibitors
- pMIR-REPORT™ miRNA Expression Reporter Vector

Frequently Updated Online miRNA Resource: www.ambion.com/miRNA

translation likely contributes to overall cell motility by supplying new actin monomers precisely at the sites where they are needed. Another set of proteins found at leading edges is the Arp2/3 complex, a stable assemblage of seven polypeptides responsible for nucleating branched actin filaments. New data indicate that upon serum induction, all seven Arp2/3 complex mRNAs are recruited to the leading protrusions of polarized fibroblasts by a mechanism requiring both actin filaments and microtubules (*34*). Such colocalization of mRNAs encoding all the components of a single macromolecular complex has numerous potential advantages. Not only is translation and degradation of colocalized mRNAs amenable to coordinate regulation, synthesis of the component parts in close physical proximity very likely facilitates assembly of the complex. The high local concentration of nascent polypeptides might even promote their cotranslational association (Fig. 2), an arranged marriage having added advantages of preventing alternate folding pathways and excluding unwanted interactions with competing cellular components.

The End of the Line (or Is It?): P-bodies and Stress Granules

Because of their key position as transient intermediates in the flow of genetic information, mRNAs have limited lifetimes. As with all other aspects of mRNA metabolism, these half-lives are subject to modulation by changing intra- and extracellular conditions. How long an mRNA lives depends on how efficiently the mRNA degradation machinery is recruited to that mRNP. In general, the core degradation machinery attacks mRNA from its ends—the 3′ poly(A) tail is removed by a host of deadenylases, while the 5′ cap is removed by specific decapping enzymes. The body of the message is then degraded by 5′→3′ and 3′→5′ exonucleases. Whether a particular mRNA is destroyed primarily in one direction or the other is a function of which set of enzymes is most active in that particular cell type and which set is recruited most efficiently to that mRNP (*35*). Of course, endonucleolytic degradation mechanisms also exist, most notably sequence-specific mRNA cleavage by the RNA-induced silencing complex (RISC) in association with endogenous small interfering RNA (siRNA) (*5*–*7*).

The general mRNA decay machinery is also required for the elimination of aberrant mRNAs containing a premature translational stop signal (nonsense mRNA) or lacking a translational signal altogether (nonstop mRNA) (*28*, *36*). Such defective mRNAs can arise through a variety of mechanisms, including genetic mutation, missplicing, and premature polyadenylation. Their efficient elimination is thought to protect cells from the potentially deleterious consequences of inappropriately terminated proteins. Recognition of nonsense and nonstop mRNAs as abnormal requires their functional engagement by ribosomes, which fail to terminate properly on both nonsense and nonstop mRNAs (*36*, *37*). This improper termination leads to recruitment of the decay machinery, presumably through interactions with ribosome release factors and/or the empty A site tRNA binding pocket on the ribosome. In mammalian cells, decay of some nonsense mRNAs is quite efficient, occurring soon after they emerge from the nucleus and are still associated with CBC20/80 (*28*). However, it remains to be determined whether this timing is true of all mRNAs or is limited to those that immediately engage the translation apparatus upon export.

Consistent with the emerging idea that many mRNPs spend their productive lives at specific subcellular addresses or in working groups with other mRNPs, recent data also suggest that mRNPs go to specific places to die. In both yeast and mammalian cells, much of the mRNA decay machinery is concentrated in discrete cytoplasmic foci. These so-called cytoplasmic processing bodies, or ‘‘P-bodies’’ (PBs), appear to form around aggregates of mRNPs not actively involved in translation (*38*). Targeting of mRNPs to these structures requires their removal from the translationally active pool, one mechanism for which appears to be interaction with miRNAs and the RISC complex (*39*). Proof that mRNA decay occurs within PBs came with the demonstration that mRNA degradation intermediates accumulate there upon either general or mRNA-specific inhibition of decay (*40*, *41*).

Whereas PBs may represent the end of the line for mRNPs, ‘‘stress granules’’ (SGs), related but distinct structures in mammalian cells, serve as temporary retirement homes. When mammalian cells are exposed to an assortment of environmental stresses, global translational arrest of ‘‘housekeeping’’ transcripts is accompanied by the formation of distinct cytoplasmic structures containing translationally inactive mRNPs, 40S ribosomal subunits, and the mRNA binding proteins TIA-1 and TIAR. Prionlike domains in TIA-1/TIAR are thought to self-oligomerize and promote SG assembly (*42*). Although translational arrest upon application of stress is widespread, selective translation of heat shock proteins, as well as some transcription factors, under these conditions allows the cell to repair the stress-induced damage while conserving anabolic energy. When the stress is relieved, SGs disassemble and the sequestered mRNAs either return to the translationally active pool or are targeted for degradation in PBs (*43*, *44*). So far, SGs have not been observed in budding yeast. Instead, it has been suggested that *S. cerevisiae* PBs serve dual roles as way stations for translationally inactive mRNPs and sites of mRNA degradation (*38*).

In summary, recent advances have greatly heightened our appreciation of the extent to which eukaryotic cells regulate gene expression at the mRNP level. In some areas, such as the control of translation by 4E interacting proteins, underlying themes have begun to emerge. In other areas, such as the spatial localization of protein synthesis and the existence of genome-wide posttranscriptional regulatory networks, we have only begun to scratch the surface. No doubt further surprises await discovery along the path from birth to death of eukaryotic mRNAs.

References and Notes

1. M. C. Costanzo *et al.*, *Nucleic Acids Res.* **29**, 75 (2001).
2. C. Maris, C. Dominguez, F. H. Allain, *FEBS J.* **272**, 2118 (2005).
3. A. C. Messias, M. Sattler, *Acc. Chem. Res.* **37**, 279 (2004).
4. R. Stefl, L. Skrisovska, F. H. Allain, *EMBO Rep.* **6**, 33 (2005).
5. E. J. Sontheimer, R. W. Carthew, *Cell* **122**, 9 (2005).
6. P. D. Zamore, B. Haley, *Science* **309**, 1519 (2005).
7. G. Hutvágner, M. Simard, Eds., poster from the special issue on RNA, *Science* **309**, following p. 1518 (2 September 2005); published online 1 September 2005 (available at www.sciencemag.org/sciext/rna).
8. P. Fechter, G. G. Brownlee, *J. Gen. Virol.* **86**, 1239 (2005).
9. D. A. Mangus, M. C. Evans, A. Jacobson, *Genome Biol.* **4**, 223 (2003).
10. M. A. Skabkin *et al.*, *Nucleic Acids Res.* **32**, 5621 (2004).
11. T. O. Tange, A. Nott, M. J. Moore, *Curr. Opin. Cell Biol.* **16**, 279 (2004).
12. J. D. Keene, S. A. Tenenbaum, *Mol. Cell* **9**, 1161 (2002).
13. H. Hieronymus, P. A. Silver, *Genes Dev.* **18**, 2845 (2004).
14. D. Greenbaum, C. Colangelo, K. Williams, M. Gerstein, *Genome Biol.* **4**, 117 (2003).
15. S. Ghaemmaghami *et al.*, *Nature* **425**, 737 (2003).
16. A. P. Gerber, D. Herschlag, P. O. Brown, *PLoS Biol.* **2**, E79 (2004).
17. G. Dreyfuss, V. N. Kim, N. Kataoka, *Nat. Rev. Mol. Cell Biol.* **3**, 195 (2002).
18. Y. Huang, J. A. Steitz, *Mol. Cell* **17**, 613 (2005).
19. M. Suntharalingam, S. R. Wente, *Dev. Cell* **4**, 775 (2003).
20. M. S. Rodriguez, C. Dargemont, F. Stutz, *Biol. Cell.* **96**, 639 (2004).
21. W. Gilbert, C. Guthrie, *Mol. Cell* **13**, 201 (2004).
22. S. Rocak, P. Linder, *Nat. Rev. Mol. Cell Biol.* **5**, 232 (2004).
23. J. Zhao, S. B. Jin, B. Bjorkroth, L. Wieslander, B. Daneholt, *EMBO J.* **21**, 1177 (2002).
24. B. Daneholt, *Chromosoma* **110**, 173 (2001).
25. J. D. Lewis, E. Izaurralde, *Eur. J. Biochem.* **247**, 461 (1997).
26. K. C. Abruzzi, S. Lacadie, M. Rosbash, *EMBO J.* **23**, 2620 (2004).
27. F. Lejeune, A. C. Ranganathan, L. E. Maquat, *Nat. Struct. Mol. Biol.* **11**, 992 (2004).
28. L. E. Maquat, *Nat. Rev. Mol. Cell Biol.* **5**, 89 (2004).
29. J. D. Richter, N. Sonenberg, *Nature* **433**, 477 (2005).
30. O. Hachet, A. Ephrussi, *Nature* **428**, 959 (2004).
31. G. B. Gonsalvez, C. R. Urbinati, R. M. Long, *Biol. Cell.* **97**, 75 (2005).
32. D. St Johnston, *Nat. Rev. Mol. Cell Biol.* **6**, 363 (2005).
33. J. Condeelis, R. H. Singer, *Biol. Cell.* **97**, 97 (2005).
34. L. A. Mingle *et al.*, *J. Cell Sci.* **118**, 2425 (2005).
35. R. Parker, H. Song, *Nat. Struct. Mol. Biol.* **11**, 121 (2004).
36. L. E. Maquat, *Science* **295**, 2221 (2002).
37. N. Amrani *et al.*, *Nature* **432**, 112 (2004).
38. D. Teixeira, U. Sheth, M. A. Valencia-Sanchez, M. Brengues, R. Parker, *RNA* **11**, 371 (2005).
39. J. Liu, M. A. Valencia-Sanchez, G. J. Hannon, R. Parker, *Nat. Cell Biol.* **7**, 719 (2005).
40. U. Sheth, R. Parker, *Science* **300**, 805 (2003).
41. N. Cougot, S. Babajko, B. Seraphin, *J. Cell Biol.* **165**, 31 (2004).
42. N. Gilks *et al.*, *Mol. Biol. Cell* **15**, 5383 (2004).
43. P. Anderson, N. Kedersha, *J. Cell Sci.* **115**, 3227 (2002).
44. N. Kedersha *et al.*, *J. Cell Biol.* **169**, 871 (2005).

10.1126/science.1111443

Ribo-gnome: The Big World of Small RNAs

Phillip D. Zamore* and Benjamin Haley

Small RNA guides—microRNAs, small interfering RNAs, and repeat-associated small interfering RNAs, 21 to 30 nucleotides in length—shape diverse cellular pathways, from chromosome architecture to stem cell maintenance. Fifteen years after the discovery of RNA silencing, we are only just beginning to understand the depth and complexity of how these RNAs regulate gene expression and to consider their role in shaping the evolutionary history of higher eukaryotes.

In 1969, Britten and Davidson proposed that RNAs specify which genes are turned on and which are turned off in eukaryotic cells (*1*). Their elegant idea was that the base-pairing rules of Watson and Crick could solve the problem of eukaryotic gene regulation. With the subsequent discovery of protein transcription factors—there are perhaps 1850 in humans—the idea that a diverse array of RNA guides sets the expression profile of each cell type in a plant or animal was abandoned.

In fact, RNAs—specifically, tiny RNAs known as "small RNAs"—do control plant and animal gene expression. Distinct classes of these small RNAs—microRNAs (miRNAs), small interfering RNAs (siRNAs), and repeat-associated small interfering RNAs (rasiRNAs)—are distinguished by their origins, not their functions [see the poster in this issue (*2*)]. One class alone, the miRNAs, is predicted to regulate at least one-third of all human genes (*3*). Small RNAs, 21 to 30 nucleotides (nt) in length, provide specificity to a remarkable range of biological pathways. Without these RNAs, transposons jump (wreaking havoc on the genome), stem cells are lost, brain and muscle fail to develop, plants succumb to viral infection, flowers take on shapes unlikely to please a bee, cells fail to divide for lack of functional centromeres, and insulin secretion is dysregulated. The production and function of small RNAs requires a common set of proteins: double-stranded RNA (dsRNA)–specific endonucleases such as Dicer (*4*), dsRNA-binding proteins, and small RNA–binding proteins called Argonaute proteins (*5*, *6*). Together, the small RNAs and their associated proteins act in distinct but related "RNA silencing" pathways that regulate transcription, chromatin structure, genome integrity, and, most commonly, mRNA stability. The RNAs may be small, but their production, maturation, and regulatory function require the action of a surprisingly large number of proteins.

Department of Biochemistry and Molecular Pharmacology, University of Massachusetts Medical School, Worcester, MA 01605, USA.

*To whom correspondence should be addressed. E-mail: phillip.zamore@umassmed.edu

A Brief History of Small RNA

In 1990, two groups overexpressed a pigment synthesis enzyme in order to produce deep purple petunia flowers, but instead generated predominantly white flowers (Fig. 1) (*7*, *8*). This phenomenon was dubbed "cosuppression" because the transgenic and endogenous genes were coordinately repressed, and its discovery quietly ushered in the study of RNA silencing. By the end of the decade, RNA silencing phenomena were discovered in a broad spectrum of eukaryotes, from fungi to fruit flies. RNA interference (RNAi) is perhaps the best known RNA silencing pathway, in part because its discovery makes it possible to block expression of nearly any gene in a wide range of eukaryotes, knowing only part of the gene's sequence (*9*, *10*). Human clinical trials testing RNAi-based drugs are currently under way.

Building on the unexpected finding that both sense and antisense RNA could silence gene expression in *Caenorhabditis elegans* (*11*), the key breakthrough in RNA silencing was the discovery that dsRNA is the actual trigger of specific mRNA destruction, with the sequence of the dsRNA determining which mRNA is destroyed (*9*). Later, the dsRNA was found to be converted into siRNAs—fragments of the original dsRNA, 21 to 25 nt in length, that guide protein complexes to complementary mRNA targets, whose expression is then silenced (*12*–*14*). Thus, the actual mechanism of RNAi is remarkably like an early model for plant cosuppression, which postulated that small RNAs derived from the overexpressed gene might guide inactivation of cosuppressed genes (*15*).

In contrast to siRNAs, which derive from dsRNA hundreds or thousands of base pairs long, miRNAs derive from long, largely unstructured transcripts (pri-miRNA) containing stem-loop or "hairpin" structures ~70 nt in length [reviewed in (*16*)]. The hairpins are cut out of the pri-miRNA by the dsRNA-specific endonuclease Drosha, acting with its dsRNA-binding protein partner DGCR8 in humans or Pasha in flies, to yield a pre-miRNA (Fig. 2) (*2*). Each mature miRNA resides in one of the two sides of the ~30–base pair stem of the pre-miRNA. The mature miRNA is excised from the pre-miRNA by another dsRNA-specific endonuclease, Dicer, again acting with a dsRNA-binding protein partner, the *tar*-binding protein (TRBP) in humans or Loquacious (Loqs) in flies. The April 2005 release of the miRNA Registry, an online database that coordinates miRNA annotation, records 1650 distinct miRNA genes, including 227 from humans and 21 from human viruses; 1648 of these were discovered in the 21st century. Whereas siRNAs are found in eukaryotes from the base to the crown of the phylogenetic tree, miRNAs have been discovered in plants and animals and their viruses only.

Ambros and co-workers discovered the first miRNA, *lin-4*, in 1993. They identified two RNA transcripts—one small and one smaller—derived from the *lin-4* locus of *C. elegans* (*17*). Earlier experiments showed that loss-of-function mutations in *lin-4* disrupted the developmental timing of worms, much as did gain-of-function mutations in the protein-coding gene *lin-14*. Noting that *lin-4* could form base pairs, albeit imperfectly, with sites in *lin-14*, Ambros and colleagues proposed that the 22-nt *lin-4* regulates the much longer *lin-14* mRNA by multiple RNA-RNA interactions between the miRNA and the 3′ untranslated region of its mRNA target. This remarkable paper predicted the contemporary miRNA pathway, suggesting that the longer 61-nt transcript corresponds to a precursor RNA that folds into a hairpin structure from which the 22-nt mature *lin-4* miRNA is excised. Eight years later, the prescient observation that "*lin-4* may represent a class of developmental regulatory genes that encode small antisense RNA products" (*17*) was amply validated by the discovery that miRNAs compose a large class of riboregulators (*18*–*23*).

The *lin-4* miRNA was discovered 3 years after the first reports of RNA silencing in plants (*7*, *8*) and 2 years before the first hint of RNAi in nematodes (*11*). However, no formal connection between miRNAs and siRNAs was made until 2001, when Dicer, the enzyme that converts long dsRNA into siRNAs (*4*, *24*), was shown to convert pre-miRNAs, such as the longer 61-nt transcript from *lin-4*, into mature miRNAs, like *lin-4* itself (*25*–*27*).

The human genome may contain ~1000 miRNAs, a few of which may not only be unique to humans, but may also contribute to making us uniquely human. Recent efforts to define the entirety of this small RNA class have uncovered 53 miRNAs unique to primates (*28*). Because miRNAs are small, they may evolve

rapidly, with new miRNA genes arising by duplication and mutation of the 21-nt miRNA sequence.

Small on Specificity

From the standpoint of binding specificity, small RNAs are truly diminutive. A mere six or seven of the 21 nucleotides within a miRNA or siRNA provide the bulk of binding specificity for the small RNA–protein complexes they guide. As first proposed by Lai (*29*), and subsequently confirmed computationally (*3*, *30*) and experimentally for miRNAs (*31–34*) and siRNAs (*35*, *36*), the 5′ end of a miRNA or an siRNA contributes disproportionately to target RNA binding. Kinetic and structural studies suggest that the first nucleotide of a small RNA guide is unpaired during small RNA function (*36–38*). The small region of the small RNA that mediates target binding has been called the "seed sequence," a term intended to suggest that the region nucleates binding between the small RNA guide and its target, and that the more 3′ regions of the small RNA subsequently zipper-up—if they can—with the 5′ regions of the binding site on the target RNA (*39*).

In truth, current experimental evidence cannot discern the order in which distinct regions of the small RNA interact with its binding site on the target RNA. Both computational and experimental approaches detect only the binding contributions of specific small RNA regions at equilibrium. But the finding that stable binding between the small RNA and its target derives from such a small region of an already puny RNA oligonucleotide implies that the manner in which the small RNA interacts with its target is very different from antisense oligonucleotide–target RNA pairing. This radical and unexpected mode of nucleic acid interaction is almost certainly a consequence of the way the small RNA—both alone and paired to its RNA target—is bound by a member of the Argonaute family of proteins. These multidomain proteins are specialized for binding the small RNAs that mediate RNA silencing; understanding the relationship of Argonaute protein structure to their functions in controlling gene expression is now the key to understanding the deeper physical meaning of the small RNA "seed sequence."

The small RNAs that act in RNA silencing pathways are like fancy restriction enzymes whose recognition sites occur at random once every ~4000 to ~65,000 nt of sequence. But unlike restriction enzymes, which cut DNA wherever they bind, small RNAs can act in two distinct ways, each of which dramatically extends their functional specificity (Fig. 3) (*2*). When a small RNA pairs extensively with its RNA target, it directs cleavage of a single phosphodiester bond in the target RNA, across from nucleotides 10 and 11 of the small RNA guide (*40*). Thus, small RNA–directed cleavage is much more specific than small RNA binding itself, as it occurs only when most of the 21 nt of the siRNA or miRNA can base pair to form at least one turn of an A-form helix with the RNA target (*36*, *41*, *42*). Even when the small RNA is fully complementary to its target RNA, cleavage only occurs when the RNA is bound to the right Argonaute protein (*43*, *44*). In humans, only one of the four Argonaute proteins examined in detail retains all the amino acids required to catalyze target RNA cleavage (*45*). Argonaute proteins contain two RNA-binding domains: the Piwi domain, which binds the small RNA guide at its 5′ end, and the PAZ domain, which binds the single-stranded 3′ end of small RNA. The endonuclease that cleaves target RNAs resides in the Piwi domain, and this domain is a structural homolog of the DNA-guided RNA endonuclease RNase H (*46*). Target RNA cleavage is commonly viewed as the siRNA or RNAi mode, but is actually the dominant mechanism by which plant miRNAs regulate their targets (*47*, *48*) and is found for at least a small number of animal (*49*, *50*) and viral miRNAs (*51*).

In *Drosophila* or human cell lysates, small RNA–programmed Argonaute2 (Ago2) acts as a multiple-turnover enzyme, with each small RNA directing the cleavage of hundreds of target molecules (*36*, *52*). Small RNA–directed mRNA cleavage cuts an mRNA into two pieces, and efficient release of these fragments requires adenosine triphosphate (ATP) (*36*). Proteins besides Ago2 may be required for release of the products of small RNA–directed target cleavage. In fact, Ago2 alone can direct a single round of target cleavage but cannot efficiently catalyze additional cycles, likely because the cleavage products remain bound to the small RNA within the enzyme (*45*). After the cleaved pieces of the target are released, the 3′ fragment is destroyed in the cytoplasm by the exonuclease Xrn1 while the 5′ fragment is degraded by the exosome, a collection of exonucleases dedicated to 3′-to-5′ RNA degradation (*53*). In plants and animals, when miRNAs direct mRNA cleavage, a short polyuridine [poly(U)] tail is subsequently added to the 3′ end of the 5′ cleavage fragment (*54*). Addition of poly(U) correlates with decapping and 5′-to-3′ destruction of the target RNA cleavage fragment, at least in plants, suggesting an alternative route to the exosome for degradation of the 5′ cleavage product.

When siRNAs or miRNAs pair only partially with their targets, they cannot direct mRNA cleavage. Instead, they block translation of the mRNA into protein (*55*, *56*). However, binding of a single miRNA alone is usually insufficient to measurably block translation; instead, several miRNAs bind to the same target—opening the door to combinatorial control of gene expression by sets of coordinately expressed miRNAs (*39*). Initially, miRNAs were proposed to repress translation at a step after ribosomes have bound the mRNA, i.e., after translational initiation (*55*). One idea was that they direct degradation of the nascent polypeptide as it emerges from the ribosome. Alternatively, they might "freeze" ribosomes in place on the mRNA, stalling elongation of the growing protein chain. Recent findings, however, call these ideas into question. For example, translational repression by miRNAs was thought to affect

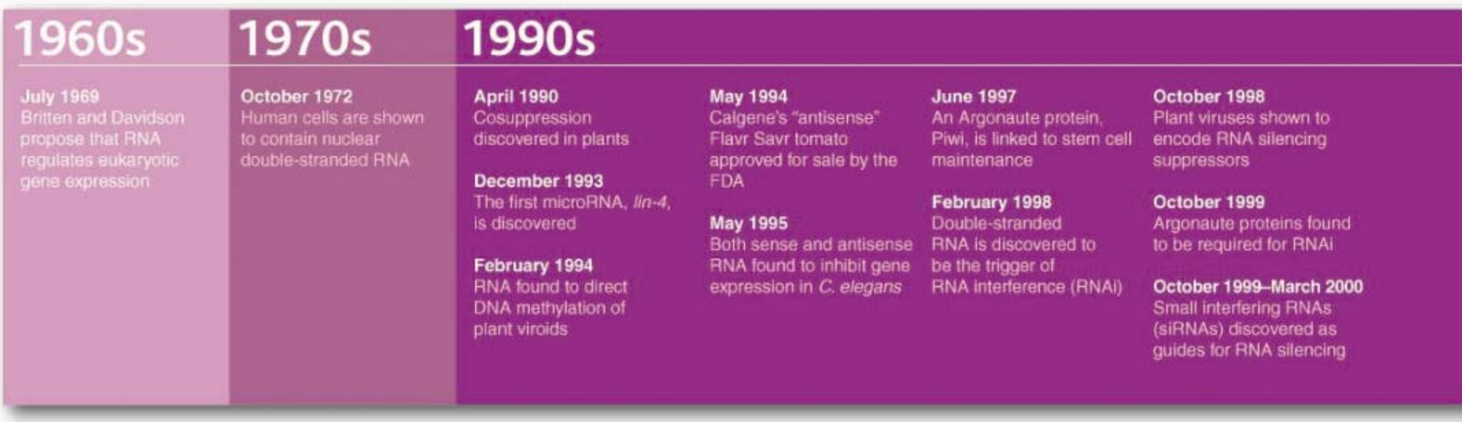

Fig. 1. A chronology of some of the major discoveries and events in RNA silencing.

only protein synthesis, not mRNA stability. Yet Lim and co-workers found that miRNAs can alter the stability of hundreds of mRNAs (*57*). And Pasquinelli and co-workers have now shown that even the founding miRNAs, worm *lin-4* and *let-7*, trigger destruction of their mRNA targets (*58*). These changes in steady-state mRNA levels are unlikely to reflect cleavage of the miRNA targets, because the complementarity between the miRNAs and their mRNA targets is restricted mainly to the seed sequence. How, then, could miRNAs make mRNA less stable? New studies offer a potential explanation.

Small RNAs, bound to Ago2, can move the mRNAs they bind from the cytosol to sites of mRNA destruction called "P-bodies" (*59*, *60*). Ago2 concentrates in P-bodies only when it binds small RNAs like miRNAs and siRNAs; Ago2 mutants that cannot bind small RNAs remain in the cytosol (*59*). Moreover, Ago2 associates with the enzymes that remove the 5′ 7-methylguanosine cap characteristic of mRNAs, a prerequisite for their destruction in the P-body (*59*, *60*). It is tempting to imagine that this new role for small RNAs, moving an mRNA to P-bodies, explains the mystery of small RNA–directed translational repression: By sequestering mRNA in the P-body, small RNAs would block translation. Subsequent destruction of the mRNA would then be a secondary consequence of relocating the mRNA from the cytosol to the P-body, which contains no ribosomal components (Fig. 4). Binding of a miRNA to the mRNA would not alter its inherent decay rate. The steady-state abundance of mRNAs that intrinsically turn over rapidly would therefore be reduced more than that of intrinsically more stable mRNAs when each is targeted by small RNA, but the translational rate of the two mRNAs would be reduced equally.

Is repression of mRNA translation by miRNAs just a consequence of the relocalization of the mRNA to the P-body? Filipowicz and colleagues argue in this issue of *Science* that translational repression comes first (*61*). They show that when bound to an mRNA target, human *let-7* miRNA blocks translational initiation. They propose that the consequence of miRNA-directed inhibition of translational initiation is relocalization of the mRNA target to the P-body. Once in the P-body, the mRNA may then be degraded, releasing the miRNA-programmed protein complex so it can return to the cytosol to begin a new round of target mRNA repression (Fig. 4). This pathway is presumed to be distinct from the small RNA–directed cleavage pathway, in which Ago2 in flies or mammals first cleaves a single phosphodiester bond in the mRNA target, and then the 5′ cleavage product is degraded by the exosome without obligate decapping.

Do all miRNAs repress gene expression? At least one human miRNA appears to act positively. Replication of hepatitis C virus (HCV) requires binding of human miR-122 to the 5′ noncoding region of the virus (*62*). Thus, for HCV, miR-122 acts as an enhancer of replication, and only cells expressing miR-122 support efficient HCV replication. Whether the positive effect of miR-122 on HCV is unique or represents an undiscovered mode of miRNA action remains unknown.

Aberrant, Unwanted

RNAi has been implicated in silencing parasitic DNA sequences, such as transposons and repetitive sequences. In many organisms, a specialized RNA silencing pathway senses the "aberrant RNA" transcribed from such sequences, and then initiates silencing posttranscriptionally and even transcriptionally. A candidate for an aberrant RNA sensor is a class of RNA silencing proteins that can copy single-stranded RNA into dsRNA. These RNA-dependent RNA polymerases (RdRPs) are found in nearly every eukaryote with a functioning RNA silencing pathway—except insects and mammals. In addition to initiating silencing responses from single-stranded trigger RNAs, RdRPs have been proposed to amplify and sustain silencing triggered by dsRNA. How RdRP enzymes distinguish between normal and aberrant transcription remains a key mystery of RNA silencing.

Meanwhile, Back in the Nucleus

RNA-directed transcriptional silencing was first identified in plants, where dsRNA corresponding to nontranscribed sequences can direct DNA methylation and transcriptional repression (*63*, *64*). Genetic studies in worms, plants, and *Schizosaccharomyces pombe* implicate small RNAs and the canonical components of the RNA silencing machinery—RdRP, Dicer, and Argonaute—in transcriptional silencing (*65*–*70*). Components of the RNAi machinery are also required for transcriptional silencing in flies (*71*, *72*). Transcriptional silencing directed by small RNAs is typically associated with the formation of heterochromatin, a transcriptionally repressed, compact form of chromatin in which the amino terminus of histone H3 is modified by methylation at lysine 9 ("H3K9"). In some organisms, such as plants and mammals, heterochromatic DNA is also hypermethylated. In *Tetrahymena*, small RNA–directed heterochromatin formation drives the deletion of specific regions of chromosomal DNA in the macronucleus (*73*, *74*).

A well-studied example of siRNA-directed assembly of heterochromatin is the outer regions of the centromere in *S. pombe*. Without this heterochromatin, *S. pombe* centromeres cannot reliably mediate chromosome segregation during cell division. Such a role for the RNA silencing machinery in assembling centromeric heterochromatin may be quite common, as chicken and mouse cells lacking Dicer also fail to assemble silent heterochromatin at their centromeres (*75*, *76*).

Repetitive, transposon-like sequences compose the outer regions of the *S. pombe* centromere. Mammalian centromeres likewise comprise repetitive sequences. Thus, how the RNA silencing machinery silences centromeric repeats may be just an example of the broader question of understanding the mechanism by which the RNA silencing machinery detects

2000s

October 2000
Double-stranded RNA shown to direct DNA methylation

January 2001
Dicer shown to make siRNAs

May 2001
RNAi discovered in human cells

July 2001
Dicer found to make microRNAs (miRNAs)

October 2001
miRNAs are established as a large class of gene regulators

July 2002
Plant miRNAs are discovered

July 2002
siRNAs are revealed as triggers of RNAi in mice

September 2002
Small RNAs guide the production of heterochromatin at centromeres

November 2002
miRNAs implicated in cancer

September 2003
It is clear that miRNA maturation begins in the nucleus

November 2003
Dicer shown to be required for mouse embryogenesis, and perhaps for stem cell production

March 2004
Human genome-wide RNAi libraries become available

April 2004
Animal viruses found to encode miRNAs

August 2004
First "investigational new drug" application filed for a therapeutic siRNA

September 2004
Argonaute is revealed as the RNAi endonuclease, "Slicer"

June 2005
miRNAs shown to act as oncogenes

July 2005
Primate-specific miRNAs identified

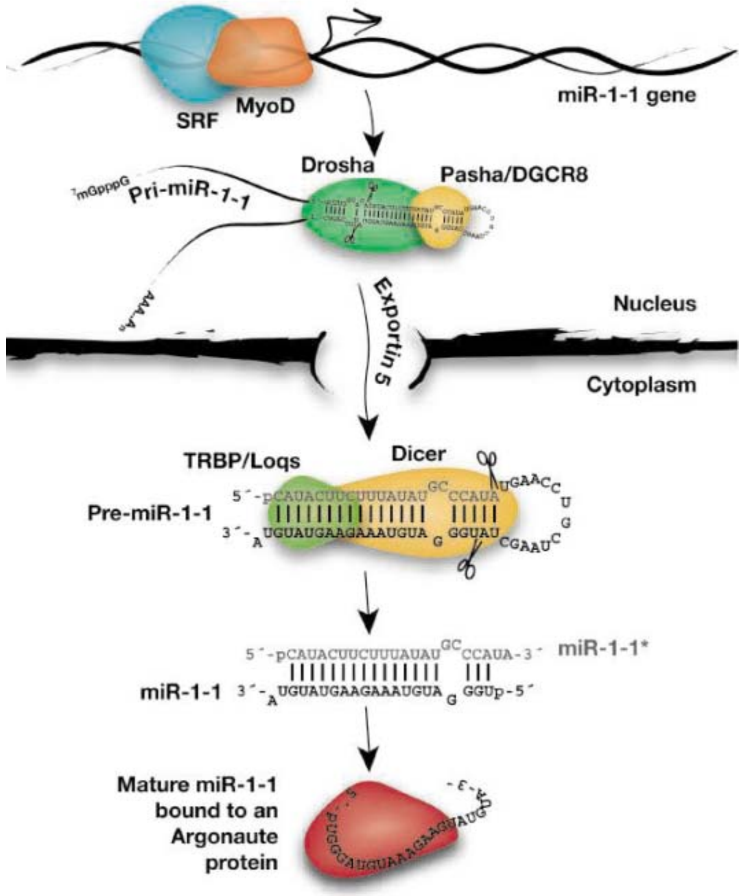

Fig. 2. A day in the life of the miRNA miR-1. In developing cardiac tissue, the transcription factors SRF (serum response factor) and MyoD promote RNA Pol II–directed transcription of pri-miR-1. In the nucleus, the RNase III endonuclease Drosha, together with its dsRNA-binding partner, Pasha/DGCR8, excises pre-miR-1 from pri-miR-1, breaking the RNA chain on both the 5′ and 3′ sides of the pre-miR-1 stem, leaving a ~2-nt, single-stranded 3′ overhang end. Exportin 5 recognizes this characteristic pre-miRNA end structure, transporting pre-miR-1 from the nucleus to the cytoplasm. In the cytoplasm, a second RNase III endonuclease, Dicer, together with its dsRNA-binding partner protein, Loqs/TRBP, makes a second pair of cuts, liberating miR-1 as a "miRNA/miRNA*" duplex. Mature, 21-nt long miR-1 is then loaded from the duplex into an Argonaute family member and miR-1* is destroyed. miR-1 guides the Argonaute protein to its target RNAs, such as the 3′ untranslated region of the *hand2* mRNA. Binding of the miR-1–programmed Argonaute protein represses production of Hand2 protein, halting cardiac cell proliferation.

and silences repetitive sequences. A coherent but speculative model of small RNA–directed transcriptional silencing emerges from recent studies in both *S. pombe* and plants. Transcripts from genomic regions to be targeted for silencing must first be converted to dsRNA. RdRPs have been assigned this role. Mutation of catalytically essential amino acids demonstrates that the polymerase activity of Rdp1, the sole *S. pombe* RdRP enzyme, is required for centromeric silencing (*77*), but what template RNA is copied by the RdRP has not been directly established in any organism. The dsRNA envisioned to be generated by the RdRP must next be converted to siRNAs, presumably by Dicer. In plants, distinct RdRP and Dicer paralogs are devoted to separate RNA silencing pathways, with RDR2, the RdRP, collaborating with DCL3, the Dicer, to generate siRNAs that target repetitive sequences for both cytosine and H3K9 methylation (*68*). Presumably the double-stranded siRNAs thus generated are unwound and the resulting single strands loaded into a member of the Argonaute family of proteins: Ago1 in *S. pombe* and AGO4, among others, in plants (*65–67*, *78*). The siRNAs, bound to the Argonaute protein within a larger complex of DNA and chromatin-modifying enzymes, guide the assembly of heterochromatin. How insects and mammals derive chromatin-silencing triggers in the absence of an RdRP is unknown.

What does it mean when we propose that siRNAs guide modifying enzymes to DNA, converting it to heterochromatin? Do we imagine that the siRNAs pair directly with single-stranded DNA, somehow separating the two strands of the chromosomal DNA, as proposed by Britten and Davidson (*1*)? Or rather, do the siRNAs bind RNA, as has been proposed for centromeric silencing in *S. pombe* (*79*)? This second model is comforting because it imagines that siRNAs interact with RNA in both

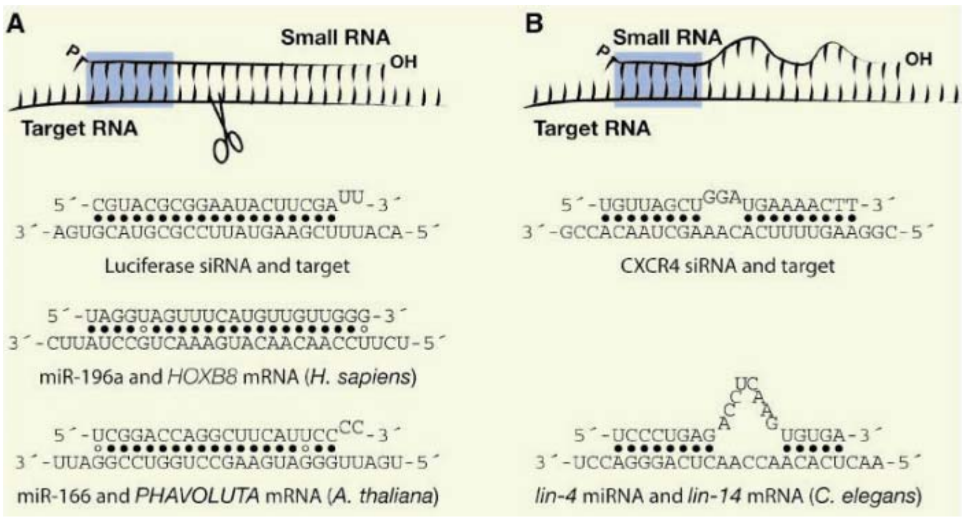

Fig. 3. Small RNA binding modes. (**A**) Extensive pairing of a small RNA to an mRNA allows the Piwi domain of a catalytically active Argonaute protein (e.g., Ago2 in humans or flies) to cut a single phosphodiester bond in the mRNA, triggering its destruction. Synthetic siRNAs typically exploit this mechanism, but some mammalian miRNAs (such as miR-196a) and most, if not all, plant miRNAs direct an Argonaute protein to cut their mRNA targets. (**B**) Partial pairing between the target RNA and the small RNA, especially through the "seed" sequence—roughly nucleotides 2 to 7 of the small RNA—tethers an Argonaute protein to its mRNA target. Binding of the miRNA and Argonaute protein prevents translation of the mRNA into protein. siRNAs can be designed to trigger such "translational repression" by including central mismatches with their target mRNAs; animal miRNAs such as *lin-4*, the first miRNA discovered, typically act by this mode because they are only partially complementary to their mRNA targets. The seed sequence of the small RNA guide is highlighted in blue.

transcriptional and post-transcriptional silencing, but it requires transcription across regions of DNA that were thought to lie untranscribed, such as promoters or intragenic regions. In plants, ''transcriptionally silenced'' DNA appears to be transcribed by a specialized type of DNA-dependent RNA polymerase, RNA polymerase IV (Pol IV) (*80–82*). RNA Pol IV may be specially adapted to transcribe silent heterochromatin, thereby providing a constant source of primary transcript to act as template for the RdRP and hence generating the dsRNA substrate required for Dicer to manufacture siRNAs (*80*). The model is appealing because it explains why siRNAs persist even after they have silenced the gene from which they arise.

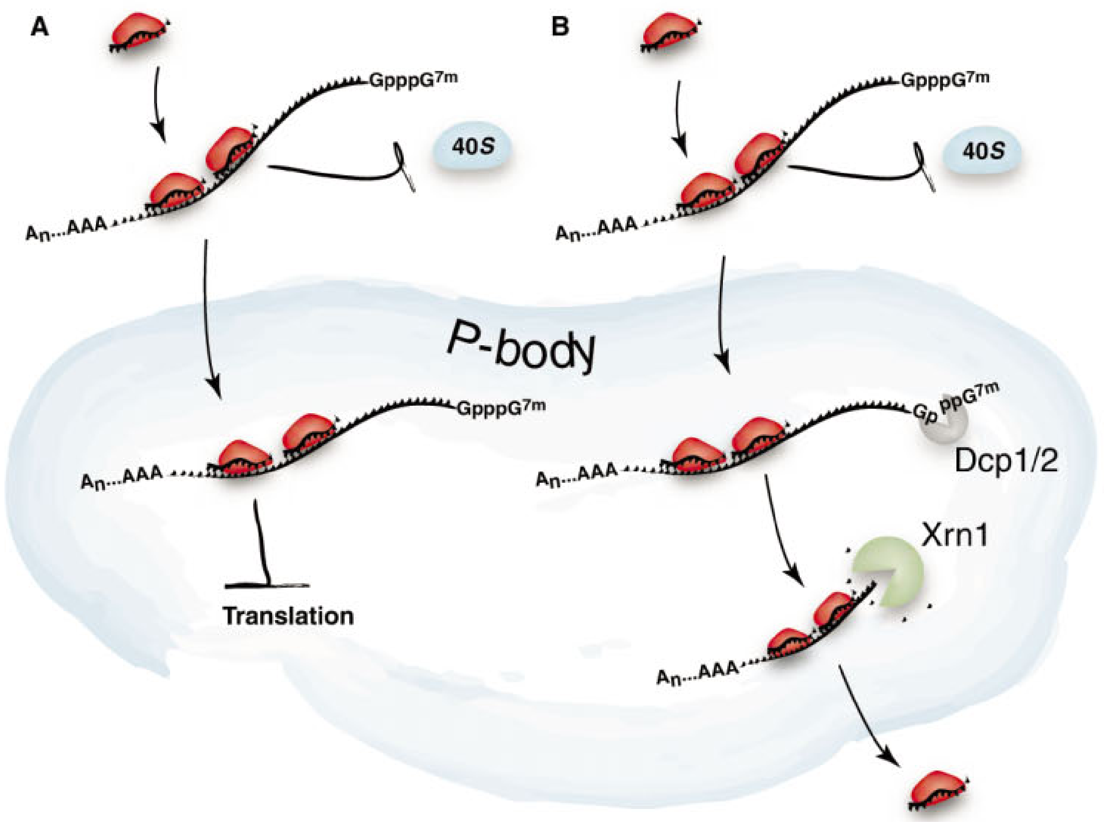

Fig. 4. A speculative model for translational repression by small RNAs: sequestration of a highly stable mRNA in the P-body. Binding of a small RNA–programmed Argonaute protein (red) to an mRNA blocks translational initiation, driving the mRNA into a P-body, the cytoplasmic site of mRNA decapping and degradation. Sequestering an mRNA in a P-body further excludes it from ribosomes, so it cannot be translated into protein. In (**A**), the mRNA is imagined to be degraded slowly in the P-body, so the miRNA appears only to repress translation. It is unknown whether mRNAs, once moved to the P-body by the binding of a small RNA, can ever return to the cytoplasm and resume translation. In (**B**), the mRNA is envisioned to be inherently prone to rapid degradation. Binding of an Argonaute-bound small RNA to an mRNA moves the mRNA to the P-body, where the decapping enzyme, Dcp1/2, is envisioned to remove its 7-methyl guanosine cap, triggering its destruction by the 5′-to-3′ exonuclease Xrn1. For the mRNA in (A), small RNAs appear to repress its translation without appreciably altering its steady-state abundance, whereas in (B), small RNAs appear to target the mRNA for exonucleolytic destruction, yet in both cases small RNAs change the cellular compartment in which the mRNA resides.

Pol IV might also supply the transcripts that provide a scaffold for siRNA-guided chromatin modification complexes to act on the adjacent DNA. Pol IV enzymes, however, occur only in plants; in *S. pombe*, formation of silent centromeric heterochromatin requires the classical RNA Pol II (*83*, *84*). This finding suggests that RNA Pol II may supply transcripts required for the production of the siRNAs themselves. For some *S. pombe* loci, perhaps even RNA Pol I provides these transcripts (*85*). Yet Pol II is required when the initial trigger of silencing is provided in trans—for example, by initiating silencing with a double-stranded hairpin—which suggests that Pol II transcription creates the target for the small RNAs as well as the trigger for small RNA production (*84*). Transcription per se is not sufficient; instead, a direct interaction between the carboxyl-terminal domain of Pol II and the RNA silencing machinery appears to help recruit the Argonaute protein, but only when loaded with siRNA, to the DNA (*84*).

These findings suggest that siRNAs interact directly with DNA and that siRNA-guided complexes can find their cognate DNA-binding sites only in the short interval during transcription of a sequence when the DNA is unpaired; when the DNA pairs again behind the polymerase, the site becomes inaccessible to the siRNA. However, most current data are also consistent with siRNAs binding nascent transcripts themselves, but in a manner that requires their being loaded on these sites by virtue of their association, through proteins, with RNA Pol II. Perhaps for genes transcribed by RNA Pol I (*85*), a similar protein-protein interaction allows the Argonaute-bound siRNA to follow closely behind the polymerase as it traverses the ''silenced'' gene.

Yet More RNA Polymerization, Just to Destroy RNA?

Template-dependent RNA polymerases are not the only RNA polymerases implicated in RNA silencing. Members of the polymerase β nucleotidyltransferase superfamily of proteins are required for RNA silencing in worms and fission yeast. This protein superfamily encompasses enzymes that either add polyadenosine to the 3′ end of RNA [poly(A) polymerases] or use ATP to make 2′-5′ polymers of adenosine monophosphate (2′-5′ oligoadenylate synthases). In worms, mutations in conserved residues in the nucleotidyltransferase domain of RDE-3 disrupt RNAi, suggesting that adenosine polymers may play a direct role in RNA silencing (*86*). In fission yeast, the putative nucleotidyl transferase Cid12 is required for heterochromatin assembly by the RNA silencing pathway (*79*). Cid12, a putative helicase protein, and Rdp1, the *S. pombe* RdRP, form a complex implicated in siRNA production. This complex also contains noncoding RNAs transcribed from centromeric DNA, the primary target of heterochromatin assembly in fission yeast, consistent with the idea that these noncoding transcripts act as templates for Rdp1, which may convert them into dsRNA, which in turn could be converted to siRNA by Dcr1, thereby triggering RNA silencing. But what do Cid12 and RDE-3 do? These enzymes may play a direct role in RNA silencing; a poly(A) tail synthesized by Cid12 may recruit enzymes that mediate heterochromatin-specific modifications to transcripts under surveillance by the RNA

silencing machinery (*79*). Alternatively, Cid12 and Rdp1 may be components of a common surveillance complex—and hence dependent on each other for their stability. This complex would contain components of two separate pathways that protect cells against "aberrant RNA"—transcripts that are misfolded, incorrectly spliced, or damaged such that they encode truncated proteins. Favoring this view, the budding yeast protein Trf4p, another polymerase β nucleotidyltransferase, adds poly(A) tails to misfolded tRNAs and to aberrant mRNAs, targeting them for destruction by the nuclear exosome, a complex of RNA-degrading enzymes (*87*–*89*). Use of a poly(A) tail as a degradation signal, rather than as a stabilizing feature that promotes mRNA translation, may be quite ancient, as bacteria use poly(A) tails to target RNA for destruction.

Stem Cells

Epigenetic marks play an important role in stem cells, which must divide to yield a daughter cell that differentiates and another that regenerates the original stem cell. RNA silencing has emerged as a vital regulatory mechanism for maintaining normal stem cell pools. Mice lacking Dicer die at embryonic day 7.5, devoid of Oct-4–expressing cells (*90*); in mammals, Oct-4 marks stem cell lineages. At least four genes in the RNA silencing pathway are required for germline stem cell function in *Drosophila melanogaster*. Piwi, an Argonaute protein, is required both to maintain female germline stem cells and to promote their proliferation (*91*). Dicer-1, which makes miRNAs and perhaps other types of small RNAs, and its dsRNA-binding protein partner, Loqs, are both required for normal germline stem cell function. In the fly ovary, germline stem cells lacking Dicer divide slowly, dramatically reducing the number of eggs generated (*92*). In contrast, in females mutant for Loqs in both the soma and the germ line, germline stem cells are lost, either because they die or because they differentiate into oocytes without replenishing the stem cell pool (*93*). It remains to be established whether these defects reflect loss of miRNAs (which require the coordinate action of Dicer-1 and Loqs for their maturation), loss of silent heterochromatin, or both.

Flies lacking Ago2 contain fewer pole cells, the germline stem cell progenitors, than do wild-type flies (*94*). The case of *ago2* mutants is particularly instructive, because loss of Ago2—like loss of the very first Argonaute protein implicated in RNA silencing, worm RDE-1 (*5*)—was originally reported to cause no cellular defects except loss of an RNAi response to exogenous dsRNA (*95*). Closer examination revealed that many aspects of early embryogenesis are defective, yet the flies somehow compensate and survive (*94*). In particular, *ago2* mutants show defects in chromosome condensation, nuclear division, spindle assembly, and nuclear timing, all perhaps caused by a loss of heterochromatin assembly normally guided by an RNA silencing pathway. It remains to be shown if Ago2 acts directly in the assembly of heterochromatin by the RNA silencing pathway, or if components common to the RNAi and transcriptional silencing pathways become unstable in the absence of Ago2 protein. But these results underscore the guiding principle of small RNA function: Small RNAs play a very big role in nearly every cellular process.

References and Notes

1. R. J. Britten, E. H. Davidson, *Science* **165**, 349 (1969).
2. G. Hutvágner, M. Simard, Eds., poster from the special issue on RNA, *Science* **309**, following p. 1518 (2 September 2005); published online 1 September 2005 (available at www.sciencemag.org/sciext/rna).
3. B. P. Lewis, C. B. Burge, D. P. Bartel, *Cell* **120**, 15 (2005).
4. E. Bernstein, A. A. Caudy, S. M. Hammond, G. J. Hannon, *Nature* **409**, 363 (2001).
5. H. Tabara *et al.*, *Cell* **99**, 123 (1999).
6. S. M. Hammond, S. Boettcher, A. A. Caudy, R. Kobayashi, G. J. Hannon, *Science* **293**, 1146 (2001).
7. C. Napoli, C. Lemieux, R. A. Jorgensen, *Plant Cell* **2**, 279 (1990).
8. A. R. van der Krol, L. A. Mur, M. Beld, J. N. M. Mol, A. R. Stuitji, *Plant Cell* **2**, 291 (1990).
9. A. Fire *et al.*, *Nature* **391**, 806 (1998).
10. S. Elbashir, J. Harborth, K. Weber, T. Tuschl, *Methods* **26**, 199 (2002).
11. S. Guo, K. J. Kemphues, *Cell* **81**, 611 (1995).
12. A. J. Hamilton, D. C. Baulcombe, *Science* **286**, 950 (1999).
13. S. M. Hammond, E. Bernstein, D. Beach, G. J. Hannon, *Nature* **404**, 293 (2000).
14. P. D. Zamore, T. Tuschl, P. A. Sharp, D. P. Bartel, *Cell* **101**, 25 (2000).
15. J. A. Lindbo, L. Silva-Rosales, W. M. Proebsting, W. G. Dougherty, *Plant Cell* **5**, 1749 (1993).
16. V. N. Kim, *Nat. Rev. Mol. Cell Biol.* **6**, 376 (2005).
17. R. C. Lee, R. L. Feinbaum, V. Ambros, *Cell* **75**, 843 (1993).
18. M. Lagos-Quintana, R. Rauhut, W. Lendeckel, T. Tuschl, *Science* **294**, 853 (2001).
19. N. C. Lau, L. P. Lim, E. G. Weinstein, D. P. Bartel, *Science* **294**, 858 (2001).
20. R. C. Lee, V. Ambros, *Science* **294**, 862 (2001).
21. C. Llave, K. D. Kasschau, M. A. Rector, J. C. Carrington, *Plant Cell* **14**, 1605 (2002).
22. W. Park, J. Li, R. Song, J. Messing, X. Chen, *Curr. Biol.* **12**, 1484 (2002).
23. B. J. Reinhart, E. G. Weinstein, M. W. Rhoades, B. Bartel, D. P. Bartel, *Genes Dev.* **16**, 1616 (2002).
24. S. W. Knight, B. L. Bass, *Science* **293**, 2269 (2001).
25. A. Grishok *et al.*, *Cell* **106**, 23 (2001).
26. G. Hutvágner *et al.*, *Science* **293**, 834 (2001).
27. R. F. Ketting *et al.*, *Genes Dev.* **15**, 2654 (2001).
28. I. Bentwich *et al.*, *Nat. Genet.* **37**, 766 (2005).
29. E. C. Lai, *Nat. Genet.* **30**, 363 (2002).
30. B. Lewis, I. Shih, M. Jones-Rhoades, D. Bartel, C. Burge, *Cell* **115**, 787 (2003).
31. J. G. Doench, P. A. Sharp, *Genes Dev.* **18**, 504 (2004).
32. A. Mallory *et al.*, *EMBO J.* **23**, 3356 (2004).
33. J. Brennecke, A. Stark, R. B. Russell, S. M. Cohen, *PLoS Biol.* **3**, e85 (2005).
34. E. C. Lai, B. Tam, G. M. Rubin, *Genes Dev.* **19**, 1067 (2005).
35. A. L. Jackson *et al.*, *Nat. Biotechnol.* **21**, 635 (2003).
36. B. Haley, P. D. Zamore, *Nat. Struct. Mol. Biol.* **11**, 599 (2004).
37. J. B. Ma *et al.*, *Nature* **434**, 666 (2005).
38. J. S. Parker, S. M. Roe, D. Barford, *Nature* **434**, 663 (2005).
39. D. P. Bartel, *Cell* **116**, 281 (2004).
40. S. M. Elbashir, W. Lendeckel, T. Tuschl, *Genes Dev.* **15**, 188 (2001).
41. Y.-L. Chiu, T. M. Rana, *Mol. Cell* **10**, 549 (2002).
42. J. Martinez, T. Tuschl, *Genes Dev.* **18**, 975 (2004).
43. J. Liu *et al.*, *Science* **305**, 1437 (2004).
44. G. Meister *et al.*, *Mol. Cell* **15**, 185 (2004).
45. F. V. Rivas *et al.*, *Nat. Struct. Mol. Biol.* **12**, 340 (2005).
46. J.-J. Song, S. K. Smith, G. J. Hannon, L. Joshua-Tor, *Science* **305**, 1434 (2004).
47. C. Llave, Z. Xie, K. D. Kasschau, J. C. Carrington, *Science* **297**, 2053 (2002).
48. G. Tang, B. J. Reinhart, D. P. Bartel, P. D. Zamore, *Genes Dev.* **17**, 49 (2003).
49. S. Yekta, I. Shih, D. P. Bartel, *Science* **304**, 594 (2004).
50. E. Davis *et al.*, *Curr. Biol.* **15**, 743 (2005).
51. S. Pfeffer *et al.*, *Science* **304**, 734 (2004).
52. G. Hutvágner, P. D. Zamore, *Science* **297**, 2056 (2002).
53. T. I. Orban, E. Izaurralde, *RNA* **11**, 459 (2005).
54. B. Shen, H. M. Goodman, *Science* **306**, 997 (2004).
55. P. H. Olsen, V. Ambros, *Dev. Biol.* **216**, 671 (1999).
56. J. G. Doench, C. P. Petersen, P. A. Sharp, *Genes Dev.* **17**, 438 (2003).
57. L. P. Lim *et al.*, *Nature* **433**, 769 (2005).
58. S. Bagga *et al.*, *Cell* **122**, 553 (2005).
59. J. Liu, M. A. Valencia-Sanchez, G. J. Hannon, R. Parker, *Nat. Cell Biol.* **7**, 719 (2005).
60. G. L. Sen, H. M. Blau, *Nat. Cell Biol.* **7**, 633 (2005).
61. R. S. Pillai *et al.*, *Science* **309**, 1573 (2005); published online 4 August 2005 (10.1126/science.1115079).
62. C. L. Jopling, M. Yi, A. M. Lancaster, S. M. Lemon, P. Sarnow, *Science* **309**, 1577 (2005).
63. M. Wassenegger, S. Heimes, L. Riedel, H. L. Sanger, *Cell* **76**, 567 (1994).
64. M. F. Mette, W. Aufsatz, J. van der Winden, M. A. Matzke, A. J. Matzke, *EMBO J.* **19**, 5194 (2000).
65. T. A. Volpe *et al.*, *Science* **297**, 1833 (2002).
66. D. Zilberman, X. Cao, S. E. Jacobsen, *Science* **299**, 716 (2003).
67. S. W. Chan *et al.*, *Science* **303**, 1336 (2004).
68. Z. Xie *et al.*, *PLoS Biol.* **2**, E104 (2004).
69. A. Grishok, J. L. Sinskey, P. A. Sharp, *Genes Dev.* **19**, 683 (2005).
70. V. J. Robert, T. Sijen, J. van Wolfswinkel, R. H. Plasterk, *Genes Dev.* **19**, 782 (2005).
71. M. Pal-Bhadra, U. Bhadra, J. A. Birchler, *Mol. Cell* **9**, 315 (2002).
72. M. Pal-Bhadra *et al.*, *Science* **303**, 669 (2004).
73. K. Mochizuki, N. A. Fine, T. Fujisawa, M. A. Gorovsky, *Cell* **110**, 689 (2002).
74. M. C. Yao, P. Fuller, X. Xi, *Science* **300**, 1581 (2003).
75. T. Fukagawa *et al.*, *Nat. Cell Biol.* **6**, 784 (2004).
76. C. Kanellopoulou *et al.*, *Genes Dev.* **19**, 489 (2005).
77. T. Sugiyama, H. Cam, A. Verdel, D. Moazed, S. I. Grewal, *Proc. Natl. Acad. Sci. U.S.A.* **102**, 152 (2005).
78. D. Zilberman *et al.*, *Curr. Biol.* **14**, 1214 (2004).
79. M. R. Motamedi *et al.*, *Cell* **119**, 789 (2004).
80. A. J. Herr, M. B. Jensen, T. Dalmay, D. C. Baulcombe, *Science* **308**, 118 (2005).
81. T. Kanno *et al.*, *Nat. Genet.* **37**, 761 (2005).
82. Y. Onodera *et al.*, *Cell* **120**, 613 (2005).
83. H. Kato *et al.*, *Science* **309**, 467 (2005).
84. V. Schramke *et al.*, *Nature* **435**, 1275 (2005).
85. H. P. Cam *et al.*, *Nat. Genet.* **37**, 809 (2005).
86. C. C. Chen *et al.*, *Curr. Biol.* **15**, 378 (2005).
87. S. Kadaba *et al.*, *Genes Dev.* **18**, 1227 (2004).
88. J. LaCava *et al.*, *Cell* **121**, 713 (2005).
89. S. Vanacova *et al.*, *PLoS Biol* **3**, e189 (2005).
90. E. Bernstein *et al.*, *Nat. Genet.* **35**, 215 (2003).
91. D. N. Cox, A. Chao, H. Lin, *Development* **127**, 503 (2000).
92. S. D. Hatfield *et al.*, *Nature* **435**, 974 (2005).
93. K. Forstemann *et al.*, *PLoS Biol.* **3**, e236 (2005).
94. G. Deshpande, G. Calhoun, P. Schedl, *Genes Dev.* **19**, 1680 (2005).
95. K. Okamura, A. Ishizuka, H. Siomi, M. C. Siomi, *Genes Dev.* **18**, 1655 (2004).
96. The authors acknowledge the support, advice, and critical comments of members of the Zamore laboratory. P.D.Z. is a W. M. Keck Foundation Young Scholar in Medical Research. Supported by NIH grants GM62862-01 and GM65236-01 (P.D.Z.). P.D.Z. is a founder of and member of the Scientific Advisory Board of Alnylam Pharmaceuticals, a biopharmaceutical company that develops therapeutic agents based on RNAi.

10.1126/science.1111444

It's a Small RNA World, After All

Matthew W. Vaughn and Rob Martienssen

Small RNAs (sRNAs) can regulate transcript and protein abundance. Previously, they have been identified using traditional cloning approaches, which has limited how many could be characterized. Now, the Meyers and Green laboratories have used massively parallel signature sequencing technology to find over 1.5 million sRNAs in *Arabidopsis thaliana*. These new sRNAs reveal a greater-than-expected potential role for sRNAs in gene regulation, preferential expression or usage of sRNAs in flowers, and the prospect of targeted sRNA-mediated regulation of pseudogenes. In addition, new plant microRNAs have been identified, some of which may be unique to *Arabidopsis*.

Small RNAs (sRNAs) are 20- to 26-nucleotide noncoding RNAs that regulate transcript and protein abundance via multiple mechanisms (*1*, *2*). MicroRNAs (miRNAs) are generated by endonucleolytic cleavage of hairpin precursor transcripts by Dicer ribonuclease (RNase) III–like proteins and can direct the cleavage of target transcripts by Argonaute RNAse H–like proteins in a sequence-specific manner. miRNAs can also inhibit translation of target mRNAs. Small interfering RNAs (siRNAs) are generated by Dicer-mediated processive cleavage of double-stranded RNA (dsRNA). They can direct cleavage of other transcripts and can also promote second-strand synthesis by RNA-dependent RNA polymerase (RdRP), resulting in dsRNAs. In addition, siRNAs are implicated in recruiting heterochromatic modifications that result in transcriptional silencing. Previously, sRNAs have been identified by means of painstaking cloning and sequencing techniques, and as a result, only a few thousand have been identified. A recent study from the laboratories of Green and Meyers (*3*) describes the use of massively parallel signature sequencing (MPSS) technology to identify over 1.5 million sRNAs from *Arabidopsis thaliana*, representing over 75,000 distinct sequences. They report that many more genes may be under the control of sRNAs than had been previously imagined.

Cold Spring Harbor Laboratory, Cold Spring Harbor, NY 11724, USA.

In *Arabidopsis*, current estimates predict that 2% of genes may be under miRNA control (*4*), but the number of genes that might be regulated by siRNAs is not known. siRNAs are known to participate in RNAi-mediated silencing of repeats and transposable elements (TEs) (*5*), so it was no surprise that the majority of sRNA sequences matched repeats and that most annotated repeats and TEs matched abundant sRNAs (*3*). Most of the remaining sRNA sequences came from intergenic regions (IGRs), including those derived from miRNAs, which is consistent with previous studies on a much smaller scale (*6*). Interestingly, 4000 protein-coding genes (15% of genes in the genome) and several hundred pseudogenes matched at least one sRNA perfectly, presumably corresponding to siRNAs (miRNAs usually match imperfectly). However, most of these genes matched only one siRNA, and only a few percent of the total sRNA sequences were from genes. It is possible therefore that many other genes may have matches that went undetected.

The number of distinct sRNA sequences for each class of genomic sequence (IGRs, TEs, and so forth) was calculated by Lu *et al.* and is shown in Fig. 1. The sRNA library from flower tissues contained over twice as many unique sRNAs as the one derived from 14-day-old seedlings, and much of that additional complexity came from IGRs. Lu *et al.* offer two possible explanations for this observation. The first is that TEs might be more strongly silenced in plant germline tissues. Consistent with this possibility, retrotransposons matched disproportionally more sRNAs in flowers than in seedlings (Fig. 1A). So perhaps the IGRs contain numerous cryptic retroelements that are more strongly silenced in flowers. The second proposed explanation for floral sRNA enrichment is that inflorescences contain a greater diversity of cell types than seedlings. Presumably these additional cell types express a wider variety of genes that could generate or be affected by sRNAs (*7*). Consistent with this data, 1.4-fold more genes are expressed in flowers than in seedlings, and some of these genes could be directly generating sRNA signatures (*8*). However, the IGRs are fourfold enriched in sRNA in flowers. What could be the source of these preferentially

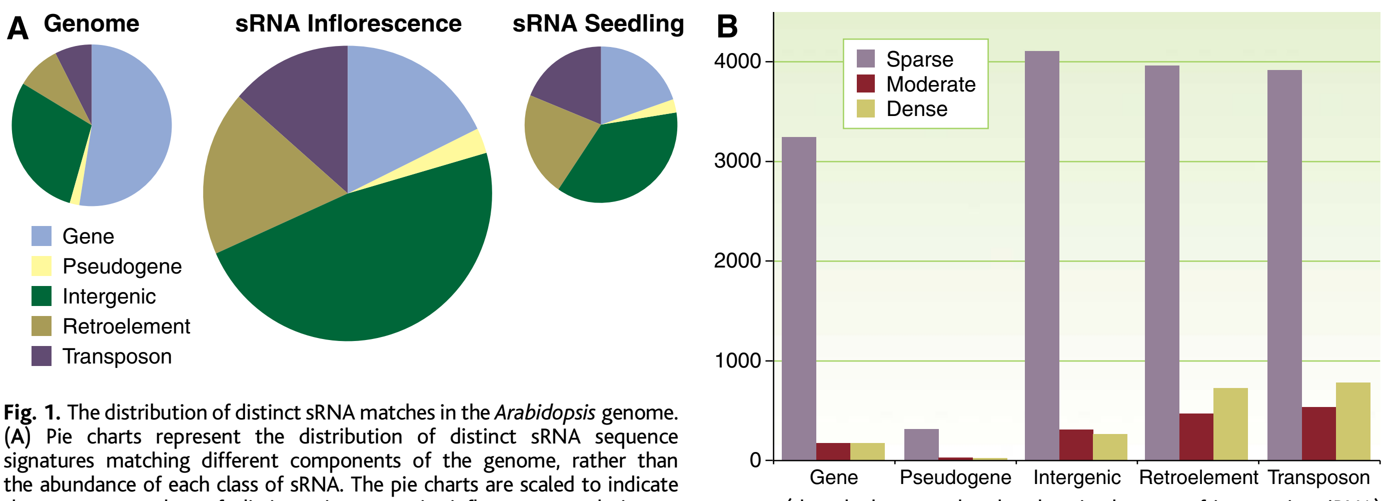

Fig. 1. The distribution of distinct sRNA matches in the *Arabidopsis* genome. **(A)** Pie charts represent the distribution of distinct sRNA sequence signatures matching different components of the genome, rather than the abundance of each class of sRNA. The pie charts are scaled to indicate the greater number of distinct signatures in inflorescence relative to seedling RNA. **(B)** Distinct signature sequences for each annotated class are grouped according to their density: Sparse clusters have only a few signatures (though these can be abundant in the case of intergenic miRNA), whereas dense clusters have many distinct signatures per kilobase and are enriched in repeats as compared to genes and intergenic regions.

expressed sequences? We know from whole-genome transcription tiling arrays that IGRs are rich with undescribed transcriptional units (*9*). These transcripts probably represent a mixture of unannotated protein coding genes and pseudogenes, members of unknown or sequence-divergent transposon families, transcribed repeats, and miRNAs.

The physical distribution of sRNAs reveals more about the composition of the IGRs. Lu *et al*. classify sRNAs as belonging to sparse, moderate, and dense clusters in the genome, where sparse clusters have 1 to 10 distinct sRNA matches within 500 base pairs (bp) and probably represent miRNA homology. Moderate clusters have 11 to 20 matches per 500 bp, whereas dense clusters contain ≥20 distinct sRNA matches. Centromeric repeats and TEs are enriched relative to genes in moderate and dense clusters. In contrast, IGRs are only slightly enriched in moderate and dense clusters, suggesting that centromeric repeats and TEs are not the predominant source of sRNAs in these domains (Fig. 1B). However, there are several hundred moderate and dense clusters in the IGRs. Because of their potential to prime iterative rounds of RdRP-mediated siRNA production and their robust association with previously cloned sRNA sequences (*10*), complex tandem repeats, which make up around 15% of the intergenic portion of the genome, merit special consideration as a potential source for these clusters. Lu *et al*. report a good correlation between tandem repeats and the presence of sRNAs. Tandem repeats have been implicated in several epigenetic phenomena, including imprinting and paramutation (*11*, *12*), and sRNAs derived from tandem repeats could be involved in regulating germline-specific genes.

Currently, 118 miRNAs are described in *Arabidopsis* that may regulate on the order of 700 genes (*13*). However, many genes that are not known or predicted targets of these miRNAs are up-regulated in RNAi-defective mutants (*14*), suggesting that additional miRNAs remain undiscovered. The sparse cluster component of IGRs reported by Lu *et al*. may contain many such miRNAs. To investigate this possibility, a set of computational filters was used to capture most known miRNAs from the MPSS data, as well as potentially undescribed miRNAs, and these sequences were used to probe Northern blots of seedling and floral RNA from the *rdr2* mutant, which is defective for an RNA-dependent RNA polymerase that is responsible for producing most heterochromatic siRNAs. For several candidates, the sRNAs were found to be independent of RDR2, suggesting that they were previously undescribed miRNAs. Some of the candidate miRNAs were not found in the rice genome, suggesting that only the most deeply conserved miRNAs have thus far been identified in *Arabidopsis*.

In plants, miRNAs act similarly to siRNAs in that they guide the cleavage of gene transcripts (*15*). Recently, a class of transitive miRNA-mediated regulation has been described. In these cases, miRNA-facilitated cleavage directs the recruitment of an RNA-dependent RNA polymerase to generate dsRNAs, which are in turn processed into siRNAs. These siRNAs are able to transitively regulate other matching transcripts by recognizing sequences outside the original miRNA binding site and are thus called trans-acting siRNAs (or ta-siRNAs) (*14*). In all characterized instances of transitive RNAi, the primary transcript recognized by the miRNA is a noncoding gene, but in principle this mechanism could occur for any miRNA target. Lu *et al*. examined this possibility by looking for evidence of siRNAs generated from 61 known or predicted miRNA target genes. Except for PPR repeat genes (which have tandem repeats in their coding sequences), most miRNA targets exhibited little or no evidence of siRNA production, indicating that transitive RNAi occurs only in special instances, if at all. However, many ta-siRNA precursors were not annotated as transcriptional units in the *Arabidopsis* genome before they were discovered, and more may lie undiscovered in the MPSS data.

Finally, nearly one in two annotated pseudogenes matched sRNAs, even when known TEs (an abundant source of pseudogenes) were excluded from the analysis. Only one in six genes matched sRNAs, suggesting that pseudogenes may be targeted specifically. What might the mechanism be? Expressed pseudogenes containing premature stop codons are expected to trigger nonsense-mediated decay (NMD) (*16*). However, the possibility that pseudogene sRNA sequences were RNA degradation products was excluded, because sRNA sequences derived from highly expressed genes with high turnover rates were not overrepresented. Instead, RNAs that experience premature termination may become substrates for RNAi through NMD. In most species, exonucleases are responsible for degrading mRNAs as part of the normal turnover process (*16*). In *Drosophila*, however, an unidentified endoribonuclease cleaves the nonsense transcript near the site of the premature termination codon (*17*). This may initiate RNAi-mediated degradation because the 5′ and 3′ ends of the cleavage products will be missing a polyA$^+$ tail and 5′ cap, respectively, resembling aberrant transcripts which are thought to be targeted by RNAi (*1*).

Regardless of mechanism, if the 20- to 24-nucleotide RNAs generated from *Arabidopsis* pseudogenes are bona fide sRNAs, they could act transitively on transcripts from paralogous protein-coding genes by promoting cleavage or interfering with translation. More than half of the pseudogene sRNAs matched sequences elsewhere in the genome, indicating that this may be the case and suggesting a mechanism for coordinated trans-acting regulation of closely related members of gene families. This may also provide a mechanism for the origin of ta-siRNA, whose noncoding precursor RNA may be derived from ancient pseudogenes that are no longer recognizable except for the sRNA homology (*14*).

What about sRNAs from genes? Small RNAs corresponding to heterochromatic transposons and repeats have been associated with chromatin modifications in the fission yeast *Schizosaccharomyces pombe* and with DNA methylation in plants, and the abundance of sRNAs from transposons and repeats supports a role in heterochromatic silencing (*18*). A significant proportion of genes in *Arabidopsis* also have some DNA methylation, although it is relatively sparse and is clustered near the 3′ end of the genes (*19*, *20*). However, our preliminary analysis indicates that partially methylated genes reported in microarray studies are not enriched in sRNAs, so that the role of sRNA from genes remains a mystery. Exceptions include *PAI1* and *PAI2*, which have dense clusters of siRNA and are subject to RNA-dependent DNA methylation (*3*, *21*).

MPSS and other high-throughput sequencing technologies have the power to reveal the prevalence of sRNAs from essentially every class of sequence in the genome. Given that components of the RNAi machinery are found in almost all eukaryotes and many archaebacteria, the possibility of an early sRNA world is one that will receive attention in the future.

References

1. D. Baulcombe, *Trends Biochem. Sci.* **30**, 290 (2005).
2. P. D. Zamore, B. Haley, *Science* **309**, 1519 (2005).
3. C. Lu *et al.*, *Science* **309**, 1567 (2005).
4. X. J. Wang, J. L. Reyes, N. H. Chua, T. Gaasterland, *Genome Biol.* **5**, R65 (2004).
5. Z. Lippman, R. Martienssen, *Nature* **431**, 364 (2004).
6. A. M. Gustafson *et al.*, *Nucleic Acids Res.* **33**, D637 (2005).
7. F. Meins Jr., A. Si-Ammour, T. Blevins, *Annu. Rev. Cell Dev. Biol.* 10.1146/annurev.cellbio.21.122303.114706.
8. B. C. Meyers *et al.*, *Genome Res.* **14**, 1641 (2004).
9. K. Yamada *et al.*, *Science* **302**, 842 (2003).
10. R. Martienssen, Z. Lippman, B. May, M. Ronemus, M. Vaughn, *Cold Spring Harbor Symp. Quant. Biol.* **LXIX**, 371 (2004).
11. T. Kinoshita *et al.*, *Science* **303**, 521 (2004).
12. M. Stam *et al.*, *Genetics* **162**, 917 (2002).
13. M. W. Jones-Rhoades, D. P. Bartel, *Mol. Cell* **14**, 787 (2004).
14. E. Allen, Z. Xie, A. M. Gustafson, J. C. Carrington, *Cell* **121**, 207 (2005).
15. G. Tang, P. D. Zamore, *Methods Mol. Biol.* **257**, 223 (2004).
16. C. R. Alonso, *Bioessays* **27**, 463 (2005).
17. M. A. Valencia-Sanchez, L. E. Maquat, *Trends Cell Biol.* **14**, 594 (2004).
18. M. A. Matzke, J. A. Birchler, *Nat. Rev. Genet.* **6**, 24 (2005).
19. Z. Lippman *et al.*, *Nature* **430**, 471 (2004).
20. R. K. Tran *et al.*, *Curr. Biol.* **15**, 154 (2005).
21. O. Mathieu, J. Bender, *J. Cell Sci.* **117**, 4881 (2004).

10.1126/science.1117805

The Functional Genomics of Noncoding RNA

John S. Mattick

Large numbers of noncoding RNA transcripts (ncRNAs) are being revealed by complementary DNA cloning and genome tiling array studies in animals. The big and as yet largely unanswered question is whether these transcripts are relevant. A paper by Willingham *et al.* shows the way forward by developing a strategy for large-scale functional screening of ncRNAs, involving small interfering RNA knockdowns in cell-based screens, which identified a previously unidentified ncRNA repressor of the transcription factor NFAT. It appears likely that ncRNAs constitute a critical hidden layer of gene regulation in complex organisms, the understanding of which requires new approaches in functional genomics.

Recent large-scale studies of the human and mouse transcriptomes have used both cDNA cloning approaches (*1*–*3*) and the interrogation of genome tiling arrays (*4*–*6*). The surprising but consistent finding of these studies has been that a huge number of observed transcripts—about half of the total—do not appear to encode proteins. Many of these transcripts appear to be developmentally regulated (*1*, *4*), and similar findings have been reported in *Drosophila* (*7*). The big and as yet largely unanswered question is whether these noncoding RNAs (ncRNAs) are meaningful or simply represent "transcriptional noise" (Fig. 1). A study by Schultz, Hogenesch, and colleagues (*8*) begins to answer this question by developing a strategy for large-scale functional screening of ncRNAs.

Willingham *et al.* (*8*) selected 512 ncRNA sequences from the RIKEN Fantom2 mouse cDNA collection (*1*, *9*) that showed significant conservation with human genomic sequences and constructed small interfering RNAs (siRNAs) (two each, expressed as short hairpin RNAs) against the human orthologs of these sequences. These siRNAs were then used to interrogate a battery of 12 cell-based assays representing key cellular processes and signaling pathways, with the use of reporter assays in microtiter plates (*10*). They identified eight functional ncRNAs: six essential for cell viability, one repressor of Hedgehog signaling, and one (termed NRON) that acts as a repressor of the transcription factor NFAT, which is itself required for T-cell receptor–mediated immune response and the development of the heart, vasculature, musculature, and nervous tissue.

Detailed analysis of NRON showed that this ncRNA, which has two blocks of near-perfect conservation between humans and mice but no substantial open reading frame, is enriched in placenta, muscle, and lymphoid tissues and exhibits a distinct tissue-specific distribution of splice variants, suggesting subtle but biologically relevant differences in its function in different tissues (*8*). By tagging NRON with an RNA hairpin that is bound by the MS2 phage protein, followed by affinity chromatography of whole-cell extracts, the authors showed that NRON interacts directly or indirectly with 11 proteins, including three members of the importin-beta superfamily, which mediate the nucleocytoplasmic transport of cargoes such as NFAT. siRNA knockdown of four of these proteins (including importin–beta 1) activated NFAT activity, whereas overexpression of these proteins repressed NFAT activity, as did siRNAs directed against NRON. Moreover, binding and ribonuclease protection experiments supported a direct association of NRON with importin–beta 1, which itself is known to associate with some of the other proteins that were identified as interacting with NRON (*8*).

These observations suggest that NRON may act as a modulator of NFAT nuclear trafficking, probably by regulating its subcellular location, a conclusion supported by the observation that NFAT nuclear localization is increased when the level of NRON is reduced by siRNA (*8*). The broader conclusion is that NRON may act as a scaffold for the assembly of protein complexes that regulate nuclear trafficking of this and probably other important transcription factors, opening a new dimension of organizational control in cell biology and development.

This elegant study not only points the way ahead but also illustrates the magnitude of the task that is in front of us, which may be an equal or greater challenge than that we already face in working out the biochemical function and biological role of all of the known and predicted proteins and their isoforms.

The cDNA and genome tiling array studies have indicated not only that there are tens of thousands of ncRNA transcripts (both polyadenylated and nonpolyadenylated) expressed from the mammalian genome in different cells and tissues but also that these transcripts comprise a complex interlaced and overlapping network from both strands, whereby even a single nucleotide may be part of multiple differently processed transcripts (*2*, *3*, *6*, *11*, *12*).

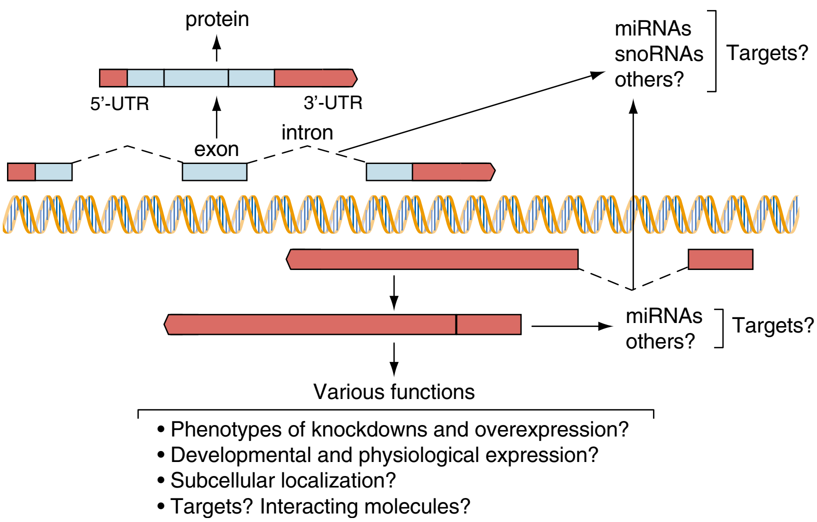

Fig. 1. The complexity of transcription of protein-coding (blue) and noncoding (red) RNA sequences. Transcripts may be derived from either or both strands, and they may be overlapping and interlaced (*2*, *3*, *6*, *11*, *12*). Many transcripts (including some noncoding transcripts) are alternatively spliced. Both exons and introns may transmit information. Many miRNAs and all small nucleolar RNAs in animals are sourced from introns [see (*13*) for a review]. The range of types and functions of noncoding RNAs is unknown.

Australian Research Council Special Research Centre for Functional and Applied Genomics, Institute for Molecular Bioscience, University of Queensland, Brisbane, QLD 4072, Australia. E-mail: j.mattick@imb.uq.edu.au

Ascribing function to these ncRNAs will not be simple, nor occur quickly, given that this will require in vivo and in vitro assays, the interpretation of which will be compromised by ambiguity in the former (for example in discriminating between mutations that affect cis-acting regulatory sequences and those that affect functional trans-acting RNAs) and in both cases by the ability to detect a phenotype when the expression of targeted ncRNA sequences is altered by siRNA-mediated knockdown or ectopic expression. Only 8 of 512 ncRNAs showed function in the assays undertaken by Willingham *et al*. (*8*), although this is not a bad rate of return given the limited scope of these assays. Nonetheless, these initial findings will have a big impact, because they reveal the involvement of hitherto unsuspected ncRNAs in already intensively studied pathways such as Hedgehog signaling and nuclear trafficking. Notably, genome tiling array studies have also revealed unknown transcript and splice variants of *sonic hedgehog* (*11*), indicating just how much remains to be done.

The selection of phenotypic assays may be guided by other studies, such as the analysis of the patterns of expression and the subcellular location of the ncRNAs under analysis, as is already routinely done for proteins with unknown functions. Indeed, most would regard tissue-specific expression as a reasonable prima facie indicator of function. On the other hand, faced with the uncomfortable implications of large numbers of such RNAs and the evidence that many are expressed only at low levels, others may suggest that these RNAs are merely transcriptional noise from illegitimate promoters, which may be variable in different cells, because of, for example, different chromatin architectures, although it also seems likely that chromatin architecture is itself controlled by RNA signaling (*13*, *14*).

Notably, evolutionary conservation may not be a reliable signature of functional ncRNAs. The ncRNAs selected by Willingham *et al*. were those that were most highly conserved between humans and mouse, a reasonable filter given that conservation is normally a good indicator of function. However, the reverse—i.e., that lack of conservation indicates lack of function—is not necessarily true. Sequence conservation is normally mandated by the preservation of structure-function relationships (as in proteins) and/or multilateral interactions (as in ribosomal RNA). If many of these newly discovered ncRNAs are regulatory, as one might reasonably suppose them to be, they may have quite different evolutionary constraints. Many microRNAs (miRNAs)—small 20- to 25-nucleotide RNAs that control many aspects of plant and animal development by sequence-specific interactions with other RNAs—are highly conserved (and have been mainly identified on this basis), but these appear to be central regulators that have many targets (making covariation difficult) and there are likely to be many more that are not so constrained (*13*).

This possibility is supported by a recent study that did not require substantial evolutionary conservation and (thereby) identified many new human miRNAs, a significant number of which appear to be primate specific (*15*). The number of known human miRNAs stands at well over 1500 and is rising rapidly (*13*, *15*, *16*). Sensitive genetic screens in *Caenorhabditis elegans* have also identified rare miRNAs with limited evolutionary conservation such as *lys-6*, which is required for left-right neuronal patterning, suggesting that many more remain to be found (*17*). Moreover, a number of well-studied ncRNAs are poorly conserved, such as XIST, which controls X-chromosome inactivation in mammals, and Air, a ncRNA of over 100 kb that is involved in imprinting of the *Igf2r* locus in mouse (*18*, *19*). All of these considerations suggest that many ncRNAs are evolving quickly (by drift under mild negative selection or under positive selection for the rewiring of regulatory circuitry in phenotypic radiation) and that those that have been identified (or prioritized for study) on the basis of evolutionary conservation are probably just the tip of a very large iceberg. Nonetheless, there is considerable scope for using more sophisticated bioinformatic approaches, including intragenomic sequence matching.

It is also clear that the majority of the genomes of animals is indeed transcribed (*12*), which suggests that these genomes are either replete with largely useless transcription or that these noncoding RNA sequences are fulfilling a wide range of unexpected functions in eukaryotic biology. These sequences include introns (Fig. 1), which account for at least 30% of the human genome but have been largely overlooked because they have been assumed to be simply degraded after splicing. However, it has been shown that many miRNAs and all known small nucleolar RNAs in animals are sourced from introns (of both protein-coding and noncoding transcripts) (*13*), and it is simply not known what proportion of the transcribed introns are subsequently processed into smaller functional RNAs. It is possible, and logically plausible, that these sequences are also a major source of regulatory RNAs in complex organisms (*20*).

The studies of Willingham *et al*. and others that have begun to explore the underworld of RNA in eukaryotes raise more questions than they answer. That complex organisms have complex genetic programming should come as no surprise. That much of this programming may be transacted by noncoding RNAs may be. However, given the sheer extent of noncoding RNA transcription, it seems more and more likely that a large portion of the human genome may be functional by means of RNA. This also means that we may have seriously misunderstood the nature of genetic programming in the higher organisms (*21*) by assuming that most genetic information is expressed as and transacted by proteins, as it largely is in prokaryotes (*22*). If so, there is a long road ahead in functional genomics.

References and Notes

1. Y. Okazaki *et al.*, *Nature* **420**, 563 (2002).
2. FANTOM Consortium and RIKEN Genome Exploration Research Group and Genome Science Group (Genome Network Project Core Group), *Science* **309**, 1559 (2005).
3. RIKEN Genome Exploration Research Group and Genome Science Group (Genome Network Project Core Group) and FANTOM Consortium, *Science* **309**, 1564 (2005).
4. S. Cawley *et al.*, *Cell* **116**, 499 (2004).
5. P. Bertone *et al.*, *Science* **306**, 2242 (2004).
6. J. Cheng *et al.*, *Science* **308**, 1149 (2005).
7. V. Stolc *et al.*, *Science* **306**, 655 (2004).
8. A. T. Willingham *et al.*, *Science* **309**, 1570 (2005).
9. K. Numata *et al.*, *Genome Res.* **13**, 1301 (2003).
10. J. B. Hogenesch, P. G. Schultz, personal communication.
11. P. Kapranov *et al.*, *Genome Res.* **15**, 987 (2005).
12. M. C. Frith, M. Pheasant, J. S. Mattick, *Eur. J. Hum. Genet.* **13**, 894 (2005).
13. J. S. Mattick, I. V. Makunin, *Hum. Mol. Genet.* **14**, R121 (2005).
14. A. H. Ting, K. E. Schuebel, J. G. Herman, S. B. Baylin, *Nat. Genet.* **37**, 906 (2005).
15. I. Bentwich *et al.*, *Nat. Genet.* **37**, 766 (2005).
16. P. D. Zamore, B. Haley, *Science* **309**, 1519 (2005).
17. R. J. Johnston, O. Hobert, *Nature* **426**, 845 (2003).
18. C. Chureau *et al.*, *Genome Res.* **12**, 894 (2002).
19. C. B. Oudejans *et al.*, *Genomics* **73**, 331 (2001).
20. J. S. Mattick, *Curr. Opin. Genet. Dev.* **4**, 823 (1994).
21. J. S. Mattick, *Nat. Rev. Genet.* **5**, 316 (2004).
22. J.-M. Claverie, *Science* **309**, 1529 (2005).
23. I am grateful for the support of the Australian Research Council, the Queensland State Government, and the University of Queensland.

10.1126/science.1117806

Fewer Genes, More Noncoding RNA

Jean-Michel Claverie

Recent studies showing that most "messenger" RNAs do not encode proteins finally explain the long-standing discrepancy between the small number of protein-coding genes found in vertebrate genomes and the much larger and ever-increasing number of polyadenylated transcripts identified by tag-sampling or microarray-based methods. Exploring the role and diversity of these numerous noncoding RNAs now constitutes a main challenge in transcription research.

A few months before the publication of the first drafts of the human genome sequence (*1*, *2*), online bids predicting the number of human protein-coding genes ranged from 30,000 to 150,000 [see (*3*)]. To the surprise of many (*4*), initial bioinformatic analyses revealed no more than 35,000 human genes, an estimate that has steadily declined to the present 25,000 genes (*5*). On the other hand, the largest estimates based on the number of distinct polyadenylated transcript 3′-ends identified through the single-pass sequencing of cDNA libraries (*6*) [i.e., expressed sequence tags (ESTs)] have not followed a diminishing trend. On the contrary, more transcripts keep being discovered, many of which do not correspond to annotated genes [e.g., (*7*)], in particular when using the serial analysis of gene expression (SAGE) approach (*8*).

Over the last 5 years, this discrepancy (*4*) between the number of recognized protein-coding genes and the apparent number of transcripts has not been reduced. As early as 1997, the then-thriving genomics industry had already sequenced several million ESTs and had come up with estimates of well over 100,000 human genes. For example, Incyte Genomics estimated 140,000 genes by grouping overlapping EST sequences [cited in (*9*)]; this total did not include more than 200,000 EST sequences seen only once.

Comparable numbers emerged a few years later in the public domain. The Human Gene Index of the Institute for Genomic Research predicted in excess of 75,000 human genes (*10*), whereas the Unigene database of the National Center for Biotechnology Information indicated 84,000 genes (*6*). These sequences are still in the databases, awaiting reconciliation with the much smaller number of human genes identified by the direct analysis of the human genome sequence.

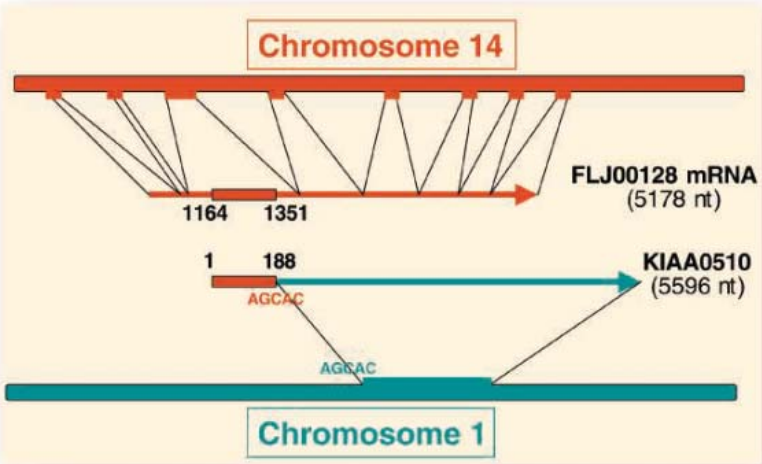

Fig. 1. Relationship between the KIAA0510 cDNA sequence and a FLJ00128 protein-encoding transcript. The FLJ00128 cDNA (GenBank identification number 18676462) looks like a standard transcript with more than 20 exons (not drawn), all mapping to human chromosome 14. This transcript encodes a large protein of more than 1500 residues without known or predicted function. The KIAA0510 cDNA sequence (GenBank identification number 3413954) corresponds to a single exon, mapping on chromosome 1 and devoid of significant open reading frames. The 3′ noncoding part of this cDNA is fused to a 188-nucleotide sequence (boxed) 100% identical to a sequence unique to chromosome 14 and encoding 62 residues of protein FLJ00128. This region does not match the boundaries of an exon (as would be expected for trans-splicing) in the gene encoding FLJ00128. Both transcript sequences were assembled from multiple independently isolated ESTs and are devoid of low-complexity regions or repeats. Thus, they cannot easily be dismissed as cloning or sequencing artifacts.

Recent results may put an end to the paradox, albeit in a rather unexpected manner: A large fraction of the human (vertebrate) genome appears to give rise to polyadenylated transcripts that do not code for proteins. The notion of noncoding RNAs is not new—for example, the 17-kb X chromosome–inactivated specific transcript (Xist) was discovered in 1991 (*11*). However, it is only recently that the sheer scale of the phenomenon has begun to be realized. Unfortunately, initial analyses of the transcriptome were based on hybridization with probes derived from predefined or predicted gene sequences, and thus they did not reveal unexpected transcripts. A vastly different picture of transcriptional activity emerged as soon as tiling arrays were introduced, allowing the interrogation of genome sequences for corresponding transcripts at fixed intervals irrespective of predicted gene locations. For instance, a tiling array with 5-nucleotide resolution that mapped transcription activity along 10 human chromosomes revealed that an average of 10% of the genome (compared to the 1 to 2% represented by bona fide exons) corresponds to polyadenylated transcripts, of which more than half do not overlap with known gene locations (*12*).

Recent data from the FANTOM 3 project (*13*, *14*) confirm and amplify these findings. Through a technical tour de force, the members of this consortium have established that a staggering 62% of the mouse genome is transcribed. They have identified more than 181,000 independent transcripts, of which half consist of noncoding RNA. Moreover, they found that more than 70% of the mapped transcription units overlap to some extent with a transcript from the opposite strand (*13*, *14*).

These results provide a solution to the discrepancy between the number of (protein-coding) genes and the number of transcripts—noncoding polyadenylated mRNA contributes to a large fraction of the 3′-EST sequences (and SAGE tags) subsequently clustered or remaining as singletons. Indeed, the noncoding Xist mRNA is abundantly represented in all EST projects. It is thus likely that sequences of noncoding transcripts have been accumulating

Structural and Genomics Information Laboratory, CNRS UPR 2589, Institut de Biologie Structurale et Microbiologie, 31 chemin Joseph Aiguier, Marseille 13402, France, and University of Méditerranée School of Medicine, Marseille 13385, France. E-mail: jean-michel.claverie@igs.cnrs-mrs.fr

in EST databases and have for the most part (including singleton and antisense ESTs) been erroneously interpreted as coming from the 3′-untranslated regions of protein-coding transcripts. Noncoding transcripts originating from intergenic regions, introns, or antisense strands have probably been right before our eyes for 8 years without having been discovered!

The notion that transcription is limited to protein-coding genes is also being challenged in microbial systems. For *Escherichia coli*, the first analysis with a genome tiling microarray revealed a substantial number of antisense and intergenic transcripts (*15*). Noncoding short-lived "cryptic" mRNAs have also recently been seen in yeast, the transcription of which may maintain chromatin in an open state (*16*). The consequences of certain RNA polymerase II mutations for the status of pericentromeric heterochromatin also suggest a direct coupling between the transcription of noncoding RNAs and chromatin structure (*17*).

The intergenic, intronic, and antisense transcribed sequences that were once deemed artifactual are now a testimony to our collective refusal to depart from an oversimplified gene model. But what if transcription is even more complex? Could it, for instance, lead to mRNAs generated from two different chromosomes (Fig. 1)? A year ago, we would have immediately suspected such sequences as further artifacts arising from large-scale cDNA sequencing programs. But now? Perhaps it's time to go back to the cDNA sequence databases and reevaluate the numerous unexpected objects they contain (*18*). Transcription will never be simple again, but how complex will it get?

References and Notes

1. E. S. Lander *et al.*, *Nature* **409**, 860 (2001).
2. J. C. Venter *et al.*, *Science* **291**, 1304 (2001).
3. Editorial, *Nat. Genet.* **25**, 127 (2000).
4. J.-M. Claverie, *Science* **291**, 1255 (2001).
5. International Human Genome Sequencing Consortium, *Nature* **431**, 931 (2004).
6. D. L. Wheeler *et al.*, *Nucleic Acids Res.* **29**, 11 (2001).
7. E. E. Schadt *et al.*, *Genome Biol.* **5**, R73 (2004).
8. K. R. Boheler, M. D. Stern, *Trends Biotechnol.* **21**, 55 (2003).
9. D. B. Davison, J. F. Burke, *IBM J. Res. Dev.* **45**, 439 (2001).
10. F. Liang *et al.*, *Nucleic Acids Res.* **28**, 3657 (2000).
11. C. J. Brown *et al.*, *Nature* **349**, 38 (1991).
12. J. Cheng *et al.*, *Science* **308**, 1149 (2005); published online 24 March 2005 (10.1126/science.1108625).
13. FANTOM Consortium and RIKEN Genome Exploration Research Group and Genome Science Group (Genome Network Project Core Group), *Science* **309**, 1559 (2005).
14. RIKEN Genome Exploration Research Group and Genome Science Group (Genome Network Project Core Group) and FANTOM Consortium, *Science* **309**, 1564 (2005).
15. D. W. Selinger *et al.*, *Nat. Biotechnol.* **18**, 1262 (2000).
16. F. Wyers *et al.*, *Cell* **121**, 725 (2005).
17. H. Kato *et al.*, *Science* **309**, 467 (2005); published online 9 June 2005 (10.1126/science.1114955).
18. J. Shendure, G. M. Church, *Genome Biol.* **3**, research0044.1 (2002).

19. The Structural and Genomics Information Laboratory is supported by CNRS and the Marseille-Nice Genopole. I thank N. Baeza for drawing my attention to the KIAA0510 transcript.

10.1126/science.1116800

VIEWPOINT

Capping by Branching: A New Ribozyme Makes Tiny Lariats

Anna Marie Pyle

The number of naturally occurring RNA enzymes has just been expanded by the discovery of a new branching ribozyme. But this ribozyme has unexpected relatives: group I introns.

Before RNA molecules are ready for action, they usually undergo splicing, whereby the noncoding sequences (introns) are removed from the coding sequences (exons) and the latter are stitched back together. In some eukaryotes and prokaryotes, two classes of specialized introns (known as group I and group II introns) fold into catalytic structures that promote their own removal from flanking exons (a process called self-splicing) (*1*). Group II introns first caught the attention of an observant investigator because of their exceptional stability. During electron microscopy studies of yeast mitochondrial RNA, Arnberg *et al.* noticed abundant RNA circles (*2*) that were later shown to result from the self-splicing activity of group II introns (*3*). These introns catalyze a branching reaction in which an unpaired adenosine within the intron uses one of its sugar groups (the 2′-hydroxyl) to join with the intron terminus, thereby freeing the adjacent exon (coding region) and creating a circular "lariat" form of the intron (Fig. 1A). Once liberated, the intron lariats can function as parasitic RNAs, or mobile genetic elements, that migrate within a genome or into new genomes (*4*).

Exceptional stability is obviously a useful trait for infectious RNAs that have their own agendas in a cell (like group II introns). However, stability is important for many other RNAs, including mRNAs that encode proteins and RNAs involved in cellular function. Most mRNAs are capped at their upstream (5′) terminus with a modified guanosine residue that protects the mRNA against predation by the abundant 5′-exonucleases that prowl the cell, ready to pounce on unprotected, linear RNA strands (*5*). In this issue, Nielsen *et al.* (*6*) report that an mRNA (called I-*Dir* I) encoded by a homing endonuclease gene (HEG) from the slime mold *Didymium iridis* is capped by a different mechanism that takes a page from the group II intron playbook. The upstream terminus of the mature I-*Dir* I mRNA is a tiny circle that results from a branching reaction in which a 2′-hydroxyl group near the beginning of the mRNA reacts with a nearby phosphodiester linkage, thereby creating a circular cap and liberating the upstream RNA (Fig. 1B). Remarkably, the branching reaction is catalyzed not by a group II intron but by an unrelated group I intron–like ribozyme that is upstream from the branch site.

This group I–like ribozyme had long been known to catalyze cleavage at its junction with the I-*Dir* I mRNA (*7*), but careful primer extension analysis of the 5′ end of the transcript revealed that the mRNA cleavage product contained an unusual RNA structure. Classic chemical and enzymatic analysis of this terminal structure, together with studies on the reversibility of the cleavage reaction, strongly suggested the existence of a tiny lariat at the mRNA terminus. Importantly, specific deletion of the 2′-hydroxyl group at the putative branch site (i.e., the nucleophile in the branching reaction) eliminates this reaction.

Implications of Branching RNAs

By finding that a group I–like ribozyme can catalyze a branching reaction, Nielsen and colleagues provide strong evidence that branching may be a common activity that is shared by many different nucleic acid molecules, regardless of their evolutionary heritage. This suggests that branching is a facile process and that branching ribozymes may have evolved independently on

Department of Molecular Biophysics and Biochemistry, Howard Hughes Medical Institute, Yale University, 266 Whitney Avenue, Bass Building Room 334, New Haven, CT 06520, USA.

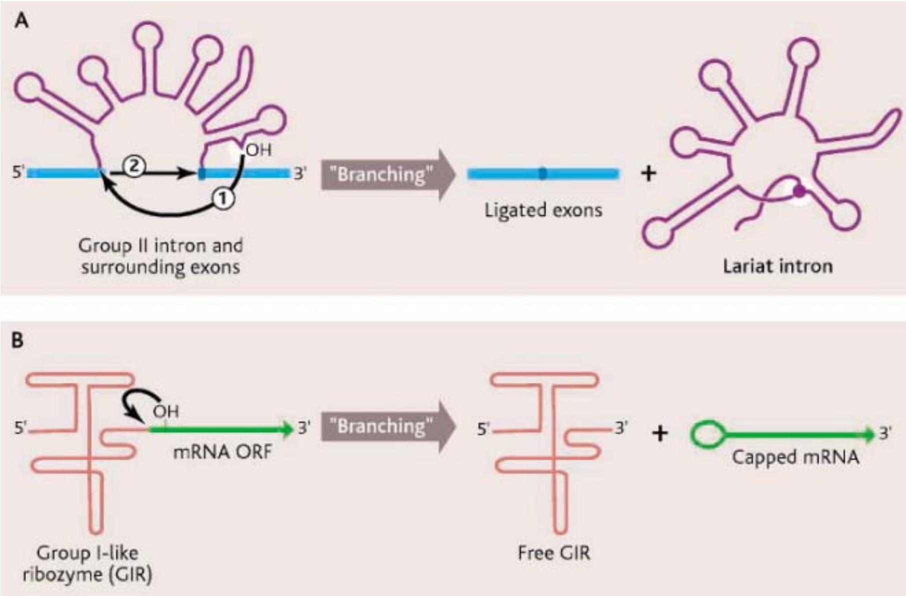

Fig. 1. (**A**) The lariat mechanism for self-splicing group II introns. Step 1, 2′-hydroxyl attacks intron terminus. Step 2, Exons are ligated together. (**B**) Branching creates a circular cap for mRNA in *D. iridus*. ORF, open reading frame.

numerous occasions. Although Nielsen *et al.*'s findings are the most clear-cut demonstration of this concept, there is precedent for this view. A role for lariat formation in retrotransposition by the yeast Ty1 element is being actively investigated (*8*, *9*). Indeed, artificial ribozymes (*10*) and even DNA molecules have been shown to catalyze branching (*11*, *12*). By using an artificial selection method in the laboratory, Silverman and colleagues have created catalytic DNA molecules (DNAzymes) that promote branching of RNA substrates. All of this recent work suggests that a wide diversity of nucleic acid enzymes can catalyze a common branching reaction.

An important aspect of activity by the group I–like ribozyme is the identity of the branch site itself. The 2′-hydroxyl group of a uridine appears to serve as the branch-site nucleophile (*6*). This is consistent with recent work by Silverman, which shows that DNAzymes can be created that promote branching from any of the four natural nucleotides (that is, the 2′-hydroxyl group of U, C, G, or A can react as a branch site) (*13*). Thus, contrary to conventional wisdom based on observation of group II introns and spliceosomal RNAs, adenosines do not have a special dispensation for participation in branching; any nucleotide can evolve to do it.

If diverse molecules catalyze branching, do they have anything in common? Although we should never rule out an ancient evolutionary connection between group II introns, group I introns, and retroelements, there is another explanation for branching activity by diverse species: Most reports of branching in natural systems involve selfish or infectious RNAs that must persist for a long time in the cell in order to carry out their biological function. That is, they are all under selective pressure for enhanced RNA stability, potentially against cellular nucleases. Indeed, the group I intron–like ribozyme reported by Nielsen *et al.* produces a branched mRNA that is highly specialized and might need to persist for a substantial length of time to carry out its function. The I-*Dir* I mRNA encodes the homing endonuclease involved in transposition of the flanking group I introns and itself, which together have parasitized the host genome (*6*). Given the many situations where enhancement of RNA stability will increase the evolutionary fitness of a parasitic RNA or even enhance the fitness of an entire organism (particularly if viability depends on the stability of certain encoded RNAs), terminal branching reactions and cyclizations are likely to be observed again in novel contexts. Thus, RNA branching reactions may be less indicative of a shared evolutionary heritage among RNAs than indicative of common modern-day functions.

Looming in the background of any report on branching are the implications for mechanistic function of the eukaryotic spliceosome, which is a gigantic ribonucleoprotein complex that uses a branching reaction to catalyze most of the splicing in eukaryotic cells. There remain many reasons, particularly those based on sequence and structural similarities, to suggest that group II introns and the spliceosome do share an evolutionary heritage (*4*). Nonetheless, the Nielsen report helps us think differently about this relationship. For example, does the release of lariat introns from spliceosomal processing confer some kind of advantage? Do these stabilized introns [which are ultimately debranched by a specialized debranching enzyme encoded by the *DBR1* gene in baker's yeast (*14*)] help regulate RNA transport between nucleus and cytoplasm or aid in homeostasis of free nucleotides? Whatever the answer, the fresh views posed by the Nielsen findings help us think more carefully about the role of ribozyme reactions in evolution and in modern RNA function.

References and Notes

1. T. R. Cech, in *The RNA World*, R. F. Gesteland, J. F. Atkins, Eds. (Cold Spring Harbor Laboratory Press, Cold Spring Harbor, NY, 1993), vol. 1, pp. 239–269.
2. A. C. Arnberg, G.-J. B. Van Ommen, L. A. Grivell, E. F. J. Van Bruggen, P. Borst, *Cell* **19**, 313 (1980).
3. C. L. Peebles *et al.*, *Cell* **44**, 213 (1986).
4. K. Lehmann, U. Schmidt, *Crit. Rev. Biochem. Mol. Biol.* **38**, 249 (2003).
5. R. Parker, H. Song, *Nat. Struct. Mol. Biol.* **11**, 121 (2004).
6. H. Nielsen, E. Westhof, S. Johansen, *Science* **309**, 1584 (2005).
7. S. Johansen, V. M. Vogt, *Cell* **76**, 725 (1994).
8. Z. Cheng, T. M. Menees, *Science* **303**, 240 (2004).
9. C. E. Coombes, J. D. Boeke, *RNA* **11**, 323 (2005).
10. T. Tuschl, P. A. Sharp, D. P. Bartel, *RNA* **7**, 29 (2001).
11. R. L. Coppins, S. K. Silverman, *J. Am. Chem. Soc.* **127**, 2900 (2005).
12. Y. Wang, S. K. J. Silverman, *J. Am. Chem. Soc.* **125**, 6880 (2003).
13. E. D. Pratico, Y. Wang, S. K. Silverman, *Nucleic Acids Res.* **33**, 3503 (2005).
14. K. B. Chapman, J. D. Boeke, *Cell* **65**, 483 (1991).
15. The author is William Edward Gilbert professor of molecular biophysics and biochemistry and a Howard Hughes Medical Institute investigator. The author thanks P. S. Perlman, G. P. Wagner, and N. Toor for helpful comments on this article.

10.1126/science.1117957

Major Biocontrol of Plant Tumors Targets tRNA Synthetase

John S. Reader,[1] Phillip T. Ordoukhanian,[1] Jung-Gun Kim,[2] Valerie de Crécy-Lagard,[1] Ingyu Hwang,[2] Stephen Farrand,[3] Paul Schimmel[1]*

Infection of plants by pathogenic strains of *Agrobacterium tumefaciens* causes crown gall tumors with devastating economic consequences. The most successful bacterial biocontrol agent, nonpathogenic *A. radiobacter* strain K84, prevents disease by production of the "Trojan horse" toxin agrocin 84 (Fig. 1A) (*1*). Because it imitates a tumor-derived substrate [agrocinopine A (fig. S1)], agrocin 84 is specifically imported into *A. tumefaciens* strains that harbor certain types of tumor-inducing (Ti) plasmids. A toxic moiety is released from agrocin 84 (Fig. 1A) that inhibits the pathogen by an unknown mechanism (*2*). Agrocin 84 has a 9-(3′-deoxy-β-D-2,3-threopentafuranosyl) adenine nucleoside-like core linked to two substituents by phosphoramidate bonds (*1*). A 5′-phosphoramidate bond links the nucleoside-like core to a D-threo-2,3-dihydroxy-4-methylpentanamide, while a second phosphoramidate bond links a D-glucofuranosyloxyphosphoryl group to the adenine base and is the only known example of a 6N phosphoramidate bond found in nature (*3*). Although this moiety is required for the selective uptake of agrocin 84 into susceptible *A. tumefaciens* cells, it is not required for toxicity (*2*).

Plasmid pAgK84 in strain K84 contains the genes for agrocin 84 production and two immunity elements (*4*). The translation product of one of these immunity genes, *agnB2*, showed >40% sequence identity between its coding sequence and many leucyl-tRNA synthetases (LeuRSs). LeuRSs catalyze attachment of leucine to its cognate tRNAs in the first step of protein synthesis (aminoacylation). Aminoacylation assays showed the recombinant AgnB2 protein exhibits robust LeuRS activity (*5*). Importantly, the *agnB2* gene is not essential for growth (*6*). The structure of the toxic moiety of agrocin 84 is similar to that of leucyl-adenylate (Leu-AMP), a critical enzyme-bound reaction intermediate (Fig. 1A), having a relatively stable 5′-phosphoramidate bond instead of the labile phosphoanhydride linkage. Plausibly, the stable toxic moiety of agrocin 84 could impart its antibiotic effect on the bacteria by binding to the catalytic domain of the *A. tumefaciens* genomic-encoded LeuRS ($LeuRS_{At}$) as a Leu-AMP mimic.

Purified agrocin 84 showed pronounced inhibition of the agrocin-supersensitive strain NTL4(pTiC58Δ*accR*) in bioassays (fig. S2) (*5*). In contrast, the toxic moiety of agrocin 84 was inactive in this assay, because the sugar group needed for uptake was removed. The toxic moiety inhibited aminoacylation by purified

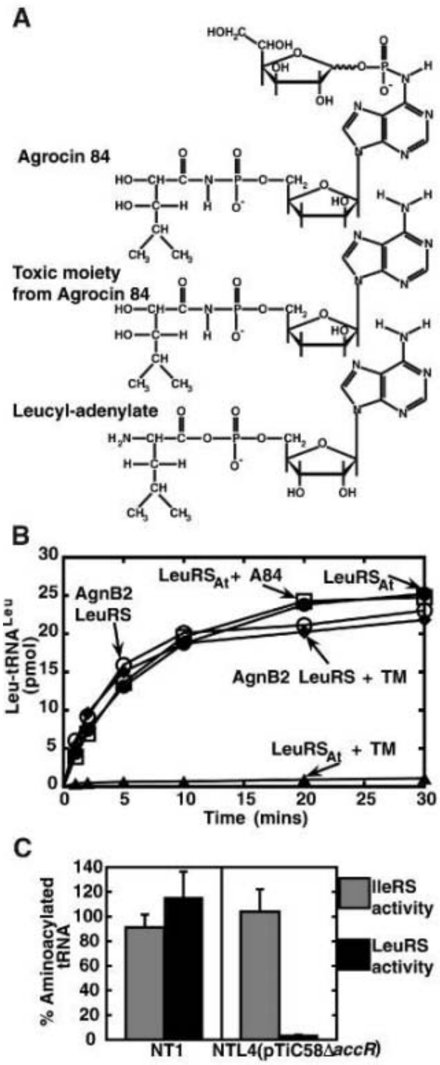

Fig. 1. (**A**) Structure of agrocin 84, the toxic moiety of agrocin 84, and Leu-AMP. (**B**) Effect of agrocin 84 (A84) and its toxic moiety (TM) on aminoacylation catalyzed by purified $LeuRS_{At}$. Aminoacylation by purified AgnB2 LeuRS in the presence or absence of the TM is also shown. (**C**) Comparison of inhibition of $LeuRS_{At}$ activity in cell-free extracts from resistant and susceptible *A. tumefaciens* strains grown with agrocin 84.

$LeuRS_{At}$ [median inhibitory concentration (IC_{50}), <10 nM], whereas the complete agrocin 84 molecule did not (Fig. 1B). Neither *Escherichia coli* alanyl- nor isoleucyl-tRNA synthetases (IleRS) were inhibited (*7*). Cell-free extracts from NTL4(pTiC58Δ*accR*) and the resistant Ti-plasmidless strain NT1 were examined for LeuRS activity, after incubation of the cells in LB containing agrocin 84 (*5*). Extracts of the sensitive strain incubated with the antibiotic showed pronounced inhibition of $LeuRS_{At}$ activity compared to extracts from strain NT1, which cannot take up the antibiotic (Fig. 1C). In contrast, the activity of IleRS in either extract was not affected by growth with the antibiotic. Purified LeuRS encoded by the *agnB2* gene was far less sensitive to inhibition by the toxic moiety (IC_{50}, 9 μM) when compared to $LeuRS_{At}$ (IC_{50}, <10 nM) (Fig. 1B). This roughly 1000-fold difference in sensitivity of the two LeuRSs to the toxic moiety supports the hypothesis that the enzyme encoded by the *agnB2* gene is responsible for immunity to the inhibitor.

Biocontrol of crown gall tumors by agrocin 84 thus targets a tRNA synthetase in the pathogen. In turn, strain K84 carries a second, self-protective copy of the synthetase. In principle, this strategy from nature could be applied to other crop diseases by delivering pathogen-specific toxins with agents that protect the delivery vehicle.

References and Notes

1. M. E. Tate, P. J. Murphy, W. P. Roberts, A. Kerr, *Nature* **280**, 697 (1979).
2. P. J. Murphy, M. E. Tate, A. Kerr, *Eur. J. Biochem.* **115**, 539 (1981).
3. W. P. Roberts, M. E. Tate, A. Kerr, *Nature* **265**, 379 (1977).
4. M. H. Ryder, J. E. Slota, A. Scarim, S. K. Farrand, *J. Bacteriol.* **169**, 4184 (1987).
5. Materials and methods are available as supporting material on *Science* Online.
6. J.-S. Shim, S. K. Farrand, A. Kerr, *Phytopathology* **77**, 463 (1987).
7. J. S. Reader, P. T. Ordoukhanian, J.-G. Kim, V. de Crécy-Lagard, I. Hwang, S. Farrand, P. Schimmel, unpublished data.
8. Supported by NIH grant nos. GM52465 (S.F.), GM15539 (P.S.), and GM23562 (P.S.); a National Foundation for Cancer Research fellowship (P.S.); and grant no. CG1412 from the Crop Functional Genomics Center (I.H.).

Supporting Online Material
www.sciencemag.org/cgi/content/full/309/5740/1533/DC1
Materials and Methods
Fig. S1
References and Notes

1 July 2005; accepted 9 August 2005
10.1126/science.1116841

[1]Skaggs Institute for Chemical Biology, The Scripps Research Institute, La Jolla, CA 92037, USA. [2]School of Agricultural Biotechnology, Seoul National University, Seoul 151-921, Korea. [3]Department of Microbiology, University of Illinois at Urbana-Champaign, Urbana, IL 61801–3838, USA.

*To whom correspondence should be addressed. E-mail: schimmel@scripps.edu

Inositol Hexakisphosphate Is Bound in the ADAR2 Core and Required for RNA Editing

Mark R. Macbeth,[1,2] Heidi L. Schubert,[1] Andrew P. VanDemark,[1] Arunth T. Lingam,[1,2] Christopher P. Hill,[1*] Brenda L. Bass[1,2*]

We report the crystal structure of the catalytic domain of human ADAR2, an RNA editing enzyme, at 1.7 angstrom resolution. The structure reveals a zinc ion in the active site and suggests how the substrate adenosine is recognized. Unexpectedly, inositol hexakisphosphate (IP_6) is buried within the enzyme core, contributing to the protein fold. Although there are no reports that adenosine deaminases that act on RNA (ADARs) require a cofactor, we show that IP_6 is required for activity. Amino acids that coordinate IP_6 in the crystal structure are conserved in some adenosine deaminases that act on transfer RNA (tRNA) (ADATs), related enzymes that edit tRNA. Indeed, IP_6 is also essential for in vivo and in vitro deamination of adenosine 37 of $tRNA^{ala}$ by ADAT1.

One form of RNA editing is catalyzed by adenosine deaminases that act on RNA (ADARs), a family of enzymes that deaminate adenosine to form inosine in double-stranded RNA (dsRNA) (Fig. 1A) (*1*). ADARs are important for proper neuronal function (*2–4*) and also are implicated in the regulation of RNA interference (RNAi) (*5–7*). Inosine is recognized as guanosine by most cellular proteins and the translation machinery, and it pairs most stably with cytidine. Therefore, editing of RNA can alter a codon, create splice sites, and change its structure. The latter occurs when an AU base pair is changed to an IU mismatch and may be important for the effects of ADARs on the RNAi pathway.

[1]Department of Biochemistry and [2]Howard Hughes Medical Institute, University of Utah, Salt Lake City, UT 84132, USA.

*To whom correspondence should be addressed. E-mail: bbass@howard.genetics.utah.edu (B.L.B.); chris@biochem.utah.edu (C.P.H.)

ADARs from all organisms have a common domain structure consisting of one to three dsRNA binding motifs (dsRBMs) near the N terminus, followed by a conserved C-terminal catalytic domain (*1*, *8*). Human ADAR2 (hADAR2) contains two dsRBMs, and its best characterized substrates are the pre-mRNAs of glutamate and serotonin receptors (*9*, *10*). Editing of codons within these RNAs leads to altered amino acids and generates receptors with altered function. hADAR2 also edits its own message to create a new splice site (*11*). Purified hADAR2 deaminates substrates in vitro (*12*) in the absence of any added cofactors, and deletions of N-terminal sequences, including dsRBM1, result in an active protein that accurately edits an RNA substrate (*13*). In addition, we found that a protein consisting of only the catalytic deaminase domain of hADAR2 (hADAR2-D, residues 299 to 701) (fig. S1A) was active in vitro, although it deaminates RNA less efficiently than full-length hADAR2 (fig. S1B).

The structure of the ADAR2 catalytic domain. To better understand the ADAR mechanism, we crystallized hADAR2-D. The structure (PDB code 1ZY7) was determined by multiple isomorphous replacement and refined at 1.7 Å resolution to an R_{factor} of 17.4% and R_{free} of 20.7% (*14*). The asymmetric unit includes 669 water molecules, one sulfate ion, and two hADAR2-D molecules that are essentially identical [root mean square deviation (RMSD) = 0.28 Å for 358 pairs of Cα atoms]. The refined hADAR2-D model contains residues 306 to 461 and 474 to 700 (462 to 473 are disordered), one zinc ion, and one molecule of inositol hexakisphosphate (IP_6).

The protein adopts a roughly spherical 40 Å diameter structure (Fig. 1B) that, consistent with sizing chromatography of hADAR2-D and equilibrium ultracentrifugation of the full-length hADAR2, appears monomeric in the crystal. The active site is indicated by an ordered zinc ion that coordinates a water molecule that presumably displaces ammonia during the deamination reaction. Coordination of the zinc ion by H394, C451, and C516, and hydrogen bonding of the water molecule by E396 (Fig. 1C), is

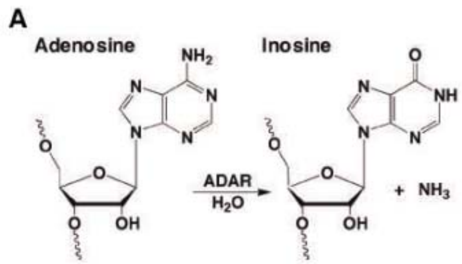

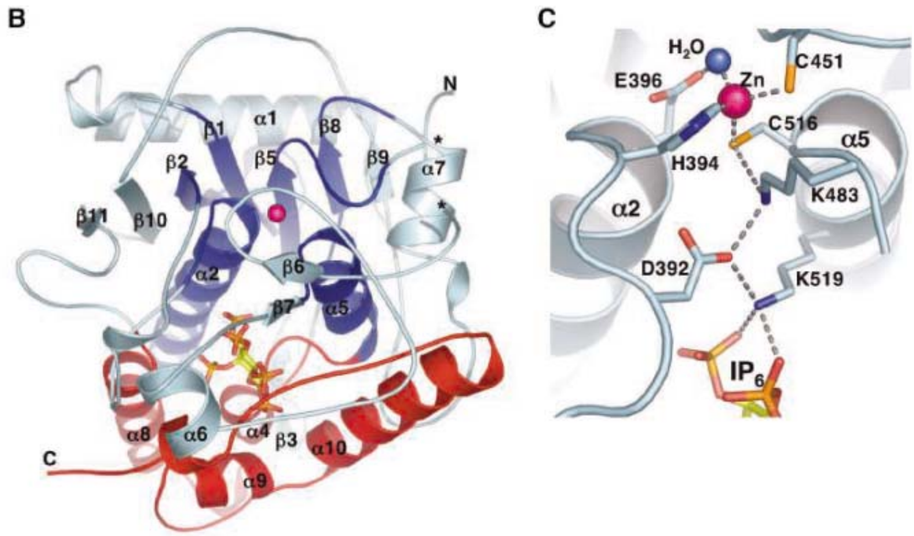

Fig. 1. (**A**) ADAR catalyzed hydrolytic deamination of adenosine to inosine in dsRNA. (**B**) Ribbon model of hADAR2-D. The active-site zinc atom is represented by a magenta sphere. The N-terminal α/β domain (residues 306 to 620) is colored cyan, with the region that shares structural similarity with CDA and TadA colored dark blue (deamination motif; residues 350 to 375, 392 to 416, 439 to 455, 514 to 525, and 542 to 551). The C-terminal helical domain (residues 621 to 700), which with contributions from the deamination motif makes the major contacts to IP_6 (ball and stick), is colored red. Ends of the disordered segment (residues 462 to 473) are indicated with asterisks. (**C**) Residue interactions at the active site. Shown are the zinc ion, coordinating residues (H394, C451, and C516), the nucleophilic water (blue sphere), and the proposed proton-shuttling residue, E396. The hydrogen-bond relay that connects the active site to the IP_6 is also indicated. Single-letter abbreviations for amino acid residues are defined in (*42*).

essentially identical to the geometry seen at the catalytic centers of cytidine deaminase (CDA) (*15*) and TadA (*16*), a member of the ADAT2 (adenosine deaminase that acts on tRNA 2) family. This similarity was predicted earlier on the basis of equivalent chemistry and sequence conservation of the four residues that coordinate zinc and water (*17*, *18*).

Superposition of zinc, water, and coordinating residues was used as the starting point to identify residues of hADAR2-D that were structurally equivalent to those in CDA and TadA (PDB codes 1CTU and 1WWR, respectively). Inspection shows that 77 residues (RMSD = 3.05 Å on Cα atoms) form a structurally conserved "deamination motif" comprising two helices (α2 and α5), four strands (β1, β2, β5, and β8), and connecting loops (Fig. 1B, dark blue). Other hADAR2-D residues do not have structural equivalents in CDA and TadA (Fig. 2A). Further emphasizing the large evolutionary separation between these enzymes, only four of the deamination motif residues have conserved identities in all three enzymes (excluding zinc/water ligands).

The active site of ADAR2. The site of nucleophilic attack during the ADAR reaction (C6 of adenine) lies deep in the major groove of the dsRNA substrate. Because this site is inaccessible to an enzyme, ADARs may use a base-flipping mechanism (*19*, *20*) like other enzymes that modify double-stranded polynucleotides (*21*). Consistent with this scenario, the catalytic zinc center is located in a deep pocket in the enzyme surface that is surrounded by positive electrostatic potential that likely serves as the dsRNA binding site (Fig. 2B). In contrast, TadA uses an alternative mechanism of substrate selection that probably involves recognition of the anticodon stem/loop of tRNA (*16*).

To model binding of substrate, we overlapped the structure of a CDA-zebularine (cytidine analog inhibitor) complex (*15*) onto the hADAR2 structure and built the adenosine monophosphate (AMP) portion of an ADAR substrate to maintain the same catalytic geometry. In this simple overlap based on zinc ion and coordinating residues, the zebularine ribose clashes with the hADAR2 loop containing T375 (Fig. 2C), thereby providing a plausible explanation for why ADARs do not deaminate cytidine. The steric clash is absent with AMP because of the additional distance afforded by the purine ring (Fig. 2D). The proposed AMP-binding geometry requires repositioning of the hADAR2 R455 side chain, although this could be accomplished through minor rearrangements that may occur upon dsRNA binding.

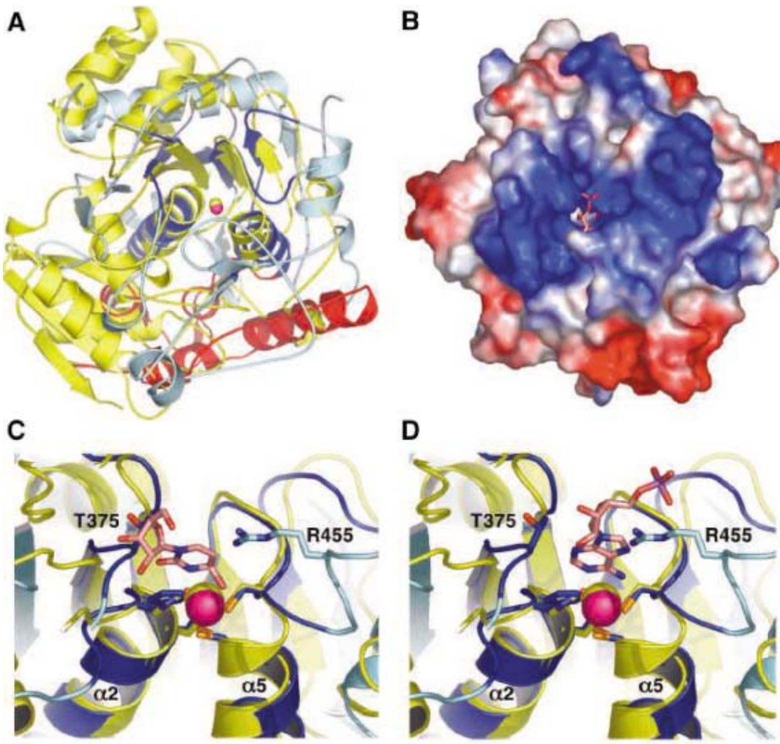

Fig. 2. (**A**) Superposition of *Escherichia coli* CDA (yellow) and hADAR2-D (color scheme as in Fig. 1B) shows that these structures are highly diverged. View direction is similar to Fig. 1B. The only hADAR2-D residues that have structural equivalents in CDA are dark blue. (**B**) Electrostatic surface potential reveals a highly basic (blue) region flanking the active site. View direction is from the top of (A). The modeled AMP (pink) and catalytic zinc ion (magenta, partially occluded) are visible in the active site cleft. (**C**) Superposition of the hADAR2 and CDA active sites. Zebularine (pink) bound to CDA would clash with the loop containing T375 of hADAR2-D. (**D**) Docking of AMP (pink) in the same chemically equivalent orientation as zebularine would not clash with the T375 loop. Single-letter abbreviations for amino acid residues are defined in (*42*).

Comparison of the ADAR and CDA/TadA structures reveals an important difference in the arrangement of the two cysteine residues that coordinate zinc (fig. S5). As often found in zinc-dependent enzymes (*22*, *23*), the two cysteines of CDA and TadA are located in a Cys-X-X-Cys motif at the N terminus of a helix. The first cysteine forms hydrogen bonds with two main-chain amide NH groups at the helix terminus; this likely contributes to catalysis by increasing the positive character of the zinc ion and nucleophilicity of the water molecule (*24*). In ADAR2, however, C451 and C516 are separated by a 64-residue loop, and hydrogen bonding to main-chain atoms is reduced to a single bond between C451 and the amide NH group of C516. However, a second hydrogen bond is observed between C516 and K483 (Fig. 3A and fig. S5), and thus ADARs may have evolved a compensating interaction; K483 is conserved in ADAR sequences but not seen in CDA or TadA.

Inositol hexakisphosphate binds in the core of the catalytic domain. One side of the deamination motif of hADAR2 contributes to a cavity, not found in CDA or TadA, that is formed mainly by C-terminal elements (Fig. 1B, red) and buries the IP_6 molecule and 29 associated water molecules. The identity of IP_6 was suggested by the strong, distinctive electron density (Fig. 3A and fig. S3) and the local electrostatic interactions, and was confirmed by (+) ion electrospray mass spectrometry [observed molecular weight (MW) of IP_6 in complex with the protein = 660.0 Da; calculated MW = 659.9 Da] (*14*). IP_6 is an abundant inositol polyphosphate implicated in many cellular functions, including RNA export, DNA repair, endocytosis, and chromatin remodeling (*25*–*29*). Intriguingly, the compound is reported to affect neuronal AMPA receptors (*30*), whose messages are edited by ADAR2 (*9*).

The IP_6 cavity is extremely basic and lined with many arginine and lysine residues (R400, R401, and R522 and K519, K629, K662, K672, and K690), as well as W523, W687, Y658, and Y668 (Fig. 3, A and B). Most of these residues are invariant among catalytically active ADARs, as well as in the ADAT1 family of enzymes, which deaminate A37 of certain tRNAs. (The ADAT2 family, of which TadA is a member, is distinct from ADAT1 and does not have the IP_6 binding pocket or its conserved residues.)

IP_6 was not added during purification or crystallization but must have been acquired during expression of the human ADAR2-D protein in *Saccharomyces cerevisiae*, which like other eukaryotes has pools of IP_6 (*31*). The presence of IP_6 in the purified protein therefore indicates a tight association, consistent with the extensive array of hydrogen bonds formed with conserved side chains (Fig. 3B) and the almost completely buried environment (Fig. 3C). The structure suggests that hADAR2 will be nonfunctional in the absence of IP_6, a view that is supported by experiments described below.

IP_6 is required for ADAR2 activity. In *S. cerevisiae*, the last step in the synthesis of IP_6 is the phosphorylation of IP_5 by Ipk1p, and yeast harboring a deletion of *IPK1* are viable but fail to produce IP_6 (*25*). To test for the IP_6 requirement of hADAR2, we expressed the protein in *ipk1*Δ yeast cells and compared its activity to hADAR2 expressed in the same strain but containing the *IPK1* gene. As substrate, we used a 27-base-pair RNA that mimics the natural arginine/glycine (R/G) editing site of the glutamate receptor B (gluR-B) pre-mRNA (Fig. 4A) and that is efficiently edited by hADAR2 in vitro (*20*). IP_6 was required for hADAR2 activity (Fig. 4B), because there was no editing of this RNA by protein expressed in the *ipk1*Δ mutant. Using reverse transcription polymerase chain reaction (RT-PCR), we determined that hADAR2 mRNA was expressed at the same levels in the wild-type and *ipk1*Δ mutant strains, although the amount of hADAR2 protein was lower by a factor of 5 to 10 in the mutant strain. Western blots were performed to determine the amount of hADAR2 protein in each extract by comparison with a standard curve generated with known amounts of purified, histidine-tagged protein (R_2D, an N-terminal truncation of hADAR2) (*13*). This information was used to normalize amounts of hADAR2 used for the in vitro assays, and a Western blot confirmed that amounts of hADAR2 in wild-type and mutant editing reactions were similar (Fig. 4C).

IP_6 is required for tRNA editing by the ADAT1 family of deaminases. ADATs are another class of enzymes that deaminate adenosine to generate inosine in RNA. These enzymes contain only the catalytic domain and deaminate tRNAs at adenosines 34 and 37 (A34 and A37) (*18*). On the basis of their sequences and substrates, there are three types of ADATs in eukaryotes. ADAT1 deaminates A37 of $tRNA^{ala}$ (*32*), and the resulting inosine is subsequently methylated at N1 in a reaction requiring a different enzyme and S-adenosylmethionine (*33*). ADAT2 and ADAT3 form a heterodimer that deaminates A34 of various tRNAs and, consistent with the fact that this is the wobble position, unlike ADAT1, these enzymes are essential (*32*, *34*). By aligning enzyme sequences, we noted that residues observed to coordinate IP_6 in the hADAR2 crystal structure were conserved in the ADAT1 family but not in the ADAT2 or ADAT3 families (Fig. 5A and fig. S6). To test the consequent prediction that ADAT1, but not ADAT2/3, requires IP_6, we monitored activity of endogenous ADAT in extracts prepared from *S. cerevisiae* wild-type or *ipk1*Δ strains. *S. cerevisiae* $tRNA^{ala}$ is deaminated at A34, as well as A37, and provided an ideal substrate with which to assay the IP_6 requirement of the different ADATs (Fig. 5B). We observed that in vitro editing of A37 by ADAT1 is severely reduced in extract prepared from the *ipk1*Δ strain compared with extract from a wild-type strain (Fig. 6A). In contrast, there was no difference for in vitro editing of A34 by the ADAT2/ADAT3 heterodimer in the mutant versus the wild-type extract (Fig. 6B). To confirm that the lack of activity in the *ipk1*Δ strain derived from a lack of IP_6 rather than a molecule downstream in the pathway, we tested ADAT1 activity in extracts prepared from a *kcs1*Δ mutant (fig. S7). The *KCS1* gene product is downstream of *IPK1* in the inositol polyphosphate synthesis pathway and phosphorylates IP_6 to form the pyrophosphate-containing IP_7 (5PP-IP_5) (*35*). The *kcs1*Δ mutation had no effect on the A37 editing activity of ADAT1, which indicates that the editing defect in the *ipk1*Δ mutant is due to the IP_6 deficiency.

The existence of the *ipk1*Δ mutant, and the fact that *S. cerevisiae* $tRNA^{ala}$ is deaminated at both A34 and A37, provided a facile system for analyzing the in vivo requirement for IP_6. RNA was prepared from wild-type or *ipk1*Δ cells, $tRNA^{ala}$ was amplified using RT-PCR, and the RT-PCR product was sequenced (Fig. 6C). Because inosine is read as guanosine by reverse transcriptase, edited adenosines were identified as guanosine in the dideoxy sequencing reaction. Consistent with the in vitro data, we observed that A34 is edited with equal efficiency in the wild-type and mutant strain, but A37 is edited

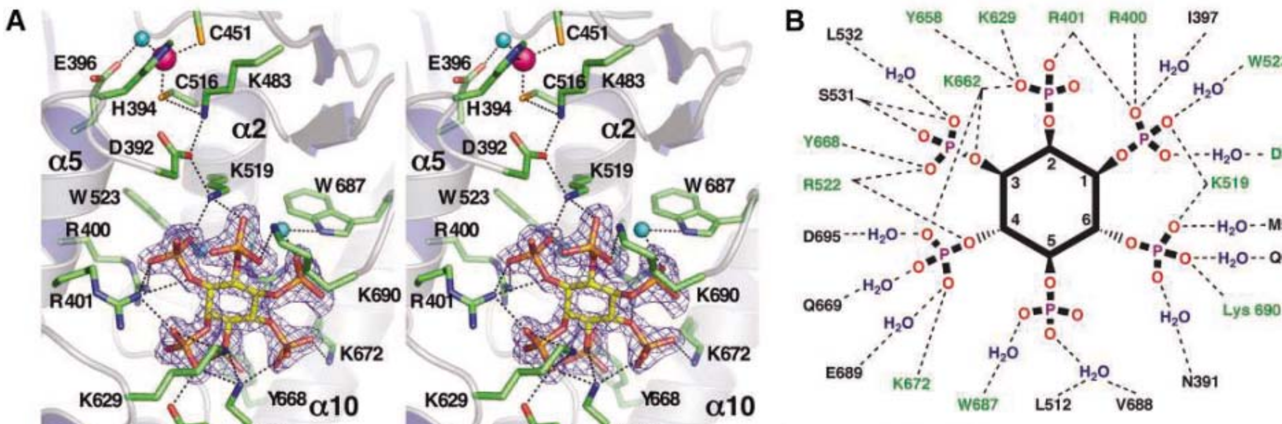

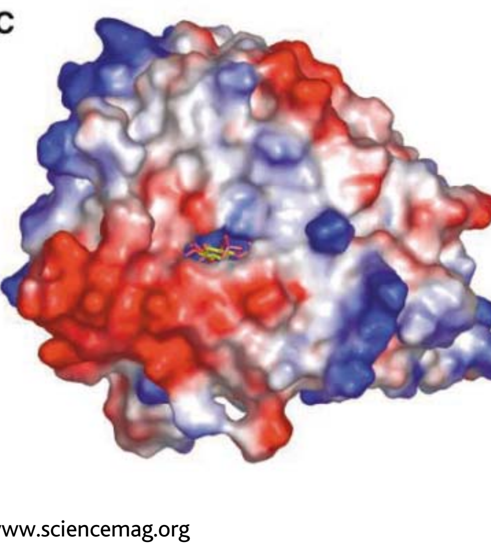

Fig. 3. (**A**) Stereo image of the active site and IP_6 binding site in hADAR2-D. The zinc ion (magenta sphere) and E396 are coordinating the nucleophilic water (aqua sphere). The hydrogen bond relay between the zinc and IP_6 (yellow sticks) is shown as dashes, as are hydrogen bonds between conserved residues (green sticks) and IP_6. IP_6 interactions with W523 and W687 are mediated by water (aqua spheres). The $2F_o - F_c$ (where F_o is the observed structure factor and F_c is the calculated structure factor) difference electron density map demonstrating the presence of the bound IP_6 is contoured at 4σ. Because IP_6 is nearly buried, part of the protein molecule in the foreground has been cut away for clarity. (**B**) Schematic diagram of residues that hydrogen-bond with IP_6 directly or through one water molecule. H bonds, dashed lines; conserved residues, green. For clarity, the inositol ring is depicted as planar, although it actually binds in the "chair" conformation. (**C**) Only view from which IP_6 (yellow) is visible from the protein exterior in a surface representation. The "window" measures 8.4 Å by 4.6 Å between van der Waal's surfaces. Single-letter abbreviations for amino acid residues are defined in (*42*).

much less efficiently in the *ipk1*Δ strain (Fig. 6C). A37 in the wild-type strain is read as a thymidine, presumably due to N[1]-methylinosine at position 37. m[1]I, like m[1]A, may pair with reduced specificity in the reverse transcription reaction, explaining the presence of a T in the PCR product (*36*).

In the crystal structure of hADAR2, IP_6 binds and fills an extremely basic hole, with the center of the inositol ring more than 10 Å from the protein surface. Thus, it seems possible that ADAR2 and, by analogy, ADAT1, are unstable without IP_6. In this regard we wondered about the nature of ADAT1 expressed in the *ipk1*Δ mutant. Was this protein trapped in an irreversible inactive state or forming a folding intermediate that could bind IP_6 to achieve its active conformation? To explore this question, we tested whether the addition of IP_6 to extracts prepared from the *ipk1*Δ mutant could recover ADAT1 activity. When added to extracts prepared from the *ipk1*Δ strain, IP_6 recovered activity to ~50% of wild-type (Fig. 7, A and C), which suggests that the protein does not require IP_6 during its synthesis and the initial stages of folding. As expected, the addition of IP_6 to wild-type extract had no effect, because these cells are capable of synthesizing IP_6 (Fig. 7, B and C). To test for the specific requirement for IP_6 by ADAT1, we performed a similar experiment, except we substituted inositol hexakissulfate (IS_6) for IP_6. Despite its similar charge and structure, IS_6 does not recover ADAT1 activity when added to *ipk1*Δ extracts (Fig. 7A). This suggests that the enzyme specifically requires IP_6 for function and can discriminate between the minor differences in phosphate/sulfate chemistry (e.g., the protonation state).

So far, we have been unable to rescue the activity of hADAR2 expressed in the *ipk1*Δ by adding IP_6. Possibly, native *S. cerevisiae* ADAT1, but not the heterologous hADAR2, is associated with a host chaperone in the extract that promotes refolding in the presence of IP_6. Alternatively, this result may hint at interesting differences between the two enzymes in IP_6 accessibility. Such a difference might explain why assays of ADAT1 in *ipk1*Δ extracts show a small (~5%) amount of A37 deamination at the highest concentrations of extract (Fig. 6A), whereas ADAR2 expressed in this strain shows no residual activity. If the IP_6 binding site in ADAT1 were more accessible than that of ADAR2, it might bind a noncognate inositol polyphosphate, such as IP_5, to allow a low level of activity.

Discussion. Burial of IP_6 may reflect a novel way of using an available cellular component to define and stabilize a protein fold. This would be analogous to the use of "structural" metal ions in stabilizing the fold of metalloproteins. To our knowledge, this represents the first example of a protein using IP_6 for this purpose. Other protein structures with bound IP_6 have been reported, such as deoxyhemoglobin (*37*) and the clathrin adaptor complex AP2 (*38*); however, unlike ADAR2-D, in these cases the IP_6 molecule is not extensively buried and does not appear to dramatically stabilize the overall structure.

In addition to the structural requirement, IP_6 may play a subtle role in modulating catalytic efficiency by indirectly ordering the side chain of K483. Two of the IP_6 phosphate groups approach within 10 Å of the catalytic zinc ion and are indirectly coordinated to zinc by a chain of hydrogen-bonded residues that includes K519, D392, and K483 (Fig. 3A). These residues are conserved among active ADARs, and K483 may contribute to tuning the pK_a of the nucleophilic water molecule through its interaction with C516 (Fig. 3A).

Sequence alignments indicate that ADAT1 enzymes are the evolutionary link between the other family members, ADAT2/3 (including TadA) and ADARs (*18*). ADAT1 apparently

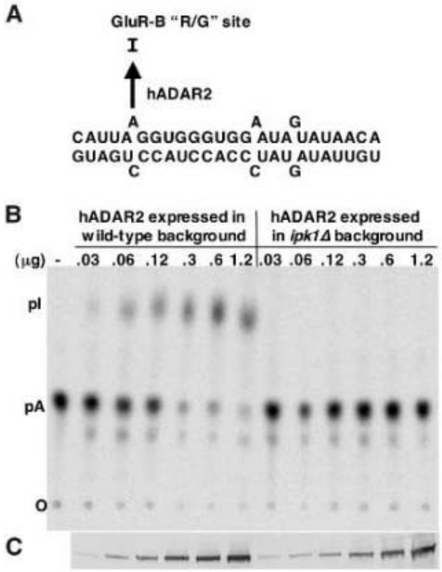

Fig. 4. (**A**) The 27-mer R/G site RNA substrate used to assay hADAR2 editing activity. (**B**) Editing of the R/G site RNA by hADAR2 expressed in wild-type or *ipk1*Δ yeast. The R/G site adenosine was labeled with ^{32}P and incubated with increasing concentrations of expressed hADAR2 in extracts. Reacted RNA was treated with nuclease P1, the resulting 5′ nucleotide monophosphates separated by thin-layer chromatography (TLC), and the plate exposed to a PhosphorImager screen. The amount of hADAR2 in each extract was determined by Western blotting, and extract was added to give the final ADAR2 concentrations as indicated. (**C**) Western blot showing the amount of hADAR2 in each reaction. Single-letter abbreviations for amino acid residues are defined in (*42*).

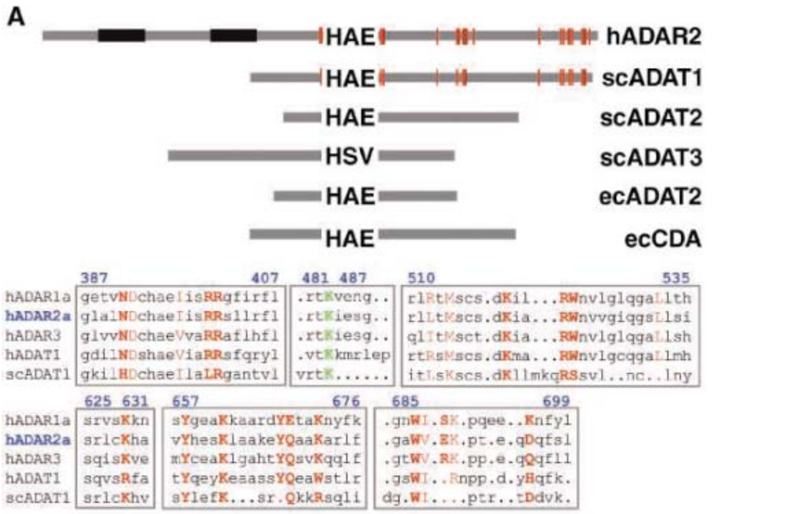

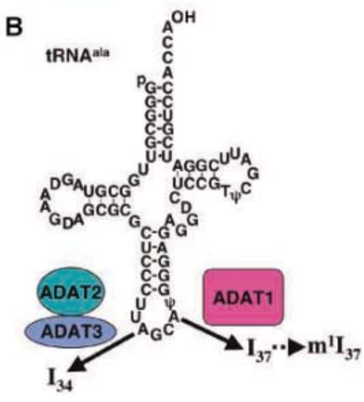

Fig. 5. (**A**) Schematic diagram showing the relative lengths and domain structures of hADAR2 and family members from *S. cerevisiae* (sc) and *E. coli* (ec). Proteins are anchored at the invariant zinc-coordinating histidine (H). Residues that coordinate IP_6 are red lines; double-stranded RNA binding motifs are in black. Alignments for regions surrounding the residues that coordinate IP_6 in hADAR2 are shown below, with blue numbering corresponding to hADAR2. IP_6 coordinating residues are in red, with side-chain contacts in bold. Residues N391, W523, Q669, W687, E689, and D695 are water-mediated contacts. The conserved K483, which is part of a hydrogen-bond relay from IP_6 to the active site zinc, is shown in green. Sequences diverge considerably in the region surrounding K483; the alignment shown was chosen because the conserved lysine of various subfamilies is aligned with K483 of hADAR2. Notably, the IP_6 coordinating residues are found in ADAR3, which suggests that inefficient IP_6 binding is not the reason this enzyme lacks deaminase activity (*43*). (**B**) The tRNA[ala] substrate used in this study showing the sites of modification by the ADAT proteins. Single-letter abbreviations for amino acid residues are defined in (*42*).

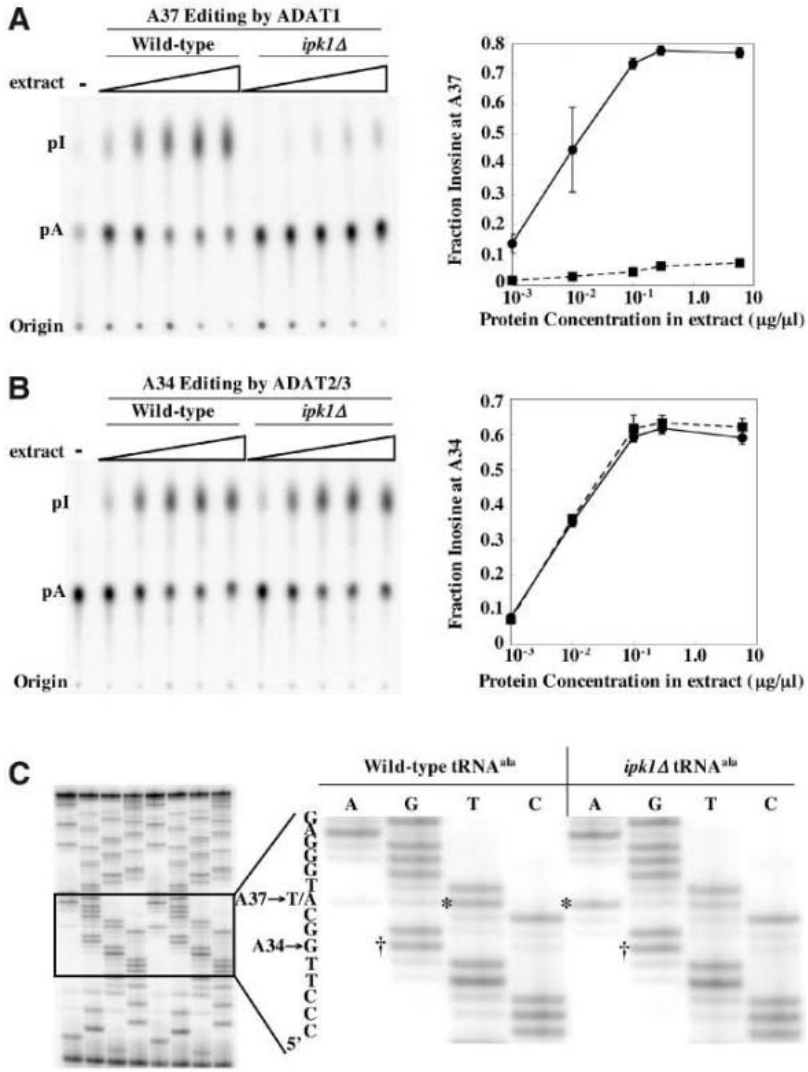

Fig. 6. (**A**) Editing of tRNA^{ala} A37 in vitro by extracts of wild-type or *ipk1*Δ yeast strains. tRNA^{ala}, labeled with ^{32}P at A37, was incubated with increasing amounts of yeast extract protein, as indicated (*14*). Reacted RNA was processed as in Fig. 4B, and nuclease P1 products were separated by TLC (left). The fraction of inosine in each lane was quantified, and the average of three determinations was plotted as a function of protein concentration (right; error bars, standard deviation; when error was very small, error bars are obscured by data point symbols). Solid line, editing by ADAT1 from wild-type extracts; dashed line, editing by ADAT1 from *ipk1*Δ extracts. (**B**) As in (A) but showing editing of A34-labeled tRNA^{ala}. Solid line, editing by ADAT2/3 from wild-type extracts; dashed line, editing by ADAT2/3 from *ipk1*Δ extracts. (**C**) Editing of endogenous tRNA in vivo. tRNA was prepared from wild-type or *ipk1*Δ strains, reverse transcribed, and amplified by PCR. PCR products were sequenced using dideoxy nucleotide triphosphates and a ^{32}P-labeled primer that anneals to the nontemplate strand at the 5′ end of the gene. The right panel shows an expanded view of the sequencing gel shown on the left. The dideoxy sequencing lanes are indicated at the top of each lane, and the 5′ to 3′ sequence to the left of the gel is read from bottom to top. Bands corresponding to A34 to G editing in the wild-type and *ipk1*Δ tRNAs are labeled with daggers, and the band representing the A37 site that is not edited in the *ipk1*Δ tRNA is labeled with an asterisk. Consistent with the observation of residual activity in the mutant extract in vitro (A), some editing of A37 in the mutant extract occurs.

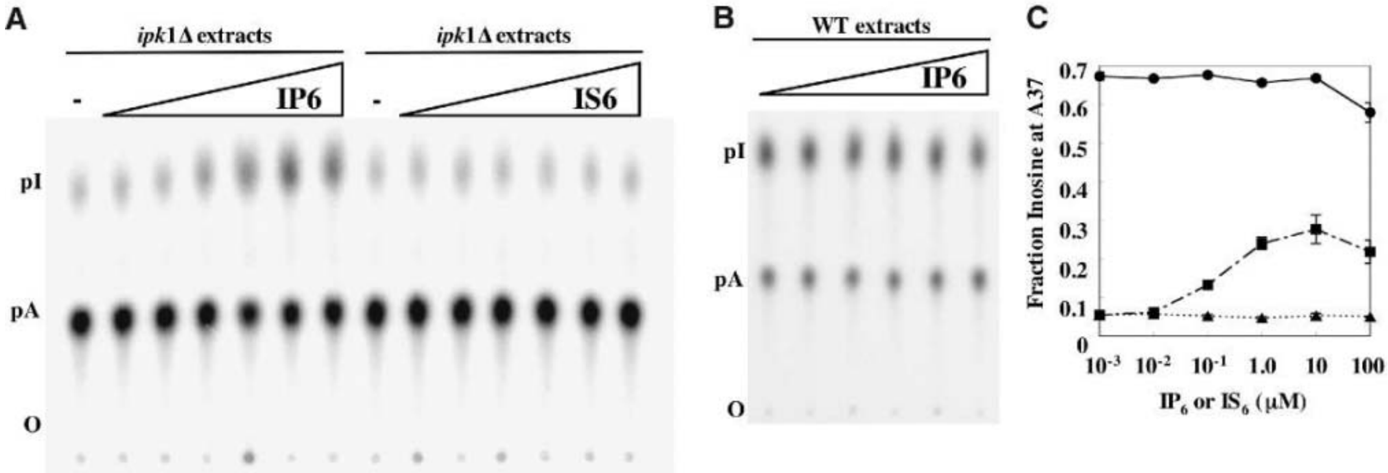

Fig. 7. (**A**) Addition of IP$_6$, but not IS$_6$, rescued ADAT1 activity in extracts prepared from *ipk1*Δ yeast. Wild-type or *ipk1*Δ protein extract (0.1 μg/μl) was incubated with IP$_6$ or IS$_6$ for 15 min at 30°C before the addition of A37-labeled tRNA^{ala}. IP$_6$ and IS$_6$ concentrations were 10-fold dilutions from 100 μM to 10^{-3} μM. The tRNA was processed as described in Fig. 4B. (**B**) Addition of IP$_6$ had no effect on ADAT1 activity in wild-type extracts using the reaction conditions of (A). Without the addition of IP$_6$, wild-type extracts gave 70% A to I conversion. (**C**) The average fraction of inosine produced in three experiments each of (A) and (B) plotted as a function of IP$_6$ or IS$_6$ concentration; error bars show the standard deviation (small error bars are obscured by the data point symbol). Circles, ADAT1 activity from wild-type extracts with IP$_6$ added; squares, activity of *ipk1*Δ extracts with IP$_6$; triangles, activity of *ipk1*Δ extracts with IS$_6$.

diverged from the ADAT2/3 family by acquiring the ability to bind IP_6, followed by the acquisition of one or more dsRBMs to generate an ADAR. ADAT1 may have evolved an IP_6 binding function as a means of regulation. IP_6 accumulates in yeast during times of stress (*39*) and thus could lead to increased ADAT1 activity, and consequently to an increased conversion of A37 to N^1-methylinosine. Modification of position 37 is predicted to increase fidelity of protein synthesis by stabilizing the codon-anticodon interaction (*40*), and thus yeast may use this modification to fine-tune protein synthesis in response to environmental conditions.

Once established as a means of regulation for ADAT1, metazoa may have extended this regulatory mode for use in ADARs, which perform important roles in the nervous system and display changes in activity during development (*41*). For example, a feedback mechanism could act through phospholipase C in response to hormones such as serotonin. Upon binding of serotonin to its 5-HT_{2c} receptor, phospholipase C is activated to cleave phosphatidyl inositol 4,5-bisphosphate (PIP_2) to form the second messengers diacylglycerol and inositol 1,4,5-triphosphate (IP_3), which is subsequently phosphorylated to form IP_6. 5-HT_{2C} receptor mRNA is edited at five distinct sites by ADAR2, with the more extensively modified receptors requiring greater concentrations of serotonin to stimulate phospholipase C. It is tempting, therefore, to speculate that the serotonin-induced production of IP_6 causes increased production of active ADAR2, which in turn edits mRNA to attenuate the serotonin signaling pathway.

The structure of the hADAR2 catalytic domain reveals the active site architecture of a zinc-catalyzed deamination reaction and suggests how ADARs discriminate between cytidine and adenosine residues. The presence of IP_6 in the protein core implied an unexpected requirement for this cofactor in ADARs, which was confirmed by assaying the RNA editing activity of enzymes lacking IP_6. The finding that IP_6 is required for ADAR and ADAT activity suggests many interesting links between RNA editing and diverse processes such as cell signaling and translation, thus setting the stage for future studies.

References and Notes

1. B. L. Bass, *Annu. Rev. Biochem.* **71**, 817 (2002).
2. M. Higuchi *et al.*, *Nature* **406**, 78 (2000).
3. M. J. Palladino, L. P. Keegan, M. A. O'Connell, R. A. Reenan, *Cell* **102**, 437 (2000).
4. L. A. Tonkin *et al.*, *EMBO J.* **21**, 6025 (2002).
5. S. W. Knight, B. L. Bass, *Mol. Cell* **10**, 809 (2002).
6. A. D. Scadden, C. W. Smith, *EMBO Rep.* **2**, 1107 (2001).
7. L. A. Tonkin, B. L. Bass, *Science* **302**, 1725 (2003).
8. S. Maas, A. Rich, K. Nishikura, *J. Biol. Chem.* **278**, 1391 (2003).
9. T. Melcher *et al.*, *Nature* **379**, 460 (1996).
10. C. M. Burns *et al.*, *Nature* **387**, 303 (1997).
11. S. M. Rueter, T. R. Dawson, R. B. Emeson, *Nature* **399**, 75 (1999).
12. M. A. O'Connell, A. Gerber, W. Keller, *J. Biol. Chem.* **272**, 473 (1997).
13. M. R. Macbeth, A. T. Lingam, B. L. Bass, *RNA* **10**, 1563 (2004).
14. Materials and methods are available as supporting material on *Science* Online.
15. L. Betts, S. Xiang, S. A. Short, R. Wolfenden, C. W. Carter Jr., *J. Mol. Biol.* **235**, 635 (1994).
16. M. Kuratani *et al.*, *J. Biol. Chem.* **280**, 16002 (2005).
17. U. Kim, Y. Wang, T. Sanford, Y. Zeng, K. Nishikura, *Proc. Natl. Acad. Sci. U.S.A.* **91**, 11457 (1994).
18. A. P. Gerber, W. Keller, *Trends Biochem. Sci.* **26**, 376 (2001).
19. A. G. Polson, B. L. Bass, *EMBO J.* **13**, 5701 (1994).
20. O. M. Stephens, H. Y. Yi-Brunozzi, P. A. Beal, *Biochemistry* **39**, 12243 (2000).
21. X. Cheng, R. J. Roberts, *Nucleic Acids Res.* **29**, 3784 (2001).
22. J. W. Schwabe, A. Klug, *Nat. Struct. Biol.* **1**, 345 (1994).
23. J. E. Wedekind, P. A. Frey, I. Rayment, *Biochemistry* **34**, 11049 (1995).
24. D. C. Carlow, C. W. Carter Jr., N. Mejlhede, J. Neuhard, R. Wolfenden, *Biochemistry* **38**, 12258 (1999).
25. J. D. York, A. R. Odom, R. Murphy, E. B. Ives, S. R. Wente, *Science* **285**, 96 (1999).
26. L. A. Hanakahi, S. C. West, *EMBO J.* **21**, 2038 (2002).
27. M. Hoy *et al.*, *Proc. Natl. Acad. Sci. U.S.A.* **99**, 6773 (2002).
28. X. Shen, H. Xiao, R. Ranallo, W. H. Wu, C. Wu, *Science* **299**, 112 (2003).
29. D. J. Steger, E. S. Haswell, A. L. Miller, S. R. Wente, E. K. O'Shea, *Science* **299**, 114 (2003).
30. B. Valastro *et al.*, *Hippocampus* **11**, 673 (2001).
31. V. Raboy, *Phytochemistry* **64**, 1033 (2003).
32. A. Gerber, H. Grosjean, T. Melcher, W. Keller, *EMBO J.* **17**, 4780 (1998).
33. H. Grosjean *et al.*, *Biochimie* **78**, 488 (1996).
34. A. P. Gerber, W. Keller, *Science* **286**, 1146 (1999).
35. A. Saiardi, J. J. Caffrey, S. H. Snyder, S. B. Shears, *J. Biol. Chem.* **275**, 24686 (2000).
36. M. Kroger, B. Singer, *Biochemistry* **18**, 3493 (1979).
37. A. Arnone, M. F. Perutz, *Nature* **249**, 34 (1974).
38. B. M. Collins, A. J. McCoy, H. M. Kent, P. R. Evans, D. J. Owen, *Cell* **109**, 523 (2002).
39. P. P. Ongusaha, P. J. Hughes, J. Davey, R. H. Mitchell, *Biochem. J.* **335**, 671 (1998).
40. H. Grosjean, C. Houssier, P. Romby, R. Marquet, in *Modification and Editing of RNA*, H. Grosjean, R. Benne, Eds. (ASM Press, Washington, DC, 1998), pp. 113–134.
41. H. Lomeli *et al.*, *Science* **266**, 1709 (1994).
42. Single-letter abbreviations for the amino acid residues are as follows: A, Ala; C, Cys; D, Asp; E, Glu; F, Phe; G, Gly; H, His; I, Ile; K, Lys; L, Leu; M, Met; N, Asn; P, Pro; Q, Gln; R, Arg; S, Ser; T, Thr; V, Val; W, Trp; and Y, Tyr.
43. C. X. Chen *et al.*, *RNA* **6**, 755 (2000).

44. We thank R. Schackmann for synthesis of oligonucleotides and N-terminal sequencing and C. Nelson for mass spectrometry analysis; both are supported by a Cancer Center Support Grant (2P30CA042014). We also thank P. Beal and S. Wente for helpful discussions. This work was supported by grants from the National Institute of General Medical Sciences, GM44073 and GM56775, to B.L.B. and C.P.H., respectively. A.P.V. is supported by a postdoctoral fellowship from the American Cancer Society. B.L.B. is a Howard Hughes Medical Institute Investigator.

Supporting Online Material
www.sciencemag.org/cgi/content/full/309/5740/1534/DC1
Materials and Methods
Figs. S1 to S8
Tables S1 and S2
References

4 April 2005; accepted 29 July 2005
10.1126/science.1113150

REPORTS

Single-Molecule Torsional Pendulum

Jannik C. Meyer,[1]* Matthieu Paillet,[2] Siegmar Roth[1]

We have built a torsional pendulum based on an individual single-walled carbon nanotube, which is used as a torsional spring and mechanical support for the moving part. The moving part can be rotated by an electric field, resulting in large but fully elastic torsional deformations of the nanotube. As a result of the extremely small restoring force associated with the torsional deformation of a single molecule, unusually large oscillations are excited by the thermal energy of the pendulum. By diffraction analysis, we are able to determine the handedness of the molecule in our device. Mechanical devices with molecular-scale components are potential building blocks for nanoelectromechanical systems and may also serve as sensors or actuators.

Carbon nanotubes (*1*, *2*) are likely to be used in future nanoscale devices because of their outstanding mechanical and electrical properties. Nanoelectromechanical devices incorporating multiwalled carbon nanotubes (MWNTs) as motion-enabling elements have been demonstrated; in these devices, the MWNT serves as a torsional spring for small angular deformations (*3*) and torsional oscillations (*4*) or as a bearing for continuous rotational operation (*5*, *6*). Here, we show that it is possible to prepare large moving objects suspended on a single molecule—a single-walled nanotube (SWNT). The cross-section of a SWNT is smaller than that of a MWNT by more than two orders of magnitude, and large deformations are possible within the elastic regime. The moving part returns to its initial position even after being turned by 180°. The ultralow torsional spring constant provided by the

[1]Max Planck Institute for Solid State Research, D-70569 Stuttgart, Germany. [2]Laboratoire des Colloïdes, Verres et Nanomatériaux, Université de Montpellier II, 34095 Montpellier, France.

*To whom correspondence should be addressed. E-mail: j.meyer@fkf.mpg.de

SWNT allows for an easily detected deflection of the pendulum from excitations as small as those from the thermal energy.

Individual SWNTs are grown on a silicon substrate with a 200-nm oxide layer by chemical vapor deposition (*7*). The tubes are located with respect to a marker structure by atomic force microscopy. The device structure, consisting of 100 nm of Au with a 3-nm Cr adhesion layer, is prepared by electron beam lithography. The substrate is cleaved so that the structure is close (<10 μm) to a cleaved edge, as illustrated in Fig. 1. These structures are etched first in 15% tetramethylammonium hydroxide (TMAH) solution for several hours. The TMAH removes the bulk silicon and undercuts the structure from the side of the cleaved edge. As a result, the structure and the oxide layer reach out across the side edge of the substrate. The TMAH etching process is monitored with an optical microscope until a sufficient part of the structure is free-standing. Afterward, buffered hydrofluoric acid is used to remove the oxide layer, followed by critical-point drying.

The advantage of preparing a free-standing structure on the corner of a substrate is that it is accessible by a transmission electron microscope (TEM). Using a similar process, we have recently combined TEM and transport measurements, including gate characteristics, on the same nanotube (*8*). Arbitrary free-standing structures can be designed in this way, and accessibility by TEM is important for understanding and optimizing novel nanoelectromechanical systems.

The devices shown in Figs. 2 and 3 consist of a metal block suspended on an individual SWNT. Although the key motion-enabling element here is a single molecule, the suspended object is large enough to be visible in an optical microscope. In the TEM, the pendulum shown in Fig. 2 is already turned by ~70° as a result of electrostatic charging from the electron beam. This effect would not affect the device in possible applications outside an electron microscope. The charging is attributed to the high-resistance contacts between the nanotube and the metal structure. It is not present in the device shown in Fig. 3, which can be actuated by an external field between the support of the pendulum and a nearby electrode. In all the investigated devices, the carbon nanotube acts as a torsional spring in a regime of fully elastic deformation. The pendulum turns back to the initial position once the potential is switched off, even though it was turned by 180°. This is one distinction from MWNT-based devices, which are reported to break the outer shells at a deflection of 20° (followed by a continuous rotational freedom) in a similar geometry.

The device in Fig. 3 has a mass of $m \approx 2 \times 10^{-16}$ kg and a moment of inertia of $J \approx 7 \times 10^{-30}$ kg·m^2 with respect to the tube axis. The torsional spring constant of the tube axis is $C \approx 3 \times 10^{-18}$ N·m per radian, calculated from values in (*9*), our device geometry, and a tube diameter of 1.5 nm. Therefore, a torsional pendulum built on a SWNT can be turned by extremely small forces. For a rotation of 1°, a torque of 5×10^{-20} N·m is necessary. This corresponds to a force of 0.1 pN acting on one end of the rotor 400 nm away from the axis. Such a deflection can be detected by optical means because the rotor is sufficiently large. Optical displacement sensing with nanometer sensitivity has been demonstrated for objects of similar size (*10*). More intriguing, however, is the possibility that the nanotube itself could be used to sense the deformation, because a torsional deformation is expected to strongly influence the tube's electronic structure (*11*).

Extremely small perturbances can also excite a visible torsional oscillation. The resonance frequency for the torsional oscillation is calculated to be $f = [1/(2\pi)][(C/J)^{1/2}] \approx 0.1$ MHz. We can observe the thermally excited oscillations at room temperature in the TEM as unsharp edges of the pendulum, also visible in Fig. 2C. The amplitude of an oscillation with an energy of $k_B T$ (where k_B is the Boltzmann constant and T is absolute temperature) is calculated to be 3° for the geometry of the device shown in Fig. 2, which has a nanotube diameter of 2.4 nm. In all investigated devices, the observed thermal vibrations are in good agreement with the cal-

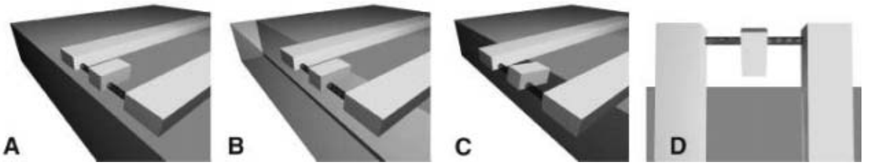

Fig. 1. Principle of sample preparation. (**A**) The structure is prepared on top of the nanotubes by electron beam lithography close to a cleaved edge of a substrate. (**B**) An etching process removes part of the substrate. (**C**) The part of the structure reaching out across the side edge is now free to move. (**D**) A view from the top shows that it is accessible by the TEM.

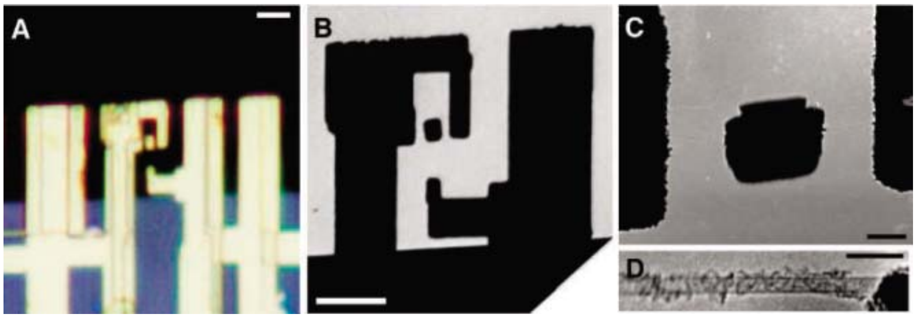

Fig. 2. A metal block suspended on one individual SWNT. (**A**) The metal block is visible in an optical microscope. (**B** and **C**) In the TEM, the suspended part rotates by up to ~70° as a result of charging by the electron beam with increasing magnification. (**D**) A high-resolution TEM image taken at the right end of the tube shows that this device is indeed built on one single molecule. Most of the amorphous carbon visible in (D) was deposited during the TEM analysis. Scale bars, 2 μm [(A) and (B)], 200 nm (C), 5 nm (D).

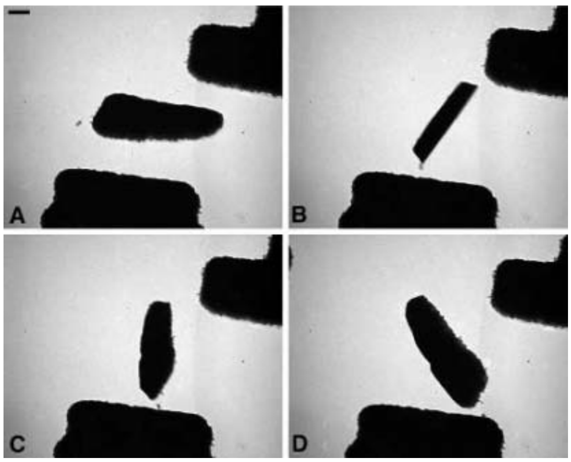

Fig. 3. A torsional pendulum built on a SWNT. (**A** to **D**) Images obtained at potentials of 0 V, 7.4 V, 9.7 V, and 22 V, respectively, between the support and the second electrode [visible in the upper left corner of (D)]. The sample is tilted by 30° for a slightly side-on view on the device. Scale bar, 100 nm. This device is also shown in movie S1.

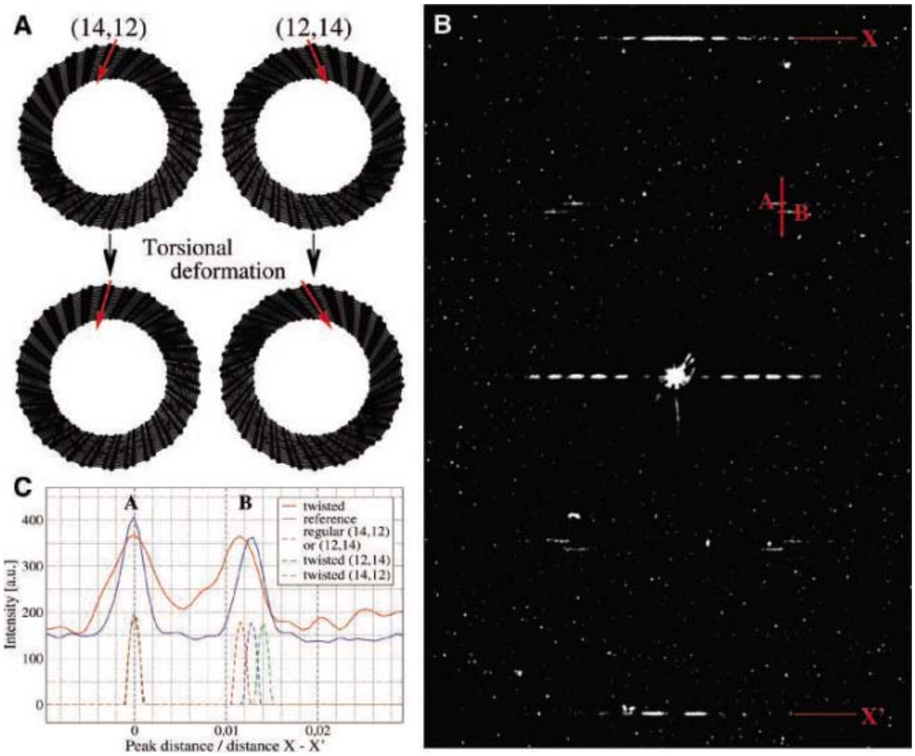

Fig. 4. (**A**) Effect of torsional deformation on the enantiomers of a (14,12) nanotube, viewed along the tube axis. The red arrows indicate a line along the graphene lattice, forming a right- or left-handed helix as it follows the cylindrical surface of the tube. The pitch of these helices is identical in the undeformed objects, but after a torsional deformation in a given direction, the pitch of the helices is different in the two enantiomers. The twisted (14,12) is no longer mirror-symmetric to the (12,14). (**B**) Diffraction pattern of a twisted nanotube. (**C**) Intensity profile along the A-B line in (B), as indicated in the pattern (solid red line) and for an undeformed (14,12) nanotube (solid blue line). Shown as dashed lines are simulated diffraction patterns of torsionally deformed nanotubes, twisted in the same direction and magnitude as in our device. The x axis is normalized to the distance between the layer lines denoted by X and X′ in (B). The angle between the tube axis and the graphene lattice can be precisely determined from the relative peak distances (*13*). All A peaks are plotted at $x = 0$. The clear difference in the peak distances, in agreement with the simulations, makes it possible to determine which enantiomer is present. Because the direction of the twist is known, we can determine that the tube structure (14,12), and not its mirror counterpart, is present in this device.

culated ones. The amplitude depends only on the diameter and length of the nanotube, not the geometry of the suspended object. Thermal vibrations up to 10° occur in devices with small-diameter (1 nm) nanotubes. The good agreement between observed and calculated values confirms that the modelization of the vibrational modes is valid and the nanotubes indeed exhibit the predicted mechanical properties.

Attaching a moving part with an individual SWNT is presumably one of the weakest couplings (i.e., one of the lowest spring constants) that can be realized. A pendulum on a SWNT 1.5 nm in diameter is supported by a total of only 40 C-C bonds (20 on each side), hence this approach is close to the limit (support by a single bond) that could be conceived for a mechanically attached object. If we consider the device as a quantum mechanical torsional harmonic oscillator, the angular uncertainty $\Delta\alpha$ of the quantum mechanical zero-point oscillation is of a magnitude $\Delta\alpha = \{[h/(2\pi)]/[(C \times J)^{1/2}]\}^{1/2}$ (where h is the Planck constant). For our device geometry, this angular uncertainty is 0.0003°, which corresponds to a position uncertainty of 2×10^{-12} m for the edge of the pendulum.

We note that a large position uncertainty requires not only a very small moving object (leading to a small mass and moment of inertia J) but also the weakest possible coupling (here in terms of the spring constant C). However, reaching a quantum-limited regime where $k_BT \approx hf$ would require microkelvin temperatures for our devices. To push the quantum limit to higher temperatures, it would be necessary to optimize the device geometry toward a higher resonance frequency (e.g., by reducing the size and mass of the moving object).

Figure 4B shows a diffraction pattern (*12*, *13*) obtained from a twisted SWNT on one side of a torsional pendulum. The tube section (300 nm in length) between the support and the rotated metal block is torsionally deformed, because one end of this tube section is turned by nearly 180°. By comparison with simulations, the nanotube can be identified as (14,12). However, there is a small deviation from the diffraction pattern of an undeformed (14,12) nanotube. In agreement with simulations for a torsionally deformed structure, this deviation shows that the tube is indeed homogeneously twisted (and not deformed, e.g., at a single defect).

Nanotubes (with the exception of the so-called armchair or zigzag types) are chiral molecules; that is, they are not identical with their mirror objects. Normally it is not possible to determine the handedness of a nanotube from a diffraction pattern. The diffraction pattern is the Fourier transform of the projected atomic potentials, and the (n,m) nanotube and its mirror counterpart [which we call (m,n)] have the same projected potential. In our case, however, the nanotube is torsionally deformed in a known direction. The two mirror-symmetric enantiomers, after deformation in a given direction, are no longer mirror-symmetric (Fig. 4A). Thus, it becomes possible to determine which type is present. From the deviation in the peak distances, we determine that in our device we have deformed the nanotube structure denoted as (14,12), and not its mirror counterpart.

Our SWNT pendulum can be reproducibly turned to any position between 0° and almost 180° with the use of a single electrostatic potential. Nanoelectromechanical systems applications include micromirrors or devices that require continuous tilting (with a precisely defined rotation axis) of any object attached to the nanotube or the pendulum. Because deflections and oscillations can be induced by extremely small forces, the pendulum can serve as a component in very sensitive nanoscale force sensors.

References and Notes

1. S. Iijima, *Nature* **354**, 56 (1991).
2. S. Iijima, T. Ichihashi, *Nature* **363**, 603 (1993).
3. P. A. Williams *et al.*, *Appl. Phys. Lett.* **82**, 805 (2003).
4. S. J. Papadakis *et al.*, *Phys. Rev. Lett.* **93**, 146101 (2004).
5. A. M. Fennimore *et al.*, *Nature* **424**, 408 (2003).
6. B. Bourlon, D. C. Glattli, C. Miko, L. Forro, A. Bachtold, *Nano Lett.* **4**, 709 (2004).
7. M. Paillet *et al.*, *J. Phys. Chem. B* **108**, 17112 (2004).
8. J. C. Meyer, D. Obergfell, S. Yang, S. Yang, S. Roth, *Appl. Phys. Lett.* **85**, 2911 (2004).
9. J. P. Lu, *Phys. Rev. Lett.* **79**, 1297 (1997).
10. D. W. Carr, S. Evoy, L. Sekaric, H. G. Craighead, J. M. Parpia, *Appl. Phys. Lett.* **75**, 920 (1999).
11. A. Pantano, D. M. Parks, M. C. Boyce, M. B. Nardelli, *J. Appl. Phys.* **96**, 6756 (2004).
12. J. C. Meyer, M. Paillet, G. S. Duesberg, S. Roth, *Ultramicroscopy*, in press (available at http://arxiv.org/cond-mat/0506356).
13. M. Gao *et al.*, *Appl. Phys. Lett.* **82**, 2703 (2003).
14. Supported by Studienstiftung des Deutschen Volkes (J.C.M.), Bundesministerium für Bildung und Forschung (BMBF) project INKONAMI, and EU projects CANAPE and CARDECOM.

Supporting Online Material
www.sciencemag.org/cgi/content/full/309/5740/1539/DC1
Movie S1

19 May 2005; accepted 27 July 2005
10.1126/science.1115067

Controlling the Kondo Effect of an Adsorbed Magnetic Ion Through Its Chemical Bonding

Aidi Zhao, Qunxiang Li, Lan Chen, Hongjun Xiang, Weihua Wang, Shuan Pan, Bing Wang, Xudong Xiao, Jinlong Yang,* J. G. Hou,* Qingshi Zhu

We report that the Kondo effect exerted by a magnetic ion depends on its chemical environment. A cobalt phthalocyanine molecule adsorbed on an Au(111) surface exhibited no Kondo effect. Cutting away eight hydrogen atoms from the molecule with voltage pulses from a scanning tunneling microscope tip allowed the four orbitals of this molecule to chemically bond to the gold substrate. The localized spin was recovered in this artificial molecular structure, and a clear Kondo resonance was observed near the Fermi surface. We attribute the high Kondo temperature (more than 200 kelvin) to the small on-site Coulomb repulsion and the large half-width of the hybridized d-level.

The Kondo effect arises from the coupling between localized spins and conduction electrons, and at sufficiently low temperatures, it can lead to change in the transport properties through scattering or resonance effects (*1*). The Kondo effect is often studied in systems where spins are permanently introduced into the sample through magnetic ions, and recently the Kondo effect has been controlled in quantum dot systems by changing their charging and hence the spin state of the dots (*2–13*).

We show here that the Kondo effect arising from magnetic ions on the surface of a nonmagnetic conductor can be controlled by changing their chemical environment. In particular, we show that Co ions, when adsorbed on a gold surface as cobalt phthalocyanine (CoPc), do not interact strongly with conduction electrons and exhibit no Kondo effect. However, after dehydrogenation of the ligand by voltage pulses from a scanning tunneling microscope (STM) tip, the Kondo effect is recovered.

Single CoPc molecules adsorbed on the terraces of an Au(111) surface exhibit a protruding four-lobed structure that is consistent with the molecular symmetry (Fig. 1, A and D) (*14*). Dehydrogenation of a CoPc molecule was realized with a local high-voltage pulse from the STM tip in a manner similar to the case of benzene on copper surfaces (*15*, *16*). We initially used a constant current mode with relatively low bias voltage and tunneling current (typically voltage $|V| < 2$ V and current $I < 0.5$ nA) to image isolated CoPc molecules. We then placed the STM tip directly over the edge of a lobe, temporarily suspended the feedback loop, and applied a positive high-voltage pulse (Fig. 1B). A typical current trace simultaneously measured during the application of a 3.6-V pulse on one of the four lobes of a CoPc molecule (Fig. 1C) shows two sudden drops in the current signal, indicating the sequential dissociation of the two H atoms from the benzene ring. We found the dehydrogenation threshold voltage to be in the range of 3.3 to 3.5 V, depending on the structure of the tip apex.

Topographic images of the dehydrogenation product show that the bright lobes disappear sequentially (Fig. 1, E to H). The apparent height of the molecular center (the Co ion) initially increases slightly (by ~0.15 Å), while the intact CoPc (Fig. 1D) is converted to a three-lobes-dehydrogenated CoPc (Fig. 1G). After the last step, when all four lobes were cut to obtain the final dehydrogenated CoPc (d-CoPc) molecule (Fig. 1H), a marked increase of ~0.8 Å in apparent height at the center indicated either a strong conformational change of the molecular structure or a redistribution of the local density of states of the molecule. Moreover, the d-CoPc molecule on the Au(111) surface was difficult to move with the STM tip, indicating a strong interaction between the molecule and substrate (figs. S1 and S2).

Typical differential conductance dI/dV spectra near the Fermi level (E_F) (Fig. 2A) were measured precisely at the center of an intact CoPc and a d-CoPc molecule with the same tip. The dI/dV spectra were obtained by sinusoidally modulating the bias voltage (4 mV in amplitude) with the first-harmonic current signal detected through a lock-in amplifier. For the intact CoPc molecule at 5 K, there is a broad resonance centered around 150 meV below E_F with a full-width at half-maximum of ~260 meV, which has been well characterized as the Co d_z^2 orbital-mediated tunneling (OMT) peak (*17–21*). This peak disappears completely in the dI/dV spectrum of d-CoPc. Instead, an intense resonance peak arises immediately below E_F (-6 ± 3 meV), with an asymmetric shape and a narrow width of ~50 meV. The amplitude of this peak decreased continuously as the dI/dV spectrum was measured at an increasing distance from the Co center. The peak eventually vanished at the edge of d-CoPc. This resonance was observed with nearly identical height and width in more than 50 d-CoPc molecules. After we elevated the temperature from 5 to 150 K, the

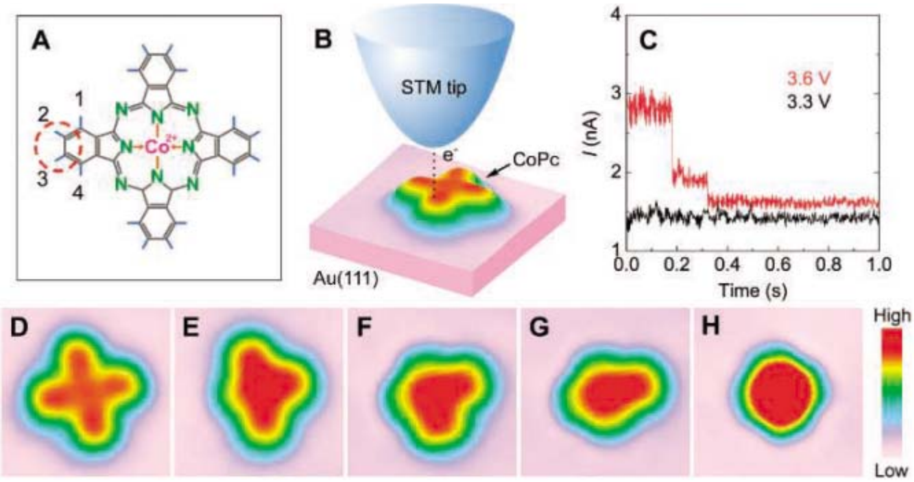

Fig. 1. STM tip–induced dehydrogenation of a single CoPc molecule. (**A**) Structural formula of the CoPc. Hydrogen atoms 2 and 3 of one lobe were dissociated in our experiments. (**B**) Diagram of the dehydrogenation induced by the STM current. (**C**) Current versus time during two different voltage pulses on the brink of one lobe. Black and red lines correspond to 3.3 V and 3.6 V, respectively. (**D** to **H**) STM images of a single CoPc molecule during each step of the dehydrogenation process, from (D) an intact CoPc to (H) d-CoPc. Image area, 25 Å by 25 Å. The color scale represents apparent heights, ranging from 0 Å (low) to 2.7 Å (high).

Hefei National Laboratory for Physical Sciences at Microscale, University of Science and Technology of China (USTC), Hefei, Anhui 230026, People's Republic of China.

*To whom correspondence should be addressed. E-mail: jghou@ustc.edu.cn (J.G.H.); jlyang@ustc.edu.cn (J.Y.)

resonance peak height for d-CoPc decreased by about a factor of 4 (Fig. 2A), but the height of the d_{z}^{2} OMT resonance peak for the intact CoPc varied by only ~15%.

The peak position, the line shape, and the temperature-dependent peak intensity all suggest that the resonance near E_F for d-CoPc molecules likely arises through the Kondo effect. The good fit of the peak at different temperatures in the Fano model (*22*), which has been successfully applied to surface Kondo systems to describe the quantum interference between a localized magnetic impurity and a continuum (*23*, *24*), further supports the notion of the Kondo effect (Fig. 2, C to E). The Fano model here can be described by the relation $\frac{dI}{dV} \propto R(\tilde{\varepsilon}) \propto \frac{(q+\tilde{\varepsilon})^2}{1+\tilde{\varepsilon}^2}$, where R is the transition rate, $\tilde{\varepsilon} = \frac{eV-\alpha}{\Gamma/2}$ represents the energy parameter as a function of the resonance energy and width, q is the interference parameter that controls the resonance shape, e is the elementary charge, α is the energy shift of the resonance center with respect to E_F, and $\Gamma = 2k_BT_K$ is the width of the resonance, where k_B is the Boltzmann constant and T_K the Kondo temperature.

At 5 K, fitting all the dI/dV spectra for different tips and d-CoPc molecules to the Fano model gives the average values $\alpha = -4 \pm 3$ meV, $\Gamma = 49 \pm 5$ meV, and $q = -9 \pm 4$ (Fig. 2C). The temperature-dependent resonance width also shows a good fit to an approximate formula [$\Gamma = 2\sqrt{(\pi k_B T)^2 + 2(k_B T_K)^2}$, where T is the measurement temperature] developed from Fermi liquid theory (*25*) and gives a T_K of ~208 K (Fig. 2D). The T_K value obtained here is much higher than any previously reported temperature for magnetic atoms (*23*, *24*, *26–29*) or clusters (*30*) on surfaces. For comparison, we also studied CuPc molecules, which have a nonmagnetic ion center, in contrast with CoPc. The CuPc molecules adsorbed on a Au(111) surface can also be dehydrogenated by the same method. The central part of an STM image of the CuPc molecule is a hole (Fig. 2B), but it is a protrusion in a fully dehydrogenated CuPc (d-CuPc), and there is no noticeable resonance appearing near E_F in the dI/dV spectra.

In order to understand qualitatively our experimental observations, we carried out first-principles studies on the structural and electronic properties of CoPc and d-CoPc molecules adsorbed on Au(111) (*31*). We used a slab model for the adsorption system, consisting of three atomic layers with 56 Au atoms each for the Au substrate and a vacuum seven atomic layers thick (Fig. 3, A and B). The distance between the molecule and the gold substrate is ~3.0 Å. The interaction between the molecule and substrate clearly changes the electronic structure and magnetic property of the CoPc molecule. In a free CoPc molecule, the Co atom has unpaired d electrons and the magnetic moment of the Co atom is 1.09 Bohr magnetons (μ_B). In the CoPc adsorption system, the magnet moment is completely quenched by the molecule-substrate interaction. The spin-polarized partial density of states (PDOS) of the Co atom in the CoPc adsorption system (Fig. 3C), and in a free CoPc molecule (Fig. 3D), revealed that the spin-down states were filled more than the spin-up states for the free CoPc molecule. However, the filling difference disappeared for the CoPc adsorbed on Au(111). The theoretical STM image of a CoPc molecule on Au(111) simulated with the Tersoff-Hamann formula (*32*) (Fig. 3E) reproduces the main feature of the experimental image (Fig. 1D).

Dehydrogenation induces a marked change of the molecular structure (Fig. 4, A and B), so that the d-CoPc molecule on Au(111) is no longer planar. The smallest separation between the end C atoms of the benzene ring and the gold substrate is ~1.9 Å, leading to a much stronger binding to the gold substrate. The central Co atom in the d-CoPc molecule shifts upward remarkably (the $d_{\text{Co-Au}}$ distance is ~3.8 Å for d-CoPc but 3.0 Å for CoPc).

More importantly, the magnetic moment is recovered for the d-CoPc adsorption system. The spin-polarized PDOS of the Co atom in the d-CoPc adsorption system (Fig. 4C) near E_F has an empty minority spin peak that comes from the magnetic quantum number $m = 0$ (d_{z}^{2}) states. This peak is consistent with our experimental spectra measured at different temperatures, in which an observable peak appears near 135 meV (fig. S3). The magnetic moment of the d-CoPc molecule is now 1.03 μ_B, very close to the value of a free CoPc molecule. The simulated STM image with a large bright spot for the d-CoPc adsorption system (Fig. 4D) agrees quite well with the observed image (Fig. 1H).

To understand the high Kondo temperature in the d-CoPc/Au(111) system, we compared its PDOS with that of a single Co adatom on an Au(111) surface (*33*) (Fig. 4E). The average spin splitting of the d-CoPc/Au(111) system is smaller than that of Co/Au(111). The on-site Coulomb repulsion U is proportional to this splitting, so the U of the d-CoPc/Au(111) system is smaller than that of the Co/Au(111)

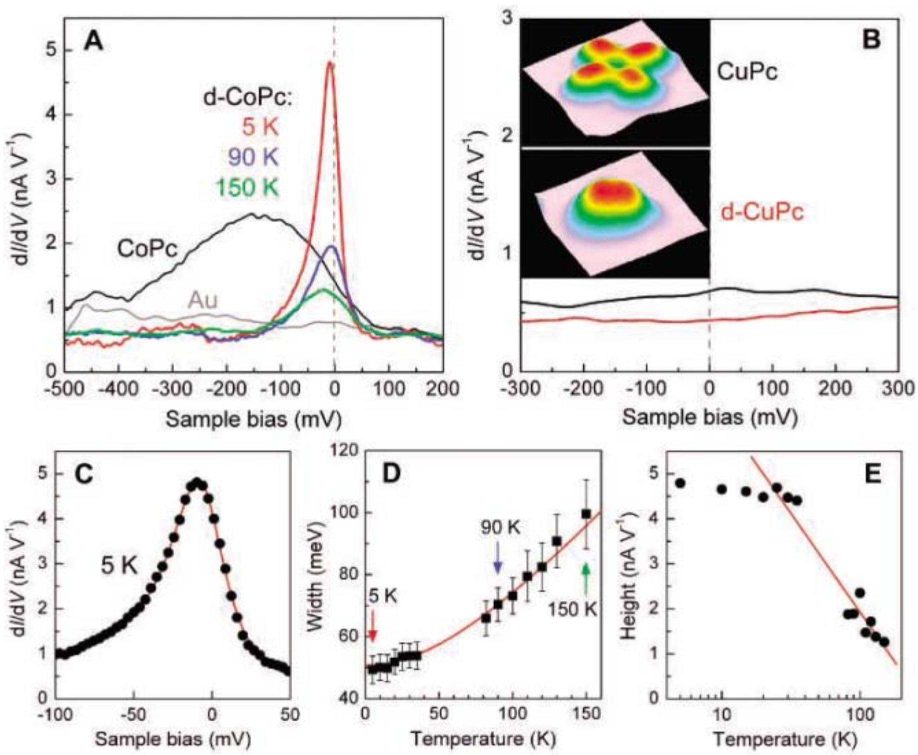

Fig. 2. Kondo resonance of d-CoPc at different temperatures. (**A**) Typical dI/dV spectra measured at the centers of a CoPc molecule at 5 K (black line), showing a d_{z}^{2} OTM resonance, and a d-CoPc molecule at 5, 90, and 150 K (colored lines), showing strong resonance near E_F. Spectra from bare Au(111) (gray line) is shown for comparison. (**B**) Topographic three-dimensional view of CuPc and d-CuPc, together with the corresponding dI/dV spectra measured at their centers. All spectra in (A) and (B) were taken with the same set point of V = 600 mV and I = 0.4 nA. (**C**) A fit (red line) to the resonance at 5 K in (A) according to the Fano model, with parameters of width ~ 44 meV, q ~ −6, and α ~ −5 meV. Black symbols indicate experimental results. (**D**) The resonance width against measured temperature. Error bars represent standard deviations. (**E**) The temperature-dependent height of the Kondo resonance peak, which decreases approximately logarithmically from 20 to 150 K and becomes nearly saturated at lower temperatures.

system. Moreover, the crystal field splitting of the Co d-level of the d-CoPc/Au(111) system is greater than that of the Co/Au(111) system (Fig. 4E), so the half-width Δ of the hybridized d-level of the d-CoPc/Au(111) system is greater than that of the Co/Au(111) system. According to theoretical models for the Kondo temperature T_K (*33*, *34*), T_K increases monotonically as U decreases or as Δ increases [$T_K = D_0 e^{-(\pi U/8\Delta M)}$, where D is a prefactor and M is the degeneracy number]. Previous experiments (*24*) reported that the T_K for Co/Au(111) is ~75 K; thus, our experimental finding of a higher T_K for the d-CoPc on Au(111) is in qualitative agreement with theory.

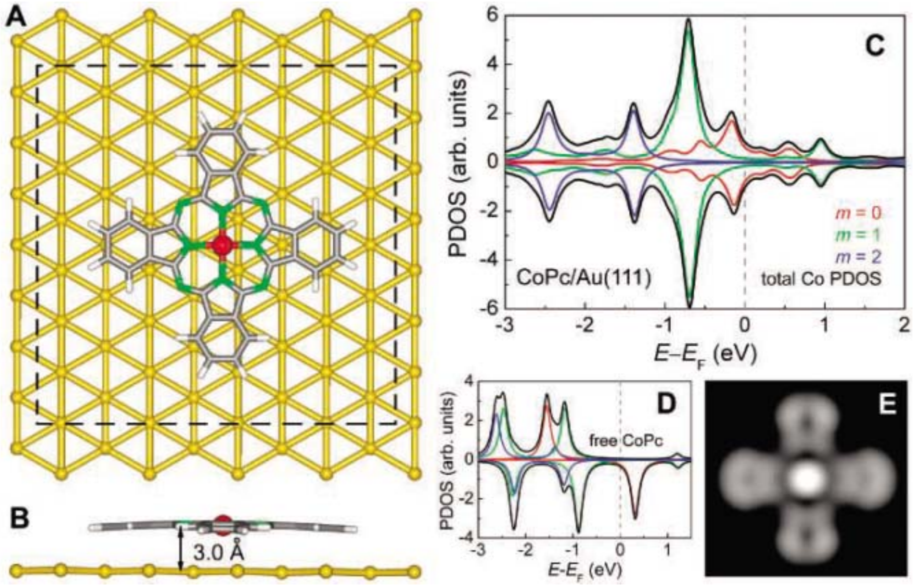

Fig. 3. The geometric and electronic structures of CoPc on Au(111). (**A** and **B**) Top and side views, respectively, of the optimized computational model for the CoPc/Au(111) adsorption system. The dashed line represents the unit cell, which contains 56 Au atoms per layer. (**C**) The PDOS of the Co atom in a CoPc molecule on a Au(111) surface. The black line is the total PDOS; the red, green, and blue lines represent its $m = 0$, $|m| = 1$, and $|m| = 2$ components, respectively. E, electron energy. (**D**) The PDOS of the Co atom in a free CoPc molecule is shown. (**E**) The simulated STM image of CoPc/Au(111). arb., arbitrary.

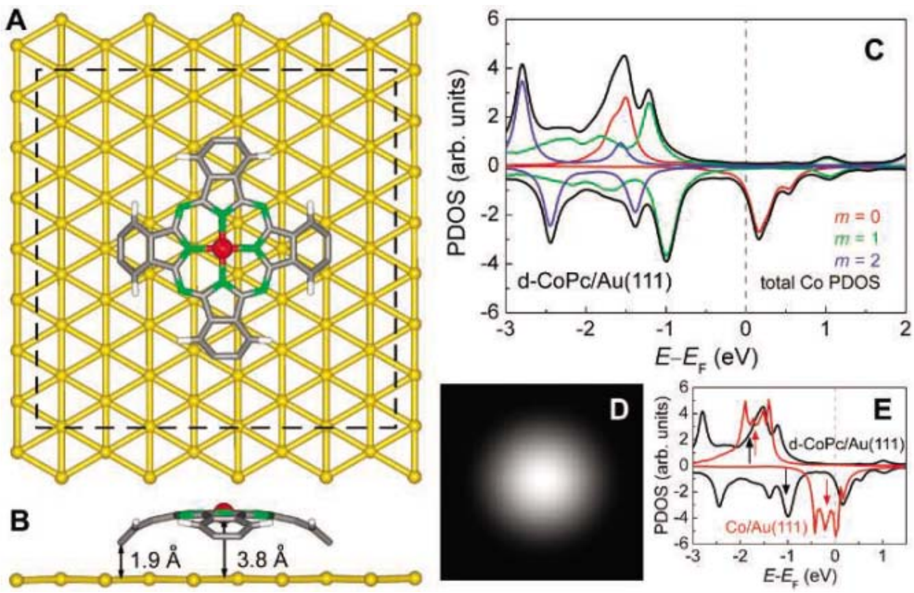

Fig. 4. The geometric and electronic structures of d-CoPc on Au(111). (**A** and **B**) Top and side views, respectively, of the optimized structure model for the d-CoPc/Au(111) adsorption system. The dashed line stands for the unit cell. (**C**) The PDOS of the Co atom in a d-CoPc molecule on a Au(111) surface. The black line is the total PDOS; the red, green, and blue lines represent its $m = 0$, $|m| = 1$, and $|m| = 2$ components, respectively. (**D**) The simulated STM image of d-CoPc/Au(111). (**E**) Comparison of the total PDOS of an isolated Co atom on a hollow site of a Au(111) surface with that of a d-CoPc molecule on Au(111). Arrows indicate the energy positions of the spin-polarized PDOS centroids of the Co atom.

References and Notes

1. A. C. Hewson, *The Kondo Problem to Heavy Fermions* (Cambridge Univ. Press, Cambridge, 1993).
2. D. Goldhaber-Gordon *et al.*, *Nature* **391**, 156 (1998).
3. S. M. Cronenwett, T. H. Oosterkamp, L. P. Kouwenhoven, *Science* **281**, 540 (1998).
4. S. Sasaki *et al.*, *Nature* **405**, 764 (2000).
5. W. G. van der Wiel *et al.*, *Science* **289**, 2105 (2000).
6. Y. Ji, M. Heiblum, D. Sprinzak, D. Mahalu, H. Shtrikman, *Science* **290**, 779 (2000).
7. J. Nygard, D. Henry Cobden, P. E. Lindelof, *Nature* **408**, 342 (2000).
8. H. Jeong, A. M. Chang, M. R. Melloch, *Science* **293**, 2221 (2001).
9. J. Park *et al.*, *Nature* **417**, 722 (2002).
10. W. Liang, M. P. Shores, M. Bockrath, J. R. Long, H. Park, *Nature* **417**, 725 (2002).
11. L. H. Yu, D. Natelson, *Nano Lett.* **4**, 79 (2004).
12. N. J. Craig *et al.*, *Science* **304**, 565 (2004).
13. A. N. Pasupathy *et al.*, *Science* **306**, 86 (2004).
14. Experiments were performed with a low-temperature STM (Omicron) operating under a base pressure of 3×10^{-11} torr. A piece of Au(111) film on mica of 180 nm in thickness was cleaned with ion sputtering and used as the substrate. CoPc molecules were thermally evaporated onto the Au(111) in ultra-high vacuum at 80 K with a typical coverage of ~0.02 monolayer. The sample was then promptly introduced into the STM cryostat, which was precooled down to 5 K.
15. L. J. Lauhon, W. Ho, *J. Phys. Chem. A* **104**, 2463 (2000).
16. T. Komeda, Y. Kim, Y. Fujita, Y. Sainoo, M. Kawai, *J. Chem. Phys.* **120**, 5347 (2004).
17. P. A. Reynolds, B. N. Figgis, *Inorg. Chem.* **30**, 2294 (1991).
18. A. Rosa, E. J. Baerends, *Inorg. Chem.* **33**, 584 (1994).
19. X. Lu, K. W. Hipps, X. D. Wang, U. Mazur, *J. Am. Chem. Soc.* **118**, 7197 (1996).
20. J. M. Assour, *J. Am. Chem. Soc.* **87**, 4701 (1965).
21. D. E. Barlow, L. Scudiero, K. W. Hipps, *Langmuir* **20**, 4413 (2004).
22. U. Fano, *Phys. Rev.* **124**, 1866 (1961).
23. J. Li, W.-D. Schneider, R. Berndt, B. Delley, *Phys. Rev. Lett.* **80**, 2893 (1998).
24. V. Madhavan, W. Chen, T. Jamneala, M. F. Crommie, N. S. Wingreen, *Science* **280**, 567 (1998).
25. K. Nagaoka, T. Jamneala, M. Grobis, M. F. Crommie, *Phys. Rev. Lett.* **88**, 77205 (2002).
26. T. Jamneala, V. Madhavan, W. Chen, M. F. Crommie, *Phys. Rev. B* **61**, 9990 (2000).
27. H. C. Manoharan, C. P. Lutz, D. M. Eigler, *Nature* **403**, 512 (2000).
28. P. Wahl *et al.*, *Phys. Rev. Lett.* **93**, 176603 (2004).
29. A. J. Heinrich, J. A. Gupta, C. P. Lutz, D. M. Eigler, *Science* **306**, 466 (2004).
30. T. W. Odom, J.-L. Huang, C. L. Cheung, C. M. Lieber, *Science* **290**, 1549 (2000).
31. Materials and methods are available as supporting material on *Science* Online.
32. J. Tersoff, D. R. Hamann, *Phys. Rev. B* **31**, 805 (1985).
33. O. Újsághy, J. Kroha, L. Szunyogh, A. Zawadowski, *Phys. Rev. Lett.* **85**, 2557 (2000).
34. H. Q. Lin, J. E. Hirsch, *Phys. Rev. B* **37**, 1864 (1988).

35. We thank Q. W. Shi, K. Wang, and T. Huang of USTC for helpful discussions and experimental support. Partially supported by the Ministry of Science and Technology of China (grant nos. G1999075305, G2001CB3095, and G2003AA302660), by the National Natural Science Foundation of China, by the USTC–Hewlett-Packard High Performance Computing Project, and by the Supercomputing Center of the Chinese Academy of Sciences.

Supporting Online Material
www.sciencemag.org/cgi/content/full/309/5740/1542/DC1
Materials and Methods
Figs. S1 to S3
References and Notes

12 April 2005; accepted 26 July 2005
10.1126/science.1113449

The Ultrasmoothness of Diamond-like Carbon Surfaces

Michael Moseler,[1,2*] Peter Gumbsch,[1,3] Cinzia Casiraghi,[4] Andrea C. Ferrari,[4] John Robertson[4]

The ultrasmoothness of diamond-like carbon coatings is explained by an atomistic/continuum multiscale model. At the atomic scale, carbon ion impacts induce downhill currents in the top layer of a growing film. At the continuum scale, these currents cause a rapid smoothing of initially rough substrates by erosion of hills into neighboring hollows. The predicted surface evolution is in excellent agreement with atomic force microscopy measurements. This mechanism is general, as shown by similar simulations for amorphous silicon. It explains the recently reported smoothing of multilayers and amorphous transition metal oxide films and underlines the general importance of impact-induced downhill currents for ion deposition, polishing, and nanopattering.

Diamond-like carbon (DLC) is an amorphous carbon with a high fraction of sp^3 bonds (*1*). Hydrogen-free DLCs with the highest density and sp^3 content are called tetrahedral amorphous carbons (ta-C) (*1*). Diamond-like carbon films are widely used as protective coatings—for instance, on magnetic and optical storage disks (*2*), optical windows (*3*), bearings (*4*), and biomedical (*5*) and microelectromechanical devices (*6*). The combination of diamond-like properties (*7*) and extreme smoothness (*8–10*) is the key factor underlying the technological importance of these films. The research on ultrathin DLCs with well-defined surface properties is driven by their use on ultrahigh storage density magnetic and optical devices (*2*, *10–14*). Despite the broad interest in the growth of DLC films, a complete understanding of the evolution of their surface profile is still lacking.

A variety of amorphous carbon films, with changing composition, structure, mechanical, and optical properties, can be produced by different deposition techniques (*1*). Subsurface implantation [subplantation (*15*)] of energetic carbon atoms can produce amorphous carbon networks with a high fraction of sp^3 sites. Filtered cathodic vacuum arc (FCVA), mass-selected ion beam deposition, and magnetron sputtering combined with energetic ion plating provide enough energy to grow ta-C films (*1*, *9*, *15*, *16*). FCVA and ion-assisted sputtering are also successfully used to produce many other coating materials, such as metals, metal oxides, nitrides, silica, and amorphous silicon [e.g., (*17*)].

[1]Fraunhofer Institute of Mechanics of Materials, Wöhlerstrasse 11, 79108 Freiburg, Germany. [2]Freiburg Materials Research Center, Stefan-Meier-Strasse 21, 79104 Freiburg, Germany. [3]Institute for Reliability of Systems and Components, IZBS, University of Karlsruhe, Kaiserstrasse 12, 76131 Karlsruhe, Germany. [4]Engineering Department, Cambridge University, Cambridge CB2 1PZ, UK.

*To whom correspondence should be addressed. E-mail: mos@iwm.fhg.de

In these deposition methods, the film growth is driven by a random hail of atomic ions. Without additional lateral relaxation processes, this would inevitably cause a rapid increase of surface roughness as a function of film thickness (*18*). Atomic force microscopy (AFM) measurements of ta-C and amorphous metal oxide coatings reveal ultrasmooth surface profiles with a root mean square (rms) roughness (R) on the order of 0.1 nm (*9*, *10*, *17*). Furthermore, the rapid smoothing of initially rough substrates by carbon deposition has been reported (*9*, *10*, *19*). Both observations indicate the presence of a very efficient lateral transport process of yet unknown origin.

An empirical local melting model (*10*) explained the smoothness of ta-C in terms of impact-induced thermal spikes accompanied by reduction of local interface curvature. However, the continuum picture of a local liquid needs an atomistic justification. The size and duration of a thermal spike in ta-C can be estimated to be on the order of 1 nm and 1 ps, respectively (*20*). Both seem too small for the establishment of a liquid-like behavior.

We present a quantitative, nonempirical, atomistic/continuum multiscale model describing the evolution of DLC surface profiles and the origin of their intrinsic ultrasmoothness. Our quantum and classical molecular dynamics (MD) simulations indicate that in ion beam deposition of DLCs there is a tendency toward subnanometer crater formation in the immediate neighborhood of the impact point, which would lead to an increase of local interface curvature. However, an efficient damping of these surface fluctuations is achieved through impact-induced downhill currents eroding hills on the film surface. A linear relation between these currents and surface slope is found in our atomistic simulations. We demonstrate that this, in combination with the particle continuity equation, results in a stochastic continuum model for the surface evolution that extends the atomistic description to mesoscopic length and time scales. This model, once fed with MD data, provides a quantitative description of several experimentally observed properties of growing DLC films, such as the evolution of the power spectral density (PSD), the smoothing of initially rough substrates (*9*, *10*, *19*), and the decrease and saturation of roughness with increasing impact energy (*8*, *19*).

This smoothing mechanism is general and not restricted only to DLCs. Tailoring of roughness and surface chemistry has become increasingly important for nanoscience and nanobiology applications. Analogous simulations of ion-beam–treated amorphous silicon show that smoothing by impact-induced downhill currents can work for any amorphous material.

The quantum MD of energetic carbon atoms impinging on an amorphous carbon substrate is simulated with density functional–based tight binding (TB) (*21*). In addition, the classical (type I) hydrocarbon bond-order potential of Brenner (*22*) with a modified cutoff function (*23*) is used to study larger systems and time scales. The initial substrate (a 2.35 nm by 2.35 nm by 2.35 nm block) is produced by melting 2000 carbon atoms at 10,000 K and by subsequent cooling to room temperature, resulting in a ta-C sample with 3.1 g/cm^3 density and 75% sp^3 fraction, in good agreement with experiments (*7*, *10*). For the TB calculations a 2.35 nm by 2.35 nm by 1.2 nm slice is generated by removing the top 1000 atoms. The full system is studied with the Brenner potential.

Periodic boundary conditions in the lateral directions are applied. The atoms in a 0.2-nm-thick bottom layer are fixed. Before each impact, the system is equilibrated to room temperature for several picoseconds using a Langevin thermostat for all mobile atoms. After that, a carbon atom with a predetermined initial velocity normal to the surface is placed in a random position 2 Å above the highest atom of the slab. The collision of this atom is then studied for 1 ps. At this stage, only atoms in a 0.3-nm layer above the fixed atom layer are thermalized to room temperature.

We first discuss the characteristics of a single impact. No evidence of a local melting is found when the quantum MD trajectories are inspected. A characteristic subplantation event is shown in the insets of Fig. 1. A carbon atom (black sphere) impinges with 100-eV kinetic energy on a ta-C film. The implantation of the new atom and the response of a few surrounding atoms last less than 1 ps and produce a small crater in the film.

To calculate the impact-induced average change of the local surface profile, we study the consecutive impact of 1000 atoms by classical MD. For each impact, the substrate is decomposed into a set of Δr = 0.025-nm

cylindrical shells centered at the impact point. The impact changes the number of carbon atoms in the shells from $n(r)$ to $n(r) + \Delta n(r)$, where r denotes the shell radius. The impact-induced change of the surface profile can be estimated by $\Delta h(r) = \Delta n(r)\Omega/(2\pi r\Delta r)$, where $\Omega = 0.0065$ nm^3 is the average atomic volume in the film. The average $\Delta h(r)$, shown in Fig. 1, reveals a trend toward crater formation even for impact energies as low as 30 eV. Recent classical MD simulations with an environment-dependent interaction potential (*20*) produce essentially the same result. These findings indicate a roughening of the surface on length scales below 1 nm. In contrast, a local surface melting model would predict a complete smoothing of the neighborhood around the impact point.

To clarify the microscopic mechanism underlying the ultrasmoothness of ta-C films, we use classical MD to study the ion-beam treatment of a film with an initial corrugation. Starting from the configuration shown in the lower left inset of Fig. 2, the evolution of an undulated surface profile during the impact of 4000 C atoms is calculated. To compare the results with experimental measurements, we perform two simulations with two different kinetic energies (30 and 100 eV). A rapid smoothing of the initial surface is observed for both energies, as reflected in the continuous decay of the initial sinusoidal profile during film growth (the upper inset in Fig. 2 shows the final configuration for the 100-eV simulation).

After each impact, the surface profile is calculated, decomposing the film into a two-dimensional (2D) array of vertical columns with lateral positions (x_1, x_2) and 0.59 nm by 0.59 nm cross sections. The height $h(x_1, x_2)$ of the columns is determined by their highest atom. The Fourier amplitude $h_{\mathbf{q}}$ (Fig. 2) of the initial sine profile decays with increasing film thickness s, paralleled by a strong decrease of the rms roughness $R(s)$. To compare the results with experimental AFM measurements, we obtain $R(s)$ by a numerical scan of the surface profile h with a 10-nm-radius sphere. The initial roughness $R(0) = 0.15$ nm of both systems drops to $R(1.5 \text{ nm}) = 0.06$ nm for 100 eV and $R(1.5 \text{ nm}) = 0.09$ nm for 30 eV, respectively.

We now consider the microscopic mechanism for the rapid smoothing of ta-C. We previously reported the smoothing of initially rough substrates by the energetic deposition of metal cluster ions (*24*, *25*). In this case, a multiscale model based on an impact-induced plastic downhill deformation of the substrate, combined with the continuity equation, was suggested to explain the observed smoothing. Here we demonstrate that even the bombardment with atomic ions induces a downhill current in a growing film. This indicates that a universal model can be derived to explain any ion-beam deposited ultrasmooth amorphous film. The surface profile of a growing DLC film is represented by a single valued function $h(x_1,x_2,t)$ of the lateral coordinates x_1, x_2. We assume that slight spatial variations in the mass density of the material below $h(\mathbf{x}, t)$ can be neglected. The equation of motion for h follows from this assumption and from the continuity Eq. (*18*):

$$\partial h(\mathbf{x},t)/\partial t = -\Omega\nabla\cdot\mathbf{j}(\mathbf{x},t) + \eta(\mathbf{x},t) \quad (1)$$

where $\mathbf{j}(\mathbf{x}, t)$ denotes a lateral particle current. The height source $\eta(\mathbf{x}, t)$ represents a particle rain with an average precipitation of r atoms per unit time on a unit area. Stochastic inhomogeneities in the distribution of particle impact points are taken into account by assuming η to be a Gaussian noise with vanishing mean and a covariance $\langle\eta(\mathbf{x},t)\eta(\mathbf{x}',t')\rangle = r\Omega^2\delta(\mathbf{x} - \mathbf{x}')\delta(t - t')$ (*18*).

Owing to the local nature of an energetic particle impact, the current $\mathbf{j}(\mathbf{x}, \mathbf{t})$ is a functional of the local shape of $h(\mathbf{x}, t)$. The lateral correlation length of the ultrasmooth profiles exceeds the size of the impinging atoms by several orders of magnitude. In this case, the current should be a simple function of the local slope, $\nabla h(\mathbf{x}, t)$. We show in the following that atomistic simulations of C deposition on a tilted DLC film provide sufficient information to determine the current-slope relationship $\mathbf{j}(\nabla h)$. Consider the inset of Fig. 3A. Here, an energetic particle impinges on an inclined surface $h = x_1 \tan\alpha$. The N atoms in the system are displaced laterally by $(d_1^{(I)}, d_2^{(I)})$ $(I = 1\ldots N)$. The strength of the related lateral current $\mathbf{j}$ is given by $|\mathbf{j}| = r\,\langle\sum_I d_1^{(I)}\rangle$. Therefore, the sum of the atomic displacements $\delta = \langle\sum_I d_1^{(I)}\rangle$ represents a simple link between the atomistic simulations and the continuum description (*24*, *26*).

The existence of an impact-driven downhill current during DLC deposition is verified by extensive quantum MD simulations. From five trajectories, each consisting of 200 consecutive 30-eV impacts on a DLC substrate with tilt angle $\alpha = 20°$, a significantly nonzero sum of atomic displacements is extracted ($\delta = 0.26 \pm 0.06$ nm, square data point in Fig. 3A). This is

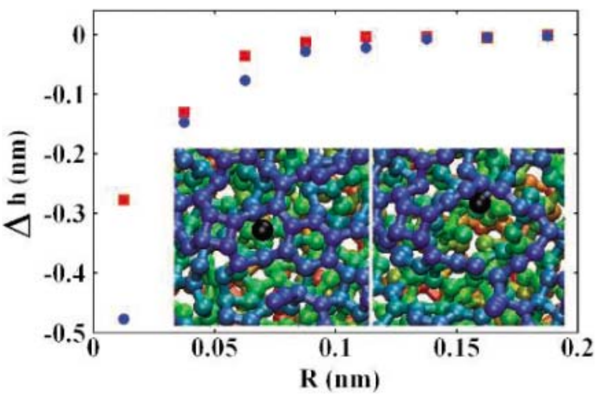

Fig. 1. Impact-induced height variation, Δh, as a function of the distance r from the impact point. The impacts of 1000 carbon atoms are simulated with classical MD for two impact energies: 30 eV (red squares) and 100 eV (blue dots). The average shape of $\Delta h(r)$ indicates a trend toward crater formation. **(Insets)** Quantum MD of a single 100-eV carbon atom (black sphere) impinging with initial velocity perpendicular to the plane. **(Left)** Snapshot of the initial configuration. **(Right)** Formation of a small crater after 1 ps. The substrate atoms are color coded according to their initial position in the film. The relative movement of the black sphere in the right inset with respect to the left inset is a consequence of multiple collisions following impact.

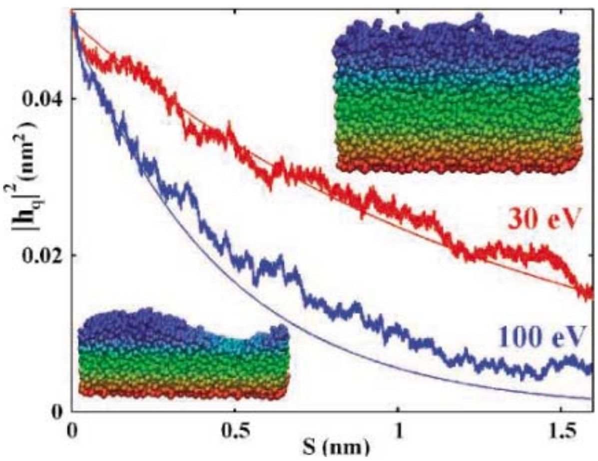

Fig. 2. Ion-beam–induced decay of a sine-shaped ta-C surface. The MD substrate of Fig. 1 is tripled in one lateral direction, resulting in a 7.05 nm by 2.35 nm by 2.35 nm block. A surface profile $h(\mathbf{x}, 0) = a \sin(qx_1)$ with $a = 0.5$ nm and $q = 2\pi/7.05$ nm is produced by removing part of the atoms. The graph plots the power spectral strength of the relevant Fourier mode as a function of film thickness s for two ion energies: 30 eV (red noisy curve) and 100 eV (blue noisy curve). The smooth curves represent the predictions of the Edwards-Wilkinson equation (Eq. 2). The values for ν in Eq. 3 are obtained from the independent MD simulations of Fig. 3. **(Insets)** Snapshots of the initial system (lower left) and after the impact of 4000 C atoms with 100-eV kinetic energy (upper right). The color coding represents the height of the atoms. Note the complete smoothing of the initial sine-shaped surface.

validated by a comparable classical MD calculation, with 3000 consecutive impacts, giving a similar outcome, with only slightly reduced displacements (red dot below the TB result in Fig. 3A).

In the experimental ta-C films, the tetrahedrally coordinated bulk layer is covered by a 1- to 2-nm layer with predominant sp^2 bonding (*7*, *15*, *27*). This is correctly reproduced in our simulations. Thus, it is quite instructive to decompose δ into contributions from sp^2- and sp^3-bound atoms. Notably, we find that roughly 90% of the displacement sum consists of sp^2 atoms, showing that the downhill currents flow in the 1- to 2-nm top layer of the film.

A linear relation between $\delta(\alpha, E)$ and the tilt angle α is observed for various impact energies E (Fig. 3A), suggesting the constitutive equation $\mathbf{j}(\mathbf{x}, t) = -r\,\nu(E)\nabla h(\mathbf{x}, t)$. The proportionality constant $\nu(E) = \delta(\alpha, E)/\tan\alpha$ measures the strength of the impact-induced smoothing. This has a peculiar energy dependence (Fig. 3B), with a linear increase for energies below 120 eV and saturation for larger energies. The saturation is likely caused by the increase of subplantation depth for higher energies (*8*, *27*, *28*). In this regime, part of the impact energy is released in the bulk and is no more available for surface currents.

The linear equation for $\mathbf{j}$ can be used to close Eq. 1, resulting in the well-known Edwards-Wilkinson (EW) stochastic differential Eq. (*29*):

$$\partial h(\mathbf{x}, s)/\partial s = \nu\nabla^2 h(\mathbf{x}, s) + \eta(\mathbf{x}, s) \qquad (2)$$

where t in Eq. 1 is replaced by the average film height $s = r\Omega t$. The PSD of EW surfaces can be calculated analytically (*24*):

$$\langle|h_{\mathbf{k}}(s)|^2\rangle = e^{-2\nu k^2 s}\langle|h_{\mathbf{k}}(0)|^2\rangle + \Omega(1-e^{-2\nu k^2 s})/(2\nu L_1 L_2 k^2) \qquad (3)$$

where $h_{\mathbf{k}}(s)$ is the Fourier transform of $h(\mathbf{x}, s)$ and $L_1 \times L_2$ are the lateral dimensions of the surface.

The validity of continuum theories should be restricted to the long-wavelength limit, i.e., to modes $h_{\mathbf{k}}$ with $|\mathbf{k}|$ not exceeding some critical value k_0. Thus, it is rather surprising that Eq. 3 accurately reproduces the evolution of our initially rough $L_1 = 7.05$ nm $\times$ $L_2 = 2.35$ nm MD model system. The relevant Fourier mode $\mathbf{k} = (2\pi/L_1, 0)$ (smooth curves in Fig. 2) has essentially the same decay as the amplitudes from our atomistic model (noisy curves in Fig. 2). This demonstrates that even nanoscale surface fluctuations on DLC films can be successfully described by the EW continuum theory. Thermally activated lateral transport processes (*30*), such as surface or bulk diffusion, as well as evaporation/condensation, are negligible for DLC deposition at room temperature.

To validate the multiscale model, we carefully analyze extensive AFM data on ta-C films deposited by FCVA with an incident ion energy of 20 to 40 eV on a ~0.2-nm rough Si substrate (*10*). In the following we focus on Eq. 3, which predicts how a PSD $\langle|h_{\mathbf{k}}(s)|^2\rangle$ evolves starting from an initial PSD $\langle|h_{\mathbf{k}}(0)|^2\rangle$. Two ta-C films, 4 and 66 nm thick, were extensively measured to obtain statistically stable estimates for the initial PSD $\langle|h_{\mathbf{k}}(s = 4\ nm)|^2\rangle$ and the final PSD $\langle|h_{\mathbf{k}}(s = 66\ nm)|^2\rangle$. These are derived by averaging eight independent AFM measurements in each of the two samples (green and red curves in Fig. 4). A very satisfactory agreement between the experimental $\langle|h_{\mathbf{k}}(s = 66\ nm)|^2\rangle$ and the corresponding theoretical PSD for 30-eV impact energy is observed (compare the red and blue lines in Fig. 4; both agree within the statistical errors), thus validating our multiscale model.

This model also provides a simple explanation of the previously observed rapid decay of an initial substrate roughness (*10*). Indeed, the first term in Eq. 3 is responsible for the exponential decay of the initial surface roughness, because the power spectrum, Eq. 3, determines the roughness via $R(s)^2 = \sum_{\mathbf{k}}\langle|h_{\mathbf{k}}(s)|^2\rangle$ (*24*).

Finally, the energy dependence of the roughness for a fixed film thickness is considered. Experimentally, for $E < 100$ eV, a strong decrease of R with increasing ion energy was reported, followed by a leveling off for $E > 100$ eV (*8*, *9*, *19*) (see, e.g., the gray squares in the inset of Fig. 4). We thus calculate the energy dependence of R in the framework of our multiscale model. We get the same trend as in the experiments (Fig. 4, inset). This suggests that the saturation of R for higher impact energies follows directly from the leveling off of $\nu(E)$ for $E > 120$ eV as seen in our atomistic simulations.

Ultrasmoothness has been reported also for amorphous transition metal oxide films grown by FCVA (*17*), as well as for amorphous silicon after low-energy Ar^+ bombardment (*31*). We thus extend our simulations to amorphous silicon by using the Tersoff interatomic potential (*32*). For various tilt angles, the MD trajectories of 1000 Si atoms impinging with 100 eV on tilted amorphous silicon substrates are calculated. As for DLC, we find a linear current-slope relationship and a comparable smoothing strength $\nu = 2.7 \pm 0.2$ nm. This indicates that the concept of ion-beam–induced

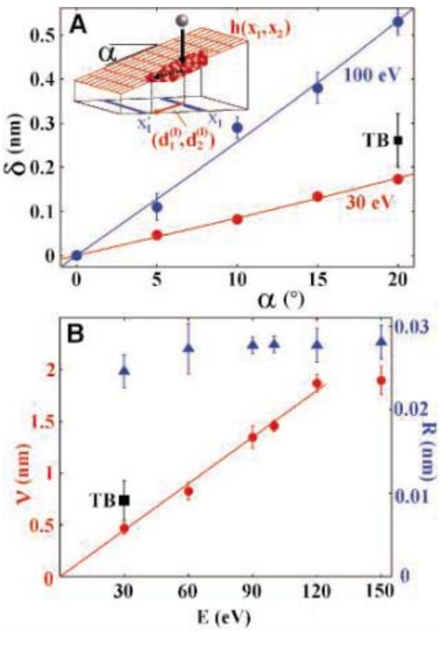

Fig. 3. Downhill current on a tilted region of the growing film. (**A**) The displacement sum $\delta(\alpha, E)$ for two different impact energies E (30 and 100 eV) depends linearly on the tilt angle α of the surface. The dots are from classical MD and the square, labeled TB, is derived from quantum MD calculations. The inset clarifies the definition of δ as given in the text. (**B**) Downhill strength $\nu(E)$ (dots, classical MD; square labeled TB, quantum MD) and steady-state nanoscale rms roughness R (triangles) as a function of impact energy. To compare with experimental AFM data, we derive R by numerically mapping the 2.35 nm by 2.35 nm surface with a 10-nm-radius tip. The slightly reduced roughness of the 30-eV sample correlates with the smaller crater size observed in Fig. 1.

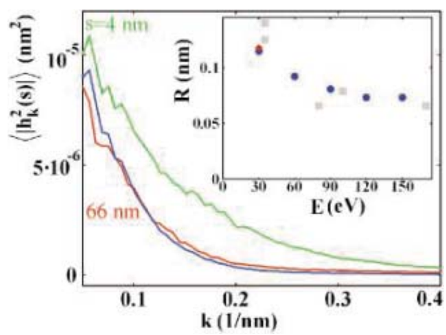

Fig. 4. Evolution of the experimental PSD compared to the prediction of our multiscale model. The green and red lines represent PSDs derived from eight independent 1-μm^2 AFM scans of 4- and 66-nm-thick ta-C films, respectively. The blue line is the multiscale prediction (Eq. 3) for the 66-nm film. The green curve has been used as the initial PSD. The overlapping error intervals of the red and blue curves are omitted for the sake of clarity. A downhill strength $\nu = 0.5$ nm is used, corresponding to ~30-eV impact energy in the MD simulations. (**Inset**) The rms roughness as a function of ion energy for a s = 66-nm-thick ta-C film. Blue dots represent the prediction based on our multiscale model. R is decomposed into a continuum and an atomistic contribution $R(s)^2 = \sum_{k<k_0}\langle|h_{\mathbf{k}}(s)|^2\rangle + \sum_{k>k_0}\langle|h_{\mathbf{k}}(s)|^2\rangle$ (*24*) with a cutoff $k_0 = 2\pi/2.35$ nm. The first sum is evaluated with the theoretical PSD given by Eq. 3 using $\nu(E)$ from our MD simulations. The second sum is approximated by the average steady-state roughness $R = 0.027$ nm of the 2.35 nm by 2.35 nm MD system as displayed in Fig. 3B. The red diamond represents the experimental roughness of our 66-nm-thick film, and the gray squares are comparable measurements from (*19*).

downhill currents is quite general and not restricted only to DLCs. However, it is important to note that the existence of downhill currents is a necessary but not sufficient condition for achieving ultrasmoothness. Amorphicity is another important prerequisite. Indeed, a transition to nanocrystallinity at higher temperatures or at higher impact energies is accompanied by considerable surface roughening also in the case of DLC films (*8*, *9*, *17*).

In summary, the multiscale theory presented here explains the origin of the ultrasmoothness of DLC coatings. Atomistic impact-induced downhill currents are responsible for the rapid erosion of asperities. Our detailed theoretical predictions are in excellent agreement with experiments. Our model is not restricted to ta-Cs. It can also be applied to explain the smoothness of other amorphous coatings deposited at high ion energy, the ion polishing of smooth surfaces, the chemical vapor deposition of hydrogenated tetrahedral amorphous carbon films, and the surface evolution of DLC films overgrown on structured substrates.

References and Notes

1. J. Robertson, *Mat. Sci. Eng. R* **37**, 129 (2002).
2. A. C. Ferrari, *Surf. Coat. Technol.* **180**, 190 (2004).
3. M. Allon-Alaluf, J. Appelbaum, M. Maharizi, A. Seidman, N. Croitoru, *Thin Solid Films* **303**, 273 (1997).
4. J. Brand, G. Beckmann, B. Blug, G. Konrath, T. Hollstein, *Ind. Lubr. Tribol.* **54**, 291 (2002).
5. R. Hauert, *Diamond Relat. Mater.* **12**, 583 (2003).
6. J. P. Sullivan, T. A. Friedmann, K. Hjort, *MRS Bull.* **26**, 309 (2001).
7. A. C. Ferrari *et al.*, *Phys. Rev. B* **62**, 11089 (2000).
8. Y. Lifshitz, G. D. Lempert, E. Grossman, *Phys. Rev. Lett.* **72**, 2753 (1994).
9. X. Shi, L. Cheah, J. R. Shi, S. Zun, B. K. Tay, *J. Phys. C* **11**, 185 (1999).
10. C. Casiraghi *et al.*, *Phys. Rev. Lett.* **91**, 226104 (2003).
11. J. Robertson, *Thin Solid Films* **383**, 81 (2001).
12. P. R. Goglia, J. Berkowitz, J. Hoehn, A. Xidis, L. Stover, *Diamond Relat. Mater.* **10**, 271 (2001).
13. D. Li, M. U. Guruz, C. S. Bhatia, *Appl. Phys. Lett.* **81**, 81 (2002).
14. T. Yamamoto, Y. Kasamatsu, H. Hyodo, *Fujitsu Sci. Tech. J.* **37**, 201 (2001).
15. Y. Lifshitz, S. R. Kasi, J. W. Rabalais, *Phys. Rev. Lett.* **62**, 1290 (1989).
16. J. Schwan *et al.*, *J. Appl. Phys.* **79**, 1416 (1996).
17. Z. W. Zhao, B. K. Tay, L. Huang, G. Q. Yu, *J. Phys. D Appl. Phys.* **37**, 1701 (2004).
18. A. L. Barabasi, H. E. Stanley, Eds., *Fractal Concepts in Surface Growth* (Cambridge Univ. Press, Cambridge, 1995).
19. X. L. Peng, Z. H. Barber, T. W. Clyne, *Surf. Coat. Technol.* **138**, 23 (2001).
20. G. Pearce, N. Marks, D. McKenzie, M. Bilek, *Diamond Relat. Mater.* **14**, 921 (2005).
21. T. Frauenheim *et al.*, *J. Phys. Condens. Matter* **14**, 3015 (2002).
22. D. W. Brenner, *Phys. Rev. B* **42**, 8458 (1990).
23. H. U. Jäger, K. Albe, *J. Appl. Phys.* **88**, 1129 (2000).
24. M. Moseler, O. Rattunde, J. Nordiek, H. Haberland, *Nucl. Instrum. Methods B* **164-165**, 522 (2000).
25. O. Rattunde *et al.*, *J. Appl. Phys.* **90**, 3226 (2001).
26. The impact of a series of atoms with random impact points $\mathbf{u} = (u_1, u_2)$ on the surface $h = x_1 \tan \alpha$ results in an average transport of
$$\delta = \int d^2u \int_{-\infty}^{0} dx_1 \int_{0}^{\infty} dx_1' \langle t(x_1 - u_1, x_1' - u_1) - t(x_1' - u_1, x_1 - u_1) \rangle = \left\langle \sum_{l} d_1^{(l)} \right\rangle$$
atoms per impact across the x_2 axis. Here, $\langle\ \rangle$ indicates the average over many impacts and $t(x_1, x_1') = \sum_{l=1}^{N} \delta(x_1^{(l)} - x_1)\delta(x_1^{(l)} + d_1^{(l)} - x_1')$ measures the number of atoms displaced from x_1 to x_1' upon the impact of an atom onto the origin $\mathbf{u} = 0$. The initial lateral coordinates of the atoms in the system are denoted by $\mathbf{x}^{(l)}$.
27. C. A. Davis, G. A. J. Amaratunga, K. M. Knowles, *Phys. Rev. Lett.* **80**, 3280 (1998).
28. S. Uhlmann, Th. Frauenheim, Y. Lifshitz, *Phys. Rev. Lett.* **81**, 641 (1998).
29. S. F. Edwards, D. R. Wilkinson, *Proc. R. Soc. London A* **381**, 17 (1982).
30. W. W. Mullins, *J. Appl. Phys.* **30**, 77 (1959).
31. E. Spiller *et al.*, *Appl. Opt.* **42**, 4049 (2003).
32. J. Tersoff, *Phys. Rev. B* **39**, 5566 (1988).

33. We thank B. Huber and P. Koskinen for technical assistance, M. Mrovec for fruitful discussions, and D. P. Chu for providing AFM facilities at the Epson Research Laboratory, Cambridge. This research is supported by the Fraunhofer MAVO for Multiscale Materials Modelling (MMM) and by the FOSTOMA project of the Wirtschaftsministerium Baden-Württemberg. Simulations were performed on the CEMI cluster of the Fraunhofer institutes EMI, ISE, and IWM. Funding from European Union project FAMOUS is acknowledged. A.C.F. acknowledges funding from The Royal Society.

9 May 2005; accepted 21 July 2005
10.1126/science.1114577

The Effect of Diurnal Correction on Satellite-Derived Lower Tropospheric Temperature

Carl A. Mears and Frank J. Wentz

Satellite-based measurements of decadal-scale temperature change in the lower troposphere have indicated cooling relative to Earth's surface in the tropics. Such measurements need a diurnal correction to prevent drifts in the satellites' measurement time from causing spurious trends. We have derived a diurnal correction that, in the tropics, is of the opposite sign from that previously applied. When we use this correction in the calculation of lower tropospheric temperature from satellite microwave measurements, we find tropical warming consistent with that found at the surface and in our satellite-derived version of middle/upper tropospheric temperature.

Much of the surface warming of Earth observed over the past century is understood to be anthropogenic (*1*, *2*). In the upper air, the situation is less clear because of the relative paucity of data and short period of observation (*3*). In situ temperature measurements made by radiosondes have limited spatial coverage, particularly over large portions of the oceans, and are subject to a host of complications, including changing instrument types, configurations, and observation practices (*4*). For the past two decades, microwave radiometers flown on a series of National Oceanic and Atmospheric Administration (NOAA) polar orbiting weather satellites have provided a complementary source of observations, which have been used to calculate temperature here. Nine microwave sounding unit (MSU) instruments have been flown, with high-quality data extending from late 1978 to mid-2004. The MSU data suffer from a number of calibration issues and time-varying biases that must be addressed if they are to be used for climate change studies. For MSU channel 2 (MSU2), the data and its associated biases have been analyzed by a number of groups, yielding warming trends over the 1979–2004 period ranging from 0.04 to 0.17 K per decade (*5*–*9*). Unfortunately, interpretation of the raw MSU2 measurements is complicated by the fact that 10 to 15% of the signal in MSU2 arises from the stratosphere, which is cooling more rapidly than either the surface or the troposphere is warming, thus canceling much of the warming signal. Recently, Fu *et al.* have used weighted combinations of different MSU channels to remove the stratospheric influence from MSU2 (*10*–*12*). However, this method is a statistical inference that depends, in part, on the vertical coherence of stratospheric trends, rather than a direct measurement of the troposphere (*13*).

A more direct measurement of the lower troposphere can be obtained by using the MSU nadir-limb contrast to extrapolate the channel 2 brightness temperatures downward and remove nearly all of the stratospheric influence (*5*, *14*, *15*) [supporting online material (SOM) text and fig. S1]. As originally constructed by Christy *et al.*, this nadir-limb product (TLT, or temperature lower troposphere) showed cooling relative to the surface in many regions of Earth, particularly in the tropics. This finding is at odds with theoretical considerations and the predictions of climate models (*16*–*18*), both of which predict that any warming at the surface would

Remote Sensing Systems, 438 First Street, Suite 200, Santa Rosa, CA 94501, USA.

be amplified in the tropical troposphere. The surface/TLT disconnect is a problem only on decadal time scales; on shorter time scales, the ratio of the temporal variability in the Christy *et al*. TLT to the temporal variability of the surface temperature agrees well with expectations (*19*, *20*).

We present results from a new TLT analysis that uses a different, model-based, method to remove spurious trends caused by the slow evolution of each satellite's local measurement time over the diurnal cycle in atmospheric temperature. Each satellite typically exhibits a slow change of the local equator-crossing time (LECT) (Fig. 1A) and a decay of orbital height over time due to drag by the upper atmosphere (*21*). The LECT is the time at which the satellite passes over the equator, moving in a northward or "ascending" direction. Changes in LECT indicate corresponding changes in local observation time for the entire orbit. If the temperature being measured changes with the time of day (e.g., the diurnal cycle of daytime heating and nighttime cooling), slow changes in observation time can cause spurious long-term trends, which must be removed from each satellite's data record before attempting to merge the data together into a single data set (*22*).

Christy *et al*. estimated the effect of the diurnal cycle by calculating the mean rate of diurnal warming and cooling by subtracting the temperature measurements on one side of the satellite measurement swath from the other (*15*). This provided an estimate of the temperature change due to the difference in local observation times from one side of the satellite swath to another, about 40 min at the equator (*23*). Unfortunately, this method is extremely sensitive to small changes in the satellite attitude, particularly the satellite roll angle, calling its accuracy into question (SOM text).

In our work on MSU2, we used a different approach to evaluate the diurnal cycle. We used 5 years of hourly output from a climate model as input to a microwave radiative transfer model to estimate the seasonally varying diurnal cycle in measured temperature for each satellite view angle at each point on the globe (*7*). For the middle/upper troposphere (MSU2) on a global scale, there are no important differences between the two methods, although there are significant latitude-dependent differences (SOM text). In this work, we extend our method to TLT. In Fig. 1, B and C, we show a color-coded time-latitude plot of the corrections applied to TLT. For most latitudes, the Christy *et al*. TLT correction is of opposite sign from our TLT correction and from the corrections applied by either group for the middle/upper troposphere (fig. S2).

We argue that the sign change exhibited by the Christy *et al*. correction is physically inconsistent with our understanding of the vertical structure of the diurnal cycle. For MSU2, the globally averaged diurnal cycle is dominated by the surface and near-surface diurnal cycle over land regions. This is supported by a number of findings: Maps of temperature differences between the ascending and descending MSU2 measurements show much larger differences over land than over ocean (*7*, *24*). When these ascending/descending differences are examined as a function of Earth incidence angle, the differences are much larger for near-nadir angles than for larger incidence angles over land, suggesting that the bulk of the signal arises at or near the surface (fig. S3 and SOM text), in general agreement with radiosonde measurements (*25*) and general circulation models, including the Community Climate Model 3 model we used to calculate our diurnal correction.

Surface and near-surface effects will be even more dominant for TLT, whose vertical weighting function peaks several kilometers closer to the surface and has a surface contribution roughly double that of MSU2. Thus, we expect the TLT diurnal cycle and diurnal correction to be similar in shape to the MSU2 diurnal cycle, but with larger amplitude. This is consistent with the diurnal correction we calculate from the climate model and is inconsistent with the Christy *et al*. correction.

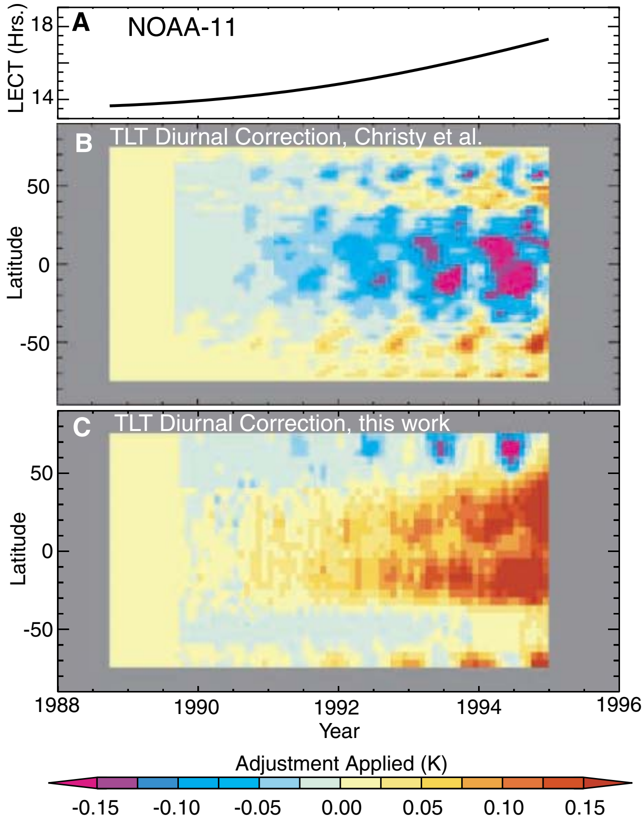

Fig. 1. Diurnal correction applied to MSU TLT for the NOAA-11 satellite. We use NOAA-11 as an example because it underwent a large drift in LECT of more than 6 hours before its ultimate failure in mid-1998. We show only the 1988–1993 period here because this is the only part of the NOAA-11 data used by Christy *et al*. NOAA-14 also underwent a similar drift, with its drift becoming more rapid after 1998, and by mid-2002, it had drifted by more than 4 hours. Most satellites in the MSU series drifted by at least 2 hours, with a few of the short-lived satellites drifting less than 1 hour. (**A**) LECT for the NOAA-11 satellite plotted as a function of time. (**B**) TLT correction applied by Christy *et al*. (**C**) TLT correction applied in this work.

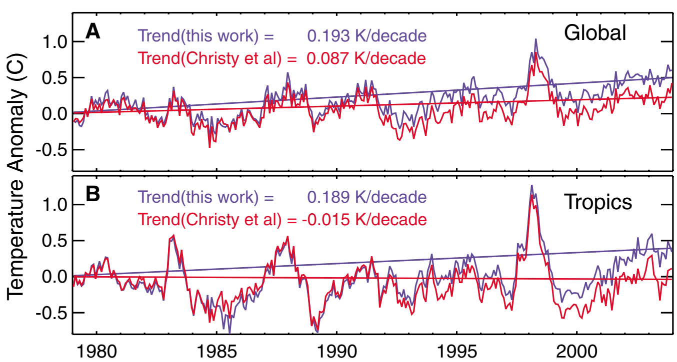

Fig. 2. TLT brightness temperature time series average over the globe (**A**), 70°S to 82.5°N, and the tropics (**B**), 20°S to 20°N, both for this work and for results from Christy *et al*. The straight lines are linear fits to the data. Our results indicate increased warming, particularly in the tropics, where the differences between the two diurnal corrections are the greatest. The differences between the time series become prominent after about 1991, when the drift in LECT for NOAA-11 begins to accelerate. A similar acceleration of drift in the NOAA-14 satellite occurs after 1998, with a corresponding increase in the difference between these time series.

The long-term behavior of a time series constructed from TLT is also dependent on the procedure used to merge the nine MSU satellites together into a single time series, in particular on the values of the parameters ("target factors") used to empirically remove the spurious dependence of the instrument calibration on the temperature of the hot calibration target (*5*, *7*, *15*) (SOM text). For the results presented below, we used exactly the same merging procedure and target factors (but different offsets) as we used when producing our results for MSU2 (*26*).

When we merge the data from the nine MSU satellites together using both our diurnal correction and target factors, we obtain a long-term time series that shows substantially more warming than the Christy *et al*. result, particularly in the tropics. In Fig. 2, we show global and tropical average monthly anomaly time series for our analysis and for Christy *et al*. Our global (70°S to 82.5°N) trend of 0.193 K per decade (1979–2003) is about 0.1 K per decade warmer than the trend calculated over the same area from the Christy *et al*. data, whereas our trend in the tropics (20°S to 20°N) of 0.189 K per decade is about 0.2 K per decade warmer (*27*). We estimate the 2σ uncertainty in these trends to be 0.09 K per decade, including both internal and structural uncertainty (SOM text).

To estimate what portion of the trend difference between our respective results is caused by the difference in diurnal correction, we performed a set of numerical experiments, where we substituted the Christy *et al*. diurnal correction into our analysis, and/or where we fixed the values of the target factors to the values used by Christy *et al*., allowing us to mimic different parts of the Christy *et al*. merging procedure separately and in combination. The results of these experiments (table S3) suggest that the difference in diurnal correction accounts for over 50% of the difference in trends for global averages and over 70% of the difference in trends for tropical averages.

In Fig. 3, we show global maps of TLT and surface trends (*28*) (1979–2003) and differences between these trends. The Christy *et al*. results indicate that the lower troposphere is cooling dramatically relative to the surface over almost all parts of the tropics, which is in sharp disagreement with both climate model output and theoretical arguments (*20*, *29*). Our results suggest that the tropical troposphere is warming slightly more than the surface in most regions, in accordance with expectations, although scenarios where the tropical troposphere is cooling relative to the surface are also possible within the range of uncertainty.

Our results are also in agreement with middle tropospheric results obtained for our data by removing the stratospheric contamination in our MSU2 data using MSU channel 4 (*10*, *11*), indicating a measure of vertical consistency in our results that is absent in the Christy *et al*. results (*12*). Also, the warming of the TLT in the tropics is in accordance with observed trends in total columnar water vapor from satellite observations made over the tropical oceans since 1988, which show an increase of more than 2% per decade (*19*, *30*). Although the correlation of total water vapor and temperature is often limited to the boundary layer, it would be difficult to explain a moistening of the tropical atmosphere without some warming within the layer measured by TLT.

In contrast, trends from temporally homogenized radiosonde data sets show less warming than our results (*31–33*) and are in better agreement with the Christy *et al*. results. However, the radiosonde record is fraught with difficulties related to changes in instrument type, observing practices, data correction, and station location. In the tropics, where they are the largest, these problems have been shown to be more likely to lead to spurious cooling trends than spurious warming trends in the unadjusted data, suggesting the possibility that any problems that were not detected during homogenization may result in a cooling bias in the homogenized radiosonde record (*32*). In the northern extratropics, there is excellent agreement between the Christy *et al*. results and a subsample of the radiosonde sites chosen to have consistent instrumentation type and thus thought to be relatively free of error (*15*). Presumably the agreement between these radiosondes and our data would be somewhat worse, although this has not been tested.

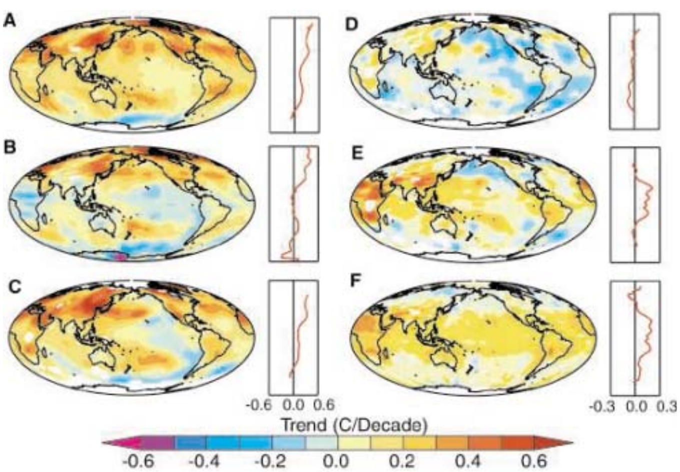

Fig. 3. Global maps and zonal averages of linear temperature trends (1979–2003). Missing data are shown as white areas. (**A**) TLT temperature trends from this work. (**B**) TLT temperature trends from Christy *et al*. (*5*). (**C**) Surface temperature trends from (*28*). Trend difference, surface minus TLT, (**D**) this work and (**E**) Christy *et al*. (**F**) TLT trend difference, this work minus Christy *et al*.

References and Notes

1. J. E. Hansen *et al.*, *J. Geophys. Res.* **106**, 23947 (2001).
2. J. T. Houghton *et al.*, *Climate Change 2001: The Scientific Basis: Contribution of Working Group I to the Third Assessment Report of the Intergovernmental Panel on Climate Change* (Cambridge Univ. Press, Cambridge, 2001).
3. J. W. Hurrell, S. J. Brown, K. E. Trenberth, J. R. Christy, *Bull. Am. Meteorol. Soc.* **81**, 2165 (2000).
4. D. J. Gaffen, M. A. Sargent, R. E. Habermann, J. R. Lanzante, *J. Clim.* **13**, 1776 (2000).
5. J. R. Christy, R. W. Spencer, W. B. Norris, W. D. Braswell, D. E. Parker, *J. Atmos. Ocean. Tech.* **20**, 613 (2003).
6. C. Prabhakara, J. R. Iaacovazzi, J.-M. Yoo, G. Dalu, *Geophys. Res. Lett.* **27**, 3517 (2000).
7. C. A. Mears, M. C. Schabel, F. J. Wentz, *J. Clim.* **16**, 3650 (2003).
8. K. Y. Vinnikov, N. C. Grody, *Science* **302**, 269 (2003).
9. N. C. Grody, K. Y. Vinnikov, M. D. Goldberg, J. T. Sullivan, J. D. Tarpley, *J. Geophys. Res.* **109**, D24104 (2004).
10. Q. Fu, C. M. Johanson, S. G. Warren, D. J. Seidel, *Nature* **429**, 55 (2004).
11. Q. Fu, C. M. Johanson, *J. Clim.* **17**, 4636 (2004).
12. Q. Fu, C. M. Johanson, *Geophys. Res. Lett.* **32**, L10703 (2005).
13. S. Tett, P. Thorne, *Nature*, published online 2 December 2004 (10.1038/nature03208).
14. R. W. Spencer, J. R. Christy, *J. Clim.* **5**, 858 (1992).
15. J. R. Christy, R. W. Spencer, W. D. Braswell, *J. Atmos. Ocean. Tech.* **17**, 1153 (2000).
16. B. D. Santer *et al.*, *Science* **287**, 1227 (2000).
17. J. M. Wallace *et al.*, *Reconciling Observations of Global Temperature Change* (National Research Council, Washington, DC, 2000).
18. B. D. Santer *et al.*, *Science* **300**, 1280 (2003).
19. F. J. Wentz, M. Schabel, *Nature* **403**, 414 (2000).
20. B. D. Santer *et al.*, *Science* **309**, 1551 (2005); published online 11 August 2005 (10.1126/science.1114867).
21. The decay of orbital height also has an important effect on measurements of long-term temperature trends (*34*). This adjustment is done in the same way in the work reported here and in (*15*). Because it is not a cause of the current discrepancy, we do not discuss it further.
22. Both at Earth's surface and in the troposphere, the diurnal cycle in temperature is dominated by the first harmonic. At a given point on Earth, the ascending and descending passes of the NOAA satellites make measurements separated by approximately 12 hours, so that averaging together the data from ascending and descending orbits has the effect of removing most of the first harmonic of the diurnal cycle. This cancellation becomes less effective as one moves toward the polar regions, where the local measurement times become closer together. We define diurnal correction to be the removal of any residual effects remaining after averaging the ascending and descending parts of the orbit together.
23. The cross-scan time difference grows slowly to about an hour at 45°N or S and to more than 2 hours in the polar regions.
24. C. A. Mears, M. Schabel, F. J. Wentz, B. D. Santer, B. Govindasamy, *Proc. Int. Geophys. Remote Sensing Symp.* **III**, 1839 (2002).
25. D. J. Seidel, M. Free, J. Wang, *J. Geophys. Res.* **110**, D09102 (2005).

26. We chose these values of the target factors to produce our final results because we have concluded that they are the most likely to be free of errors. They are calculated from oceanic observations to reduce errors from uncorrected diurnal variations, and we use unweighted MSU channel 2 data (T2 in SOM) to avoid additional noise due to the differencing procedure used to calculate TLT. The values of the intersatellite offsets needed to be recalculated to remove obvious intersatellite differences. In the supporting online material, we discuss the impact of using different data subsets to determine the target factors. This information is used to help determine the structural uncertainty.
27. We obtain this estimate of the tropical TLT trend when we recalculate the intersatellite offsets to optimize them for tropical data. If this reoptimization is not performed, as it is not in producing maps such as those shown in Fig. 3, we obtain a smaller trend value of 0.164 K per decade.
28. T. M. Smith, R. W. Reynolds, *J. Clim.* **18**, 2021 (2005).
29. J. W. Hurrell, K. E. Trenberth, *J. Clim.* **11**, 945 (1998).
30. K. E. Trenberth, J. Fasullo, L. Smith, *Clim. Dyn.*, in press; published online 11 May 2005 (10.1007/s00382-005-0017-4).
31. J. Lanzante, S. Klein, D. Seidel, *J. Clim.* **16**, 224 (2003).
32. J. Lanzante, S. Klein, D. Seidel, *J. Clim.* **16**, 241 (2003).
33. P. W. Thorne *et al.*, *J. Geophys. Res.*, in press.
34. F. J. Wentz, M. Schabel, *Nature* **394**, 661 (1998).
35. This work was supported by the NOAA Climate and Global Change Program. We thank J. Christy and R. Spencer for providing numerical values for their diurnal adjustment.

Supporting Online Material
www.sciencemag.org/cgi/content/full/1114772/DC1
SOM Text
Figs. S1 to S4
Tables S1 to S3
References and Notes

12 May 2005; accepted 27 July 2005
Published online 11 August 2005;
10.1126/science.1114772
Include this information when citing this paper.

Amplification of Surface Temperature Trends and Variability in the Tropical Atmosphere

B. D. Santer,[1*] T. M. L. Wigley,[2] C. Mears,[3] F. J. Wentz,[3] S. A. Klein,[1] D. J. Seidel,[4] K. E. Taylor,[1] P. W. Thorne,[5] M. F. Wehner,[6] P. J. Gleckler,[1] J. S. Boyle,[1] W. D. Collins,[2] K. W. Dixon,[7] C. Doutriaux,[1] M. Free,[4] Q. Fu,[8] J. E. Hansen,[9] G. S. Jones,[5] R. Ruedy,[9] T. R. Karl,[10] J. R. Lanzante,[7] G. A. Meehl,[2] V. Ramaswamy,[7] G. Russell,[9] G. A. Schmidt[9]

The month-to-month variability of tropical temperatures is larger in the troposphere than at Earth's surface. This amplification behavior is similar in a range of observations and climate model simulations and is consistent with basic theory. On multidecadal time scales, tropospheric amplification of surface warming is a robust feature of model simulations, but it occurs in only one observational data set. Other observations show weak, or even negative, amplification. These results suggest either that different physical mechanisms control amplification processes on monthly and decadal time scales, and models fail to capture such behavior; or (more plausibly) that residual errors in several observational data sets used here affect their representation of long-term trends.

Tropospheric warming is a robust feature of climate model simulations that include historical increases in greenhouse gases (*1–3*). Maximum warming is predicted to occur in the middle and upper tropical troposphere. Atmospheric temperature measurements from radiosondes also show warming of the tropical troposphere since the early 1960s (*4–7*), consistent with model results (*8*). The observed tropical warming is partly due to a step-like change in the late 1970s (*5*, *6*).

Considerable attention has focused on the shorter record of satellite-based atmospheric temperature measurements (1979 to present). In both models and observations, the tropical surface warms over this period. Simulated surface warming is amplified in the tropical troposphere, corresponding to a decrease in lapse rate (*2*, *3*, *9*). In contrast, a number of radiosonde and satellite data sets suggest that the tropical troposphere has warmed less than the surface, or even cooled, which would correspond to an increase in lapse rate (*4–12*).

This discrepancy may be an artifact of residual inhomogeneities in the observations (*13–19*). Creating homogeneous climate records requires the identification and removal of nonclimatic influences from data that were primarily collected for weather forecasting purposes. Different analysts have followed very different data-adjustment pathways (*4–7*, *12*, *14*, *17*). The resulting "structural uncertainties" in observed estimates of tropospheric temperature change (*20*) are as large as the model-predicted climate-change signal that should have occurred in response to combined human and natural forcings (*16*).

Alternately, there may be a real disparity between modeled and observed lapse-rate changes over the satellite era (*9–11*, *21*). This disparity would point toward the existence of fundamental deficiencies in current climate models (and/or in the forcings used in model experiments), thus diminishing our confidence in model predictions of climate change.

This scientific puzzle provides considerable motivation for revisiting comparisons of simulated and observed tropical lapse-rate changes (*10*, *13*, *21*, *22*) with more comprehensive estimates of observational uncertainty and a wide range of recently completed model simulations. The latter were performed in support of the Fourth Assessment Report of the Intergovernmental Panel on Climate Change (IPCC), and involve 19 coupled atmosphere-ocean models developed in nine different countries. Unlike previous model intercomparison exercises involving idealized climate-change experiments (*23*), these new simulations incorporate estimated historical changes in a variety of natural and anthropogenic forcings (*24*, *25*).

Our focus is on the amplification of surface temperature variability and trends in the free troposphere. We study this amplification behavior in several different ways. The first is to compare atmospheric profiles of "scaling ratios" in the IPCC simulations and in two new radiosonde data sets: HadAT2 (Hadley Centre Atmospheric Temperatures, version 2) and RATPAC (Radiosonde Atmospheric Temperature Products for Assessing Climate). These were compiled (respectively) by the UK Met Office (UKMO) (*6*) and the National Oceanic and Atmospheric Administration (NOAA) (*7*). The scaling factor is simply the ratio between the temperature variability (or trend) at discrete atmospheric pressure levels and the same quantity at the surface (*26*). Observed trends and variability in tropical surface temperatures (T_S) were obtained from the NOAA (*27*) and HadCRUT2v data sets (*28*, *29*).

[1]Program for Climate Model Diagnosis and Intercomparison, Lawrence Livermore National Laboratory, Livermore, CA 94550, USA. [2]National Center for Atmospheric Research, Boulder, CO 80303, USA. [3]Remote Sensing Systems, Santa Rosa, CA 95401, USA. [4]National Oceanic and Atmospheric Administration (NOAA)/Air Resources Laboratory, Silver Spring, MD 20910, USA. [5]Hadley Centre for Climate Prediction and Research, UK Met Office, Exeter, EX1 3PB, UK. [6]Lawrence Berkeley National Laboratory, Berkeley, CA 94720, USA. [7]NOAA/Geophysical Fluid Dynamics Laboratory, Princeton, NJ 08542, USA. [8]Department of Atmospheric Sciences, University of Washington, Seattle, WA 98195, USA. [9]NASA/Goddard Institute for Space Studies, New York, NY 10025, USA. [10]NOAA/National Climatic Data Center, Asheville, NC 28801, USA.

*To whom correspondence should be addressed. E-mail: santer1@llnl.gov

Our second method for estimating scaling ratios uses the weighted-average temperatures of deep atmospheric layers (*12*, *17*). These temperatures are available from the satellite-based Microwave Sounding Unit (MSU), which monitors atmospheric microwave emissions from the lower stratosphere (T_4) and the troposphere (T_2). MSU T_2 data have also been used to retrieve lower tropospheric temperatures (T_{2LT}). We calculate synthetic MSU temperatures from the IPCC simulations, and then compare these with actual MSU temperatures produced by research groups at the University of Alabama in Huntsville (UAH) (*12*) and Remote Sensing Systems (RSS) in California (*14*, *17*). Synthetic T_4, T_2, and T_{2LT} data are also computed from the HadAT2 and RATPAC radiosonde data sets (*25*).

T_2 receives a contribution from the cooling stratosphere (*30*). This hampers its use for estimating the amplification of surface temperature changes in the free troposphere. We therefore focus on T_{2LT}, which is relatively unaffected by the stratosphere (*15*). Until recently, only UAH provided a satellite-based T_{2LT} product (*12*). The RSS group has now independently derived a second T_{2LT} data set (*14*).

Another strategy for removing stratospheric influences on T_2 relies on a linear combination of T_4 and T_2 (*15*, *25*). This procedure yields T_{Fu} [named for the first author of (*15*)], which is representative of temperatures in the bulk troposphere. Relative to T_{2LT}, T_{Fu} receives more of its signal from higher regions of the troposphere. On the basis of simple moist adiabatic lapse rate (MALR) theory (*31*), we expect scaling ratios in the deep tropics to increase with increasing height and to peak at roughly 200 mbar. Comparison of the amplification factors estimated with T_{2LT} and T_{Fu} data allows us to verify whether models and observations confirm this theoretical expectation.

Before discussing the scaling ratio results, it is instructive to examine the variability and trends in layer-averaged atmospheric temperatures and T_S. Our analysis period (January 1979 through December 1999) is constrained by the start date of observed satellite data and the end date of the IPCC historical forcing experiment. A total of 49 realizations of this experiment were available (*24*).

Time series of tropical T_4 changes in UAH, RSS, and the IPCC simulations are characterized by overall cooling trends and volcanically induced stratospheric warming signals (Fig. 1A). High-frequency variability associated with the quasi-biennial oscillation is evident in the observations but not in the model simulations (*5*, *25*). Satellite T_4 trends lie within the range of model results, but the larger cooling trends estimated from radiosondes do not (Fig. 2A). Part of this discrepancy may be caused by residual stratospheric and upper tropospheric cooling biases in the tropical radiosonde data (*18*, *19*).

In observations, the tropical variability of tropospheric and surface temperatures is dominated by the large El Niño events in 1982/83, 1987/88, and 1997/98 (Fig. 1, B and C). Because the IPCC runs are coupled-model simulations, they cannot reproduce the time sequence of observed El Niño and La Niña events, except by chance (*2*, *16*). The range of simulated El Niño/Southern Oscillation (ENSO) variability spans an order of magnitude. Models with very strong ENSO variability have fluctuations in surface and tropospheric temperatures that are noticeably larger than observed.

The observed tropical T_S trends in the NOAA and HadCRUT2v data sets (0.12 and 0.14°C per decade, respectively) are very similar to $\overline{X}$, the average warming over all model simulations (Fig. 2E) (*32*). In the troposphere, however, model-observed trend agreement is sensitive to the atmospheric layer examined and the choice of observational data set. In both radiosonde data sets used here, T_2 cools over the years 1979 to 1999, and trends are outside the spread of model results (Fig. 2B). Large stratospheric cooling biases in the radiosonde data probably contribute to this disparity (*18*, *19*). The use of T_{Fu} removes most of the stratospheric influence on T_2 and yields positive temperature trends in all observed data sets (Fig.

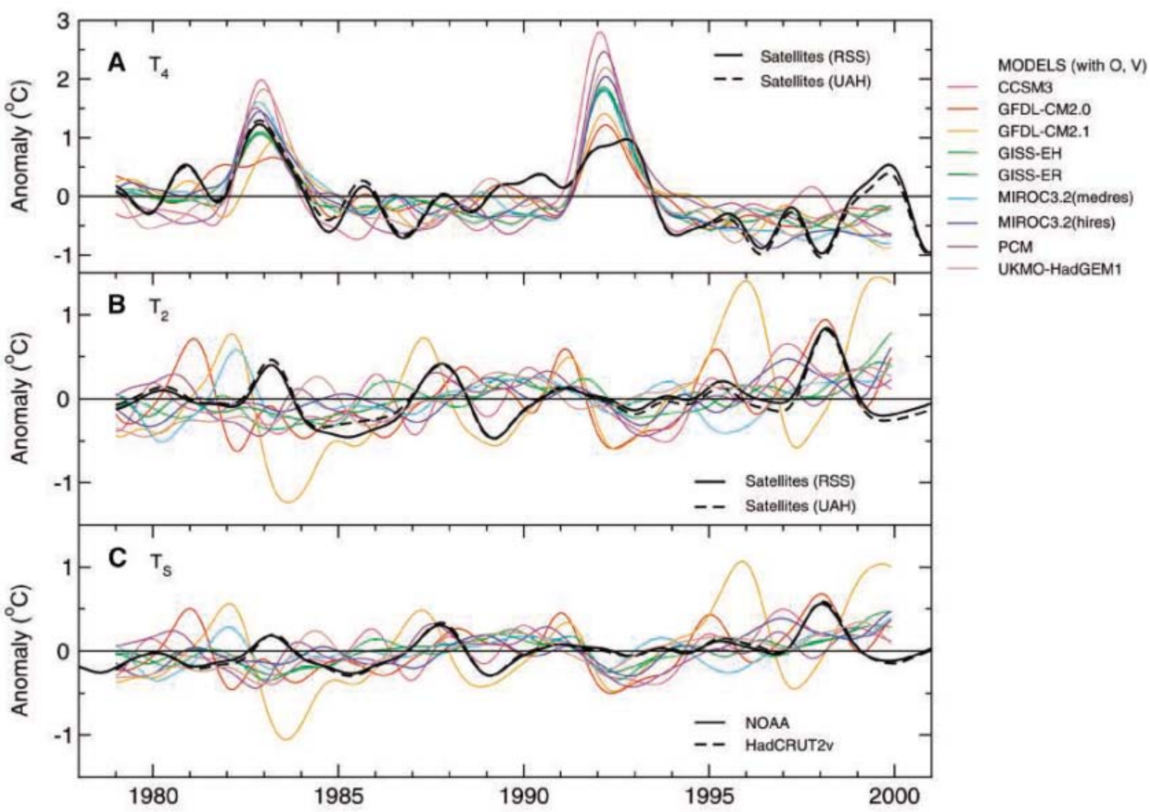

Fig. 1. Time series of monthly-mean tropical temperature anomalies in (**A**) T_4, (**B**) T_2, and (**C**) T_S. Observed T_4 and T_2 data are from UAH (*12*) and RSS (*17*). Observed T_S results are from the NOAA (*27*) and HadCRUT2v datasets (*28*). The latter were subsampled at the locations of HadAT2 radiosonde data (*6*). Model T_S results and synthetic MSU temperatures are from the IPCC historical forcing runs (*25*). Results shown are restricted to those models that included forcing by both stratospheric ozone depletion (O) and volcanic aerosols (V). All data were spatially averaged over 20°N to 20°S, expressed as anomalies relative to climatological monthly means over the years 1979 to 1999, and low-pass filtered. To facilitate model observation and model-model variability comparisons involving models with different ensemble sizes, only the first realization is plotted from each model.

2C) (*5*, *15*, *30*). All observed T_{Fu} trends are within the envelope of model values.

In the tropical lower troposphere, all data sets except UAH have positive T_{2LT} trends (Fig. 2D). The difference between the UAH and RSS trends (~ 0.13°C per decade) is a factor of two larger than the claimed 95% confidence interval for the UAH global T_{2LT} trend (*12*). This difference is primarily attributable to the different ways in which the two groups account for the effects of orbital drift on the sampling of the diurnal temperature cycle (*14*). The UAH T_{2LT} trend lies outside the range of model solutions. The disparate behavior of T_{2LT} and T_{Fu} in the UAH data (the former cools, whereas the latter warms) is not evident in any other data set (*14*, *15*, *30*).

Both model and satellite data indicate that variability in T_S is amplified in the tropical troposphere (Fig. 1, B and C). Amplification of surface warming is a direct result of moist thermodynamic processes (*31*). We examine two different amplification metrics: $R_S(z)$, the ratio between the temporal standard deviations of monthly-mean tropospheric and T_S anomalies, and $R_\beta(z)$, the ratio between the multidecadal trends in these quantities, where z denotes a height coordinate (pressure in mbars). Because most of the monthly timescale variability in tropical surface and tropospheric temperatures is driven by interannual fluctuations in ENSO, $R_S(z)$ largely reflects amplification processes acting on annual time scales (fig. S1) (*33*).

Figure 3A shows $R_S(z)$ values in models and radiosondes. The theoretically expected profile is also displayed (*34*). In all cases, $R_S(z)$ increases above the boundary layer, with maximum amplification at ~200 mbar. Below ~400 mbar, there is close agreement between the scaling ratios in models, radiosondes, and theory. Between 400 and 150 mbar, the theoretical scaling ratios are consistently larger than they are in either the radiosondes or the IPCC simulations. Such departures may be due to the fact that MALR theory is applicable to regions of the tropical ocean experiencing deep convection. In contrast, the model and radiosonde temperature data used to calculate $R_S(z)$ include many convectively inactive areas, where the surface-air temperature change is not constrained by the moist adiabat set by the convectively active regions. Furthermore, active moist convection does not always penetrate above 400 hPa, which would weaken the connection to a moist adiabat above this level.

When scaling ratios are calculated for multidecadal linear trends, both radiosonde data sets are clear outliers. HadAT2 and RATPAC $R_\beta(z)$ values never exceed 0.82, indicating damping of the surface warming trend in the free atmosphere (Fig. 3B). None of the 49 model realizations demonstrates such behavior. The shapes of the radiosonde-based scaling ratio profiles also differ from model and theoretical results, with peak values at generally lower atmospheric levels. Subsampling the HadCRUT2v T_S data at the locations of the HadAT2 radiosonde stations has little impact on the observed $R_S(z)$ or $R_\beta(z)$ values (*25*).

In the low- to mid-troposphere, model $R_\beta(z)$ results are in good agreement with theoretical expectations. Model scaling ratios are therefore consistent with theory on both monthly and multidecadal time scales, whereas the radiosonde data are only consistent with theory on monthly time scales.

A qualitatively similar picture emerges from scatter plots of the individual components of $R_S(z)$ and $R_\beta(z)$ (Fig. 4). These display scaling behavior for layer-averaged atmospheric temperatures rather than for temperatures at discrete atmospheric levels. Figure 4A shows $s(T_S)$ and $s(T_{2LT})$, the temporal standard deviations of monthly-mean tropical T_S and T_{2LT} data. Both vary by a factor of ≥ 5 over the 19 IPCC models. Values of $s(T_{Fu})$ span a comparable range (Fig. 4B). These large ranges are primarily dictated by model differences in the amplitude of ENSO variability.

Despite this large spread of model variability estimates, the tropospheric amplification of $s(T_S)$ is internally consistent across a wide range of models and observed data (Fig. 4, A and B). The regression between the model $s(T_S)$ and $s(T_{2LT})$ values has a slope of 1.3, in accord with the theoretically expected scaling ratio at the peak of the T_{2LT} weighting function. The regression line for $s(T_S)$ and $s(T_{Fu})$ is steeper (1.5). This is because the T_{Fu} weighting function peaks higher in the atmosphere, where scaling ratios are larger (Fig. 3A) (*25*). All model and observational results in Fig. 4, A and B, are tightly clustered around the fitted (red) regression lines, which is consistent with the close agreement between

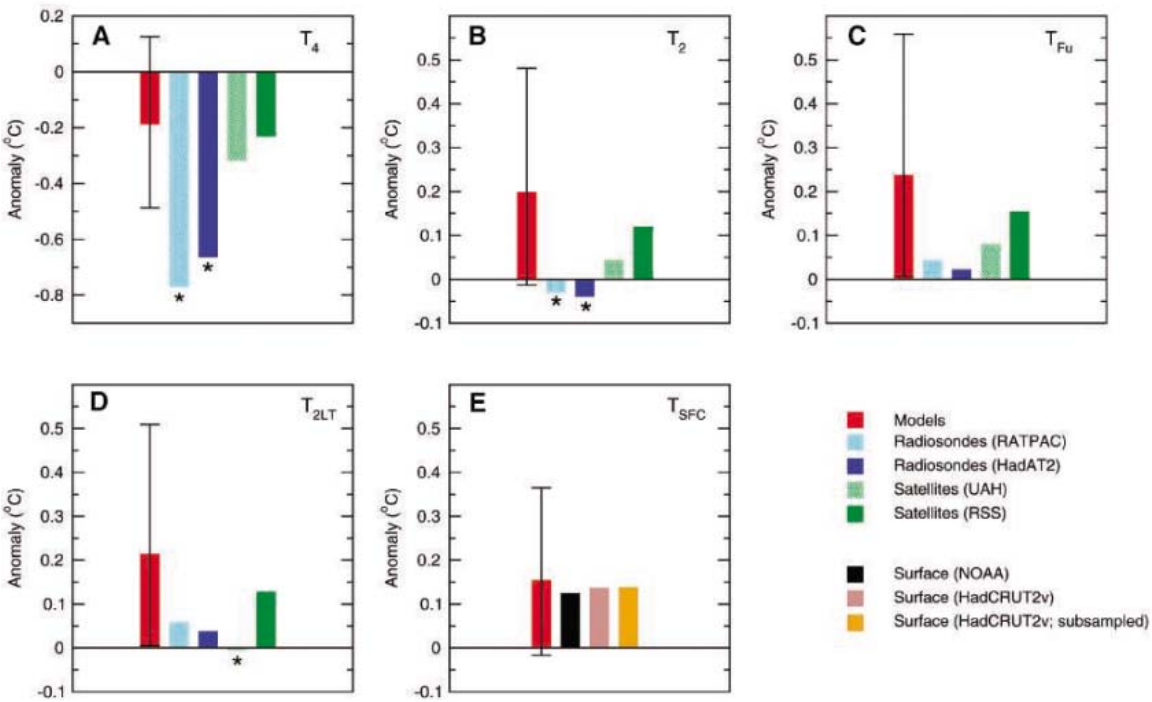

Fig. 2. Simulated and observed least-squares linear trends in tropical (**A**) T_4, (**B**) T_2, (**C**) T_{Fu}, (**D**) T_{2LT}, and (**E**) T_S. Red bars represent $\overline{X}$, the mean of the model results (*32*). The black lines that encompass $\overline{X}$ are the maximum and minimum values from 49 realizations of the IPCC historical forcing experiment (*25*). Asterisks identify observational trends outside the range of model results. All trends were calculated from spatially-averaged (20°N to 20°S) anomaly data over the 252-month period January 1979 to December 1999. For anomaly definition and data sources, see Fig. 1. The orange bar in panel (E) is the T_S trend based on HadCRUT2v T_S data that were subsampled at the locations of HadAT2 radiosonde data (*6*).

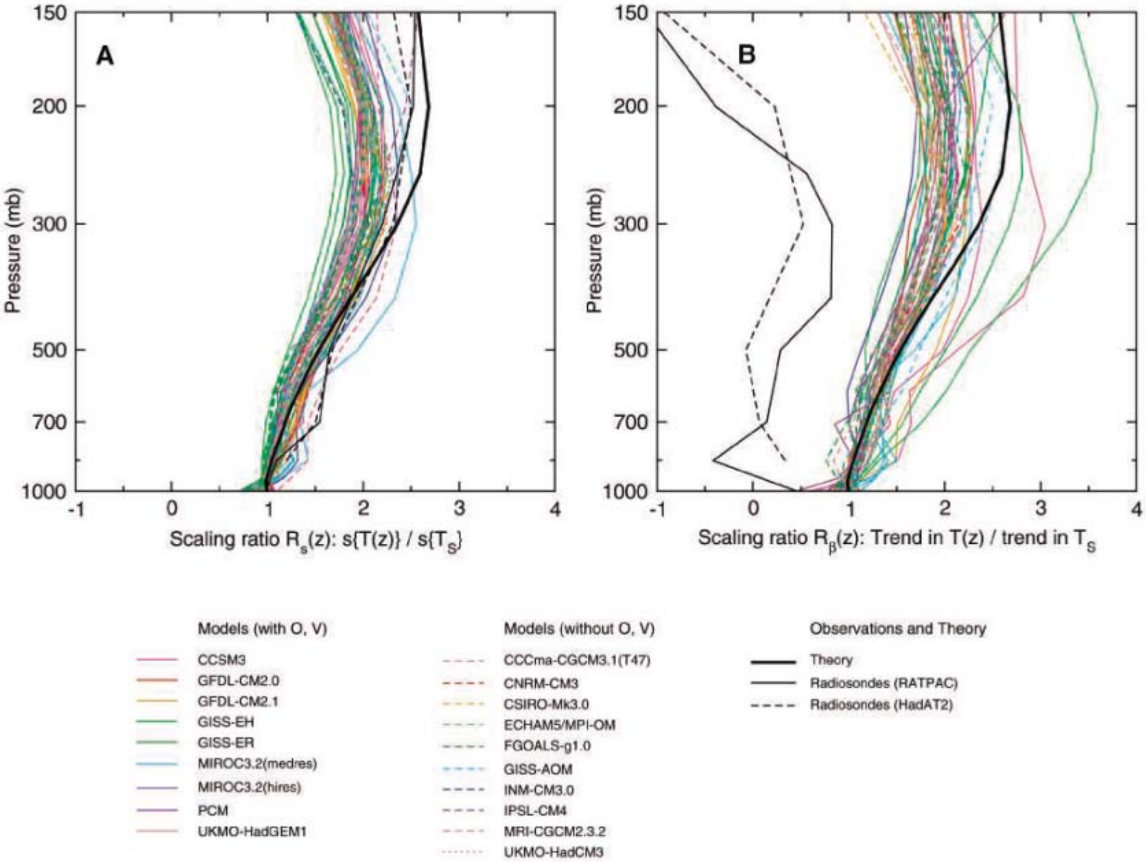

Fig. 3. Atmospheric profiles of temperature scaling ratios in models, theory, and radiosonde data. (**A**) $R_S(z)$ is the ratio between the temporal standard deviations of $T(z)$, the temperature at discrete pressure levels, and the surface temperature T_S. (**B**) $R_\beta(z)$ is similarly defined, but for trends over 1979 to 1999. Model results are from 49 realizations of the IPCC historical forcing experiment. Radiosonde scaling ratios were calculated with HadAT2 and RATPAC $T(z)$ data (*6*, *7*). Scaling ratios for HadAT2 are based on unsubsampled HadCRUT2v T_S data. HadCRUT2v T_S data subsampled with HadAT2 coverage yield virtually identical scaling ratios (not shown). RATPAC-derived scaling ratios use spatially complete NOAA T_S data. Theoretically expected values of $R_S(z)$ and $R_\beta(z)$ are also shown (*34*). All standard deviations in panel (A) were calculated with linearly detrended data. $R_\beta(z)$ results in panel (B) are not plotted for three model realizations with surface warming close to zero (*25*). All results are for spatial averages over 20°N to 20°S. For anomaly definition, data sources, and further processing details, see Fig. 1 and (*25*).

modeled and observed $R_S(z)$ values in the lower troposphere (Fig. 3A).

Amplification factors estimated from multidecadal trends in T_S, T_{2LT}, and T_{Fu} also display considerable internal consistency in the 19 IPCC models (Fig. 4, C and D). This consistency occurs despite large intermodel differences in convective parameterizations, boundary layer formulation, and resolution, all of which affect the simulation of tropical convection and tropospheric lapse rates. Furthermore, the model-model consistency in $R_\beta(z)$ ratios is robust to differences in the natural and anthropogenic forcings applied by each group (*24*, *25*). Many of these forcings are heterogeneous in space and time (*2*, *3*, *35*). These differences in forcings and physics do not cause appreciable displacement of model results from the regression line in Fig. 4, C and D. The regression slopes are similar to those estimated from monthly-timescale variability, with T_{Fu} results again yielding a steeper slope than does T_{2LT}.

The real conundrum in Fig. 4 is the complex behavior of the observations. On monthly timescales, the amplification behavior of models and observations is consistent. On decadal timescales, however, only the RSS-based T_{2LT} and T_{Fu} trends have scaling factors that are in reasonable accord with model results (Fig. 4, C and D) (*25*). Despite sustained warming of the tropical land and ocean surfaces, the UAH T_{2LT} trend is negative—i.e., $R_\beta(z) < 0$. The UAH $R_\beta(z)$ value seems physically implausible (*14*, *15*). Prolonged surface warming should destabilize tropical temperature profiles, thus enhancing conditions for moist convection and readjustment of atmospheric temperatures to an MALR.

In contrast to the model results and theoretical expectations, both radiosonde data sets used here have $R_\beta(z)$ ratios $\ll 1.0$ (Fig. 4, C and D). As in the case of the satellite data sets, there are large structural uncertainties in radiosonde estimates of tropospheric temperature change (*4–7*). Comparisons of tropical temperature data from day- and night-time radiosonde ascents suggest that the error arising from solar heating of temperature sensors has decreased over time (*18*, *19*). Inadequate correction for this effect may account for a residual cooling bias in tropospheric temperature changes.

The existence of residual inhomogeneities in the observational data is likely. Current atmospheric observing systems were designed for real-time monitoring of weather rather than long-term monitoring of climate. The construction of reliable climate records from radiosondes is hampered by the above-noted changes in instrumentation (*18*, *19*) along with changes in observing practices and network density (*4–7*, *11*, *13*). Similar concerns apply to satellite data, which are influenced by intersatellite biases, orbital drift and decay, and uncertainties in instrument calibration coefficients (*11–14*, *17*).

Adjustments for these and other effects are applied at discrete points in an observational time series, such as times of transition to a new satellite. None of these corrections is precisely known. Small errors in adjustments can introduce systematic errors in the time series. These errors have little impact on monthly and interannual variability, which account for most of the variance of tropospheric temperature fluctuations in the deep tropics (Fig. 1B). However, systematic errors can have a pronounced effect on interdecadal variability. This helps to explain why model/data comparisons of $R_\beta(z)$ ratios are sensitive to observational uncertainty, whereas $R_S(z)$ ratios are not.

We have demonstrated that all observed data sets and model results are remarkably consistent in terms of their relation between monthly– and annual–time scale temperature variations at the surface and in the free troposphere. This is a strong verification of the

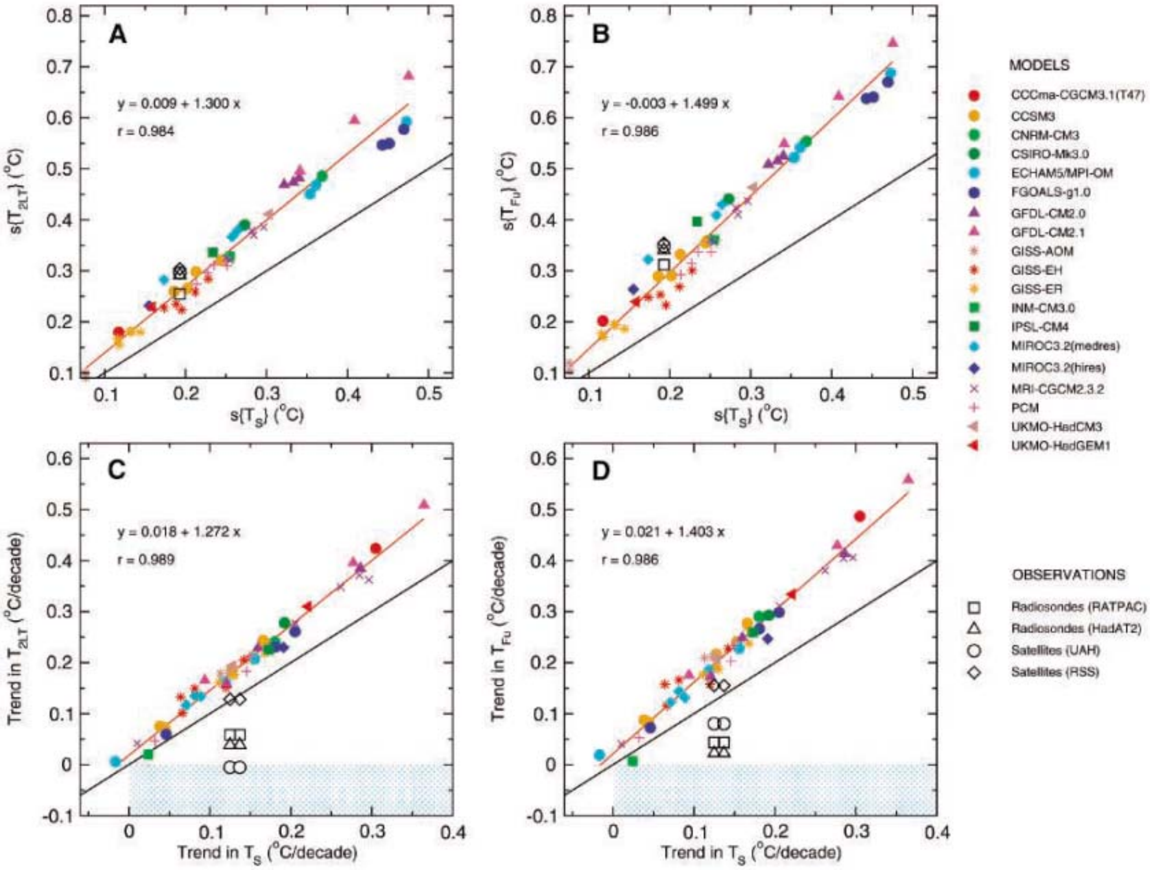

Fig. 4. Scatter plots of the individual components of the $R_S(z)$ and $R_\beta(z)$ scaling ratios. Results are for the deep tropics (20°N to 20°S). The two upper panels provide information on amplification of the monthly-timescale T_S variability in (**A**) T_{2LT} and (**B**) T_{Fu}. The two bottom panels show the relation between decadal-timescale trends in (**C**) T_S and T_{2LT} and in (**D**) T_S and T_{Fu}. Each scatter plot has 49 pairs of model results. The fitted regression lines (in red) are based on model data only. The black lines denote a slope of 1. Values above the black lines indicate tropospheric enhancement, and values below the black line indicate tropospheric damping of surface temperature changes. There are two columns of observational results in (C) and (D). These are based on the NOAA and HadCRUT2v T_s trends (0.12 and 0.14°C per decade, respectively). Because $s(T_S)$ (the temporal standard deviation of T_S) is very similar in the NOAA and HadCRUT2v data sets, observed results in (A) and (B) use NOAA $s(T_S)$ values only. The blue shading in the two bottom panels defines the region of simultaneous surface warming and tropospheric cooling. For anomaly definition, analysis period, and data sources, refer to Fig. 1 and (*25*).

model physics that governs the amplification of tropical surface temperature changes. On decadal time scales, however, only one observed data set (RSS) shows amplification behavior that is generally consistent with model results. The correspondence between models and observations on monthly and annual time scales does not guarantee that model scaling ratios are valid on decadal time scales. However, given the very basic nature of the physics involved, this high-frequency agreement is suggestive of more general validity of model scaling ratios across a range of time scales.

The RSS T_{2LT}, T_2, and T_{Fu} trends are physically consistent (all three layers warm as the surface warms), whereas the UAH data show trends of different sign in the lower- and midtroposphere. These results support the contention that the tropical warming trend in RSS T_{2LT} data is more reliable than T_{2LT} trends in other observational data sets. This conclusion does not rest solely on comparisons with climate models. It is independently supported by the empirical evidence of recent increases in tropospheric water vapor and tropopause height (*26*, *36*), which are in accord with warming but not cooling of the free troposphere.

We have used basic physical principles as represented in current climate models, for interpreting and evaluating observational data. Our work illustrates that progress toward an improved understanding of the climate system can best be achieved by combined use of observations, theory, and models. The availability of a large range of model and observational surface and atmospheric temperature data sets has been of great benefit to this research, and highlights the dangers inherent in drawing inferences on the agreement between models and observations without adequately accounting for uncertainties in both.

References and Notes

1. B. D. Santer *et al.*, *Nature* **382**, 39 (1996).
2. J. E. Hansen *et al.*, *J. Geophys. Res.* **107**, ACL-2, 10.1029/2001JD001143 (2002).
3. S. F. B. Tett *et al.*, *J. Geophys. Res.* **107**, 10.1029/2000JD000028 (2002).
4. J. R. Lanzante, S. A. Klein, D. J. Seidel, *J. Clim.* **16**, 241 (2003).
5. D. J. Seidel *et al.*, *J. Clim.* **17**, 2225 (2004).
6. P. W. Thorne *et al.*, *J. Geophys. Res.* in press.
7. M. Free *et al. J. Geophys. Res.*, in press.
8. P. W. Thorne *et al.*, *Geophys. Res. Lett.* **29**, 10.1029/2002GL015717 (2002).
9. B. D. Santer *et al.*, *Science* **287**, 1227 (2000).
10. D. J. Gaffen *et al.*, *Science* **287**, 1242 (2000).
11. J. M. Wallace *et al.*, *Reconciling Observations of Global Temperature Change* (National Academy Press, Washington DC, 2000).
12. J. R. Christy, R. W. Spencer, W. B. Norris, W. D. Braswell, *J. Atmos. Ocean. Tech.* **20**, 613 (2003).
13. J. W. Hurrell, K. E. Trenberth, *J. Clim.* **11**, 945 (1998).
14. C. A. Mears, F. J. Wentz, *Science* **309**, 1548 (2005); published online 11 August 2005 (10.1126/science.1114772).
15. Q. Fu, C. M. Johanson, *Geophys. Res. Lett.* **32**, L10703, 10.1029/2004GL022266 (2005).
16. B. D. Santer *et al.*, *Science* **300**, 1280 (2003).
17. C. A. Mears, M. C. Schabel, F. W. Wentz, *J. Clim.* **16**, 3650 (2003).
18. S. C. Sherwood, J. R. Lanzante, C. L. Meyer, *Science* **309**, 1556 (2005); published online 11 August 2005 (10.1126/science.1115640).
19. W. J. Randel, F. Wu, in preparation.
20. P. W. Thorne, D. E. Parker, J. R. Christy, C. A. Mears, *Bull. Am. Met. Soc.*, in press.
21. G. C. Hegerl, J. M. Wallace, *J. Clim.* **15**, 2412 (2002).
22. N. P. Gillett, M. R. Allen, S. F. B. Tett, *Clim. Dyn.* **16**, 49 (2000).
23. G. A. Meehl, G. J. Boer, C. Covey, M. Latif, R. J. Stouffer, *Bull. Am. Met. Soc.* **81**, 313 (2000).
24. Whereas all 19 modeling groups used very similar changes in well-mixed greenhouse gases, the changes in other forcings were not prescribed as part of the experimental design. In practice, each group applied different combinations of 20th century forcings and often used different data sets for specifying individual forcings. End dates for the experiment varied between groups and ranged from 1999 to 2003. Some modeling centers performed ensembles of the historical forcing simulation (*25*). An ensemble contains multiple realizations of the same experiment, each initiated from slightly different initial conditions, but with identical changes in external forcings (*2*). This yields many different realizations of the climate "signal" (the response to the imposed forcing changes) plus climate noise. Averaging over multiple

realizations reduces noise and facilitates signal estimation.
25. Materials and methods are available as supporting material on *Science* Online.
26. F. J. Wentz, M. Schabel, *Nature* **403**, 414 (2000).
27. T. M. Smith, R. W. Reynolds, *J. Clim.* **18**, 2021 (2005).
28. P. D. Jones, A. Moberg, *J. Clim.* **16**, 206 (2003).
29. HadCRUT2v is the designation for version 2 of the (variance-corrected) Hadley Centre/Climatic Research Unit surface temperature data set.
30. Q. Fu, C. M. Johanson, S. G. Warren, D. J. Seidel, *Nature* **429**, 55 (2004).
31. P. H. Stone, J. H. Carlson, *J. Atmos. Sci.* **36**, 415 (1979).
32. Here, we define $\overline{X}$ as the arithmetic mean of the ensemble means, i.e., $\overline{X} = \frac{1}{N}\sum_{j=1}^{N} \overline{X}_j$, where N is the total number of models in the IPCC archive and $\overline{X}_j$ is the ensemble mean signal of the jth model. This weighting avoids undue emphasis on results from a single model with a large number of realizations.
33. One measure of ENSO variability is $s(T_{\text{NIÑO}-3.4})$, the standard deviation of sea-surface temperatures in the Niño 3.4 region of the equatorial Pacific. Values of $s(T_S)$ in the 49 IPCC realizations are closely correlated with $s(T_{\text{NIÑO}-3.4})$ (correlation coefficient $r = 0.92$).
34. The theoretical expectation plotted in Fig. 3 was computed by taking the difference of two pseudo-adiabats calculated from surface air parcels with temperatures of 28.0° and 28.2°C and 80% relative humidity. These are conditions typical of deep convective regions over the tropical oceans. The pseudo-adiabats correspond to equivalent potential temperatures of 353.2 and 354.1 K. The assumed temperature difference of 0.2°C corresponds approximately to the total change in tropical ocean temperature over the years 1979 to 1999. Theoretical scaling ratios are relatively insensitive to reasonable variations in the baseline values of surface air temperature and relative humidity, as well as to the magnitude of the surface air temperature increase.
35. V. Ramaswamy *et al.*, in *Climate Change 2001: The Scientific Basis*, J. T. Houghton *et al.*, Eds. (Cambridge Univ. Press, Cambridge, 2001), pp. 349–416.
36. B. D. Santer *et al.*, *Science* **301**, 479 (2003).
37. Work at Lawrence Livermore National Laboratory (LLNL) was performed under the auspices of the U.S. Department of Energy (DOE), Environmental Sciences Division, contract W-7405-ENG-48. A portion of this study was supported by the U.S. DOE, Office of Biological and Environmental Research, as part of its Climate Change Prediction Program. T.M.L.W. was supported by NOAA Office of Climate Programs (Climate Change Data and Detection) grant NA87GP0105. P.W.T. and G.J. were funded by the UK Department of the Environment, Food, and Rural Affairs. We acknowledge the international modeling groups for providing their data for analysis, the Joint Scientific Committee/Climate Variability and Predictability Working Group on Coupled Modeling and their Coupled Model Intercomparison Project and Climate Simulation Panel for organizing the model data analysis activity, and the IPCC WG1 TSU for technical support. The IPCC Data Archive at LLNL is supported by the Office of Science, U.S. DOE. The static MSU weighting functions and UAH MSU data were provided by J. Christy (UAH). We thank I. Held, T. Delworth (both Geophysical Fluid Dynamics Laboratory), D. Easterling (National Climatic Data Center), B. Hicks (NOAA Air Resources Laboratory), and two anonymous reviewers for useful comments. O. Boucher (Hadley Centre), G. Flato (Canadian Climate Centre), and E. Roeckner (Max-Planck Institute for Meteorology) supplied information on the historical forcings used by CNRM-CM3, CCCma-CGCM3.1(T47), and ECHAM5/MPI-OM.

Supporting Online Material
www.sciencemag.org/cgi/content/full/1114867/DC1
Materials and Methods
Fig. S1
Table S1
References and Notes

16 May 2005; accepted 27 July 2005
Published online 11 August 2005;
10.1126/science.1114867
Include this information when citing this paper.

Radiosonde Daytime Biases and Late–20th Century Warming

Steven C. Sherwood,[1]* John R. Lanzante,[2] Cathryn L. Meyer[1]

The temperature difference between adjacent 0000 and 1200 UTC weather balloon (radiosonde) reports shows a pervasive tendency toward cooler daytime compared to nighttime observations since the 1970s, especially at tropical stations. Several characteristics of this trend indicate that it is an artifact of systematic reductions over time in the uncorrected error due to daytime solar heating of the instrument and should be absent from accurate climate records. Although other problems may exist, this effect alone is of sufficient magnitude to reconcile radiosonde tropospheric temperature trends and surface trends during the late 20th century.

Atmospheric models and simple thermodynamic arguments indicate that tropospheric and surface temperature changes should be closely linked (*1*). Radiosonde data during the late 20th century, however (*2–5*), have not shown warming commensurate with that reported for the surface (*1*, *6*, *7*). The main discrepancy is in the Tropics during the last two decades of the 20th century.

A number of design changes to radiosonde systems over the years may have affected trends (*8*). Indeed, the spread of trends among stations well exceeds that implied by satellite data (*9*), suggesting that trends in the observation bias typically exceed those of the actual temperature at individual stations.

[1]Department of Geology and Geophysics, Yale University, New Haven, CT 06520, USA. [2]National Oceanic and Atmospheric Administration/Geophysical Fluid Dynamics Laboratory, Princeton University, Princeton, NJ 08542, USA.

*To whom correspondence should be addressed. E-mail: ssherwood@alum.mit.edu

Among the most serious known problems is bias due to solar heating of the temperature sensor (*10*). For many radiosonde designs this can elevate the temperature several °C above ambient during daylight, an effect that must be removed via an estimated correction. For other designs no correction is standard even though the effect may not be completely absent. Adjustment of climate records for instrument changes using their documented histories is problematic (*8*, *11*).

One can try to remove undocumented artifacts by careful examination of the data itself. Several such efforts have detected hundreds or thousands of apparent artifacts (*3–5*, *12*). Their net effect on trends was found to be large only in the stratosphere. Revised trends were still lower than those indicated by the Microwave Sounding Unit (MSU) in both the troposphere and stratosphere (*13*). Because empirical separation of artificial discontinuities from genuine variability is extremely challenging in correlated time series (*14*, *15*), especially as changes can probably occur in many small steps (*16*), it is not clear how successful the above efforts may have been in detecting discontinuities—or avoiding false adjustments—of amplitudes well below 1°C.

Here we adopt a strategy for quantifying trend errors that does not require identifying specific change events. The strategy applies only to the solar heating error and does not detect other errors. It relies on the fact that the diurnal temperature range in the free troposphere, hence its expected trend, is small and has known characteristics that differ from those expected from a radiation error.

The diurnal temperature variation in Earth's atmosphere is a tide arising from its direct solar heating and from diurnal variations of convective heating driven by the diurnal variation of surface temperature. Atmospheric heating, which occurs primarily in the stratosphere via ozone absorption, drives migrating resonant oscillations that cause temperature fluctuations of several °C in the upper stratosphere. In the troposphere, weaker solar heating occurs due mainly to near-infrared absorption by water with a contribution from dark aerosols. These influences produce diurnal temperature fluctuations of 1°C or less in the free troposphere (*17*). Near the land surface, variations of 5° to 15°C occur due to surface diurnal heating (*18*); over oceans, variations are $\sim$1°C.

Because atmospheric tides are a linear phenomenon (*19*), the diurnal variation of temperature is proportional to that of the heating, though the two need not be in phase. Trends of ~ -0.2°C per decade are evident in the land surface diurnal temperature range (DTR) (*20*), which amount to about 2% of the mean DTR per decade. Tropospheric water vapor and stratospheric ozone changes do not exceed a few percent per decade in recent decades (*21*, *22*), and absorption increases

weakly with concentration due to line saturation (*23*). It follows that tides could not have changed by more than a few percent, or ~ 0.01° to 0.02°C per decade. Because of this, trends in the observed day minus night difference in radiosonde temperatures should provide a sensitive detector of changes in the daytime observation bias.

We examine the diurnal range using the CARDS data set with no adjustments (*24*). We calculated a quantity ΔT equal to the temperature difference between adjacent 0000 UTC and 1200 UTC sonde flights, wherever such pairs were available. Pairs were used regardless of which time of day came first, but ΔT was always defined as temperature at 0000 minus temperature at 1200. At all CARDS stations with sufficient data, we fitted linear trends to ΔT for the same periods (1959 to 1997 and 1979 to 1997) documented by Lanzante *et al*. (LKS) (*3*). LKS considered temperature trends at 87 stations denoted here as the "LKS subset."

Figure 1 shows the 1979 to 1997 trend in stratospheric ΔT at tropical stations plotted by longitude, together with a sinusoid representing the local time of day at 0000. These data show that the trend is in phase with solar heating, with daytime readings growing cooler compared to nighttime readings, and is pervasive.

Although clearest in the stratosphere, these characteristics appear also at tropospheric levels. Indeed, tropospheric and stratospheric ΔT trends are highly correlated in general: for example, r = 0.85 between 50 and 300 hPa over 1959 to 1997. This is not true for natural temperature variability, which tends to be anticorrelated below and above the tropopause in both low and high latitudes (*25*), nor is it true of the tide itself. According to wind data, tidal fluctuations in the troposphere should lag those at 50 hPa by about 6 hours (*26*); this is also simulated by the National Center for Atmospheric Research (NCAR) Community Atmosphere Model (CAM3) (not shown) and appears (albeit with slightly less shift) in carefully selected radiosonde temperature data (*17*). Consequently, we expect peak ΔT magnitudes near 90°E and 90°W. However, before the 1980s ΔT peaked broadly around 0° and 180°, where solar heating was greatest. Only by the late 1990s did the pattern in the troposphere begin to appear as expected.

To quantify the anomalous signal, we defined an additional quantity $\Delta T'$, equal to $\pm\Delta T$ with sign determined by longitude to make it daytime (6 am to 6 p.m.) minus nighttime. To minimize sunrise-time ambiguities, we did not compute $\Delta T'$ at stations within 10° of the 90°E/W meridians.

A map of the trend in upper tropospheric $\Delta T'$ (Fig. 2) reveals regional variations. The largest trends occurred in the Tropics, particularly among Indian, African, and island stations where transitional problems have been reported previously (*3*, *4*, *27*). Trends were small in North America and most of Asia. We see no evidence in Fig. 2 that the ΔT trends at stations in the LKS subset differed systematically from those at neighboring, non-LKS stations. However, the most affected stations tend to be in sparsely sampled areas where they would be strongly weighted in any spatially representative climatology. We omitted all Indian stations from subsequent analysis, because these show anomalously large ΔT and have other problems (*3*, *4*).

Following LKS, we averaged $\Delta T'$ over three belts: the Tropics, the Northern Hemisphere extratropics (NH), and the Southern Hemisphere extratropics (SH). Because tropospheric temperature is expected to lag insolation by about 6 hours, the zonal means $\langle\Delta T'\rangle$

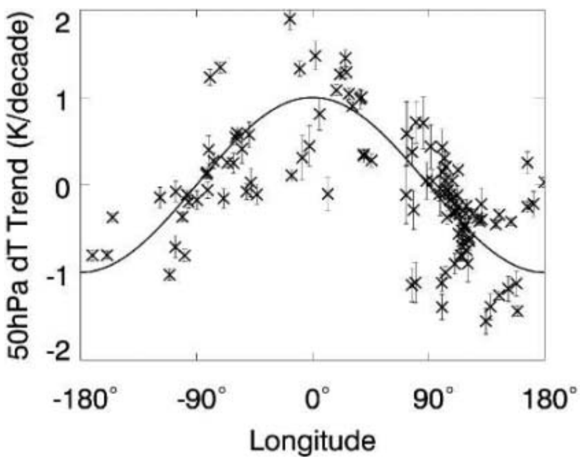

Fig. 1. Trend in 50-hPa ΔT (0000 UTC T minus 1200 UTC T) during 1979 to 1997 versus longitude at all Tropical stations. Sine wave (not a curve fit) represents the negative of solar forcing of ΔT, peaking where 0000 UTC falls at midnight and troughing where it falls at noon. Error bars are 1σ sampling uncertainties.

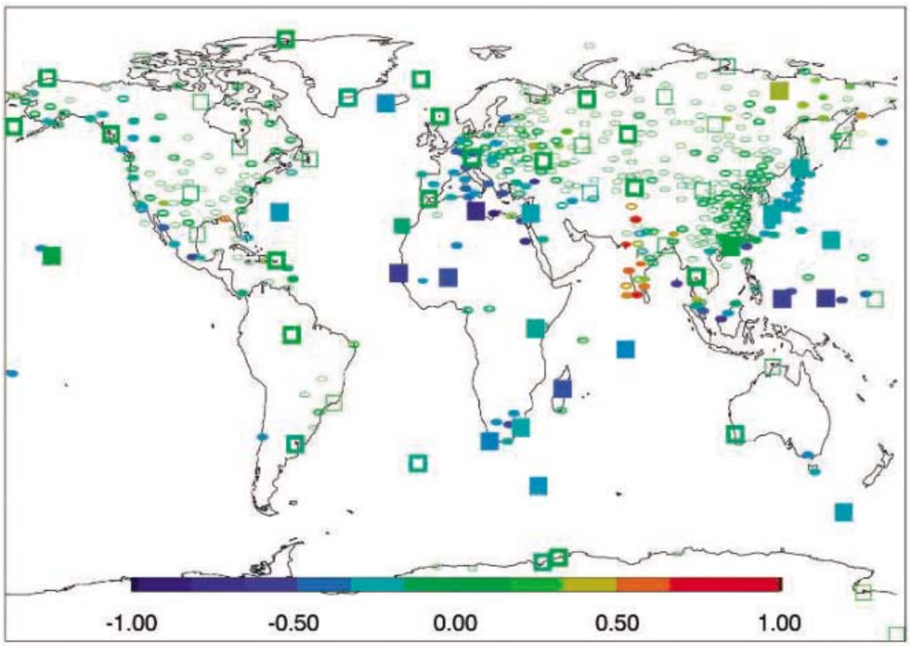

Fig. 2. Trends in 300-hPa day-night difference $\Delta T'$ during 1979 to 1997, in K per decade. LKS station subset is indicated by large squares. One station (Mumbai) is off scale (not shown). Solid symbols are significant at 95% confidence level; thick open symbols do not pass the test at 300 hPa but are significant in the stratosphere (50 hPa).

Table 1. Mean difference in ΔT trend from 1979 to 1997, vertically weighted according to the MSU channel 2 profile, sonde minus MSU (first two columns) among LKS stations; the differences in this quantity between the two station types (third column); and prediction of the latter based on assumptions in text (last column). All quantities are in °C per decade. Figures in parentheses are the number of stations used (*29*).

Daytime only	Twice daily	Difference	Predicted difference
	Tropics		
−0.228 (17)	−0.102 (8)	0.130	0.120 (18)
	Extratropics		
−0.052 (4)	−0.029 (43)	0.023	0.050 (38)

should be small due to near-cancellation of different longitudes.

The time series of tropical upper tropospheric $\langle \Delta T' \rangle$ (Fig. 3), however, shows significant long-term variations. Daytime temperatures warmed before about 1971, reaching values near 0.5°C above nighttime temperatures, then began a slow cooling trend. By the mid- to late 1990s, $\langle \Delta T' \rangle$ finally dropped to a level commensurate with predictions. The trend was particularly strong during the satellite era beginning in 1979. Since 1997 the trend has leveled off.

The linear trend in $\langle \Delta T' \rangle$ is shown by altitude in Fig. 4 for the two LKS time periods, for all three belts. It increases rapidly in the stratosphere, is weak in NH but strong in the other two belts, and is much stronger during the 1979 to 1997 period than the longer period starting in 1959.

This trend appears unrealistic in several respects. First, it is almost two orders of magnitude larger than can be justified physically based on the known forcings. (A run of the CAM3 general circulation model with half-normal ozone, an unrealistically large change, caused tropospheric ΔT to change by only 13%.) Indeed, if a 0.5°C change in diurnal temperature range were caused by a change in daytime heating from any source, then the radiative relaxation time scale of ~1 month for deep perturbations (*28*) would imply a change in equilibrium temperature of 10° to 20°C. Clearly, nothing like this has happened. Moreover, the spatial patterns of this trend are inconsistent with absorbing aerosol (which decreases with height and is scanty in SH) or convective heating (absent in the stratosphere) as a cause. Finally, the strong correlation of the ΔT trend between the troposphere and stratosphere is unnatural.

We are left to propose that the trends are caused by decreases over time in the uncorrected heating of the sensor. This is plausible a priori given the history of radiosonde development and improvement efforts and is fully consistent with all characteristics of the trend here documented: strong in the stratosphere (due mainly to the low thermal diffusivity of thin air) and in phase with solar heating. The smaller effect in NH is consistent with the expected superior stability of those stations.

The trend reported from a particular set of stations can be adjusted to a nighttime-only value by adding an adjustment δ_{sol} equal to the trend in $\langle \Delta T' \rangle$ multiplied by a factor f representing the fraction of the reported trend coming from daytime data (*29*). This assumes that stations that do not collect nighttime data are just as susceptible to spurious daytime trends, on average, as those that do.

MSU Channel 2 data can be used to test this assumption. We require only trend differences between sites, which are much more robust to analysis method than the overall MSU trend itself. We use diurnal-mean MSU trends from the University of Alabama at Huntsville at LKS station locations (*3*). Our assumption implies that daytime-only stations will cool more compared to colocated MSU retrievals than will twice-daily stations. The calculated differences, given in Table 1 (we combine SH and NH here because there are no daytime-

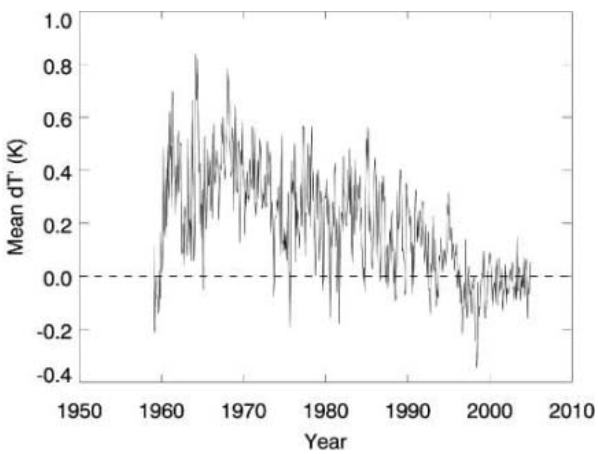

Fig. 3. Monthly mean 300-hPa $\langle \Delta T' \rangle$, the average day-night temperature difference, at the 10 LKS tropical stations spanning the 1959 to 1997 period.

Table 2. Layer-average tropospheric and stratospheric temperature trends (in K per decade) reported by LKS for unhomogenized data ("orig"), and with solar heating bias removed ("new"). Factor f is specific to LKS station subset. Uncertainties are 1σ sampling uncertainty in the solar heating bias correction only.

	Tropics	NH extratropics	SH extratropics
	1979–1997		
f	0.84	0.50	0.67
50–100 hPa (orig)	−1.30	−0.85	−1.04
50–100 hPa (new)	−0.81 ± 0.08	−0.78 ± 0.03	−0.67 ± 0.08
850–300 hPa (orig)	−0.02	+0.10	−0.07
850–300 hPa (new)	+0.14 ± 0.04	+0.14 ± 0.02	+0.01 ± 0.04
	1959–1997		
50–100 hPa (orig)	−0.71	−0.43	−0.50
50–100 hPa (new)	−0.52 ± 0.06	−0.38 ± 0.02	−0.30 ± 0.07
850–300 hPa (orig)	+0.17	+0.06	+0.25
850–300 hPa (new)	+0.23 ± 0.03	+0.07 ± 0.01	+0.30 ± 0.03

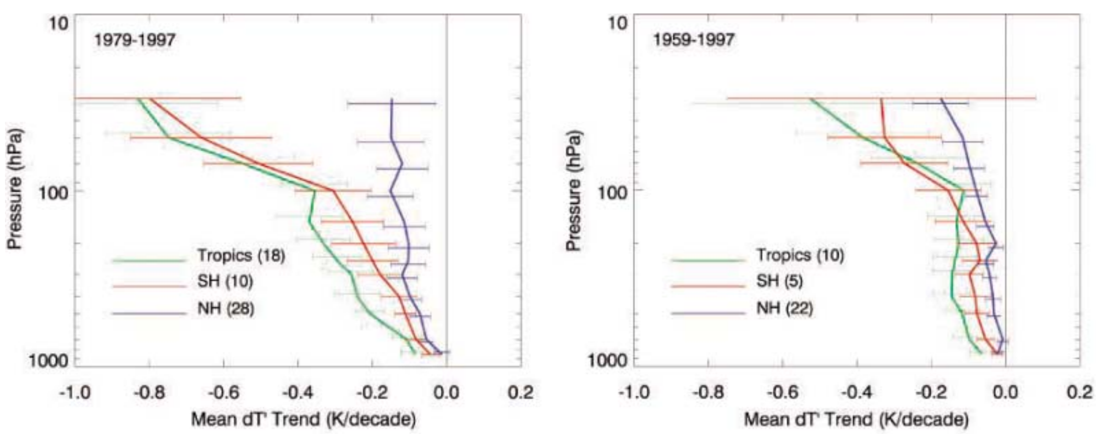

Fig. 4. Trend in $\langle \Delta T' \rangle$ during 1979 to 1997 (top) and 1959 to 1997 (bottom) at LKS stations. Green, Tropics (30°N to 30°S); red, Southern Hemisphere (90°S to 30°S); blue, Northern Hemisphere (30°N to 90°N). Error bars are 1σ sampling uncertainty. Figures in parentheses are the number of stations used.

only LKS stations in NH), are fully consistent with this assumption, particularly for the tropical stations. In the extratropics there are only four daytime-only stations so the MSU test is less meaningful, but the two independent estimates do agree within 0.03°C per decade.

To illustrate the importance of the heating bias, we have computed its impact δ_{sol} on the trends at LKS stations. The LKS f factors, unhomogenized trends, and trends adjusted only for solar heating are given for the middle troposphere and lower stratosphere in Table 2. In the stratosphere, our δ_{sol} is similar to the total adjustments by LKS and others, with trends moving closer to those from MSU (*13*). At the tropical tropopause (of relevance to stratospheric water vapor), δ_{sol} is somewhat smaller than LKS's. In the troposphere, however, δ_{sol} is much larger than previous adjustments. Indeed, the tropical trend with this adjustment (0.14°C per decade over 1979 to 1997) would be consistent with model simulations driven by observed surface warming, which was not true previously (*1*). One independent indication that the solar-adjusted trends should be more accurate is their consistency across latitude belts: for the period 1979 to 1997, the spread of values fell by 70% in the lower stratosphere and 25% in the troposphere.

Though this is encouraging, our confidence in these nighttime trends is still limited given that other radiosonde errors have not been addressed. SH trends from 1958 to 1997 seem unrealistically high in the troposphere, especially with the δ_{sol} adjustment, although this belt has by far the worst sampling. Previous homogenization efforts typically produced small changes to mean tropospheric trends, which could mean that other error trends cancel out δ_{sol} in the troposphere. In our judgment, however, such fortuitous cancellation of independent errors is unlikely compared to the possibility that most solar artifacts were previously either missed or their removal negated by other, inaccurate adjustments. To be detected easily, a shift must be large and abrupt, but δ_{sol} was spread out over so many stations (79% of stations during 1979 to 1997 and 90% during 1959 to 1997 experienced ΔT trends significant at 95% level), at such modest levels, and of sufficient frequency at many stations that many may have been undetectable. Most important, jumps in the difference between daytime and nighttime monthly means would be detectable at only a few tropical stations because most lack sufficient nighttime data. In any case, we conclude that carefully extracted diurnal temperature variations can be a valuable troubleshooting diagnostic for climate records, and that the uncertainty in late–20th century radiosonde trends is large enough to accommodate the reported surface warming.

References and Notes

1. B. D. Santer *et al.*, *Science* **309**, 1551 (2005); published online 11 August 2005 (10.1126/science.1114867).
2. J. K. Angell, *J. Clim.* **16**, 2288 (2003).
3. J. R. Lanzante, S. A. Klein, D. J. Seidel, *J. Clim.* **16**, 241 (2003).
4. D. E. Parker *et al.*, *Geophys. Res. Lett.* **24**, 1499 (1997).
5. P. W. Thorne *et al.*, *J. Geophys. Res.*, in press.
6. D. H. Douglass, B. D. Pearson, S. F. Singer, P. C. Knappenberger, P. J. Michaels, *Geophys. Res. Lett.* **31**, L13207 (2004).
7. D. J. Gaffen *et al.*, *Science* **287**, 1242 (2000).
8. D. E. Parker, D. I. Cox, *Int. J. Climatol.* **15**, 473 (1995).
9. M. Free, D. J. Seidel, *J. Geophys. Res.* **110**, D07101 (2005).
10. J. K. Luers, R. E. Eskridge, *J. Appl. Meteorol.* **34**, 1241 (1995).
11. I. Durre, T. C. Peterson, R. S. Vose, *J. Clim.* **15**, 1335 (2002).
12. L. Haimberger, "Homogenization of radiosonde temperature time series using ERA-40 analysis feedback information," Tech. Rep. European Center for Medium Range Weather Forecasting (2005), ERA-40 Project Report Series 23.
13. D. J. Seidel *et al.*, *J. Clim.* **17**, 2225 (2004).
14. P. R. Krishnaiah, B. Q. Miao, *Handbook of Statistics*, P. R. Krishnaiah, C. R. Rao, Eds. (Elsevier, New York, 1988), vol. 7.
15. M. Free *et al.*, *Bull. Am. Meteorol. Soc.* **83**, 891 (2002).
16. W. J. Randel, F. Wu, in preparation.
17. D. J. Seidel, M. Free, J. Wang, *J. Geophys. Res.* **110**, D09102 (2005).
18. A. Dai, K. E. Trenberth, T. R. Karl, *J. Clim.* **12**, 2451 (1999).
19. S. Chapman, R. S. Lindzen, *Atmospheric Tides* (D. Reidel, Norwell, MA, 1970).
20. D. R. Easterling *et al.*, *Science* **277**, 364 (1997).
21. D. J. Gaffen, R. J. Ross, *J. Clim.* **12**, 811 (1999).
22. W. J. Randel *et al.*, *Science* **285**, 1689 (1999).
23. K. N. Liou, T. Sasamori, *J. Atmos. Sci.* **32**, 2166 (1975).
24. R. E. Eskridge *et al.*, *Bull. Am. Meteorol. Soc.* **76**, 1759 (1995).
25. H. Riehl, *Tropical Meteorology* (McGraw Hill, New York, 1954).
26. S. C. Sherwood, *Geophys. Res. Lett.* **27**, 3525 (2000).
27. J. R. Christy, R. W. Spencer, W. B. Norris, W. D. Braswell, D. E. Parker, *J. Atmos. Oceanic Technol.* **20**, 613 (2003).
28. T. Sasamori, J. London, *J. Atmos. Sci.* **23**, 543 (1966).
29. Data files and further information on methods, uncertainty, and interpretation of our results are available as supporting material on *Science* Online.

30. S.C.S. thanks J. Risbey and K. Braganza for useful discussions. This work was supported by the National Oceanic and Atmospheric Administration Climate and Global Change Program award NA03OAR4310153, and by NSF ATM-0134893.

Supporting Online Material

www.sciencemag.org/cgi/content/full/1115640/DC1
Methods
SOM Text
Data files
References and Notes

2 June 2005; accepted 27 July 2005
Published online 11 August 2005;
10.1126/science.1115640
Include this information when citing this paper.

The Transcriptional Landscape of the Mammalian Genome

The FANTOM Consortium* and RIKEN Genome Exploration Research Group and Genome Science Group (Genome Network Project Core Group)*

This study describes comprehensive polling of transcription start and termination sites and analysis of previously unidentified full-length complementary DNAs derived from the mouse genome. We identify the 5′ and 3′ boundaries of 181,047 transcripts with extensive variation in transcripts arising from alternative promoter usage, splicing, and polyadenylation. There are 16,247 new mouse protein-coding transcripts, including 5154 encoding previously unidentified proteins. Genomic mapping of the transcriptome reveals transcriptional forests, with overlapping transcription on both strands, separated by deserts in which few transcripts are observed. The data provide a comprehensive platform for the comparative analysis of mammalian transcriptional regulation in differentiation and development.

The production of RNA from genomic DNA is directed by sequences that determine the start and end of transcripts and splicing into mature RNAs. We refer to the pattern of transcription control signals, and the transcripts they generate, as the transcriptional landscape. To describe the transcriptional landscape of the mammalian genome, we combined full-length cDNA isolation (*1*) and 5′- and 3′-end sequencing of cloned cDNAs, with new cap-analysis gene expression (CAGE) and gene identification signature (GIS) and gene signature cloning (GSC) ditag technologies for the identification of RNA and mRNA sequences corresponding to transcription initiation and termination sites (*2*, *3*). A detailed description of the data sets generated, mapping strategies, and depth of coverage of the mouse transcriptome is provided in supporting online material (SOM) text 1 (Tables 1 and 2). We have identified paired initiation and termination sites, the boundaries of independent transcripts, for 181,047 independent transcripts in the transcriptome (Table 3). In total, we found 1.32 5′ start sites for each 3′ end and 1.83 3′ ends for each 5′ end (table S1). Based on these data, the number of transcripts is at least one order of magnitude larger than the estimated 22,000 "genes" in the mouse genome (*4*) (SOM text 1), and the

large majority of transcriptional units have alternative promoters and polyadenylation sites. The use of genome tiling arrays (*5*–*7*) in humans has also implied that the number of transcripts encoded by the genome is at least 10 times as great as the number of "genes." To extend the mouse data, two HepG2 CAGE libraries, one constructed with random primers and the other with oligo-dT primers, were combined to produce 1,000,000 CAGE tags. Mapping of these tags to the human genome identified the likely promoters and transcriptional starting site (TSS) of many of the gene models identified by tiling array, also called transfrags (*5*), and clearly indicates that the same level of transcriptional diversity occurs in humans as in mice (table S2).

The mapping of ends of transcripts can be used to identify the genomic span of the primary transcript. Figure 1A shows length distributions of the predicted genomic regions spanned by mouse cDNAs showing a bimodal distribution and compares them with one peak for unspliced and another for spliced RNAs. At the upper end of the distribution are candidate mega transcripts (transcripts originating from genomic regions in the order of millions of base pairs). For example, we located six pairs of genome signature cloning (GSC) ditags to RIKEN clone ID 9330159J16 and corresponding RIKEN expressed sequence tags (ESTs). This clone encodes for a previously unidentified large transcript that is similar to a protein tyrosine phosphatase, receptor type D (accession no. BC086654), the genomic structure of which has not been previously reported (*8*). The predicted mRNA is 2475 base pairs in length but spans a genomic region of 2.2 megabases (Mb).

We previously coined the term transcriptional units (TUs), which groups mRNAs that share at least one nucleotide and have the same genomic location and orientation (*9*). However, TU fusions can join unrelated and differently annotated transcripts (SOM text 2). Therefore, we define a transcriptional framework (TK) as grouping transcripts that share common expressed regions as well

The FANTOM Consortium:
P. Carninci,† T. Kasukawa, S. Katayama, J. Gough,† M. C. Frith,† N. Maeda, R. Oyama, T. Ravasi,† B. Lenhard,† C. Wells,† R. Kodzius, K. Shimokawa, V. B. Bajic,† S. E. Brenner, S. Batalov, A. R. R. Forrest, M. Zavolan, M. J. Davis, L. G. Wilming, V. Aidinis, J. E. Allen, A. Ambesi-Impiombato, R. Apweiler, R. N. Aturaliya, T. L. Bailey, M. Bansal, L. Baxter, K. W. Beisel, T. Bersano, H. Bono, A. M. Chalk, K. P. Chiu, V. Choudhary, A. Christoffels, D. R. Clutterbuck, M. L. Crowe, E. Dalla, B. P. Dalrymple, B. de Bono, G. Della Gatta, D. di Bernardo, T. Down, P. Engstrom, M. Fagiolini, G. Faulkner, C. F. Fletcher, T. Fukushima, M. Furuno, S. Futaki, M. Gariboldi, P. Georgii-Hemming, T. R. Gingeras, T. Gojobori, R. E. Green, S. Gustincich, M. Harbers, Y. Hayashi, T. K. Hensch, N. Hirokawa, D. Hill, L. Huminiecki, M. Iacono, K. Ikeo, A. Iwama, T. Ishikawa, M. Jakt, A. Kanapin, M. Katoh, Y. Kawasawa, J. Kelso, H. Kitamura, H. Kitano, G. Kollias, S. P. T. Krishnan, A. Kruger, S. K. Kummerfeld, I. V. Kurochkin, L. F. Lareau, D. Lazarevic, L. Lipovich, J. Liu, S. Liuni, S. McWilliam, M. Madan Babu, M. Madera, L. Marchionni, H. Matsuda, S. Matsuzawa, H. Miki, F. Mignone, S. Miyake, K. Morris, S. Mottagui-Tabar, N. Mulder, N. Nakano, H. Nakauchi, P. Ng, R. Nilsson, S. Nishiguchi, S. Nishikawa, F. Nori, O. Ohara, Y. Okazaki, V. Orlando, K. C. Pang, W. J. Pavan, G. Pavesi, G. Pesole, N. Petrovsky, S. Piazza, J. Reed, J. F. Reid, B. Z. Ring, M. Ringwald, B. Rost, Y. Ruan, S. L. Salzberg, A. Sandelin, C. Schneider, C. Schönbach, K. Sekiguchi, C. A. M. Semple, S. Seno, L. Sessa, Y. Sheng, Y. Shibata, H. Shimada, K. Shimada, D. Silva, B. Sinclair, S. Sperling, E. Stupka, K. Sugiura, R. Sultana, Y. Takenaka, K. Taki, K. Tammoja, S. L. Tan, S. Tang, M. S. Taylor, J. Tegner, S. A. Teichmann, H. R. Ueda, E. van Nimwegen, R. Verardo, C. L. Wei, K. Yagi, H. Yamanishi, E. Zabarovsky, S. Zhu, A. Zimmer, W. Hide, C. Bult,† S. M. Grimmond, R. D. Teasdale, E. T. Liu,† V. Brusic, J. Quackenbush,† C. Wahlestedt,† J. S. Mattick,† D. A. Hume†
RIKEN Genome Exploration Research Group and Genome Science Group (Genome Network Project Core Group):
C. Kai, D. Sasaki, Y. Tomaru, S. Fukuda, M. Kanamori-Katayama, M. Suzuki,† J. Aoki, T. Arakawa, J. Iida, K. Imamura, M. Itoh, T. Kato, H. Kawaji, N. Kawagashira, T. Kawashima, M. Kojima, S. Kondo, H. Konno, K. Nakano, N. Ninomiya, T. Nishio, M. Okada, C. Plessy, K. Shibata, T. Shiraki, S. Suzuki, M. Tagami, K. Waki, A. Watahiki, Y. Okamura-Oho, H. Suzuki, J. Kawai.
General Organizer:
Y. Hayashizaki†‡

*Affiliations can be found on *Science* Online (available at www.sciencemag.org/cgi/content/full/309/5740/1559/DC1).
†These authors are core authorship members.
‡To whom correspondence should be addressed. E-mail: yosihide@gsc.riken.jp

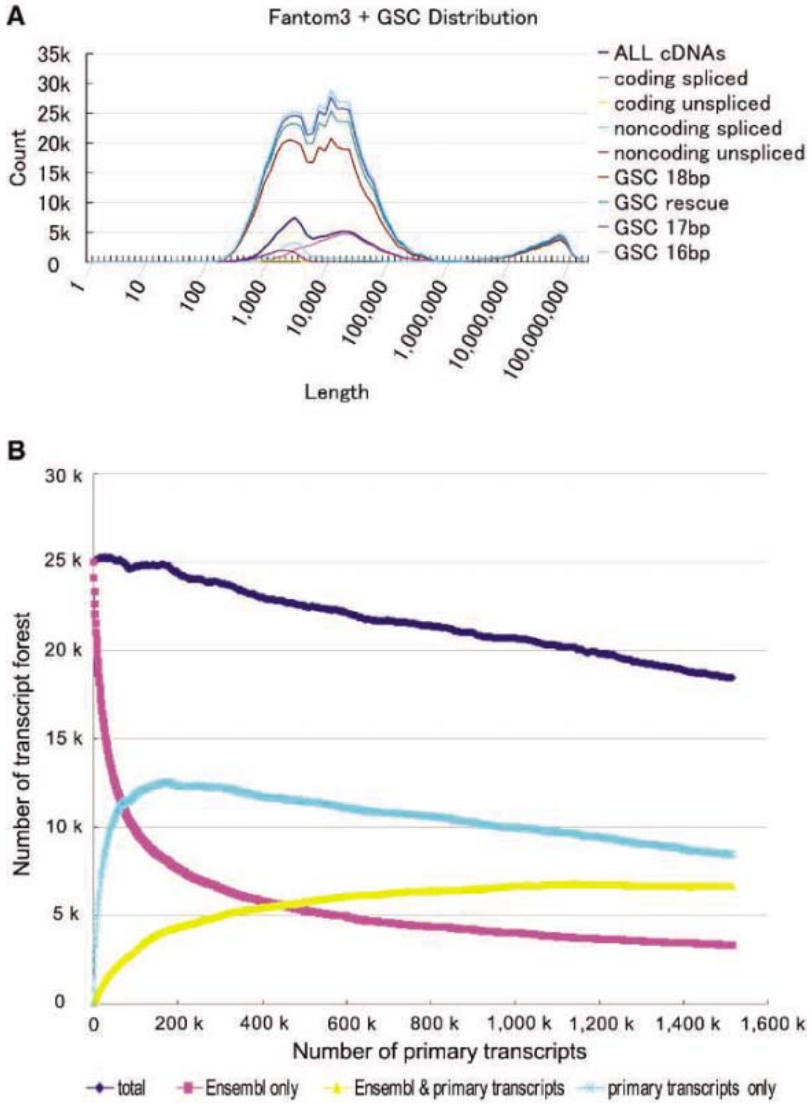

Fig. 1. Genome-transcriptome relation. (**A**) Genome span covered by full-length cDNA and GIS/GSC ditags shows similar distribution with two main peaks. Ditags mapping follows the same distribution profile at various mapping thresholds, with a minimum around 2 to 2.5 Mb. Mapping events above this genomic span are nonspecific. Count displays the number of events in the size interval. (**B**) Asymptotic unit collapse. Due to extensive overlap of the genome, transcripts overlap to the extent that they collapse to a few GFs. Simulating addition of ditags shows the collapsing rate of the known annotated genes into 9976 elements only. Primary transcripts only, GFs identified by GSC ditags only; Ensembl only, GFs produced by the 3332 Ensembl-only annotated transcripts; total, the total number of GFs.

as splicing events, TSS, or termination events (SOM text 1).

TKs can be clustered together into transcript forests (TFs), genomic regions that are transcribed on either strand without gaps. TFs encompass 62.5% of the genome (table S1) and are separated by regions devoid of transcription, or transcription deserts. With the inclusion of GSC tags in addition to full-length cDNA and paired EST sequences, the estimated total number of transcript forests is 18,461,which will collapse further with increasing depth of coverage (Fig. 1B).

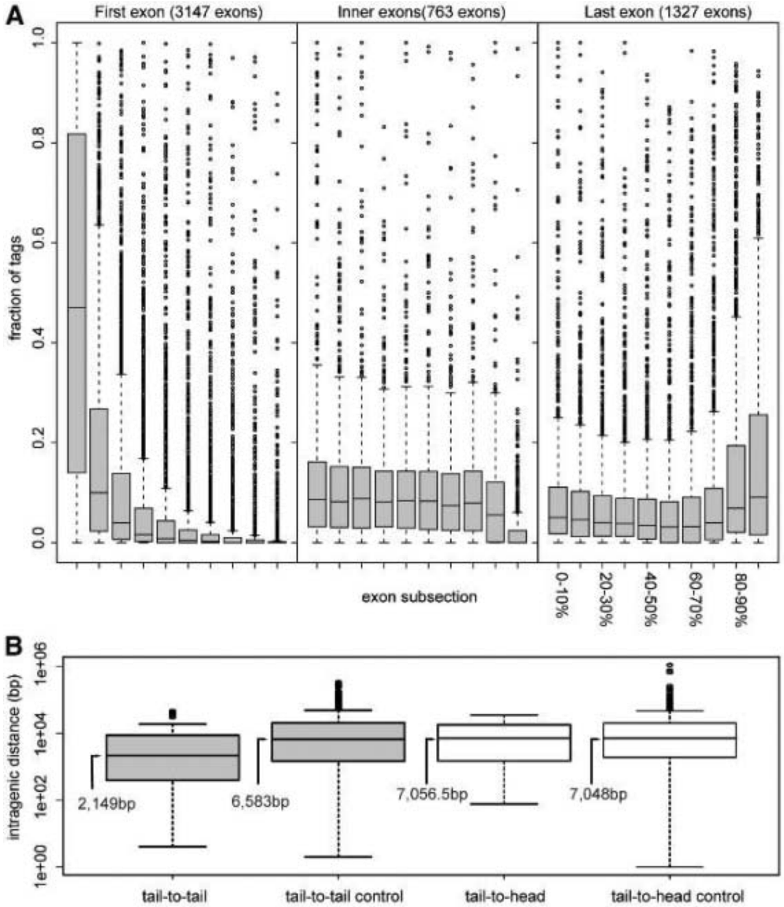

Fig. 2. Transcription originating in 3′UTRs. (**A**) For each analyzed exon, the fraction of tags mapped to 10 equally large subsections of the exon was calculated. (Left) CAGE tags mapping to the first exon are prevalently located in the first part of the exon. (Middle) CAGE tags mapping to internal exons are uniformly distributed. (Right) Last exons show a distinct overrepresentation of CAGE tags mapping close to the 3′ end. (**B**) Distance to the closest downstream gene for the set of highly expressed TUs that have extreme tag density in the 3′ of the terminal exons. Transcript pairs were grouped into tail-to-head (3′ exon and downstream TU on same strand) or tail-to-tail (3′ exon and downstream TU on opposite strand) configurations. Remaining TUs were used as control groups. For TUs with strong 3′ transcriptional activity, the distance to the next TU is significantly smaller than expected when the gene pair is in a tail-to-tail configuration ($P \leq 0.001107$, Wilcoxon test), suggesting regulatory mechanisms based on natural antisense influencing the downstream gene (*26*).

Table 1. Data set resources.

	Total	Number of libraries	Safely mapped
RIKEN full-length cDNAs	102,801	237	100,313
Public (non-RIKEN) mRNAs	56,009		52,119
CAGE tags (mouse)	11,567,973	145	7,151,511
CAGE tags (human)	5,992,395	24	3,106,472
GIS ditags	385,797	4	118,594
GSC ditags	2,079,652	4	968,201
RIKEN 5′ESTs	722,642	266	607,462
RIKEN 3′ESTs	1,578,610	265	907,007
5′/3′EST pairs of RIKEN cDNA	448,956	264	277,702

The approach used to isolate full-length cDNAs, based on library subtraction and previously unidentified 5′/3′ end selection before full-insert sequencing, was weighted toward identification of representative transcripts. Nevertheless, 78,393 different splicing variants were identified, such that 65% of TUs contain multiple splice variants (Table 2), an increase from our previous estimate (41%) (*9*). This is still expected to be an underestimate, and new approaches will be necessary for a full evaluation of exon diversity (*10*).

Transcript diversity also arises through alternative termination. Little is known about sequence motifs that control alternative polyadenylation. We identified 27 motif families with six or more nucleotides that were statistically overrepresented within 120 base pairs of the polyadenylation site of individual transcripts in our data set. These motifs represent candidate modulators of polyadenylation site for eight unconventional alternative polyadenylation signals (*1*) (table S3). In addition, we found a widespread motif family with sequence TTGTTT, which was associated with both the canonical (AAUAAA and AUUAAA) and unconventional signals (*1*, *11*).

Gene names of 56,722 transcripts that were protein coding were assigned according to annotation rules (*9*, *12*). Their encoded protein sequences were combined with the publicly available proteins supported by cDNA sequences (*8*). This generated a nonredundant set of 51,135 proteins with experimental evidence [isoform protein set (IPS)], 36,166 of which are complete (complete IPS). By comparison, the mammalian gene collection (http://mgc.nci.nih.gov) has cloned, as of July 2005, only ~16,700 transcripts (11,514 nonredundant). In the FANTOM3 data set, 16,274 protein sequences are newly described. Their splice variants were grouped together into 13,313 TKs. For 9002 of these, a previously known sequence maps to the same TK (locus), but 4311 clusters (5154 different proteins) map to new TKs (SOM text 3).

There are a total of 32,129 protein-coding TKs on the genome, of which 19,197 have only a single protein splice form, although 2525 of those do have an alternative noncoding splice variant. The SUPERFAMILY analysis of structural classification of protein database (SCOP) domain architectures (*13*) was carried out for each sequence. Of the 12,932 TKs that show variation in splicing, 8365 showed variation in SCOP domain prediction. Of the 12,932 variable TKs, 2392 produce proteins with different observed contents of InterPro entries. More than two alternatives were observed in 439 of the 2392 InterPro-variable TKs. Thus, in the majority of variable loci, splicing controls some aspect of domain content or organization. To seek evidence for such an impact in specific sets of regulatory proteins, we compared a representative protein set

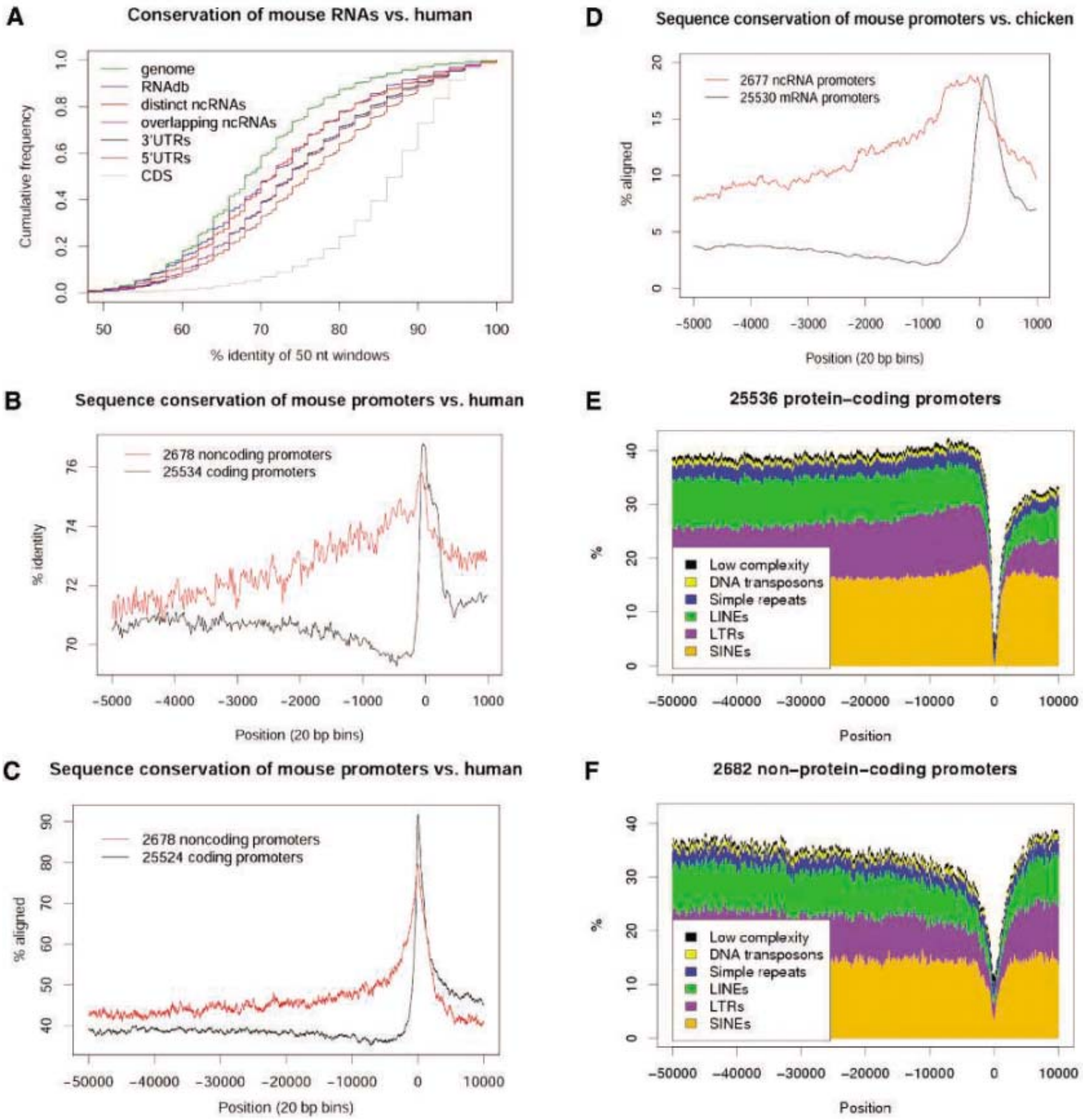

Fig. 3. Noncoding RNA promoters are highly conserved. (**A**) Human-mouse conservation of coding and noncoding RNAs compared with random genome sequence. (**B** and **C**) Promoters conservation of noncoding and coding mRNA evaluated (B) by identity and (C) by alignment. (**D**) Overlap of promoters of ncRNAs. (**E** and **F**) Promoters of coding mRNAs contain a larger fraction of low complexity and repeats than noncoding promoters. LINE, long interspersed nuclear elements; LTR, long terminal repeats; SINEs, short interspersed nuclear elements.

(RPS) and a variant protein set (VPS) of phosphatases and kinases that have been comprehensively annotated (*14*) by looking at domain composition counts (table S4). These phosphoregulators could be functionally modulated through alteration in their intracellular location. Among the 21 receptor tyrosine phosphatase loci, we identified 23 variant transcripts from 14 loci with predicted changes to the subcellular localization and function of the encoded peptides. Of these, we identified two noncatalytic classes: secreted (10) and tethered (3). Furthermore, we identified two catalytic classes that lack the extracellular domains: catalytic only (5) and tethered catalytic (5). Similarly, among the 77 receptor kinase loci, we identified 41 variant transcripts from 33 loci which encode secreted (16), tethered (10), catalytic only (7), or other tethered catalytic (8) peptides. We then analyzed the membrane organization splicing variants class within the full set of TUs (table S5), which revealed 1287 TUs that exhibit alternative initiation, splicing, and termination, likely to yield variant isoforms of membrane proteins that differ in their cellular location.

Of the 102,281 FANTOM3 cDNAs, 34,030 lack any protein-coding sequence (CDS) and are annotated as non–protein coding RNA (ncRNA) (*6*, *15*) (table S1). Many putative ncRNAs were singletons in the full-length cDNA set. Among the FANTOM3 cDNA set there was additional support from ESTs, CAGE tags, or other cDNA clones overlapping both the starting and termination sites for 41,025 cDNAs, of which only 3652 were ncRNAs. This supported ncRNA set includes many known ncRNAs (SOM text 4), and many are dynamically expressed (SOM text 5). Following these same criteria, 3012 from 8961 cDNAs previously annotated as truncated CDS were supported as genuine transcripts and are believed to be ncRNA variants of protein-coding cDNAs.

Many ncRNAs appear to start from initiation sites in 3′ untranslated regions (3′UTRs) of protein-coding loci (*16*). The normalized distribution of CAGE tags along annotated exons of known transcripts with more than 300 mapped tags each is shown in Fig. 2A. As expected, the highest tag density on average occurs at the 5′ end, but there is also a substantial increase of tags in the last one-fifth of the 3′UTR. Strong evidence of 3′ end initiation was correlated with a short intergenic distance when in tail-to-tail orientation with a neighboring gene (Fig. 2B), suggesting a possible role in an intergenic regulatory interaction.

The function of ncRNAs is a matter of debate (*17*). Some ncRNAs are highly conserved even in distant species: 1117 out of 2886

Table 2. Transcript grouping and classification. The extent of splice variation was calculated by excluding T-cell receptor and immunoglobulin genes from the transcripts. The remaining 144,351 transcripts were grouped in 43,539 TUs, of which 18,627 (42.8%) consist of single-exon transcripts, 8110 (18.6%) contain a single multiexon transcript, and the remaining 16,802 TUs (38.6%) contain at least two spliced transcripts. Among these TUs, 5862 (34.9%) show no evidence of splice variation, whereas 10,940 (65.1%) contain multiple splice forms.

	Total	Average per TU cluster	Average per TK cluster
Total number of transcripts	158,807	7.59	7.30
RIKEN full-length	102,801		
Public (non-RIKEN) mRNAs	56,006		
GFs	25,027	1.20	1.15
Framework clusters	31,992	1.53	1.47
TUs	44,147	2.11	2.03
With proteins	20,929	1.00	0.96
Without proteins	23,218	1.11	1.07
TK	45,142	2.16	2.07
With proteins	21,757	1.04	1.00
Without proteins	23,385	1.12	1.07
Splicing patterns	78,393	3.75	3.60

Table 3. Determination of transcripts start/end accuracy. Two pieces of evidence (cDNA, tags, ditags, EST, and 5′-3′ EST pairs) are required when TSS/terminations lie inside larger transcripts, and one piece of evidence is required when they extend or identify new transcripts. Reliable indicates that both ends are associated with reliable tag clusters.

	Total	Reliable
Total 5′/3′-end pair sequence	1,507,122	1,336,397
5′/3′-end pair cluster	313,821	181,047

overlap chicken sequences, of which 780 do not overlap known CDS and 438 do not overlap known mRNAs on either strand, whereas 68 out of 2886 have BLAST-like alignment tool (BLAT) alignments to the Fugu genome, of which 40 do not overlap known CDS on either strand. These ncRNAs are at least as conserved as a reference set of known ncRNAs (Fig. 3A), contrary to a previous study (*17*). However, ncRNAs are slightly less conserved on average than 5′ or 3′UTRs. In contrast, the promoter regions of ncRNAs are generally more conserved than the promoters of the protein-coding mRNA, not only between human and mouse but also down in the evolutionary scale to chicken (Fig. 3, B to F), and they contain binding sites for known transcription factors (*18*). We conclude that the large majority of ncRNAs that we analyzed display positional conservation across species. In considering function, one might conclude that the act of transcription from the particular location is either important or a consequence of genomic structure or sequence (for example, enhancers such as that of the globin locus can act as promoters), the transcript may function through some kind of sequence-specific interaction with the DNA sequence from which it is derived, or many noncoding RNAs have other targets but are evolving rapidly (*19*, *20*).

New databases have been created for cDNA annotation, expression, and promoter analysis (http://fantom3.gsc.riken.jp/db/ and SOM text 6). The databases integrate common gene and tissue ontologies like eVOC mouse developmental ontologies (*21*), cross mapped to Edinburgh Mouse Atlas Project (EMAP) ontology terms (*22*). These eVOC terms allow analysis standardization of RNA samples used for cDNA and CAGE libraries in both mouse and human and were included into the DNA Database of Japan (DDBJ) data submission (*23*).

Analysis of the output of FANTOM2 suggested that there were many more transcripts still to be discovered (*24*). Here, we have confirmed that the majority of the mammalian genome is transcribed, commonly from both strands. Such transcriptional complexity implies caveats in interpretation of microarray experiments (*25*) and genome manipulation in mice, because these will commonly interrupt or interrogate more than one TK. Although the current overview gives us an indication of the complexity of the mammalian transcriptional landscape and a new set of tools to begin to understand transcriptional control (for example a very large set of promoters that can be ascribed to distinct classes) (*16*), we also gain insight into the scale of the task that remains. The ditag data indicate the existence of very long transcripts whose isolation and sequencing will require new cloning and sequencing strategies. Although we have isolated and sequenced many putative ncRNAs, the FANTOM3 collection only contains 40% of those already known. Finally, the focus has been on polyadenylated mRNAs that are processed and exported to the cytoplasm. Recently, Gingeras and colleagues (*5*) have shown that the set of nonpolyadenylated nuclear RNAs may be very large, and that many such transcripts arise from so-called intergenic regions (*7*). The future can only reveal additional complexity in the mammalian transcriptome.

References and Notes

1. P. Carninci *et al.*, *Genome Res.* **13**, 1273 (2003).
2. T. Shiraki *et al.*, *Proc. Natl. Acad. Sci. U.S.A.* **100**, 15776 (2003).
3. P. Ng *et al.*, *Nat. Methods* **2**, 105 (2005).
4. R. H. Waterston *et al.*, *Nature* **420**, 520 (2002).
5. D. Kampa *et al.*, *Genome Res.* **14**, 331 (2004).
6. P. Bertone *et al.*, *Science* **306**, 2242 (2004).
7. J. Cheng *et al.*, *Science* **308**, 1149 (2005).
8. R. L. Strausberg *et al.*, *Proc. Natl. Acad. Sci. U.S.A.* **99**, 16899 (2002).
9. Y. Okazaki *et al.*, *Nature* **420**, 563 (2002).
10. A. Watahiki *et al.*, *Nat. Methods* **1**, 233 (2004).
11. V. Bajic, in preparation.
12. N. Maeda, R. Oyama, in preparation.
13. J. Gough, in preparation.
14. A. R. Forrest *et al.*, *Genome Res.* **13**, 1443 (2003).
15. Materials and methods are available as supporting material on *Science* Online.
16. P. Carninci *et al.*, in preparation.
17. J. Wang *et al.*, *Nature* **431**, 1 p following 757; discussion following 757 (2004).
18. S. Cawley *et al.*, *Cell* **116**, 499 (2004).
19. T. Ravasi, D. A. Hume, in *Encyclopedia of Genetics, Genomics, Proteomics, and Bioinformatics*, L. B. Jorde, P. F. R. Little, M. J. Dunn, S. Subramaniam, Eds. (John Wiley & Sons, Chichester, UK, in press), part 2.3.
20. J. S. Mattick, I. V. Makunin, *Hum. Mol. Genet.*, in press.
21. J. Kelso *et al.*, *Genome Res.* **13**, 1222 (2003).
22. R. A. Baldock *et al.*, *Neuroinformatics* **1**, 309 (2003).
23. All sequences (CAGE, and cDNA) are available through DDBJ to other public databases. The cDNA clones are available.
24. Y. Okazaki, D. A. Hume, *Genome Res.* **13**, 1267 (2003).
25. E. Marshall, *Science* **306**, 630 (2004).
26. RIKEN Genome Exploration Research Group and Genome Science Group (Genome Network Project Core Group) and the FANTOM Consortium, *Science* **309**, 1564 (2005).

27. We thank H. Atsui, A. Hasegawa, Y. Hasegawa, K. Hayashida, H. Himei, F. Hori, T. Iwashita, S. Kanagawa, C. Kawazu, M. Aoki, K. Murakami, M. Murata, H. Nishida, M. Nishikawa, K. Nomura, M. Ohno, Y. Onodera, N. Sakazume, H. Sato, Y. Shigemoto, N. Suzuki, Y. Takeda, Y. Tsujimura, K. Yoshida for discussion, encouragement, and technical assistance. We thank A. Wada, T. Ogawa, M. Muramatsu, and all the members of RIKEN Yokohama Research Promotion Division for support and encouragement. We also thank the Laboratory of Genome Exploration Research Group for secretarial and technical assistance, Yokohama City University for providing human samples, and computational resources of the RIKEN Super Combined Cluster (RSCC). This work was mainly supported by Research Grant for the Genome Network Project from MEXT, the RIKEN Genome Exploration Research Project from MEXT (Y.H.), Advanced and Innovational Research Program in Life Science (Y.H.), National Project on Protein Structural and Functional Analysis from MEXT (Y.H.), Presidential Research Grant for Intersystem Collaboration of RIKEN (P.C. and Y.H.) and a grant from the Six Framework Program from the European Commission (P.C.).

Supporting Online Material
www.sciencemag.org/cgi/content/full/309/5740/1559/DC1
Materials and Methods
SOM Text
Figs. S1 to S4
Tables S1 to S10
References
DDBJ Accession Codes

9 March 2005; accepted 4 August 2005
10.1126/science.1112014

Antisense Transcription in the Mammalian Transcriptome

RIKEN Genome Exploration Research Group and Genome Science Group (Genome Network Project Core Group) and the FANTOM Consortium

Antisense transcription (transcription from the opposite strand to a protein-coding or sense strand) has been ascribed roles in gene regulation involving degradation of the corresponding sense transcripts (RNA interference), as well as gene silencing at the chromatin level. Global transcriptome analysis provides evidence that a large proportion of the genome can produce transcripts from both strands, and that antisense transcripts commonly link neighboring "genes" in complex loci into chains of linked transcriptional units. Expression profiling reveals frequent concordant regulation of sense/antisense pairs. We present experimental evidence that perturbation of an antisense RNA can alter the expression of sense messenger RNAs, suggesting that antisense transcription contributes to control of transcriptional outputs in mammals.

The sense strand of DNA generally provides the template for production of mRNA, which in turn encodes proteins. Transcription from the opposite (antisense) strand can produce transcripts that hybridize with the coding DNA strand, or with the antisense transcript, to interfere with transcription or mRNA stability.

Although previous analysis of the mammalian transcriptome suggested that up to 20% of transcripts may contribute to sense-antisense (S/AS) pairs (*1–3*), large-scale cDNA sequencing in the FANTOM3 project (*4*) suggests that antisense transcription is more widespread. To elucidate the function of S/AS pairs, we used the FANTOM3 data set to analyze their location in the mouse genome, the extent and position of their overlap, and promoter architecture and regulation (*4*).

Analysis of the imprinted *gnas* locus in mice demonstrated numerous sense and antisense transcripts expressed selectively depending on parental chromosomal origin (*5*). However, paired S/AS expression is not restricted to imprinted loci. For example, fig. S1 shows the complex transcript overlap patterns of the HoxA locus and complex transcript overlap patterns. To analyze such complex loci on a genomewide scale, we generated a cDNA set comprising 158,807 full-length transcripts obtained by merging the 102,801 Fantom-3 cDNA set (http://fantom3.gsc.riken.jp/db/) with mouse cDNAs from GenBank (www.ncbi.nlm.nih.gov/Genbank/) and clustering the cDNAs into transcriptional units (TUs), in which members share sequence transcribed from the same strand. There were 50,111 overlapping transcript pairs, grouped into 29,780 nonredundant different overlapping regions in 8331 TU pairs (9713 distinct representative overlapping regions).

In the accompanying paper (*4*), transcription and termination sites were identified. On the basis of this information, more than 72% of all genome-mapped TUs (43,553) overlap with some cDNA, 5′ or 3′ expressed sequence tag (EST) sequence, or tag or tag-pair region mapped to the opposite strand (Table 1). From the above data, 4520 TU pairs contain full-length transcripts, which form S/AS pairs on exons (Table 2). S/AS interaction might also occur between immature RNAs (heterogeneous nuclear RNA, hnRNA) in the nucleus. Furthermore, introns themselves can originate smaller RNA with biological activity (*6*). In addition to transcript pairs that share exons in opposite orientations, 4129 TU pairs were transcribed from different strands of the same locus without apparently sharing overlapping exons (Table 2). Although conservative, the combined S/AS prediction is 1.5- to 2-fold greater than that from previous studies of mouse (*1*) and human (*2*, *3*, *7*) transcripts.

Overlaps of cis S/AS pairs can target different portions of the corresponding TU, giving rise to three basic types of S/AS pairs (fig. S2): head-to-head or divergent (D), tail-to-tail or convergent (C), and fully overlapping (F). The relative abundance of these classes is shown in Table 3. The divergent (head-to-head) classes are the most prevalent, contrasting to previous studies emphasizing convergent cis S/AS pairs (3′-3′ end) (*2*, *8*, *9*). For example, the insulin-like growth factor 1 receptor (IGF1R) shows a very strong antisense CAGE tag overlapping the promoter of the sense transcript, which provides a parallel to the AIR noncoding RNA (ncRNA) in the IGF2R loci (*10*).

S/AS phenomena affect different types of genes (tables S1 and S2) and are unevenly distributed across the genome (table S3). Mouse chromosomes 4 and 17 show a S/AS pair density that is greater than average, whereas chromosomes 6, 9, and 13 show a S/AS pair density that is significantly lower than average (table S3). Chromosome 6 is largely homologous to human chromosome 7, which is known to be rich in RNAs transcribed by RNA polymerases I and III, a facet not captured by our approach (*11*). The X chromo-

RIKEN Genome Exploration Research Group and Genome Science Laboratory (Genome Network Project Core Group) and the FANTOM Consortium:
S. Katayama,[1]* Y. Tomaru,[1]* T. Kasukawa,[1] K. Waki,[1,2] M. Nakanishi,[1] M. Nakamura,[1] H. Nishida,[1] C. C. Yap,[1] M. Suzuki,[1] J. Kawai,[1,2] H. Suzuki,[1] P. Carninci,[1,2]† Y. Hayashizaki,[1,2]‡ C. Wells,[3] M. Frith,[1,3] T. Ravasi,[3] K. C. Pang,[3,4] J. Hallinan,[3] J. Mattick,[3] D. A. Hume,[3] L. Lipovich,[5] S. Batalov,[6] P. G. Engström,[7]* Y. Mizuno,[7]* M. A. Faghihi,[7,8] A. Sandelin,[7] A. M. Chalk,[7] S. Mottagui-Tabar,[7,8] Z. Liang,[7] B. Lenhard,[7] C. Wahlestedt[7,8]‡

[1]Laboratory for Genome Exploration Research Group, RIKEN Genomic Sciences Centre (GSC), RIKEN Yokohama Institute, 1-7-22 Suehiro-cho, Tsurumi-ku, Yokohama, 230-0045, Japan. [2]Genome Science Laboratory, Discovery and Research Institute, RIKEN Wako Main Campus, 2-1 Hirosawa, Wako, 351-0198, Japan. [3]Australian Research Council Special Research Centre for Functional and Applied Genomics, Institute for Molecular Bioscience, The University of Queensland, Brisbane Qld, 4072, Australia. [4]T Cell Laboratory, Ludwig Institute for Cancer Research, Austin and Repatriation Medical Centre, Heidelberg VIC 3084, Australia. [5]Genome Institute of Singapore, 60 Biopolis Street #02-01, Singapore 138672. [6]Genomics Institute of the Novartis Research Foundation (GNF), 10675 John Jay Hopkins Drive, San Diego, CA 92121, USA. [7]Center for Genomics and Bioinformatics, Karolinska Institutet, Berzelius v. 35, S-171 77 Stockholm, Sweden. [8]Scripps Florida, Jupiter, FL 33458, USA.

*These authors contributed equally to this work.
†To whom technical correspondence should be addressed.
‡To whom general correspondence should be addressed.

Table 1. Number of individual TUs showing S/AS overlap. "Single or multiple evidence": at least one type of evidence was used for classification. "Multiple evidence": at least two independent transcripts were detected. "Overlapping cDNA": overlap using only the cDNA data set. Noncoding TUs do not have any coding cDNA in the cluster. Coding TUs may contain noncoding variants of coding transcripts.

TU	Total no. of TUs	TUs potentially involved in S/AS pair		
		Overlapping cDNA, tag, or tag pair. Single or multiple evidence	Multiple evidence	TUs with overlapping cDNA evidence
Coding TU	20,714	18,021 (87.0%)	13,711 (66.2%)	7,223 (34.9%)
Noncoding TU	22,839	13,401 (58.7%)	8,593 (37.6%)	5,296 (23.2%)
Total	43,553	31,422 (72.1%)	22,304 (51.2%)	12,519 (28.7%)

some contains the fewest bidirectional pairs, which could be related to monoallelic inactivation because S/AS pairs are also enriched in imprinted regions (*5*). We have identified 2114 transcripts (1985 TUs) that are potentially imprinted (*12*). Among them, on the basis of directly overlapping cDNAs, EST, CAGE tags, and GSC/GIS ditags, 1281 (23% more than expected, $P = 2.26 \times 10^{-15}$) showed S/AS pairs, and up to 81% of all imprinted TUs showed S/AS pairs when AS sequences to introns were included. This result suggests that S/AS pairing is almost universally associated with candidate imprinted loci. In view of the low frequency of S/AS pairs on the X chromosome, it should be noted that random allelic inactivation also occurs on the autosomes, albeit at lower density than on the X-chromosome (*13*).

Together with microarray analysis (table S4), CAGE tag frequency data represent a de facto expression profiling approach, and allowed further validation of the coexpression of S/AS pairs (table S5). Randomly primed CAGE libraries identified more S/AS pairs than did oligo-dT primed CAGE libraries, suggesting that some polyadenylate [poly(A)] minus RNA transcripts or very long noncoding RNA transcripts are involved in S/AS (fig. S3, table S5). In keeping with an earlier report (*14*), S/AS CAGE tags were detected concordantly at greater than the expected frequency. These coexpressed S/AS pairs (table S6) show complex and tissue-specific regulation. Specific examples are considered in fig S4. Different types of genes are preferentially involved in S/AS regulation, with particular overrepresentation for cytoplasmic proteins and underrepresentation for membrane and extracellular proteins (tables S1 and S2) (*15*).

Possible regulatory interactions between S/AS pairs can be assessed by monitoring correlation of expression with time. To assess such patterns of regulation, we selected S/AS pairs for transcripts where the expression was substantially increased or decreased during the activation of bone marrow–derived macrophages by bacterial lipopolysaccharide (LPS) (*16*). Out of 15 S/AS pairs tested, 7 showed various patterns of reciprocal regulation (Fig. 1). Three S/AS pairs showed proportional coregulation, where both members of the S/AS pair decreased with time. Two pairs showed reciprocal regulation, where one transcript concentration was induced while the other declined in response to LPS. Two more regulated S/AS pairs showed no obvious connection. A transcriptional map of these transcripts is available in fig. S5.

Although concordant regulation is more frequent in S/AS pairs, there are many examples in which the two transcripts are expressed reciprocally. Examples were chosen to test the effect of disturbing the expression of one or the other partner in the S/AS pair. Out of five S/AS pairs selected from expression profiling (*17*), two produced divergent coregulation. Figure 2A shows an example of reciprocal regulation of two coding transcripts, Ddx39 (AK012002) and CD97 [a G protein–coupled receptor (AK004577)]. Targeted small interfering RNA (siRNA) inhibition of Ddx39 led to an increase in CD97 mRNA, but the reciprocal effect was not observed (Fig. 2A).

CAGE data identified potentially coregulated S/AS pairs in mouse hepatocyte Hepa1-6 cells. In contrast with the above correlation, the inhibition of sense hypothetical aminoacyl–tRNA synthetase class II–containing protein (I530027A02) resulted in decreased antisense C/EBP delta expression, but the reverse interaction was not observed (Fig. 2B). The association between these two transcripts was tested further by transiently overexpressing I530027A02 (Fig. 2C), which caused induction of CEBP/delta expression. This finding argues against the simplistic assumption of a negative regulatory role of antisense transcription.

Similarly, the cytoplasmic level of CDC23 was decreased by siRNA against the AS transcript Kif20a for 48 hours (Fig. 2D). Here, the RNA concentration in the nucleus was diminished, suggesting moderate reduction at a nuclear level as well. Another example is shown in the human HeLa cell line, in which siRNA-mediated ablation of an antisense thymidylate synthetase transcript produced a marginal, but reproducible, elevated level of the thymidylate synthetase mRNA (Fig. 2E).

The examples above involve S/AS pairs in which both partners encode protein, and the

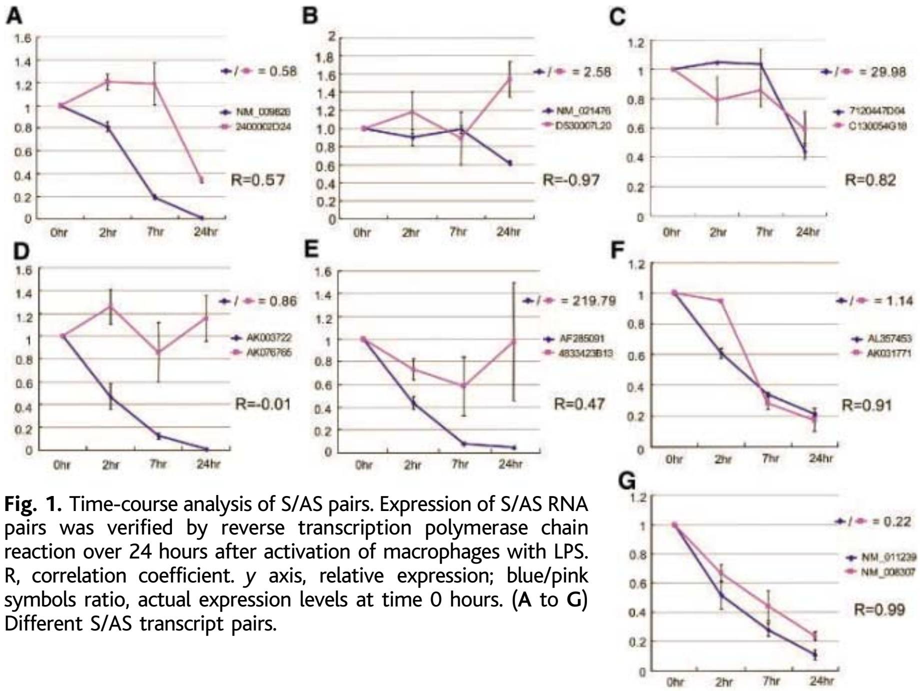

Fig. 1. Time-course analysis of S/AS pairs. Expression of S/AS RNA pairs was verified by reverse transcription polymerase chain reaction over 24 hours after activation of macrophages with LPS. R, correlation coefficient. *y* axis, relative expression; blue/pink symbols ratio, actual expression levels at time 0 hours. (**A** to **G**) Different S/AS transcript pairs.

Table 2. Pairwise analysis of S/AS TUs with cDNA support. Nonexon overlapping bidirectional pairs indicate S/AS pairs having exons overlapping introns of the counterpart, but no exon-exon overlaps, including TUs within antisense TUs.

TU pairing types	Cis-S/AS pairs	Nonexon overlapping S/AS pairs
Coding-coding	1687	1081
Coding-noncoding	2478	2452
Noncoding-noncoding	355	596
Total	4520	4129

Table 3. Directionality of S/AS TUs. Type of S/AS pairs overlap, as in fig. S2. Convergent S/AS pairs overlap tail to tail (3′-3′), and divergent S/AS pairs overlap on the promoter (5′-5′ overlap). Numbers in parentheses: relative difference from expected values (coefficient of variation). The plus or minus sign indicates direction of deviation. Discrepancies from Table 2 derive from counting in all corresponding columns TUs having more than one transcript overlap.

TU pairing types	Divergent	Convergent	Full overlap
Coding-coding	727 (+0.03)	885 (+0.31)	375 (−0.38)
Coding-noncoding	1092 (0.00)	832 (−0.20)	1129 (+0.22)
Noncoding-noncoding	113 (−0.18)	132 (+0.01)	140 (+0.20)
Total	1932 [+0.07]	1849 [+0.02]	1644 [−0.09]

transcripts are processed and exported to the cytoplasm. We also manipulated the expression of six pairs in which one partner is noncoding, and in four of them there was a slight positive correlation (*18*). In three other S/AS pairs in the two different cellular systems tested, there was no evidence that ablation of the AS transcript altered the level of the sense transcript. This finding is consistent with the unaffected phenotype in ROSA-26 locus knockout mice, in which ablation of ncRNA did not alter expression of overlapping coding transcripts (*19*).

S/AS hybrids can potentially provide the templates for transcript cleavage involving the enzyme Dicer, which forms the molecular basis for so-called RNA interference (RNAi) (*20*). Dicer cleaves the RNA duplex to produce siRNAs, which in turn catalyze cleavage of the corresponding mRNA. siRNAs can also participate in transcriptional gene silencing in the nucleus (*21–23*). In addition, Dicer seems to be essential for heterochromatin formation in vertebrate cells (*24*). In addition to siRNA-mediated activities, noncoding antisense RNAs apparently contribute to local chromatin modification or methylation when they overlap the sense promoter (*25–27*).

Both RNAi and RNA-dependent heterochromatin assembly, as the basis for function in S/AS pairs, would predict that the transcripts display divergent regulation, but most S/AS pairs in our study were positively correlated in their expression. Alternatively, coexpression would occur if the transcription of the S/AS pair was controlled by the same enhancer elements (*28*). If antisense transcripts do reflect the transcriptional activity of enhancers, the act of transcription from the antisense promoter may generate the regulatory interaction. In the imprinted IGF2R locus, the antisense transcript, AIR, does not imprint the overlapping *Mas1* gene, and elimination of the transcriptional overlap with IGF2R in a transgene does not prevent silencing (*29*). Hence, some effects of antisense transcription may not require the formation of an RNA duplex.

The large-scale transcriptome profiling of the mouse by the Fantom3 Consortium reveals that antisense transcription is widespread in the mammalian genome. Although there are some examples in which the pairs are discordantly regulated, and some experimental evidence of a direct regulatory interaction, generally the S/AS pairs are positively correlated. Whether concordant or discordant regulation reflects common or divergent regulation, or cis/trans-acting regulatory interactions, will require detailed analysis of the kind presented here for each of the pairs of transcripts under a wide range of conditions.

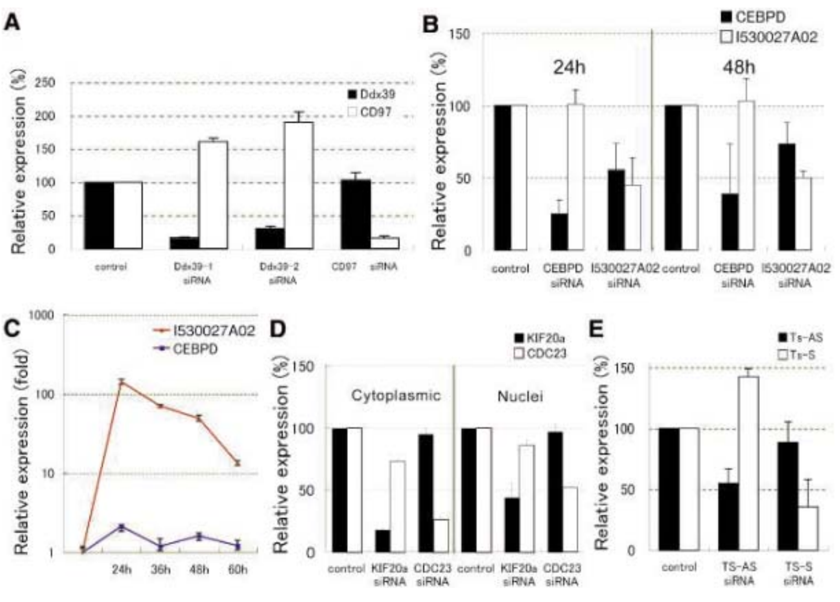

Fig. 2. Expression perturbation of S/AS pairs. siRNAs were designed against the indicated transcripts to specifically inhibit only the target transcripts without producing an off-target effect. (**A**) Relative expression of the coding transcripts Ddx39 and CD97 24 hours after transfection. The Ddx39 transcript was silenced by siRNA designed to inhibit the transcript at two positions, Ddx39-1 and Ddx39-2, outside the CD97 overlap. (**B** to **D**) Hepa1-6 mouse cells. (B) siRNA perturbation of CEBPD (CCAAT/enhancer-binding protein related) and I530027A02 (hypothetical aminoacyl–tRNA synthetase class II). (C) Overexpression of I530027A02 transcript induces overexpression of CEBPD. (D) Perturbation of KIF20a (rabkinesin-6) and CDC23 (cell division cycle 23 yeast homolog) testing both cytoplasmic and nuclear RNA. (**E**) HeLa cell. Ts-S, thymidylate synthase; TS-AS, thymidylate synthase antisense. Results represent the mean ±SE of three independent experiments performed in triplicate relative to GAPDH (glyceraldehyde-3-phosphate dehydrogenase) controls. Controls, no siRNA added.

References and Notes

1. H. Kiyosawa, I. Yamanaka, N. Osato, S. Kondo, Y. Hayashizaki, *Genome Res.* **13**, 1324 (2003).
2. R. Yelin *et al.*, *Nat. Biotechnol.* **21**, 379 (2003).
3. J. Chen *et al.*, *Nucleic Acids Res.* **32**, 4812 (2004).
4. FANTOM Consortium and RIKEN Genome Exploration Research Group and Genome Science Group (Genome Network Project Core Group), *Science* **309**, 1559 (2005).
5. R. Holmes *et al.*, *Genome Res.* **13**, 1410 (2003).
6. J. S. Mattick, I. V. Makunin, *Hum. Mol. Genet.* **14**, R121 (2005).
7. J. Shendure, G. M. Church, *Genome Biol* **3**, RESEARCH0044.1 (2002).
8. V. Veeramachaneni, W. Makalowski, M. Galdzicki, R. Sood, I. Makalowska, *Genome Res.* **14**, 280 (2004).
9. B. Lehner, G. Williams, R. D. Campbell, C. M. Sanderson, *Trends Genet.* **18**, 63 (2002).
10. F. Sleutels, R. Zwart, D. P. Barlow, *Nature* **415**, 810 (2002).
11. P. Carninci *et al.*, *Genome Res.* **13**, 1273 (2003).
12. I. Nikaido *et al.*, *Genome Res.* **13**, 1402 (2003).
13. N. Singh *et al.*, *Nat. Genet.* **33**, 339 (2003).
14. S. Cawley *et al.*, *Cell* **116**, 499 (2004).
15. Databases displaying S/AS pairs and tag-based expression in the genomic viewers are available at http://fantom31p.gsc.riken.jp/s_as/ and http://fantom32p.gsc.riken.jp/gev-f3/gbrowse/mm5, respectively.
16. C. A. Wells *et al.*, *BMC Immunol.* **4**, 5 (2003).
17. H. Kiyosawa, N. Mise, S. Iwase, Y. Hayashizaki, K. Abe, *Genome Res.* **15**, 463 (2005).
18. RIKEN Genome Exploration Research Group and Genome Science Group (Genome Network Project Core Team) and the FANTOM Consortium, data not shown.
19. T. Ravasi, D. A. Hume, *Non-Coding RNAs in Mammals*, in *Encyclopedia of Genetics, Genomics, Proteomics and Bioinformatics* (Wiley, UK, in press), part 2.3.
20. V. Ambros, *Nature* **431**, 350 (2004).
21. M. A. Matzke, J. A. Birchler, *Nat. Rev. Genet.* **6**, 24 (2005).
22. H. Kawasaki, K. Taira, *Nature* **431**, 211 (2004).
23. K. V. Morris, S. W. Chan, S. E. Jacobsen, D. J. Looney, *Science* **305**, 1289 (2004).
24. T. Fukagawa *et al.*, *Nat. Cell Biol.* **6**, 784 (2004).
25. T. Imamura *et al.*, *Biochem. Biophys. Res. Commun.* **322**, 593 (2004).
26. A. Murrell, S. Heeson, W. Reik, *Nat. Genet.* **36**, 889 (2004).
27. A. A. Andersen, B. Panning, *Curr. Opin. Cell Biol.* **15**, 281 (2003).
28. H. Tagoh *et al.*, *EMBO J.* **23**, 4275 (2004).
29. F. Sleutels, G. Tjon, T. Ludwig, D. P. Barlow, *EMBO J.* **22**, 3696 (2003).
30. We thank A. Wada, T. Ogawa, M. Muramatsu, and all the members of RIKEN Yokohama Research Promotion Division for support and encouragement. We also thank the Laboratory for Genome Exploration Research Group for secretarial and technical assistance. We thank the computational resources of the RIKEN Super Combined Cluster (RSCC). This work was mainly supported by Research Grant for the Genome Network Project from the Ministry of Education, Culture, Sports, Science and Technology of Japan (MEXT), the RIKEN Genome Exploration Research Project from MEXT (to Y.H), Advanced and Innovational Research Program in Life Science (to Y.H), National Project on Protein Structural and Functional Analysis from MEXT (to Y.H.), Presidential Research Grant for Intersystem Collaboration of RIKEN (to Y.H.), and a grant from the Wallenberg Foundation (WCN, Sweden) on natural antisense transcripts and a grant from the Swedish Research Council to C.W. All the sequences (CAGE and cDNA) are available through the DNA Data Bank of Japan (DDBJ) to other public databases. The Fantom 3 cDNAs are available through Y.H. (e-mail: yosihide@gsc.riken.jp).

Supporting Online Material

www.sciencemag.org/cgi/content/full/309/5740/1564/DC1
Materials and Methods
Figs. S1 to S5
Tables S1 to S6
References and Notes
DDBJ Accession Codes

9 March 2005; accepted 4 August 2005
10.1126/science.1112009

Elucidation of the Small RNA Component of the Transcriptome

Cheng Lu,[1] Shivakundan Singh Tej,[1] Shujun Luo,[4] Christian D. Haudenschild,[4] Blake C. Meyers,[1,2*] Pamela J. Green[1,2,3*]

Small RNAs play important regulatory roles in most eukaryotes, but only a small proportion of these molecules have been identified. We sequenced more than two million small RNAs from seedlings and the inflorescence of the model plant *Arabidopsis thaliana*. Known and new microRNAs (miRNAs) were among the most abundant of the nonredundant set of more than 75,000 sequences, whereas more than half represented lower abundance small interfering RNAs (siRNAs) that match repetitive sequences, intergenic regions, and genes. Individual or clusters of highly regulated small RNAs were readily observed. Targets of antisense RNA or miRNA did not appear to be preferentially associated with siRNAs. Many genomic regions previously considered featureless were found to be sites of numerous small RNAs.

Small RNAs [21 to 24 nucleotides (nt)] function to silence genes by multiple mechanisms and are present in diverse eukaryotic organisms. Among these molecules, small interfering RNAs (siRNAs) and microRNAs (miRNAs) are the two major types, and both are produced by RNase III–like enzymes called DICERs (*1*, *2*). Whereas siRNAs are processed from longer double-stranded RNA molecules and represent both strands of the RNA, miRNA molecules originate from "hairpin" precursors transcribed from one strand of distinct genomic loci. Existing methods do not sequence deeply enough to sample the full complexity of small RNAs in plant and animal systems, nor do they quantify small RNA abundances.

To investigate the complexity of small RNAs, we adapted massively parallel signature sequencing (MPSS) for these molecules (fig. S1). MPSS sequences hundreds of thousands of molecules per reaction and provides quantitative information. Briefly, small RNA molecules are isolated by size fractionation on a polyacrylamide gel; RNA adapters are sequentially ligated to the 5′ and 3′ ends; and reverse transcriptase generates the first strand of cDNA, which is amplified and used as the template for MPSS (*3*). We generated libraries using small RNA of *Arabidopsis* inflorescence or seedlings, resulting in 721,044 (67,528 distinct) and 686,124 (27,833 distinct) 17-nucleotide sequences or "signatures," respectively (Table 1A; see SOM for the second round of sequencing on seedlings in Table 1B). For the two libraries, 77% of the total distinct small RNA sequences matched the genome [the Institute for Genomic Research (TIGR) version 5.0] (*4*), representing 84% of the nearly 1.5 million total signatures (Table 1A) and exceeding by more than 10-fold the total distinct sequences from all previous *Arabidopsis* studies (*5*). The unmatched signatures may be derived from genomic gaps such as ribosomal RNA (rRNA) repeats or centromeres or may result from sequencing errors (*6*). Signatures matching to rRNAs, transfer RNAs (tRNAs), small nucleolar RNAs (snoRNAs), or small nuclear RNAs (snRNAs) made up 5.9% of the inflorescence library and 31.9% of the seedling library (table S1), lower levels compared with those previously reported (*7*, *8*). Even after removing these RNAs from consideration, the inflorescence library was proportionally more complex (Table 1A). The increased levels and diversity of small RNAs in inflorescence could reflect stronger silencing of transposons in the germline tissue, similar to that of *Caenorhabditis elegans* (*9*). Of the distinct signatures in the inflorescence and seedling libraries, 68.7 and 52.4%, respectively, matched unique sites in the genome (table S2).

We examined the distribution of small RNAs on the five *Arabidopsis* chromosomes and compared this with repeat and mRNA abundance distributions (Fig. 1, A and B; and fig. S2). The small RNAs from both libraries were highly concentrated in the pericentromeric regions of each chromosome, similar to the repeats. In contrast, mRNA levels were greatest in the euchromatic regions (fig. S2). The small RNA data for these and other specific genomic locations are best examined via the Web (*10*); the site provides detailed information about each signature that can be accessed by clicking on the corresponding triangle.

More than half of the genomic sequences matching the small RNAs in the two libraries were transposons or retrotransposons (table S3a). However, the small RNAs matching these sequences accounted for less than half the number of distinct small RNAs (Fig. 2) because more than 80% of these predicted siRNAs matched multiple locations in the genome. The corresponding small RNA signatures were predominantly found at moderate abundances (11 to 100 TPQ, transcripts per quarter million). At least half of the 11,324 retrotransposon or transposon-related sequences in the *Arabidopsis* genome had matches to small RNAs in each library, and small RNAs matched to 41% of 572 pseudogenes (table S3a).

The relative number of distinct small RNAs per megabase of sequence was lower for genes than for other genomic features (Fig. 2, table S3, a and b). About two-thirds of the genes that were matched had relatively few small RNAs (1 to 10 TPQ). These low-abundance signatures could represent perfectly matched miRNAs, or siRNAs targeted to silenced genes, unannotated pseudogenes, unannotated repeats, or other unknown sources of siRNAs (Fig. 1C). Matching the small RNAs to genes in different GO functional categories indicated that the small RNAs were well distributed among a broad range of cellular processes and molecular functions (table S4). A comparison of mRNA and small RNA MPSS data for highly expressed genes suggested that

Table 1. Summary statistics for small RNA MPSS libraries. The signatures sequenced for each library reflect the sum of two sequencing reactions. "Distinct" refers to the number of different sequences found within the set. "Total" refers to the union of the different libraries. "Genome matches" refers to distinct signatures that perfectly match to at least one location in the genome, and includes signatures matching to tRNAs, rRNAs, snRNAs or snoRNAs.

No.	Library	Signatures sequenced	Distinct signatures	Genome matches
	A. Inflorescence and seedling signatures			
1	Inflorescence	721,044	67,528	56,920
2	Seedling	686,124	27,833	17,101
Total of rows 1 and 2		1,407,168	91,445	70,633
	B. Additional signatures from a second round of sequencing from seedlings			
3	Seedling	802,978	33,640	20,379
4	Combined seedling	1,489,102	42,062	24,650
Total of all libraries		2,210,146	104,800	77,434

[1]Delaware Biotechnology Institute, [2]Department of Plant and Soil Sciences, and [3]College of Marine Studies, University of Delaware, Newark, DE 19711, USA. [4]Solexa, Inc., 25861 Industrial Boulevard, Hayward, CA 94545, USA.

*To whom correspondence should be addressed. E-mail: meyers@dbi.udel.edu (B.C.M.); green@dbi.udel.edu (P.J.G.)

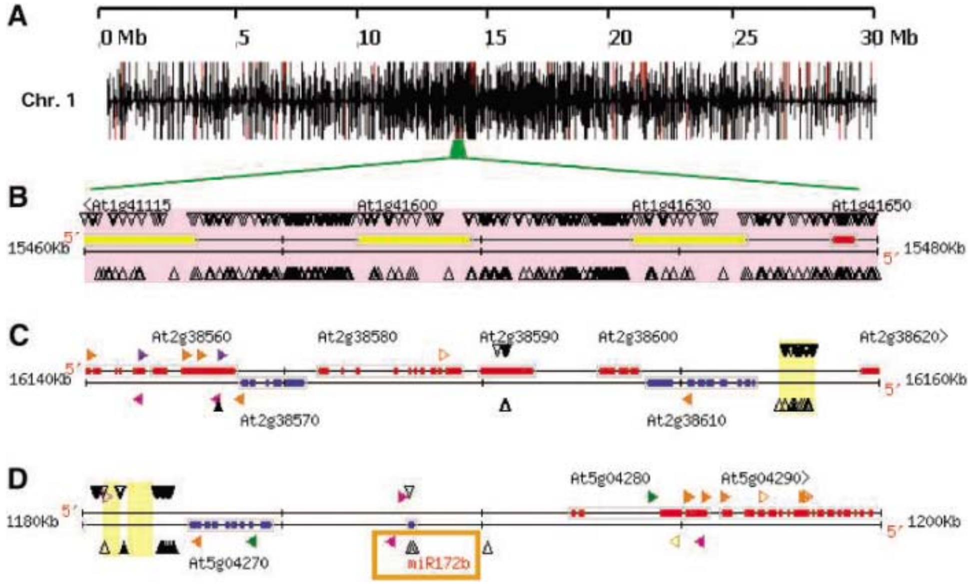

Fig. 1. Small RNAs map to numerous chromosomal locations. (**A**) Inflorescence small RNAs matched to chromosome 1. The height of the vertical lines indicates the abundance of the small RNA. Maximum height of black bar, >25 TPQ; red bar maximum >125 TPQ. (**B**) A pericentromeric region from Chr. 1. Retrotransposon-related sequences identified by RepeatMasker are highlighted in pink, and this entire region was found to be repetitive, including the spaces between annotated retrotransposons. Black triangles above or below the matching strands, small RNAs; hollow triangles, signatures mapping to more than one location; red or blue boxes, exons on top or bottom strands, respectively; colored triangles, poly(A) (MPSS from polyadenylated RNA) MPSS signatures; retrotransposons, thin yellow bars. (**C**) A typical genic region; most small RNAs map to intergenic regions which are often unannotated transposon-related sequences. Yellow shading, DNA transposon-related sequences identified by RepeatMasker. (**D**) An intergenic region of chr. 5. Orange box, small RNAs and poly(A) MPSS signatures that correspond to mir172.

the small RNA data contained only a very low level of degradation products of the longer mRNAs.

The number of distinct small RNAs that matched to intergenic regions exceeded the numbers that matched to genes, pseudogenes, transposons, or retrotransposons (Fig. 2), an observation that cannot be explained by the fraction of the genome that these entities comprise. Inflorescence small RNAs matching intergenic regions were about four times as complex as those from seedlings, and this complexity difference was evident to a slightly lesser extent for small RNAs in other categories (Fig. 2; table S3, a and b). Small RNAs in the intergenic regions potentially represent miRNAs or siRNAs from unannotated repeats such as tandem or inverted genomic repeats (*11*). We observed good correlations for tandem repeats (r = 0.5986) and inverted repeats (r = 0.4955) and small RNAs, based on comparisons of the repeat scores (representing the size and percent sequence identity) versus the total numbers of matching small RNA signatures for each repeat.

Repetitive sources of siRNAs should produce numerous small RNAs that match nearby sequences, whereas each miRNA derives from a specific sequence within the corresponding *miR* gene(s). We developed a proximity-based algorithm to build clusters of small RNAs, so that clusters with overlapping genomic locations could be compared across libraries. Moreover, the characteristics of these clusters may help differentiate novel miRNAs from siRNAs, as sparse clusters may characterize miRNAs and dense clusters may characterize siRNAs.

Genes matched by small RNAs contained an average of one sparse cluster (table S3c).

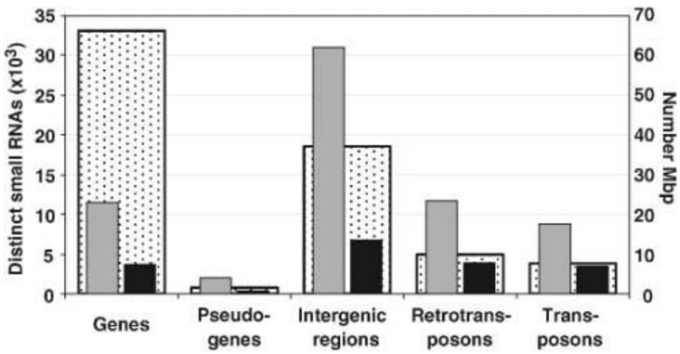

Fig. 2. Small RNAs matching classes of genomic features. Stippled bars indicate the total number of base pairs of the *Arabidopsis* genome (scale on the right) that are found in the indicated genomic features. Retrotransposon and transposon categories are from RepeatMasker. Gray vertical bars, total number of distinct small RNAs matched from the inflorescence library; black vertical bars, total number of distinct small RNAs matched from the seedling library; the scale for distinct small RNAs is on the left.

In contrast, many transposons contained more than one cluster, typically dense. In the intergenic, unannotated regions of the *Arabidopsis* genome, more than 4600 clusters of small RNAs were identified in the inflorescence library alone, which suggests a previously unrecognized activity for a large proportion of the intergenic space. A comparison of genes with and without antisense transcripts for small RNAs indicated no correlation (table S7), consistent with and extending previous arguments against small RNA involvement in general antisense control (*12*, *13*). Nevertheless, the impact of small RNAs may be far greater than this analysis of perfectly matching signatures reflects, because small RNAs are active against imperfectly matched targets (*14*, *15*), and such interactions may be numerous (table S5).

Of the 4067 genes matched by small RNAs, 693 (17%) contained small RNAs found in only one of the two libraries (table S6). Four times as many of these sequences were specific to inflorescence as to seedling (SOM file 2), which may reflect a greater variety of specialized cell types or an increased use of small RNAs in all cell types within the inflorescence. We selected representative known miRNAs or new small RNAs for validation by RNA gel-blot analysis. Figure 3A includes examples of signatures that were specific to or highly preferential for inflorescence or seedlings (signal in only one library, or >100-fold greater in one library). These include AS02, which is a known siRNA (*16*), and five new small RNAs (sm18, sm19, sm1, sm35, and sm39). Clear differential expression recapitulating the MPSS results was detected for all probes. We also examined several small RNAs that exhibited 10- to 100-fold differences in accumulation, represented in Fig. 3A by mir172, a known miRNA, sm14, and sm38. The correlation between RNA gel blots and MPSS was strong, but not always perfectly proportional, particularly for small differences or low abundances (see SOM).

Most siRNAs in *Arabidopsis* are dependent on the RNA-dependent RNA polymerase, RDR2 and are absent in an *rdr2* mutant (*16*). RNA isolated from the inflorescence of the *rdr2* mutant was also included in our

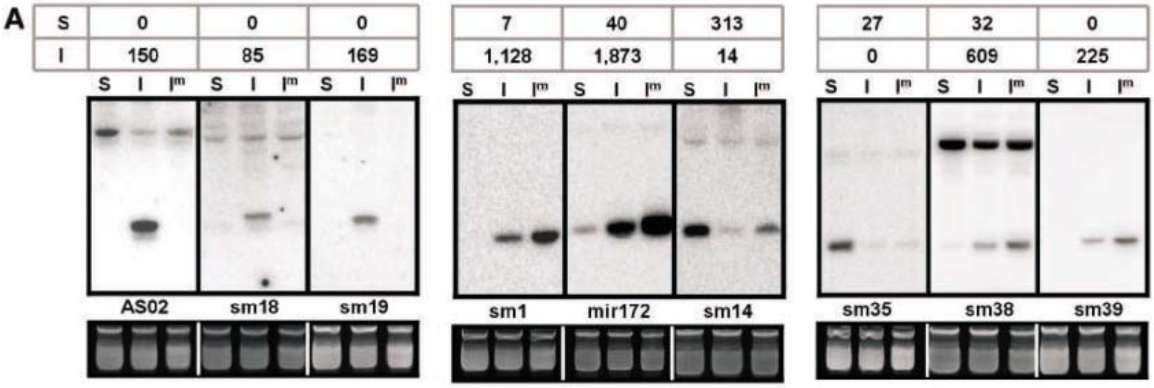

Fig. 3. Regulation and identification of new miRNA candidates. (A) Differential control of miRNAs and siRNA. RNA gel blots of low-molecular-weight RNA isolated from inflorescence tissues (I) and 2-week-old seedlings (S) were probed with labeled oligonucleotides. The blots also included RNA from inflorescence tissues of the *rdr2* mutant (I^m). The normalized abundance level from the MPSS data for each small RNA is listed above the blots, and ethidium bromide staining of the 5S/tRNA region of the gels is shown below. (B) Five-way Venn diagram of selection criteria for miRNAs. The number of distinct signatures matching the criteria is indicated in each box numbered in upper right as mentioned in the text and table S8. The figure excludes 39,622 distinct signatures that did not pass any of the criteria. See SOM and text for descriptions of the paired, sparse, and abundance filters and application of the *At*Set1 and *At*Set2 data sets (*20*). Probes for the right-hand blots in (A) are from box 3.

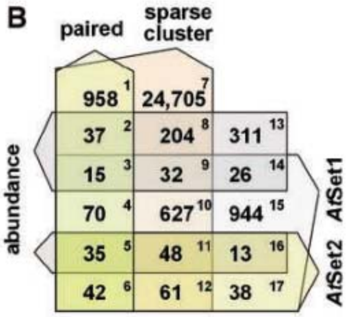

blots (I^m in Fig. 3A and fig. S3) to help distinguish new siRNAs and miRNAs. As expected, siRNA AS02 is lacking in this mutant as reported previously (*16*), as are sm18 and sm19 (Fig. 3A, left). The other new small RNAs in Fig. 3A and fig. S3 are not diminished in *rdr2*. These are presumably miRNAs, although it is possible that they belong to a specialized class of siRNAs dependent on another RDR such as RDR6 (*16*). Indeed, of these RDR2-independent small RNAs, several derive from regions that can form typical pre-miRNA hairpin structures (see fig. S4 for examples) and, thus, fit the requirements for annotation as new miRNAs (*17*).

Most of the miRNAs known at the time of this analysis (*18*) were found in our data set (77 of 92). Signatures exactly matching 73 miRNAs accounted for ~40% of the total abundance of genome-matched signatures from the inflorescence library, and 72 known miRNAs accounted for ~62% of seedling signatures (SOM file 1, Fig. 1D). We examined 61 known or predicted mRNA targets of *Arabidopsis* miRNAs for evidence of transitivity, the production of secondary siRNAs that match a target gene outside the sequence originally targeted. Although transitivity is common for transgene miRNA targets (*19*), most endogenous targets had no matching small RNAs other than miRNAs, or the only matching small RNAs were few, of very low abundance, or corresponded to repeats (see SOM).

To enrich for new miRNAs, we developed a set of filters that captured the majority of the 77 known miRNAs present in the small RNA MPSS data. Our abundance and sparse cluster filters captured 71 and 58, respectively, and the "paired" filter, designed to identify small RNAs near another small RNA that could be a miRNA (the complementary molecule produced from the opposite arm of the miRNA precursor), identified 39 known miRNAs (table S8). These filters were applied in combination with hairpin folding (*At*Set1) and rice conservation (*At*Set2) data sets (*20*) to generate the five-way Venn diagram in Fig. 3B. Among those that form hairpins, the sequences in box 3 were retained by all of the three filters and represent good candidates for novel miRNAs (right, Fig. 3A). None were lacking in the inflorescence of the *rdr2* mutant as expected. This is also true for representatives of box 9 retained by the sparse and abundance filters and box 2, which had paired and sparse configurations but was not identified by the *At*Set1 filter (fig. S3b). The absence of these sequences in *At*Set2 indicates that filters based on MPSS data can enhance miRNA prediction capability even when cross-species conservation is lacking.

Our data indicate that the small RNA component of the genome and its regulatory role is more extensive and complex than previously demonstrated. Many regions of the genome considered inactive or featureless were found in our analyses to be sites of considerable small RNA activity. Insight into the functional basis for this complexity will result from detailed analyses of the *Arabidopsis* small RNAs and application of this approach in diverse treatments, small RNA mutants, and other species.

References and Notes

1. E. Bernstein, A. A. Caudy, S. M. Hammond, G. J. Hannon, *Nature* **409**, 363 (2001).
2. A. Grishok *et al.*, *Cell* **106**, 23 (2001).
3. S. Brenner *et al.*, *Nat. Biotechnol.* **18**, 630 (2000).
4. J. R. Wortman *et al.*, *Plant Physiol.* **132**, 461 (2003).
5. A. M. Gustafson *et al.*, *Nucleic Acids Res.* **33**, D637 (2005).
6. B. C. Meyers *et al.*, *Genome Res.* **14**, 1641 (2004).
7. W. Park, J. Li, R. Song, J. Messing, X. Chen, *Curr. Biol.* **12**, 1484 (2002).
8. R. Sunkar, J. K. Zhu, *Plant Cell* **16**, 2001 (2004).
9. T. Sijen, R. H. Plasterk, *Nature* **426**, 310 (2003).
10. http://mpss.udel.edu/at
11. R. A. Martienssen, *Nat. Genet.* **35**, 213 (2003).
12. C. H. Jen, I. Michalopoulos, D. R. Westhead, P. Meyer, *Genome Biol.* **6**, R51 (2005).
13. X. J. Wang, T. Gaasterland, N. H. Chua, *Genome Biol.* **6**, R30 (2005).
14. A. L. Jackson, P. S. Linsley, *Trends Genet.* **20**, 521 (2004).
15. L. P. Lim *et al.*, *Nature* **433**, 769 (2005).
16. Z. Xie *et al.*, *PLoS Biol.* **2**, E104 (2004).
17. V. Ambros *et al.*, *RNA* **9**, 277 (2003).
18. S. Griffiths-Jones, *Nucleic Acids Res.* **32**, D109 (2004).
19. E. A. Parizotto, P. Dunoyer, N. Rahm, C. Himber, O. Voinnet, *Genes Dev.* **18**, 2237 (2004).
20. M. W. Jones-Rhoades, D. P. Bartel, *Mol. Cell* **14**, 787 (2004).
21. We are grateful to M. Nakano and D. Lee for the web interface, J. Carrington for the *rdr2* mutant, F. Souret and B.-C. Yoo for comments on the manuscript, and S. Jacobsen for helpful discussions. This work was supported primarily by NSF SGER #0439186, with additional support from the NSF Plant Genome Program (B.C.M.), DOE DE-FG02-04ER15541 (P.J.G.), and NIH P20 RR16472-04.

Supporting Online Material

www.sciencemag.org/cgi/content/full/309/5740/1567/DC1
SOM Text
Materials and Methods
Figs. S1 to S9
Tables S1 to S4
References and Notes
Data files 1 and 2

7 April 2005; accepted 28 July 2005
10.1126/science.1114112

A Strategy for Probing the Function of Noncoding RNAs Finds a Repressor of NFAT

A. T. Willingham,[1] A. P. Orth,[2] S. Batalov,[2] E. C. Peters,[2] B. G. Wen,[2] P. Aza-Blanc,[2] J. B. Hogenesch,[2]*† P. G. Schultz[1,2]†

Noncoding RNA molecules (ncRNAs) have been implicated in numerous biological processes including transcriptional regulation and the modulation of protein function. Yet, in spite of the apparent abundance of ncRNA, little is known about the biological role of the projected thousands of ncRNA genes present in the human genome. To facilitate functional analysis of these RNAs, we have created an arrayed library of short hairpin RNAs (shRNAs) directed against 512 evolutionarily conserved putative ncRNAs and, via cell-based assays, we have begun to determine their roles in cellular pathways. Using this system, we have identified an ncRNA repressor of the nuclear factor of activated T cells (NFAT), which interacts with multiple proteins including members of the importin-beta superfamily and likely functions as a specific regulator of NFAT nuclear trafficking.

Noncoding RNAs (ncRNAs) are surprisingly prevalent. A systematic analysis of transcription observed ~10 times more transcriptional activity than can be accounted for by predicted protein-coding genes (*1*). Much of this activity was subsequently shown to be regulated (*2*). Moreover, large-scale cDNA analysis and genome annotations predict thousands of ncRNAs (*3*–*6*), and computational analysis suggests that over 20% of human genes are regulated by ncRNAs known as microRNAs (*7*). Whereas several strategies have been used to identify probable ncRNAs (*8*, *9*), a systematic approach to explore their biological functions is lacking. Traditional genetic studies with chemical mutagens are unsatisfactory because ncRNAs are likely resistant to the nonsense and frameshift mutations typically generated in such screens. Furthermore, many of the biochemical methods used to characterize protein complexes are not useful for identifying RNA components. Consequently, we have developed a genomics-based strategy to computationally identify ncRNAs conserved between mouse and human, and we subsequently characterized their biological function by knockdown of the ncRNA transcripts with RNA interference (RNAi) in a series of cell-based pathway screens (*10*).

In a large-scale analysis of full-length mouse cDNAs, the Functional Annotation of the Mouse (FANTOM) Consortium identified 454 mouse ncRNAs with significant human genome homology (*3*, *11*). We used a de novo analysis and expanded searches to more recent versions of both the Celera and the public assemblies of the human genome (*12*). Ultimately, 512 ncRNAs with significant human homology were identified; 88 were overlapping with the FANTOM data set and four were independently identified in a genome-wide analysis of ultraconserved elements (*13*). These ncRNAs are significantly larger (averaging ~2 kb) than many characterized small ncRNAs and, given their initial isolation in the FANTOM cDNA cloning project, are likely transcribed by RNA polymerase II. Because these longer ncRNAs do not have readily identifiable functional domains (unlike tRNA or microRNA), a priori classification of the mouse-human conserved ncRNA data set is not practical. Instead, their cellular function was explored using an RNAi-based approach. Two DNA vector-encoded short hairpin RNAs (shRNAs) were designed for each of the mouse-human conserved ncRNAs, for a total of 1024 shRNAs (*12*); human ncRNAs were selectively targeted because of the many available cell-based assays that use human cell lines. This shRNA collection was arrayed in 384-well tissue culture plates and screened to identify genes that modulate the activity of nuclear factor of activated T cells (NFAT) by using an NFAT-responsive luciferase (luc) reporter (*12*).

NFAT, a remarkably sensitive transcription factor responsive to local changes in calcium signals, is essential for T cell receptor–mediated immune response and plays a critical role in the development of the heart and vasculature, musculature, and nervous tissue (*14*). Upon stimulation, the calcium-regulated phosphatase calcineurin dephosphorylates cytoplasmic subunits of NFAT complexes, thus promoting accumulation of NFAT in the nucleus, where it becomes transcriptionally active. The calcium ionophore ionomycin increases intracellular calcium levels, which promotes NFAT translocation to the nucleus, while low levels of the phorbol ester PMA (phorbol 12-myristate 13-acetate) lead to moderate activation of the activating protein 1 (AP1) transcription factor, which binds cooperatively with NFAT. Because shRNAs were used to knock down putative ncRNAs, "activators" in this screen represent ncRNAs whose actual function is repressive in nature. One ncRNA was found, which, when targeted with shRNAs, resulted in a dramatic activation of NFAT activity. This noncoding repressor of NFAT (NRON) was then further characterized.

When human embryonic kidney (HEK) 293 cells were stimulated with ionomycin and PMA, shRNA knockdown of NRON resulted in significantly increased NFAT activity (Fig. 1A and fig. S1), which was blocked by the addition of the calcineurin inhibitor cyclosporine A. A different set of shRNAs directed against mouse NRON also showed activity in mouse 3T3 cells (fig. S1). Furthermore, shRNA knockdown of NRON in the T cell–derived Jurkat cell line elevated NFAT activity in cells stimulated by both chemical (Fig. 1B)

Table 1. NRON-interacting proteins identified by an RNA-protein affinity purification strategy using the long splice form (2.7 kb) of exon 3 (*12*). Recovered proteins were identified by mass spectrometry [see (*12*) for peptide sequences and quality scores]. trans., transport; CAS, cellular apoptosis susceptibility protein; JNK, Jun N-terminal kinase; ATP, adenosine triphosphate; CaM, calmodulin.

Unigene	Function	Description	Genbank
CSE1L	Nucleocytoplasmic trans.	Importin-alpha export (CAS)	AAC35008
KPNB1	Nucleocytoplasmic trans.	Importin-beta 1 (karyopherin)	NP_002256
TNPO1	Nucleocytoplasmic trans.	Importin-beta (transportin1)	AAB68948
EIF3S6	Protein biosynthesis	Translation initiation factor	AAH17887
CUL4B	Proteolysis	Cullin-based E3 ligase complex	AAK16812
PSMD11	Proteolysis	Proteasome 26S non-ATPase	NP_002806
UREB1	Proteolysis	E3 ubiquitin protein ligase	BAC06833
DDX3X	RNA helicase	DEAD-box protein	O00571
IQGAP1	Signal transduction	CaM-binding scaffolding protein	NP_003861
PPP2R1A	Signal transduction	Protein phosphatase 2 subunit A	P30153
SPAG9	Signal transduction	JNK-assoc. leucine-zipper protein	AAN61565

[1]Department of Chemistry, Scripps Research Institute, 10550 North Torrey Pines Road, La Jolla, CA 92037, USA. [2]Genomics Institute of the Novartis Research Foundation, 10675 John Jay Hopkins Drive, San Diego, CA 92121, USA.

*Present address: Scripps Florida, 5353 Parkside Drive—RF1, Jupiter, FL 33458, USA.
†To whom correspondence should be addressed. E-mail: hogenesch@scripps.edu (J.B.H.); schultz@scripps.edu (P.G.S.)

and T cell receptor activation. To address potential shRNA and interferon related artifacts, small interfering RNAs (siRNAs) corresponding to the shRNA sequences were also tested and shown to be active (fig. S1). In addition, little activity was seen in an interferon-responsive reporter with the NRON shRNAs. Quantitative polymerase chain reaction (PCR) was used to confirm siRNA-mediated knockdown of NRON, and a ~40% reduction was observed (Fig. 1C). Transfection efficiency of siRNAs was shown to be over 90% for these experiments; lentiviral delivery of an shRNA (with nearly 100% infection rate) also reduced NRON transcript a comparable amount. Because NRON is likely a rare transcript (see below), moderate changes in transcript levels may have pronounced cellular effects.

To gain further insight into the function of NRON, we characterized its gene structure and expression. Based on rapid amplification of cDNA ends (RACE) and cDNA sequence data, we found that the NRON gene is composed of three exons, which can be alternatively spliced to yield transcripts ranging in size from 0.8 to 3.7 kb (Fig. 2A). The NRON gene also has two large 300-to-400–base pair (bp) regions of near-perfect sequence conservation between rodents and primates (fig. S2). An analysis of the coding potential of NRON transcripts and the surrounding genomic interval further supports the FANTOM Consortium's classification of NRON as an ncRNA (*12*). The expression of NRON was analyzed by reverse transcription (RT)–PCR, and the high number of amplification cycles required to detect NRON suggests that it is a relatively rare transcript (Fig. 2 and fig. S2). A survey of total RNA from a variety of human and mouse tissues showed that NRON is enriched in placenta, muscle, and lymphoid tissues such as the thymus, spleen, and lymph node (Fig. 2, B and C). Furthermore, all three mouse FANTOM cDNA clones were originally isolated from thymus libraries. A Northern blot of mouse RNA showed significant NRON expression in the embryo and the thymus (Fig. 2D), which is consistent with the enrichment in the placenta and the thymus seen by RT-PCR. Finally, NRON transcripts have a distinct tissue-specific distribution of splice forms, which likely serve a currently unknown biological function. NRON's tissue-specific expression, particularly its enrichment in lymphoid tissues, is consistent with its role as a modulator of NFAT signaling.

In order to define the molecular mechanism by which NRON represses NFAT activity, a biochemical approach was used to identify possible RNA-protein interactions. The 3′ terminus of exon 3 of NRON was tagged with an RNA hairpin, which itself was bound tightly by the MS2 phage protein (*15*). An MS2/maltose binding-protein fusion was then used to purify NRON-interacting proteins from a whole-cell protein extract, and their identities were determined by mass spectrometry (*12*). After comparison to a nonspecific RNA control, 11 proteins were found to bind NRON specifically (Table 1), including three members of the importin-beta superfamily, factors which directly mediate the nucleocytoplasmic transport of cargoes such as NFAT (*16*). siRNAs directed against four of these 11 putative interactors—a calmodulin-binding protein (IQGAP1), a nuclear transport factor (KPNB1), the structural subunit of a phosphatase (PPP2R1A), and a component of the proteasome (PSMD11)—all activated NFAT activity (a two- to sixfold

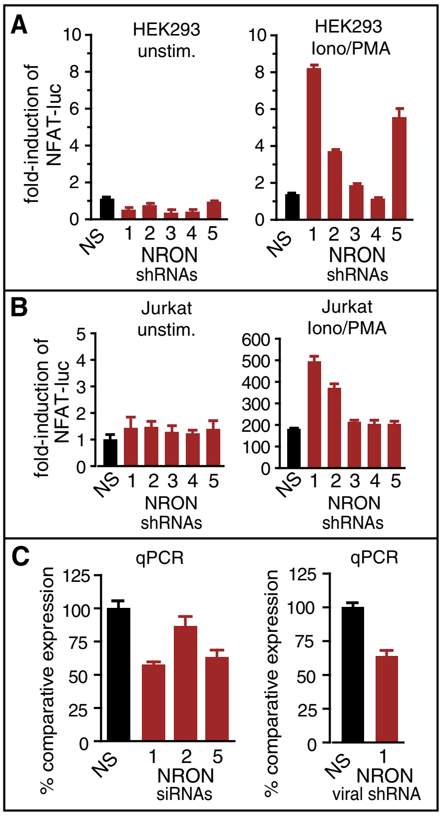

Fig. 1. Noncoding repressor of NFAT (NRON). (**A**) Five different shRNAs (shRNA1 and shRNA5 share 17 bp of overlap) targeting NRON were tested with and without ionomycin (Iono) and PMA stimulation. Three shRNAs showed significant activation of an NFAT-responsive luciferase reporter (mean ± SD). Samples were normalized to a nonspecific shRNA (NS) in unstimulated cells. Similar results were observed with human U2OS and mouse 3T3 cell lines (fig. S1). (**B**) These shRNAs were also tested in T cell–derived Jurkat cells, with two shRNAs showing ~2-fold or greater activation of the NFAT-luc reporter. Cells were either chemically stimulated with Iono/PMA or activated via a T cell receptor with antibodies targeting CD3 (data not shown). (**C**) Quantitative real-time PCR (qPCR) measure of NRON transcript knockdown by siRNA in HEK293 cells. Transfection efficiency for siRNAs was greater than 90%. NRON siRNAs caused a reduction in NRON RNA, compared with a nonspecific control siRNA: siRNA1, 42.4% reduction; siRNA2, 13.2%; and siRNA5, 36.7% (mean ± SD). Transcript knockdown was also measured by lentiviral delivery of shRNA1 (with nearly 100% transfection transduction efficiency), which reduced NRON RNA 36.0%, compared with a nonspecific shRNA.

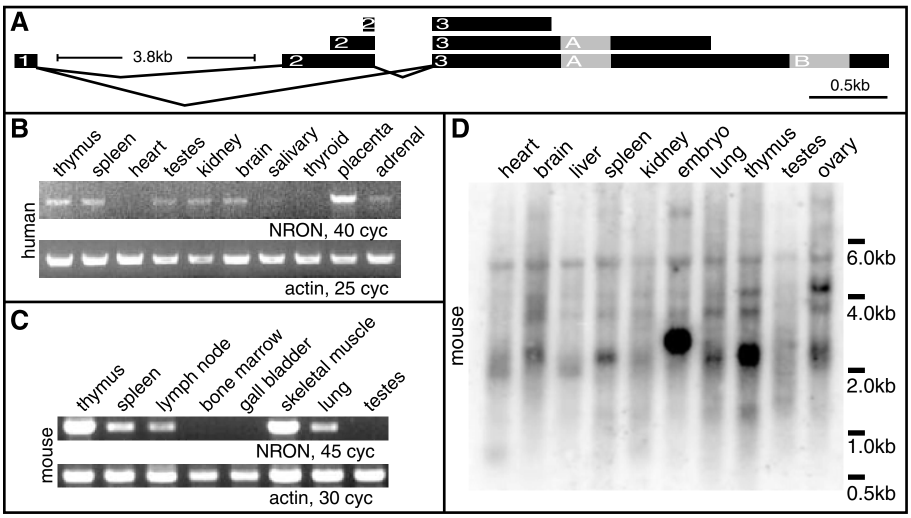

Fig. 2. NRON expression data. (**A**) Gene structure for mouse NRON based on 5′ RACE analysis and RIKEN cDNA clones (*12*). Gray bars in exon 3 indicate regions highly conserved between human, chimp, mouse, and rat (fig. S2): region A (298 bp, 90% identity) and region B (400 bp, 89% identity). Most of the siRNA or shRNA sequences used in this study target areas near region B. (**B**) RT-PCR of NRON from human tissues showed relative enrichment in the placenta, thymus, and spleen, with detectable expression in the testes, kidney, brain, and adrenal glands. (**C**) RT-PCR of NRON from mouse tissues showed elevated expression in skeletal muscle and the thymus, with expression also seen in the spleen, lymph node, and lung. (**D**) A Northern blot of mouse poly-A+ mRNA probed with the long splice form of NRON exon 3 showed significant NRON expression in the embryo and thymus, with lower expression in other tissues. The size differences in transcripts, ranging from 2 to 4 kb, are consistent with probable splice variants.

increase in NFAT activity was observed in a sensitized setting where NRON was also knocked down). cDNA overexpression of these four interactors had the opposite effect and repressed NFAT activity. Therefore, these four proteins, together with NRON, have a repressive effect on NFAT signaling (Fig. 3A and fig. S3).

In vitro RNA protein-binding assays (*12*) were used to further characterize the interaction between NRON and the four proteins that showed NFAT modulatory effects. Protein open reading frames were cloned into mammalian expression vectors containing an N-terminal FLAG tag. Then, protein extracts from cells expressing these plasmids were incubated with radiolabeled NRON, and tagged proteins were precipitated. Cell extracts containing overexpressed importin-beta 1 (KPNB1) bound significantly more NRON than did a nonspecific RNA control, suggesting that importin-beta 1 and NRON directly associate (Fig. 3B). This interaction is supported by ribonuclease (RNase) protection experiments, which show that NRON is protected from digestion by extracts containing high levels of KPNB1 (Fig. 3B). Furthermore, interactions between PPP2R1A and KPNB1 (*17*), as well as between PPP2R1A and IQGAP1 (*18*), have been previously reported. Altogether, this data argues that NRON functions as an RNA component of a protein complex that acts to repress NFAT activity.

The initial isolation of three importin-beta family members and the subsequent demonstration that importin-beta 1 can bind NRON and alter NFAT activity suggests that NRON may act as a modulator of NFAT nuclear trafficking. Furthermore, NRON acts on multiple NFAT family members; cotransfection of NFAT cDNAs and NRON shRNA showed that NRON modulates the calcium-regulated transcriptional activity of NFATc1, NFATc2, NFATc3, and NFATc4 (fig. S1). shRNAs targeting NRON were also assayed with p53, nuclear factor κB (NFκB), AP1, and the forkhead FOXO1 reporters, which are transcription factors that translocate from cytoplasm to nucleus (Fig. 3, C and E). No NRON-dependent phenotypes were seen, suggesting that NRON is specific for NFAT translocation. Finally, using an NFATc1–green fluorescent protein (GFP) fusion as a visible marker for NFAT subcellular localization (*19*), it was shown that an NRON shRNA results in a significant increase in nuclear levels of NFAT protein (Fig. 3E and fig. S4). NRON knockdown elevated nuclear NFAT even in the absence of Ca^{2+} stimulation, which is probably a direct result of elevated cellular levels of NFAT protein from the introduction of the NFATc1-GFP fusion. This is consistent with the observation that overexpression of NFAT cDNAs obviates the need for chemical stimulation for NRON shRNA activity (fig. S1) (*20*, *21*). Therefore, rather than directly modulating the transcriptional activity of NFAT itself, NRON likely regulates NFAT's subcellular localization.

The interaction of NRON with nuclear import factors suggests that NRON exists in a complex with importin-beta and specifically regulates the nuclear trafficking of NFAT, a hypothesis supported by studies of NFATc1-GFP translocation. In light of the complicated networks of nuclear-cytoplasmic transport and the seemingly limited number of available importin-beta family members, specific ncRNAs may play a role in regulating the complexity of intracellular trafficking. The interplay between importins, the nuclear localization signal of

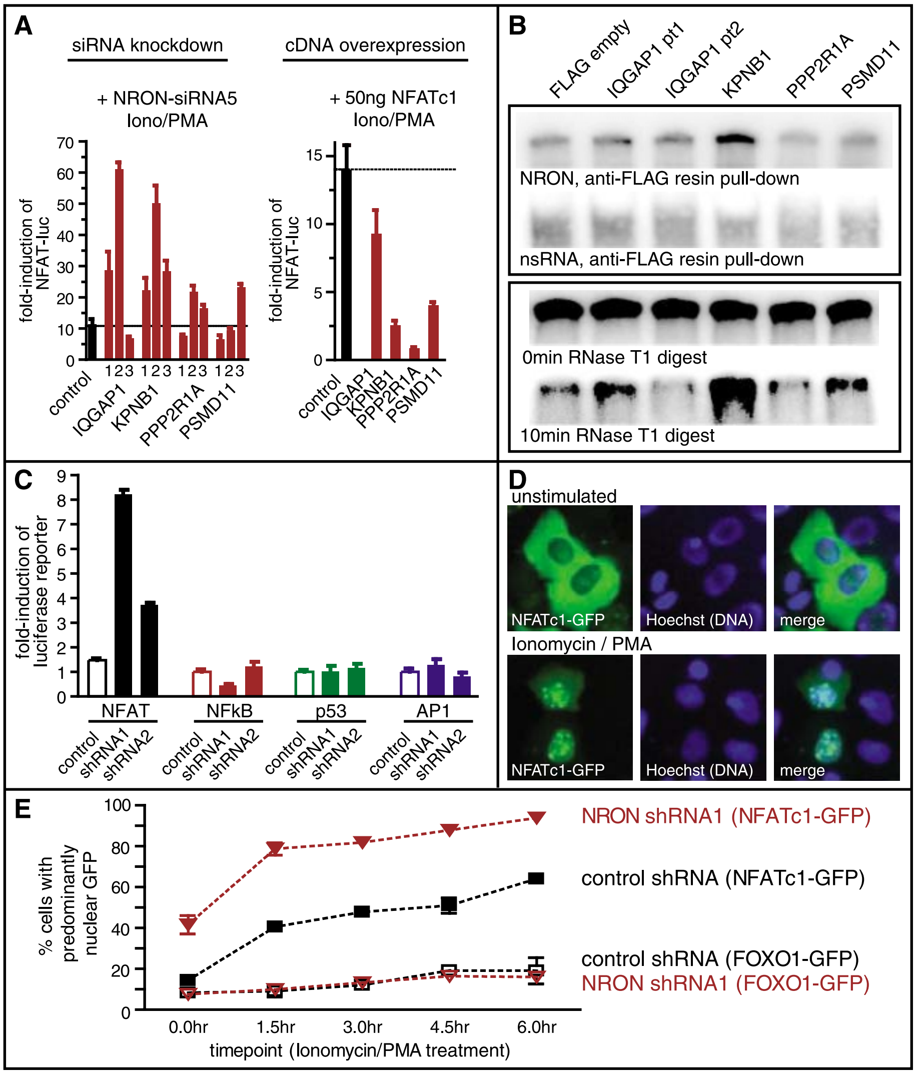

Fig. 3. NRON interacts with nuclear transport factors. (**A**) For each NRON-interacting protein, three unique siRNAs were assayed for their activity on the NFAT-luc reporter. The siRNAs by themselves had no effect (fig. S3); however, in the presence of an siRNA targeting NRON (siRNA5), significant stimulation-dependent synergy was observed (mean ± SD). These same proteins were also identified as repressors of NFAT when overexpressed in the presence of a small amount of NFAT cDNA to stimulate basal levels of activity. See fig. S3 for further controls and qPCR data. (**B**) In vitro RNA-binding experiments show that NRON interacts with KPNB1. The precipitation of epitope-tagged proteins (because of its size, IQGAP1 was split into two fragments) from cell extracts incubated with radiolabeled NRON (2.7 kb of exon 3) demonstrated that NRON specifically coprecipitates with KPNB1, when compared with a nonspecific RNA (nsRNA). In an RNase T1 protection experiment, protein extracts containing overexpressed KPNB1 protected radiolabeled NRON from digestion. (**C**) Two NRON shRNAs show no effects on reporters for NFκB, p53, and AP1 transcription. NFAT data are from stimulated cells. (**D**) U2OS cells were selected for microscopy analysis because of their morphology and adherence. NFATc1 fused to GFP is an effective reporter (*19*), localizing from cytoplasm to nucleus upon stimulation. (**E**) Cotransfection with NRON shRNA1 results in significantly increased NFAT nuclear localization (NFATc1-GFP), compared with a control shRNA (mean ± SD). The forkhead transcription factor FOXO1, which also shuttles from cytoplasm to nucleus (*24*), was used as a control and was shown to be unaffected by NRON knockdown.

NFAT, and NRON remains unknown, as does whether the native function of NRON is to repress nuclear import or to promote the nuclear export of NFAT. In addition, given the effects of both calcium and phosphorylation on NFAT activity, the interactions of NRON with the structural subunit of the phosphatase PP2A and the calmodulin binding IQGAP1 may also be significant. Further characterization of all 11 putative NRON interactors may identify more complex interactions and regulatory features for this presumed RNA-protein macromolecular complex.

NRON is but one of the potentially thousands of RNA regulators, which, through RNA-RNA, RNA-DNA, or RNA-protein interactions, may effectively amplify the complexity of a human genome with a limited number of protein-coding genes (*22*, *23*). The application of this library of ncRNA-specific shRNAs to additional cellular pathway and phenotypic screens is likely to reveal additional functional roles for these transcribed RNAs. Preliminary experiments have identified seven other functional ncRNA genes: six essential for cell viability and one repressor of Hedgehog signaling.

References and Notes

1. P. Kapranov *et al.*, *Science* **296**, 916 (2002).
2. S. Cawley *et al.*, *Cell* **116**, 499 (2004).
3. Y. Okazaki *et al.*, *Nature* **420**, 563 (2002).
4. S. W. Scherer *et al.*, *Science* **300**, 767 (2003).
5. K. C. Pang *et al.*, *Nucleic Acids Res.* **33**, D125 (2005).
6. S. Griffiths-Jones *et al.*, *Nucleic Acids Res.* **33**, D121 (2005).
7. X. Xie *et al.*, *Nature* **434**, 338 (2005).
8. S. R. Eddy, *Nat. Rev. Genet.* **2**, 919 (2001).
9. G. Storz, S. Altuvia, K. M. Wassarman, *Annu. Rev. Biochem.* **74**, 199 (2005).
10. A. T. Willingham, Q. L. Deveraux, G. M. Hampton, P. Aza-Blanc, *Oncogene* **23**, 8392 (2004).
11. K. Numata *et al.*, *Genome Res.* **13**, 1301 (2003).
12. Materials and methods are available as supporting material on *Science* Online.
13. G. Bejerano *et al.*, *Science* **304**, 1321 (2004).
14. P. G. Hogan, L. Chen, J. Nardone, A. Rao, *Genes Dev.* **17**, 2205 (2003).
15. Z. Zhou, L. J. Licklider, S. P. Gygi, R. Reed, *Nature* **419**, 182 (2002).
16. D. Gorlich, U. Kutay, *Annu. Rev. Cell Dev. Biol.* **15**, 607 (1999).
17. E. J. Lubert, K. D. Sarge, *Biochem. Biophys. Res. Commun.* **303**, 908 (2003).
18. E. Nakajima, K. Suzuki, K. Takahashi, *Biochem. Biophys. Res. Commun.* **326**, 249 (2005).
19. R. H. Kehlenbach, A. Dickmanns, L. Gerace, *J. Cell Biol.* **141**, 863 (1998).
20. J. Trama, Q. Lu, R. G. Hawley, S. N. Ho, *J. Immunol.* **165**, 4884 (2000).
21. J. P. Northrop *et al.*, *Nature* **369**, 497 (1994).
22. J. S. Mattick, *Nat. Rev. Genet.* **5**, 316 (2004).
23. International Human Genome Sequencing Consortium, *Nature* **431**, 931 (2004).
24. N. Nakamura *et al.*, *Mol. Cell. Biol.* **20**, 8969 (2000).

25. We thank L. Miraglia, S. Chanda, S. White, C. Cooper, M. Hancock, J. Liu, and Q. Huang for their assistance in cell-based assays and screenings; J. Walker for sharing RNAs from mouse and human tissues; J. Grbic for help with experiments; L. Linford, M. Medina, and B. Smith for help preparing the shRNA library; and P. DeJesus and J. Graziano for aid with proteomics efforts. The NFATc1-GFP construct was a generous gift from L. Gerace, as was FOXO1-GFP provided by W. Sellers. This work was supported by the Novartis Research Foundation and an NIH Kirschstein National Research Service Award for A.T.W. This is manuscript 17361-CH of the Scripps Research Institute and is dedicated to Peter B. Dervan on the occasion of his 60th birthday.

Supporting Online Material

www.sciencemag.org/cgi/content/full/309/5740/1570/DC1

Materials and Methods

Figs. S1 to S4

Tables S1 to S5

References

9 June 2005; accepted 20 July 2005

10.1126/science.1115901

Inhibition of Translational Initiation by Let-7 MicroRNA in Human Cells

Ramesh S. Pillai,[1] Suvendra N. Bhattacharyya,[1] Caroline G. Artus,[1] Tabea Zoller,[1] Nicolas Cougot,[2] Eugenia Basyuk,[2] Edouard Bertrand,[2] Witold Filipowicz[1]*

MicroRNAs (miRNAs) are ~21-nucleotide-long RNA molecules regulating gene expression in multicellular eukaryotes. In metazoa, miRNAs act by imperfectly base-pairing with the 3′ untranslated region of target messenger RNAs (mRNAs) and repressing protein accumulation by an unknown mechanism. We demonstrate that endogenous let-7 microribonucleoproteins (miRNPs) or the tethering of Argonaute (Ago) proteins to reporter mRNAs in human cells inhibit translation initiation. M^{7}G-cap-independent translation is not subject to repression, suggesting that miRNPs interfere with recognition of the cap. Repressed mRNAs, Ago proteins, and miRNAs were all found to accumulate in processing bodies. We propose that localization of mRNAs to these structures is a consequence of translational repression.

Initial studies of the function of lin-4 RNA during development of *Caenorhabditis elegans* indicated that this miRNA down-regulates protein accumulation without affecting mRNA concentrations and mRNA association with polysomes, suggesting that either translation is repressed at the step downstream of its initiation or proteins undergo synthesis but are rapidly degraded (*1*, *2*). Subsequent work performed in *Drosophila* and mammalian cells has confirmed that decreased protein accumulation is not due to mRNA degradation (*3*–*6*). However, miRNAs can also affect metazoan gene expression in other ways, as indicated by the involvement of miR-16 in AU-rich element–mediated mRNA turnover (*7*).

To investigate how miRNAs inhibit protein accumulation in mammalian cells, we used mRNA reporters, whose translation is regulated by either the tethering of human Argonaute 2 (hAgo2) or the endogenous let-7 microribonucleoprotein (miRNP). The use of the tethering approach follows the observation that the repressive effect of miRNAs can be mimicked in HeLa cells by tethering of Ago proteins, established components of miRNPs, to the mRNA reporter (*8*). For assaying let-7 effects, we constructed *Renilla reniformis* (RL) and firefly (FL) luciferase reporters containing in the 3′ untranslated region (3′-UTR) either one (1xBulge) or three (3xBulge) sequences able to form bulged duplexes with the let-7 RNA; RL-Perf and FL-Perf contain a single site perfectly complementary to let-7 RNA (Fig. 1A and fig. S1A). We found that expression of RL-3xBulge and RL-Perf was inhibited up to 10-fold when compared with control RL mRNA (RL-Con) (fig. S1B). The inhibition was largely eliminated upon co-transfection of a 2′-*O*-Me oligonucleotide complementary to let-7 but not to control miR-122a RNA, consistent with the effect being mediated by let-7 miRNP (fig. S1C). The amount of RL-Perf mRNA was decreased about fivefold, whereas that of RL-3xBulge mRNA was reduced by only 20%; expression of RL-1xBulge mRNA was not decreased when compared with RL-Con mRNA (fig. S1). The data are in agreement with the findings that endogenous miRNAs can cleave an RNA containing a single perfectly complementary site and that translational repression generally requires several miRNA target sites (*6*).

We investigated whether let-7 miRNP or tethered hAgo2 inhibits the translation process per se or induces the proteolysis of nascent polypeptides. Toward this we tested the effect of targeting the reporter RL proteins to the endoplasmic reticulum (ER), arguing that co-translational insertion of the signal sequence–containing, hemagglutinin-tagged RL (ER-HA-RL) to the ER should make nascent proteins inaccessible to proteolysis. Inhibition of

[1]Friedrich Miescher Institute for Biomedical Research, 4002 Basel, Switzerland. [2]Institut de Génétique Moléculaire de Montpellier, 34000 Montpellier, France.

*To whom correspondence should be addressed. E-mail: Filipowi@fmi.ch

ER-HA-RL expression was similar to that of HA-RL by both let-7 and the hAgo2 tethering (Fig. 1B). Western analysis performed with purified ER fractions indicated that, as expected, the ER-HA-RL protein was targeted into the ER lumen (fig. S2). We also tested the effect of the proteasome inhibitors MG132 and Z-Leu-Leu-Leu-al. Neither relieved the repression (*9*). Together, these results suggest that translation itself is the target of the inhibition.

To determine which translation step is inhibited by miRNAs, we analyzed polysome profiles of reporter mRNAs undergoing repression by let-7 (Fig. 1, C to G) or tethered hAgo2 (fig. S3A). In both cases the repression was accompanied by a strong shift of reporter mRNAs toward the top of the gradient, similar to that seen upon addition of NaF or harringtonine, known inhibitors of translation initiation (fig. S3, B and C). The shift was largely eliminated when cells were co-transfected with anti-let-7 but not control oligonucleotide or when RL-3xBulgeMut [this RNA contains nonfunctional let-7 sites (fig. S9B)] was used as a reporter (Fig. 1, F and G). The distribution of endogenous β-actin mRNA remained unchanged, arguing for a specificity of the effect. These results suggest that miRNAs in mammalian cells inhibit the loading of mRNA to polysomes, possibly resulting from a block in initiation.

To investigate the mechanism of miRNA repression in more detail, we synthesized RNA reporters bearing different 3′-UTRs in vitro and studied their expression in transfected HeLa cells. We found that activity of the m^{7}GpppN-capped RL-Perf or RL-3xBulge reporters, with or without a polyadenylate [poly(A)] tail, was about 10-fold lower than that of control RL RNAs (Fig. 2A). Similar results were obtained with FL reporters (fig. S4A). Co-transfection of the anti-let-7 but not of control oligonucleotide markedly increased the activity of 3xBulge RNAs, indicating that the effect was specific (fig. S4, B and C). When tested for translation in reticulocyte or wheat germ extracts [these extracts do not recapitulate the let-7–mediated repression (*10*)], the FL- and RL-3xBulge, FL- and RL-Perf, and FL- and RL-Con RNAs showed similar activity (fig. S4, D to G). We conclude that the let-7–mediated repression of capped mRNAs can be reproduced in HeLa cells transfected with RNA and that a poly(A) tail is not required for the repression.

We examined whether translation initiated at the internal ribosome entry site (IRES) is subject to the repression. Translation starting at the IRES is not dependent on the 5′-terminal m^{7}G cap, and its requirements for initiation factors differ from the cap-initiated reaction (*11*). In contrast to cap-dependent translation, the activity of transfected RNAs containing the IRES of the encephalomyocarditis virus (EMCV), EMCV-RL, and EMCV-FL, or the IRES of the hepatitis C virus (HCV-FL) was not down-regulated by the insertion of let-7 sites. Moreover, co-transfection of the anti-let-7 oligonucleotide had no effect on the activity of IRES-containing mRNAs bearing let-7 sites (Fig. 2B and fig. S5A). We also compared the effect of let-7 site insertion on EMCV-IRES– and cap-mediated translation by co-transfecting both classes of RNA. For both the RL and FL reporters, only activity of the capped RNA was inhibited (fig. S5, B to H). These results argue against the possibility that resistance of IRES-containing mRNAs to the inhibition is due to saturation of the available let-7 miRNP.

Resistance of IRES-mediated translation to let-7 inhibition implied that the miRNA machinery targets an early step in protein synthesis, a step required for the cap- but not the IRES-dependent initiation. To substantiate this possibility, we constructed dicistronic reporters in which translation of the downstream RL cistron is driven by the initiation factors eIF4E or eIF4G directly tethered at the intercistronic region via either two or six BoxB hairpins (Fig. 2C and fig. S6). For tethering, mutant forms of both factors were expressed as fusions with the N peptide, which binds to BoxB hairpins. Prior experiments (*12*) have indicated that tethering of either factor promotes cap-independent translation. Consistently, we found that tethering of eIF4E or eIF4G, but not of lacZ used as a control, promoted translation of the downstream cistron without having any effect on the cap-dependent synthesis of FL. Most importantly, insertion of three let-7 sites down-regulated synthesis of FL by about threefold (in a let-7–RNA–dependent process) (fig. S6A) but had no effect on a cap-independent translation started internally in response to eIF4E or eIF4G tethering (Fig. 2C and fig. S6). These data suggest that the miRNA machinery interferes with the step upstream of eIF4E recruitment of eIF4G during initiation, possibly with the recognition of the m^{7}G cap by eIF4E.

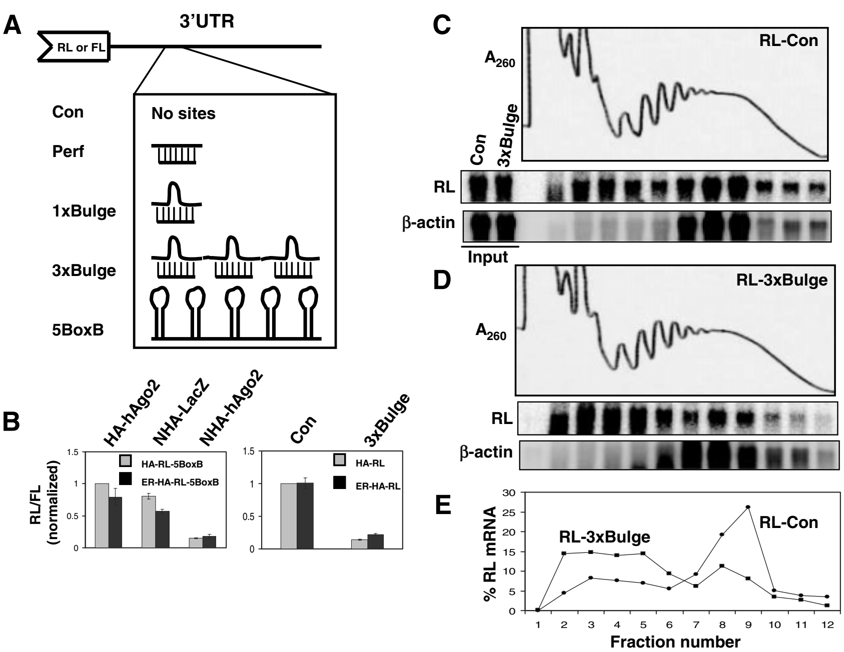

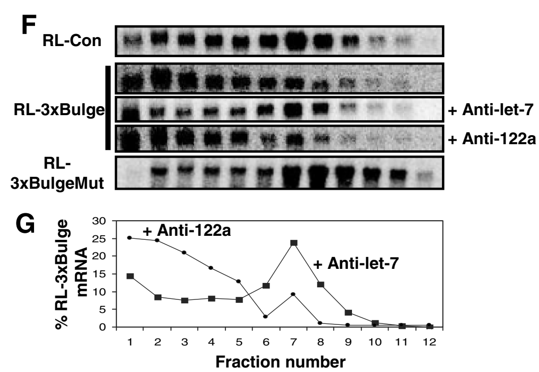

Fig. 1. The miRNA-mediated repression targets translational initiation. (**A**) Schematic representation of mRNA reporters used for most experiments. (**B**) Targeting of the protein to ER does not interfere with repression. Cells were transfected with RL reporters, which express RL that is either cytoplasmic (HA-RL) or targeted to the ER lumen (ER-HA-RL). Activity of reporters regulated by tethered NHA-hAgo2 (but not HA-hAgo2 or NHA-LacZ) and endogenous let-7 is shown in the left and right, respectively. (**C** and **D**) Polysomal distribution of RL mRNAs in extracts prepared from cells transfected with either pRL-Con (C) or pRL-3xBulge (D). RNA extracted from individual fractions was analyzed with probes specific for RL and endogenous β-actin mRNAs. (**E**) Quantification of mRNA distribution, expressed as a percentage of total radioactivity present in each fraction. (**F** and **G**) The shift of RL-3xBulge mRNA to the top of the gradient is specifically eliminated upon co-transfection of anti-let-7 oligonucleotide. (F) Transfected reporters and oligonucleotides are indicated. The bottom row represents analysis of RL-3xBulgeMut, containing nonfunctional let-7 sites. (G) Quantification of RL-3xBulge mRNA distribution in the presence of 2′-*O*-Me oligonucleotides.

We analyzed the intracellular localization of the miRNP components. Previous work has indicated that translationally repressed mRNAs can be sequestered in specific cellular structures such as germline (*13*) or stress (*14*) granules. Immunofluorescence analysis indicated that HA-tagged hAgo2-4 proteins, expressed in transfected HeLa and human embryonic kidney (HEK) 293 cells (fig. S7) or in stable HeLa cell lines (figs. S8, A to C, and S9A), localize to processing bodies (PBs; visualized as structures enriched in the marker proteins Lsm1, Dcp1a, and Xrn1), suborganelles identified as sites of mRNA degradation (*15*). Association of Ago proteins with PBs was further confirmed by co-immunoprecipitation experiments (fig. S8, D and E). Notably, the GFP-tagged Dcp1 was found to interact with HA-hAgo2 but not HA-hAgo2$^{\Delta PRP}$, a mutant of hAgo2 that does not function as a repressor (*8*) (fig. S8E).

Next, we analyzed the cellular distribution of reporter mRNAs by in situ hybridization in HeLa cells. The RL-3xBulge mRNA but not its mutant version, RL-3xBulgeMut, co-localized with the PB marker Dcp1a, expressed as a fusion with green fluorescent protein (GFP) (Fig. 3A and table S1). The co-localization of RL-3xBulge mRNA with PBs was let-7–dependent (table S2). Moreover, RL-3xBulgeMut RNA accumulated in PBs when co-transfected with the siRNA-like duplex, let-7Mut, which carries mutations restoring base pairing between let-7 and RL-3xBulgeMut RNAs (Fig. 3A and fig. S10). The RL-Perf mRNA could not be visualized in PBs, arguing against a possibility that RL-3xBulge or RL-3xBulgeMut signals in PBs originate from an mRNA targeted for degradation (fig. S11). Closer examination of the images provided additional evidence that RL-3xBulge RNA localization is not related to the degradative function of PBs. RL-3xBulge RNA was often found adjacent to Dcp1 foci and not overlapping with them (Fig. 3A, fig. S11, and table S3). Furthermore, we also observed that some Dcp1 foci did not contain detectable amounts of RL-3xBulge RNA and, conversely, that a few mRNA foci were negative for Dcp1 (*9*). These data point to some heterogeneity and/or compartmentalization of PBs.

We used HeLa cells stably expressing either RL-3xBulge or RL-3xBulgeMut reporters (fig. S9, B and C) to further document the association of repressed mRNAs with cellular structures. The cells were permeabilized with digitonine, and the resulting S14 supernatant and pellet fractions were analyzed for the presence of mRNAs and PB and miRNP components. The RL-3xBulgeMut RNA was enriched in a soluble fraction, but the RL-3xBulge reporter was found almost exclusively in the pellet fraction containing cellular structures. Likewise, endogenous N-Ras and K-Ras mRNAs, recently established targets of let-7 RNA (*16*), were enriched in the pellet as were all tested PB and miRNP components (fig. S12). Importantly, treatment of cells with anti-let-7 oligonucleotide specifically released a substantial fraction of the pellet-associated mRNAs to the supernatant (fig. S12A).

Lastly, we investigated whether miRNAs localize to specific cellular structures. The let-7 and miR-122a probes stained dot-like structures in HeLa and human hepatoma Huh7 cells, respectively, but not in control cells known not to express these miRNAs (*16*, *17*) (Fig. 3B). No staining was observed with the mutant or pre-miRNA–specific probes (fig. S13). Because the in situ hybridization was not compatible with the antibody labeling of PBs, we microinjected the in vitro–transcribed, Cy3-labeled pre–let-7 RNA into nuclei of HeLa cells and analyzed its distribution. Remarkably, exported let-7 RNA accumulated in PB foci also labeled with antibodies against Dcp1 (Fig. 3C). The presence of let-7 in the cytoplasm was inhibited by wheat germ agglutinin, indicating that export of pre-miRNA from the nucleus occurred by a physiological mechanism (fig. S14). As with the RL-3xBulge RNA foci, let-7 foci were frequently adjacent to, rather than exactly co-localizing with, Dcp1 foci. Some let-7 foci not labeled by Dcp1, and vice versa, were also observed (Fig. 3C and tables S1 and S3).

Our data indicate that, in mammalian cells, let-7 miRNP inhibits translation at the initiation step. The observation that the cap-independent translation is immune to the repression suggests that miRNPs target an early step of initiation, likely involving the m^{7}G cap. Importantly, the results of experiments involving an entirely independent methodology—a direct tethering of hAgo2 to mRNA reporters, an approach that mimics the miRNP-mediated inhibition (*8*)—are consistent with the above interpretation. Inhibition of initiation by factors binding to the mRNA 3′-UTR is a common theme in translational regulation. Such inhibition may involve interference either with the recruitment of eIF4E to the m^{7}G cap or with the eIF4E-eIF4G interaction (*18*–*20*). Our findings that the polysomal status of mRNAs repressed by let-7 in mammalian cells differs from that of mRNAs repressed by lin-4 in *C. elegans* (*1*, *2*) suggest that the inhibition of productive translation by different miRNAs, or in different organisms, can follow diverse routes.

After initial submission of this work, other reports implicating PBs in miRNA-mediated repression have appeared (*21*, *22*). Our data extend these findings by directly demonstrating that miRNAs and repressed mRNAs localize to PBs. We believe that relocalization of the repressed mRNA to PBs is a consequence rather

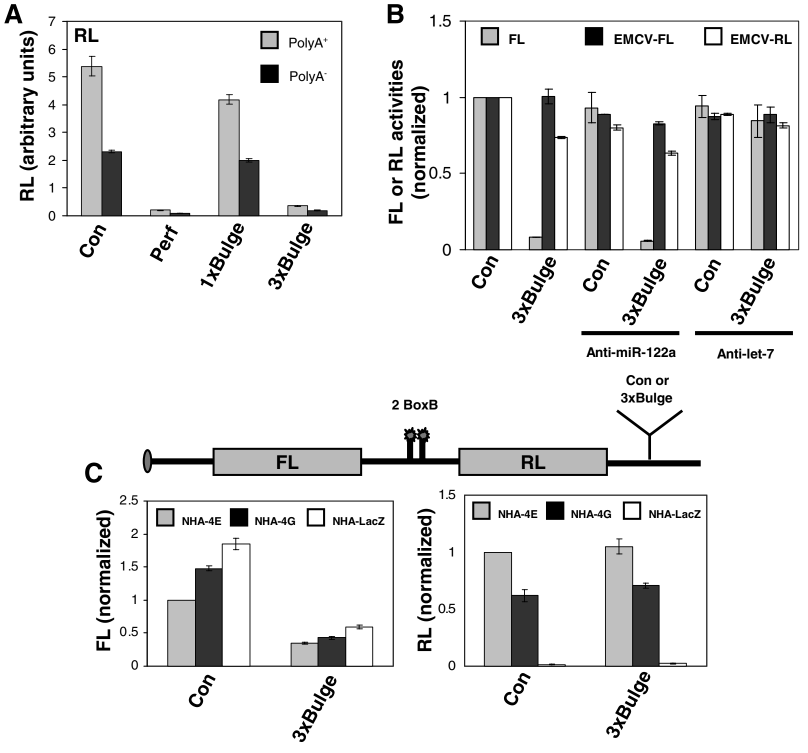

Fig. 2. Cap-dependent but not cap-independent translation is repressed by let-7. The values represent means of three transfections ± SD. (**A**) Translation of the in vitro–transcribed capped RL-RNA reporters, either poly(A)$^+$ (200 ng) or poly(A)$^-$ (400 ng), in transfected HeLa cells. (**B**) IRES-mediated translation is immune to repression by let-7. HeLa cells were transfected with 200 ng of the indicated noncapped EMCV-FL or -RL RNAs or capped FL RNA. Oligonucleotides were included as indicated. (**C**) Translation driven by the tethered initiation factor eIF4E or eIF4GI is immune to let-7 repression. Cells were transfected with 100 and 500 ng of plasmids expressing dicistronic reporters and indicated NHA fusions. Activities in co-transfections performed with pFL-2BoxB-RL-Con and pNHA-eIF4E were set to 1.

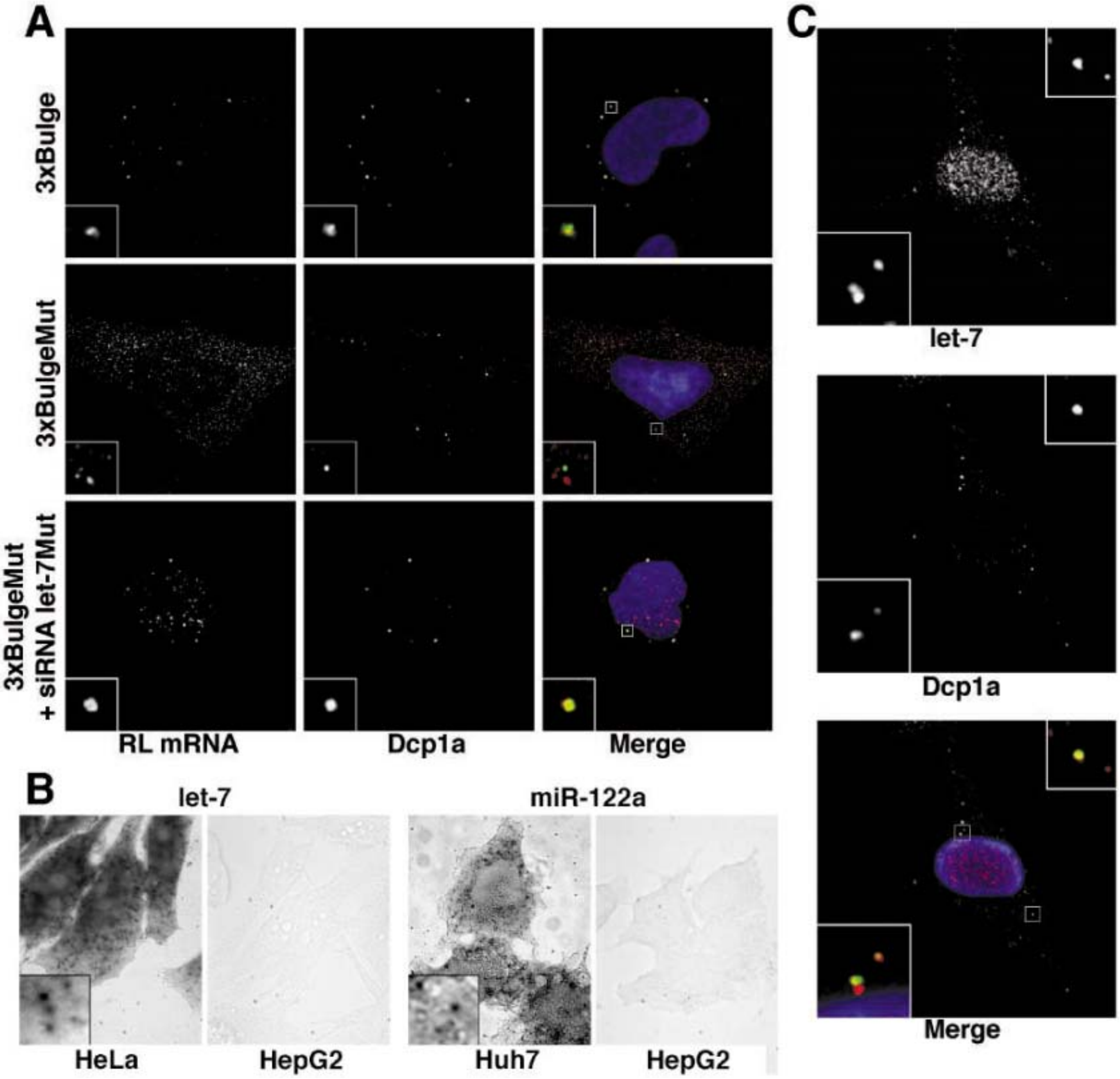

Fig. 3. Localization of translationally repressed mRNA and miRNAs to discrete foci adjacent to or overlapping with PBs. Insets represent enlargements of indicated regions, representative of localization of RL reporters, miRNAs, and Dcp1a. (**A**) HeLa cells were cotransfected with the indicated RL reporters and a plasmid expressing GFP-Dcp1a. Cells shown in a lowest row we additionally cotransfected with the let-7Mut duplex. RL mRNAs were detected by in situ hybridization with Cy3-conjugated probes (red), and Dcp1a was visualized by GFP fluorescence (green). The nucleus was stained with 4′,6′-diamidino-2-phenylindole (DAPI, blue). (**B**) Enrichment of endogenous miRNAs let-7 and miR-122a in dot-like structures. The indicated cells were stained with digoxigenin-labeled complementary probes. (**C**) Accumulation of let-7 RNA in foci adjacent to or overlapping with PBs. Nuclei of HeLa cells were microinjected with an in vitro–transcribed Cy3-labeled RNA (red), which self-cleaves to produce authentic pre–let-7 RNA (*26*). Cells were counterstained with anti-Dcp1a antibody to locate PBs (green). The Cy3 staining of the nucleus likely originates from the 5′ cleavage fragment of the ribozyme.

than a cause of the repression. However, the relocalization could contribute to the repression by maintaining the mRNA in an environment unfavorable for translation (*15*, *23*, *24*). Inhibition of translation initiation leads to the appearance of stress granules and the concomitant recruitment of repressed mRNAs to these structures (*24*). PBs were originally identified as sites of mRNA degradation (*15*), but a role in mRNA storage has recently been suggested (*23*). Our results provide experimental evidence that PBs could act as a storage compartment for translationally repressed mRNAs. The observation that the repressed reporter mRNA, and also let-7 RNA, do not always precisely co-localize with a PB marker protein, Dcp1p, suggests that PBs may comprise two subcompartments, one dedicated to the storage of mRNA and the other to its degradation. Close proximity of the compartments might explain why mRNAs subjected to miRNP-mediated repression may also undergo limited degradation (*25*).

References and Notes

1. P. H. Olsen, V. Ambros, *Dev. Biol.* **216**, 671 (1999).
2. K. Seggerson, L. Tang, E. G. Moss, *Dev. Biol.* **243**, 215 (2002).
3. J. G. Doench, C. P. Petersen, P. A. Sharp, *Genes Dev.* **17**, 438 (2003).
4. Y. Zeng, R. Yi, B. R. Cullen, *Proc. Natl. Acad. Sci. U.S.A.* **100**, 9779 (2003).
5. J. Brennecke, D. R. Hipfner, A. Stark, R. B. Russell, S. M. Cohen, *Cell* **113**, 25 (2003).
6. D. P. Bartel, *Cell* **116**, 281 (2004).
7. Q. Jing *et al.*, *Cell* **120**, 623 (2005).
8. R. S. Pillai, C. G. Artus, W. Filipowicz, *RNA* **10**, 1518 (2004).
9. R. S. Pillai *et al.*, data not shown.
10. R. S. Pillai *et al.*, unpublished results.
11. C. U. Hellen, P. Sarnow, *Genes Dev.* **15**, 1593 (2001).
12. E. De Gregorio, J. Baron, T. Preiss, M. W. Hentze, *RNA* **7**, 106 (2001).
13. G. Seydoux, S. Strome, *Development* **126**, 3275 (1999).
14. P. Anderson, N. Kedersha, *J. Cell Sci.* **115**, 3227 (2002).
15. U. Sheth, R. Parker, *Science* **300**, 805 (2003).
16. S. M. Johnson *et al.*, *Cell* **120**, 635 (2005).
17. J. Chang *et al.*, *RNA Biol.* **1**, 2 (2004).
18. F. Gebauer, M. W. Hentze, *Nat. Rev. Mol. Cell Biol.* **5**, 827 (2004).
19. J. D. Richter, N. Sonenberg, *Nature* **433**, 477 (2005).
20. P. F. Cho *et al.*, *Cell* **121**, 411 (2005).
21. G. L. Sen, H. M. Blau, *Nat. Cell Biol.* **7**, 633 (2005).
22. J. Liu, M. A. Valencia-Sanchez, G. J. Hannon, R. Parker, *Nat. Cell Biol.* **7**, 719 (2005).
23. D. Teixeira, U. Sheth, M. A. Valencia-Sanchez, M. Brengues, R. Parker, *RNA* **11**, 371 (2005).
24. M. A. Andrei *et al.*, *RNA* **11**, 717 (2005).
25. L. P. Lim *et al.*, *Nature* **433**, 769 (2005).
26. F. A. Kolb *et al.*, *Methods Enzymol.* **392**, 316 (2005).

27. We thank T. Hobman, R. Lührmann, J. Lykke-Andersen, A. Prats, B. Seraphin, and N. Sonnenberg for providing plasmids and antibodies and F. Rage, S. Fumagalli, N. Sonenberg, and members of the Filipowicz group for help and discussions. This work was supported by grant 3109 of l'Association de la Recherche Contre le Cancer to E.B. S.N.B. is a recipient of a long-term fellowship from the Human Frontier Science Program. The Friedrich Miescher Institute is supported by Novartis Research Foundation.

Supporting Online Material

www.sciencemag.org/cgi/content/full/1115079/DC1
Materials and Methods
Figs S1 to S14
Tables S1 to S3
References

20 May 2005; accepted 22 July 2005
Published online 4 August 2005;
10.1126/science.1115079
Include this information when citing this paper.

Modulation of Hepatitis C Virus RNA Abundance by a Liver-Specific MicroRNA

Catherine L. Jopling,[1] MinKyung Yi,[2] Alissa M. Lancaster,[1] Stanley M. Lemon,[2] Peter Sarnow[1]*

MicroRNAs are small RNA molecules that regulate messenger RNA (mRNA) expression. MicroRNA 122 (miR-122) is specifically expressed and highly abundant in the human liver. We show that the sequestration of miR-122 in liver cells results in marked loss of autonomously replicating hepatitis C viral RNAs. A genetic interaction between miR-122 and the 5′ noncoding region of the viral genome was revealed by mutational analyses of the predicted microRNA binding site and ectopic expression of miR-122 molecules containing compensatory mutations. Studies with replication-defective RNAs suggested that miR-122 did not detectably affect mRNA translation or RNA stability. Therefore, miR-122 is likely to facilitate replication of the viral RNA, suggesting that miR-122 may present a target for antiviral intervention.

MicroRNAs (miRNAs) are a class of small RNA molecules, ~21 to 22 nucleotides (nt) in length, that have been detected in many plant and animal species (*1*). Even certain animal viral RNA genomes encode miRNAs (*2–4*). Cloning efforts and computational predictions have indicated that there are ~800 miRNA-encoding genes in humans (*5*), which together regulate more than 5300 genes (*6*, *7*). Interaction of miRNAs with target mRNAs results in mRNA cleavage if the bound miRNA engages in perfect base complementarity with its target (*8*, *9*). However, in a few cases, imperfect base complementarity between a miRNA and target mRNA leads to translational repression (*10–15*). In all of these examples, the miRNA interacts with sequences within the 3′ noncoding region (NCR) of the target mRNA.

Certain miRNAs are expressed ubiquitously, whereas others are expressed in a highly tissue-specific manner (*16*, *17*). MiR-122 is specifically expressed in the liver, where it constitutes 70% of the total miRNA population (*16*, *18*). To examine the role of miR-122 in regulating mRNA function, we first monitored the expression of miR-122 in liver tissue and liver cell lines. MiR-122 was detected in mouse and human liver, in cultured human Huh7 and mouse Hepa 1-6 liver cells, but not in human cervical carcinoma-derived HeLa

[1]Department of Microbiology and Immunology, Stanford University, Stanford, CA 94305, USA. [2]Center for Hepatitis Research, Department of Microbiology and Immunology, University of Texas Medical Branch, Galveston, TX 77555–1019, USA.

*To whom correspondence should be addressed. E-mail: psarnow@stanford.edu

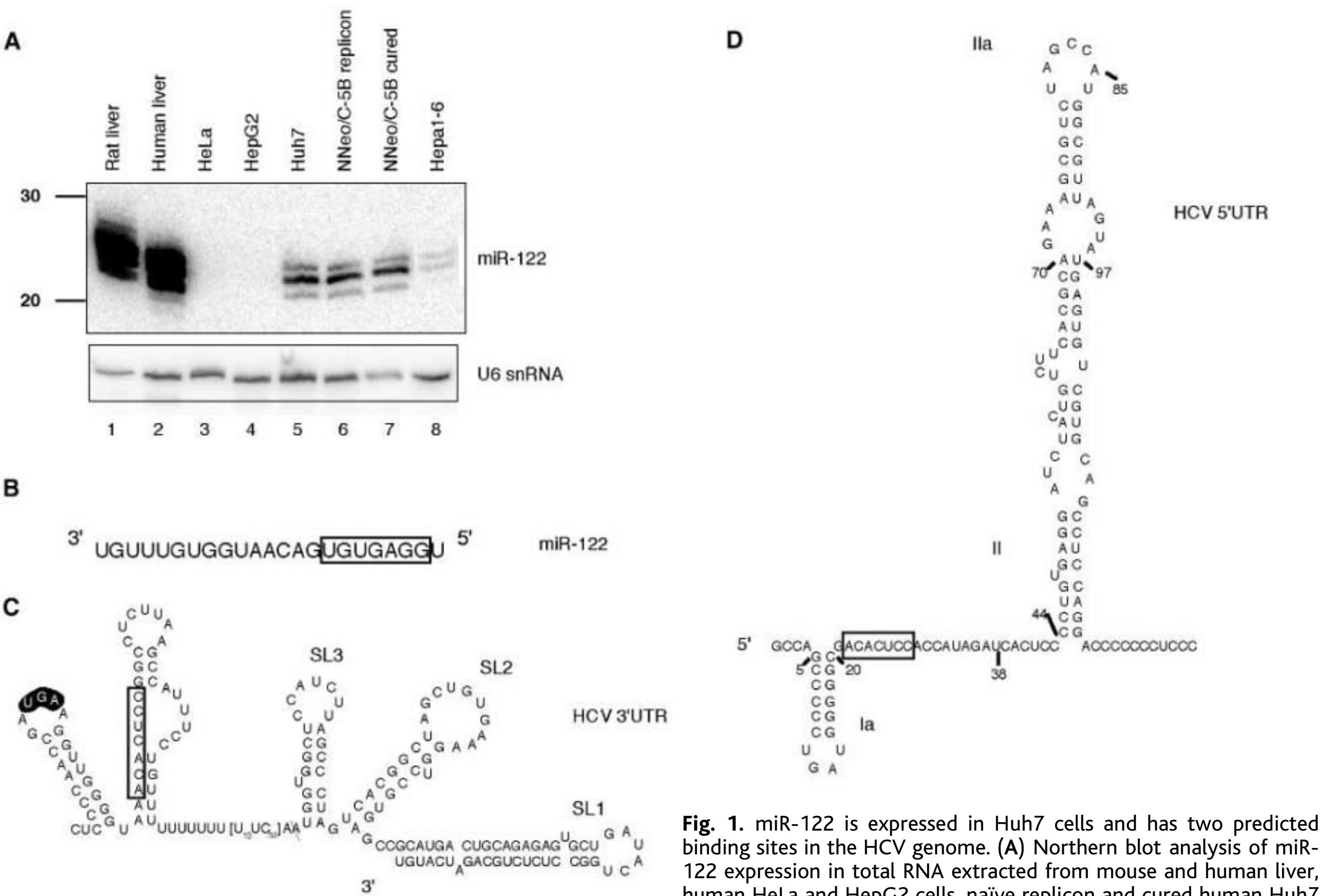

Fig. 1. miR-122 is expressed in Huh7 cells and has two predicted binding sites in the HCV genome. (**A**) Northern blot analysis of miR-122 expression in total RNA extracted from mouse and human liver, human HeLa and HepG2 cells, naïve replicon and cured human Huh7 cells, and mouse Hepa1-6 cells. Expression of U6 small nuclear (sn) RNA was used as a loading control. (**B**) Sequence of miR-122 with the seed sequences surrounded by a box. (**C** and **D**) Secondary structure of the (C) 3′ and (D) 5′ noncoding regions of the HCV genotype 1a strain H77c, with predicted miR-122 binding sites indicated. The seed matches are enclosed in boxes. SL, stem-loop; UTR, untranslated region.

cells or even in human liver-derived HepG2 cells (Fig. 1A).

Hepatitis C virus (HCV) is a hepatotropic, positive-stranded RNA virus belonging to the family *Flaviviridae*; it is a major cause for chronic liver disease with an estimated 170 million people infected (*19*). Although both Huh7 and HepG2 cells are derived from human hepatocytes, HCV RNA constructs can only replicate in Huh7 cells. To explore whether this could be related to the presence of miR-122 in permissive Huh7 cells, we inspected the 9600-nt, positive-strand, viral RNA genome for potential miR-122 binding sites that fulfill the rules for a successful miRNA-target mRNA interaction. We searched for sequences in the viral mRNA that could engage in Watson and Crick base pairing with nucleotides 2 through 8, the "seed sequence" of miR-122 (*6*, *20*), and we noted two predicted binding sites for miR-122 (Fig. 1B) in the viral NCRs. One is located within the viral 3′ NCR of the genotype 1a (Fig. 1C). Although this sequence is in the "variable region" of the 3′ NCR, the seed match sequence itself is highly conserved among the six HCV genotypes (table S1). The second miR-122 binding site is also conserved and is located within the 5′ NCR, only 21 nt from the 5′ end of the viral genome (Fig. 1D). With the exception of genotype 2, the putative seed match sequence is flanked by adenosines (table S1), indicative of a high confidence miRNA-binding site (*6*).

To determine whether miR-122 regulates HCV gene expression, we tested whether its inactivation would alter the abundance of an autonomously replicating, dicistronic HCV RNA replicon. Huh7 cells stably expressing the genotype 1b strain HCV-N replicon NNeo/C-5B were used (Fig. 2A) (*21*). To inactivate miR-122 in this cell line, NNeo/C-5B cells were transfected with a 2′-O-methylated RNA oligonucleotide (122-2′OMe) with exact complementarity to miR-122. Such oligonucleotides have been shown to sequester miRNAs (*22*, *23*). As a control for functional inactivation of miR-122, we monitored the expression of enhanced green fluorescent protein (eGFP) sensor mRNAs that contained sequences complementary to miR-122 in their 3′ NCR (eGFP-122). Because of its complete complementarity, miR-122 should lead to the nucleolytic degradation of the eGFP mRNAs. Indeed, little full-length eGFP-122 RNA was detected in cells transfected with plasmids encoding eGFP-122 (Fig. 2A, lane 3), although a similar RNA that contained sites complementary to the brain-specific miR-124 was expressed at high levels (Fig. 2A, lane 2). Upon transfection with 122-2′OMe, the amount of eGFP-122 RNA markedly increased (Fig. 2A, lane 4), whereas a randomized oligomer (Rand-2′OMe, lane 5) and an oligomer complementary to miRNA

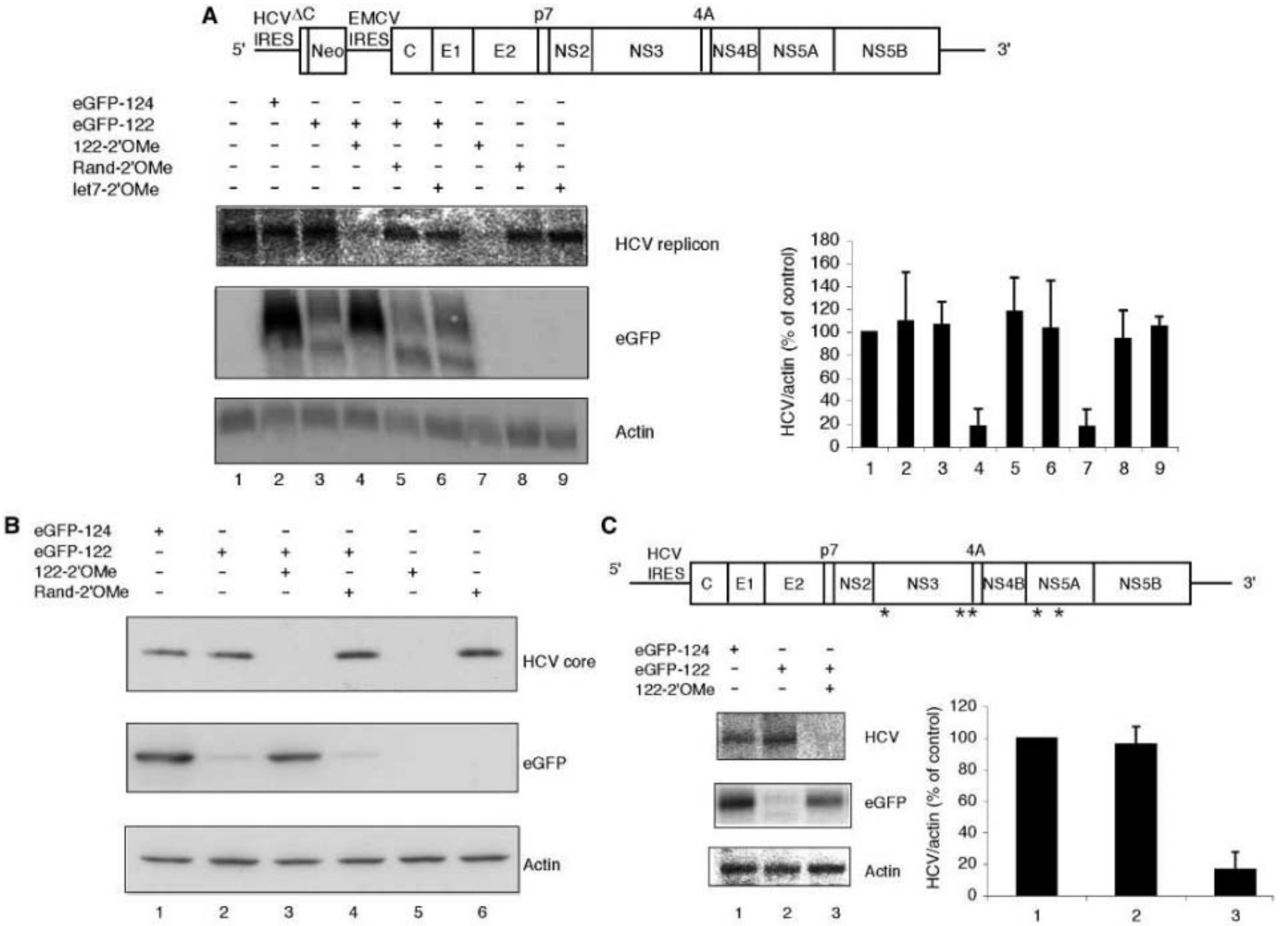

Fig. 2. Sequestration of miR-122 reduces HCV RNA and protein abundance in replicon cells. (**A**) Northern blot analysis of HCV, eGFP, and actin RNA in the NNeo/C-5B replicon cell line. In these replicon RNAs (*21*), the HCV internal ribosome entry site (IRES) directs the synthesis of the neomycin resistance gene product, and the encephalomyocarditis viral IRES (EMCV) directs the synthesis of the structural and nonstructural (NS) proteins of the HCV-N 1b strain. The eGFP sensor plasmids and 2′-O-methylated oligonucleotides were introduced into cells by lipofectamine 2000–mediated transfection, and total RNA was extracted 48 hours later. Quantitation of the HCV-actin mRNA ratios from three independent Northern blot experiments and the standard deviations are shown. (**B**) Western blot showing levels of HCV core protein, eGFP, and actin 48 hours post-transfection with the indicated eGFP sensor plasmids and 2′-O-methylated oligomers. (**C**) Northern analysis of HCV, eGFP, and actin RNA in Huh7 cells containing the genome-length genotype 1a H77c RNA and transfected with eGFP-122 and 122-2′OMe. Quantitation of the HCV-actin mRNA ratios from three independent Northern blot experiments and the standard deviations are shown. The locations of cell culture–acquired adaptive mutations in the viral RNA are indicated by asterisks in the top diagram.

let-7a (let7-2′OMe) had no effect (Fig. 2A, lane 6). The level of HCV viral replicon RNA was specifically reduced by ~80% when miR-122 was inactivated (Fig. 2A, lanes 4 and 7). Reduced mRNA abundance resulted in a decrease in HCV protein expression in cells transfected with the 122-2′OMe oligomer, whereas the level of eGFP protein increased under this experimental condition (Fig. 2B, lane 3).

To determine whether miR-122 would similarly affect RNA accumulation in cells newly transfected with replication-competent HCV RNA, RNA transcripts were synthesized from a cDNA that encodes the full-length genotype 1a strain H77c genome. Five adaptive mutations in the cDNA (Fig. 2C, top) promote efficient RNA replication in Huh7 cells (*24*). Introduction of these RNAs into Huh7 cells led to accumulation of viral RNA in the presence of endogenous miR-122 (Fig. 2C, lanes 1 and 2); in contrast, viral RNA failed to accumulate when miR-122 was sequestered by 122-2′OMe oligomers (Fig. 2C, lane 3). Furthermore, the 122-2′OMe oligomer did not affect total protein synthesis in transfected cells, excluding the possibility that the 122-2′OMe oligomer induced antiviral effects (fig. S1). Thus, miR-122 is required to maintain the abundance of both genotypes 1a and 1b RNA, both in a stable cell line supporting autonomous replication of a dicistronic replicon and upon direct transfection of minimally modified genomic RNA.

To investigate whether the putative miR-122 binding sites are required for the miR-122 effects on RNA abundance, we introduced mutations into the H77c cDNA. Transfection of H77c RNAs containing a 4-nt substitution mutation, m3′, in the predicted seed match in the 3′ NCR (Fig. 3A, left) did not diminish RNA accumulation (Fig. 3B, lane 2). In contrast, RNAs that contained single-nucleotide substitution mutations at the p3 and p6 positions in the seed match in the 5′ NCR or double mutations at the p3-p4 position failed to accumulate (Fig. 3B, lanes 4, 9, and 11). However, RNAs with mutations at p1 accumulated to similar levels (Fig. 3B, lane 8) as wild-type RNA (lane 6), supporting the idea that p1 does not contribute to formation of microRNA-mRNA complexes (*6*). These findings suggest that failure to recruit miR-122 to the HCV 5′ NCR caused loss of viral RNA or that the mutations affected translation, stability, or replication of HCV RNA.

If mutations in the HCV 5′ NCR reduced RNA accumulation because of poor binding of miR-122, ectopic expression of miR-122 RNAs that contain base complementary mutations should restore mutant microRNA–mutant RNA complexes. Ectopic expression of wild-type miR-122 RNAs did not rescue p3, p6, or p3-4 mutated viral RNAs (Fig. 3B, lanes 4, 9, and 11) but did enhance the abundance of wild-type viral RNAs (lane 7) and replicon RNAs (fig. S2). This demonstrated that the introduced miR-122 RNAs entered the cellular machinery as functional miRNA molecules and that the

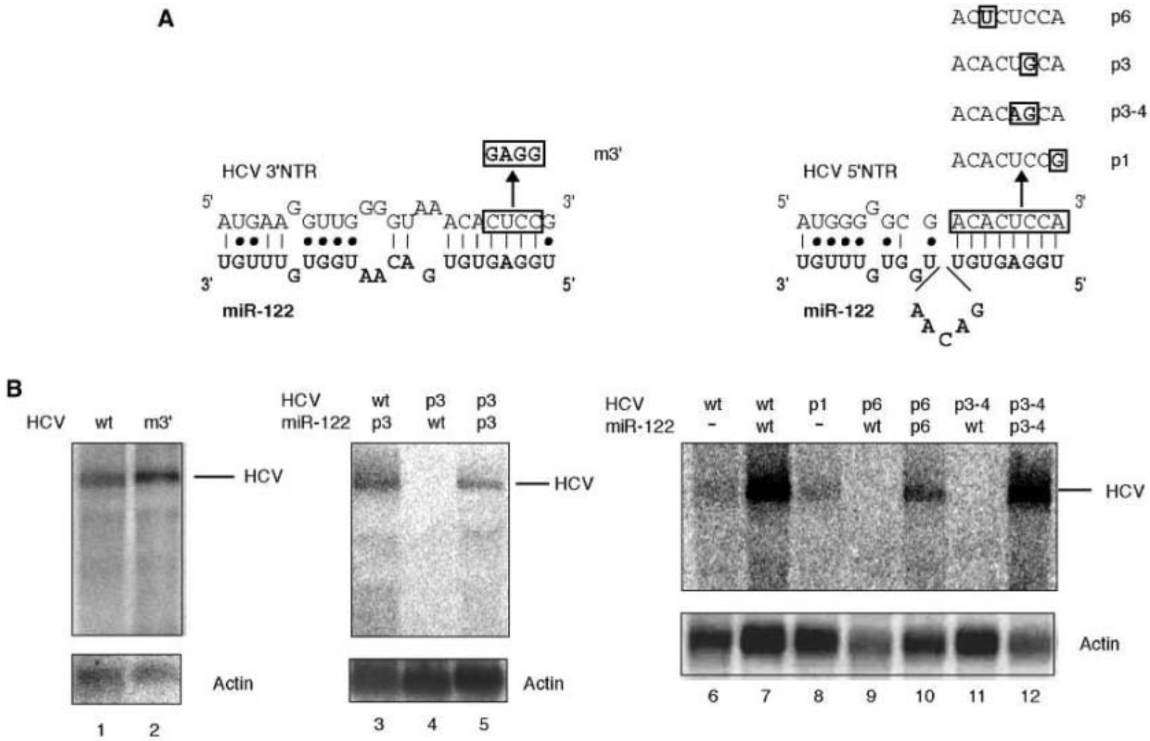

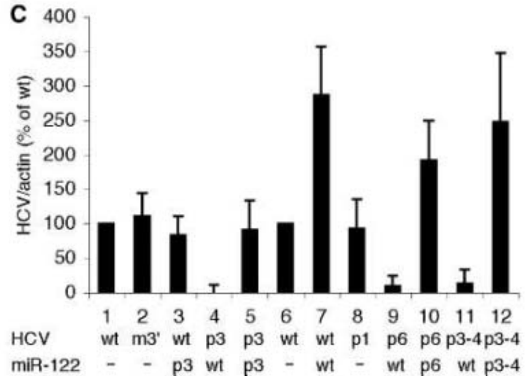

Fig. 3. The predicted miR-122 binding site in the 5′ noncoding region of HCV is required for viral RNA maintenance and directly interacts with miR-122. (**A**) Position of the mutations introduced into the H77c full-length RNA. The locations of a 4-nt substitution mutation in the seed match in the 3′ noncoding region (m3′) and single- or double-substitution mutations in the 5′ noncoding region seed match (p1, p3, p6, and p3-4) are shown. The mutated nucleotides are enclosed in boxes. (**B**) RNA was synthesized by in vitro transcription and introduced into Huh7 cells by electroporation, and HCV RNA levels were determined by Northern blotting 5 days later. Levels of actin mRNAs were determined as loading controls. Cells were transfected with synthetic duplexes corresponding to wild-type miR-122 (wt) or miR-122 with mutations in the seed complementary to the seed match mutations, with the opposite strand of the duplex based on the miR-122 precursor hairpin. The duplexes were introduced into cells 1 day before electroporation with wild-type H77c RNAs or mutant RNAs, and again at 1 and 3 days post-electroporation. Total RNA was harvested 5 days post-electroporation, and HCV and actin RNA levels were determined by Northern blotting. (**C**) Quantitation of the HCV-actin mRNA ratios from three independent Northern blot experiments and the standard deviations are shown.

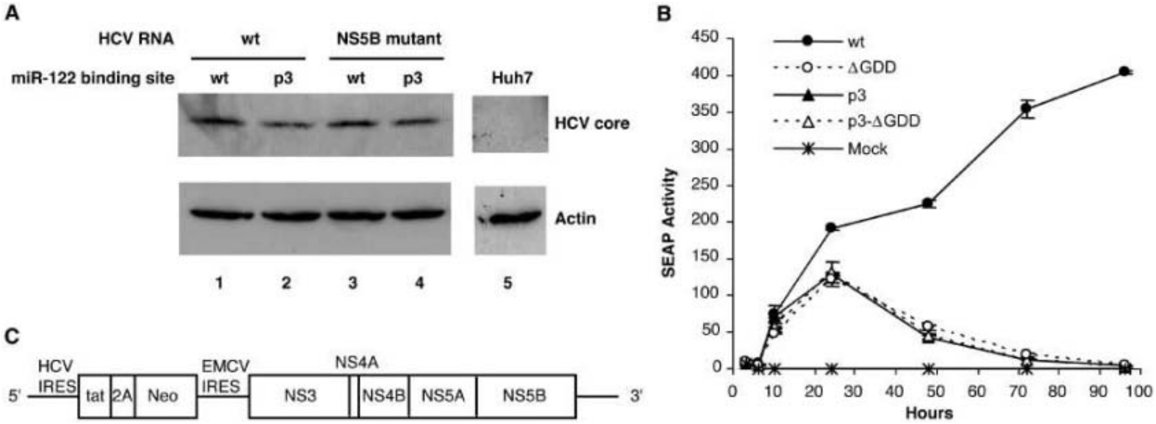

Fig. 4. Effects of mutation of the miR-122 binding site on mRNA translation and RNA stability. (**A**) Mutation of the miR-122 binding site does not affect HCV mRNA translation. The p3 mutation was introduced into a replication-deficient mutant of H77c, containing amino acid changes GDD to AAG at positions 2737 to 2739 in the viral polymerase NS5B (*24*). Lysates were harvested 20 hours after transfection of the wild-type and mutant RNAs, and HCV core protein and actin expression was determined by Western blotting. (**B**) Time course of SEAP production (activity displayed as arbitrary units) after transfection of En5-3 cells with various Ntat2ANeo replicon RNAs (*35*). The p3 mutation in the miR-122 binding site was introduced into both wild-type and the ΔGDD replication-deficient replicon. (**C**) The Ntat2ANeo replicon.

endogenous pool of miR-122 that mediates the accumulation of viral RNA is limiting. In contrast, expression of mutated p3, p6, and p3-4 miR-122 duplexes allowed accumulation of mutated viral RNAs (Fig. 3B, lanes 5, 10, and 12, and Fig. 3C), arguing for a genetic interaction between miR-122 and the 5′ NCR of the HCV genome. Furthermore, the rescue of mutated viral RNAs by miR-122 RNAs carrying complementary mutations provides evidence for a direct HCV RNA–miR-122 interaction, rather than an indirect effect through another miR-122 target.

It has been speculated that microRNAs reduce the accumulation of proteins encoded by target mRNAs by modulating translational efficiency of the mRNAs (*1*). Thus, we examined whether miR-122 modulates translation of HCV RNA, which occurs by an internal ribosome entry mechanism (*25–27*). We monitored the production of HCV core protein from transfected replicating and nonreplicating viral RNAs, containing or lacking miR-122 binding sites. Slightly greater amounts of core protein accumulated by 20 hours after transfection with wild-type (Fig. 4A, lane 1) versus p3-mutant RNA (Fig. 4A, lane 2). This difference is likely due to early replication of wild-type RNA. However, we were unable to detect full-length viral RNA by Northern analysis at this time point. To examine production of core protein from input RNAs in the absence of replication, we monitored translation of replication-defective viral RNAs. Both wild-type (Fig. 4A, lane 3) and p3-mutant (lane 4) RNAs containing a replication-lethal mutation in the viral RNA polymerase (GDD to AAG) produced similar amounts of core protein. These data may indicate that p3-mutant RNAs are less stable yet more efficiently translated than wild-type RNAs. An alternative interpretation suggests that mutant and wild-type RNAs display similar stabilities and translational efficiencies at 20 hours after transfection.

To distinguish between these two possibilities, we monitored the abundance of wild-type and mutated genotype 1b replicon RNAs derived from the strain HCV-N after their transfection into En5-3 cells. These replicon RNAs (Fig. 4C) express the human immunodeficiency virus tat protein and induce secretion of alkaline phosphatase (SEAP) in these cells in a manner that quantitatively reflects the intracellular abundance of the replicon RNAs (*28*). The mutant p3 replicon failed to accumulate over time after transfection compared to the wild-type replicon (Fig. 4B). Furthermore, the SEAP secretion profile of the p3 replicon mirrored that of cells transfected with the replication-deficient ΔGDD mutant, arguing that translation and stability of mutant p3-replicon RNAs are not affected by the p3 mutation (Fig. 4B). Taken together, these findings suggest that mutation of the seed match sequence for miR-122 in the HCV 5′ NCR does not primarily affect RNA translation or stability, at least at early times after RNA transfection, and likely affects viral RNA replication. In the absence of miR-122, core-encoding sequences have been reported to interact with nucleotides 24 to 38 in the viral 5′ NCR, resulting in translational inhibition in dicistronic mRNAs (*29*). However, mutations encompassing the miR-122 binding site have been shown to primarily affect replication of replicon RNAs (*30*) in cells expressing miR-122, suggesting that miR-122 may aid in RNA folding or RNA sequestration in replication complexes.

Although two plant miRNAs interact with the 5′ NCR of their target mRNAs (*31*), this has not been observed for animal miRNAs (*6*). Thus, our finding that the HCV genome recruits miR-122 to its 5′ end raises the question of whether 5′ NCRs in other viral or host cell mRNAs can also be targeted by microRNAs and whether such interactions regulate mRNA translation, mRNA turnover, or possibly RNA localization. HCV RNA can replicate in nonhepatic cells (*32–34*), raising the question of whether the role of miR-122 in regulating HCV gene expression is liver-specific. What are the natural targets for miR-122 in the liver, and is their expression affected by HCV infection? Finally, current therapies against HCV are frequently ineffective; thus, there is a need to search for alternative antiviral targets. Sequestration of host-encoded miR-122 could provide a possible antiviral tool against a rapidly evolving viral genome.

References and Notes

1. Y. Tomari, P. D. Zamore, *Genes Dev.* **19**, 517 (2005).
2. Y. Bennasser, S. Y. Le, M. L. Yeung, K. T. Jeang, *Retrovirology* **1**, 43 (2004).
3. S. Pfeffer *et al.*, *Science* **304**, 734 (2004).
4. C. S. Sullivan, A. T. Grundhoff, S. Tevethia, J. M. Pipas, D. Ganem, *Nature* **435**, 682 (2005).
5. I. Bentwich *et al.*, *Nat. Genet.* **37**, 766 (2005).
6. B. P. Lewis, C. B. Burge, D. P. Bartel, *Cell* **120**, 15 (2005).
7. X. Xie *et al.*, *Nature* **434**, 338 (2005).
8. G. Hutvagner, P. D. Zamore, *Science* **297**, 2056 (2002).
9. S. Yekta, I. H. Shih, D. P. Bartel, *Science* **304**, 594 (2004).
10. X. Chen, *Science* **303**, 2022 (2004).
11. J. G. Doench, C. P. Petersen, P. A. Sharp, *Genes Dev.* **17**, 438 (2003).
12. J. G. Doench, P. A. Sharp, *Genes Dev.* **18**, 504 (2004).
13. P. H. Olsen, V. Ambros, *Dev. Biol.* **216**, 671 (1999).
14. S. Saxena, Z. O. Jonsson, A. Dutta, *J. Biol. Chem.* **278**, 44312 (2003).
15. Y. Zeng, R. Yi, B. R. Cullen, *Proc. Natl. Acad. Sci. U.S.A.* **100**, 9779 (2003).
16. M. Lagos-Quintana *et al.*, *Curr. Biol.* **12**, 735 (2002).
17. L. F. Sempere *et al.*, *Genome Biol.* **5**, R13 (2004).
18. J. Chang *et al.*, *RNA Biol.* **1**, 106 (2004).
19. J. H. Hoofnagle, *Hepatology* **36**, S21 (2002).
20. B. P. Lewis, I. H. Shih, M. W. Jones-Rhoades, D. P. Bartel, C. B. Burge, *Cell* **115**, 787 (2003).
21. M. Ikeda, M. Yi, K. Li, S. M. Lemon, *J. Virol.* **76**, 2997 (2002).
22. G. Hutvagner, M. J. Simard, C. C. Mello, P. D. Zamore, *PLoS Biol.* **2**, E98 (2004).
23. G. Meister, M. Landthaler, Y. Dorsett, T. Tuschl, *RNA* **10**, 544 (2004).
24. M. Yi, S. M. Lemon, *J. Virol.* **78**, 7904 (2004).
25. H. Ji, C. S. Fraser, Y. Yu, J. Leary, J. A. Doudna, *Proc. Natl. Acad. Sci. U.S.A.* **101**, 16990 (2004).
26. G. A. Otto, J. D. Puglisi, *Cell* **119**, 369 (2004).
27. T. V. Pestova, I. N. Shatsky, S. P. Fletcher, R. J. Jackson, C. U. Hellen, *Genes Dev.* **12**, 67 (1998).
28. M. Yi, F. Bodola, S. M. Lemon, *Virology* **304**, 197 (2002).
29. Y. K. Kim, S. H. Lee, C. S. Kim, S. K. Seol, S. K. Jang, *RNA* **9**, 599 (2003).
30. P. Friebe, V. Lohmann, N. Krieger, R. Bartenschlager, *J. Virol.* **75**, 12047 (2001).
31. R. Sunkar, J. K. Zhu, *Plant Cell* **16**, 2001 (2004).

32. S. Ali, C. Pellerin, D. Lamarre, G. Kukolj, *J. Virol.* **78**, 491 (2004).
33. T. Kato *et al.*, *J. Virol.* **79**, 592 (2005).
34. Q. Zhu, J. T. Guo, C. Seeger, *J. Virol.* **77**, 9204 (2003).
35. Materials and methods are available as supporting material on *Science* Online.
36. We thank K. Kirkegaard for discussions and critical reading of the manuscript. Supported in parts by NIH grant nos. AI47365 and GM069007 (P.S.), AI40035 (S.M.L.), and AI63451 (MK.Y) and by International Research Fellowship 066592/Z/01/Z from the Wellcome Trust (C.L.J.).

Supporting Online Material
www.sciencemag.org/cgi/content/full/309/5740/1577/DC1
Materials and Methods
Figs. S1 and S2
Table S1

8 April 2005; accepted 8 August 2005
10.1126/science.1113329

Recombination Regulation by Transcription-Induced Cohesin Dissociation in rDNA Repeats

Takehiko Kobayashi[1,2]* and Austen R. D. Ganley[1]

Organisms maintain ribosomal RNA gene repeats (rDNA) at stable copy numbers by recombination; the loss of repeats results in gene amplification. Here we report a mechanism of amplification regulation. We show that amplification is dependent on transcription from a noncoding bidirectional promoter (E-pro) within the rDNA spacer. E-pro transcription stimulates the dissociation of cohesin, a DNA binding protein complex that suppresses sister-chromatid–based changes in rDNA copy number. This transcription is regulated by the silencing gene, *SIR2*, and by copy number. Transcription-induced cohesin dissociation may be a general mechanism of recombination regulation.

In most organisms, recombination is necessary for DNA repair, chromosome segregation, and the rescue of stalled replication forks. If not properly regulated, however, recombination can lead to genomic instability (*1*) and can be toxic to cells (*2*). It is not clear how cells maintain only the positive effects of recombination.

In repeated-gene families, such as the ribosomal RNA (rRNA) gene repeats (rDNA), recombination helps maintain copy number (*3*) and the evolutionary stability of the repeats (*4*). The number of rDNA copies is tightly regulated; if repeats are deleted or inserted, copy number is quickly restored to that of the wild type (*5*, *6*). One way that copy number is maintained is by gene amplification after deletional recombination. In the yeast *Saccharomyces cerevisiae,* this amplification is dependent on the replication-fork blocking protein, *FOB1*, and a ~520–base pair (bp) *cis*-acting factor called EXP, which is found in the rDNA intergenic spacer (IGS) (Fig. 1A) (*6*, *7*). In a recent *Saccharomyces* species phylogenetic footprinting study, we found a highly conserved sequence that corresponds to a previously identified bidirectional RNA polymerase II (pol II) promoter (*8*) in EXP (*9*). This EXP promoter (named E-pro) does not appear to be associated with any coding function, and its position and conservation suggested it might play a role in rDNA amplification.

To determine whether E-pro is involved in rDNA amplification, we replaced it with galactose-inducible pol II promoters (unidirectional *GAL7* and bidirectional *GAL1/10* promoters) (fig. S1) in an *S. cerevisiae* strain containing only two rDNA copies (two-copy strain), and we observed the effects on amplification. Reintroduction of a plasmid-borne *FOB1* gene into the two-copy strain stimulated rDNA amplification, and the resulting rDNA copy-number increase can be visualized by an increase in the size of chromosome XII (chr XII) by using pulsed-field gel electrophoresis [contour-clamped homogeneous electric field (CHEF)] (*7*). The deletion of E-pro abolished amplification ability (Fig. 1, B and C), and when E-pro was replaced with the *GAL7* promoter in either direction, amplification ability was not rescued. However, when E-pro was replaced with the bidirectional *GAL1/10* promoter (GAL1/10 strain), the introduction of *FOB1* resulted in amplification.

To confirm that amplification depends on E-pro transcription, we changed the carbon source from galactose to glucose to inhibit transcription in the GAL1/10 strain. The size of chr XII continued to increase in galactose-grown cells, but did not increase in glucose-grown cells over 150 generations (Fig. 1D). Furthermore, the chr XII bands of cells grown in glucose were sharp, indicating the inhibition of rDNA recombination (*6*). To investigate whether read-through transcription or another function of E-pro is required for amplification, we blocked each direction of GAL1/10 transcription by using a transcriptional terminator. Blockage in either direction resulted in the loss of amplification ability (Fig. 1D). Therefore, bidirectional E-pro transcription is essential for rDNA amplification.

How can transcription from E-pro trigger recombination and hence amplification? One way is through cohesin association. Cohesin is a multifunctional protein complex involved in chromatin structure (*10*), and its localization is inversely correlated with transcription, suggesting that transcription disrupts cohesin association (*11*, *12*). Cohesin association is thought to hold chromatids in place, leading to equal (versus unequal) sister-chromatid recombination and thereby preventing changes in copy number after the formation of double-strand breaks (DSBs) (*13*). Thus, E-pro transcription may result in cohesin dissociation, allowing a change in copy number. Chromatin immunoprecipitation (ChIP) assays were performed with a GAL1/10 strain carrying hemagglutinin (HA) epitope–tagged Mcd1p (a cohesin complex component) in conjunction with seven rDNA primer combinations (Fig. 2). In the wild-type strain grown in both glucose and galactose, the cohesin associating region (CAR) gave the strongest signal of cohesin association, as found previously (*13*, *14*), and the pattern in the galactose-grown GAL1/10 strain was similar. However, when grown in glucose, the GAL1/10 strain showed much stronger cohesin association throughout the IGS. Thus, the repression of E-pro transcription leads to increases in cohesin association on both sides of E-pro, not just in CAR. This increase is consistent with bidirectional transcription dissociating cohesin in both IGS1 and 2, and it suggests that unidirectional transcription leaves cohesin association on the opposite side, inhibiting unequal sister-chromatid recombination. We also tested the effect of a cohesin mutation, *smc1-2* (*15*), in the GAL1/10 strain, and we confirmed that the amplification rate was increased (fig. S2).

The silencing gene *SIR2* suppresses rDNA copy-number change through effects on cohesin association, because *SIR2* loss results in the loss of cohesin association in the IGS (*13*). *SIR2* represses pol II–transcribed genes integrated in the rDNA (*16*, *17*). We therefore speculated that *SIR2* regulates recombination by repressing E-pro transcription. To test this,

[1]National Institute for Basic Biology and [2]The Graduate University for Advanced Studies, SOKENDAI, School of Life Science, 38 Nishigonaka, Myodaijicho, Okazaki, 444-8585 Japan.

*To whom correspondence should be addressed. E-mail: koba@nibb.ac.jp

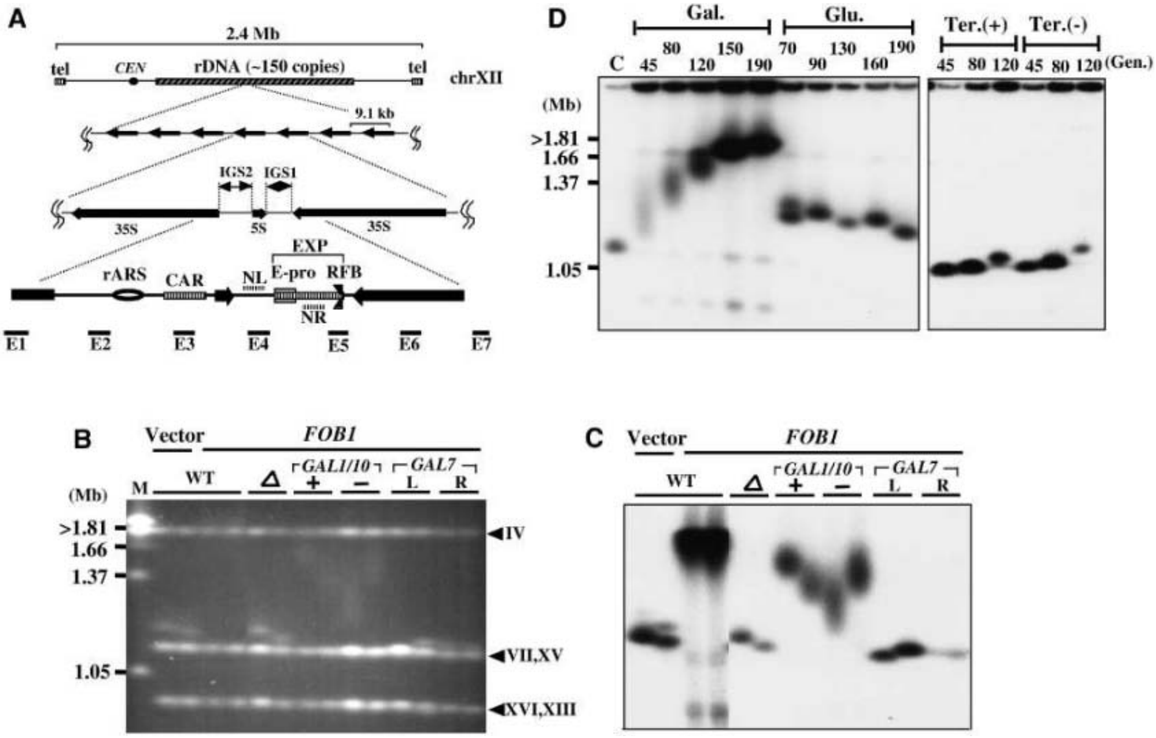

Fig. 1. Bidirectional E-pro transcription is required for rDNA amplification. (**A**) rDNA occupies ~60% of chr XII in *S. cerevisiae*. The 35S and 5S rRNA genes, IGS1 and 2, the origin of replication (rARS), the RFB, EXP, E-pro, and the CAR are indicated. Locations of Northern probes (NL and NR) and ChIP primers (E1 to E7) are shown. (**B** and **C**) CHEF gel showing chr XII sizes of various two-copy strains ~45 generations after *FOB1* or control plasmid (vector) transformation. WT, wild-type two-copy strain (TAK201). E-pro was replaced with the following: (i) an empty cassette (Δ, strain TAK222); (ii) a bidirectional Gal promoter in both orientations (*GAL1/10* +/−, strains TAK223 and TAK224); and (iii) a unidirectional Gal promoter (*GAL7*), with transcription in the RFB (R, strain TAK225) and rARS (L, strain TAK226) directions (*25*). Two independent transformants were analyzed for each mutant. M is the *Hansenula wingei* marker. (B) is an ethidium bromide–stained gel and (C) is an autoradiogram of (B), probed with an rDNA probe showing chr XII position. (**D**) CHEF gel showing the effects of repressing the *GAL1/10* promoter and of transcription termination on rDNA amplification. In the left panel, amplification was induced as in (B), and after ~45 generations, half of the cultures were shifted to glucose media. Chr XII sizes were observed as in (C) at various generations after *FOB1* transformation. The right panel shows *GAL1/10* transcription inhibited in each direction by a pol II (*URA3*) terminator (fig. S1). Termination (Ter.) +/− (strains TAK227 and TAK228) indicate directions of transcription termination. C indicates the strain before *FOB1* transformation.

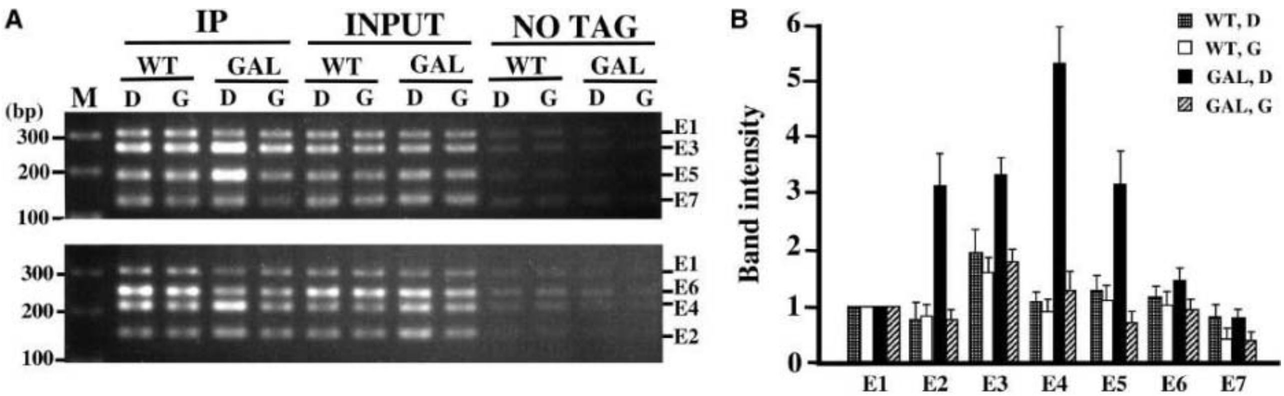

Fig. 2. Cohesin association within the IGS using ChIP assays. Wild-type (WT) (strain TAK1005) and GAL1/10 strains (TAK1006) with HA-tagged *MCD1*, as well as control strains without tag (labeled "NO TAG"), were grown in glucose and galactose (D and G, respectively). After formaldehyde treatment, rDNA fragments (sheared to ~500 bp) were coimmunoprecipitated using antibodies to HA. Seven rDNA regions (E1 to E7, Fig. 1A) were analyzed by polymerase chain reaction (PCR) in two groups. Primer set E1 was used in both as a control. PCR reactions were terminated in the logarithmic phase of amplification. (**A**) Representative ethidium bromide–stained gels of the PCR products. IP, tagged immunoprecipitated samples; INPUT, nonimmunoprecipitated controls. (**B**) Quantification of cohesin association from three independent experiments. PCR products were quantified, values were corrected using NO-TAG results, and then normalized using respective INPUT values.

we used Northern blots to measure E-pro transcription levels by using wild-type and *SIR2*-disrupted strains with endogenous E-pro (Fig. 3, A and B). E-pro transcript levels were increased ~16.5-fold in the ribosomal autonomously replicating sequence (rARS) direction and ~9.5-fold in the replication fork barrier (RFB) direction when *SIR2* was deleted. Transcripts could be detected in an RNA pol I mutant, suggesting that E-pro is transcribed by RNA pol II (fig. S3).

If *SIR2* is responsible for copy-number change by regulating E-pro transcription, then the deletion of *SIR2* should not effect recombination in a glucose-grown GAL1/10 strain, because transcription is already repressed. To test this, we analyzed the rDNA stability of GAL1/10 and wild-type strains with and without *SIR2* (Fig. 3C). As previously observed (*13*), the chr XII bands of a wild-type strain lacking *SIR2* are smeared. In contrast, the chr XII bands in the glucose-grown GAL1/10 strain remain sharp, even after *SIR2* deletion.

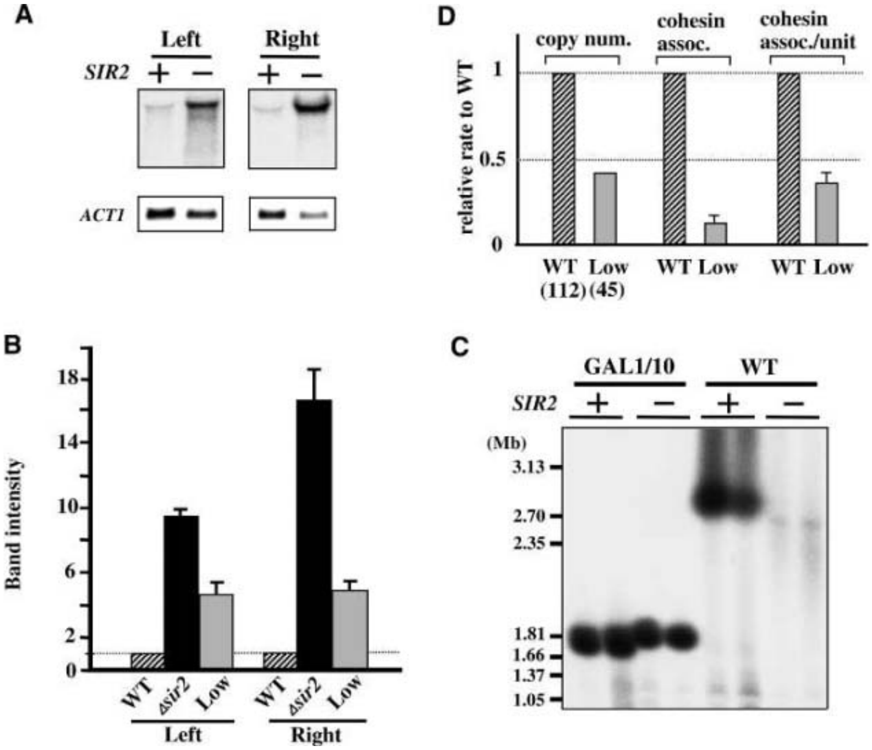

Fig. 3. Regulation of E-pro transcription and rDNA stability by *SIR2* and rDNA copy number. (**A** and **B**) Northern blot analysis of E-pro transcripts. The total RNA from wild-type (WT) (strain NOY408-1b), Δ*sir2* (labeled *SIR2*, strain TAK190), and amplifying low-copy (low) strains was hybridized with probes to the rARS-facing (Left) and RFB-facing (Right) transcripts, and an *ACT1* control probe. (A) shows a representative Northern blot and (B) shows the quantification of E-pro transcript levels. Results were normalized using *ACT1*. (**C**) CHEF gel probed with an rDNA probe showing the effects of *SIR2* deletion on chr XII stability. GAL1/10 (strains TAK2004 and TAK2005) and wild-type strains with and without *SIR2* were grown in glucose (two independent colonies were analyzed for each). DNA loading was similar in each lane. Separation conditions differ from Fig. 1. Positions of *H. wingei* markers are indicated at the left. (**D**) rDNA copy number (*6*), the level of cohesin association using ChIP analyses with pooled E2 to E5 PCR products (Fig. 1A), and the cohesin association corrected by copy number were determined for wild-type (TAK1005) and low-copy (TAK1008) strains. Cohesin association is relative to wild-type. Absolute copy numbers are in parentheses.

Finally, we tested the relationship between rDNA copy number and E-pro regulation. A strain undergoing amplification (low-copy strain) should show increased E-pro transcription and decreased cohesin association. To generate low-copy strains, we introduced a plasmid-borne *FOB1* gene into two-copy strains. After 45 generations, there were ~45 rDNA copies, indicating active amplification. Analysis with Northern blots showed that E-pro transcription in the low-copy strain was enhanced ~4.5-fold over that in the wild-type in both directions, and the value per rDNA unit will be even higher (Fig. 3B). Furthermore, ChIP analysis with an HA-tagged *MCD1* low-copy strain revealed that cohesin association was reduced to 35% of the wild-type level per unit of rDNA (Fig. 3D). Therefore, when the rDNA is amplifying, E-pro is activated and cohesin dissociates, indicating that E-pro is the major regulator of rDNA amplification.

These results suggest a model of amplification regulation where transcription of E-pro stimulates unequal recombination by disrupting cohesin association in the rDNA, thus allowing for a change in copy number (Fig. 4). Sir2p is a negative regulator of E-pro transcription, and in normal situations, its activity allows cohesin to associate throughout the IGS and thereby prevents unequal sister-chromatid recombination that leads to copy-number change. This model explains the stimulatory effects of *SIR2* deletion and why the absolute level of rDNA recombination is the same, regardless of *SIR2* status (*13*). The

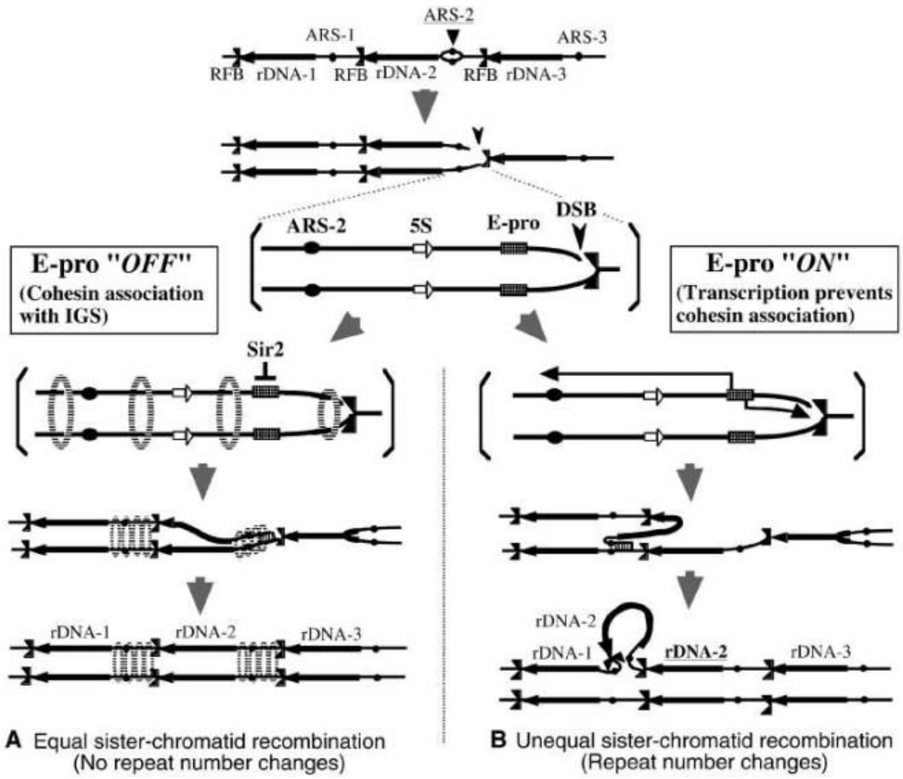

Fig. 4. Transcription-induced cohesin dissociation model of rDNA amplification. (**A**) In normal situations, such as wild-type rDNA copy number, *SIR2* represses E-pro activity, allowing cohesin to associate throughout the IGS. DSBs, formed by replication forks pausing at the RFB site, are repaired by equal sister-chromatid recombination, with no change in the rDNA copy number. (**B**) When *SIR2* repression is removed, such as with *sir2* mutation or low copy number, E-pro becomes active and transcription displaces cohesin. Unequal sister chromatids can then be used as templates for DSB repair, resulting in changes in the rDNA copy number. Lines represent single chromatids (double-stranded DNA). The IGS in which the replication fork is paused is expanded in the bracket.

model is supported by evidence that Sir2p alters chromatin structure within EXP (*18*). DSBs in the IGS are expected to recruit cohesin (*19*), countering the effect of transcription. However, because not many DSBs form in the rDNA repeats (*20*), this effect is likely to be minor. Also, DSB formation at the RFB was similar in the GAL1/10 strain when grown on glucose/galactose (0.89/1.00, relative values). Therefore, cohesin dissociation appears to be the major role of E-pro transcription activity.

Transcription-induced cohesin dissociation provides a potential mechanism for the well-established link between transcription and recombination (*21*), the molecular mechanism(s) of which have remained controversial. For instance, in immune cells, antibody gene recombination requires the transcription of flanking genes (*22*, *23*), and this transcription-dependent recombination may be mediated through cohesin dissociation. Given the large amount of noncoding transcription recently found in higher eukaryotes (*24*), some of these transcripts may be involved in the regulation of cohesin association, allowing cells to regulate recombination.

References and Notes

1. L. H. Hartwell, M. B. Kastan, *Science* **266**, 1821 (1994).
2. F. Fabre, A. Chan, W.-D. Heyer, S. Gangloff, *Proc. Natl. Acad. Sci. U.S.A.* **99**, 16887 (2002).
3. R. S. Hawley, C. H. Marcus, *Annu. Rev. Genet.* **23**, 87 (1989).
4. G. P. Smith, *Cold Spring Harbor Symp. Quant. Biol.* **38**, 507 (1973).
5. K. D. Rodland, P. J. Russell, *Biochim. Biophys. Acta* **697**, 162 (1982).
6. T. Kobayashi, D. J. Heck, M. Nomura, T. Horiuchi, *Genes Dev.* **12**, 3821 (1998).
7. T. Kobayashi, M. Nomura, T. Horiuchi, *Mol. Cell. Biol.* **21**, 136 (2001).
8. G. M. Santangelo, J. Tornow, C. S. McLaughlin, K. Moldave, *Mol. Cell. Biol.* **8**, 4217 (1988).
9. A. R. D. Ganley, K. Hayashi, T. Horiuchi, T. Kobayashi, *Proc. Natl. Acad. Sci. U.S.A.* **102**, 11787 (2005).
10. C. H. Haering, K. Nasmyth, *Bioessays* **25**, 1178 (2003).
11. E. F. Glynn *et al.*, *PLoS Biol.* **2**, e259 (2004).
12. A. Lengronne *et al.*, *Nature* **430**, 573 (2004).
13. T. Kobayashi, T. Horiuchi, P. Tongaonkar, L. Vu, M. Nomura, *Cell* **117**, 441 (2004).
14. S. Laloraya, V. Guacci, D. Koshland, *J. Cell Biol.* **151**, 1047 (2000).
15. A. V. Strunnikov, V. L. Larionov, D. Koshland, *J. Cell Biol.* **123**, 1635 (1993).
16. J. S. Smith, J. D. Boeke, *Genes Dev.* **11**, 241 (1997).
17. M. Bryk *et al.*, *Genes Dev.* **11**, 255 (1997).
18. C. E. Fritze, K. Verschueren, R. Strich, R. E. Esposito, *EMBO J.* **16**, 6495 (1997).
19. E. Unal *et al.*, *Mol. Cell* **16**, 991 (2004).
20. H. Zou, R. Rothstein, *Cell* **90**, 87 (1997).
21. A. Aguilera, *EMBO J.* **21**, 195 (2002).
22. T. K. Blackwell *et al.*, *Nature* **324**, 585 (1986).
23. M. S. Schlissel, D. Baltimore, *Cell* **58**, 1001 (1989).
24. P. Bertone *et al.*, *Science* **306**, 2242 (2004).
25. Materials and methods are available as supporting material on *Science* Online.
26. We thank M. Nomura (University of California, Irvine) and D. Koshland (Carnegie Institute) for strains and M. Inagaki (National Institute for Basic Biology, Okazaki) for technical support. This work was supported in part by grants 13141205, 14380332, 17080010, and 17370065 from the Ministry of Education, Science and Culture, Japan, and by a Human Frontier Science Program grant to T.K.

Supporting Online Material

www.sciencemag.org/cgi/content/full/309/5740/1581/DC1

Materials and Methods

Figs. S1 to S3

Table S1

References

14 June 2005; accepted 5 August 2005

10.1126/science.1116102

An mRNA Is Capped by a 2′,5′ Lariat Catalyzed by a Group I–Like Ribozyme

Henrik Nielsen,[1,2]* Eric Westhof,[3] Steinar Johansen[2]

Twin-ribozyme introns are formed by two ribozymes belonging to the group I family and occur in some ribosomal RNA transcripts. The group I–like ribozyme, GIR1, liberates the 5′ end of a homing endonuclease messenger RNA in the slime mold *Didymium iridis*. We demonstrate that this cleavage occurs by a transesterification reaction with the joining of the first and the third nucleotide of the messenger by a 2′,5′-phosphodiester linkage. Thus, a group I–like ribozyme catalyzes an RNA branching reaction similar to the first step of splicing in group II introns and spliceosomal introns. The resulting short lariat, by forming a protective 5′ cap, might have been useful in a primitive RNA world.

RNA splicing is found in most prokaryotic and eukaryotic organisms and different RNA splicing mechanisms have evolved for different classes of genes (*1*, *2*). Group I introns (*3*) carry out splicing in a structurally and chemically distinct way from that of group II introns and the spliceosomal introns found widespread in higher eukaryotes. The group I twin-ribozyme intron found in the extrachromosomal ribosomal DNA (rDNA) of the myxomycete *Didymium iridis* (Dir.S956-1) consists of two self-catalytic units, a conventional group I splicing ribozyme (GIR2) and a group I–like cleavage ribozyme (GIR1) (Fig. 1A). A homing endonuclease gene (HEG) encoding the I-*Dir*I mRNA is found inserted downstream of GIR1 (*4*–*6*). The 5′ end of the I-*Dir*I mRNA is formed by cleavage catalyzed by the GIR1 ribozyme (*7*). Primer extension analyses have led to the suggestion of two cleavage sites located three nucleotides apart (*5*, *8*) referred to as IPS1 (internal processing site 1), and IPS2, respectively (Fig. 1B). Cleavage at IPS1 was shown to be hydrolytic (*5*, *9*). IPS2 has not been characterized in detail. Primer extension analyses of cellular RNAs exclusively show a stop at IPS2 (*10*, *11*), whereas the primer extension stop at IPS1 is only observed in analysis of full-length intron (*7*) or deletion constructs in vitro.

We found the processing pattern to be strongly dependent on sequences at both the 5′ and 3′ ends of the ribozyme and selected two variants for a study of IPS2 cleavage (*12*). The length variants 166.22 [including 166 nt (nucleotides) upstream and 22 nt downstream of IPS1 Fig. 1, A and B] and 157.22 have comparable cleavage kinetics (fig. S1), but primer extension analysis shows a distinct difference in processing pattern. A primer extension stop at IPS1 accumulates over time in 166.22 and a stop at IPS2 accumulates in 157.22 (Fig. 1C). In a parallel cleavage analysis with 3′ end-labeled RNA (Fig. 1D) the 3′ fragment that accumulates from cleavage of both 166.22 and 157.22 is of the same length (22 nt). This is inconsistent with cleavage at IPS2, and we conclude that the observed primer extension stop at IPS2 is a structural stop.

Incubation of a 22-nt 3′ fragment isolated from cleavage of 157.22 (IPS2) with the 166-nt 5′ fragment results in a complete conversion of the primer extension signal from IPS2 to IPS1 (Fig. 1E) because of ligation and recleavage by hydrolysis. Ligation of the 22-nt fragment onto the 3′ end of the 5′ fragment followed by recleavage is shown in Fig. 1F. The ligation reaction is fast and is dependent on the presence of G229 because the removal of this nucleotide by β-elimination inhibited the reaction (fig. S2). The ligation experiments suggest that the IPS2 modification conserves the energy from the cleavage reaction.

The 5′ ends of the two 22-nt RNAs were analyzed by treatment of 3′ end-labeled RNA with modifying enzymes (Fig. 2A). Incubation of the 3′ fragment carrying the IPS2 modifica-

[1]Department of Medical Biochemistry and Genetics, The Panum Institute, University of Copenhagen, DK-2200N Copenhagen, Denmark. [2]Department of Molecular Biotechnology-RNA Research Group, Institute of Medical Biology, University of Tromsø, N-9037 Tromsø, Norway. [3]Institut de Biologie Moléculaire et Cellulaire, CNRS, Université Louis Pasteur, 67084 Strasbourg Cedex, Strasbourg, France.

*To whom correspondence should be addressed. E-mail: hamra@imbg.ku.dk

tion [(157)22 RNA] with AP (alkaline phosphatase) or AP and PNK (polynucleotide kinase), or PNK alone all shifted the mobility of the fragment one position upward in the gel, which was consistent with the removal of the 3′-phosphate of the pCp label. In contrast, a 3′ fragment that resulted from cleavage at IPS1 without the IPS2 modification [(166)22 RNA] was shifted two positions upward with AP, one position when phosphorylated with PNK after AP treatment, and one position with PNK alone. This is consistent with removal of the 3′-phosphate (from the pCp) as well as an additional phosphate at the 5′ end left by IPS1 cleavage. Thus, the phosphate at the 5′ end of the 22-nt 3′ fragment is accessible to phosphatase in the absence of the IPS2 modification but inaccessible when the IPS2 modification is present. This feature of the IPS2 modification could be removed by incubation of (157)22 RNA with 166 RNA before the analysis, as shown in the last panel in Fig. 2A. Thus, both the primer extension stop at IPS2 and blocking of the 5′ end are reversible. An explanation for these observations is that GIR1 cleavage occurs by a transesterification reaction in which cleavage at IPS1 is coupled to formation of a 2′,5′-phosphodiester bond between C230 and U232. This explains the primer extension stop at IPS2, the blocking of the 5′ end, the conservation of internal energy after cleavage, and the reversibility of the reaction. Consistent with the engagement of the 2′OH of U232, this nucleotide is resistant to alkaline hydrolysis in (157)22 RNA, in contrast to (166)22 RNA (fig. S3).

Branches in RNA are resistant to digestion with various RNases including mung bean nuclease (*13*). A resistant fragment was found in mung bean nuclease digests of body-labeled (157)22 RNA but not (166)22 RNA (fig. S4 and SOM text). Digestion of (157)22 RNA with the exonuclease snake venom phosphodiesterase resulted in a resistant fragment corresponding to the 4-nt lariat circle (Fig. 2B) that could subsequently be cleaved by the endonuclease mung bean nuclease to release the branched nucleotide and pA (Fig. 2C). These analyses are consistent with the presence of the proposed 2′,5′-phosphodiester bond between C230 and U232. The sequence of the branch was verified by thin-layer chromatography (TLC) analysis of the nucleotides liberated by snake venom phosphodiesterase cleavage of purified branch nucleotide (Fig. 2D).

Formation of the branched nucleotide implies a reaction mechanism in which the 2′OH of U232 makes a nucleophilic attack at the phosphodiester bond at IPS (Fig. 3A). To test this mechanism, we made cleavage analyses combining a ribozyme truncated in L9 (157.-7) and site-specifically deoxy-substituted substrates that complemented the truncated ribozyme (7.22). Only the dU232 substrate did not support cleavage (Fig. 3B). Weak cleavage with the dA231 substrate is ascribed to a critical structural role of this nucleotide. The cleavage in the all-RNA, dC230, dA231, and dC233 substrates was by transesterification as shown by primer extension analysis (fig. S5).

We have shown here that GIR1 cleaves by transesterification, not by hydrolysis as proposed previously (*5*). The reaction leaves a 5′ fragment containing a fully active ribozyme with a 3′OH, and a 3′ fragment in which the first and the third nucleotides are linked by a 2′,5′-phosphodiester bond. A 4-nt lariat was found by nuclear magnetic resonance (NMR) imaging to have an unusual structure with the sugars in the lariat ring locked in a rigid South-type conformation (*14*). We refer to the similarly sized lariat in *Didymium* as the lariat cap because it is found to cap the cellular I-*Dir* I mRNA (Fig. 3C). Other studies have shown that IPS1-cleaved RNA cannot be reactivated for modification at IPS2, which suggests a mechanistic coupling of the two reactions. Hydrolytic IPS1 cleavage thus appears as a failure to link the 5′-phosphate of C230 to the 2′OH of U232 and is considered an in vitro phenomenon. We propose that IPS1 is denoted IPS, and that IPS2 is replaced by BP (branch point) in line with the nomenclature used for group II and spliceosomal introns.

Our results show that a ribozyme with a group I intron–like architecture can carry out an RNA branching reaction similar to the first step of splicing in group II introns and spliceosomal introns. The GIR1 ribozyme has clear structural distinctions from group I self-splicing ribozymes including the lack of a P1 helix carrying the 5′ splice site (*5*, *6*). The two known GIR1 ribozymes from *Didymium* and *Naegleria* show striking similarity to individual members of group I eubacterial transfer RNA (tRNA) introns to which the similarity in the core structure is in the 60 to 80% range (*6*). Therefore, GIR1 ribozymes may have arisen from splicing ribozymes several times during evolution. The rearrangements that led to the evolution of GIR1 transformed a conventional 3′ splice site (G↓) into a 5′ splice site AG↓ [incidentally the consensus sequence of the exon part of the 5′ splice site of the major class of

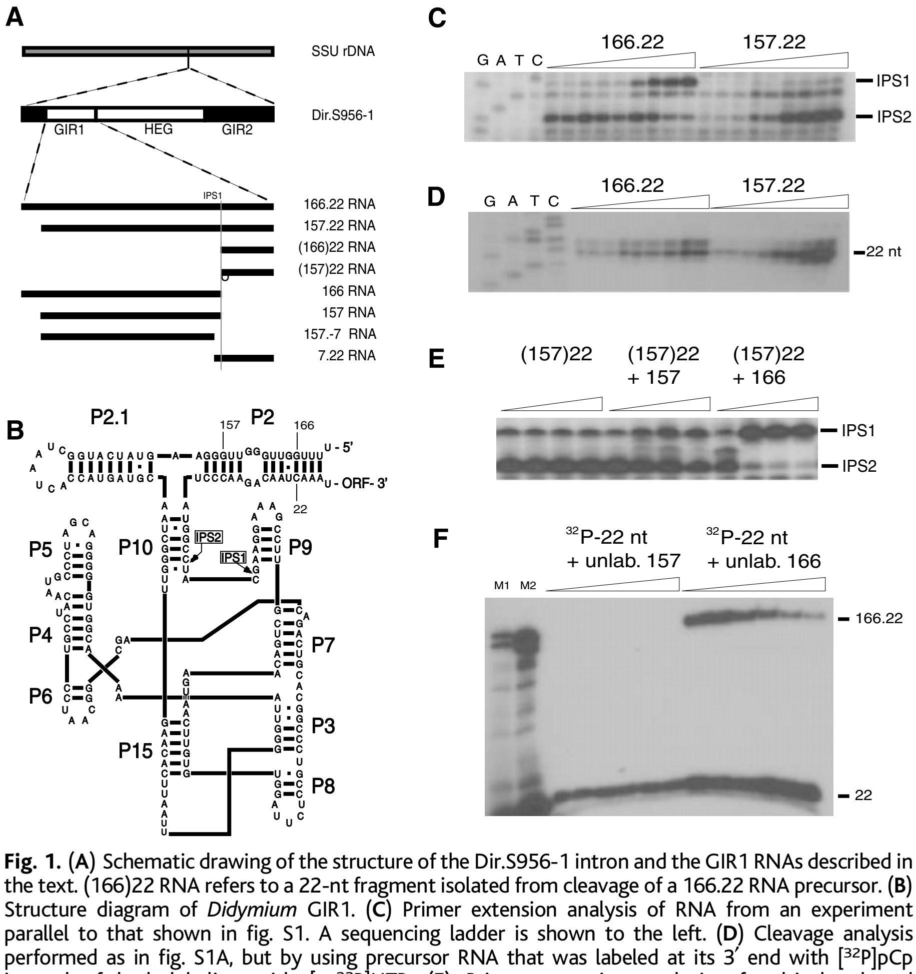

Fig. 1. (**A**) Schematic drawing of the structure of the Dir.S956-1 intron and the GIR1 RNAs described in the text. (166)22 RNA refers to a 22-nt fragment isolated from cleavage of a 166.22 RNA precursor. (**B**) Structure diagram of *Didymium* GIR1. (**C**) Primer extension analysis of RNA from an experiment parallel to that shown in fig. S1. A sequencing ladder is shown to the left. (**D**) Cleavage analysis performed as in fig. S1A, but by using precursor RNA that was labeled at its 3′ end with [^{32}P]pCp instead of body-labeling with [α-^{32}P]UTP. (**E**) Primer extension analysis of gel-isolated and reincubated (157)22 RNA alone, with 157 RNA, and with 166 RNA. The time points are 0, 1, 4, and 8 hours. (**F**) Ligation of a 22-nt 3′ fragment to a 166-nt 5′ fragment. The 3′ fragment was labeled at its 3′ end with [^{32}P]pCp. The 5′ fragment was unlabeled. The time points are 0 and 20 min, and 1, 2, 3, and 4 hours. M1 and M2: 166.22 and 157.22, respectively, cleaved and labeled with [^{32}P]pCp.

spliceosomal introns (*1*)]. Thus, the evolution of GIR1 ribozymes illustrates a possible step in the evolution of spliceosomal introns.

The homing endonuclease is expressed from I-*Dir*I mRNA formed by precursor ribosomal RNA (rRNA) processing (*10*). The formation of the 5′ end of the I-*Dir*I mRNA by cleavage of the spliced out intron precludes the normal cotranscriptional addition of a cap nucleotide. The cap nucleotide in typical messengers serves several functions, including protection from degradation by 5′→3′ exonucleases, and recruitment of protein factors in initiation of translation (*15*). The reaction at IPS in GIR1 results in protection of the 5′ end of the I-*Dir*I mRNA against the activity of 5′→3′ exonucleases by formation of a lariat cap. This potentially substitutes for one of the features of the missing cap nucleotide. GIR1 processed RNAs are stable when expressed in *Escherichia coli* and yeast (*11*, *16*), which supports this idea of 5′ stabilization by lariat formation.

The present observations extend the diversity of natural ribozymes (*3*) and connect the group I and group II introns, two major structural classes of self-splicing RNAs. Despite its overall structural similarity with other natural group I introns, the GIR1 ribozyme is distinct from the group I splicing ribozymes not only in key structural features but also in the type of reaction catalyzed and in the derived function.

References and Notes

1. C. B. Burge, T. Tuschl, P. A. Sharp, in *The RNA World, Second Edition*, R. F. Gesteland, T. R. Cech, J. F. Atkins, Eds. [Cold Spring Harbor Laboratory (CSHL) Press, Cold Spring Harbor, New York, 1999], pp. 525–560.
2. C. R. Trotta, J. Abelson, in *The RNA World, Second Edition*, R. F. Gesteland, T. R. Cech, J. F. Atkins, Eds. (CSHL Press, Cold Spring Harbor, New York, 1999), pp. 561–584.

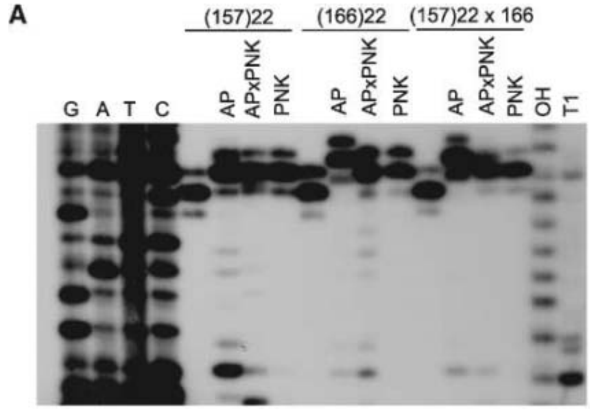

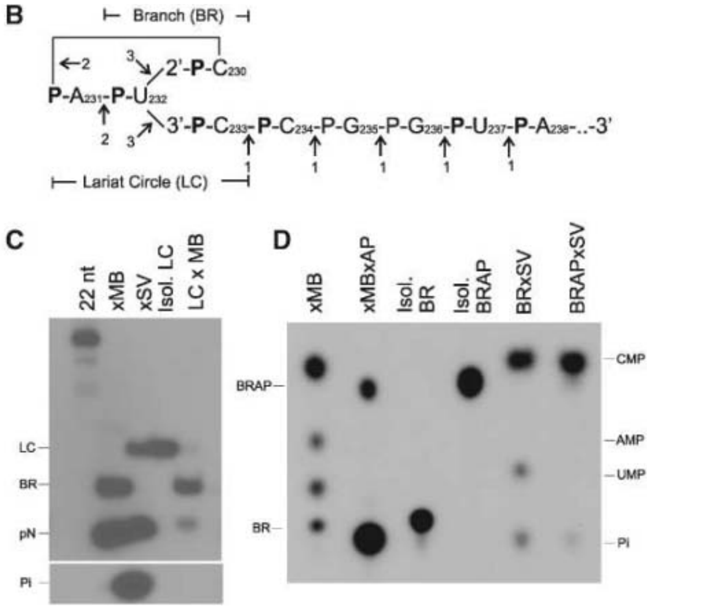

Fig. 2. (**A**) Characterization of the 5′ end of the 22-nt 3′ fragment. [^{32}P]pCp-labeled 3′ fragment was isolated from 157.22 and 166.22 and subjected to treatment with alkaline phosphatase (AP), AP followed by rephosphorylation with T4 polynucleotide kinase (APxPNK), or treatment with PNK alone (PNK). The sample denoted (157)22 × 166 was preincubated at reaction conditions for 30 min before the analysis. OH and T1: Alkaline ladder and T1 digest of [^{32}P]pCp–labeled precursor 157.22. (**B**) Diagram of the 22 nt lariat used for experiments in (C) and (D). The RNA was body-labeled at the phosphates in bold by incorporation of ^{32}P. Arrows indicate potential cleavage sites for mung bean nuclease (MB) and snake venom phosphodiesterase (SV). Cleavage of the 22-nt fragment at sites labeled 1 with SV results in a protected lariat circle (LC). Cleavage at sites labeled 1 and 2 with MB results in a protected branched nucleotide (BR). Subsequent cleavage of BR with SV at sites labeled 3 releases the nucleotides involved in the branch. (**C**) Characterization of the lariat circle by gel purification and subsequent digestion with MB (LCxMB). The 22-nt fragment and digests with MB or SV serves as markers. (**D**) Characterization of the branched nucleotide by purification of its phosphorylated and dephosphorylated form, and subsequent TLC analysis of nucleotides liberated by digestion with SV. The first two runs show digests of the 22-nt fragment. The following show the isolated branch (BR), and dephosphorylated branch (BRAP), respectively. Finally, the last two runs show the subsequent digests of these with SV (BRxSV and BRAPxSV).

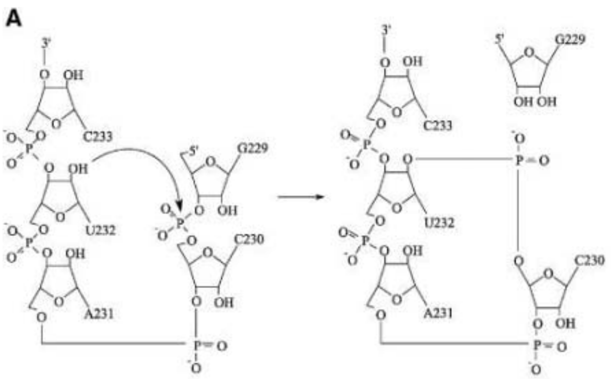

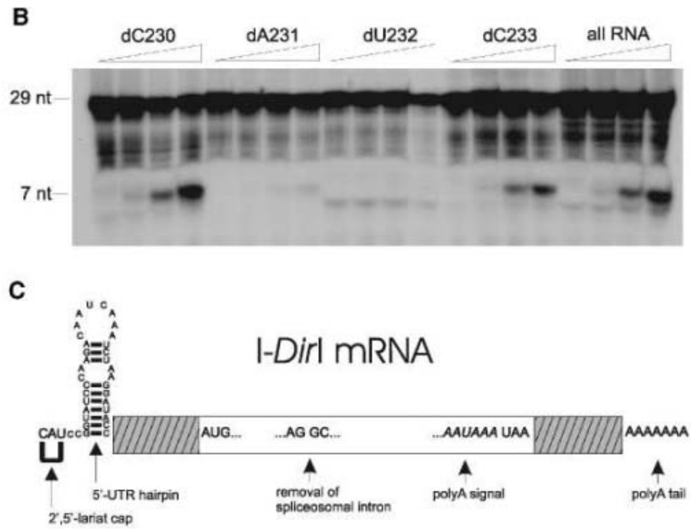

Fig. 3. (**A**) Outline of the reaction catalyzed by GIR1. The 2′OH of the internal residue U232 makes a nucleophilic attack at the IPS. Bond lengths are not drawn to scale. (**B**) Cleavage experiment using 157.-7 ribozyme combined with four different deoxy-substituted substrates each containing 7 nucleotides upstream and 22 nucleotides downstream of IPS. Numbering of nucleotides is according to their position in the intron. (**C**) Diagram showing the structure of the fully processed I-*Dir* I mRNA that encodes the homing endonuclease.

3. B. L. Golden, T. R. Cech, in *The RNA World, Second Edition*, R. F. Gesteland, T. R. Cech, J. F. Atkins, Eds. (CSHL Press, Cold Spring Harbor, New York, 1999), pp. 321–349.
4. W. A. Decatur, C. Einvik, S. Johansen, V. M. Vogt, *EMBO J.* **14**, 4558 (1995).
5. C. Einvik, H. Nielsen, E. Westhof, F. Michel, S. Johansen, *RNA* **4**, 530 (1998).
6. S. Johansen, C. Einvik, H. Nielsen, *Biochimie* **84**, 905 (2002).
7. S. Johansen, V. M. Vogt, *Cell* **76**, 725 (1994).
8. C. Einvik, W. A. Decatur, T. M. Embley, V. M. Vogt, S. Johansen, *RNA* **3**, 710 (1997).
9. E. Jabri, S. Aigner, T. R. Cech, *Biochemistry* **36**, 16345 (1997).
10. A. Vader, H. Nielsen, S. Johansen, *EMBO J.* **18**, 1003 (1999).
11. W. A. Decatur, S. Johansen, V. M. Vogt, *RNA* **6**, 616 (2000).
12. Materials and Methods are available as supporting material on *Science* Online.
13. J. D. Reilly, J. C. Wallace, R. F. Melhem, D. W. Kopp, M. Edmonds, *Methods Enzymol.* **180**, 177 (1989).
14. P. Agback *et al.*, *J. Biochem. Biophys. Methods* **27**, 229 (1993).
15. N. Cougot, E. van Dijk, S. Babajko, B. Séraphin, *Trends Biochem. Sci.* **29**, 436 (2004).
16. A. B. Birgisdottir, S. Johansen, *Nucleic Acids Res.* **33**, 2042 (2005).
17. This paper is dedicated to Jan Engberg, who died of cancer on 20 December 2004. The work was supported by grants (to H.N.) from Vera and Carl Johan Michaelsens Fund, the NOVO Nordic Foundation, and the Carlsberg Foundation. We thank F. Frenzel for technical assistance, J. Kjems and B. Hove-Jensen for supplying reagents, and J. Christiansen for helpful suggestions to the manuscript. E.W. thanks the Institut Universitaire de France for support.

Supporting Online Material
www.sciencemag.org/cgi/content/full/309/5740/1584/DC1
Materials and Methods
SOM Text
Figs. S1 to S5
References and Notes

15 April 2005; accepted 29 July 2005
10.1126/science.1113645

Structural Evidence for a Two-Metal-Ion Mechanism of Group I Intron Splicing

Mary R. Stahley and Scott A. Strobel*

We report the 3.4 angstrom crystal structure of a catalytically active group I intron splicing intermediate containing the complete intron, both exons, the scissile phosphate, and all of the functional groups implicated in catalytic metal ion coordination, including the 2′-OH of the terminal guanosine. This structure suggests that, like protein phosphoryltransferases, an RNA phosphoryltransferase can use a two-metal-ion mechanism. Two Mg^{2+} ions are positioned 3.9 angstroms apart and are directly coordinated by all six of the biochemically predicted ligands. The evolutionary convergence of RNA and protein active sites on the same inorganic architecture highlights the intrinsic chemical capacity of the two-metal-ion catalytic mechanism for phosphoryl transfer.

Divalent metal ions are used in the active sites of a variety of protein phosphoryltransfer enzymes, including those required for replication, transcription, and cell signaling (*1*–*3*). Structural and biochemical studies of these proteins have shown that many, including all polymerases, use a two-metal-ion mechanism to promote catalysis (*4*, *5*). In these enzymes, a pair of divalent metals, located 3.8 to 5.0 Å apart, are used to position substrates, activate the nucleophile, and stabilize the charge on both the leaving group and the scissile phosphate (*6*–*8*).

Many RNA-based phosphoryltransferases also require direct coordination to active-site Mg^{2+} ions, including self-splicing introns, ribonuclease P, and the spliceosome when it catalyzes pre-mRNA splicing (*9*). Both chemical steps of group I intron splicing require divalent metals, and several of the ligands for these metals have been biochemically identified (Fig. 1B) (*10*–*15*). What has remained unclear are the structural details of metal-ion coordination in the RNA active site. Recent crystal structures have provided information on the fold of the group I intron and the structural basis for splice site selection (*16*–*19*); however, each of these structures included only one active-site Mg^{2+}, and all were inactive (Fig. 1B and fig. S1) (*20*). An independent model derived from biochemical analysis invokes three active-site metals and a coordination geometry for these metals different from that observed in protein enzymes (Fig. 1C) (*21*, *22*).

We have determined the crystal structure of an intron splicing intermediate that includes all metal-ion ligands and thereby retains the ability to catalyze exon ligation at a slow rate. We formed this crystallization construct by annealing a transcript comprising the majority of the *Azoarcus sp.* pre-tRNA^{Ile} group I intron with two oligonucleotides, capturing the intron just before the second step of splicing (pre-2S) (Fig. 1A) (*23*). One 22-residue oligonucleotide, rcirc, represents the 3′-end of the intron and the 3′-exon. The second, a trimer (CAT), mimics the 5′-exon. The critical difference between this construct and the previously reported *Azoarcus* group I intron structure is the inclusion of the ribose at the terminal guanosine (ωG) position. The ωG O2′ has been biochemically identified as an essential ligand for a catalytic metal ion that increases the rate of splicing at least a millionfold (*24*, *25*). In order to slow the reaction sufficiently for crystallization, the complex contains a single 2′-deoxy substitution at the last nucleotide of the 5′-exon, U-1. This functional group contributes ~1000-fold to chemistry through a hydrogen bonding network that appears to be independent of metal-ion coordination (*19*, *26*, *27*). Crystals of the ribo-ωG intron in complex with the RNA binding protein U1A were obtained under conditions similar to those reported for the deoxy-ωG complex (*19*, *23*).

The crystallized RNA was able to promote exon splicing when the ribo-ωG pre-2S crystals were soaked with a radiolabeled 5′-exon substrate containing either a ribose (CAU) or a 2′-deoxyribose (CAT) at U-1 (Fig. 2A) (*28*). For this reaction to occur, the labeled substrate must have displaced the CAT cocrystallized in the intron complex. For crystals soaked with CAU or CAT, the extent of reaction after 50 hours was similar to that observed in solution under conditions designed to mimic those within the crystal (~15% and ~3% reacted, respectively) (Fig. 2, A and B). Incomplete reaction is likely to reflect the stoichiometry of the reactants and the equilibrium between the forward and reverse splicing reactions (*19*, *29*). No spliced exon product resulted from the combination of oligonucleotides used in the previous structure determination (Fig. 2A, lane 4). The crystals did not change in appearance upon addition of CAU, but diffraction was substantially reduced, likely resulting from an increase in heterogeneity of the RNA. These data demonstrate that the ribo-ωG pre-2S complex is in a catalytically accessible conformation within the crystals.

We determined the 3.4 Å structure of the ribo-ωG pre-2S group I intron complex using the experimental phases from the deoxy-ωG structure followed by refinement (supporting text) (*23*). Because the RNA in the ribo-ωG structure is primarily in the unspliced form because of the inclusion of a deoxy at U-1, the model is exclusively of the pre–second step reaction state. Although the overall architecture of the ribo-ωG pre-2S complex was essentially unchanged, the identity and position of metal ions in the active site were substantially different from those observed in the deoxy-ωG pre-2S structure (*16*).

An F_O-F_C difference map calculated before metal modeling revealed two large peaks (5σ)

Department of Molecular Biophysics and Biochemistry, Yale University, 260 Whitney Avenue, New Haven, CT 06520–8114, USA.

*To whom correspondence should be addressed. E-mail: scott.strobel@yale.edu

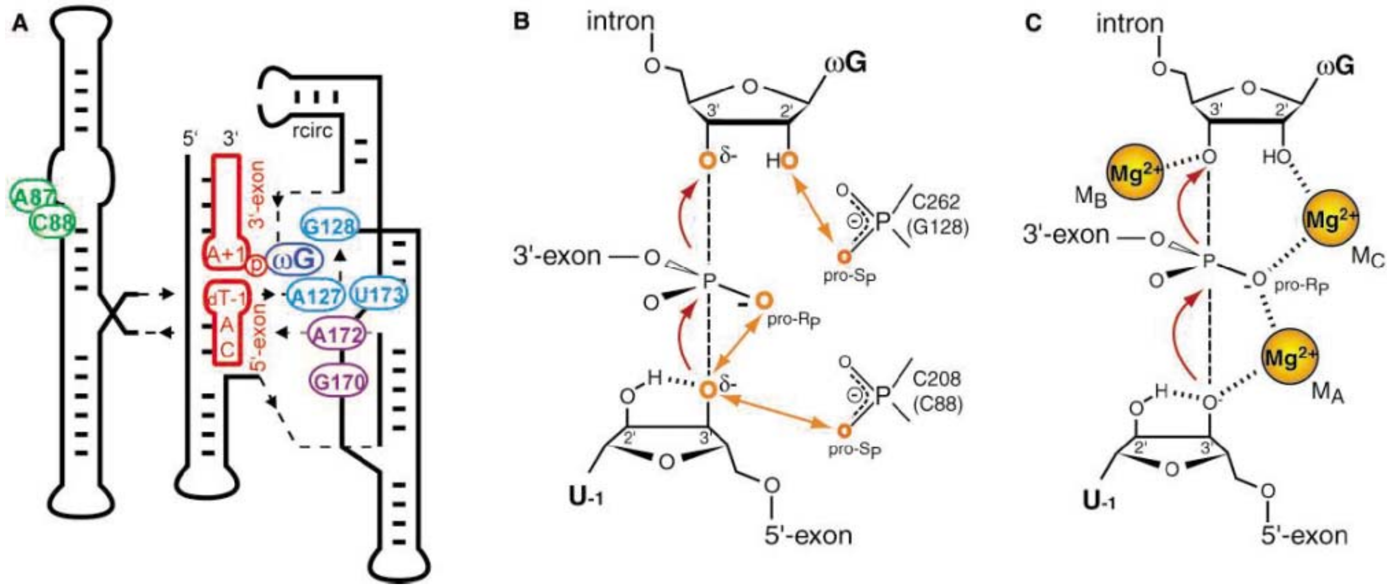

Fig. 1. The group I intron splicing reaction. (**A**) Secondary structure of the pre-2S crystallization construct. The residues discussed in the text are shown superimposed on the secondary structure. RNA connectivity is depicted with a dashed line with small arrows to show the 5′ to 3′ orientation. Exons are shown in red. The coloring of other residues corresponds to the structural element in which they are located: P4 to P6 (green), P3 to P9 (blue), and J8/7 (purple). (**B**) Summary of the biochemically defined ligands for active-site metal coordination. The six oxygens shown in orange have been implicated in metal-ion coordination on the basis of metal specificity switch experiments (*10–15*), including four in the substrates and two in the intron. Ligands biochemically shown to coordinate the same metal are depicted with double-ended arrows. The exon splicing reaction involving attack of the U-1 O3′ on the scissile phosphate with loss of the ωG O3′ is shown with curved arrows. (**C**) Proposed three-metal-ion mechanism based on differential Mn^{2+} affinity to sulfur/amino-substituted substrates (*21*, *22*). The four substrate ligands in (B) are coordinated to three metal ions, M_A, M_B, and M_C.

of native electron density in the active site (Fig. 3A). These peaks were assigned as Mg^{2+} ions based on the anomalous density observed for binding of a Mg^{2+} mimic at each site. Yb^{3+} bound at site M_1, and Mn^{2+} bound at site M_2 [(*30*) and supporting text]. The bond distances (all ~2.1 Å) and octahedral coordination geometry also indicate Mg^{2+} binding at both sites (Fig. 3B). The two metals have inner sphere coordination to nine oxygens, including all six of the biochemically predicted ligands (Figs. 1B and 3, B and C). In both cases, five of the metals' six possible coordination positions were satisfied by direct contacts to RNA functional groups. In each case, an additional phosphate oxygen (U173 pro-S_P oxygen for M_1 and A87 pro-S_P oxygen for M_2) appeared to make an outer sphere contact, fully satisfying the metals' octahedral coordination geometry. Density for the bridging waters was not visible at this resolution.

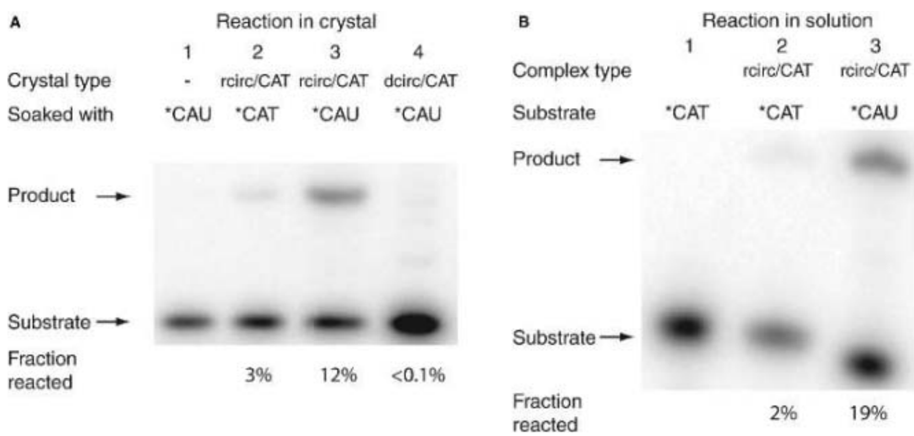

Fig. 2. Activity of the group I intron crystals. (**A**) Pre-2S crystals were soaked with an excess of ^{32}P-radiolabeled 5′-exon substrate with ribose or 2′-deoxy at U-1 (CAU or CAT, respectively). The crystals were assayed for exon ligation as described (*28*). The pair of oligonucleotides used in the original crystallization and the identity of the soaked, radiolabeled, 5′-exon substrate are indicated above the autoradiogram. (**B**) Reactivity of the complex in solution (*28*). In both panels, the fraction reacted is shown below each lane.

The two metals are well positioned to promote catalysis of the exon ligation reaction (Fig. 3B). M_1 shows direct coordination to the nucleophile (O3′ of U-1) and the scissile phosphate pro-R_P oxygen; it is equivalent to the metal observed in the deoxy-ωG pre-2S complex (*16*). Substantial changes in the identity and location of the second metal ion were observed upon inclusion of the ωG 2′-OH. A K^+ was bound near site M_2 in the deoxy-ωG structure, but it was too far away to make direct contact with the scissile phosphate (*16*). In the native ribo-ωG complex, the Mg^{2+} at M_2 was 2.5 Å closer to the scissile phosphate and the ωG O3′ leaving group. This Mg^{2+} ion makes inner sphere contacts to the scissile phosphate's nonbridging pro-R_P oxygen and both the O2′ and the O3′ leaving group of the ωG (Fig. 3B). This change in metal positioning and identity is coupled with movements of nucleotides A127 and G128 within the active site. These changes resulted in a decreased metal-to-metal distance from 5.4 Å in the deoxy-ωG structure to 3.9 Å in the ribo-ωG structure. The observed changes in metal-ion identity and coordination likely account for the more than a millionfold loss of activity observed upon 2′-deoxy ωG substitution during either step of splicing (*24*, *25*).

The coordination of M_1 and M_2 in this structure satisfies all the biochemically predicted catalytic metal-ion ligands, including four provided by the substrates and two within the intron active site (*10–15*) (Figs. 1B and 3B). In the three cases for which data are available, the biochemically predicted coordination of one metal by two ligands was also observed in the structure (*13–15*). Furthermore, the orientation of the O3′-nucleophile and scissile phosphate are ideal for inline nu-

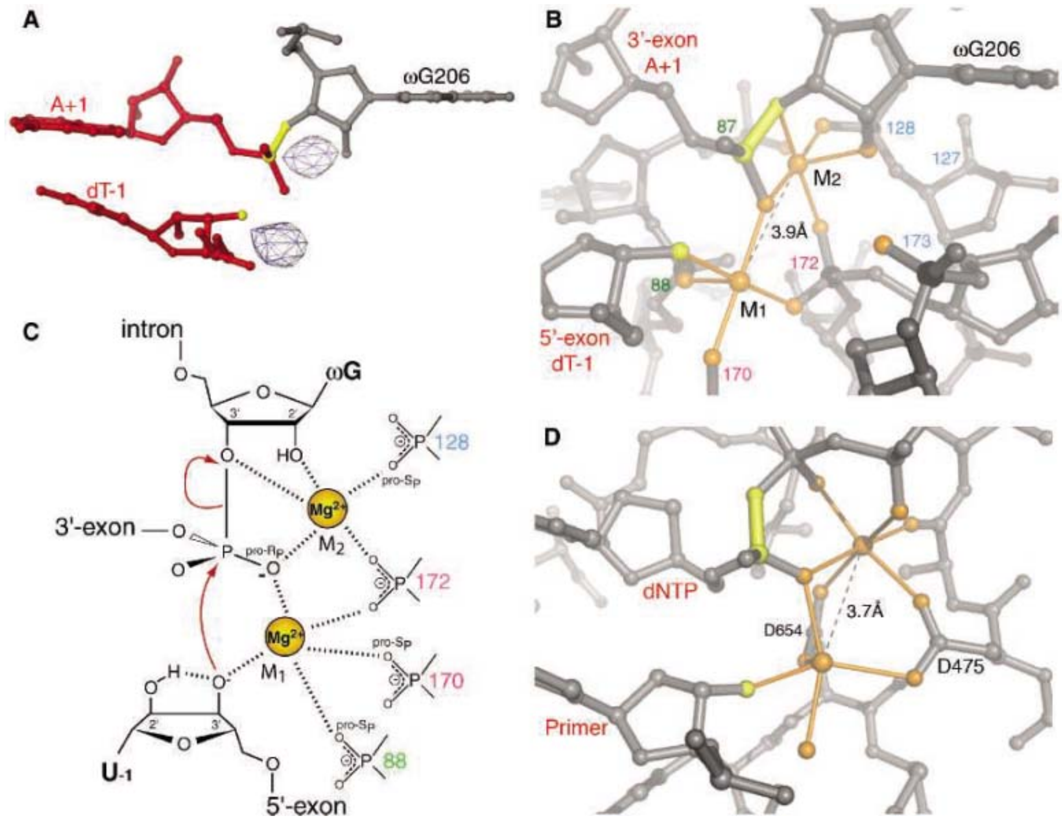

Fig. 3. A two-metal mechanism for group I intron splicing. (**A**) F_O-F_C omit map (active-site metals were not included in the model) used to assign M_1 and M_2 positions, superimposed on the refined structure. The native density (5σ) for each metal is depicted in blue. The other residues are as labeled. In (A), (B), and (D), the scissile bond, nucleophile, and leaving group are shown in yellow. (**B**) Active-site coordination to M_1 and M_2. In this and (D), the active-site Mg^{2+} ions are shown as large orange spheres, the predicted inner and outer sphere ligands are shown as small orange spheres, and the metal-to-metal distance is labeled. Orange lines indicate inner sphere coordinations. Labels for the individual nucleotides are as in Fig. 2A. All the coordinations depicted in Fig. 1B are satisfied in this structure. (**C**) Model of the group I intron transition state stabilized by a two-metal mechanism. (**D**) Two-metal active-site coordination within the T7 DNA polymerase (*1*). The incoming deoxy-nucleotide triphosphate (dNTP), the primer oligonucleotide, and active-site aspartates are labeled. The nucleophile was not present in the crystal structure but is modeled here for comparison.

cleophilic attack (the O3′–P distance is 3.2 Å, and the O3′–P–O3′ angle is 175°).

There is no evidence within this structure for a third active-site metal ion. A three-metal-ion mechanism was proposed on the basis of a difference in Mn^{2+} concentration needed to rescue different sulfur or amino substitutions of substrate functional groups. These experiments were performed on a "ground state complex" in which neither of the exons nor the critical guanosine were bound (Fig. 1C) (*21*, *22*). In this model, two different metals, M_B and M_C, are proposed to coordinate the O3′ and O2′ ligands of the ωG, respectively, resulting in different roles for the catalytic metals from those predicted by the ribo-ωG structure. Most notably, none of the metals bridge between the scissile phosphate and the leaving group in the three-metal model. Although we cannot exclude the possibility that a third metal ion is disordered in the crystal structure, the majority of the biochemical data are explained by the two metals that are observed. If a third metal is modeled near the O3′ of ωG opposite M_2, the position that is predicted in the three-metal model, the closest phosphates (ωG206 and C+2) are more than 3.5 Å away, too large a distance to make direct metal-ion coordination. Additionally, these two phosphates have never been implicated in metal-ion coordination, and it has long been established that the absence of these phosphates does not alter the activity of the reaction (*31*).

The two-metal architecture observed in this ground state structure and the bulk of the biochemical data on catalytic metal ions in group I intron splicing support a two-metal-ion mechanism for transition state stabilization, similar to that originally proposed by Steitz and Steitz based on analogy to exonuclease and phosphatase mechanisms (Fig. 3C) (*7*). M_1 (biochemically titled M_A) (*10*) activates the nucleophile, whereas M_2 (which has the dual characteristics of the biochemically titled metals M_B and M_C) (*11*, *12*) stabilizes the leaving group. Both metals bridge to the scissile phosphate, where they counterbalance the development of negative charge. In this mechanism, the active-site metal ions are symmetrical, which is consistent with a forward and reverse equilibrium for group I intron phosphoryl transfer of approximately one under standard reaction conditions (*29*). The reversible nature of the group I reaction suggests that the intron completes both steps of splicing in a similar active site. In the first step of splicing, the roles of the U-1 O3′ and G O3′ are reversed from what is observed here, in that U-1 O3′ is the leaving group and the exogenous G O3′ is the nucleophile. The roles of nucleophilic and leaving group activation for the two metals are also likely to be reversed between the two splicing reactions.

The location, coordination, and function of the active-site metals observed in this RNA active site are equivalent to a generalized two-metal-ion mechanism of catalysis employed by a wide variety of protein enzymes for the promotion of phosphoryltransfer reactions (*8*). The M_1 to M_2 distance is 3.9 Å, a hallmark of the two-metal mechanism. M_1 and M_2 share a scissile phosphate ligand and coordinate the two conjugated phosphate oxygens of A172 (Fig. 3, B and C) (*13*). Shared ligands are seen in two-metal-ion protein enzymes where both catalytic metals coordinate the scissile phosphate and bidentate carboxylates of conserved aspartate or glutamate residues (*8*, *32*). Because conjugated and shared ligands of two metals are bound less tightly than other ligands, this coordination geometry is expected to increase the Lewis acidity of the metal toward the nucleophile or leaving group and promote the reaction (*32*). The conservation of this feature between RNA and protein enzymes highlights its importance. Further, two-metal-ion mechanisms sometimes use a metal-bound water to protonate the leaving group of the reaction (*6*). M_2 has a single apical position available for a water ligand that may protonate the ωG O3′ leaving group.

There is marked similarity between this RNA active site and the active sites of RNA and DNA polymerases (Fig. 3, B and D) (*5*). The 5′-exon is analogous to the primer strand, the 3′-exon to the incoming nucleotide, and the ωG to the pyrophosphate leaving group (*33*). Both active sites contain two metal ions and coordinate those metals in a similar man-

ner. The simultaneous coordination of the scissile phosphate pro-R_P oxygen, ωG O2′, and ωG O3′ by M_2 is analogous to coordination of a single metal to the alpha, beta, and gamma phosphates of the incoming nucleotide in polymerases (*1*). RNA enzymes and protein enzymes are not evolutionarily related, so the equivalence of group I intron and polymerase active sites must be an example of convergent evolution. That macromolecular evolution arrived independently at the same solution in RNA and proteins implies an intrinsic chemical capacity of the two-metal-ion catalytic architecture for phosphoryl transfer. It is possible that this mechanism was used by the prebiotic RNA-based RNA polymerase and that it continues to be employed by other RNA splicing systems, including the spliceosome.

References and Notes

1. S. Doublie, S. Tabor, A. M. Long, C. C. Richardson, T. Ellenberger, *Nature* **391**, 251 (1998).
2. G. Zhang *et al.*, *Cell* **98**, 811 (1999).
3. R. X. Xu *et al.*, *Science* **288**, 1822 (2000).
4. N. Strater, W. N. Lipscomb, T. Klabunde, B. Krebs, *Angew. Chem. Int. Ed. Engl.* **35**, 2024 (1996).
5. L. S. Beese, T. A. Steitz, *EMBO J.* **10**, 25 (1991).
6. N. C. Horton, J. J. Perona, *Nat. Struct. Biol.* **8**, 290 (2001).
7. T. A. Steitz, J. A. Steitz, *Proc. Natl. Acad. Sci. U.S.A.* **90**, 6498 (1993).
8. N. Strater, W. N. Lipscomb, T. Klabunde, B. Krebs, *Angew. Chem. Int. Ed. Engl.* **35**, 2024 (1996).
9. M. J. Fedor, *Curr. Opin. Struct. Biol.* **12**, 289 (2002).
10. J. A. Piccirilli, J. S. Vyle, M. H. Caruthers, T. R. Cech, *Nature* **361**, 85 (1993).
11. L. B. Weinstein, B. C. Jones, R. Cosstick, T. R. Cech, *Nature* **388**, 805 (1997).
12. A. S. Sjogren, E. Pettersson, B. M. Sjoberg, R. Stromberg, *Nucleic Acids Res.* **25**, 648 (1997).
13. A. Yoshida, S. Sun, J. A. Piccirilli, *Nat. Struct. Biol.* **6**, 318 (1999).
14. A. A. Szewczak, A. B. Kosek, J. A. Piccirilli, S. A. Strobel, *Biochemistry* **41**, 2516 (2002).
15. J. L. Hougland, A. V. Kravchuk, D. Herschlag, J. A. Piccirilli, *PLoS Biol.* **3**, e277 (2005).
16. P. L. Adams, M. R. Stahley, A. B. Kosek, J. Wang, S. A. Strobel, *Nature* **430**, 45 (2004).
17. F. Guo, A. R. Gooding, T. R. Cech, *Mol. Cell* **16**, 351 (2004).
18. B. L. Golden, H. Kim, E. Chase, *Nat. Struct. Mol. Biol.* **12**, 82 (2005).
19. P. L. Adams *et al.*, *RNA* **10**, 1867 (2004).
20. Two recently reported group I intron crystal structures each contained one active-site metal ion identified by soaks with an anomalous scattering metal. The P3-P9 apo-enzyme form of the *Tetrahymena* group I intron crystal structure contained what appeared to be metal M_2. The metal was coordinated to the O2′ and O3′ of the ωG (*17*). This structure included the ωG but did not include the scissile phosphate, the 5′- or 3′-exon, or the internal guide sequence to which the exons bind. The ribozyme product form of the *Twort* intron included a single metal that appeared to be equivalent to M_1 (*18*). The metal coordinated the O3′ of U-1. This structure included the nucleophile (O3′) and the ωG but not the scissile phosphate or the 3′-exon (fig. S1).
21. S. Shan, A. Yoshida, S. Sun, J. A. Piccirilli, D. Herschlag, *Proc. Natl. Acad. Sci. U.S.A.* **96**, 12299 (1999).
22. S. Shan, A. V. Kravchuk, J. A. Piccirilli, D. Herschlag, *Biochemistry* **40**, 5161 (2001).
23. CAT and rcirc were added to a 185-nucleotide transcript before crystallization. Crystal screens were set up as described previously (*16*). Optimal crystallization conditions were 30% 2-methyl-2,4-pentanediol (MPD), 40 mM MgOAc, 40 mM KOAc, 50 mM NaCac at pH 6.7, and 0.2 mM CoHex. Crystals appeared in 2 days and reached full size in 2 weeks. Data were collected at 100 K at 1.1 Å wavelength on beamline X25 at the National Synchrotron Light Source and were processed in HKL2000 (*34*). Experimental phases were used from the deoxy-ωG structure (*16*). Refinement was performed in the program CNS (*35*), and model building was performed with the program O (*36*). Figures were made with Ribbons (*37*) and Pymol (*38*).
24. B. L. Bass, T. R. Cech, *Biochemistry* **25**, 4473 (1986).
25. S. Moran, R. Kierzek, D. H. Turner, *Biochemistry* **32**, 5247 (1993).
26. S. A. Strobel, L. Ortoleva-Donnelly, *Chem. Biol.* **6**, 153 (1999).
27. D. Herschlag, F. Eckstein, T. R. Cech, *Biochemistry* **32**, 8312 (1993).
28. Crystal activity assays were performed by washing ribo-ωG crystals in a stabilization solution of 30% MPD, 10 mM MgOAc, 10 mM KOAc, 50 mM NaCac at pH 6.8, and 0.2 mM CoHex to remove noncrystallized intron RNA. Crystals were transferred to 10 μL of this stabilization solution containing 150 μM CAU or CAT, mixed with a trace amount of ^{32}P 5′-end labeled CAU or CAT. Crystals in labeled substrate were incubated at room temperature for 2 days. The crystals were then washed extensively to remove any unbound ligation product and dissolved in a formamide denaturing buffer. The product was separated from the substrate through denaturing polyacrylamide gel electrophoresis. Ligation assays of the complex in solution were performed in the same buffer under conditions expected to mimic those found in the crystal activity assay; i.e., 1 μM transcript was mixed with 1 μM rcirc and 1 μM CAT and incubated for 30 min. To this solution was added 5 μM CAU or CAT, a trace portion of which was radiolabeled. The mixture was allowed to react for 50 hours and analyzed as described above.
29. R. Mei, D. Herschlag, *Biochemistry* **35**, 5796 (1996).
30. Crystals were soaked in 0.1 mM MnOAc or 0.5 mM $YbCl_3$ for 3 hours. Data were collected at 1.4 Å and 1.3550 Å, respectively. The Mn^{2+} soaked crystal showed a 5σ anomalous peak located over the M_2 site. The Yb^{3+} soaked crystal showed a 14σ anomalous peak located over the M_1 site. Anomalous difference maps are included as supplementary information.
31. T. R. Cech, A. J. Zaug, P. J. Grabowski, *Cell* **27**, 487 (1981).
32. G. C. Dismukes, *Chem. Rev.* **96**, 2909 (1996).
33. J. A. Doudna, J. W. Szostak, *Nature* **339**, 519 (1989).
34. Z. Otwinowski, W. Minor, *Methods Enzymol.* **276**, 307 (1997).
35. A. T. Brunger *et al.*, *Acta Crystallogr. D Biol. Crystallogr.* **54**, 905 (1998).
36. T. A. Jones, J. Y. Zou, S. W. Cowan, M. Kjeldgaard, *Acta Crystallogr. A* **47**, 110 (1991).
37. M. Carson, *J. Appl. Crystallogr.* **24**, 958 (1991).
38. DeLano Scientific (www.pymol.org).

39. We thank J. Wang for assistance with structure refinement; M. Becker and the staff at Brookhaven National Laboratory Beamline X25 for help with data collection; and T. Steitz, J. Cochrane, and L. Szewczak for critical comments on the manuscript. Supported by NSF grant no. MCB315329. Coordinates for the ribo-ωG *Azoarcus* group I intron structure are deposited in the Protein Data Bank under accession no. 1ZZN.

Supporting Online Material
www.sciencemag.org/cgi/content/full/309/5740/1587/DC1
SOM Text
Figs. S1 to S3
Tables S1 and S2
References and Notes

18 May 2005; accepted 1 August 2005
10.1126/science.1114994

Albumin and IgG Removal
Albumin and gammaglobulin (IgG) can constitute more than 50% of total serum proteins, obscuring other proteins and making the resolution of low-abundant proteins difficult. Two new kits, one antibody-based and one dye-based, efficiently remove albumin and IgG from samples. The ProteoSeek Antibody Based Albumin/IgG Removal Kit contains an immobilized anti-IgG/anti-albumin gel for the removal of human serum albumin and all major subclasses of IgG from human serum, plasma, or spinal fluids. The dye-based ProteoSeek Albumin/IgG Removal Kit contains a mixed bed matrix of immobilized cibacron blue and high-capacity immobilized protein A and provides an efficient, economical method for depleting excess abundant proteins while enriching the lower molecular weight proteins, peptides, and other small components.
Pierce For information 815-968-0747 www.piercenet.com

DNA Damage System
The Comet Assay IV is an interactive video-based software system that measures the DNA damage detected using single-cell gel electrophoresis. Using a high-definition video camera attached to a microscope, Comet Assay IV provides real-time cell scoring by transferring a live video image to a computer screen with no time lag. The comet assay is one of the standard methods of assessing DNA damage and uses fluorescent microscopy to examine it at the single-cell level in a wide range of applications, including genotoxicity testing, ecotoxicology, clinical diagnostics, food processing and nutrition, mechanistic research, and health and safety testing. The system can be incorporated into existing protocols and data can be saved to Microsoft Excel or an Oracle database.
Perceptive Instruments For information +44 (0)1440 730773 www.perceptive.co.uk

Quantitative Proteomics Software
Proteineer-LC 1.1 is a unique liquid chromatography-mass spectrometry/mass spectrometry (LC-MS/MS) based quantitative proteomics solution. ProteinScape 1.3 is new bioinformatics software. Stable isotope labeling experiments and user-defined isotopic labels are fully supported in these new software releases. The Proteineer software suite extends the existing workflow support from two-dimensional gel to LC-MS/MS-based protein identification and quantitation using Bruker Daltonics' Ultraflex II matrix-assisted laser desorption ionization-time of flight and HCTultra ion trap mass spectrometers.
Bruker Daltonics For information 978-667-9580 www.bruker-biosciences.com

For more information visit GetInfo, *Science*'s new online product index at *http://science.labvelocity.com*

From the pages of GetInfo, you can:
- Quickly find and request free information on products and services found in the pages of *Science*.
- Ask vendors to contact you with more information.
- Link directly to vendors' Web sites.

Stackable Shaking Cabinets
The Certomat BS-1 line of high-capacity, stackable environmental shaking cabinets has been redesigned for improved user-friendliness and longevity. Requiring less than 10 square feet of floor space, up to three cabinets can be stacked without any reduction in shaking speeds. The interior chamber can hold up to six-liter Erlenmeyer flasks. All key parameters are programmable though a digital controller. Clean-up of spills is easy because of a hygienic, polished stainless steel interior and removable spill tray.
Sartorius For information 800-258-9000 www.sartorius-bbi-systems.com

Electronic Pipettors


The line of Biopette E Electronic Pipettors has been expanded to 12 models available in single-, 8-, and 12-channel configurations. The new 8-channel and 12-channel, 1200-μl instruments are well-suited for efficient pipetting into 96-well plates. Pipetting modes include multiple dispensing, mixing, sequential dispensing, sequential aspiration, and serial dilution. The instruments feature a lightweight, ergonomic design and fully motorized piston drive to reduce the potential for repetitive stress injury.
Labnet International For information 888-522-6381 www.labnetlink.com

Membrane Protein Plates
CrystalQuick Plus combines the optical properties of a flat crystallization well bottom with superior surface features, rendering a format especially conducive to crystallography of cell membrane proteins. The hydrophobic plate surface effectively prevents drop deformation, even when surface-tension–reducing substances such as detergents or ethanol are contained within. In addition, the hydrophobic surface significantly reduces meniscus formation of reservoir screening solutions, thereby minimizing the risk for screening solution to spread from the reservoir into the crystalization well. CrystalQuick Plus permits screening of up to 288 crystallization setups per plate. Each screening reservoir contains an elevated platform with three square, flat bottom crystallization wells to perform multiple sitting drop vapor diffusions within a 96-well framework. Designed to facilitate high-throughput protein crystallography in automated system, the plates enable the investigation of optimal crystal growth conditions and subsequent x-ray diffraction at reduced cost.
Greiner Bio-One For information 800-884-4703 www.gbo.com/bioscience

Literature
Endogen Applications Handbook and Catalog 2005/2006 is an 82-page publication with technical sections on enzyme-linked immunosorbent assays, Searchlight multiplex assays and custom array development, enzyme-linked immunospot kits, and primer sets. It also features information for recombinant proteins, recombinant active kinases, antibodies, and supporting reagents.
Pierce For information 815-968-0747 www.piercenet.com

Newly offered instrumentation, apparatus, and laboratory materials of interest to researchers in all disciplines in academic, industrial, and government organizations are featured in this space. Emphasis is given to purpose, chief characteristics, and availability of products and materials. Endorsement by *Science* or AAAS of any products or materials mentioned is not implied. Additional information may be obtained from the manufacturer or supplier by visiting www.science.labvelocity.com on the Web, where you can request that the information be sent to you by e-mail, fax, mail, or telephone.

» advances in:

Biochips

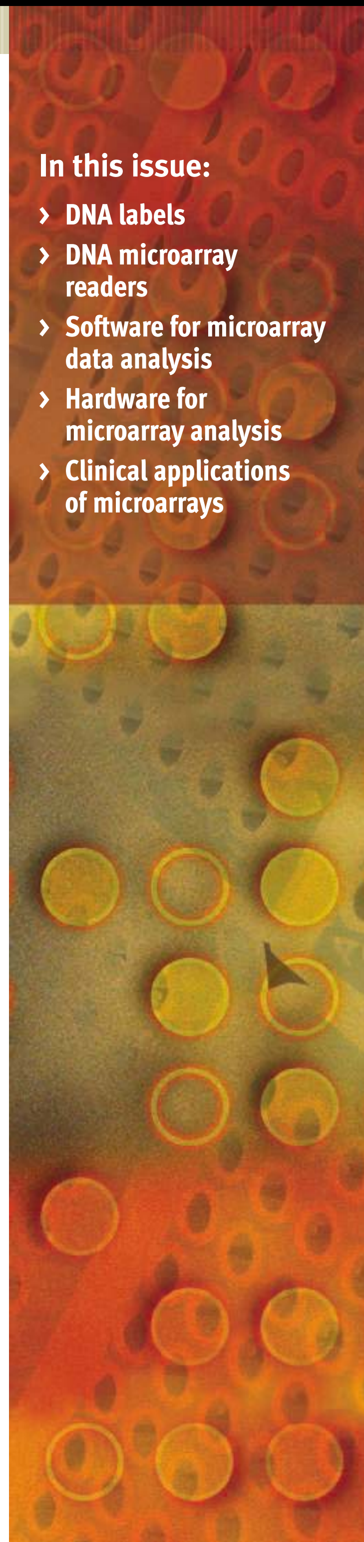

Data Delivery for DNA Microarrays

As their technology has advanced, DNA microarrays have started to find fresh applications in biomedicine. To facilitate those uses, vendors have had to develop new approaches to storing and analyzing the data that microarrays produce.

BY PETER GWYNNE AND GARY HEEBNER

During the past half decade, DNA microarrays have undergone a transformation from laboratory curiosities to devices that permit scientists to probe entire genomes at an exquisitely detailed level. They have also begun to move from studies of gene expression profiling into broader areas of biomedicine. "Microarrays are now actively used in clinical trials and are needed for drug development because they permit you to assess quickly how a particular drug is working; you can see early what kinds of genes are responding," explains Irene Gabashvili, technical lead for computational biosciences at **Hewlett-Packard** (HP). "They are also used in diagnostics."

This expansion of applications stems in large measure from developments in DNA microarray technology. "There have been improvements in the robustness of the systems," says Jordan Stockton, marketing manager for informatics at **Agilent Technologies**. "Users have gone from spotted complementary DNAs [cDNAs] to direct synthesis on slides or arrays. The content of arrays has improved dramatically as sequences have become available."

Walter Koch, head of research for **Roche Molecular Diagnostics**, adds to that list. "There have been substantial improvements over the past five years in microarray manufacturing technologies that allow the reproducible, larger scale manufacture of higher-density microarrays with smaller feature size," he says. "Concomitantly, advances in laser scanning technology have resulted in smaller pixel resolution to take advantage of the ever-smaller feature sizes." Gabashvili, meanwhile, sees a continuing process of improvement. "We have better quality control. We have cheap fabrication technologies," she says. "And the main improvements are yet to come, via nanotechnology research at **MIT**, HP, and other technology innovators."

Herbert Auer, director of the functional genomics core at **Columbus Children's Research Institute** and chair of the **ABRF Microarray Research Group** (MARG), an organization that undertakes regular surveys of microarray users, has his own take on advances in the technology. "What's happening now is almost not comparable with what happened five years ago," he says. "Now, scientists can examine all the transcripts of an organism rather than a few thousand. Another thing that has definitely changed is the reproducibility of commercially available microarrays. And the equipment used for home-made microarrays has become better. The probes that I use are much more specific now. Five years ago, pretty much everybody used cDNAs; now they use oligonucleotides for more specificity."

Massive Amounts of Genetic Information

Stephen Fodor and his colleagues invented the microarray in the late 1980s. Fodor, founder, chairman and CEO of **Affymetrix**, the first company to commercialize microarrays, summarizes the impact of the recent advances. "The frame- MORE ›››

Inclusion of companies in this article does not indicate endorsement by either AAAS or Science*, nor is it meant to imply that their products or services are superior to those of other companies.*

This is the final one of four special supplements this year on Advances in Biochips. The first three appeared in the 4 March, 6 May, and 19 August issues of Science.

» advances in: Biochips

work for growth of the field is there," he says. "Today, scientists have the ability to look at massive amounts of genetic information simultaneously in a single experiment."

Those huge amounts of data create an obvious challenge: They have no value until scientists can analyze and make sense of them. "The biggest problem is still as it was through the years: bioinformatics and data analysis," Auer says. Dealing with that problem demands a combination of sophisticated hardware and software, as well as tools such as microarray readers and scientific software that are user-friendly for bench scientists.

Users of microarrays face other issues. "The number two challenge, according to surveys by MARG, is funding of operations," Auer says. "Microarray technology is still relatively expensive – a few hundred dollars per experiment." Siamak Baharloo, marketing manager with the bioinformatics and e-business group at **Invitrogen**, pinpoints another problem. "The challenge is a lack of standards in platforms, protocols, and analysis," he explains. "You can follow the exact same protocol, but if you change a single reagent or the platform, you get entirely different data. Two labs down the same corridor can get entirely different results by using different platforms."

Two Types of Labels

Sample processing for microarrays involves labeling, detection, and data interpretation. Scientists can tag the DNA attached to a microarray with some type of label and then detect it with laser scanners or other devices specifically designed for use with microarrays. Scientists have a choice of two types of label. Radioactive labels, imaged with a phosphorimager or autoradiography film, make up in effectiveness what they may lack in glamour. Companies such as **MP Biomedicals** and **PerkinElmer Life and Analytical Sciences** offer the most common radiolabels for this procedure. Radiolabels most often find use with nylon membrane macroarrays, such as those offered by **BD Biosciences Clontech** and **Millipore**.

Scientists tend to prefer fluorescent labels, which offer less risk of radiation exposure, easier disposal, and greater sensitivity when compared with radioactive labels. To identify multiple samples, a researcher can multiplex experiments on a single microarray, using several different compounds that each emit a different wavelength. Companies that produce fluorescent labels include **GE Healthcare**, Invitrogen, and **Sigma-Aldrich**.

Fluorescent imaging systems for microarrays perform several basic operations. They excite the fluorescent labels attached to the samples, collect emitted light, and generate digital images of the fluorescent signal. To collect the fluorescent images, scientists can opt for scanning or imaging. Scanning involves laser excitation with a photomultiplier tube detector while imaging uses filtered white light excitation with a charge coupled device detector. Affymetrix, **Hitachi Genetic Systems/MiraiBio**, **Molecular Devices**, and other companies offer DNA microarray readers based on these detection systems.

Affymetrix has developed the GeneChip Scanner 3000 7G, related to the company's GeneChip Scanner 3000 series, for use with next-generation higher density arrays. It scans 5 µm features, enabling an increase in genomic content of 500 percent over the previous arrays. The scanner supports the latest high density, high information content microarrays for tiling, and up to 500,000 SNP genotyping research. Combined with Affymetrix's GeneChip AutoLoader, the 3000 7G provides sample tracking, temperature control, and walk-away freedom from scanning.

The scanner processes vast amounts of information. "At a 5 micron feature size, our standard 1-cm. square chip contains about 6.5 million probes," Fodor says. "That's a lot of data, and the 7G is capable of reading it."

Interpreting the Results

Having scanned the array, scientists need to interpret the results. Storing and analyzing information from microarrays that contain thousands of samples or spots offer a serious challenge. "Data analysis represents a bottleneck today," says Scott Cole, marketing manager for Agilent. Scientists typically spend many hours at their desks, working with computers and specialized software to store and manage sequence data, design microarray formats, and analyze the data gathered from those studies.

The situation is improving, however. "A few years ago, scientists didn't know what questions to ask," Cole's colleague Stockton explains. "Now we have tools to guide them." Several companies, including Agilent, Invitrogen, **Premier BioSoft**, **Spotfire**, and **TeleChem International**, offer software and other products for microarray design and analysis.

Through its InforMax subsidiary, Invitrogen offers Vector NTI Advance and Vector Xpression software packages for microarray data analysis. And in June, the company released iPath, a bioinformatics system that consists of 225 high-level, annotated, validated maps of human cell signaling and metabolic pathways compiled by **GeneGo, Inc**. "iPath has very useful and rich bioinformatics content," Baharloo explains. "Customers can search the signaling and metabolic pathways by the name of the pathway. They'll land at a very user-friendly graphical interface with proteins and other objects in the pathway indicated by symbols. The software also indicates bindings, translocations, phosphorylations, and other reactions symbolically."

In practice, users can seek pathways by querying the software with a keyword, a gene's name or ID, or IDs from specific arrays. "We have associated the IDs with the genes, and then associated them MORE ›››

with the pathways the genes are involved with," Baharloo explains. "It deconvolutes the various pathways." To update pathways, a group at GeneGo combs through the peer-reviewed literature. "We'll update significant changes instantly and minor ones shortly," Baharloo says. Affymetrix, meanwhile, recently launched a GeneChip Compatible Software Partners Program that provides users of microarrays with a broad spectrum of integrated solutions for biomedical research and development.

Software and Hardware

Agilent's Silicon Genetics unit specializes in software for expression data analysis and management. Its GeneSpring software product is a powerful visualization and analysis solution, designed for use with genomic expression data from virtually any source, that can display and analyze large datasets on a typical desktop computer. "GeneSpring is the center of our code base. We're aiming to add new applications and uses for any high throughput technologies," Stockton says "Data generated from many different types of microarray applications tend to be useful in the same experiment," Cole adds. "So it's becoming important to leverage many pieces of microarray data. We're working on tools to do that in the GeneSpring platform."

Microarray applications are clearly pressing the limits of conventional computing power. Hardware companies such as **Apple**, HP, and **IBM** are working on ways to obtain more power from existing computers, to develop more powerful computers, and to devise more capable software. "We are doing our own research and supporting research at academic institutions," HP's Gabashvili says. "For real-time results you need good middleware, which we are designing. Ours is unique in that our customers can decide just what they want."

The firm also takes a highly customized approach to bioinformatics, aiming to determine the optimum high performance architectures for its customers' needs. "Every bioinformatics company says that it offers customized software," Gabashvili says. "But we are supporting the IEEE standardization initiative for bioinformatics – in particular in microarrays – to increase productivity in the field."

HP also encourages a move of microarraying into the diagnostic arena. "One of our collaborators, Harvard Partners Centers for Genetics and Genomics, is using microarrays to diagnose certain diseases such as deafness, particularly in babies," Gabashvili says. "And another partner, at the Biomedical Engineering department of the Georgia Institute of Technology and Emory University, is integrating the microarray technology with bionanotechnology in cancer research for uses such as early detection, diagnosis, prognosis, and therapeutics."

Diagnostic Applications in View

Roche Molecular Systems has taken that movement a stage further. The **U.S. Food and Drug Administration** has cleared its first microarray based test, the AmpliChip CYP450 Test, powered by Affymetrix microarray technology, for diagnostic use in the United States. "The test detects variations in the CYP2D6 and CYP2C19 genes, which play a primary role in the metabolism of many widely prescribed drugs," Koch explains. "The test also provides a predicted phenotype – that is, poor, intermediate, extensive, or ultrarapid metabolizer."

That represents just a start. "We are continuing to develop other innovative clinical diagnostic AmpliChip tests based on the Affymetrix high-density oligonucleotide microarray platform," Koch says. "Several other companies are also working on developing microarrays for diagnostic use, so one might say a trend is beginning."

Microarrays have proven their utility for research in several areas, including expression profiling, SNP analysis, and tumor sub-typing. The data from these devices just keeps on coming as microarrays gain popularity with researchers worldwide. And as progress continues in developing standards and more application-specific arrays come to market, these new tools will become increasingly useful in revealing more and more scientific data from less and less sample.

Peter Gwynne (pgwynne767@aol.com) is a freelance science writer based on Cape Cod, Massachusetts, U.S.A. Gary Heebner (gheebner@cell-associates.com) is a marketing consultant with Cell Associates in St. Louis, Missouri, U.S.A.

FEATURED COMPANIES

Affymetrix, DNA microarrays, http://www.affymetrix.com

Agilent Technologies, lab-on-a-chip systems, http://www.agilent.com

Apple Computer, Inc., computers and operating systems, http://www.apple.com

Association of Biomolecular Resource Facilities (ABRF), scientific society, http://www.abrf.org

BD Biosciences Clontech, nylon membrane arrays, http://www.clontech.com

Columbus Children's Research Institute, nonprofit research institute, http://www.ccri.net

GE Healthcare, products for microarray fabrication, http://www.gehealthcare.com

GeneGo, Inc., bioinformatics software, http://www.genego.com

Georgia Institute of Technology, university, http://www.gatech.edu

Harvard Partners Center for Genetics and Genomics, research institute, http://www.hpcgg.org

Hewlett-Packard, computers and operating systems, http://www.hp.com

Hitachi Genetic Systems/MiraiBio, products for microarray fabrication, http://www.miraibio.com

IBM Healthcare and Life Sciences, computers and operating systems, http://www.ibm.com

Invitrogen Corporation, scientific software, http://www.invitrogen.com

LION Bioscience AG [Germany], bioinformatics software, http://www.lionbioscience.com

Massachusetts Institute of Technology (MIT), university, http://www.mit.edu

Millipore Corporation, nylon membrane arrays, http://www.millipore.com

Molecular Devices, image detection systems, http://www.moldev.com

MP Biomedicals, radiolabeled biochemical, http://www.mpbio.com

PerkinElmer Life and Analytical Sciences, radiolabeled biochemical, http://las.perkinelmer.com

Premier BioSoft, bioinformatics software, http://www.premierbiosoft.com

Roche Molecular Diagnostics, diagnostic kits and reagents, http://www.roche.com

Sigma-Aldrich Corporation, products for microarray fabrication, http://www.sigma-aldrich.com

Spotfire, Inc., bioinformatics software, http://www.spotfire.com

Telechem International, Inc., bioinformatics software, http://www.arrayit.com

U.S. Food and Drug Administration (FDA), government organization, http://www.fda.gov

POSITIONS OPEN

FACULTY POSITIONS IN BIOPSYCHOLOGY
The University of Chicago

The University of Chicago is seeking to fill **SENIOR** or **JUNIOR POSITIONS** in biopsychology. Our primary goal is to understand behavior and the mind in relation to biological mechanisms. We construe biological mechanisms to include the interactions among the nervous, endocrine, and immune systems, and we are particularly interested in those who study effects of mental and behavioral processes on biological mechanisms. The Institute for Mind and Biology, housed in a new biopsychological sciences research facility, is dedicated to behavioral studies in animals and humans, with fully accredited animal care facilities and communal research equipment.

Ideal candidates are those whose research interests bridge to other strengths in the Department of Psychology, and are enthusiastic about engaging in collaborative transdisciplinary research within a highly interactive research community both inside and outside the Department of Psychology. We invite applications from individuals who primarily study animals and employ an integrative approach incorporating multiple biological mechanisms (e.g., genetic, molecular, neurochemical, hormonal, immune, electrophysiological) that complement their behavioral research. Of particular interest is research in the developmental, emotional, social, and cognitive aspects of psychological processes.

Evaluation of applicants will begin November 1, 2005. Applicants should submit curriculum vitae, a conceptual summary of research, a statement of teaching interests/philosophy, representative publications, and three letters of reference. Please send all materials to: **Biopsychology Search Committee, 5730 Woodlawn Avenue, Room 101, Chicago, IL 60637.** *The University of Chicago is an Affirmative Action/Equal Opportunity Employer.*

UC DAVIS SCHOOL OF MEDICINE
Department of Psychiatry and Behavioral Sciences

ASSISTANT/ASSOCIATE/FULL PROFESSOR of psychiatry. The Department of Psychiatry and Behavioral Sciences and the Center for Neuroscience, University of California, Davis, invite applications for a Neuroscientist at the Assistant/Associate/Full Professor level, to begin July 1, 2006.

Specialization within any area of cellular or molecular neuroscience consistent with the broad goals of the Department and Center is open but candidates with backgrounds in the neuropathology of schizophrenia are encouraged to apply, especially if their research can interact productively with existing and developing programs on the neuropathology of major mental illnesses in the School of Medicine. The successful candidate will be expected to demonstrate leadership in their research specialty, obtain extramural funds, and participate in teaching, and University and public service. Candidate will teach graduate students, medical students, and psychiatry residents. Candidates must possess a Ph.D. or M.D. degree. Some clinical responsibilities possible for qualified applicants but not essential.

Applicants should send a letter, in response to search #3824, describing their research and teaching interests, curriculum vitae, copies of representative publications, and the names of at least five persons from whom references can be obtained to: **Edward G. Jones M.D., Ph.D., Director, Center for Neuroscience and Distinguished Professor of Psychiatry and Behavioral Sciences, 1544 Newton Court, University of California, Davis, CA 95616-8659.** All materials must be received by November 30, 2005, to be assured of consideration. The search will continue until the position is filled. *The University of California is an Affirmative Action/Equal Opportunity Employer.*

POSITIONS OPEN

FACULTY POSITION, IMMUNOLOGY
Department of Microbiology and Immunology
University of Oklahoma Health Sciences Center
Oklahoma City, Oklahoma

The Department of Microbiology and Immunology at the University of Oklahoma Health Sciences Center invites applications for a 12-month, tenure-track position at the **ASSISTANT** or **ASSOCIATE PROFESSOR** level with emphasis in immunology. Outstanding scientists in all areas of immunology are encouraged to apply. Applicants at the Assistant Professor level must have a Ph.D. or equivalent degree with at least two years of postdoctoral training. At the Associate Professor level, the candidate is expected to have an independent, extramurally funded research program. In addition to developing their own research program, the successful candidate will have the opportunity to interact with strong existing programs in basic immunology, cancer, and microbial pathogenesis. Close ties exist with immunologists at the adjacent Oklahoma Medical Research Foundation. Teaching responsibilities will involve participation in the immunology portions of the team-taught graduate, medical, and/or dental curricula within the Department. The Department currently has 14 full-time, tenured, or tenure-track faculty, more than 40 extramural grants and contracts, and ranks in the top 10 medical school microbiology departments in NIH funding. For an overview of the Department, visit our **website: http://w3.ouhsc.edu/mi.** Submit curriculum vitae, description of research interests and teaching experience, and the names and contact information, including e-mail addresses, of three references to **e-mail: immuno-search@ouhsc.edu** or mail to: **Dr. Frank Waxman, Chair of the Search Committee, Department of Microbiology and Immunology, BMSB-1053, 940 S. L. Young Boulevard, Oklahoma City, OK 73104.** Applications will be reviewed as they are received and the position will remain open until filled. *The University of Oklahoma is an Equal Opportunity/Affirmative Action Employer. Applications from women and ethnic minorities are strongly encouraged.*

The Department of Chemistry at Lehman College of The City University of New York (CUNY) invites applications for the position of **DEPARTMENT CHAIR** beginning September 1, 2006; compensation commensurate with the applicant's qualifications. The successful candidate will have a distinguished record of research and scholarly activity that is sufficient to merit appointment in the rank of **FULL PROFESSOR** with tenure, and have a significant record of extramural funding. The applicant should have expertise in either environmental chemistry or structural biochemistry. Applicants should hold a Doctorate in chemistry or biochemistry and should have excellent oral and administrative skills and a commitment to teaching at the undergraduate and graduate levels. The Chair is expected to provide leadership in expanding and further developing the Department, and to participate fully in the life of the College, including teaching, research, and faculty leadership groups. The position will be part of the University's Flagship Initiative in either the Urban Environment or Structural Biology, and the successful applicant will be expected to participate in collaborative CUNY-wide efforts in one of these areas. Applications containing a cover letter; curriculum vitae; statements of research experience, vision for undergraduate and graduate education, and departmental leadership philosophy; and the names of three references should be submitted before December 31, 2005, to: **Search Committee for the Chair of the Department of Chemistry, Office of the Dean of Natural and Social Sciences, Lehman College, The City University of New York, 250 Bedford Park Boulevard West, Bronx, NY 10468-1589.** Please check the Lehman College **website: http://www.lehman.cuny.edu** for upcoming faculty announcements. *Lehman College/CUNY is an Equal Employment Opportunity/Affirmative Action/ADA/IRCA Employer.*

Careers at the National Institutes of Health

BY PETER GWYNNE

Training Programs for Young Scientists

The National Institutes of Health's Office of Intramural Training and Education provides a range of opportunities for individuals to learn the nature of the biomedical research profession.

DR. MICHAEL M. GOTTESMAN

The National Institutes of Health (NIH) has a worldwide reputation for conducting and funding research related to biomedicine. But the organization has another significant role: training young people who want to make their careers in science. "Our focus is on the training, which is basically related to teaching people how to conduct scientific research," says Michael M. Gottesman, Deputy Director for Intramural Research. "We have tried to develop fairly seamless pathways for training, starting at the high school level, going all the way to postdoctoral research, and then on to transitional or bridge training as people go on from training programs to scientific positions." Adds Joan P. Schwartz, assistant director of the Office of Intramural Research and acting deputy director of the Office of Intramural Training and Education: "The goal is to provide training at various levels of entry into science."

That training consists of several separate programs, each with their own objectives. For example, the training can provide a route into the research lab for women and members of disadvantaged populations who have faced extreme difficulties becoming scientists in the past. "The idea is to give an opportunity to be involved in and contribute to research to people who may not otherwise have that opportunity," explains Alfred C. Johnson, director of the NIH's Undergraduate Scholarship Program and its Loan Repayment Programs. According to Mary J. DeLong, director of the NIH Graduate Partnerships Program, the home of graduate students in NIH laboratories, "Students and university faculty in research collaborations gain access to the incredible research resources of the NIH, with a potential for faculty to expand into new areas of research." In addition, says Frederick P. Ognibene, director of the NIH Clinical Research Training Program: "We want to get people engaged in careers in clinical research."

National Institutes of Health
http://www.nih.gov

NIH Office of Intramural Training and Education
http://www.training.nih.gov

NIH Clinical Research Training Program
http://www.training.nih.gov/crtp/index.asp

NIH Graduate Partnerships Program
http://gpp.nih.gov

NIH Loan Repayment Programs
http://www.lrp.nih.gov

NIH Research and Training Opportunities
http://www.training.nih.gov

NIH Undergraduate Scholarship Program
http://ugsp.info.nih.gov

DR. JOAN P. SCHWARTZ

Career Development The programs have a marked effect on trainees' career development. "Just being at the NIH is a remarkable experience," Schwartz says. "There is nowhere else you can work where you have the opportunity to see what is happening and have collaboration possibilities." DeLong extends that thought. "Graduate training at NIH gives students the training experience that can serve as a model for the future collaborative and interdisciplinary research careers that are rapidly becoming the norm," she explains. "There is also the broad network of colleagues established during the students' training that is required for success in the science world."

The training can also give emerging scientists a direct entrée to careers within NIH. For trainees, Gottesman says, "The world is their oyster. So is NIH. We have 1,200 principal investigators and a fair amount of turnover. So we have about 30 tenure track positions open per year on average."

The programs provide an obvious benefit to the organization. "Students bring a new 'energy' and dimension to research teams at NIH," DeLong says. "Our idea," Ognibene adds, "is to enhance the pipeline of clinical researchers." Schwartz points out the value of the programs to the United States, whose taxpayers have doubled government support for NIH during the past decade. "We will get a better educated, more eager, and hopefully more diverse scientific work force," she says.

NIH's 21 individual institutes and centers run the training programs and pay trainees' expenses. However, the Office of Intramural Training and Education has the responsibility of overseeing the targeted programs and placing trainees in them. Several of the programs run throughout the year, while others focus on summer training. Within the course of a single year, NIH's institutes and centers host more than 5,000 trainees at different levels of training and from a variety of locations, including high schools from across the United States and American and overseas universities. The organization also awards scholarships for undergraduates to study science at accredited four-year universities.

General to Particular The programs run the gamut from the general to the specific. They range from giving teenagers a diversity of scientific experiences that they can't obtain in their CONTINUED »

National Human Genome Research Institute

Investigator Recruitment in Bioinformatics and Computational Biology

The Genome Technology Branch (GTB) of the National Human Genome Research Institute (NHGRI) is seeking to recruit outstanding tenure-track or tenured investigators to pursue innovative, independent research using computational approaches to study complex biological problems. General areas of interest include, but are not limited to:

- Comparative and/or large-scale sequence analysis
- Computational functional genomics
- Genome annotation
- Structural prediction, protein folding, and molecular dynamics
- Modeling and simulation of complex biological networks
- Expression profiling
- Evolutionary biology
- Database design and data mining

The successful candidate will be able to take advantage of interactions with a highly collegial group of scientists within NHGRI, the NIH Intramural Sequencing Center (NISC), the National Center for Biotechnology Information (NCBI), and the NIH campus as a whole. In addition, the candidate will have access to NHGRI's established and robust bioinformatics infrastructure, as well as resources made available through NIH's Center for Information Technology (CIT).

This position includes a generous start-up allowance, an ongoing resource commitment of research support and space, laboratory resources (as needed), and positions for support of personnel and trainees. Candidates must have a Ph.D. or equivalent degree, as well as comprehensive, advanced training and accomplishment in one of the targeted areas. Interested applicants should submit a curriculum vitae, a three-page description of proposed research, and three letters of recommendation through our online application system at **http://research.nhgri.nih.gov/apply**

The closing date for this position is **December 1, 2005.**

For more information on GTB and NHGRI's Intramural Program, please see **http://www.genome.gov/Research/** Specific questions regarding the recruitment may be directed to **Dr. Andy Baxevanis (Search Chair) at andy@nhgri.nih.gov or by fax (301-480-2634).**

Tenured Investigator Position
Molecular Pathogenesis and Epidemiology of Influenza Virus

The Respiratory Viruses Section of the Laboratory of Infectious Diseases seeks an M.D. scientist to establish a research program on Molecular Pathogenesis and Epidemiology of influenza virus. This is a broad mandate that will include studies of molecular archeology of the influenza viruses, pathogenesis of influenza A virus for diverse host species, and viral evolution and adaptation in human and animal hosts. The person will interact with and likely provide some guidance to the recently established influenza genomics project. The scientist will translate epidemiological observations and insights into the study of the molecular biology of the virus using reverse genetic systems to investigate molecular determinants of host range and of pathogenesis. This work will be multi-dimensional involving molecular epidemiological studies, analysis of viral genomes, molecular virology, and pathogenesis in a variety of animals. Trials of influenza viruses in human volunteers and epidemiological studies in humans will be possible.

The scientist will head a research team group that will consist of up to eight members including professional and technical staff. The group will be located in Building 33, a building under construction that contains BSL2 and BSL3 laboratory and animal space. The BSL2 research laboratory space will be located adjacent to space occupied by a Principal Investigator engaged in pandemic influenza virus research, and it will therefore be possible for both groups to collaborate and to share equipment. Space, technical and postdoctoral Fellow support, supply budget, and salary are committed.

To be considered for this position, you will need to submit curriculum vitae, bibliography, a detailed statement of research interests, and selected publications preferably via email to Felicia Braunstein at braunsteinf@niaid.nih.gov. In addition, three letters of recommendation must be sent to **Alan Sher, Ph.D., Chairperson, NIAID Search Committee, c/o Ms. Felicia Braunstein, DIR Committee Manager, 10 Center Drive MSC 1349, Building 10, Rm. 4A-30, Bethesda, Maryland 20892-1349**. Completed applications MUST be received by **September 16, 2005**. For additional information on this position, and for instructions on submitting your application, please see our website at: **www.niaid.nih.gov.**

NIMH
National Institute of Mental Health

Postdoctoral Position in Psychology or Psychiatry
Mood and Anxiety Disorders Research Program

The Section of Developmental Genetic Epidemiology in the Mood and Anxiety Disorders Program at the National Institute of Mental Health is recruiting a postdoctoral fellow in experimental psychology, biological psychology/psychiatry, clinical psychology, neuro-psychology/psychiatry, or related field. The focus of the section is genetic epidemiologic and community studies, particularly family and high-risk studies of the correlates and risk factors for the development of mood and anxiety disorders. The candidate must have a Ph.D. in psychology or an M.D. with psychiatry residency, and some research experience is preferred. Preference will be given to candidates with a background and interest in the fundamentals of stress, the autonomic nervous system, and/or reproductive endocrinology/hormones. Applicants should send a curriculum vitae, statement of research interests, and three letters of reference to **Dr. Kathleen R. Merikangas, Chair Search Committee, National Institute of Mental Health, 35 Convent Drive, Bldg 35 Room 1A201, MSC-2370, Bethesda, MD 20892-3720.**

Sallie Rosen Kaplan Fellowship for Women in Basic, Clinical, Epidemiological or Prevention Science

National Cancer Institute®

The Sallie Rosen Kaplan Fellowship for Women Scientists in Cancer Research is made possible by a generous bequest to the Foundation for NIH (FNIH). This is a competitive program for postdoctoral fellows applying to train in any of the National Cancer Institute's intramural research settings, including basic, clinical, epidemiological, and prevention science.

The postdoctoral fellowship experience at the NCI can serve as a first postdoctoral training assignment, or offer more experienced postdoctoral scientists an opportunity to further their training in more advanced methods, to acquire new research capabilities, to make changes in the direction of their research, or to receive training in fundamental sciences and clinical disciplines for the purpose of enhancing the transfer of biotechnology to cancer clinical programs.

Program duration is normally 2 to 5 years. Fellows will be supported by a Cancer Research Training Award (CRTA), with an augmented stipend in the first year provided by the FNIH. The CRTA Fellowship stipend range is $38,500 to $66,100 commensurate with level of experience. Standard self and family health insurance is provided and high option coverage is available.

Candidates for the Sallie Rosen Kaplan Fellowship must be female, must possess a doctoral degree, and have less than 5 years postdoctoral research experience. U.S. citizenship or U.S. permanent residency (green card) is required. Candidates selected for the fellowship will be notified by March 1, 2006 and the starting date will be no earlier than May 1, 2006. Applicants are required to apply online at **http://generalemployment.nci.nih.gov**. by December 15, 2005.

NIDDK National Institute Of Diabetes And Digestive And Kidney Diseases

Postdoctoral positions are available in the Liver Diseases Branch (http://intramural.niddk.nih.gov/research/labbranch.asp?Org_ID=610) of NIDDK. Candidates should hold a D.V.M., M.D., Ph.D., M.D./Ph.D., or equivalent degree conferred less than 5 years before beginning the fellowship. Candidates must have a record of outstanding research productivity and familiarity with a wide range of relevant research techniques. The scientific atmosphere of the NIH Intramural Program offers multiple opportunities for education and training. Please send a resume, statement of career goals and names of 3 references to the appropriate investigator.

T. Jake Liang, M.D. (jliang@nih.gov): molecular pathogenesis of virus-cell/host interactions, vaccine development for hepatitis C, animal models for hepatitis B and C, molecular pathways of host antiviral defense, and identifying and characterizing molecular targets for antiviral development.

Caroline C. Philpott, M.D. (carolinep@intra.niddk.nih.gov): This laboratory uses genetic and cell biological approaches to study iron uptake and utilization in eukaryotic cells. Our work in budding yeast has led to the discovery of new genes involved in iron metabolism, novel systems of iron uptake, and unexpected interactions with other metabolic pathways. Newer projects include the use of yeast expression systems to identify novel human genes of iron metabolism.

Barbara Rehermann, M.D. (Rehermann@nih.gov); Basic and clinical immunology research on the pathogenesis of hepatitis B and hepatitis C virus infection and immune-mediated liver disease. Areas of interest include mechanisms of virus-host interaction, correlates of spontaneous and treatment-induced recovery and mechanisms of disease pathogenesis and progression using immunological, molecular and biochemical techniques and experimental animal models.

Marc Ghany M.D. (marcg@intra.niddk.nih.gov): Basic and clinical research on the pathogenesis and therapy of hepatitis B and C . Areas of interest include molecular biology of hepatitis B virus mutants and mechanisms of antiviral resistance of hepatitis B and C.

Theo Heller, M.D., (theller@nih.gov): The virology of acute hepatitis C, utilizing a model of hepatitis C virion production to elucidate the biology of virion assembly and release, and to explore novel therapeutics.

United States
National Institute of Diabetes & Digestive & Kidney Diseases
of the National Institutes of Health

Research Opportunity at the NIH, DHHS
DIRECTOR, OBESITY CLINICAL RESEARCH CENTER AND CHIEF, DIABETES BRANCH, NIDDK

The Intramural Research Program (IRP) of NIDDK invites applications for the combined position of Chief of the Diabetes Branch and Director of a newly established, NIH-wide initiative in patient-oriented research in obesity ("Obesity Clinical Research Center" – OCRC). The Diabetes Branch, NIDDK conducts basic, translational and clinical research in the areas of diabetes mellitus and obesity. The Chief is responsible for all activities of the Branch, in particular, for integrating the research programs of the several senior investigators and the career development of junior investigators. The goal of the OCRC, which will involve researchers from all Institutes and Centers within the NIH IRP, is to generate knowledge of the pathophysiology, prevention and treatment of obesity and its multisystem co-morbidities, especially type 2 diabetes mellitus. The approach is: 1) to create a center in which to conduct state-of-the-art, patient-oriented obesity research, including metabolic analysis and imaging capabilities, that would support IRP scientists and serve as a magnet facility to foster collaborations with extramural researchers; and 2) to foster multidisciplinary approaches to obesity research, including metabolism, endocrinology, nutrition, gastroenterology, hepatology, imaging, genetics and behavioral sciences.

Priority will be given to applicants at the Professor or Associate Professor level in clinical departments of traditional academic medical centers, or in equivalent positions. The applicant must have a proven record of accomplishments, including evidence of significant, competitively obtained funding for extramural investigators. The appointment will be as a tenured Principal Investigator within NIDDK. The successful candidate will be expected to coordinate the multidisciplinary research proposed for the OCRC and the Diabetes Branch. The position offers unparalleled opportunity to lead a state of the art program in diabetes/obesity research. Salary and benefits are commensurate with the experience of the applicant.

The Diabetes Branch laboratories are in the Warren G. Magnuson Clinical Center and the OCRC Patient Care Unit is a self-contained, metabolic unit located in the new Mark O. Hatfield Clinical Research Center, which are contiguous on the main intramural campus of the NIH in Bethesda, Maryland, a suburb of Washington, D.C.

Interested applicants should send a Curriculum Vitae and list of publications, copies of three major publications, a summary of research accomplishments, a plan for future research and three letters of recommendation to **Dr. James E. Balow, Chair, Search Committee, c/o Ms. Giulia Verzariu, Office of the Scientific Director, NIDDK, Building 10, Room 9N222, NIH, Bethesda, MD 20892.**

Closing Date: October 1, 2005

Department of Health and Human Services
National Institutes of Health
National Institute of Diabetes and Digestive and Kidney Diseases
Equal Opportunity Employers

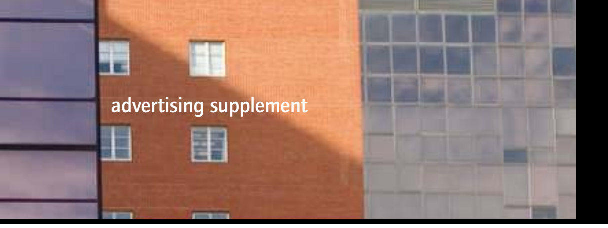

DR. ALFRED C. JOHNSON

high schools and providing support for science undergraduates from underprivileged backgrounds to setting up specialized research programs on disparities in the health of different ethnic groups and introducing medical and dental students to clinical research.

Training starts at the high school level. "We have a competitive program for high school students in the Washington, D.C., area; about 150 schools can nominate up to two students each. We also have about 200 high school students from all over the country who come here for summer study," Gottesman explains. "The concept is that virtually all of us who do science had a formative experience. That suggests it may be necessary, if not sufficient, for a good scientific career."

At the next level comes the Undergraduate Scholarships Program. "Its purpose is to provide support and training for students from disadvantaged backgrounds," Johnson says. "On average we give out about 15 new scholarships per year, with an annual value of up to $20,000 depending on the scholars' needs." Students majoring in the biomedical and behavioral sciences are eligible for the awards. They can fill out their own applications and persuade advisers to send letters of recommendations that attest to their scientific skills. Recipients spend summers at NIH, and have an obligation to work a year at NIH for each year's award.

Another program targets life scientists with recently minted Bachelor's degrees. "We have about 600 students who have graduated from college in the last one or two years and stay at NIH for one or perhaps two years, doing research in the lab," Schwartz says. The program aims to attract students interested in going on to graduate work or medical school. "It gets students at a time when they are deciding what they want to do," Gottesman says. "It gives students a chance to experience life in a real laboratory situation."

DR. MARY J. DELONG

Graduate Programs A special segment of the postbaccalaureate program is the NIH Academy for Health Disparities, which studies the reasons for demographic differences in vulnerability to various diseases. "We have 16 students living together, attending a three-hour course once a week, and doing research on the issue," Schwartz says. "This group is highly diverse; about half the members come from underrepresented minorities."

At the next academic level, the Graduate Partnerships Program links NIH laboratories with universities in collaborative training of about 400 talented Ph.D. students from over 100 universities, including such overseas institutions as Oxford and Cambridge Universities in the United Kingdom and Sweden's Karolinska Institute. "Students complete most of the academic course work at their home universities and then carry out their dissertation research either predominantly at the NIH or in collaboration between an NIH mentor and a university mentor," DeLong explains. "Exposing students early in their training to two distinct institutions, both committed to cutting-edge science though different in structure and operation, fast-forwards the scientific maturation of the student. This experience also creates opportunities for interdisciplinary research, and doubles the number of scientific colleagues and networking contacts."

Clinical research also features on the NIH's list. "The Clinical Research Training Program is targeted at medical and dental students who have completed clinical parts of their training," Ognibene says. "It's a one-year program to do mentored clinical research. Students are also exposed to a formal academic program that teaches them about clinical research." Identified as a significant program in the road map prepared by NIH director Elias Zerhouni, the program has expanded in the last academic year from 15 students to 30 annually. "The idea from the road map is strengthening the clinical research pipeline," Ognibene says. "Through this early capture mechanism we hope that students who seemingly have an interest will pursue careers in clinical research."

DR. FREDERICK P. OGNIBENE

Postdoctoral Fellowships Finally, NIH offers fellowships to postdoctoral students. "They cover scientists within five years of getting their graduate degree," Schwartz says. "We have about 2,600 fellows, roughly 1,800 of them foreign nationals, spread out across all the institutes. We don't target any specific countries, but the reality is that China, Japan, India, South Korea, and Italy have the most fellows."

The fellowships are nominally three years with extension up to five years, although the average stay is three-and-a-half years, and fellows can earn senior fellowships lasting three more years if their supervisors want them to continue. Gottesman outlines the basic approach to subject matter. "We've tried to focus the program around exciting new opportunities, interdisciplinary studies, and translational research," he says.

NIH regards translational research, which focuses on moving results and treatments from bench to bedside, as critical enough to warrant a special course. "A lot of the postdoctoral fellows who come in are interested in doing that," Gottesman says. "We're also developing a more formal program to include the application of physical science to biomedicine." NIH postdocs have other opportunities to move away from conventional research. "If they think they're interested in something other than bench science, we provide internship opportunities in science writing, technology transfer, policy studies, or handling grant reviews," Schwartz says.

And the ultimate goal of the postdoctoral work? "The continuum for clinical fellows includes the possibility of increasing independence," Gottesman says. "For lab fellows it includes learning how to be a research scientist. We don't want them to leave until they can run their own labs."

Getting to that stage can cost a great deal of money, as well as sweat equity. At this point the Loan Repayment Program comes in. "It provides opportunities for young researchers with a lot of student loans to pursue careers in research; we can repay their student loans," Johnson says. One program applies to scientists who join the NIH staff; their applications for loan repayment go through a committee that judges them on scientific merit and potential. The program also has an extramural segment, to repay loans of scientists working in specified research areas.

Whether they receive scholarships, fellowships, or loans, scientists involved with the NIH Intramural Program gain unique insights into the nature of research. As Schwartz puts it, "We offer these people an incredibly rich experience."

A former science editor of Newsweek, *Peter Gwynne (pgwynne767@aol.com) covers science and technology from his base on Cape Cod, Massachusetts, U.S.A.*

IZI

Fraunhofer Institut Zelltherapie und Immunologie

Das Fraunhofer-Institut für Zelltherapie und Immunologie wird ab Oktober 2005 seine Arbeit in der BioCity in Leipzig aufnehmen und sucht aus diesem Grund wissenschaftliche Mitarbeiter (m/w) als

Arbeitsgruppenleiter (m/w)

Das Fraunhofer-Institut für Zelltherapie und Immunologie ist eines von 58 Instituten der Fraunhofer-Gesellschaft. Als eine der führenden Organisationen für angewandte Forschung in Europa bietet sie engagierten Bewerberinnen und Bewerbern anspruchsvolle Aufgaben mit Verantwortung und Gestaltungsspielraum.

zur Durchführung von Forschungs- und Entwicklungsprojekten in den Bereichen Zelltherapie, Transplantations- und Transfusionsmedizin, Immuntherapie, Gewebetherapie (tissue engineering), Immun- und Zelldiagnostik, Biosensorik und Prozessentwicklung, Zellsteuerung und Gewebezucht, molekulare Bildgebung (Imaging) von Regenerationsprozessen.

Da wir uns in der Aufbauphase befinden, sollte der/die Bewerber/in bereits über bewilligte Drittmittel verfügen. Dabei setzen wir einschlägige Forschungserfahrung nach abgeschlossener Promotion sowie die Fähigkeit zur selbstständigen Leitung einer Arbeitsgruppe voraus.

Im Gegenzug bieten wir Ihnen:

- Selbstständige Forschungsarbeit, integriert in ein wissenschaftliches Netzwerk und eine aufzubauende Abteilungsstruktur
- Einen modernen Arbeitsplatz in einem neugegründeten Institut mit eigenem Gestaltungsspielraum
- Bereitstellung der Laborräume, Basisausstattung, Infrastruktur und Zugang zu GMP-Reinsträumen
- Möglichkeit zur freien personellen Gestaltung der Arbeitsgruppe
- Zugang zur akademischen Lehre und Weiterbildung
- Vielfältige Unterstützung durch eine renommierte Forschungsorganisation in Bezug auf Verwaltung, Öffentlichkeitsarbeit und Projektbetreuung

Die Fraunhofer-Gesellschaft hat sich die berufliche Förderung von Frauen zum Ziel gesetzt und ist daher besonders an Bewerbungen von Frauen interessiert. Schwerbehinderte werden bei gleicher Qualifikation bevorzugt eingestellt.

Anstellung, Vergütung und Sozialleistungen richten sich nach dem Bundes-Angestelltentarifvertrag (BAT-O). bzw. dem neuen Tarifvertrag für den öffentlichen Dienst (TVöD). Die Stellen sind zunächst auf ca. 2-3 Jahre (projektgebunden) befristet. Bitte richten Sie Ihre Bewerbung mit allen wichtigen Unterlagen (CV, Publikationsverzeichnis, Drittmittelaufstellung, 2 Referenzschreiben, Forschungsprogramm) unter Angabe der Kennziffer IZI-131-05-006 an:

Fraunhofer-Institut für Zelltherapie und Immunologie IZI, Deutscher Platz 5, 04103 Leipzig.
Fragen zu dieser Position beantwortet gern Herr Hark Kemlein-Schiller,
E-Mail: hark.kemlein-schiller@izi.fraunhofer.de
www.fraunhofer.de

THE OHIO STATE UNIVERSITY
UNIVERSITY MEDICAL CENTER

Director of Research with Endowed Chair

The Department of Surgery at The Ohio State University Medical Center is seeking a tenured full-time faculty member at the level of Professor to direct research in the Division of Cardiothoracic Surgery. The successful candidate is an MD and/or PhD with substantial record of active extramural research funding and publications in tissue repair and remodeling. The position is supported by an endowed chair. The successful candidate will function in the rich environment of the Davis Heart and Lung Research Institute. Candidates with proven expertise in the fields of stem or progenitor cell biology, imaging or tissue engineering applied to heart failure and related problems are desirable. This position holds a co-appointment in the Biomedical Engineering program.

Applicants should send a resume and a statement of current research/funding activities to the **Chair of the Search Committee, Professor Chandan K. Sen, Vice Chairman of Research, Department of Surgery, sen-1@medctr.osu.edu. Ph: 614-247-7786, Fax 614-247-7818.**

The Ohio State University is an Equal Opportunity Affirmative Action Employer; women, minorities, and individuals with disabilities are encouraged to apply.

Tenure-track positions are open for outstanding individuals to establish research programs at Institute of Molecular Biology, Academia Sinica, Taipei, Taiwan.

Applicants should have a Ph. D. degree and sufficient postdoctoral experience. Individuals with demonstrated records of research accomplishments and scientific creativity in all areas of **molecular and cellular biology** are strongly encouraged to apply. Junior scientists for the level of Assistant Research Fellow are most favorable. Senior members with excellent scientific performance are also welcome. Deadline for application is December 31, 2005.

Interested individuals should send Curriculum Vitae, a description of past research accomplishments and future research interests, and three letters of reference to:

Director's Office, c/o Fei Chen
Institute of Molecular Biology
Academia Sinica
Nankang, Taipei 115, Taiwan

Further information can be obtained from **Ms Fei Chen at feichen@ccvax.sinica.edu.tw** or from: **http://www.sinica.edu.tw/imb**

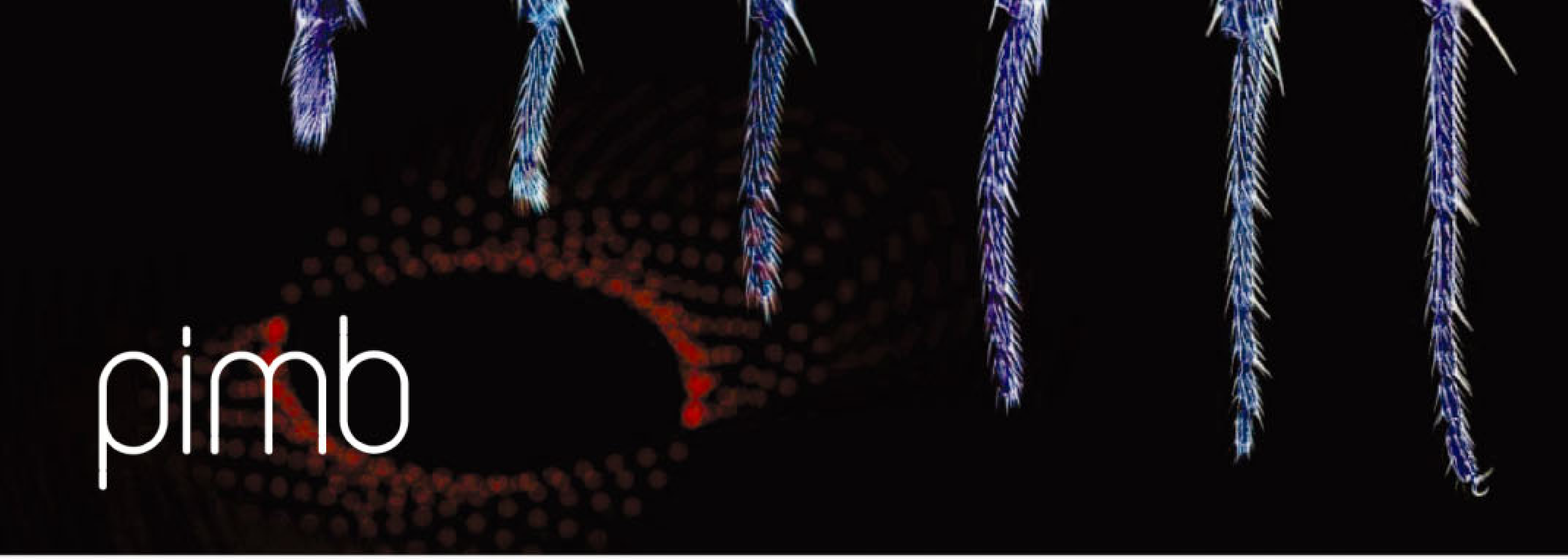

The Program in Integrative Molecular Biology

Introducing PIMB

The University of Pittsburgh is launching the **Program in Integrative Molecular Biology (PIMB)**, an innovative new course of Ph.D. training for students with a highly focused and developed interest in integrative biology.

Innovative Curriculum

PIMB is designed to quickly immerse students in a challenging research environment and mentor them to become independent scientific practitioners with the creative and technical skills required to address some of the most important questions in the life sciences.

Exceptional Training

Intensive rotations in multiple laboratory environments with diverse technologies and scientific disciplines, specialized coursework, integrated career mentoring, a broad choice of advanced electives, and training in the ethics of scientific exploration are among PIMB's most notable features.

- Class size is limited to 6 to 10 students for optimal interaction with faculty.
- Successful applicants will receive financial support in the form of tuition plus a stipend.
- The program, which will begin in June 2006, is designed for completion in approximately four years. Applications will be received beginning in August 2005.

Outstanding Faculty

An outstanding panel of acclaimed scientists with a broad range of investigative approaches has been assembled from laboratories across the University of Pittsburgh to serve as the faculty for this program.

Susan G. Amara, Ph.D.
Gerard Apodaca, Ph.D.
Karen Arndt, Ph.D.
Ivet Bahar, Ph.D.
Jeffrey L. Brodsky, Ph.D.
Gerard Campbell, Ph.D.
J. Richard Chaillet, M.D., Ph.D.
Yuan Chang, M.D.
Deborah Chapman, Ph.D.
Donald B. DeFranco, Ph.D.
Susan Gilbert, Ph.D.
Paula Grabowski, Ph.D.
Angela M. Gronenborn, Ph.D.
Graham Hatfull, Ph.D.
Roger W. Hendrix, Ph.D.
Jeffrey Hildebrand, Ph.D.
Neil A. Hukriede, Ph.D.
Judith H. Klein-Seetharaman, Ph.D.
Jeffrey Lawrence, Ph.D.
Patrick S. Moore, M.D., M.P.H.
James M. Pipas, Ph.D.
William Saunders, Ph.D.
Thomas E. Smithgall, Ph.D.
Linton M. Traub, Ph.D.
Ora A. Weisz, Ph.D.
Richard D. Wood, Ph.D.

For More Information

Program in Integrative Molecular Biology

Graduate Office
524 Scaife Hall
3550 Terrace Street
Pittsburgh, PA 15261

412-648-8957
PIMBinfo@medschool.pitt.edu
http://www.pimb.pitt.edu

University of Pittsburgh
School of Arts and Sciences
School of Medicine

Breast Cancer Basic Science Research
Associate Professor

The Cardinal Bernardin Cancer Center of Loyola University Medical Center, under the leadership of Drs. Patrick J. Stiff as Director and Brian J. Nickoloff as Deputy Director, is seeking outstanding candidates to fill a faculty position at the Associate Professor level within our Breast Cancer Basic Science Program. Candidates must have developed an innovative research program, and demonstrate a strong publication and funding track record.

This laboratory based program, under the direction of Dr. Lucio Miele, is one of the four primary research programs within the Cancer Center's Oncology Institute, and is complemented by an established clinical program in this area. Areas of research interest include experimental therapeutics and target identification, tumor progression biology, metastasis/angiogenesis, cancer stem cells and hormone and growth factor effects in breast carcinogenesis. We are interested in investigators addressing these research areas in clinically relevant model systems.

The successful candidate will be expected to develop and maintain an independently funded laboratory research program as part of the Breast Cancer Basic Science program. In addition to a generous start up package and laboratory space, the Cardinal Bernardin Cancer Center provides a highly interactive research environment, including opportunities for translational research in association with a strong clinical program in breast oncology.

Located in the west suburbs of Chicago, the 125,000 sq. ft. Cancer Center houses both research laboratories and outpatient facilities. The Medical Center campus is also the site of Loyola University's Stritch School of Medicine and Foster G. McGaw Hospital. Additional information about the Oncology Institute can be found online at www.luhs.org/oncinstitute .

Interested applicants may send CV, publications list, funding history, statement of research interests, and the names of three references to:

LOYOLA UNIVERSITY CHICAGO

AD·MAJOREM·DEI·GLORIAM 1870

Lucio Miele, M.D., Ph.D.
Director, Breast Cancer Basic Science Program
c/o Maggie Storti
Administrative Assistant
Cardinal Bernardin Cancer Center
Loyola University Medical Center
2160 S. First Avenue
Maywood, IL 60153

An Equal Opportunity Employer/Educator

U.S. Environmental Protection Agency
National Health and Environmental Effects Research Laboratory
Mid-Continent Ecology Division
Duluth, Minnesota

The U.S. Environmental Protection Agency (EPA) is recruiting to fill the position of **Supervisory Biologist/Toxicologist/Environmental Scientist, GS-0401/0415/1301-14/15**.

This vacancy is for the Chief of the Ecotoxicology Analysis Research Branch at the National Health and Environmental Effects Research Laboratory's Mid-Continent Ecology Division in Duluth, Minnesota. The branch chief provides scientific and administrative leadership for the branch, which is engaged in environmental toxicological research. Research foci include biologically based toxicokinetic and toxicodynamic modeling, species and dose extrapolation, chemical bioavailability, mixtures and multiple stressors, avian toxicology, population response, contaminated sediments, and other issues relevant to the interpreting and predicting the environmental effects of toxic chemicals. This branch is a focal point for delivery of ecotoxicology databases and toxicological modeling approaches to EPA and to the States, Tribes, and other partners, and is heavily engaged in providing technical consultation to these same entities. Ideal candidates will have strong quantitative/analytic skills in biology, toxicology, natural resources, environmental sciences or a closely related field, and have demonstrated leadership skills in a research context. This position supervises senior scientists, bench scientists, and technicians working in interdisciplinary teams.

This is a permanent, full-time position. U.S. citizenship is required. Candidates must meet U.S. Office of Personnel Management (OPM) qualifications as described in the announcements referenced below. Salary ranges from $85,123 to $130,173. A full benefits package, including relocation expenses, is included.

Application instructions are posted at **http://www.usajobs.opm.gov** and **http://www.epa.gov/ezhire** under the titles and announcement numbers: **Supervisory Biologist/Toxicologist/Environmental Scientist - RTP-DE-2005-0150** and **RTP-MP-2005-0264**. The application deadline is **October 15, 2005**. For further information, contact **Rena Sawyer** at **800-433-9633** or **sawyer.rena@epa.gov**.

The U.S. EPA is an Equal Opportunity Employer.

The Jackson Laboratory

FACULTY RECRUITING

The Jackson Laboratory, an independent, mammalian genetics research institution, and an NCI-designated Cancer Center, is engaged in a major research expansion. New faculty will be recruited in the following areas:

- **Neurobiology**
- **Cancer Biology**
- **Reproductive/Developmental Biology**
- **Immunology/Hematology**
- **Metabolic Disease Research**
- **Computational Biology/Bioinformatics**

We are recruiting scientists at all levels who hold a Ph.D., M.D. or D.V.M., completed postdoctoral training, have a record of research excellence and have the ability to develop a competitive, independently funded research program, taking full advantage of the mouse as a research tool. We also encourage applications from scientists with a background in cross-disciplinary approaches.

The Jackson Laboratory offers a unique scientific research opportunity, including excellent collaborative opportunities with our staff of 35 Principal Investigators, unparalleled mouse and genetic resources, outstanding scientific support services, highly successful Postdoctoral and Predoctoral training programs, and a major meeting center, featuring courses and conferences centered around the mouse as a model for human development and disease.

For more information, please visit our web site: www.jax.org.

Applicants for faculty positions should send a curriculum vitae, 2-3 page statement of research interests and plans, and arrange to have three letters of reference sent to facultyjobs@jax.org. Applications should be mailed to Director's Office, The Jackson Laboratory, 600 Main Street, Bar Harbor, Maine 04609, or email (preferred method): facultyjobs@jax.org
Application deadline is October 15, 2005.

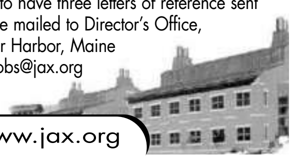

The Jackson Laboratory is an EOE/AA Employer

www.jax.org

ÉCOLE POLYTECHNIQUE FÉDÉRALE DE LAUSANNE

Faculty Position in Physics and Technology of Quantum Nanodevices

at Ecole Polytechnique Fédérale de Lausanne (EPFL)

EPFL invites applications for a tenure track assistant professor position to be named jointly between the School of Basic Sciences and the School of Engineering.

The field of research may be broadly defined as **physics and technology of nanoscale devices. Possible orientations include research in III-V materials, silicon, or other materials relevant for nanoscale systems.** The new professor is expected to develop strong interactions with industry and other research institutions in the field and in particular with the National Center of Competence in Research in Quantum Photonics (NCCR-QP) established with EPFL as the leading house.

We seek applicants with an interdisciplinary vision, a strong record of scientific accomplishments and a commitment to excellence in teaching at both the undergraduate and graduate levels. Substantial start-up resources will be available, in addition to the wide range of characterization tools and processing facilities present at EPFL. We offer internationally competitive salaries and benefits.

Applications with curriculum vitae, publication list, concise statement of research and teaching interests as well as the names and addresses (including e-mail) of at least five references should be submitted as a single PDF file via the website http://sb.epfl.ch/photonsearch by **October 15, 2005.**

For additional information, please contact **Prof. B. Deveaud-Plédran** in the School of Basic Sciences benoit.deveaud-pledran@epfl.ch or **Prof. A. Ionescu** in the School of Engineering adrian.ionescu@epfl.ch or visit the following web sites:
http://sb.epfl.ch/en, http://sti.epfl.ch/index.en.html,
http://www.epfl.ch/Eplace.html, http://nccr-qp.epfl.ch

EPFL is an equal opportunity employer.

The University of Alaska Fairbanks

TWO TENURE-TRACK FACULTY POSITIONS IN MICROBIOLOGY
UNIVERSITY OF ALASKA FAIRBANKS

The Department of Biology and Wildlife and the Institute of Arctic Biology at the University of Alaska Fairbanks seek applications for TWO joint tenure-track faculty positions in microbiology at the assistant professor level. Applicants must have earned a Ph.D. and postdoctoral and teaching experiences are preferred. Successful applicants for both positions will be expected to establish independent and externally funded research programs. Teaching duties will be two courses per year. We seek microbiologists with a background in either of the following two areas:

(1) Applicants working on microorganisms, preferably prokaryotes, with research interests in molecular biology, ecology, biogeochemistry, or digestive physiology. We expect this hire to develop a research program relevant to high-latitude biology. Teaching duties could include an undergraduate general microbiology course and opportunities at the advanced undergraduate/graduate level. Please reference **PCN # 204206/REQ # FF204206-01**.

(2) Applicants working on infectious agents, particularly those causing zoonotic diseases. Preference will be for applicants with research interests relevant to biomedical research. Teaching duties could include an undergraduate microbiology or an infectious disease course and opportunities at the advanced undergraduate/graduate level. Please reference **PCN # 247945/REQ # FF247945-01**.

Field and laboratory facilities include the DNA and Proteomic Core Facility, the Alaska Stable Isotope Facility, a new animal research facility, the R.G. White Large Animal Research Station, Toolik Field Station, Bonanza Creek LTER site, and instrument facilities that house transmission and scanning electron microscopes, a confocal microscope, and a FACS Aria flow cytometer. Our Bioinformatics Program provides access to the Arctic Region Supercomputing Center. A State of Alaska Public Health Diagnostic Laboratory is adjacent to the Institute of Arctic Biology. The Biology and Wildlife Department and the Institute of Arctic Biology have approximately 50 faculty, 20 postdoctoral fellows, and 300 undergraduate and 120 graduate students, including 40 Ph.D. students.

Applicants are encouraged to consult the Institute/Departmental websites and faculty profiles at **http://mercury.bio.uaf.edu**. Applications will be reviewed starting 6 October 2005. Please provide a signed application form (**http://www.alaska.edu/hr/forms/PDF_ent/applicant_form_ent.pdf**), cover letter, curriculum vitae, statements of teaching and research interests, letters from three references and submit to: **Terry Chapin, C/O UAF Human Resources, P.O. Box 757860, Fairbanks, Alaska 99775-7860, Phone (907) 474-7700, Fax (907) 474-5859**. If you have specific questions about this announcement, please contact **Terry Chapin** at **(907) 474-7922, terry.chapin@uaf.edu**.

The University of Alaska Fairbanks is an Equal Opportunity/Affirmative Action Employer and Educational Institution.
Women, protected, and minority applicants are encouraged to apply.

ÉCOLE POLYTECHNIQUE
FÉDÉRALE DE LAUSANNE

Faculty Position in Theoretical High-Energy Physics

at Ecole Polytechnique Fédérale de Lausanne (EPFL)

The EPFL invites applications for a tenure-track assistant professorship in theoretical high-energy physics. Experienced candidates seeking a higher-level position may be considered.

We seek outstanding scientists with interests in particle cosmology, physics beyond the standard model, and particle phenomenology.

The successful candidate will establish and lead a vigorous, independent research program, interact with existing projects in particle physics and cosmology, and be committed to excellence in teaching at both the undergraduate and graduate levels. Significant start-up resources and research infrastructure will be available.

We offer international competitive salaries and benefits.

Applications including a curriculum vitae, publication list, concise statement of research and teaching interests as well as the names and addresses (including email) of at least five references should be submitted in PDF format via the website http://sb.epfl.ch/partphyssearch by **December 15, 2005.**

For additional information, please contact Professor **M. Shaposhnikov** (mikhail.shaposhnikov@epfl.ch) or consult the following websites: http://sb.epfl.ch/en, http://itp.epfl.ch and http://www.epfl.ch/Eplace.html

The EPFL is an equal opportunity employer.

“Our work is more than a job,

it's a career of mission-focused investigation.”

Krystal Williams, Research Analyst,
M.S., Applied Mathematics

Bradford Ng, Research Analyst.
Ph.D., Chemistry

Kathleen Ward, Research Analyst,
Ph.D., Physiology and Biophysics

Work that matters.

The CNA Corporation is a non-profit institution that operates on the principle of conducting impartial, accurate, actionable research and analysis to inform the important work of public sector leaders.

It’s work that matters, and that reflects a commitment to serve the public’s interests and the common good.

We offer career opportunities for people with degrees in engineering, mathematics, economics, physics, chemistry, international relations, national security, history, and many other scientific and professional fields of study.

Diverse views, objectivity, imaginative techniques, process driven, results oriented – committed to the common good. Join us.

The CNA Corporation

Research that works, for work that matters

www.cna.org

ÉCOLE POLYTECHNIQUE FÉDÉRALE DE LAUSANNE

Faculty Positions in Physics

at Ecole Polytechnique Fédérale de Lausanne (EPFL)

The EPFL anticipates making several faculty appointments at the level tenure-track assistant professor in physics. Outstanding scientists with recognized accomplishments in any field of experimental or theoretical physics will be considered. We particularly encourage applications in the fields of theoretical and experimental quantum photonics, condensed matter physics and biophysics. Experienced candidates seeking a higher-level position may be considered.

The successful candidate will establish and lead a vigorous, independent research program, interact with existing projects and be committed to excellence in teaching at both the undergraduate and graduate levels. Significant start-up resources and research infrastructure will be available.

We offer internationally competitive salaries and benefits.

Applications including a curriculum vitae, publication list, concise statement of research and teaching interests as well as the names and addresses (including email) of at least five references should be submitted as a single PDF via the website http://sb.epfl.ch/physearch by **October 15, 2005.**

For additional information, please contact **Professor Jean-Jacques Meister** jean-jacques.meister@epfl.ch or visit the following websites: http://sb.epfl.ch/en, http://www.epfl.ch/Eplace.html.

The EPFL is an equal opportunity employer.

Assistant Professor Microbiology University of Washington

The Department of Microbiology is conducting a search for an Assistant Professor whose research interests employ the power and logic of genetics to address complex microbiological problems. The position is a 12-month tenure track position in the School of Medicine. In addition to research, all University of Washington faculty engage in teaching and service. Possible research areas include, but are not limited to, bacterial development, phage biology, microbial evolution, host-microbe interactions, chromosome mechanics, and regulatory mechanisms.

Applicants with a minimum of two years postdoctoral experience should send their CV, a statement of up to two pages of research interests, and names and contact information for three letters of reference to: **Chair, Search Committee, Department of Microbiology, Box 357242, University of Washington, 1959 NE Pacific St., Seattle, WA 98195**. Application deadline: **November 1, 2005**. Salary and benefits are competitive and commensurate with qualifications and experience.

The University of Washington is an Affirmative Action, Equal Opportunity Employer and is building a culturally diverse faculty. Applications from female and minority candidates are strongly encouraged.

THE AMERICAN UNIVERSITY IN CAIRO

Founded in 1919, AUC's campus is currently located in Cairo, Egypt, but will be moving to a new, state-of-the-art campus in New Cairo beginning Fall Semester, 2007 (see the New Campus website at www.aucegypt.edu/ncd/New%20Campus.html). AUC's degree programs are accredited by the Commission on Higher Education of the Middle States Association of Colleges and Schools. For more information see our website at www.aucegypt.edu. One- two- or three-year appointments subject to mutual agreement will begin September 2006. Renewal of an appointment depends upon institutional needs and/or the appointee's performance. The normal teaching load is three courses per semester and English is the language of instruction. Salary and rank are according to scale based on qualifications and professional experience. For expatriates, benefits include housing, annual round-trip air travel for appointee and qualifying dependents, plus schooling for the equivalent of up to two children at Cairo American College. In view of AUC's protocol agreement with the Egyptian Government, which requires specific proportions of Egyptian, U.S., and third-country citizen faculty, at this time preference will be given to qualified applicants who are U.S. citizens.

Department of Biology

The Department of Biology anticipates one vacancy. The successful candidate will teach in the Undergraduate Program.

Comparative Anatomist. Successful candidate must be able to teach Comparative Vertebrate Anatomy, Physiology and Developmental Biology. Candidates with experience in applied Quantitative Biology are highly encouraged. Candidates are also expected to teach introductory level courses in general biology for science and non-science majors.

APPLICATION INSTRUCTIONS: E-mail a letter of intent specifying **Position # BIOL #1** with a current C.V. to **facultyaffairs@aucnyo.edu** and arrange to have three letters of recommendation and transcripts mailed to:

Dr. Earl (Tim) Sullivan, Provost
American University in Cairo
420 Fifth Avenue, Fl. 3
New York, N.Y. 10018-2729

For full consideration, candidates must also complete the Personnel Information Form provided at **http://forms.aucegypt.edu/provost/pif3.html.** Deadline for applications is November 30th.

The American University in Cairo is an equal opportunity employer.

DUQUESNE UNIVERSITY

CHAIR OF BIOLOGICAL SCIENCES

The Bayer School of Natural and Environmental Sciences invites applications and nominations for the position of Professor and Chair of the Department of Biological Sciences. Our collegial and dynamic department currently has 14 research faculty, 3 teaching faculty, and 45 graduate students, and over 270 undergraduate Biology majors. Faculty research interests are in the areas of cellular and molecular biology, microbiology, cellular and systems physiology, genetics, and evolution. The Department offers B.S., M.S., and Ph.D. programs with a strong emphasis on research. Additional information regarding our programs and this position can be found at the Department's (www.science.duq.edu/biology/) and the Bayer School's Web sites (www.science.duq.edu).

We are seeking an accomplished scientist with imagination and energy, as well as the leadership ability to enable us to continue strengthening our educational and research programs. The preferred candidate will have an excellent record of publication and extramural support, a commitment to education, and strong leadership skills. The University's strategic plan identifies biotechnology as a particular focus area for development. The successful candidate will therefore be expected to collaborate with the endowed Edward Fritzky Chair in Biotechnology Leadership and to foster interactions within the University community and with the burgeoning biotechnology initiatives in the Pittsburgh area. Salary will be commensurate with qualifications and experience. Review of applicants will begin **September 26** and will continue until the position is filled.

Applicants should submit a letter of interest, curriculum vitae, and a list of three references to:

Dr. Jana Patton-Vogt, Chair Search Committee
Department of Biological Sciences
Duquesne University
Pittsburgh, PA 15282

Founded and sponsored by the Holy Spirit Fathers in 1878, Duquesne University is Catholic in mission and ecumenical in spirit. The University values equality of opportunity both as an educational institution and as an employer.

OVERCOMING
INFECTIOUS DISEASES

VaxGen Inc. is a biopharmaceutical company focused on the development, manufacture and commercialization of biologic products for the prevention and treatment of human infectious disease. Our business strategy emphasizes the development & commercialization of vaccine candidates for the prevention of potential bioterrorism threats, specifically anthrax and smallpox.

Senior Manager/Director QA
Quality Systems/Operations
South San Francisco, CA

We have a great opportunity for an experienced QA professional to coordinate QA activities relating to GMP manufacturing and control operations at the VaxGen Manufacturing Facility (VMF) in South San Francisco and at contract manufacturing facilities. Specifically, you will ensure compliance with GMPs; direct/coordinate QA 'person-in-the-plant' activities at CMOs; provide strategic input to senior management; hire/supervise QA staff; and ensure the timely resolution of deviations and investigations related to manufacturing & control operations. Requires a BA/BS/MS in a related scientific discipline; 8-15 years of experience in a GMP-regulated industrial setting; and experience with the development, implementation and management of quality systems/programs in support of pharmaceutical manufacturing for biologics/biotechnology products/vaccines.

VaxGen offers full benefits and a competitive salary package. To apply, please reference Job Code **EBQA-SCI** and email your resume to: **jobs@vaxgen.com** *(text only)*, or FAX: **(650) 624-4782**. No phone calls please. *EOE*

VaxGen

View complete job description at:

www.VaxGen.com

ETH

Eidgenössische Technische Hochschule Zürich
Swiss Federal Institute of Technology Zurich

Assistant Professor in Neural Stem Cell Biology

The Neuroscience Center Zurich, located at the University of Zurich and the Swiss Federal Institute of Technology Zurich (ETH), seeks applications for the position of an Assistant Professor (6 years) in Neural Stem Cell Biology. This assistant professorship has been established to promote the careers of younger scientists.

The successful candidate is expected to develop an internationally recognized line of research and should have an avid interest in both, basic science and applied research on neural stem cells. The new professor will be located at the Institute of Cell Biology, Department of Biology, ETH Zurich. He or she will benefit from the excellent general infrastructure of the Institute and the Department of Biology, as well as from the ample opportunities within the Neuroscience Center Zurich and Life Science Zurich. He or she will also be integrated in the teaching program of the Institute of Cell Biology and the Neuroscience Center at the undergraduate and graduate levels.

Please submit your application together with curriculum vitae, list of publications, and research plan to the **President of ETH Zurich, Prof. Dr. O. Kübler, ETH Zentrum, CH-8092 Zurich, no later than October 31, 2005**. The National Center of Neuroscience specifically encourages female candidates to apply with a view towards increasing the proportion of female professors.

FACULTY POSITION IN VERTEBRATE BIOLOGY (ZEBRAFISH)
Department of Biology
Indiana University, Bloomington

The Department of Biology invites applications for a tenure-track faculty position working with zebrafish. Well-qualified candidates at both assistant professor and senior ranks will be considered. We seek candidates with research interests in any of several areas: developmental biology, neurobiology, behavior, or evolutionary-developmental biology.

This position is part of a major expansion of IU-Bloomington's life sciences. The expansion includes construction of two major research buildings, a new NSF IGERT program in genomics, evolution and development, new program initiatives including METACyt, a $53 million dollar project in molecular and cellular life sciences, a program in human biology, and hires in microbiology, biochemistry, cell and developmental biology, molecular evolution, and ecology.

The successful candidate will be provided with a competitive start-up package, including a new zebrafish facility currently under construction that will support two faculty. The candidate will be expected to establish a vigorous externally funded research program and to participate in teaching undergraduate and graduate courses. For information about the Biology Department and for links to the campus and the Bloomington community, see: **http://www.bio.indiana.edu**.

Candidates should send a curriculum vitae, a statement of research, and representative publications, and arrange to have three (or more) letters of recommendation sent to: **Prof. Rudolf Raff, Vertebrate Biology Faculty Search, Department of Biology, Indiana University, Myers Hall 150, 915 E. Third Street, Bloomington, IN 47405-7107**. Review of applications will begin **October 31, 2005** and will continue until suitable candidates are identified.

Indiana University is an Affirmative Action/Equal Opportunity Employer. Women and minority candidates are encouraged to apply.

POSITIONS OPEN

FACULTY POSITION, ANALYTICAL CHEMISTRY

The University of Alaska Fairbanks (UAF) Department of Chemistry and Biochemistry invites applications for a tenure-track position at the **ASSISTANT** or **ASSOCIATE PROFESSOR** level in the area of analytical chemistry. Teaching duties include undergraduate and graduate courses in analytical chemistry, and advanced courses in the candidate's field of expertise. The candidate is expected to establish an externally funded research program in an area related to analytical chemistry with an emphasis on environmental and/or biochemical applications. The candidate is expected to mentor graduate and undergraduate students in research projects. A Ph.D. in chemistry or related discipline is required, postdoctoral experience is highly preferred. For information about the Department of Chemistry and Biochemistry at the University of Alaska Fairbanks, please visit **website: http://www.uaf.edu/chem/.** To apply, send a letter of interest, curriculum vitae, graduate and undergraduate transcripts, description of research plan, a statement of teaching philosophy, and at least three letters of reference to: **William R. Simpson, Search Committee Chair, Human Resources, University of Alaska Fairbanks, P.O. Box 757860 Fairbanks, AK 99775-7860.** Review of applications begins on November 15, 2005. The candidate must also complete the UAF application found at **website: http://www.alaska.edu/hr/forms/hr_employmentforms.xml.** *The University of Alaska is an Equal Opportunity/Affirmative Action Employer and Educational Institution. Minorities and women are encouraged to apply.*

CHAIR, DEPARTMENT OF BIOLOGY
Emory University

The Department of Biology in Emory College of Emory University invites applications for the position of Department Chair and Professor of Biology. Emory is an internationally known research university and will soon begin a comprehensive fund-raising campaign to strengthen its research and teaching programs. The Biology Department is currently composed of 23 tenure-track faculty and seven senior lecturers and lecturers. The successful candidate for this position will have a distinguished record of extramurally funded research and scholarly activity sufficient to merit appointment at the rank of tenured **FULL PROFESSOR** in Emory College. Applicants must have a doctoral degree or its equivalent in biology, or other appropriate discipline and should have a research focus in one of the three areas of research strengths in the Department: population biology, ecology, and evolution; computational neuroscience; genetics, cell, and developmental biology. Applicants should have excellent communication, leadership, and administrative skills and should have a strong commitment to undergraduate and graduate teaching. The successful candidate will oversee the continued growth of the Department via the hiring of new faculty, the development of the undergraduate curriculum, and the possible reconfiguration of the departmental graduate program.

Please submit a cover letter, curriculum vitae, statement of research interests, experience, and future plans, teaching philosophy, and departmental leadership philosophy. Materials should be submitted to: **Chair, Search Committee, Department of Biology, 1510 Clifton Road, Emory University, Atlanta, GA 30322.** Documents may be submitted electronically to **e-mail: george.h.jones@emory.edu.** The review of applications will begin in mid-September 2005 and will continue until a suitable candidate is identified. Please visit the departmental **website: http://www.biology.emory.edu** to learn more about biology at Emory. *Emory University is an Equal Opportunity Employer.*

POSITIONS OPEN

FACULTY POSITIONS, SYSTEMS BIOLOGY/MICROBIOLOGY
Department of Biology and Biocomplexity Institute
Indiana University, Bloomington

The Department of Biology and the Biocomplexity Institute invite applications for two tenure-track faculty positions in experimental and/or computational systems biology. We anticipate an appointment at the **ASSISTANT PROFESSOR** level, but outstanding **SENIOR**-level candidates will also be considered. We will be especially interested in individuals whose research will enhance our current strengths in: (1) mechanisms of bacterial cell function, (2) cell differentiation and developmental biology, and (3) biomolecular networks, including signaling, gene regulatory, and metabolic networks.

The successful candidate will have strong interdisciplinary interests and will benefit from opportunities to collaborate with scientists in the Departments of Biology, Medical Sciences, Physics, Chemistry, Mathematics, the School of Informatics, the Center for Genomics and Bioinformatics, and the Biocomplexity Institute. While his/her primary appointment will be in the Department of Biology, joint appointments with other departments are possible.

This position is part of a major expansion of Indiana University (IU)-Bloomington's research efforts in the life sciences. That expansion includes construction of two research buildings, a new National Science Foundation Integrative Graduate Education and Research Traineeship program in genomics, evolution, and development, new program initiatives including Metabolomics and Cytomics Initiative, a $53 million dollar project in molecular and cellular life sciences, a program in human biology, and new hiring in microbiology, biochemistry, cell and developmental biology, molecular evolution, and ecology.

The successful candidate will be expected to establish a vigorous, externally funded research program and to participate in teaching undergraduate and graduate courses. For information about the Biology Department and the Biocomplexity Institute, and for links to the campus and the Bloomington community, see **websites: http://www.bio.indiana.edu** and **http://biocomplexity.indiana.edu/.**

Candidates should send curriculum vitae, a statement of research (past, present, and planned) and teaching interests, and representative publications, and arrange to have at least four letters of recommendation sent to: **Yves Brun, Systems Biology/Microbiology Faculty Search, Department of Biology, Indiana University, Jordan Hall 142, 1001 E 3rd Street, Bloomington, IN 47405-7005.** Review of applications will begin as soon as possible, and will continue until suitable candidates are identified.

Indiana University is an Affirmative Action/Equal Opportunity Employer. Women and minority candidates are encouraged to apply.

SENIOR FACULTY, NEUROSCIENCE

Two tenure-track positions for **FULL** or **ASSOCIATE PROFESSOR** are available in the Department of Neuroscience and Physiology, Upstate Medical University. The Department has a focus in developmental neuroscience. Researchers interested in cell fate, neurogenetics, neurite outgrowth, and plasticity are encouraged. Successful candidates must have record of research productivity, an independent extramurally supported research program, participation in medical/graduate education. Candidates should send curriculum vitae, statement of research plans, and names of references to: **Michael Miller, Department of Neuroscience and Physiology, Upstate Medical University, 750 E. Adams Street, Syracuse, NY 13210.** Applications will be considered until positions are filled. *Applications from women and minority candidates are especially welcome. The State University of New York is an Affirmative Action/Equal Employment Opportunity Employer.*

POSITIONS OPEN

BIOINFORMATICS AND MOLECULAR BIOLOGY
Department of Biology
University of Vermont

Applications are invited for a **RESEARCH FACULTY** member in the Department of Biology in the area of molecular genetics and bioinformatics. This faculty member will be supported by the Vermont Genetics Network, an NIH-sponsored program, and will be expected to work with baccalaureate college faculty and students in colleges around Vermont to bring technology at the University of Vermont (UVM), such as microarrays and proteomics, into undergraduate classrooms.

All applicants are expected to hold a Ph.D. degree, have experience in the general area of bioinformatics and molecular biology, and have an interest in teaching or working with undergraduates.

Candidates must apply online at **website: http://www.uvmjobs.com** and must attach to that application curriculum vitae, a statement of interest in working with undergraduates in molecular biology settings, and names with contact information of three references. We will be accepting applications until Friday, September 16, 2005.

The University of Vermont is an Affirmative Action/Equal Opportunity Employer. The Department is committed to increasing faculty diversity and welcomes applications from women and underrepresented ethnic, racial, and cultural groups and from people with disabilities.

The Albert Einstein College of Medicine (AECOM) seeks a **TENURE-TRACK FACULTY** member in bioinformatics to both establish an independent research program and to serve as the Faculty Supervisor of AECOM's Bioinformatics Shared Facility (BSF). The BSF is a data management and mining facility, serving the research needs of the entire medical school faculty. The successful applicant in his/her faculty supervisor role will direct data management and bioinformatics analysis support for, and foster collaborations among, basic and clinical science researchers and the BSF. The BSF collaborates closely with statisticians, other bioinformatics research faculty, and various AECOM shared facilities for proteomics, genetics, and clinical research. The faculty supervisor position is highly collaborative in nature. Screening of applications will be continuous. Appointment will be considered at a rank appropriate to the candidate's experience. Applications received by October 7, 2005, are assured full consideration.

How to apply: Please send detailed curriculum vitae with bibliography and contact details (telephone number, e-mail address) for at least three references to **e-mail: omendoza@aecom.yu.edu.** Subject: "Director of BSF." Attn: Chair, Faculty Search Committee for BSF. *Equal Opportunity Employer.*

ASSISTANT/ASSOCIATE PROFESSOR
Department of Ophthalmology
Emory University
School of Medicine

Invites applications for a tenure-track faculty member at the rank of Assistant/Associate Professor. We seek an outstanding scientist to perform research in a field relevant to glaucoma or neural science, with opportunities to interface with leading researchers in visual sciences and related fields. Endowed funds are available to support the position.

Please send curriculum vitae, a one- to two-page summary of your research contributions with plans for future work, and a list of three references to: **Mrs. Patricia Bennett, Emory Eye Center, Emory University, 1365B Clifton Road, NE, Suite B4500, Atlanta, GA 30322.** *Emory University is an Affirmative Action/Equal Opportunity Employer.*

THE STATE UNIVERSITY OF NEW JERSEY

RUTGERS

Faculty Position in Human Genetics
Rank Open

The Department of Genetics (**http://lifesci.rutgers.edu/~genetics**) and the Human Genetics Institute of Rutgers University seek an outstanding scientist to fill one of several new positions in human genetics. Researchers seeking a well-funded, diverse, and interactive department are encouraged to apply. Research areas of interest include but are not limited to: population genetics, computational genetics, developmental genetics, chromatin remodeling and epigenetics, complex disease gene discovery, cancer genetics, neurogenetics and neuropsychiatric genetics, and functional genomics.

Candidates must have either a Ph.D. or M.D., or both, a demonstrated ability to conduct and publish significant independent research, and an interest in teaching at the undergraduate and graduate levels. Senior level candidates must have a strong record of grant support. Appointments will be made at a tenured or tenure-track level, consistent with the candidate's credentials.

Laboratory space will be provided in the newly constructed, state-of-the-art Genetics/Human Genetics Institute on Rutgers' Busch Campus. We are part of a vibrant life sciences community including the Waksman Institute, the Center for Advanced Biotechnology and Medicine, the Center of Alcohol Studies, the Environmental and Occupational Health Sciences Institute, and the Robert Wood Johnson Medical School. The campus is located in central New Jersey, close to New York City, Philadelphia, beaches, and countryside.

Applicants should send a CV, a statement of research interests, and full contact information for three individuals willing to provide a detailed evaluation of the candidate to: **genetics_search@biology.rutgers.edu**, or to **Jay Tischfield, Chair, Department of Genetics, Rutgers University, 145 Bevier Road, Room 136, Piscataway, NJ 08854-8082**. Review of applications will begin **October 1, 2005**. The starting date is flexible.

Rutgers University is an Equal Opportunity/Affirmative Action Employer.

Tenure-Track Position in Microbiology

The Department of Microbiology at Southern Illinois University Carbondale invites applications for a tenure-track position as an Assistant Professor with a start date of August 16, 2006. Applicants must hold a Ph.D. or other appropriate doctoral degree and have a record of relevant postdoctoral research training by the time of appointment. The applicant must also have an externally funded research program or the potential for developing one, as well as a significant record of peer-reviewed publication. The successful candidate will contribute to an area of existing strength in Microbiology, such as microbial evolution, diversity, physiology, or bioremediation, and have particular expertise in an aspect of quantitative microbiology such as bioinformatics, proteomics, genomics, or metabolomics. The candidate will be encouraged to collaborate with quantitative biology faculty in other departments and colleges such as the biological mathematician sought by the Department of Mathematics, the systematics expert sought by the Department of Plant Biology and the genomics specialist sought by the College of Agriculture. The successful applicant is expected to teach a portion of a course in introductory microbiology as well as an advanced undergraduate or graduate course in an area of expertise.

Review of applications will begin **October 15, 2005** and continue until the position is filled. Applicants should submit a curriculum vitae, a statement of teaching and research interests, and the names and addresses of at least three references to: **Dr. Laurie Achenbach, Search Committee Chair, Department of Microbiology, Mailcode 6508, 1125 Lincoln Dr., Southern Illinois University Carbondale, Carbondale, IL 62901**. E-mail: **microbiology@micro.siu.edu**.

Southern Illinois University Carbondale is a large, public, comprehensive research-intensive university situated in a pleasant small-town setting southeast of St. Louis. SIUC is seeking to enhance interdisciplinary research and become a leading public research university (**http://news.siu.edu/s150/**). The Department of Microbiology, with a faculty of six, offers the M.S and Ph.D through the interdisciplinary Molecular Biology, Microbiology, and Biochemistry Graduate Program, as well as an undergraduate Microbiology degree. Please visit our website at **http://www.science.siu.edu/microbiology/**.

SIUC is an Affirmative Action/Equal Opportunity Employer that strives to develop a diverse faculty and staff and to increase its potential to serve a diverse student population. All applications are encouraged and will receive consideration.

Computational Chemistry and Biology Opportunities at D. E. Shaw Research and Development

Extraordinarily gifted computational chemists, biologists, and other computational scientists are sought to join a rapidly growing New York-based research group that is pursuing an ambitious, long-term strategy aimed at fundamentally transforming the process of drug discovery.

Candidates should have world-class credentials in computational chemistry, biology, or physics, or in a relevant area of computer science or applied mathematics, and must have unusually strong research skills. Relevant areas of experience might include protein structure prediction, the computation of protein-ligand binding affinities, the study of biologically important systems using molecular dynamics and/or Monte Carlo simulation, and the application of statistical mechanics to biomolecular systems—but specific knowledge of any of these areas is less critical than exceptional intellectual ability and a demonstrated track record of achievement. Current areas of interest within the group include molecular dynamics simulation of functionally significant globular and membrane proteins, the prediction of protein structures and binding free energies, structure- and ligand-based drug design, characterization of protein-protein, protein-nucleic acid and protein-lipid interactions, and the development of algorithms for biomolecular simulations.

This research effort is being financed by the D. E. Shaw group, an investment and technology development firm with approximately $16 billion in aggregate capital. The project was initiated by the firm's founder, Dr. David E. Shaw, and operates under his direct scientific leadership.

We are eager to add both senior- and junior-level members to our world-class team, and are prepared to offer above-market compensation to candidates of truly exceptional ability. Please send your CV (including list of publications, thesis topic, and advisor, if applicable) to sciencemag-cc@desrad.deshaw.com.

D. E. Shaw Research and Development, L.L.C. does not discriminate in employment matters on the basis of race, color, religion, gender, national origin, age, military service eligibility, veteran status, sexual orientation, marital status, disability, or any other protected class.

D E Shaw & Co

FACULTY POSITION
Cell Biology: Neuroscience

The Department of Biology invites applications for a tenure-track **ASSISTANT PROFESSOR** position in cell biology, beginning in the fall of 2006. The successful candidate will contribute to our general biology curriculum and a successful and growing interdisciplinary neuroscience program. Area of specialization is open and might include neurophysiology, neuroendocrinology, cell signaling, receptor biology, neural plasticity, or cell-cell communication.

Applicants must have a Ph.D. in biology or a related discipline, teaching experience, a successful independent research program, and a primary interest in teaching undergraduates at a liberal arts and science institution; postdoctoral experience is required. Yearly course load will be selected from among foundation courses in biology and neuroscience, exploration courses for nonmajors, and specialty courses in the candidate's area of expertise. Establishment of a strong research program that involves undergraduates is expected. Excellent teaching, research, and imaging facilities are available. Send curriculum vitae, statements of teaching and research interests, and three letters of recommendation to: **Corey R. Freeman-Gallant, Chair, Department of Biology, Skidmore College, Saratoga Springs, NY 12866, Cell Biology Search.** Review of applications will begin on October 7, 2005. Refer to our **website: http://www.skidmore.edu/academics/biology.**

Skidmore encourages applications from women and men of diverse racial, ethnic, and cultural backgrounds.

FACULTY POSITION
Molecular Prokaryotic Microbiology

The Department of Biology invites applications for a tenure-track **ASSISTANT PROFESSOR** position in molecular prokaryotic microbiology, beginning in the fall of 2006. The successful candidate will contribute to our general biology curriculum and an emerging interdisciplinary program in biological chemistry and have particular expertise in immunology or virology.

Applicants must have a Ph.D. in biology or a related discipline, teaching experience, a successful independent research program, and a primary interest in teaching undergraduates at a liberal arts and science institution; postdoctoral experience is required. Yearly course load will be selected from among foundation courses in biology, exploration courses for nonmajors, and specialty courses in the candidate's area of expertise. Establishment of a strong research program that involves undergraduates is expected; excellent teaching and research facilities and support are available. Send curriculum vitae, statements of teaching and research interests, and three letters of recommendation to: **Corey R. Freeman-Gallant, Chair, Department of Biology, Skidmore College, Saratoga Springs, NY 12866, Molecular Microbiology Search.** Review of applications will begin on October 7, 2005. Refer to our **website: http://www.skidmore.edu/academics/biology.**

Skidmore encourages applications from women and men of diverse racial, ethnic, and cultural backgrounds.

The Department of Chemistry at The University of Chicago invites applications from outstanding individuals for the position of **ASSISTANT PROFESSOR** of chemistry. This search is in the areas broadly defined as inorganic, organic, and physical chemistry. Applicants must mail hard copies of curriculum vitae, a list of publications, and a succinct outline of their research plans; and arrange for three letters of recommendation to be sent by mail to: **Michael D. Hopkins, Chairman, Department of Chemistry, The University of Chicago, 5735 S. Ellis Avenue, Chicago, IL 60637.** Review of completed applications will begin October 1, 2005; to ensure full consideration, all materials should be submitted by that date. *An Equal Opportunity/Affirmative Action Employer.*

POSITIONS OPEN

IOWA STATE UNIVERSITY

DEPARTMENT OF VETERINARY MICROBIOLOGY AND PREVENTIVE MEDICINE
College of Veterinary Medicine

Applications are invited for a **BACTERIOLOGIST** to fill a tenure-track position at the **ASSISTANT** or **ASSOCIATE PROFFSSOR** level. The successful candidate will be expected to establish and maintain an independent, extramurally funded research program focused on the pathogenesis of bacterial diseases (60 percent effort); teach and mentor graduate and professional students (35 percent); and perform University service (5 percent). A Ph.D., or an equivalent degree, in a relevant discipline is required. A minimum of two years of postdoctoral training is preferred. Although a D.V.M. is preferred, it is not required. For consideration at the Associate Professor level, the candidate must be nationally/internationally recognized with records of sustained publication and extramural funding. Applications received by October 1, 2005, will be guaranteed for review for an employment start date of Summer 2006. Applications must be submitted online at **website: http://www.iastate.edu/jobs/,** vacancy ID#: 050325. Questions about the position may be directed to: **Dr. Greg Phillips, Bacteriologist Search Committee Chair, 1802 Elwood Drive, VMRI #6, College of Veterinary Medicine, Iowa State University, Ames, IA 50011. Telephone: 515-294-1525; e-mail: gregory@iastate.edu.**

Iowa State University is an Affirmative Action/Equal Opportunity Employer.

ASSISTANT PROFESSOR
BIOLOGY

Full-time, tenure-track Biologist. Responsibilities include courses in human biology, human anatomy, and physiology, developmental biology, and an advanced-level course. Must have a Ph.D. and commitment to excellence in teaching; teaching and a focus on student learning are primary duties of faculty. Department offers collegial work environment and relatively small classes. Research, particularly projects involving undergraduates, is encouraged. Tenure-track faculty are eligible for a one semester sabbatical during their first three years to carry out research and other preparations for tenure review. Start date is January 2006 (preferable) or September 2006, pending budget approval.

Forward cover letter, curriculum vitae, transcripts, statement of teaching philosophy, long-term goals, and three letters of reference. Screening will begin September 30, 2005, and will continue until the position is filled. Additional information on the Department at **website: http://biology.wsc.ma.edu.** Send materials to:

Dr. David Doe
Chair, Biology Search Committee
Department of Biology
Westfield State College
577 Western Avenue
Westfield, MA 01086-1630

Affirmative Action/Equal Opportunity Employer. Women, persons of color, and persons with disabilities are encouraged to apply.

The Department of Chemistry at the University of Chicago invites applications from qualified individuals for positions of **POSTDOCTORAL RESEARCH ASSOCIATE** in chemistry. These searches are in the areas broadly defined as inorganic, organic, and physical chemistry. For details about specific job opportunities and how to apply visit **website: http://jobopportunities.uchicago.edu.** Qualified applicants will have a Ph.D. degree or will have completed the Ph.D. requirements in the related areas prior to hire. *The University of Chicago is an Equal Opportunity/Affirmative Action Employer.*

POSITIONS OPEN

MOLECULAR BIOLOGIST
TENURE-TRACK ASSISTANT PROFESSOR
Colgate University

We seek a tenure-track Assistant Professor to start August 2006. Ph.D. or expectation of completion this academic year required; teaching and postdoctoral research experience desirable. The successful candidate will contribute to a foundation course called molecules, cells, and genes, teach elective courses including microbiology, contribute to a capstone seminar in molecular biology, and participate in University-wide programs. The appointee will join a biology faculty deeply committed to a strong, research-oriented program involving undergraduate students and will add to this effort by offering a research tutorial in their area of interest; opportunities also exist to lead a semester-long program at the NIH. Applications are especially encouraged from candidates whose research is focused in the area of microbiology, virology, or immunology. Please forward a letter of application with curriculum vitae, transcripts, and separate statements of teaching philosophy and research interests to: **Dr. Barbara Hoopes, Department of Biology, Colgate University, 13 Oak Drive, Hamilton, NY 13346-1398** and also arrange to have three letters of recommendation sent to this address. Review of applications will begin October 7, 2005, and continue until the position is filled. We intend to begin interviewing candidates by the end of October. *Colgate University is an Equal Opportunity/Affirmative Action Employer. Developing and maintaining a diverse faculty and staff further the University's academic mission. Women and minorities are especially encouraged to apply.*

TENURE-TRACK FACULTY POSITIONS
Delaware State University

Delaware State University seeks applicants for two 12-month, tenure-track faculty positions (75 percent research and 25 percent teaching) at the **ASSISTANT PROFESSOR** level. Positions are part of a National Science Foundation-Experimental Program to Stimulate Competitive Research Infrastructure Improvement (**website: http://www.epscor.dbi.udel.edu/**) program to develop a center for the study of environmental issues related to agriculture and aquatic ecosystems. The University seeks one faculty member from any area of plant biology and a second with a chemical or biochemical background. Candidates must hold a Ph.D. and have demonstrated excellence in innovative research including biotechnological approaches. A competitive salary and state-of-the-art facilities in house and at collaborating institutions are available. Applicants should send curriculum vitae, a statement of research interests and future plans, and a statement of their teaching philosophy, and have three letters of reference sent to: **Plant biology/Agronomy search committee chair, Maria Labreveux, c/o Lisa Hopkins, Department of AGNR, Delaware State University, 1200 N Dupont Highway, Dover, DE 19901.**

Chemistry search committee chair, Andrew Goudy, c/o Rose Dabney, Department of Chemistry, Delaware State University, 1200 N Dupont Highway, Dover, DE 19901.

The review of applications will begin September 1, 2006, and continue until a suitable candidate is identified. The application package will be shared with University faculty. *Delaware State University is an Equal Opportunity Employer.*

ASSISTANT PROFESSOR

The Department of Nutrition and Food Sciences at Utah State University invites applications for an Assistant Professor with 50 percent teaching and 50 percent research assignment. We seek applicants who employ molecular and cellular approaches to study nutrition and health issues. Candidates must have a Ph.D. in nutrition science or related field. See **website: http://www.usu.edu/jobs** (2-129-05) for full job description and application information. *Affirmative Action/Equal Opportunity Employer.*

Faculty Position in Cancer Biology & Genetics

Memorial Sloan-Kettering Cancer Center invites applications for tenure-track faculty positions in the Cancer Biology and Genetics Program of the Sloan-Kettering Institute. (http://www.mskcc.org/mskcc/html/15422.cfm). The new faculty members will join an interactive, interdisciplinary community of scientists and clinicians at the Center, which offers an outstanding basic and translational research environment within expanded state-of-the-art research facilities. Faculty will be eligible to hold graduate school appointments in the newly established Gerstner Sloan-Kettering Graduate School of Biomedical Sciences, as well as the Weill/SKI Graduate School of Medical Sciences of Cornell University.

Successful candidates will carry out independent research on the genesis, progression, prognosis, prevention and treatment of cancer that synergize with ongoing efforts at the Center. Areas of special interest include but are not limited to: tumor-host microenvironment, genetics/epidemiology, cancer-specific translational research and animal models of cancer. A representative list of research and clinical expertise of the program members and their clinical associates follows:

CANCER BIOLOGY & GENETICS FACULTY
Robert Benezra, PhD - Angiogenesis/Differentiation
Eric Holland, MD/PhD - Glioma Mouse Models
Anna Kenney, PhD - Neural Stem Cells/Brain Tumors
Johanna Joyce, PhD - Tumor Microenvironment
Joan Massague, PhD- Cell Regulation/Metastasis
Pier Paolo Pandolfi, MD/PhD -Molecular Genetics of Cancer
Harold Varmus, MD -Molecular Mechanisms of Oncogenesis

CLINICAL ASSOCIATES/ADVISORS
George Bosl, MD -Germ Cell Tumors
Lisa DeAngelis, MD - Primary CNS Tumors
Yuman Fong, MD - Hepatic Oncology
David Kelsen, MD - Gastrointestinal Cancers
Mark Kris, MD/Valerie Rusch, MD - Lung Cancers
Stephen Nimer, MD - Leukemia, Lymphoma
Larry Norton, MD - Breast Cancer
Kenneth Offit, MD - Genetics/Epidemiology
Richard O'Reilly, MD - Pediatric Cancers
Howard Scher, MD - Prostate and other GU Tumors
Jatin Shah, MD - Head and Neck Malignancies
David Spriggs, MD - Ovarian, Developmental Chemotherapy

Interested parties should forward their Curriculum Vitae, a description of their past research accomplishments and proposed research program, selected reprints, and three letters of recommendation via e-mail to **cancerbio@mskcc.org.** Application materials can also be submitted to **Joan Massagué, Ph.D, c/o Maria Beckles, Memorial Sloan-Kettering Cancer Center, 1275 York Avenue, Box 494, New York, NY, 10021.** Application deadline is November 1, 2005. EOE/AA.

Memorial Sloan-Kettering Cancer Center
The Best Cancer Care. Anywhere.
www.mskcc.org

PLANT ECOLOGIST

The Department of Botany at the University of Toronto invites applications for a tenure-track faculty position at the Assistant Professor level in the area of **Plant Ecology** to begin July 1, 2006. Specialists in all areas of plant ecology are encouraged to apply. Applicants who are using, or will develop, experimental approaches to understanding ecological pattern and process will be given priority.

The successful candidate will have demonstrated excellence in teaching and research and will be expected to participate in undergraduate and graduate teaching of ecology, plant biology and field courses at the University of Toronto. She or he would also be expected to interact with faculty across campus working in related fields. Salary to be commensurate with qualifications and experience.

Applicants should arrange to have four reference letters sent directly to the address below. In addition, applicants should forward their *curriculum vitae*, copies of significant publications, and statements of research and teaching interests to the **Chair, Plant Ecology Search Committee, Department of Botany, University of Toronto, 25 Willcocks Street, Toronto, ON M5S 3B2 Canada before October 24, 2005**. Inquiries should be directed to **Dr. Rowan Sage** at **Rsage@botany.utoronto.ca**.

All qualified candidates are encouraged to apply; however, Canadians and permanent residents will be given priority. The University of Toronto offers the opportunity to teach, conduct research and live in one of the most diverse cities in the world and is strongly committed to diversity within its community. The University especially welcomes applications from visible minority group members, women, aboriginal persons, persons with disabilities, members of sexual minority groups, and others who may contribute to the further diversification of ideas.

Karolinska Institutet, Stockholm, Sweden
Researcher / Post-doctoral position
Ref-no: 3950/2005

KASPAC is a joint venture arising from collaboration between **Sumitomo Pharmaceuticals Co Ltd, Japan and the Karolinska Institutet, Sweden** with the designation of identifying novel targets for Alzheimer's disease therapeutics.

KASPAC is under the directorship of Professor Bengt Winblad and is based at the Novum Research Park, Huddinge.

The research at KASPAC is focussed on four sub-projects:
- The Presenilin in Mitochondria project
- The Human g-secretase project
- The CLAC project
- The Genomics project

We are seeking a **post-doctoral scientist** with expertise in cell biology and protein biochemistry, to join a group studying functions of Alzheimer's disease associated proteins. The successful applicant has a strong background in work using animal models, breeding transgenic animals and dissecting organs etc.

The position is a full time research position for one year, with a possibility of prolongation.

For **information**, contact Professor Bengt Winblad,
+46 70 632 67 71 or +46 8 585 836 17.
SACO: Karin Bergström, +46 8 5248 38 33,
karin.bergstrom@neurotec.ki.se.

To apply, please send a personal letter including your full CV, Publication list and references to:
Karolinska Institutet, Professor Bengt Winblad, Neurotec, KASPAC, Novum, S-141 57 Sweden
or by email: b.winblad.kaspac@neurotec.ki.se.

Closing date for applications: September 15, 2005.

POSITIONS OPEN

FACULTY POSITION: THEORETICAL ECOLOGY/EVOLUTION

The Department of Ecology and Evolutionary Biology at the University of Tennessee, Knoxville, seeks to fill a tenure-track position in theoretical/computational ecology and/or evolution at the **ASSISTANT** or **ASSOCIATE PROFESSOR** level, to start August 1, 2006. Attractive research areas include complex ecological or evolutionary systems, problems at multiple spatial scales, and analysis of evolutionary and ecological data at broad spatial or temporal extent. Teaching will include courses in theoretical ecology or evolution.

For information about the Department visit **website: http://eeb.bio.utk.edu.** Candidates should apply to:

Dr. Sergey Gavrilets
Department of Ecology and Evolutionary Biology
University of Tennessee
Knoxville, TN 37996

Applicants should send curriculum vitae, statements of research and teaching goals, up to five reprints, and arrange for three reference letters to be submitted. Applications will be reviewed beginning September 30, 2005.

The University welcomes and honors people of all races, creeds, cultures, and sexual orientations, and values intellectual curiosity, pursuit of knowledge, and academic freedom and integrity.

The University of Tennessee is an Equal Employment Opportunity/Affirmative Action/Title VI/Title IX/Section 504/ADA/ADEA Institution in the provision of its education and employment programs and services.

TENURE-TRACK FACULTY POSITION MICROBIOLOGY
Indiana University, Bloomington

The Department of Biology (**website: http://www.bio.indiana.edu**) and Indiana University (IU) Interdisciplinary Human Biology Program invite applications for a position in prokaryotic cell and molecular biology, including pathogenesis and cellular microbiology. The successful candidate will join a strong microbiology program in the Department of Biology and comprehensive interdisciplinary initiatives in human biology and biotechnology, receive a competitive startup package and salary, and have outstanding research resources. The successful candidate will be expected to develop an externally funded research program and to participate in undergraduate and graduate teaching. Appointment is expected to be at the **ASSISTANT PROFESSOR** level, but outstanding **SENIOR**-level candidates will also be considered. Applicants should send curriculum vitae, statement of research and teaching interests, reprints/preprints, and arrange to have at least four letters of recommendation sent to: **Malcolm E. Winkler, Department of Biology, Indiana University, Jordan Hall, Room 142, Bloomington, IN 47405.** Address questions by **e-mail: mwinkler@bio.indiana.edu.** Review of applicants will begin as soon as possible and continue until the position is filled. *Indiana University is an Affirmative Action/Equal Opportunity Employer. Women, minority candidates, and couples are encouraged to apply.*

TIME FOR A CAREER CHANGE?

CPE Communications, a leader in pharmaceutical healthcare communications, is looking for an enthusiastic, self-motivated **MEDICAL WRITER.** If you enjoy writing and learning about the pharmacologic management of disease, have excellent communication and presentation skills, can adhere to deadlines, and manage multiple projects, this job may be for you! Send inquiries, curriculum vitae, and salary requirements to **e-mail: hr@dpmadvert.com** referring to code #MW-805. Advanced degree required (Ph.D., Pharm.D., or M.D.). Immunology, oncology, or pharmacology expertise preferred. Must be willing to work in Chicago, Illinois. CPE will train. Experience a plus.

POSITIONS OPEN

The Molecular Cardiology Program at Weill Medical College of Cornell University seeks independent investigators as **TENURE-TRACK/TENURED FACULTY MEMBERS.** The Molecular Cardiology program is a vibrant multidisciplinary group with diverse interests including cardiovascular genetics, cardiovascular development, vascular biology, stem cell biology, signal transduction, and cellular electrophysiology. Successful candidates (M.D., M.D./Ph.D., or Ph.D.) should have an established track record of extramural funding and will be provided with newly renovated research space and a generous startup package. Salary and rank will be commensurate with experience. Applicants should forward curriculum vitae, research plan, and three references to: **Ann Grgas, Assistant to the Molecular Cardiology Search Committee, Division of Cardiology, Cornell Medical College, Starr 4, 525 East 68th Street, New York, NY 10021. Telephone: 212-746-2169; fax: 212-746-6951; e-mail: ang2010@med.cornell.edu.** *Cornell is an Equal Opportunity Employer.*

VERTEBRATE PHYSIOLOGY

The Department of Biology at Middlebury College invites applications for a tenure-track position at the rank of **ASSISTANT PROFESSOR** beginning September 2006 with a focus on the integrative analysis of vertebrate physiology. Teaching responsibilities include courses in animal physiology and vertebrate biology, both with laboratory, and an upper-level course in the candidate's area of specialization. The successful candidate will also be expected to participate in the Neuroscience Program and to establish an active research program that includes undergraduates. Candidates must have completed a Ph.D. in a relevant discipline, and should provide evidence in their application of commitment to excellence in teaching and scholarship. The application should include a statement of both teaching and research interests, curriculum vitae, copies of undergraduate and graduate transcripts (unofficial copies are acceptable), and samples of scholarly work. The application materials and three letters of recommendation, which should be sent under separate cover and must collectively speak to both teaching and research ability, should be sent to: **Dr. Sallie Sheldon, Vertebrate Physiology Search Committee Chair, Department of Biology, Middlebury College, Middlebury, VT 05753. E-mail: sheldon@middlebury.edu.**

See **website: http://www.middlebury.edu/academics/ump/majors/bio/default.htm** for more details about the position, the Biology Department, the Program in Neuroscience, and the College. Review of applications will begin October 15, 2005, and will continue until a successful candidate is identified. *Middlebury College is an Equal Opportunity Employer, committed to hiring a diverse faculty to complement the increasing diversity of the student body.*

ASSISTANT PROFESSOR, BIOLOGY
Mercer University (Macon, Georgia)

Mercer University seeks a tenure-track Assistant Professor for August 2006 with a Ph.D. in biological sciences, broad training in genetics and molecular biology, and promise of excellence in teaching and scholarly activity. Candidates should be able to contribute to general science education and/or the University's interdisciplinary studies programs.

Duties will consist of teaching five undergraduate courses per academic year, including introductory biology, genetics, and upper-division specialty. Research involving undergraduates is encouraged. For full announcement and to apply online, access **website: http://www.mercerjobs.com.** *Affirmative Action/Equal Opportunity Employer/ADA.*

POSITIONS OPEN

COGNITIVE NEUROSCIENTIST
Wake Forest University
School of Medicine

The Department of Neurobiology and Anatomy invites applications for a tenure-track faculty position. Applicants should have a minimum of two years of postdoctoral experience and a strong record of scholarship; the level of appointment will be commensurate with experience. The Department is seeking an outstanding individual using modern approaches in cognitive neuroscience at the systems, cellular, molecular, and/or behavioral/psychophysical level. Preference will be given to applicants with experience and interests that overlap those of current departmental members. The successful candidate will become part of the large and active neuroscience community at the University, which includes the Departmental Program and an interdisciplinary program in neuroscience, as well as an NIH-funded training program focused on multiple sensory systems. For more information on the Department and areas of research emphasis, visit our **website: http://www.wfubmc.edu/nba.** Candidates should send curriculum vitae, statement of research interest, and three letters of recommendation to:

Search Committee
Department of Neurobiology and Anatomy
Wake Forest University
School of Medicine
Winston-Salem, NC 27157-1010

Wake Forest University is an Affirmative Action/Equal Opportunity Employer.

CELL BIOLOGIST. Kalamazoo College invites applications for a tenure-track position to begin in fall 2006 at the **ASSISTANT PROFESSOR** level. Ph.D. required. Postdoctoral experience preferred. Salary is competitive and commensurate with experience. Teaching responsibilities will include evolution and genetics (an introductory-level core course), cell and molecular biology (a mid-level core course), and upper-level courses compatible with the candidate's interest and the curriculum. Candidates are expected to have a high aptitude and interest in undergraduate teaching, a commitment to the liberal arts, and a desire to involve undergraduates in scholarship both inside and outside the classroom. Kalamazoo College is a highly selective, nationally recognized liberal arts college that takes pride in its outstanding undergraduate science education program. A recent Higher Education Data Sharing consortium survey ranked the College fourth nationally among all institutions in the proportion of its graduates who ultimately receive Doctorates in the life sciences. Completed applications received by November 15, 2005, will receive full consideration with later applications reviewed as needed until the position is filled. Send letter of application, curriculum vitae, undergraduate and graduate transcripts (unofficial acceptable), statement of teaching philosophy and research interests, and three letters of recommendation to: **Dr. Paul Sotherland, Chair, Department of Biology, 1200 Academy Street, Kalamazoo, MI 49006-3295.** *Kalamazoo College encourages candidates who will contribute to the cultural diversity of the College to apply and to identify themselves if they wish. Equal Opportunity Employer.*

POSTDOCTORAL ASSOCIATE

Stony Brook University's Division of Cancer Prevention is seeking a Postdoctoral Associate. Required: Ph.D. in molecular biology or related field. Experience in protein analysis with chemotherapeutic agents. Use of Ciphergen system is desirable. Good communication skills. To apply, send curriculum vitae, three letters of reference, and salary history to: **Dr. B. Rigas, Chief, Division of Cancer Prevention, L5-LICC, Stony Brook University Hospital, Stony Brook, NY 11794-7547. E-mail: diana.giarraputo@stonybrook.edu.** Visit **website: http://www.stonybrook.edu/cjo** for employment information. *Affirmative Action/Equal Opportunity Employer.*

POSITIONS OPEN

BIOMATERIALS/BIOTECHNOLOGY/ TISSUE ENGINEERING FACULTY POSITION University of Michigan

The University of Michigan seeks nominees and applicants to fill a tenure-track position at the **ASSISTANT** or **ASSOCIATE PROFESSOR** level. The appointment is based in the Department of Biologic and Materials Sciences, the Basic Science Department in the School of Dentistry and recipient of over $8 million per year in federal funding. The successful candidate may obtain a joint appointment in an appropriate department in the College of Engineering. An especially important aspect of this position is that excellent resources are available University-wide to support this position. There is a long history of multidisciplinary interaction in the areas of biomaterials, bioengineering, and tissue engineering at the University of Michigan. The successful candidate will have the opportunity to become an integral faculty member and will have access to high quality graduate students in established Ph.D. programs in biomedical engineering and oral health sciences, as well as emerging University initiatives in nanotechnology, cellular, and molecular biotechnology, regenerative medicine, and organogenesis.

Applicants should hold a Ph.D. or equivalent degree in bioengineering, materials engineering, or related field, or in a biological science with strong background interests and postdoctoral experience in materials science. Qualified applicants should be able to establish an independent and extramurally funded research program. They should also possess a strong commitment to teaching biomaterials and training doctoral students.

Research areas of particular interest include, but are not limited to, organic and inorganic biomaterials, biomolecular engineering, nanotechnology, surface science and cell-surface interactions, microfluidics, biosensors, cellular biomechanics, and/or biofilms.

For best consideration, applications should be received by November 30, 2005. Application, curriculum vitae, two- to three-page research plan, and names of at least five references should be sent to:

David H. Kohn, Ph.D.
Chair, Search Committee for Biomaterials
Department of Biologic and Materials Sciences
School of Dentistry
University of Michigan
Ann Arbor, MI 48109-1078
Telephone: 734-764-2206
Fax: 734-647-2110
E-mail: dhkohn@umich.edu

The University of Michigan is an Equal Opportunity Employer.

FACULTY POSITION, PHYSIOLOGY

The Department of Physiology at Loyola University Chicago Stritch School of Medicine seeks applicants for tenure-track positions at the **ASSISTANT** or **ASSOCIATE** or **FULL PROFESSOR** level. Applicants (with Ph.D., M.D., or equivalent) are expected to establish a strong and interactive research program. More senior applicants should have a strong record of research productivity and extramural support. Applicants whose research complements and extends existing research strengths in cellular and molecular aspects of cell signaling mechanisms in cardiovascular or neuroscience are especially encouraged (see **website: http://www.luhs.org/depts/physio/index2.cfm**). Send letter, curriculum vitae including research plans, and names of three references to:

Donald Bers, Ph.D.
Department of Physiology
Loyola University Chicago
2160 South First Avenue
Building #102, Room #4644
Maywood, IL 60153

Loyola University Chicago is an Equal Opportunity/ Affirmative Action Employer.

POSITIONS OPEN

ASSISTANT PROFESSOR: The Department of Biology at Denison University invites applications for a tenure-track position with emphasis in plant biology to begin August 2006. Research system and specialization within plant biology are open, excluding genetics and systematics. A strong potential for excellence in teaching and for a productive research program involving undergraduates is essential. Ph.D. is required; postdoctoral experience and demonstrated teaching ability are assets. Teaching responsibilities include advanced courses (junior/senior level) in the candidate's area of specialty and introductory courses for both majors and nonmajors. In addition, shared oversight of the Denison greenhouse is expected.

Denison offers competitive startup funds, summer support for student and faculty research, a 350-acre biological reserve with field station near campus and the new Talbot Hall of Biological Science. See our **website: http://www.denison.edu/biology** for more detailed descriptions of the position and the program. Candidates should send a cover letter addressing their interest in liberal arts education; curriculum vitae; statements of teaching philosophy and research interests; copies of transcripts (graduate and undergraduate); and the names, e-mail addresses, and telephone numbers of three references to:

Chair, Plant Biologist Search Committee
Biology Department
Denison University
Granville, OH 43023

Review of applications will begin October 10, 2005. *Denison is an Affirmative Action/Equal Opportunity Employer. Women and minorities are especially encouraged to apply.*

Saint Mary's College of California seeks a leader who will build upon a record of success and lead the School of Science to its next level of academic excellence. With strong institutional support, the **DEAN** will continue to develop our outstanding undergraduate science and mathematics programs and our national reputation as a leader in undergraduate science education.

An independent institution, Saint Mary's draws upon three principle traditions: the liberal arts, Catholicism, and the "Lasallian" education vision of Saint John Baptist DeLaSalle. The faculty is committed to maintaining lives of current and vigorous teaching and research/scholarship. This allows us to provide our students with an outstanding educational experience characterized by vibrant and innovative teaching, personal contact between professor and student, and frequently highlighted collaborative research projects that convey the excitement and hands-on nature of all scientific investigations.

The Dean is the primary academic advocate and administrative officer of the School, which has a full-time faculty of nearly 50, representing the disciplines of biology, chemistry, computer science, mathematics, physics, psychology, environmental science, and 3+2 engineering, as well as a consortium arrangement with Samuel Merritt College of Nursing. The Dean promotes the vitality, integrity, and advancement of all programs and ensures that the programs and the policies of the School are consistent with the College's mission.

POSTDOCTORAL POSITION IMMUNOLOGY

Applications are invited for a Postdoctoral position to investigate the molecular mechanisms underlying development of neonatal immunity and T cell memory (for details see **website: http://www.missouri.edu/~mmiwww/habib/hz.php**). Candidates should possess a Ph.D. and/or M.D. and a good background in molecular biology. Salary is competitive and Columbia is a quality living city. Please send curriculum vitae and the names of three references to: **H. Zaghouani, University of Missouri School of Medicine, Department of Molecular Microbiology and Immunology, DC044, Columbia, MO 65212, U.S.A.** Or, **e-mail: zaghouanih@health.missouri.edu.**

Affirmative Action/Equal Opportunity Employer.

POSITIONS OPEN

ANIMAL BEHAVIOR Indiana University, Bloomington

The Department of Biology of Indiana University invites applications for an open rank, tenure-track **FACULTY POSITION** in animal behavior. We seek candidates with a conceptually driven research program to complement existing strengths in the evolution, ecology, and behavior program. The specific focus within animal behavior is open, but we especially encourage applicants whose research uses evolutionary or ecological approaches to understand the function and diversity of behavior and/or neuroethological, endocrinological, or genetic approaches to understanding the mechanisms of behavior. Indiana University is widely recognized for its outstanding interdisciplinary programs in behavior, including the Center for the Integrative Study for Animal Behavior (**website: http://www.indiana.edu/~animal/**) and a new NIH Training Program in Common Themes in Reproductive Diversity (**website: http://www.indiana.edu/~reprodiv/**). Strong applicants are expected to have postdoctoral research and/or teaching experience and established research productivity. The successful candidate will be provided with a competitive startup package and will be expected to establish a vigorous, externally funded research program and to participate in teaching undergraduate and graduate courses. For information about the Biology Department and for links to the campus and the Bloomington community, see **website: http://www.bio.indiana.edu.** Candidates should send curriculum vitae, a statement of research, and representative publications and should arrange to have three letters of recommendation sent to: **Chair, Animal Behavior Search, Department of Biology, Indiana University, 1001 East Third Street, Bloomington, IN 47405-3700.** Review of applications will begin October 15, 2005, and will continue until suitable candidates are identified. *Indiana University is an Affirmative Action/Equal Opportunity Employer. Women and minority candidates are encouraged to apply.*

RESEARCH ASSISTANT PROFESSOR

Southern Illinois University (SIU) School of Medicine welcomes applications for a position as a Research Assistant Professor. Responsibilities: Perform research to collect and analyze behavioral, electrophysiological, biochemical, genetic, and other data as necessary to study the regulation of sleep during infectious and inflammatory disease in rodent models. Position also involves teaching in relevant subject areas to SIU School of Medicine students. Requirements: Ph.D. degree or equivalent in pharmacology, physiology, neuroscience, genetics, immunology, or a related field. Salary Range: $38,500 to $41,796 annually. Full-time position. Regular hours 8:30 a.m. to 5:00 p.m. To apply: To assure full consideration, applicants should send curriculum vitae to: **Richard Herndon, Business Manager, Department of Pharmacology, Southern Illinois University School of Medicine, P.O. Box 19629, Springfield, IL 62794-9629.** Applications will be accepted for this position through October 3, 2005. *SIU School of Medicine is an Affirmative Action/ Equal Opportunity Employer.*

POSTDOCTORAL RESEARCH ASSOCIATE: To participate as a member of the team conducting research to investigate the roles of dietary fatty acids and phytochemicals in modulating inflammatory responses and chemoprevention. Successful candidate will require hands-on experience in molecular biological techniques including transgenic mice, bioinformatics, and gene manipulation. A strong background in molecular biology is highly desirable. Recent doctoral degree in biological sciences is required: good potential to advance to faculty rank. Send application materials to: **Dr. Daniel Hwang, Department of Nutrition, Meyer Hall, University of California, Davis, CA 95616-4160. Telephone: 530-754-4838; e-mail: dhwang@whnrc.usda.gov.**

University of California, Davis is an Equal Opportunity Provider and Employer.

PROTEIN CRYSTALLOGRAPHER

Department of Biochemistry & Molecular Biology
Oregon Health & Science University

The Department of Biochemistry & Molecular Biology at OHSU is seeking faculty candidates with expertise in protein crystallography to be appointed at the rank of Associate or Full Professor.

Applicants should have an established record of outstanding scientific achievement, interest in participating in an interactive research environment within the scientific community at OHSU, and be committed toward teaching and mentoring the next generation of biochemists.

Substantial start-up funds and an endowed professorship will be available to support the successful candidate's research program. Applicants should send *curriculum vitae* and names and addresses of four references by November 15, 2005 to:

Chair, Faculty Search Committee
Biochemistry & Molecular Biology
Oregon Health & Science University
3181 SW Sam Jackson Park Road
Mail code L224
Portland, Oregon 97239-3098

OHSU is an Affirmative Action/Equal Opportunity Employer

Faculty Position in Molecular/Cellular Neuroscience

Washington University in St.Louis

Department of Anatomy and Neurobiology

Two faculty positions at Washington University School of Medicine in St. Louis, MO are available for individuals taking innovative approaches to fundamental questions in molecular neuroscience. These positions are in the Department of Anatomy and Neurobiology (**http://thalamus.wustl.edu/**) and will be at the Assistant Professor or Associate Professor level. The department houses 20 active research labs in neurobiology, and is part of a much larger inter-departmental neuroscience program (program website **http://neuroscience.wustl.edu/**). Excellent shared facilities are available for molecular and cellular neuroscience, including imaging (electron and optical microscopy) and mouse genetics (generation and behavioral analysis of transgenic and knockout lines). Both the department and the neuroscience program offer numerous opportunities for scientific interactions and collaborations.

To apply: Send by email attachment **one PDF or Word document** that includes your cover letter, CV, research summary, and names and email addresses of three references. **Send one document only**, limited to 10 pages to **susan@brainvis.wustl.edu**. In addition, please arrange for three letters of recommendation to be sent to **Dr. David Van Essen**, via email to **susan@brainvis.wustl.edu**. Applications and letters must be received by **December 1, 2005**.

AA/EOE M/F/D/V.

EXHIBIT DEVELOPERS
Full Time Temporary

The Museum of Science and Industry, Chicago is currently seeking two Exhibit Developers. The first is for a large-scale science exhibition about physics and chemistry. The second is for an exhibition about human biology and health. Each position requires deep subject-related knowledge in its respective topic areas. General responsibilities include, but are not limited to, the following:

- Provide creative exhibit development activities to develop interactive concepts
- Interpret and translate science content into outstanding hands-on experiences
- Work with consultants to produce units for prototyping, evaluation, and testing
- Manage and coordinate collaborative academic partnerships to gain useful feedback and creative ideas

The Exhibit Developer for the Science Storms project must be able to effectively communicate scientific principles related to chemistry, physics, materials science, and nanotechnology to the general public. A Master's degree in chemistry, physics or materials science and/or four- to 10-years related experience is required.

The Exhibit Developer for the Body Human project must be able to effectively communicate scientific principles related to biology, physiology, and neuroscience to the general public. A Master's degree in the biological sciences and/or four- to 10-years related experience is required. Emphasis in physiology or neuroscience is preferred.

For each position a Ph.D. is a plus. Previous experience producing informal, hands-on educational learning experiences is highly desired. To apply for the Science Storms or Body Human position, please send a letter of interest, curriculum vitae, and three references to: **Museum of Science and Industry, Human Resources, 57th Street and Lake Shore Drive, Chicago, IL 60637; www.human.resources@msichicago.org; Fax: 773-684-0019.**

AA/EOE/ADA

Founding Director, Mills Breast Cancer Institute

Carle Foundation Hospital, Carle Clinic Association, College of Medicine at Urbana-Champaign University of Illinois

The Mills Breast Cancer Institute, partnered by Carle Foundation Hospital, the University of Illinois, College of Medicine, and Carle Clinic Association is seeking to fill an innovative new position to nucleate this institute focused on breast cancer treatment and research. This position provides an opportunity for someone to assume the leadership of a completely new research program that has received outside funding to ensure that the program is fully staffed, functioning and operating in a new facility by March 2008. Duties include: Development of the Institute, hiring and directing staffing, identifying and initiating research projects, and providing input on creation of a new $30 million facility. Administrative direction of MBCI to identify quality issues in areas of cancer care; clinical patient care and teaching activities will also be included. Research activities will be at both Carle Foundation Hospital in establishing the new research program for the Mills Breast Cancer Institute as well as research and teaching in the College of Medicine at Urbana-Champaign, in conjunction with a faculty position. The successful candidate will be a physician and have previous healthcare administrative experience; board certification in practicing specialty; and have a proven research track record, with demonstrated funding on a national level. Champaign-Urbana, Illinois offers the residential advantages of a medium-sized university city; excellent cultural opportunities; and easy access to Indianapolis, Chicago and St. Louis.

The starting date will be a mutually agreed upon date on or before May 2006. For fullest consideration, candidates should submit curriculum vitae with a complete list of publications and a summary of research interests and future plans, and should arrange to have at least 3 letters of reference sent on or before **November 15, 2005** to: **Founding Director MBCI Search, Attn: Cathy Emanuel, (217)383-4505, Carle Foundation Hospital, 611 W. University Avenue, Urbana, IL 61801.**

TENURE-TRACK FACULTY POSITIONS
Biochemistry/All Ranks
Indiana University
Bloomington, Indiana

The Department of Chemistry at Indiana University has a distinguished record of scientific achievement and is in the midst of significant additions to its faculty. Several new initiatives are underway in Bloomington, Indiana, including the construction of a new center for interdisciplinary research. We invite applications for tenure-track faculty in biochemistry beginning August 2006. Successful candidates will possess outstanding credentials and be expected to develop a vigorous, independent research program. All faculty members contribute to teaching and curricular development. Candidates with interests in all aspects of biochemistry but especially areas such as chemical biology, structural biology, and proteomics will be considered in a new human biology program. Individuals of advanced stature with proven performance in research and teaching are encouraged to apply and will be considered at the **ASSOCIATE** or **FULL PROFESSOR** level.

Applicants must specify the area or areas in which they have special competence and include curriculum vitae. **ASSISTANT PROFESSOR** candidates should include a summary of future research plans and arrange to have four letters of recommendation forwarded to the Department. Review of applications will begin upon receipt and will continue until the positions are filled. Send applications to:

Chairman, Department of Chemistry
800 E. Kirkwood Avenue
Indiana University
Bloomington, IN 47404
Fax: 812-856-5050
E-mail: chemchair@indiana.edu

Indiana University is an Affirmative Action/Equal Opportunity Employer and especially encourages applications from women and members of minority groups.

TENURE-TRACK FACULTY POSITION
Biochemistry and Molecular Biology

The Department of Biochemistry and Molecular Biology at Southern Illinois University Carbondale, School of Medicine invites applications for a tenure-track position at the **ASSISTANT** or **ASSOCIATE PROFESSOR** level. The candidate's research program should be in gene regulation and its involvement in development or disease. Applicants must have an M.D. or Ph.D. in life sciences or related area. We will give preference to those with two or more years of postdoctoral experience. The ability to develop an active, externally funded research program and to contribute to teaching medical and graduate students is required. The position is a 12-month appointment with a competitive salary, excellent facilities, and substantial startup funds. All applicants should submit a cover letter, curriculum vitae, research plan, and arrange for three letters of reference to be sent to:

Dr. Joseph C. Schmit
Chair, Department of Biochemistry and Molecular Biology
1245 Lincoln Drive
Neckers Room 229C
Southern Illinois University
School of Medicine
Carbondale, IL 62901
E-mail: jschmit@siumed.edu

Application review will begin November 1, 2005, and continue until the position is filled.

This is a security-sensitive position. Before any offer of employment is made, the University will conduct a pre-employment background investigation, which includes a criminal background check.

Southern Illinois University Carbondale is an Equal Opportunity/Affirmative Action Employer that strives to enhance its ability to develop a diverse faculty and staff and to increase its potential to serve a diverse student population. All applications are welcomed and encouraged and will receive consideration.

POSITIONS OPEN

University of Massachusetts
UMASS Medical School

TENURE-TRACK FACULTY POSITION
Department of Cell Biology
University of Massachusetts
Medical School
Worcester, Massachusetts

Applications are invited for a tenure-track faculty position at the **ASSISTANT PROFESSOR** level. Candidates of outstanding research potential are being sought to develop an extramurally funded program within the areas of developmental biology and genetics, particularly related to mammalian systems (mouse and human) from a cellular perspective and/or as linked to cancer. The position is highly competitive with regard to salary, startup funds, and new laboratory space.

The University of Massachusetts Medical School and Graduate School of Biomedical Sciences are undergoing rapid growth. Excellent core facilities, including genomics, proteomics, microscopy, digital imaging, and transgenic/knockout mice are provided. The Department has been ranked among the top cell biology research programs in the country. Send letter of application with curriculum vitae, statement of accomplishments and research plans, and the names and addresses of three references as a PDF file to: **Dr. Jane B. Lian, Search Committee Chair** or **Dr. Gary S. Stein, Department Chair** at **e-mail: cellbiosearch@umassmed.edu.** *An Equal Opportunity/Affirmative Action Employer.*

ASSISTANT PROFESSOR, evolutionary developmental biology. Augustana College invites applications for a tenure-track position in the Department of Biology beginning September 2006. Duties include teaching two courses each semester. These are developmental biology, evolutionary biology, team-taught introductory biology courses, and possibly a course in the candidate's specialty during our January term. While teaching is a major component of the position, productive research involving undergraduates is expected and is a long-standing tradition in the Department. The College is situated in an area experiencing rapid growth in biomedical, biotech, agricultural, and environmental research; offering collaboration opportunities in various research areas. Applicants must possess a Ph.D. A commitment to the mission of a church-related liberal arts college is expected. Visit us at **website: http://www.augie.edu** or contact the chair at **e-mail: mike.wanous@augie.edu, telephone: 605-274-4712.** Salary is competitive and dependent upon qualifications. Excellent fringe benefits are included. Review of applications will begin October 7, 2005. Send a letter of application, including goals for teaching and professional development, copies of undergraduate and graduate transcripts, curriculum vitae, and three letters of reference, and the e-mail addresses and telephone numbers of references to: **Dr. Bob Kiner, Dean of the College, Box 763, Sioux Falls, SD 57197. Telephone: 605-274-5545; fax: 605-274-5547.** Applicants must comply with the Immigration Reform and Control Act, and are required to submit official transcripts upon employment. *Augustana College is an Equal Opportunity/Affirmative Action/Title IX Employer. Qualified minority applicants are encouraged to apply.*

UNIVERSITY OF FLORIDA

One **POSTDOCTORAL POSITION** is available immediately to study proteins imported into mitochondria for conversion of cholesterol to steroid hormones. Candidates with Ph.D. in molecular cell biology or protein biochemistry using spectroscopic tools should send curriculum vitae with contact information of three references to: **Himangshu Bose (e-mail: hbose@ufl.edu), Department of Physiology and Functional Genomics, P.O. Box 100274, University of Florida, Gainesville, FL 32610-0274.** Visit our laboratory at **website: http://www.med.ufl.edu/phys/hbose.shtml.** *Equal Employment Opportunity Institution.*

POSITIONS OPEN

ASSISTANT PROFESSOR, cell biology-biochemistry. Augustana College invites applications for a tenure-track position in the Department of Biology beginning September 2006. Duties include teaching two courses each semester. These are cell biology, biochemistry, team-taught introductory biology courses, and possibly a course in the candidate's specialty during our January term. While teaching is a major component of the position, productive research involving undergraduates is expected and is a long-standing tradition in the Department. The College is situated in an area experiencing rapid growth in biomedical, biotech, agricultural, and environmental research; offering collaboration opportunities in various research areas. Applicants must possess a Ph.D. A commitment to the mission of a church-related liberal arts college is expected. Visit us at **website: http://www.augie.edu** or contact the chair at **e-mail: mike.wanous@augie.edu, telephone: 605-274-4712.** Salary is competitive and dependent upon qualifications. Excellent fringe benefits are included. Review of applications will begin October 7, 2005. Send a letter of application, including goals for teaching and professional development, copies of undergraduate and graduate transcripts, curriculum vitae, and three letters of reference, and the e-mail addresses and telephone numbers of references to: **Dr. Bob Kiner, Dean of the College, Box 763, Sioux Falls, SD 57197. Telephone: 605-274-5545; fax: 605-274-5547.** Applicants must comply with the Immigration Reform and Control Act, and are required to submit official transcripts upon employment. *Augustana College is an Equal Opportunity/Affirmative Action/Title IX Employer. Qualified minority applicants are encouraged to apply.*

ASSISTANT PROFESSOR OF STRUCTURAL BIOLOGY
Department of Structural Biology
Stanford University
School of Medicine

Applications are invited for a tenure-track junior faculty appointment in the Department of Structural Biology, Stanford University School of Medicine. **Website: http://www.med.stanford.edu/school/structuralbio/.**

Candidates must have a Ph.D. and have expertise and a commitment to future research in the broad area of structural biology and biophysics. The predominant criterion for tenure-track University appointment is a major commitment to research and teaching. Applicants should send curriculum vitae, description of research interests and future research goals, representative reprints, and the names of three references to:

Chair, Faculty Search Committee
Department of Structural Biology
Stanford University
School of Medicine
299 Campus Drive West
D105 Fairchild Building
Stanford, CA 94305-5126

Evaluation of applications will begin on November 15, 2005; applications received after this date may not receive full consideration. *Stanford University is an Equal Opportunity/Affirmative Action Employer.*

POSTDOCTORAL POSITION
NANOFABRICATION

A Postdoctoral position is available to use genetically engineered polypeptides that can selectively recognize and bind to inorganics for the self-assembly of nanoscale electronic devices. The preferred background for this exciting multidisciplinary project is physical chemistry, biochemistry, or electrical engineering, but all candidates with interest in crossing the conventional boundaries of these fields will be considered. Please send a complete curriculum vitae, a brief description of career goals, and the names of three references to: **Dr. Babak Parviz, Campus Box 352500, Department of Electrical Engineering, University of Washington, Seattle, WA 98195, U.S.A. E-mail: babak@ee.washington.edu.**

Faculty Position in Macromolecular Crystallography

The Wistar Institute, an independent non-profit research institute with a primary focus on cancer research, is seeking outstanding candidates for the rank of Assistant (or possibly Associate) Professor.

The successful candidate is expected to develop a vigorous, independent, extramurally funded research program addressing contemporary biomedical problems. Preference will be given to candidates who can combine biochemical and/or biophysical techniques with X-ray crystallography, to study mechanisms of protein and/or nucleic acid function in areas complementing existing programs in Gene Expression and Regulation, Molecular and Cellular Oncogenesis, and Immunology. The Wistar Institute is an NCI-designated Basic Cancer Center. Its Core grant supports several facilities, including proteomics, protein expression, genomics, microarray, bioinformatics and microscopy facilities (www.wistar.org). The Institute's location on the University of Pennsylvania campus provides convenient access to abundant academic resources, including graduate and undergraduate students and many potential academic and clinical collaborators.

Highly competitive laboratory start-up support, salary, and fringe benefits will be offered. Candidates should have a Ph.D., M.D. or an equivalent degree, and advanced training in structural biology. Applicants should submit a curriculum vitae, brief summary of past and future research interests, and the names of three references to: **Ronen Marmorstein, Ph.D., Search Committee Chair, The Wistar Institute, 3601 Spruce Street, Philadelphia, PA 19104; e-mail: marmor@wistar.org.** Electronic applications are preferred. Applications will be accepted through October 15, 2005. EOE/AA/M/F/D/V.

www.wistar.org

THE WISTAR INSTITUTE

COLUMBUS Children's RESEARCH INSTITUTE

THE OHIO STATE UNIVERSITY COLLEGE OF MEDICINE AND PUBLIC HEALTH

FACULTY POSITION IN PEDIATRIC INFECTIOUS DISEASES

Henry G. Cramblett Chair in Medicine

Columbus Children's Research Institute and The Department of Pediatrics at The Ohio State University seek an outstanding MD or MD/PhD scientist to hold the Henry G. Cramblett Chair in Medicine. Candidates must have a distinguished record of research accomplishment and experience in the care of pediatric infectious diseases. It is anticipated that the position will be filled at the Professor level. Excellent research space and facilities are available at Columbus Children's Research Institute on the campus of Columbus Children's Hospital. Exceptional opportunities exist for collaboration in the Center for Microbial Pathogenesis and the Center for Vaccines and Immunity based at Columbus Children's Research Institute and the Center for Microbial Interface Biology located on The Ohio State University campus.

Columbus Children's Research Institute is a 300,000 sq ft dedicated research facility with more than 90 full-time research faculty and an ambitious plan to continue the exciting growth trajectory established in recent years. The Institute is equipped with a state-of-the-art mouse facility and DNA sequencing, informatics, histopathology, transgenic, microarray, ES cell, and viral vector cores. Joint appointments in graduate departments of The Ohio State University are available.

For more information, please visit our websites at **www.ccri.net** and **http://www.medicine.osu.edu.** Address correspondence and curriculum vitae to:

John Barnard, MD
Columbus Children's Research Institute
700 Children's Drive
Columbus, OH 43205
Phone: (614) 722-2880 FAX: (614) 722-5892
E-mail: BarnardJ@ccri.net

Columbus Children's Hospital, Inc. and The Ohio State University are Equal Opportunity/ Affirmative Action Employers. Women, minorities, veterans, and individuals with disabilities are encouraged to apply.

DEPARTMENT HEAD

Neuroscience and Experimental Therapeutics
College of Medicine
The Texas A&M University System
Health Science Center

The Texas A&M University System Health Science Center College of Medicine, invites applications and nominations for the position of Head, Department of Neuroscience and Experimental Therapeutics. The Head will assume the leadership of a newly realigned department, and thus will have the opportunity to direct its development, including the recruitment of new faculty to build upon current research and teaching strengths within the Department and College. These include a flourishing multidisciplinary basic and clinical neurosciences group. New research space will become available in January 2006 on a competitive basis. In addition, commitment to a new research building is the number one legislative priority of the College and Health Science Center, presenting an exciting and unique opportunity for the new Head. The successful applicant should possess the following: (1) a doctorate in the Neurosciences or related fields and/or a MD degree; (2) an established record of exemplary research achievement; (3) a reputation for effective interpersonal and leadership skills; and (4) a strong commitment to excellence and innovation in medical education. The Head will guide and facilitate the continued development of programs/centers of excellence that will further enhance the national reputation of the Department and College. This necessarily includes fostering research collaborations within the College and its clinical academic partners, Scott & White Memorial Hospital & Clinic and the Central Texas Veterans Health Care System, as well as other components of the Health Science Center and The Texas A&M University System. Applications from female and minority candidates are strongly encouraged. Review of applications will begin as they are received.

Applicants should submit a current curriculum vitae and a statement of administrative philosophy, research goals and teaching interests, along with names and addresses of at least four references to: **Dr. Kelly Hester, Associate Dean for Academic Affairs, The Texas A&M University System College of Medicine, 164 Reynolds Medical Building, College Station, TX 77843-1114**. The College of Medicine's website is **http://medicine.tamhsc.edu**.

The Texas A&M University System Health Science Center is an Affirmative Action/Equal Opportunity Employer.

THE UNIVERSITY OF IOWA

GENETICS

Department of Biological Sciences
The University of Iowa

Applications are invited for a tenure-track position at the Assistant Professor level. We are seeking candidates that are addressing fundamental problems in genetics at the molecular, cellular, organismal, or population level. We invite individuals working on plant, animal, fungal or microbial systems to apply. The Department has seen significant growth over the last five years, including establishment of the Roy J. Carver Center for Comparative Genomics, and additional growth is anticipated during the next five years. More about the Department and the Center for Comparative Genomics may be viewed at **www.biology.uiowa.edu** and **www.biology.uiowa.edu/ccg**.

Candidates must have post-doctoral experience and a recognized record of accomplishment as reflected in publications in leading journals. The successful candidate will be expected to establish and maintain an extramurally funded research program and participate in the department's teaching mission. Recently renovated space and a competitive start-up package will be made available. Applicants should send a curriculum vitae, statement of research objectives, selected reprints, a description of teaching interests, and the names of three references to: **Genetics Search Committee, c/o Becky Birch, Department of Biological Sciences, 143 Biology Building, The University of Iowa, Iowa City, IA 52242-1324.** Review of applications will begin **November 1, 2005** and continue until the position is filled.

The University of Iowa is an Affirmative Action/Equal Opportunity Employer. Women and minority candidates are especially encouraged to apply.

FACULTY POSITION, VIROLOGY
Department of Microbiology and Immunology
University of Oklahoma Health Sciences Center
Oklahoma City, Oklahoma

The Department of Microbiology and Immunology at the University of Oklahoma (OU) Health Sciences Center invites applications for a 12-month, tenure-track position at the **ASSISTANT** or **ASSOCIATE PROFESSOR** level with emphasis in cancer virology. Applicants for the Assistant Professor position must have a Ph.D. or equivalent degree with at least two years of postdoctoral training. At the Associate Professor level, the successful candidate is expected to have an independent extramurally funded research program. Although outstanding scientists in all areas of virology are encouraged to apply, special consideration will be given to those applicants whose research focus is related to the viral etiology of cancer. The successful candidate will join a well-funded interdisciplinary group of virologists and will also have opportunities to interact with other scientists involved in cancer research and contribute to the scientific development of the new OU Cancer Center. Teaching responsibilities will involve participation in the virology portions of the team-taught graduate, medical, and dental curricula within the Department. The Department currently has 13 full-time, tenured, or tenure-track faculty, more than 40 extramural grants and contracts, and ranks in the top 20 NIH-sponsored medical school microbiology departments. For an overview of the Department, visit our **website: http://w3.ouhsc.edu/mi.** Submit curriculum vitae, description of research interests and teaching experience, and the names and contact information, including e-mail addresses, of three references to **e-mail: virology-search@ouhsc.edu** or mail information to: **Chair of the Search Committee, Department of Microbiology and Immunology, BMSB-1053, 940 S. L. Young Boulevard, Oklahoma City, OK 73104.** Applications will be reviewed as they are received. *The University of Oklahoma is an Equal Opportunity/Affirmative Action Employer. Applications from women and ethnic minorities are strongly encouraged.*

BIOINFORMATICS POSITION. Tenure-track **ASSISTANT PROFESSOR** level position, University of Nebraska-Lincoln Department of Statistics. Start January 2006 or later (negotiable), pending final approval. Ph.D. in statistics. Emphasis on bioinformatics/biotechnology. Outstanding research/teaching potential. Applicants should complete the faculty administrative information at **website: http://employment.unl.edu.** Application materials required and mailing address at **website: http://employment.unl.edu.** Review of applications begins October 1, 2005, and continues until a suitable candidate is found or search is closed. More at **website: http://statistics.unl.edu.** *The University of Nebraska is committed to a pluralistic campus community through Affirmative Action and Equal Opportunity, and is responsive to the needs of dual career couples. We assure reasonable accommodation under the Americans with Disabilities Act: contact Barbara Pike at telephone: 402-472-7214 for assistance.*

POSTDOCTORAL FELLOWSHIPS in Neurobiology of Disease at University of California, Davis. Postdoctoral fellowships are available immediately, Department of Neurology and the Neurosciences graduate program at the University of California at Davis. Projects include genomic/microarray studies of stroke and intracerebral hemorrhage; neurogenesis following stroke; cell death and survival signaling pathways following stroke; and blood genomics of neurological diseases. Animal surgery experience, molecular biology skills, and computer and writing skills are essential. Send curriculum vitae and names and addresses of three references to: **Frank R. Sharp, M.D., Department of Neurology, MIND Institute, University of California at Davis, 2805 50th Street, Sacramento, CA 95817. E-mail: frsharp@ucdavis.edu.** *The University of California is an Affirmative Action/Equal Opportunity Employer.*

POSITIONS OPEN

FRED HUTCHINSON CANCER RESEARCH CENTER
A LIFE OF SCIENCE

FACULTY POSITION

The Fred Hutchinson Cancer Research Center is recruiting a faculty physician/scientist (M.D. or M.D./Ph.D.) with active laboratory research and clinical expertise in a breast cancer–related discipline. Candidates with translational research interests and a desire to join a strong cross-disciplinary research team in breast cancer are encouraged. Candidates at **ASSISTANT, ASSOCIATE,** or **FULL MEMBER** levels will be considered. The primary appointment will be in the Clinical Research Division of the Fred Hutchinson Cancer Research Center. If desired, a joint appointment may be made to other divisions at the Center and to the full-time faculty in an appropriate department at the University of Washington. Interested individuals should forward their curriculum vitae, including a research plan and the names of five references, to: **Suzanne Lentz, Fred Hutchinson Cancer Research Center, 1100 Fairview Avenue N., mail stop: C1-015, P.O. Box 19024, Seattle, WA 98109.** The closing date for applications is December 15, 2005.

The Fred Hutchinson Cancer Research Center is an Affirmative Action, Equal Opportunity Employer. We are dedicated to building a culturally diverse faculty and strongly encourage applications from women, minorities, individuals with disabilities, and covered veterans.

AQUATIC PLANT BIOLOGIST
TENURE-TRACK ASSISTANT PROFESSOR
Colgate University

We seek a tenure-track Assistant Professor to start August 2006. Ph.D. or expectation of completion this academic year required; teaching and postdoctoral research experience desirable. The successful candidate will contribute to a foundation course in evolution, ecology, and diversity, teach elective courses in their specialty and contribute to interdisciplinary and University-wide programs, including environmental studies. The appointee will join a biology faculty deeply committed to a strong, research-oriented program involving undergraduate students and will add to this effort by offering a research tutorial in their area of interest. Please forward a letter of application with curriculum vitae, transcripts, and separate statements of teaching philosophy and research interests to: **Dr. Randy Fuller, Department of Biology, Colgate University, 13 Oak Drive, Hamilton, NY 13346-1398** and also arrange to have three letters of recommendation sent to this address. Review of applications will begin October 7, 2005, and continue until the position is filled. We intend to begin interviewing candidates by the end of October. *Colgate University is an Equal Opportunity/Affirmative Action Employer. Developing and maintaining a diverse faculty and staff further the University's academic mission. Women and minorities are especially encouraged to apply.*

The Department of Chemistry and Biochemistry at The University of Texas at Austin is seeking to expand its faculty with the addition of two tenure-track **ASSISTANT PROFESSOR** positions starting September 1, 2006. We seek the best candidates with interests in teaching and research. Applicants with expertise in the areas of bioanalytical chemistry and structural biology (X-ray or nuclear magnetic resonance) are particularly encouraged to apply. Exceptional candidates in other areas and at other ranks may also be considered. Visit **website: http://www.cm.utexas.edu** for further information. Applications should be received by October 1, 2005, for full consideration. Candidates should forward curriculum vitae, a description of future research plans, a statement of teaching philosophy, and three letters of reference to: **Biochemistry Faculty Search Committee, Department of Chemistry and Biochemistry, The University of Texas at Austin, 1 University Station A5300, Austin, TX 78712-0165.** *Equal Opportunity/Affirmative Action Employer.*

POSITIONS OPEN

ASSISTANT PROFESSOR
BIOLOGY

Full-time, tenure-track Biologist. Responsibilities include courses in human biology, human anatomy and physiology, developmental biology, and an advanced-level course. Must have a Ph.D. and commitment to excellence in teaching; teaching and a focus on student learning are primary duties of faculty. Department offers collegial work environment and relatively small classes. Research, particularly projects involving undergraduates, is encouraged. Tenure-track faculty are eligible for a one semester sabbatical during their first three years to carry out research and other preparations for tenure review. Start date is January 2006 (preferable) or September 2006, pending budget approval.

Forward cover letter, curriculum vitae, transcripts, statement of teaching philosophy, long-term goals, and three letters of reference. Screening will begin September 30, 2005, and will continue until the position is filled. Additional information on the Department at **website: http://biology.wsc.ma.edu.** Send materials to:

Dr. David Doe
Chair, Biology Search Committee
Department of Biology
Westfield State College
577 Western Avenue
Westfield, MA 01086-1630

Women, persons of color, and persons with disabilities are encouraged to apply. Affirmative Action/Equal Opportunity Employer.

Two **TENURE-TRACK** positions at the **ASSISTANT PROFESSOR** level for (A) a physiologist and (B) a vertebrate zoologist. (A) Must have a Ph.D. in biology, physiology, or zoology with an emphasis in physiology. Must be qualified to teach upper-level human physiology, human anatomy-physiology to nursing students, and advanced courses in specialty of interest. (B) Must have a Ph.D. in biology, zoology, or wildlife biology with an emphasis in vertebrate zoology. Must be qualified to teach herpetology or ichthyology or mammalogy, and human anatomy-physiology to nursing students, comparative vertebrate zoology, and advanced courses in specialty of interest. Postdoctoral experience preferred. Must participate in graduate program and establish a modest research program. Salary commensurate with experience. Review of applicants will begin immediately, with a deadline of October 10, 2005, or until position is filled. Starting date: August 2006. Applicants should send application materials to address below. To access more information, click here at **website: http://www.sfasu.edu/biologypositions.html.** Send letter of application, curriculum vitae, transcripts, three letters of recommendation, and a statement of teaching and research philosophies and career objectives to: **Dr. Don A. Hay, Chair, Department of Biology, Box 13003, Stephen F. Austin State University, Nacogdoches, TX 75962-3003. Telephone: 936-468-3601. E-mail: dhay@sfasu.edu.** Applications subject to disclosure under Texas Open Records Act. Security-sensitive position: Criminal background check required for successful candidate. *Equal Opportunity/Affirmative Action Employer.*

POSTDOCTORAL FELLOW

The Basic Science Research Group in the Department of Dermatology at Columbia University seeks to hire a Postdoctoral Fellow to contribute to ongoing projects to study the mechanism of ultraviolet-induced cell cycle alterations and signal transduction in skin tumorigenesis. Applicants should have a Ph.D. degree or equivalent in biological or related fields with strong background in molecular biology, general laboratory techniques, experience in manipulation of mice. Send curriculum vitae and three references to: **Mohammad Athar, Ph.D./David R. Bickers, M.D., 630 West 168th Street, VC 15-204, New York, NY 10032. E-mail: ak309@columbia.edu; fax: 212-305-7391.**

We take Affirmative Action toward Equal Employment Opportunity.

POSITIONS OPEN

ANIMAL ECOLOGY
University of Wyoming

The Department of Zoology and Physiology at the University of Wyoming invites applications for a tenure-track position in animal ecology beginning August 2006 at the level of **ASSISTANT PROFESSOR,** or at a higher rank for an individual with an outstanding research and funding record. Research interests can involve any aspect of animal ecology, although a focus on spatial aspects of population dynamics and habitat use would complement existing areas of expertise in our Department. Applicants should have peer-reviewed publications and evidence of teaching potential. Teaching responsibilities include an introductory course in either general biology, ecology, or fisheries and wildlife biology plus an upper-division course in the candidate's area of expertise. Teaching responsibilities also include supervision of graduate student research. The candidate will be expected to advise undergraduates in our wildlife and fisheries biology major and to develop an extramurally funded research program. Ph.D. required for faculty rank.

Review of applications will begin on October 7, 2005. Applicants should send curriculum vitae and statements of research and teaching interests, and should arrange to have three letters of reference sent to: **Chair, Animal Ecology Search Committee, Department of Zoology and Physiology, Department 3166, 1000 E. University Avenue, University of Wyoming, Laramie, WY 82071. Website: http://uwadmnweb.uwyo.edu/Zoology.** *The University of Wyoming is an Affirmative Action/Equal Opportunity Employer.*

SYSTEMS NEUROSCIENTIST
The University of Texas at Dallas

The Cognition and Neuroscience Program of the School of Behavioral and Brain Sciences at The University of Texas at Dallas (UTD) seeks a Systems Neuroscientist whose research interests directly address issues of plasticity in nervous systems. This individual will add to our multidisciplinary research programs investigating sensory systems, neural plasticity, aging, computational and neural modeling, memory, etc. (see **website: http://www.utdallas.edu/dept/bbs**). Appointment is tenure track at the **ASSISTANT** (or, if qualified, **ASSOCIATE**) **PROFESSOR** level, beginning in the 2006 academic year. For information (no e-mail applications), contact: **Dr. Aage Moller, Neuroscience Search Chair (e-mail: amoller@utdallas.edu).** We have a strong and growing undergraduate (B.S.) and graduate (Ph.D.) program, with top academic ratings, excellent research facilities, and competitive startup packages. Send curriculum vitae and three letters of reference to: **Academic Search #580, The University of Texas at Dallas, P.O. Box 830688—AD23, Richardson, TX 75083-0688.** *Indication of sex and ethnicity for Affirmative Action statistical purposes is requested as part of the application but not required. UTD is an Affirmative Action/Equal Opportunity Employer and strongly encourages applications from candidates who would enhance the diversity of the University's faculty.*

SCIENTIFIC DIRECTOR, Damon Runyon Cancer Research Foundation. Nationally respected nonprofit committed to supporting young, basic, and clinical investigators in cancer research seeks Scientific Director to oversee its grant programs (currently $11 million), serve as liaison to the scientific community, and develop communications and participate in activities to promote awareness about the Foundation. Ph.D., M.D., or equivalent advanced scientific degree, experience with research grant processes, and outstanding oral and written communications skills required. Position description can be viewed at **website: http://www.drcrf.org.** Please submit a letter of application and curriculum vitae to: **Lorraine Egan, Damon Runyon Cancer Research Foundation, 675 Third Avenue, New York, NY 10017.** Or **e-mail: lorraine.egan@drcrf.org.**

POSITIONS OPEN

FACULTY POSITIONS
DEPARTMENT OF ECOLOGY AND EVOLUTIONARY BIOLOGY
DEPARTMENT OF BIOCHEMISTRY AND MOLECULAR BIOPHYSICS
University of Arizona

Two **TENURE-TRACK POSITIONS** are available as part of a new initiative in genome-based microbial science at the University of Arizona. We are searching for applicants with independent research programs within each of two broad areas: (1) microbial evolution and/or ecology, including emphases such as comparative genomics, evolution and ecology of infectious disease agents, or environmental genomics, and (2) protein structure and function on a genomic scale, including systems biology and proteomics in microbial systems. In both positions, computational and/or experimental research programs are welcome. Research organisms can be bacterial, archaeal, or eukaryotic. The positions may begin as early as January 2006. Curriculum vitae and statements of research and teaching interests must be submitted online at **website: http://www.uacareertrack.com.** The first position (#33412) will be in the Department of Ecology and Evolutionary Biology (EEB). Three letters of recommendation should be sent to: **Amanda Burke, Microbial Genomics Search, EEB Department BSW 310, 1041 E. Lowell, University of Arizona, Tucson AZ 85721.** The second position (#33450) will be in the Department of Biochemistry and Molecular Biophysics (BMB). Three letters of recommendation should be sent to: **Margaret Gomez, Microbial Genomics Search, BMB Department BSW 362B2, 1041 E. Lowell, University of Arizona, Tucson AZ 85721.** Applicants may apply to both positions. Review of applications will begin October 14, 2005, and continue until position is filled. *The University of Arizona is an Equal Employment Opportunity/Affirmative Action Employer. Minorities/Women/Persons with Disabilities/Veterans.*

ASSOCIATE CHIEF OF STAFF

The Department of Veterans Affairs Northern California Health Care System is currently recruiting for a full-time Associate Chief of Staff for Research and Development (ACOS/R&D), to head its research program. VA Northern California is an integrated health care system, which provides a full range of health care services to veterans in Northern California. VA Northern California has two major campuses and nine locations in the Northern California area. Clinical and nonclinical research is conducted at our two main campuses located at Sacramento and Martinez, California. The Sacramento campus is the site of our new medical center, which includes 16,000 square feet of basic research laboratory space and a nine-bed, 8,000 square foot NIH-funded General Clinical Research Center in collaboration with University of California, Davis (UCD). Applicants for the ACOS/R&D position must have an M.D. and/or Ph.D. degree. The successful candidate is expected to maintain an outstanding research program and facilitate the growth of new and existing intramural research programs as well as building interdisciplinary collaborations with researchers at our affiliate, UCD. The selected applicant will be provided research space at the VA Sacramento campus. Candidates should possess previous experience in administrative or leadership positions, preferably in the VA, a record of research excellence, and be eligible for academic appointment at the level of Associate Professor or Professor at our university affiliate, UCD. Candidates should forward a letter of interest describing their research and teaching background and current interests, curriculum vitae, reprints of three publications, and names and addresses of at least three references to: **VA Research Office, Attn: ACOS Search Committee, 10535 Hospital Way, Mather, CA 95655.** For full consideration applications must be received by October 11, 2005. *VA is an Equal Opportunity Employer.*

POSITIONS OPEN

FACULTY POSITIONS
Department of Chemistry
Boston College

Applications are invited for two tenure-track faculty positions, effective September 2006. Areas of interest include, but are not limited to: experimental physical, theoretical, materials, analytical, organic, inorganic, and biological chemistry, as well as related interdisciplinary areas. Successful applicants are expected to establish a prominent, externally funded research program and will join a department of approximately 100 doctoral students, 25 postdoctoral fellows, and an internationally recognized faculty. Boston College is located in a residential community bordering Boston, Massachusetts, and within 20 minutes of the other major universities in the Boston/Cambridge area. Applicants at the beginning Assistant Professor level should indicate their area or areas of research and their teaching interests by submitting both a detailed research plan and a brief statement of teaching interests, along with their curriculum vitae and a summary of previous research accomplishments. In addition, applicants should arrange to have three letters of reference transmitted. Established investigators should send a letter of application and appropriate supporting materials. All materials should be sent to: **Chair, Faculty Search Committee, Department of Chemistry, Boston College, Chestnut Hill, MA 02467-3860.** The application deadline is October 15, 2002. **Website: http://chemserv.bc.edu. Fax: 617-552-2705.** *Boston College, a university of 14 schools and colleges, is an Equal Opportunity Employer and supports Affirmative Action.*

ASSISTANT PROFESSOR

The Department of Physiological Sciences, College of Veterinary Medicine, Oklahoma State University (OSU), invites applications for a tenure-track position at the rank of Assistant Professor (Ph.D.) in physiology, cell biology, pharmacology or toxicology. Primary responsibilities include development of an extramurally supported research program and participation in the Veterinary Biomedical Sciences graduate program. Interested individuals should submit an application including curriculum vitae, statement of professional goals, and names of three references to: **Dr. Carey Pope, Interim Head, Department of Physiological Sciences, 264 McElroy Hall, Center for Veterinary Health Sciences, Stillwater, OK 74078-2014. Telephone: 405-744-6257; e-mail: carey.pope@okstate.edu.** To ensure full consideration, applications should be received by November 1, 2005. Review of applications will continue until a suitable candidate is identified. *OSU is an Equal Opportunity/Affirmative Action Employer that encourages applications from members of minority groups.*

ENVIRONMENTAL BIOTECHNOLOGY

The Cooperative Institute for Marine and Atmospheric Studies (CIMAS) of the University of Miami invites applications for two **POSTDOCTORAL POSITIONS** to work with scientists at the Rosenstiel School for Marine and Atmospheric Science (RSMAS) and the National Oceanic and Atmospheric Administration Atlantic Oceanographic and Meteorological Laboratory (AOML). The successful applicants will develop rapid methods for detection, quantification, and source tracking of aquatic fecal contamination. One applicant will develop Luminex technology and the other will develop portable and in-situ electrochemical biosensors to detect nucleic acid signatures in coastal waters. The positions require solid molecular biology skills and the ability to develop and test novel molecular methods and instruments. Excellent oral and written communication and effective collaboration with multiple partners is required. Positions require a Ph.D. degree in molecular biology, environmental science, or related field. Please apply online at **website: http://www.miami.edu/careers.**

NEW

Save money and promote your event easily!

Go to www.ScienceMeetings.org

Post your meeting or announcement ad directly to our website. It is quick, easy, and economical.

Rate: $299 per posting (commissionable to approved ad agencies). Credit card orders only.

Duration: Your ad will remain up until the end date of the meeting or one year, whichever comes first. It will be included in our searchable database within one business day of posting.

Specs: You can also include a hyperlink back to your website or your event information.

Visit: www.ScienceMeetings.org and click on Post your Meeting or Announcement or contact your sales representative.

U.S. Kathleen Clark
phone: 510-271-8349
e-mail: kclark@aaas.org

Europe and International
Tracy Holmes
phone: +44 (0) 1223 326 500
e-mail: ads@science-int.co.uk

Science
AAAS

POSITIONS OPEN

POSTDOCTORAL POSITION

Identifying human genes essential for HIV-1 replication and Developing RNA inhibitors of HIV-1. A postdoctoral position is available immediately to work in exciting HIV research projects. One project is on identifying human genes that are essential to HIV replication. The candidate will characterize the specific step in which the human protein participates and delineating the molecular mechanisms involved. The second project is on developing RNA aptamers directed to HIV-1 RT, Tat, Rev and other vital targets. This basic research project is aimed at measuring efficacy, understanding resistance, delineating the mechanism of action and ultimately geared towards bringing the aptamers to the clinic.

Individuals interested in learning more, can visit the laboratory website at: **http://www.aecom.yu.edu/prasadlab/**.

Candidates must have experience in more than one of the following areas: Molecular Biology, Virology, Nucleic acid/Protein biochemistry and Cell Biology. Candidates with at least 2 years of Postdoctoral research experience are preferred. Selected candidates are expected to develop their own research projects in 2-3 years (independent or mentored).

Interested individuals should directly email their curriculum vitae and names of three references to: **Prasad@aecom.yu.edu, Albert Einstein College of Medicine, Jack and Pearl Resnick Campus, 1300 Morris Park Avenue, Bronx, NY 10461.** EOE.

ALBERT EINSTEIN COLLEGE OF MEDICINE
Advancing science, building careers

Position Available at the University of Vermont In the Area of Neurobiology Department of Biology

Applications are invited for a tenure-track Assistant Professor position in the Department of Biology in the area of Neurobiology, to augment the research in the department in this area. Successful candidates will have experience with and research interests in neurobiology, and teaching interests in neurobiology. Candidates taking a molecular or biochemical approach and who exploit modern technologies to investigate mechanisms of biological function will be strongly considered.

All applicants are expected to (1) hold a Ph.D. degree and have two or more years of postdoctoral experience; (2) develop a competitively funded program; and (3) teach undergraduate and graduate level courses. Candidates must apply online at **www.uvmjobs.com** and must attach to that application a curriculum vitae, representative publications, and a statement of research and teaching interests. In addition, three (3) hardcopy letters of recommendation should be sent to: **Dr. Rona Delay, Department of Biology, University of Vermont, 120A Marsh Life Science Building, Burlington, VT 05405-0086.** Review of applicants will begin on **October 1, 2005**.

The University of Vermont is an Affirmative Action/Equal Opportunity Employer. The Department is committed to increasing faculty diversity and welcomes applications from women and underrepresented ethnic, racial and cultural groups and from people with disabilities.

POSTDOCTORAL POSITION IN CARDIOVASCULAR PHARMACOLOGY

PCOM

PCOM, Department **of Pathology, Microbiology and Immunology has a Postdoctoral position in cardiovascular pharmacology.** The position involves studying the role of specific Protein kinase C isoform activators/inhibitors in splanchic ischemia/reperfusion in the anesthetized rat using intravital microscopy technology. The animal model is applicable to clinical circulatory shock. The position involves setting up the animal model to evaluate leukocyte-endothelial interaction. It is desirable that the applicant has demonstrated proficiency in microscopy and in vivo animal models. The position also involves scientific writing for publication submission and aptitude in various computer software programs applicable to recording and analyzing data. In addition, the applicant should be familiar with other assays conducted in the lab such as the isolated perfused rate heart, measurement of leukocyte superoxide release and chemotaxis, endothelial nitric oxide release and histological and western blotting techniques.

Please submit detailed resume **including salary history and salary requirements** to:

PCOM
4190 City Avenue
Human Resources Department
Philadelphia, PA 19131
Fax: 215-871-6505
E-mail: hr@pcom.edu
EEO

w w w . p c o m . e d u

UNIVERSITY OF MINNESOTA

ECOLOGY AND ECONOMIC POSTDOCTORAL RESEARCHERS

Two Postdoctoral Research positions are available for scholars with skills in ecology and/or economics to work on quantification and valuation of ecosystem services in relation to agriculture and renewable energy. Positions are annually renewable for up to three years and may begin immediately. The researchers would join a multidisciplinary team led by **David Tilman** (ecology) and **Steve Polasky** (economics). Applications including curriculum vitae, list of three references, writing sample, and statement of research interests, should be sent to: **Nancy Larson, Department of Ecology, Evolution and Behavior, University of Minnesota, 1987 Upper Buford Circle, St. Paul, MN 55108.** *The University of Minnesota is an Equal Opportunity Employer.*

POSTDOCTORAL RESEARCH SCIENTIST

Lamont-Doherty Earth Observatory of Columbia University and the Department of Microbiology of the Columbia University Medical Center are recruiting for a Postdoctoral Research Scientist to carry out research in the broadly defined area of Earth microbiology. This position will be supported for two years in conjunction with the establishment of a new program in Earth Microbiology at Columbia University. Particular areas of interest include the development of novel methods for the detection and phylogenetic analysis of bacterial species inhabiting deep subsurface sediments; studies of the contribution of microbial activity to global biogeochemical cycles; and studies on the microbial contribution to the formation of gas hydrates. Individuals with backgrounds in geochemistry or a relevant area of microbiology are encouraged to apply. Excellent interpersonal and written communication skills in English are required. Search will remain open for at least 30 days after the ads appear and until position is filled. Applicants should send a cover letter specifying Search Number LD 670 05 016, curriculum vitae (please include e-mail address), and a statement of research interests to: **Ms. M. Mokhtari, Manager of Human Resources, Lamont-Doherty Earth Observatory, Palisades, NY 10964.** Or **e-mail: personnel@admin.ldeo.columbia.edu.**

Columbia University is an Equal Opportunity/Affirmative Action Employer. Minorities and women are encouraged to apply.

POSTDOCTORAL POSITIONS, molecular/cell biology of bacterial toxins. Postdoctoral positions are available in the laboratory of **Dr. Randall Holmes** at the University of Colorado School of Medicine. We are currently investigating the structure, function, and trafficking of cholera toxin and *E. coli* heat-labile enterotoxins, characterizing the roles of the metalloregulatory proteins DtxR and IdeR in iron-dependent global regulation of gene expression and virulence in *C. diphtheriae* and *M. tuberculosis*, and applying structure-based methods for development of vaccines and drugs for prevention and treatment of bacterial infectious diseases. Research facilities, grant funding, and training environment are excellent. We have new research facilities that include a BSL-3 laboratory. Recreational facilities of the beautiful Rocky Mountains are easily accessible. Salary is commensurate with training and experience. Submit curriculum vitae, bibliography, and names of three professional references to: **Dr. Randall Holmes, Microbiology Department, The University of Colorado DHSC, Mail Stop 8333, P.O. Box 6511, Aurora, CO 80045** or **e-mail: randall.holmes@uchsc.edu.** *The University of Colorado is committed to diversity and equality in education and employment. Citizens and permanent residents of the United States may be considered for positions on an NIH-funded training grant, and individuals from underrepresented groups are encouraged to apply.*

POSITIONS OPEN

POSTDOCTORAL POSITIONS (four) to study the membrane organization of glycosphingolipids and their intermembrane trafficking by transfer/binding proteins. Sphingolipid interactions with membrane lipids to be studied by fluorescence, monolayer, calorimetric, and nuclear magnetic resonance approaches. Sphingolipid transfer protein structure and function will be analyzed by X-ray diffraction, fluorescence, and circular dichroism in combination with point mutagenesis. Experience with noted approaches preferred as applied to lipid-lipid and lipid-protein interactions and/or in cloning, protein purification, and crystallization. One position focused on cellular function(s) of sphingolipid transfer proteins, including potential roles in apoptosis and cell growth/cycling. Strong background in cloning, two-hybrid analysis, protein post-translational modification, kinase-related signaling, and/or transcriptional regulation preferred. Require M.D. or Ph.D. in biophysics, biochemistry, molecular biology, or related discipline. Send curriculum vitae and names of three references to: **Professor Rhoderick E. Brown, The Hormel Institute, University of Minnesota, 801 16th Avenue, N.E., Austin, MN 55912. E-mail: rebrown@hi.umn.edu.** *The University of Minnesota is committed to the policy that all persons shall have equal access to its programs, facilities, and employment without regard to race, color, creed, religion, national origin, sex, age, marital status, disability, public assistance status, veteran status, or sexual orientation.*

POSTDOCTORAL RESEARCH POSITION

A Postdoctoral Research position is available immediately to study combined effects of neurotoxicants and environmental stress at the Environmental and Occupational Health Sciences Institute (EOHSI), a joint institute of the Robert Wood Johnson Medical School, University of Medicine and Dentistry of New Jersey, and of Rutgers, the State University of New Jersey. The research takes place in a collaborative group setting with multiple technologies operative. Experience in psychology, operant behavior, and neurochemistry is highly desirable. Salary will be commensurate with experience. Send curriculum vitae along with names and telephone numbers of three references to:

Dr. Deborah Cory-Slechta
Environmental and Occupational
Health Sciences Institute
170 Frelinghuysen Road
Piscataway, NJ 08854
E-mail: dcs@eohsi.rutgers.edu

The Environmental and Occupational Health Sciences Institute is an Equal Opportunity/Affirmative Action Employer and actively encourages interest from women and minorities.

POSTDOCTORAL RESEARCHER
(One or more positions)
Department of Biological Sciences

One or more Postdoctoral Research positions are available to study the biogenesis and metabolism of iron-sulfur proteins under cellular oxidative stress conditions. Required qualifications: Ph.D. or equivalent degree; experience in molecular biology and protein biochemistry. Additional qualification desired: working on the structure and function of metalloproteins. Application deadline is September 16, 2005, or until candidate is selected. An offer of employment is contingent on a satisfactory pre-employment background check. Interested candidates should send a cover letter, the curriculum vitae (including e-mail address), and names and addresses of three references to: **Huangen Ding, 202 Life Sciences Building, Department of Biological Sciences, Louisiana State University, Reference Log #0442, Baton Rouge, LA 70803. E-mail: hding@lsu.edu.**

Louisiana State University is an Equal Opportunity/Equal Access Employer.

POSITIONS OPEN

UNIVERSITY OF Nebraska Medical Center

POSTDOCTORAL FELLOWSHIP
Molecular Genetics of Retinal Development

Postdoctoral position available immediately to study photoreceptor development. Experience in microarray, transgenics, and proteomics is highly desirable. A strong background in genetics and molecular biology, with a Ph.D., M.D., or D.V.M. in genetics or related field is required. Competitive salary based on experience. Interested applicants should e-mail complete curriculum vitae including research interests, bibliography, names, and contact information for three references to: **Neena Haider, Ph.D.,** at **e-mail: nhaidern@unmc.edu. Website: http://www.unmc.edu/genetics.**

The University of Nebraska is an Equal Opportunity/Affirmative Action Employer. Individuals of culturally diverse backgrounds and women are encouraged to apply.

RESEARCH LABORATORY MANAGER
Center for Innovations in Medicine
Biodesign Institute
Arizona State University

The Center for Innovations in Medicine (CIM), led by **Stephen Albert Johnston,** Director, is seeking a research laboratory manager for this unique new research center. Center researchers innovate blue-sky solutions to fundamental problems in biomedicine. The CIM laboratory manager will be involved with 20 or more scientists with chemistry, biology, and/or engineering backgrounds to assure optimal infrastructure operations as well as integrating new systems, technologies, and instruments into the Center. The manager will also integrate operations with other centers and be proactive in negotiations with vendors. CIM is part of the Biodesign Institute and located in new facilities that epitomize the interdisciplinary, use-inspired science of the future. The manager will be involved in multiple projects requiring frequent priority changes to immediately respond to research needs/issues.

Deadline is September 9, 2005; if not filled, weekly thereafter until search closed. For qualification/application information, see SR #O-121265 at **websites: http://www.asu.edu/hr/jobs** or **http://www.asu.edu/biodesign** for more information about CIM and the Biodesign Institute. *Affirmative Action/Equal Opportunity Employer.*

POSTDOCTORAL POSITION, STEM CELL BIOLOGY
Harvard Institutes of Medicine

A position is available in the laboratory of **Dr. Peter Oettgen** at the Harvard Institutes of Medicine in Boston, Massachusetts. The focus of the projects include the identification of the molecular mechanisms of endothelial differentiation from pluripotent stem cells into endothelial progenitor cells and mature endothelial cells, with a particular focus on the role of specific transcription factors in this process. The successful applicant will work as part of team with broad expertise in a variety of experimental techniques and animal model systems. These studies will provide new insights into treating diseases such as ischemic heart disease and cancer.

Previous experience with embryonic stem cells or flow cytometry desirable.

Website: http://www.bidmc.harvard.edu/oettgenlab.

Please forward curriculum vitae to **e-mail: vascularbiology@bidmc.harvard.edu.**

MARKETPLACE

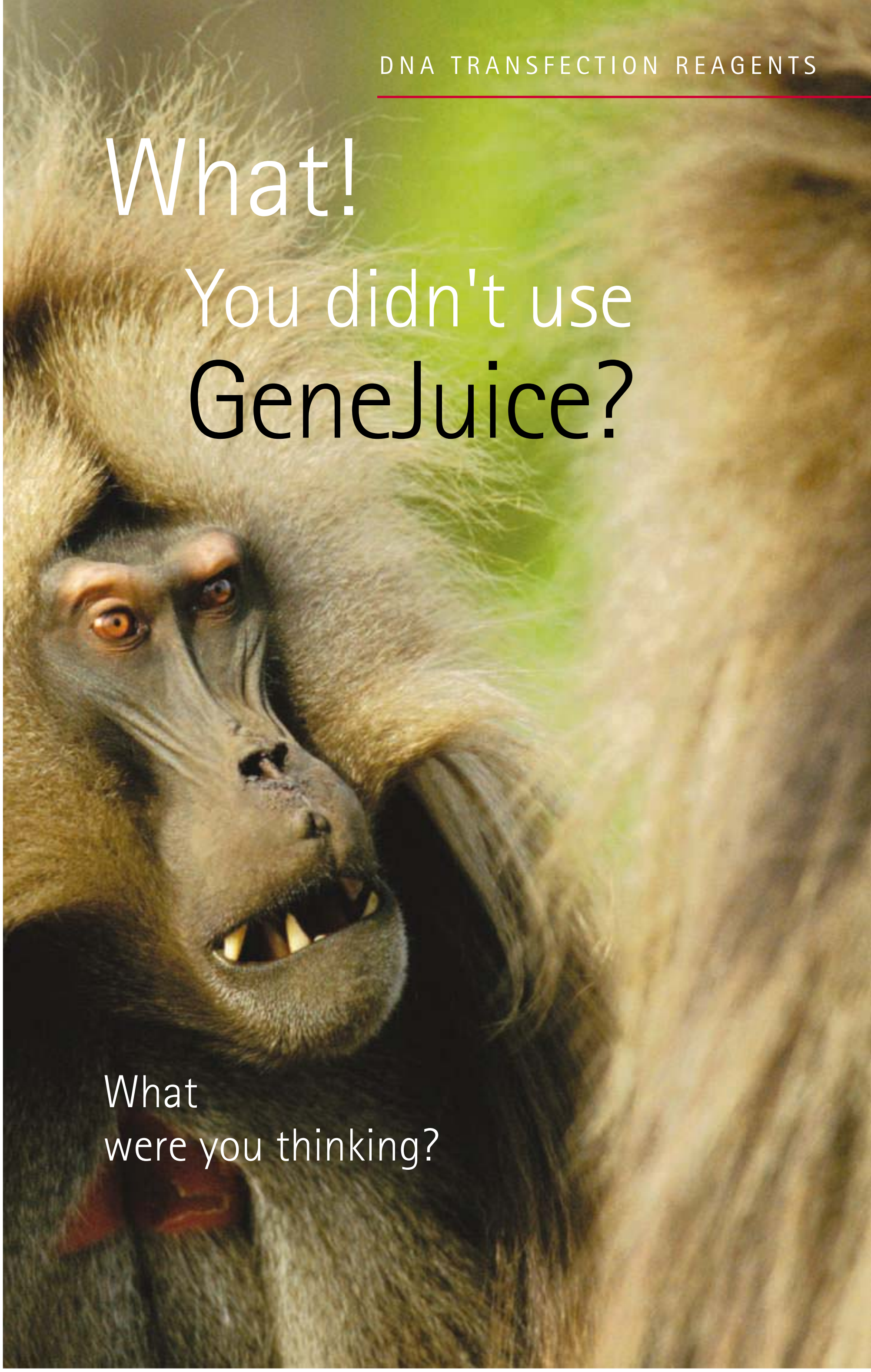
DNA TRANSFECTION REAGENTS
What!
You didn't use
GeneJuice?
What
were you thinking?